NASA Technical Memorandum 80625

Current Problems in Stellar Pulsation Instabilities

David Fischel, Janet Rountree Lesh,
and Warren M. Sparks

MAY 1980

NASA

NASA Technical Memorandum 80625

Current Problems in Stellar Pulsation Instabilities

David Fischel, Janet Rountree Lesh,
and Warren M. Sparks
Goddard Space Flight Center
Greenbelt, Maryland

National Aeronautics
and Space Administration

**Scientific and Technical
Information Office**

1980

Preface

The fourth meeting in the series of stellar pulsation conferences sponsored alternately by the Los Alamos Scientific Laboratory and the Goddard Space Flight Center was held at GSFC in Greenbelt, Maryland, on 1-2 June 1978. In contrast to previous conferences in this series, the topics of discussion included all kinds of pulsating variable stars, rather than Cepheids alone. In recognition of this broader scope, this conference was entitled "Current Problems in Stellar Pulsation Instabilities."

The Scientific Organizing Committee consisted of Drs. Morris L. Aizenman, Annie Baglin, Arthur N. Cox, David Fischel, R. Edward Nather, Kurt von Sengbusch, and Warren M. Sparks (chairman). On the Local Organizing Committee were Drs. David Fischel, Warren M. Sparks, and Janet Rountree Lesh (chairman). We made a concerted effort to gain international participation in the meeting, and about 60 scientists from 10 countries attended.

Dr. Adriaan J. Wesselink, whose pioneering work is the basis of many modern variable star studies, was an honored guest at the conference. We wish to thank Dr. Wesselink for his many perceptive comments during the discussion periods, and also for his concluding remarks.

Thanks are also due to the session chairmen, and to Dr. Norman Baker for his witty contribution to the conference dinner. We gratefully acknowledge financial support for this meeting from the National Aeronautics and Space Administration.

The Editors

Greenbelt, Md.
February 1979

CONTENTS

List of Participants

Thomas F. Adams	Los Alamos Scientific Lab.
Morris L. Aizenman	National Science Foundation
B. Altner	Rutgers University
Norman H. Baker	Columbia University
Thomas G. Barnes	University of Texas
Wallace R. Beardsley	University of Pittsburgh
Emilia P. Belserene	Maria Mitchell Observatory
J. Robert Buchler	University of Florida
C. John Butler	Armagh Observatory
Julius H. Cahn	University of Illinois
P. W. Cole	Boston University
Leo P. Connolly	Sierra Nevada College
Arthur N. Cox	Los Alamos Scientific Lab.
John P. Cox	JILA
Cecil G. Davis	Los Alamos Scientific Lab.
Robert G. Deupree	Boston University
Joel A. Eaton	Pennsylvania State University
Nancy Remage Evans	University of Toronto
Richard P. Fahey	Goddard Space Flight Center
J. Donald Fernie	David Dunlap Observatory
David Fischel	Goddard Space Flight Center
R. Gingold	Cambridge University
Marcel Goossens	University of Louvain
Henry A. Hill	University of Arizona

Richard W. Hillendahl	Science Applications, Inc.
Stephen W. Hodson	Los Alamos Scientific Lab.
Douglas A. Keeley	Science Applications, Inc.
Charles F. Keller	Los Alamos Scientific Lab.
David S. King	University of New Mexico
Yoji Kondo	Goddard Space Flight Center
Janet Rountree Lesh	Goddard Space Flight Center
Kam-Ching Leung	Office of Energy Research, DOE
Stephen P. Maran	Goddard Space Flight Center
John T. McGraw	University of Texas
David D. Meisel	Geneseo State College
Andrew G. Michalitsianos	Goddard Space Flight Center
R. Edward Nather	University of Texas
Jan Willem Pel	University of Groningen
Edward L. Robinson	University of Texas
Jeffrey D. Rosendhal	NASA Headquarters
Jean-Pierre Sareyan	Nice Observatory
Richard Scuflaire	University of Liege
Barry M. Schlesinger	Goddard Space Flight Center
Edward G. Schmidt	University of Nebraska
Henry L. Shipman	University of Delaware
Edward M. Sion	Villanova University
Paul Smeyers	University of Louvain
Myron A. Smith	University of Texas
Yousef Sobouti	Pahlavi University
Sabatino Sofia	Goddard Space Flight Center

William H. Spangenberg	Los Alamos Scientific Lab.
Warren M. Sparks	Goddard Space Flight Center
S. Ranga Sreenivasan	University of Calgary
Robert F. Stellingwerf	Rutgers University
Allen V. Sweigart	Goddard Space Flight Center
Hugh M. Van Horn	University of Rochester
Adriaan Wesselink	Yale University
Lee Anne Willson	Iowa State University
Robert F. Wing	Ohio State University
Charles L. Wolff	Goddard Space Flight Center
H. John Wood	Indiana University
Peter R. Wood	Mt. Stromlo Observatory
Chi-Chao Wu	Goddard Space Flight Center
Eugene R. Zizka	University of Pittsburgh

OBSERVATIONS OF CLASSICAL CEPHEIDS

J.W. Pel

Kapteyn Astronomical Institute
University of Groningen
Groningen, The Netherlands

Reviewing the observations of Cepheids, I feel like a man who is holding a wide-angle camera out of the window, in order to get a picture of the large and complex building in which he is living himself. You know what can be expected of such an attempt: at best a highly distorted picture, with aberrations that are closely related to the photographer's position. I will do my best to reach out of the window as far as I can, but please be aware of the distorted perspective! It is obviously not possible to get all sides of the building into one picture, so I will limit myself to the "classical" Cepheids, leaving out the W Virginis and RR Lyrae variables.

New observations

In Table 1 I have listed the most important observational studies of Cepheids that have been made in the last five years. Rather arbitrarily I let this compilation start in 1973, and I should add that this table does not pretend to be a complete list of *all* Cepheid observations since 1973: only the more extensive sets of new data are given.

Two aspects of these recent observations are immediately clear: the concentration on photometry - both photoelectric and photographic - of the continuous spectra, and the emphasis on the southern hemisphere. Of course the Magellanic Clouds constantly draw our attention to the south, but also the southern galactic Cepheids have been observed extensively during the last few years. In fact, we have now reached the situation that the

Table 1. Important sets of new observations of classical Cepheids since 1973

AUTHORS	REFERENCES	REMARKS
R. Wielen	1974, A&A Suppl. 15, 1 (also: 1973, A&A 25, 285	Space velocities for 45 nearby Cepheids.
B.F. Madore	1975, Ap. J. Suppl. 29, 219 (also: 1976, M.N.R.A.S. 177, 215)	UBV for 22 LMC, 15 SMC, and 46 southern galactic Cepheids ($P > 11^d$).
E.G. Schmidt	1976, Ap. J. 203, 466	R,I and b,y for 14 field Cepheids and 9 in open clusters, also 34 giants in or near clusters.
C.J. Butler	1976, A&A Suppl. 24, 299	Photographic B,V for 72 SMC Cepheids.
J.W. Pel	1976, A&A Suppl. 24, 413 (also: 1978, A&A 62, 75 and Walraven et al. 1964 B.A.N. 17, 520)	VBLUW for 170 galactic Cepheids and 238 supergiants ($\delta < +15^o$).
E. Janot-Pacheco	1976, A&A Suppl. 25, 159	UVBGR for 13 southern Cepheids.
N.R. Evans	1976, Ap. J. Suppl. 32, 399 (also: 1976, Ap. J. 209, 135)	UBVR and v_{rad} for 15 Cepheids.
K.A. Feltz, D.H. McNamara	1976, P.A.S.P. 88, 699, 709	*uvbyβ* and *khg* for B and A stars near 12 Cepheids.
J.F.Dean, A.W.J.Cousins, R.A. Bywater, P.R.Warren	1977, Mem. R.A.S. 83, 69 1977, M.N.A.S.S.A. 36, 3 and paper in preparation	BVI for 60 southern galactic Cepheids.
O.J. Eggen	1977, Ap. J. Suppl. 34, 1, 33	UBVRI for 10 SMC, 11 LMC, 5 galactic, and 6 glob. cluster Cepheids, 50 glob. cluster (sub)giants; *uvbyβ* for associations of ℓ CAR and RS PUP.
A.M. van Genderen	1977, A&A 54, 737 (also: 1969, B.A.N. 20, 317)	VBLUW for 25 Cepheids in SMC.
L. Szabados	1977, Comm. Hungarian Acad. Sc. 70	UBV for 38 northern Cepheids ($P < 5^d$), more work for longer periods in progress.
C.J. Butler	1978, A&A Suppl. 32, 83	Photographic B,V for 98 LMC Cepheids (larger LMC material in preparation by Wayman and Stift).
W.L. Martin	work in progress at SAAO	Photographic B,V for large number of Cepheids in LMC

Cepheids in the southern Milky Way have been observed more thoroughly than their northern counterparts!

Table 1 represents an enormous effort by many observers, and in half an hour it is impossible to do justice to the many new results that can be found in these papers. I will try to summarize the main progress that has been made, and point out some of the problems that still have to be solved.

Colour excesses

The first problem that one encounters in the study of the continuum colours of Cepheids is that of interstellar extinction. From the extensive literature and the continuing discussions on this subject it is clear that, at least in our own galaxy, this first step towards the temperature scale is by no means the easiest one.

Although the different methods of reddening determination have not yet converged to generally accepted colour excesses, some progress has been made during the last five years. We still find differences in zeropoint, in the sense that on the whole all colour excesses of method A may differ by a fixed amount from those of method B. But there used to exist also much more serious systematic discrepancies between different reddening scales, that depended on the periods, or on the amount of reddening. One important result of the more recent photometric studies is, that these latter effects have largely disappeared now.

This is demonstrated most clearly by the two new southern surveys with the largest overlap, the BVI program of the SAAO observers (Dean, Warren, Cousins, and collaborators), and my own photometry in the Walraven VBLUW system. These studies have about 60 Cepheids in common, over the whole range of periods. When we compare these two extensive sets of reddening values, we note only a small zeropoint difference: the VBLUW excesses, transformed to $E(B-V)_J$, are on the average about $0^m.05$ smaller than the colour excesses derived by Dean et al. in the BVI system. This zeropoint difference should not be taken too seriously, however, as it could be resolved by taking slightly different reddenings for the Cepheids in clusters and associations that were used in both studies to define the zeropoints of the intrinsic Cepheid colours. More important than this minor disagreement is the small r.m.s. scatter in the relation between both sets of reddenings ($\pm 0^m.03$), and in particular the absence of period-dependent

effects.

Both methods use passbands at about 5500 and 4300 Å, but the VBLUW method combines these with L at 3840 Å to construct an intrinsic Cepheid locus, while the BVI system uses I at 8100 Å. Considering the very large difference in line-blocking between the L and I regions, I find it most reassuring that both methods produce reddening results that agree very well, regardless of the periods of the Cepheids.

The overlap of the BVI and the VBLUW colour excesses with those derived from six-colour data by Parsons and Bell (1975) is limited, but the agreement between these three reddening scales seems satisfactory, with only small differences in zeropoint, and no signs of period-dependent effects. On the other hand, these three studies all differ significantly from the colour excesses used by Sandage and Tammann (1968) in their calibration of the P-L-C relation. The latter excesses are essentially in the Kraft system.

This situation confirms the trend towards smaller reddenings that has been apparent for some years already. Since the pioneering work by Kraft in the early sixties, several investigators have pointed out that the reddenings based on the original Kraft calibration were probably overestimated, particularly for the longer periods. Not only the three papers mentioned above, but also much other recent work supports smaller reddening values, e.g. Canavaggia et al. (1975), Feltz and McNamara (1976), Schmidt (1975).

Cepheids in clusters and associations

As indicated above, the zeropoint of the intrinsic colours of Cepheids ultimately rests upon the Cepheids in open clusters and associations. But even for these calibrating Cepheids the intrinsic colours and luminosities are not always as accurately known as one would like. This is partly due to the patchiness of interstellar extinction, partly to photometric inaccuracies. I expect therefore that a completely consistent system of absolute magnitudes and intrinsic colours for galactic Cepheids can only be established by doing more photometry of the open clusters and associations that contain Cepheids. Although a lot of work in this field has been done in the last few years, these few calibrating Cepheids are in so many respects a keystone in all studies of classical Cepheids, that new observ-

ational work on these objects is still fully justified. It would especially be valuable if some clusters could be re-observed with properly chosen photometric systems that do not suffer from complications due to bandwidth effects, and with reddening-free indices such as H_β; one obviously should try to go as faint as possible on the main-sequence, in order to reduce the uncertainty in the main-sequence fitting.

Schmidt (1976) has recently studied eight Cepheids in clusters with R,I and Strömgren b,y photometry, but his observations do not cover the cluster main-sequences. At the Leiden Southern Station we are working on VBLUW photometry for clusters with Cepheids, but results are not yet available. Eggen (1977) discusses uvbyβ photometry for the associations that have been suggested as parent associations for the long-period Cepheids ℓ CAR and RS PUP. Unfortunately, the observations by Eggen indicate that these associations do not exist. This bad news is compensated somewhat by the recent evidence for the membership of the 11-day Cepheid TW NOR of the open cluster Lyngå 6 (Madore, 1975[a], 1975[b]; Van den Bergh and Harris, 1976; Lyngå, 1977; Thé, 1977). Van den Bergh (1977) gives a list of 14 cluster/association Cepheids. For this list he rejects as less reliable the Cepheids in binaries (ℓ CAR, Polaris) and in reflection nebulae (SU CAS, RS PUP), and the four Cepheids that are thought to be members of h+χ PER (UY PER, VY PER, VX PER, SZ CAS). On the other hand, a number of new cluster/association members appear in this table that were not among the well-known 13 of Sandage and Tammann (1969): V367 SCT, CS VEL, CV MON, T MON, TW NOR, VY CAR, SV VUL (for references see Van den Bergh, 1977).

The case of V367 SCT is particularly important, as this Cepheid is a double-mode pulsator (Efremov and Kholopov, 1975; Madore and Van den Bergh, 1975; Madore et al., 1978). As the only known double-mode cluster Cepheid, this star is very valuable in view of the well-known mass problems that exist for Cepheids in general and for beat-Cepheids in particular. Stobie (1977) shows that the pulsation mass derived for V367 SCT is consistent with the pulsation masses for other cluster Cepheids, but that it leads again to discrepancies with the evolutionary and double-mode mass estimates.

Compared to the 13 Cepheids of Sandage and Tammann, the longer periods may be represented slightly better in Van den Bergh's list, but the fact

remains that we still have only a very small number of calibrating Cepheids at our disposal. This stresses once more: 1) that we should observe these Cepheids and their parent clusters as accurately as possible, 2) that the reliability of the dubious cluster/association Cepheids should be checked with additional observations (radial velocities and/or proper motions!), 3) that the search for new calibrating Cepheids should continue. Considering the fact that most massive stars are probably formed in associations, it is surprising how few long-period Cepheids have been found to be association members. This probably just means that our methods to detect such cases have not been very efficient.

Duplicity among Cepheids

A problem that has become somewhat prominent only relatively recently is that of duplicity among Cepheids. Since the early value by Abt (1959), who estimated that about 2% of the Cepheids are in binaries, the numbers have gone up considerably. Lloyd Evans (1968) estimates $\geq$ 15% for the binary percentage, while Janot-Pacheco (1976), Madore (1977) and Pel (1978) give values around 25%. As is shown by Madore (1977) it may be possible in many cases to correct for the presence of the companion, but this needs either rather detailed information about the observed composite energy distribution, or a priori assumptions. In any case we should keep in mind that part of the scatter in our empirical relations for Cepheids will be due to duplicity.

The existence of binary Cepheids also has its positive aspects: they are interesting from the point of view of stellar evolution, and, provided that detailed information can be obtained for the companions, they can even yield independent mass and luminosity estimates for the Cepheids.

As the binary companions of Cepheids are likely to be bluer than the Cepheids in most cases, their contribution to the combined colours will usually become smaller towards longer wavelengths. This is one advantage of photometry in the red part of the spectrum.

Ultraviolet colours

The red part of the spectrum has other advantages too: less line-blocking, less interstellar reddening, and good separation of temperature effects and interstellar reddening. Indeed we see that compared to the

"UBV-era" of ten, fifteen years ago, an increasing amount of Cepheid photometry is being done in the R and I bands. On the other hand, if we abandon the complex blue and ultraviolet part of the Cepheid spectrum altogether in favour of spectral regions that behave more like black-body radiation, the only photospheric parameter that we can determine is the effective temperature. Information on other physical parameters such as surface gravity and chemical composition is of course obtained best from those parts of the spectrum that deviate most from Planck's law. In this particular case this means that if we want photometric effective gravities for Cepheids, we need at least one passband shortward of the Balmer jump. One naturally thinks of the UBV U-band, and of the large body of UBV data that has been collected over the years.

The interpretation of (U-B) colours of Cepheids has always been problematic, however, due to complications with the U band that arise mainly from its great width and from the fact that the red flank of U extends slightly beyond the Balmer jump. It is therefore worthwhile to investigate whether the wealth of new photometric data that is now available (mostly in other systems than UBV) could possibly help us to solve the old problems with the UBV U-band.

To give you the answer right away: I am pessimistic in this respect! Let me make this clear in the following figure (Fig. 1), which shows a comparison of (U-B) with the three ultraviolet colours of the VBLUW photometry. The UBV data used here are from Wampler et al. (1961) and from Cousins and Lagerweij (1968).

In the region of the UBV U-band the Walraven system has three bands: one (L, with λ_{eff} at 3840 Å) just longward of the Balmer jump in the region of the higher Balmer lines, and two bands in the Balmer continuum (U at 3630 Å, and W at 3255 Å). Going across the Balmer jump from L to U and W, we note a drastic change in the temperature and gravity dependence of the colours. For F-G supergiants of a given composition, (B-L) is almost exclusively temperature-sensitive (the VBLUW and UBV B-bands are very similar), while (B-U) and (U-W) - Balmer jump and slope of the Balmer continuum, respectively - depend mostly on gravity. This explains the very different behaviour of these three colours during the Cepheid cycle.

Comparing the VBLUW data now with $(U-B)_{UBV}$, we see that the $(U-B)_{UBV}$ curves are nearly identical with (B-L)! This means that the integral over

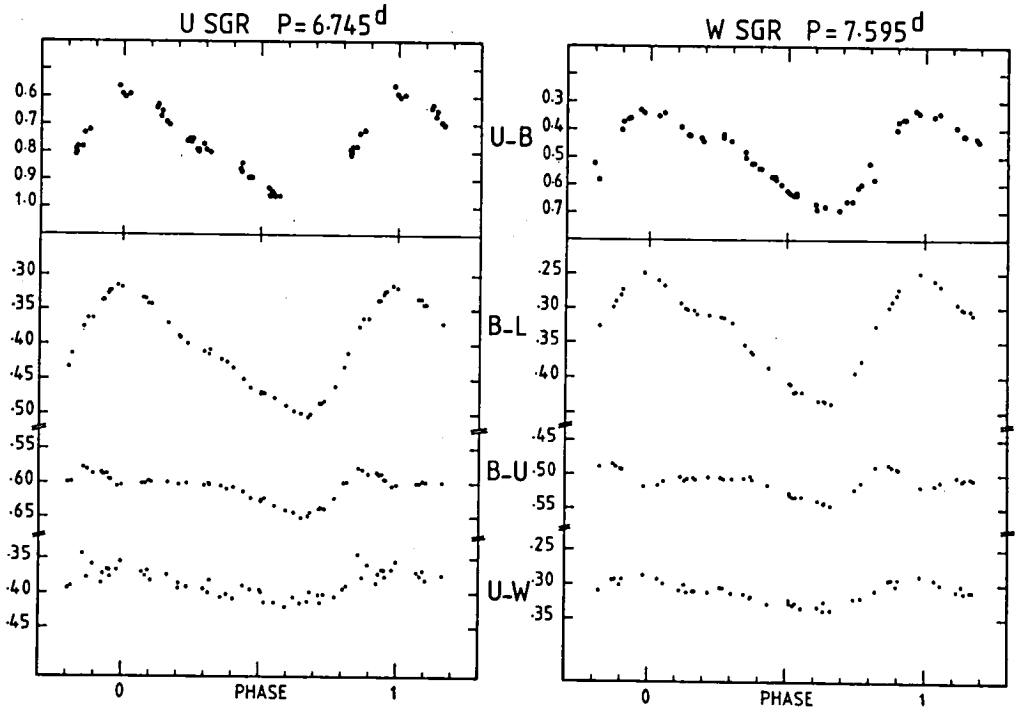

Fig. 1. Cepheid colour curves in the ultraviolet colours (B-L), (B-U) and (U-W) of the VBLUW system compared with the UBV (U-B)-curves. The $\log_{10}$(intensity) scale of the VBLUW data has been adjusted to the UBV magnitude scale.

the U_{UBV} band is completely dominated by the flux in the long-wavelength tail, just longward of the Balmer jump. So for Cepheids and supergiants later than type A, this band, which was originally meant to give information about the Balmer jump, effectively is still in the Paschen continuum. This is quite understandable if we realize how steep the intensity drops below the Balmer jump for these cooler supergiants, but it makes $(U-B)_{UBV}$ practically useless as source of physical information for these stars. Even if we would solve the photometric complications caused by the varying effective wavelength of U_{UBV}, and the systematic differences between observers due to slightly different red wings of various U-filters, the contribution of log g in (U-B) could hardly be disentangled from the dominating temperature sensitivity.

I discuss this problem in some detail in order to underline a more general warning, both to future observers of Cepheids and to theorists who

compute light and colour curves for hydrodynamic Cepheid models: 1^{o} take care to use passbands with accurately known response curves, that fit well to the main features in the stellar spectra, and 2^{o} beware of the Balmer jump!

Temperature-colour relations, mass discrepancies

In Fig. 2 I have collected most of the temperature-colour relations that exist in the literature for Cepheids and intermediate to late-type supergiants. These relations have been obtained with widely different methods, and I will not go into any of the details of these, but it is striking that at both ends of the colour range the general agreement in temperature is quite reasonable, while in between there exist large differences. Around $(B-V)_o = 0^m.9$ the temperature estimates for class I supergiants may differ by as much as 800 K! Even for Cepheids, which form a much more sharply defined subgroup of supergiants, the differences between various authors are surprisingly large.

These differences are probably mostly due to uncertainties in the temperature calibrations, but partly also to the problems with colour excesses and intrinsic colours that we discussed before. It should be noted that the problem of interstellar extinction may enter the temperature determination for a Cepheid even twice. Firstly, the calibration of a temperature-colour relation often implies reddening corrections for one or more calibrating stars. Secondly, the reddening correction that we apply to a Cepheid determines where this star will lie on the temperature-colour relation.

Up to now I assume implicitly that there exists a unique relation between $(B-V)_o$ and T_{eff} for Cepheids, but some authors have questioned this uniqueness. Schmidt has pointed out in several papers (e.g. Schmidt, 1973) that $(B-V)_o$ may not be a good temperature indicator, and for this reason he has advocated the use of $(R-I)_o$. Schmidt's arguments against $(B-V)_o$ are supported qualitatively by my own temperature determinations for Cepheids, but quantitatively I find the non-uniqueness of the T_{eff} - $(B-V)_o$ relation less severe than suggested by Schmidt. This is illustrated in Fig. 3.

The effective temperatures and gravities for Cepheids that I derived from the VBLUW photometry are based upon a calibration of the VBLUW

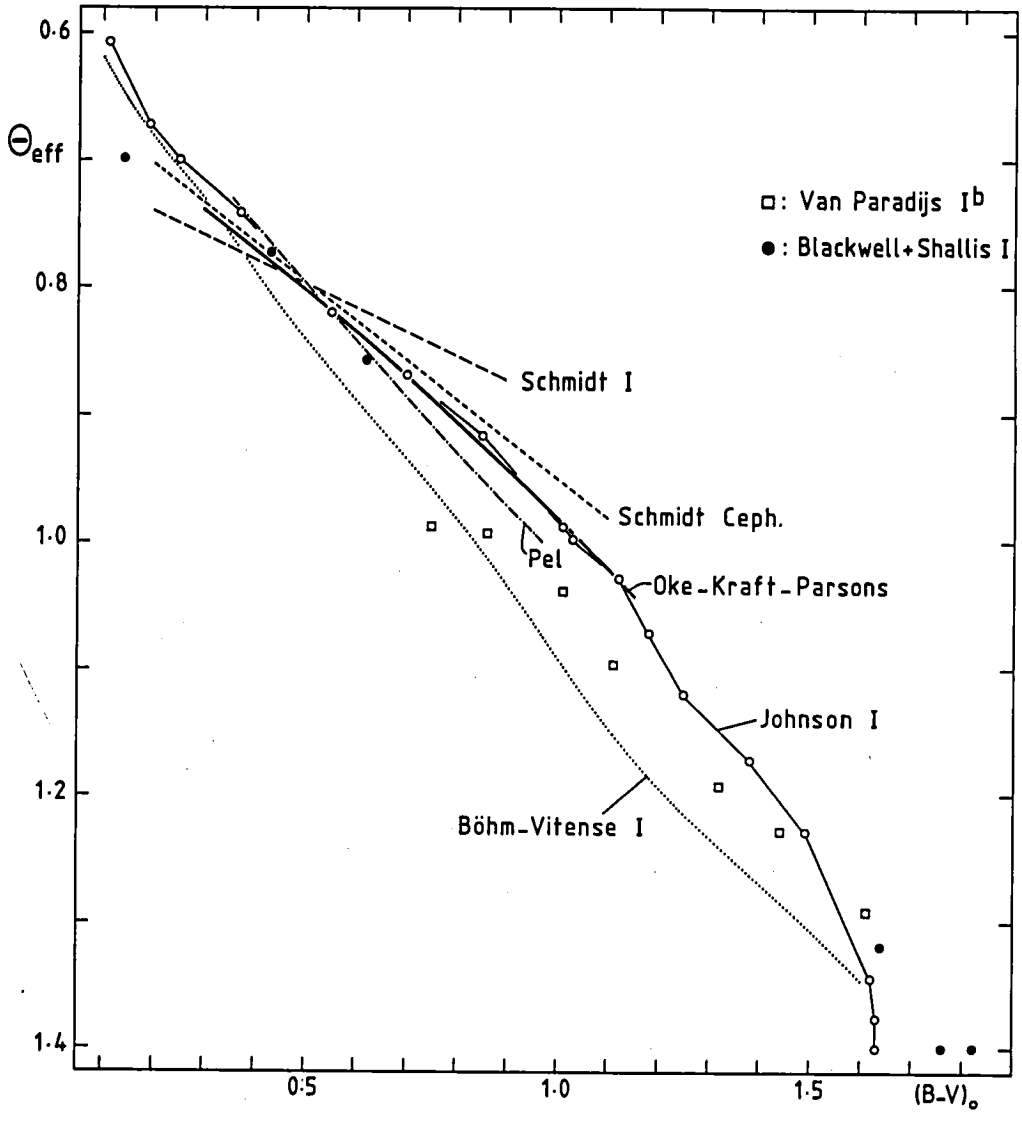

Fig. 2. Temperature-colour relations for Cepheids and supergiants.

Class I supergiants:

Johnson I : Johnson (1966).
Böhm-Vitense I : Average for I^a and I^b supergiants from Böhm-Vitense (1972).
Schmidt I : Schmidt (1972).
Van Paradijs I^b : 7 individual I^b supergiants. Van Paradijs (1973).
Blackwell + Shallis I : 6 individual class I supergiants from Blackwell and Shallis (1977). For one star (δ CMa, at $(B-V)_o$ = 0.62) E(B-V) was derived from VBLUW data, the other stars are within 200 pc, and small corrections were made according to E(B-V) = $0^m.3$ kpc^{-1}.

Cepheids:

Oke-Kraft-Parsons : Oke (1961); Kraft (1961); Parsons (1971, 1974).
Schmidt Ceph. : Schmidt (1972).
Pel : average relation derived from Pel (1978).

The relation by Rodgers (1970) is not shown separately, as it lies very close to the Oke-Kraft-Parsons relation.

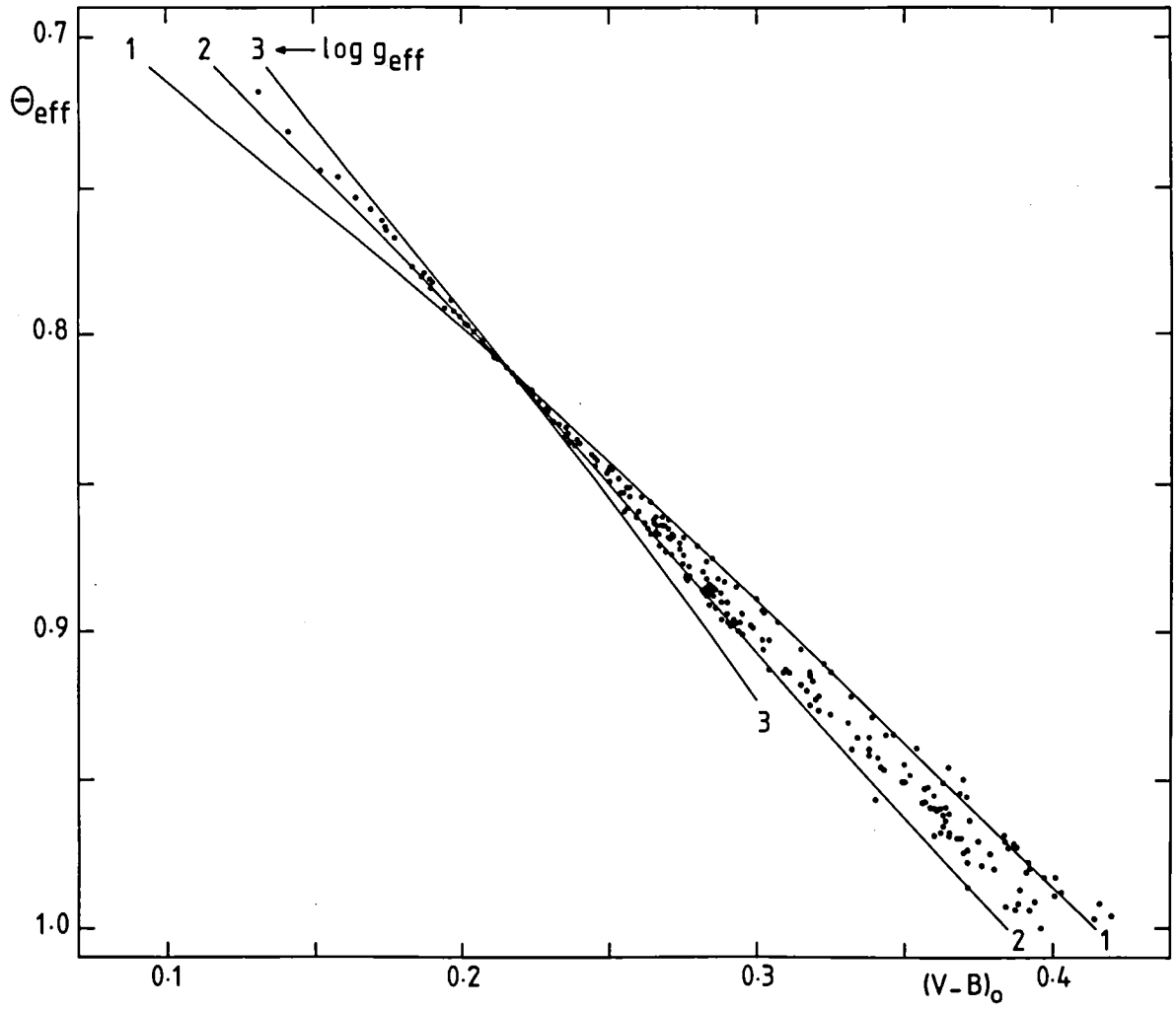

Fig. 3. Theoretical temperature-colour relations for $(V-B)_o$ (in $\log_{10}$ units) of the VBLUW system, for three different values of the effective gravity. The dots are the individual measurements for 10 bright Cepheids.

colours (Lub and Pel, 1977) by means of the model atmosphere fluxes of Kurucz (1975, 1978). These theoretical fluxes are for hydrostatic, plane-parallel atmospheres in LTE, but they include the blanketing by nearly one million atomic lines by means of opacity distribution functions. Fig. 3 gives the theoretical relations between inverse effective temperature and $(V-B)_o$ for different values of surface gravity. $(V-B)_o$ is the VBLUW equivalent of $(B-V)_o$ in the UBV system. The plotted points are the individual measurements for ten bright Cepheids that cover the whole range of periods. The theoretical colours do not cover the minima of the long-period

Cepheids completely, so points cooler than $\Theta = 1$ have been omitted. The divergence for different gravities at the cool end in Fig. 3 is clear, but the spread around the mean temperature-colour relation for Cepheids is not too disturbing. Near $(V-B)_o = 0.4$ the detailed temperature determinations scatter around the mean relation by ± 75 K at most. To make the comparison with other relations in Fig. 2, I adopted the following mean temperature-colour relation (V-B in $\log_{10}$ units):

$$\Theta_{eff} = 0.552 + 1.331(V-B)_o - 0.582(V-B)_o^2$$

The transformation of this relation into $(B-V)_o$ is probably slightly gravity-dependent, but this uncertainty can be neglected for the present purpose.

The temperature scale for Cepheids automatically leads us to the well-known "mass-discrepancy" problem. Since the various kinds of Cepheid mass-discrepancies appeared in the literature, around 1970, a very large number of papers have dealt with the problem of Cepheid masses. In fact, the mass-discrepancies are responsible for a considerable part of the recent revival in Cepheid research. However, as the subject will be discussed in detail in the next session of this meeting, I will make a few short remarks only.

There are several ways of estimating Cepheid masses: "pulsation masses" M_{puls} (from the pulsation equation for Cepheids with known luminosities and temperatures), "bump masses" M_{bump} (from non-linear Cepheid models and observed phases of bumps in light- and velocity-curves), and "double-mode masses" M_{beat} (from period ratios of mixed-mode pulsators). As is well-known, each of these masses usually turns out to be smaller than evolutionary masses M_{ev}, derived from evolutionary tracks (for more detailed discussions see e.g. Fricke et al., 1972; Iben and Tuggle, 1972[a]; Cox et al., 1977; Stobie, 1977).

The temperature scale has no effect on M_{bump}, M_{beat} and M_{ev}, but M_{puls} depends strongly on the temperature ($P \propto L^{0.83}.M^{-0.66}.T_{eff}^{-3.45}$, see Iben and Tuggle, 1972[b]). As I pointed out at the Russell Symposium last year (Pel and Lub, 1978), it is possible to remove most of the discrepancy between M_{ev} and M_{puls} if we adjust the luminosities of Cepheids to the revised distance of the Hyades, and use the new smaller colour excesses and

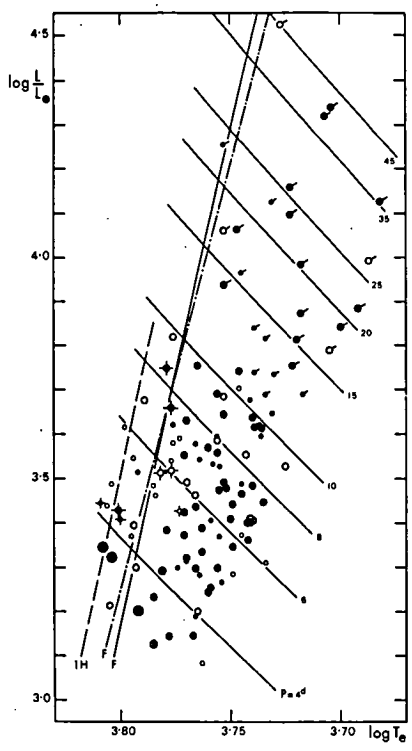

Fig. 4. Cepheids from the VBLUW survey in the HR-diagram. Luminosities were computed from the observed periods and temperatures, the pulsation equation, and a mass-luminosity relation for Cepheids (both relations taken from Iben and Tuggle, 1975). The composite fundamental ("F", full curve) and first harmonic ("1H", dashed) blue edges from Iben and Tuggle are given, as well as the fundamental blue edge ("F, dot-dash) from King et al. (1975); all for Y = 0.28, Z = 0.02, and the M-L relation of Iben and Tuggle (1975).
Open symbols: stars with known or suspected companions; ✓: long-period Cepheids for which the equilibrium temperature was computed from appropriate time-averages of the observed colours; ⊙: double-mode Cepheids; ✦: likely overtone pulsators, plotted at the position corresponding to P_o.

lower temperatures from the VBLUW survey. The change in the adopted temperatures is the most important factor here. Not only are the VBLUW temperatures lower than most previous temperature scales (particularly that of Schmidt), but the difference increases for longer periods. This is just what we need to remove the increase of $(M_{ev} - M_{puls})$ towards longer periods.

When adjustments are made to the luminosities and temperatures of Cepheids, we should check of course whether this does not create a new discrepancy between the observed and theoretical blue edges in the HR-diagram. Of the several ways of locating a Cepheid in the theoretical HR-diagram, I have chosen the following. Assuming that the Cepheid masses are consistent with evolutionary masses, we can adopt a Cepheid mass-luminosity relation from evolution theory (e.g. the M-L relation from Iben and Tuggle, 1975) to eliminate M from the pulsation equation. With known period and temperature we can then solve for the luminosity, which fixes the Cepheid's position in the HR-diagram. The result is shown in Fig. 4 (see also: Pel and Lub, 1978). The agreement of the distribution of the observed Cepheids with the theoretical blue edges of Iben and Tuggle (1975) and King et al. (1975) is very satisfactory. Of the 14 stars that lie to the left of the fundamental blue

edge, 7 are suspected to have blue companions, 2 are double-mode Cepheids, and 4 may be overtone pulsators (I will come back to these later).

It seems therefore that we may solve the general Cepheid mass problem from the observational side, by properly calibrating the observed data in terms of luminosity and effective temperature. We are stil left, however, with two other mass discrepancies where little can be done observationally: in both cases the important observables are rather well established numbers (a period and a phase for M_{bump}, and two periods for M_{beat}).

Cox et al. (1977) have recently proposed inhomogeneous envelope models with helium-enriched surface layers as a way to solve both the M_{bump} and the M_{beat} mass anomalies. In a subsequent paper, Cox et al. (1978) discuss Cepheid winds as a mechanism that can produce the high helium abundance ($Y \sim 0.75$!) that is needed in the hydrogen and helium ionization zones to change M_{beat} and M_{bump} in the right direction (upwards). A very attractive aspect of this idea is that two mass problems may be solved at once, but there are problems too, as the authors of the theory point out themselves (e.g. instability of heavy helium layers on top of layers with normal composition). Although it is not easy to determine the abundance of helium in the spectra of cool supergiants, it is obviously very important that the observers try to check whether a Y-value as high as 0.75 is consistent with spectroscopic evidence.

There is one observational remark that I would like to make about the bump Cepheids. It is often stated that the bump phenomenon disappears around periods of 17 days, but I think that this statement is mainly based on photometry that is not complete or accurate enough to show sufficient detail. Not only are the bumps for 17 and 18 days Cepheids often very pronounced, but there clearly exist bumps at longer periods as well, with phases that fit to the Herzsprung sequence. Good examples from the VBLUW survey are: RZ VEL ($20^d.4$), WZ SGR ($21^d.8$), WZ CAR ($23^d.0$), VZ PUP ($23^d.2$), RY VEL ($28^d.1$). Even at the longest periods one finds signs of bumps, which start climbing the descending branch of the lightcurve again. I mention this point, as the existence of long-period bump-Cepheids is relevant to the theory of surface helium enrichment by Cepheid winds (no significant He-enrichment can be obtained above 8 $M_\odot$, so more massive Cepheids with bumps may still be a problem), and also to the identification of bumps with resonances between fundamental and second overtone (Simon and Schmidt,

1976; Simon, 1977).

Radial velocity studies and radius determinations

Up to now I have been discussing mainly photometric results, as most observational work on Cepheids of the last five years has been photometric. There are, however, a number of important studies on radial velocity curves that have appeared since 1973. The only reason that I included only one of these in Table 1 is, that most discussions of Cepheid radial velocity curves are based on velocity data that have been in the literature for quite some time already.

When discussing radial velocity curves, we all think of the Baade-Wesselink method to obtain Cepheid radii. The virtues of this method are well known: by combining radial velocity curves with photometric light- and colour-curves we can in principle obtain all basic parameters of a Cepheid without needing direct distance information. The method has its problems too, as is equally well-known. Evans (1976) has analyzed in detail the effects of many different observational errors on the Wesselink radius solutions, and her results are not too reassuring about the accuracy that can be obtained. To quote some examples: an uncertainty of 1 km s^{-1} in the γ-velocity can cause a 10% error in R; a change of only $0^m.01$ in the descending branch of a colour-curve results even in 15% radius error.

Several authors have tried to avoid some of these problems by modifications of the original Baade-Wesselink method. Balona (1977) has applied a maximum likelihood method to solve R from observed V,(B-V) and radial velocity curves for 54 well-observed Cepheids. This work was not listed in Table 1, but I should mention that it is partly based on new radial velocity observations by Lloyd Evans, which are however not published.

A very interesting method to determine Cepheid radii and distances has been applied by Barnes et al. (1977). Instead of deriving the surface brightness F_V from $(B-V)_o$, as Wesselink did (Wesselink, 1969), they use the linear relation between $(V-R)_o$ and F_V discovered by Barnes and Evans (1976). As they point out, the method is nearly independent of interstellar extinction. The scatter in some of the resulting radius curves is large, mainly due to insufficient accuracy of the photometry, but there is no reason why this should not be improved. The method has clearly great potential value, as it yields radii and distances in a straightforward way,

avoiding some of the problems related to the calibration of Cepheid luminosities.

Once the radius of a pulsating star is known, we can fix its mass from the period and the pulsation relation. This gives us again a mass estimate which can be compared with the various other mass determinations. Dr. A.N. Cox has just completed a comparison in this context of the radius determinations by Balona, Evans, and Barnes et al. As he will discuss his results in the next session of this conference, I will not go into this aspect of Cepheid radii here.

One problem that all Baade-Wesselink and related radius determinations have in common, is the necessity of accurate phase-matching between light- and radial velocity curves. This phase-matching is of course done most accurately by simultaneous photometric and spectroscopic observations, but here one is hampered by the fact that spectroscopic observations are usually so much slower than photometry. The situation would improve considerably if more Griffin-type radial velocity machines would become available. Dr. Balona informed me that at the SAAO the Griffin technique is presently being used for radial velocity measurements of pulsating stars while photometry is carried out simultaneously. If sufficient observing time is available for this work, we may soon have accurate radius curves for many more Cepheids.

The Magellanic Clouds

Let me finally say a few words about the nearest extragalactic Cepheids. Compared to the problems with distance and interstellar extinction for Cepheids in our own galaxy, the Magellanic Cepheids have the great advantage of being at essentially the same distance and of much less interstellar reddening. But this is where the advantages stop: in all other respects the observers have to struggle with the faintness of most Cepheids in the clouds, and with the problems of crowding. Although progress has been made through the large amount of photometry that has become available in the last few years, we are still far from a clear picture about the basic parameters of the Magellanic Cepheids, and there is probably much more hard work needed before we can solve some of the most frustrating uncertainties.

The discussions of Magellanic Cloud Cepheids concentrate mostly on comparisons of the P-L-C, P-L and P-C relations in the clouds and in the

galaxy. There is no time to discuss the many determinations of these relations in any detail, but let me give some representative numbers to give an impression about the present state of affairs. The coefficient of the colour term in the empirical P-L-C relation is still very uncertain, both in the clouds and in the galaxy. According to Feast (1977) the work by Martin on the LMC indicates a value in the range of 1.5 to 3.5. Assuming a mean value of this coefficient of 2.52, Feast lists a number of recent determinations for the log P coefficient in the P-L-C relation. These range between 3.4 and 4.0 (values for the clouds and the galaxy). Again quoting Feast, the slope of the P-L relation ranges from 2.3 (for the galaxy, from Balona's work) to 3.1 (Gascoigne, for the LMC). It is obviously unfair to compare numbers in this manner, without discussing the details, but this gives at least some idea about the level of accuracy that we have to consider.

One problem that has become more and more outstanding during the last few years, is that of possible composition differences between LMC, SMC and the galaxy. As Gascoigne has pointed out (1974), a difference in metal abundance may have a noticeable effect on the luminosity that we derive for a Cepheid. I expect that the VBLUW photometry of cloud Cepheids by Van Genderen may provide important clues here, as the VBLUW system allows a very interesting way of estimating metallicity that is largely independent of temperature, gravity and reddening (see Pel and Lub, 1978). Unfortunately the method works best for the maxima of the short-period Cepheids, which means that very long integrations on faint stars are needed.

Another subject where conflicting results have been given recently, is that of pulsation amplitudes. From photometry in the clouds both Yakimova (1973) and Madore (1976[b]) find the Cepheids with largest light- and colour-amplitudes on the cool side of the instability strip, while Butler (1976[b]) finds a small effect in the opposite direction. The behaviour of the pulsation amplitude in the instabilaty strip is important as amplitude may be a useful extra parameter to locate a Cepheid in the HR-diagram (Kraft, 1960; Sandage and Tammann, 1971), and furthermore because the amplitude may provide information about the mode of pulsation.

In relation to this problem I would like to mention a result that I obtained recently from the VBLUW data of galactic Cepheids (see also Pel and Lub, 1978). This is shown in Fig. 5. Here I have plotted the photometric

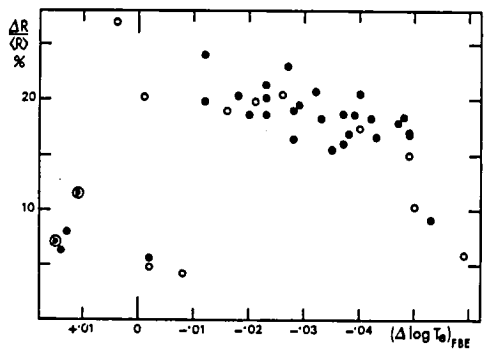

Fig. 5. The behaviour of radius amplitude across the instability strip. The amplitudes of the radius curves ($\Delta R/\langle R\rangle$) are derived from the VBLUW photometry of galactic Cepheids. Symbols as in Fig. 4. $(\Delta \log T_e)_{FBE}$ is the distance in effective temperature at constant L from the fundamental blue edge (Y = 0.28, Z = 0.02) of Iben and Tuggle (1975). Note the increase in amplitude towards the blue edge, and the discontinuity at the blue edge ($\Delta \log T_e = 0$).

radius amplitudes of the bright Cepheids in the interval $3.24 < \log L/L_\odot < 3.60$ as a function of distance in temperature to the fundamental blue edge of Iben and Tuggle (1975), with $\Delta \log T_e$ measured at constant luminosity (see Fig. 4). In Fig. 5 we note an increase in amplitude towards the blue edge, and then a discontinuity to a small group of hot stars with small amplitudes. Two of these are double-mode Cepheids, I suspect that the others are overtone pulsators. The diagram reminds very much of the behaviour of type-ab and type-c RR Lyrae stars. The overtone candidates in Fig. 5 all belong to the class of Cepheids with symmetric, small-amplitude lightcurves that are sometimes called "s-Cepheids", and which have often been thought to be first-harmonic pulsators (e.g. Ivanov and Nikolov, 1976). From Fig. 5 we can draw three conclusions: 1) amplitude is not a very suitable parameter to locate a Cepheid inside the strip, 2) the double-mode Cepheids are found near the blue edge, and may be related to the fundamental-overtone transition, 3) this result for galactic Cepheids supports the result of Butler for the Magellanic Clouds.

Coming back to the extragalactic Cepheids now, you have noticed that I scetched the situation in the Magellanic Clouds as still rather unsatisfactory, and it is clear that for Cepheids in other galaxies, at even greater distances, the observational problems will even become worse. Many extragalactic Cepheids have been observed only once, and I am sure that we will run into discrepancies as soon as these stars are re-observed with slightly different methods.

These observational uncertainties may look rather disturbing, but on the other hand I am optimistic. We know more about Cepheids than about most other types of stars. There is probably no other field in stellar astronomy

where theory and observation touch in so many details, and where both sides are bound by so many consistency requirements. If we just keep trying to get all pieces of this chinese puzzle together, we may eventually be rewarded by an extremely rigid framework of distances and basic stellar parameters.

References

Abt, H.A.: 1959, Astrophys. J. 130, 769

Balona, L.A.: 1977, Monthly Notices Roy. Astron. Soc. 178, 231

Barnes, T.G., Evans, D.S.: 1976, Monthly Notices Roy. Astron. Soc. 174, 489

Barnes, T.G., Dominy, J.F., Evans, D.S., Kelton, P.W., Parsons, S.B., Stover, R.J.: 1977, Monthly Notices Roy. Astron. Soc. 178, 661

Blackwell, D.E., Shallis, M.J.: 1977, Monthly Notices Roy. Astron. Soc. 180, 177

Böhm-Vitense, E.: 1972, Astron. Astrophys. 17, 335

Butler, C.J.: 1976[a], Astron. Astrophys. Suppl. 24, 299

Butler, C.J.: 1976[b], Roy. Obs. Bull. 182, 159

Butler, C.J.: 1978, Astron. Astrophys. Suppl. 32, 83

Canavaggia, R., Mianes, P., Rousseau, J.: 1975, Astron. Astrophys. 43, 275

Cousins, A.W.J., Lagerweij, H.C.: 1968, Monthly Notices Astron. Soc. S. Africa 27, 138

Cox, A.N.: 1978, Astrophys. J., to be published

Cox, A.N., Deupree, R.G., King, D.S., Hodson, S.W.: 1977, Astrophys. J. 214, L127

Cox, A.N., Michaud, G., Hodson, S.W.: 1978, Astrophys. J., in press

Dean, J.F.: 1977, Monthly Notices Astron. Soc. S. Africa 36, 3

Dean, J.F., Cousins, A.W.J., Bywater, R.A., Warren, P.R.: 1977, Mem. Roy. Astron. Soc. 83, 69

Dean, J.F., Warren, P.R., Cousins, A.W.J.: 1978, Monthly Notices Roy. Astron. Soc., to be published

Efremov, Yu.N., Kholopov, P.N.: 1975, Perem. Zvezdy 20, 133

Eggen, O.J.: 1977, Astrophys. J. Suppl. 34, 1, 33

Evans, N.R.: 1976, Astrophys. J. Suppl. 32, 399

Feast, M.W.: 1977, review given at ESO workshop on the Magellanic Clouds, Geneva April 1977, unpublished

Feltz, K.A., 1976, Publ. Astron. Soc. Pacific 88, 709

Feltz, K.A., McNamara, D.H.: 1976, Publ. Astron. Soc. Pacific 88, 699

Fricke, K., Stobie, R.S., Strittmatter, P.A.: 1972, Astrophys. J. 171, 593

Gascoigne, S.C.B.: 1974, Monthly Notices Roy. Astron. Soc. 166, 25P

Iben, I., Tuggle, R.S.: 1972a, Astrophys. J. 173, 135

Iben, I., Tuggle, R.S.: 1972b, Astrophys. J. 178, 441

Iben, I., Tuggle, R.S.: 1975, Astrophys. J. 197, 39

Ivanov, G.R., Nikolov, N.S.: 1976, Astrophys. Letters 17, 115

Janot-Pacheco, E.: 1976, Astron. Astrophys. Suppl. 25, 159

Johnson, H.L.: 1966, Ann. Rev. Astron. Astrophys. 4, 193

King, D.S., Hansen, C.J., Ross, R.R., Cox, J.P.: 1975, Astrophys. J. 195, 467

Kraft, R.P.: 1960, Astrophys. J. 132, 404

Kraft, R.P.: 1961, Astrophys. J. 134, 616

Kurucz, R.L.: 1975, in *Multicolour Photometry and the Theoretical HR-diagram*, A.G. Davis Philips, D.S. Hayes (eds), Dudley Observatory Reports 9, 271

Kurucz, R.L.: 1978, Astrophys. J. Suppl., to be published

Lloyd Evans, T.: 1968, Monthly Notices Roy. Astron. Soc. 141, 109

Lub, J., Pel, J.W.: 1977, Astron. Astrophys. 54, 137

Lyngå, G.: 1977, Astron. Astrophys. 54, 311

Madore, B.F.: 1975a, Astron. Astrophys. 38, 471

Madore, B.F.: 1975b, Astrophys. J. Suppl. 29, 219

Madore, B.F.: 1976a, Monthly Notices Roy. Astron. Soc. 177, 215

Madore, B.F.: 1976b, Roy. Obs. Bull. 182, 151

Madore, B.F.: 1977, Monthly Notices Roy. Astron. Soc. 178, 505

Madore, B.F., Van den Bergh, S.: 1975, Astrophys. J. 197, 55

Madore, B.F., Stobie, R.S., Van den Bergh, S.: 1978, Monthly Notices Roy. Astron. Soc. 183, 13

Oke, J.B.: 1961, Astrophys. J. 134, 214

Parsons, S.B.: 1971, Monthly Notices Roy. Astron. Soc. 152, 121

Parsons, S.B.: 1974, in: *Stellar Instability and Evolution*, P. Ledoux, A. Noels, A.W. Rodgers (eds), D. Reidel Publishing Company, Dordrecht, IAU Symp. No. 59, 56

Parsons, S.B., Bell, R.A.: 1975, in *Multicolour Photometry and the Theoretical HR-diagram*, A.G. Davis Philip, D.S. Hayes (eds), Dudley Observatory Reports 9, 73

Pel, J.W.: 1976, Astron. Astrophys. Suppl. 24, 413

Pel, J.W.: 1978, Astron. Astrophys. 62, 75

Pel, J.W., Lub, J.: 1978, in *The HR diagram - The 100th Anniversary of Henry Norris Russell*, A.G. Davis Philip, D.S. Hayes (eds), D. Reidel publishing company, Dordrecht, in press

Rodgers, A.W.: 1970, Monthly Notices Roy. Astron. Soc. 151, 133

Sandage, A.R., Tammann, G.A.: 1968, Astrophys. J. 151, 531

Sandage, A.R., Tammann, G.A.: 1969, Astrophys. J. 157, 683

Sandage, A.R., Tammann, G.A.: 1971, Astrophys. J. 167, 293

Schmidt, E.G.: 1972, Astrophys. J. 174, 605

Schmidt, E.G.: 1973, Monthly Notices Roy. Astron. Soc. 163, 67

Schmidt, E.G.: 1975, Monthly Notices Roy. Astron. Soc. 170, 39^{P}

Schmidt, E.G.: 1976, Astrophys. J. 203, 466

Simon, N.R., Schmidt, E.G.: 1976, Astrophys. J. 205, 162

Simon, N.R.: 1977, Astrophys. J. 217, 160

Stobie, R.S.: 1977, Monthly Notices Roy. Astron. Soc. 180, 631

Szabados, L.: 1977, Comm. Hungarian Acad. Sc. 70

Thé, P.S.: 1977, Astron. Astrophys. 60, 423

Turner, D.G.: 1977, Astron. J. 82, 163

Van den Bergh, S., Harris, G.L.H.: 1976, Astrophys. J. 208, 765

Van den Bergh, S.: 1977, in *Décalages vers le Rouge et Expansion de l'Univers*, C. Balkowski, B.E. Westerlund (eds), éditions du C.N.R.S., Paris, IAU Coll. No. 37, 13

Van Genderen, A.M.: 1969, Bull. Astron. Inst. Neth. 20, 317

Van Genderen, A.M.: 1977, Astron. Astrophys. 54, 737

Van Paradijs, J.A.: 1973, Astron. Astrophys. 23, 369

Walraven, J.H., Tinbergen, J., Walraven, Th.: 1964, Bull. Astron. Inst. Neth. 17, 520

Wampler, J., Pesch, P., Hiltner, W.A., Kraft, R.P.: 1961, Astrophys. J. 133, 895

Wesselink, A.J.: 1969, Monthly Notices Roy. Astron. Soc. 144, 297

Wielen, R.: 1974, Astron. Astrophys. Suppl. 15, 1

Yakimova, N.N.: 1973, Soobshch. Gos. Astron. Inst. Shternberga 177, 19

Fernie: You pointed out the advantages of the Walraven photometric system. Do you think that it is almost an ideal system? For example, how does it compare with the Stromgren system?

Pel: They are very similar. You cannot transform Stromgren and Walraven photometry directly, because the transformations are very complicated. When you look at the two-color diagrams, calibrated for temperature, gravity and composition, the features found in one system are found in the other. I think that in the case of the hotter (OB) stars, the extra band in the Balmer continuum of the Walraven system offers clear advantages. For the intermediate temperature range, they are more or less equivalent. Both, of course, lack a band at longer wavelength. We are thinking of trying to extend the present system with a band somewhere around R, since photometry at long wavelengths should be done. In fact, it is very important to do. However, the UV region must not be neglected.

A. Cox: Do you have a simple explanation or speculation for the discrepancies of Kraft's color excesses?

Pel: He calibrated his color excesses at the shorter periods only, and he had to extrapolate his G-band photometry for the longer period stars. There is a zero-point difference of the more recent color excess scales relative to all systems based on the Kraft system. However, that's not hard to get and it's not a serious problem. At the longer periods, the differences are really large, $0^{m}.15$ to $0^{m}.18$! I think that is because the G-band photometry runs into gravity problems there.

Sareyan: Do you check transmission of the red window in U filter?

Pel: That was one more complication I didn't mention.

THE PERIODS AND AMPLITUDES OF TU CAS

Stephen W. Hodson and Arthur N. Cox
Theoretical Division
Los Alamos Scientific Laboratory

ABSTRACT

Light curve observations of the double-mode Cepheid TU Cas obtained by 10 different sets of observers on several photometric systems over a time span of 67 years have been carefully studied to determine the fundamental and first overtone periods and their amplitudes on the V magnitude scale. The presence of a second overtone radial pulsation is discussed, and it is concluded that a previous detection of this mode was spurious due to the lack of a proper zero point correction for two groups of observations. The amplitudes of the two modes are shown to possibly vary during the entire observing period with the fundamental mode amplitude of 0.69 ± 0.03 and the overtone amplitude decreasing about 0.2 or 0.3 magnitude. If this Cepheid displays the two pulsation modes because it is mode switching, this switching time scale might be less than a hundred years.

Our motivation for this investigation is the reported existence by Faulkner (1977) of a third radial pulsation mode in the double-mode Cepheid TU Cas. At least one other Cepheid-type variable, AC And, and many of the δ Scuti variables have three radial pulsation modes, so it is perhaps not surprising to find another. There are two problems, however, TU Cas appears to be like the dozen or so double-mode Cepheids with a first overtone to fundamental mode period ratio $\cong 0.71$, unlike AC And with a ratio of almost 0.74. In addition the reported third period is abnormally long with respect to the primary and secondary periods, making it very difficult to explain in terms of reasonable stellar models. The AC And model is within the normal range of composition and structure according to Cox, King, and Hodson (1978).

Another motivation for studying TU Cas is to see if the amplitudes of the two modes are changing with respect to each other over the 67 years spanned by the available observations. Double-mode Cepheids, which might comprise one-third of all short period Cepheids (< 5 days) according to Stobie (1977), have yet to be adequately explained. Stellingwerf (1975) suggested that double-mode behavior resulted at temperatures near the red edge of the instability strip where the two modes switched toward each other. Unfortunately, Hodson and Cox (1976) found no double-mode behavior at these cooler temperatures. Currently, the only other cause of double-mode Cepheids predicted by theory is mode switching at the transition line between fundamental mode pulsation to the red and first overtone pulsation to the blue.

Observational evidence tends to support double-mode Cepheid pulsation near the transition line. Results from Rogers and Gingold (1973) on U Tr A, Schmidt (1972) on TU Cas, Pel and Lub (1978), and Cogan (1978) all arrived at temperatures placing most of these variables near the transition line. However, if double-mode behavior is the result of mode switching, we would expect to find a complete range of amplitude ratios between the two modes. As the evidence currently stands, only AX Vel has a first overtone amplitude larger than the fundamental.

Amplitude changes over a span of 67 years would support the rapid mode switching rates predicted by Stellingwerf (1975) and by unpublished results at Los Alamos, whereas no change would be more consistent with a possible slow change or just a stable permanent mixed mode.

The observations used in our TU Cas analysis are given in Table 1. The set used by Faulkner contains 290 points and consist of the four groups ranging from 1946 to 1959 (denoted by *). We attempted a period search on 302 white light observations by Osterhoff (1957), but were unsuccessful due to poor phase distribution of this data. For the amplitude analysis, we added 111 observations starting from 1962 to the present, which include 60 new visual magnitudes by Schmidt observed from 1976-78. For a more sensitive mode switching search, we converted observations by van Biesbroeck and Casteels (1914) from visual estimates to the modern V magnitude system with reasonably good results.

TABLE 1

OBSERVATIONS OF TU CASSIOPEIAE

REFERENCE	EPOCHS (JD 2400000+)	YEAR	NUMBER OF MEASURES	OBSERVING SYSTEM
Van Biesbroeck & Casteels (1914)	19198-19481	1911-1912	192	Visual
Gordon & Kron* (1947)	32039-32163	1946	28	Δm_{5000}
Oosterhoff (1957)	32424-32471	1947	265	Δm white light
	32606-32615	1948	37	
	32272-33608	1950	350	
Worley & Eggen* (1957)	33146-33206	1949	11	V_E, $(P-V)_E$
	34334-34369	1952	4	
	35063-35113	1954	102 means	
	35388-35404	1955	74 means	
Oosterhoff* (1960)	36751-36849	1959	45	UBV
Weaver, Steimetz & Mitchell (1960)*	36742-36858	1959	26	UBV
Williams (1966)	37936-37940	1962	6	UBV
Kwee & Braun (1967)	38219-38235	1963	14	UBV
Takase (1969)	38776-39079	1965	20	UBV
	39358-39433	1966	11	UBV
Schmidt (private communication)	43015-43126	1976	26	UBVRI
	43403-43500	1977-1978	34	

* Observations used by Faulkner (1977).

For our periodicity search we fitted the Faulkner data group by least squares to a sinusoidal series

$$\frac{L(t)}{\langle L \rangle} = 1 + \sum_{i=1}^{m} A_i \cos 2\pi(ift-\phi_i) \qquad (1)$$

made up of a single frequency plus m-1 harmonics taken over a specified frequency range. The quality of the fit and, consequently, the significance of any frequency is measured by σ, the standard deviation of the observations from the fit. When $m = 1$, the amplitude is related to σ by $A^2 = 2(\Delta\sigma^2)$. Equation 1 can be expanded to include two or more

frequencies, not harmonically related, and their cross coupling terms. The luminosity variations for the triple mode case are fit by

$$\frac{L(t)}{<L>} = 1 + \sum_{|i|+|j|+|k|=1}^{m} A_{ijk} \cos 2\pi[(if_0 + jf_1 + kf_2)t - \phi_{ijk}]. \quad (2)$$

The appropriate order of a fit is determined when the variance of fit, order m + 1, is not appreciably smaller than the variance of m^{th} order fit. In addition, the fit will yield small changes in amplitude (A_{ijk}) and phase angle (ϕ_{ijk}) with increasing order as suggested by Fitch. From Equation 2 we can directly obtain the amplitude and shape of each natural frequency.

Third order Fouriergrams on the Faulkner data group yield the same primary and secondary period values as Faulkner obtained. We used these values to construct the double-mode fit, and then searched the residual for any remaining periodicity. In Figure 1 we see, in the upper curve, the first order Fouriergram of the fourth order residual which is identical to Faulkner's results. The change in σ of the central minimum corresponds to an amplitude of ~ 0.014 for $\Pi_2 \sim 1.25247$ days. The sidelobes are due to the gap of ~ 1450 days between the 1959 and 1954-55 epochs. The lower curve is the Fouriergram of the fifth order residual, and, although the central minimum still persist, its depth gives an amplitude of ~ 0.009, down by 35% from the fourth order amplitude.

In Figure 2, we see the same Fouriergram over a larger frequency range, expanded in the direction of slightly higher, but more theoretically plausible frequencies. In the fifth order residual, we find at

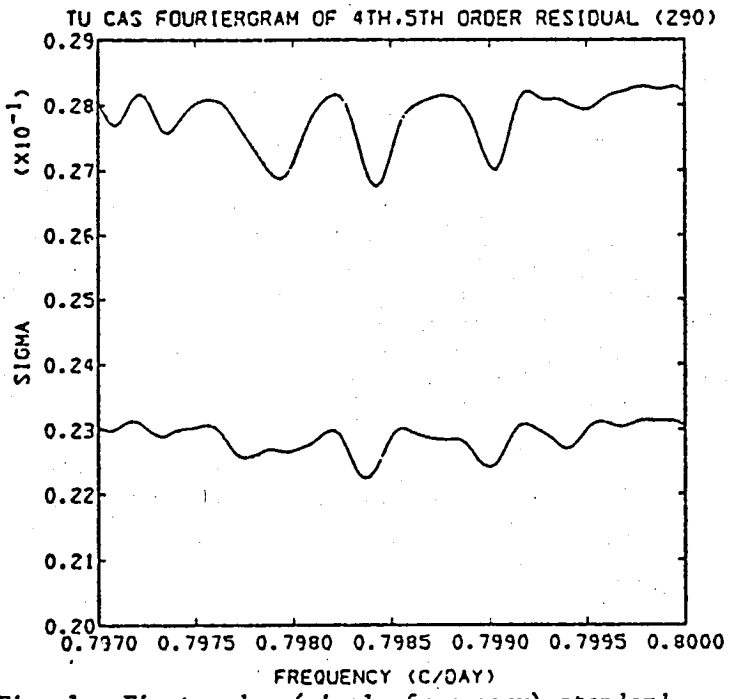

Fig. 1. First order (single frequency) standard deviation of the fourth and fifth order residuals versus frequency using the basic 290 data points.

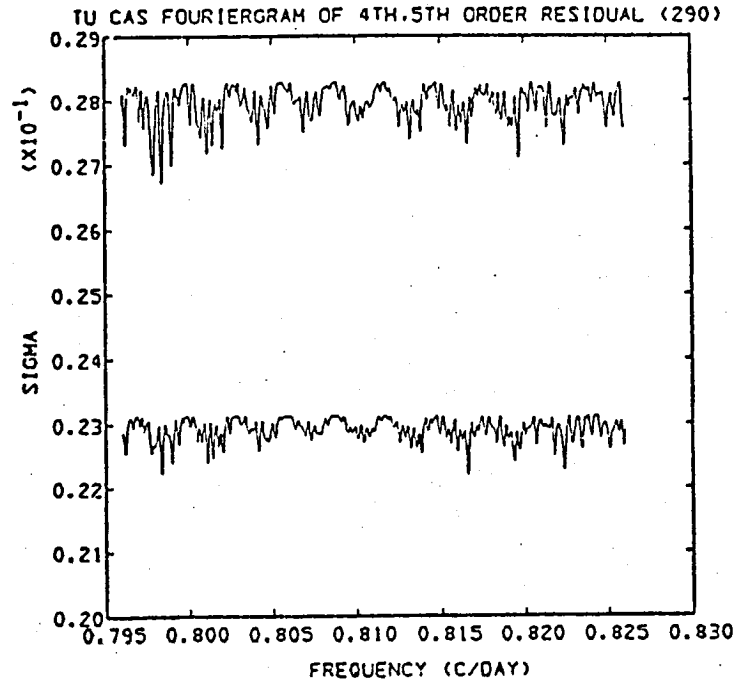

Fig. 2. First order (single frequency) standard deviation of the fourth and fifth order residuals versus frequency. This figure shows the same data as in Fig. 1 but over a larger frequency range.

least one frequency at $\sim 0.816^{-d}$ with a deeper minimum than Faulkner's in the far left portion of the curve, suggesting that perhaps his longer period may be an artifact of data noise.

To test the quality of the data, we calculated the standard deviation of each epoch, grouped by year, about a fourth-order double-mode fit through all 290 points. The results are given in Table 2. From the σ's in the first column, we see that the 1949 data have rather large scatter. The 1952 data may also be noisy, but with only four observations, its sigma value may be spurious. But the 1949 data remain suspect, especially considering the small scatter of the 1954-55 Worley and Eggen data. This epoch could be intrinsically noisy, or it may not share the same zero point with the other epochs.

We were able to confirm Faulkner's magnitude zero point adjustments between observers, and ran a subsequent check on the zero point between different observing epochs. Our check centered around Worley and Eggen

TABLE 2

EPOCH STANDARD DEVIATIONS

FOURTH ORDER DOUBLE-MODE FIT

EPOCH	No Shift (290)	1955 Shift* (290)	1949 Shift† (290)	1955 + 1949 Shift (290)	No Shift - 1949 (279)	1955 Shift - 1949 (279)
ALL (290)	0.0283	0.0271	0.0267	0.0254	0.0231	0.0214
GK 1946 (28)	.0260	.0246	.0257	.0234	.0252	.0234
WE 1949 (11)	.0835	.0841	.0713	.0724	.0000	.0000
WE 1952 (4)	.0567	.0553	.0544	.0552	.0552	.0555
WE 1954 (102)	.0205	.0180	.0212	.0187	.0208	.0180
WE 1955 (74)	.0156	.0095	.0151	.0089	.0145	.0077
O+WSM 1959 (71)	0.0323	0.0332	0.0308	0.0314	0.0299	0.0307

* 1955 Shift $\Delta V = -0.044$

† 1949 Shift $\Delta V = 0.066$

data, as it is the only group with more than one epoch. We performed various trial shifts on the three epochs in this group in an attempt to reduce the relative and total standard deviation.

From the third column, we see that by shifting the 1955 epoch by $\Delta V = -0.044$, the total σ is reduced, and σ for this epoch is down almost by a factor of two. A ΔV change of $+0.066$ in the 1949 data also gave some reduction in the total sigma, and in the fifth column, we see that the combined effects of shifting both 1949 and 1955 epochs results in an ever smaller total deviation.

Removing the 1949 epoch from the unshifted 290 points produces, by itself, a larger reduction in total sigma than does any of previous shifting. ($\sim$ 18% reduction in σ for a 4% point reduction). Removing this epoch and shifting the 1955 epoch gives the largest reduction in sigma, almost 24% lower than for the original Faulkner data.

In Figure 3 we have Fouriergrams of fourth order fit residuals in the region of Faulkner's third period for each trial listed on the table. The uppermost curve is the same Fouriergram as you saw in Figure 1, showing the central minimum surrrounded by aliases. By shifting 1955 epoch this pattern almost disappears (second curve from top). However, in the next curve, we see that 1949 epoch shift alone, produces only small changes from the original pattern of the top curve. The fourth curve shows the combined effect of the two shifts, and is similar to the second curve because of the large effect of the 1955 epoch shift. The fifth curve results from removing 1949 epoch from the data, and in spite of a substantial reduction in σ, the original pattern still persists. This pattern again disappears when we

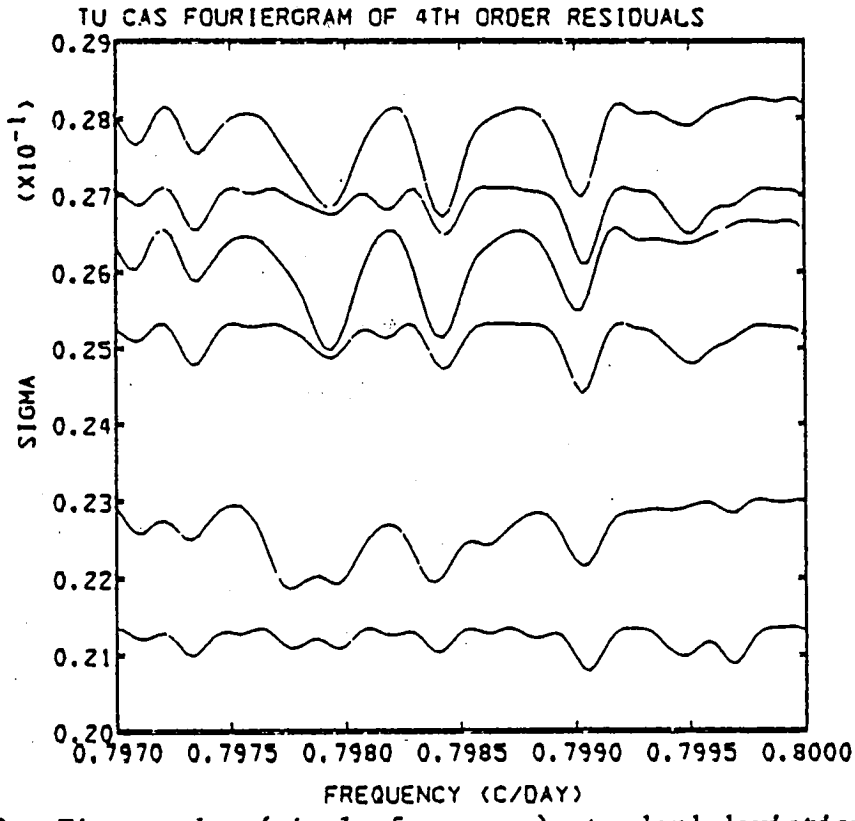

Fig. 3. First order (single frequency) standard deviation of the several fourth order fit residual cases of Table 2 versus frequency.

introduce the 1955 data shift as seen in the bottom curve.

Expanding the frequency range in Figure 4, as we did before, shows that shifting 1955 data removes the cyclic pattern of curves one, three and five, which corresponds to the 291 day interval between the 1954 and 1955 epochs. Faulkner's proposed third period, at the far left, appears to be only a deeper member of this pattern that disappears with the appropriate zero point shift.

Fitch noted the amplitude given by Faulkner's limited triple mode fit was a factor of two larger than the amplitude predicted by the depth of the minimum in the Fouriergram (about 0.025 to 0.014). We can explain this discrepancy in Figure 5 with two plots of fundamental and first overtone prewhitened data and mean curves as a

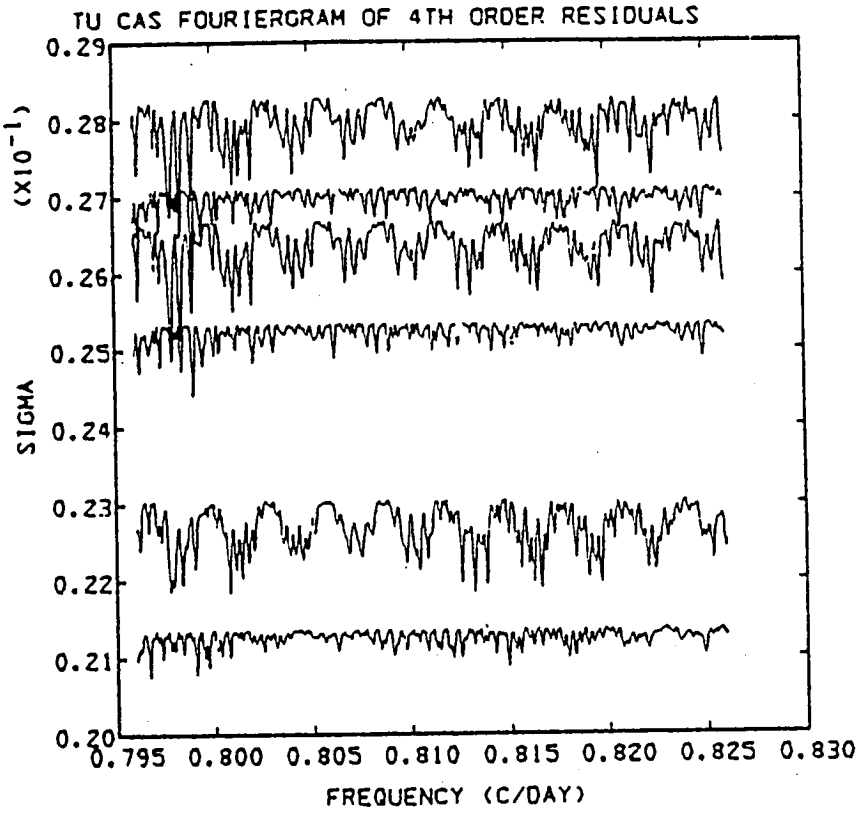

Fig. 4. First order (single frequency) standard deviation of the several fourth order fit residual cases of Table 2 versus frequency. This figure shows the same data as in Fig. 3 but over a larger frequency range.

function of phase. In both cases we have used the original, uncorrected Faulkner data set. We produced the upper plot by removing all the triple-mode fit terms except the Π_2 sine term, and phasing the residual to Π_2. This plot is identical to Faulkner's (Figure 4, 1977) and confirms his amplitude for Π_2 given by the triple-mode fit. The lower plot is the phased residual of the fourth order-double mode fit, with the amplitude estimated by a spline fit. It gives an amplitude value of $\sim$ 0.017 which is much closer to the predicted value of 0.014, with the difference of 20% due to uncertianties in the spline fit such as the number of knots and order. In general, we have noticed when any new natural mode (real or spurious) is introduced into the multimode

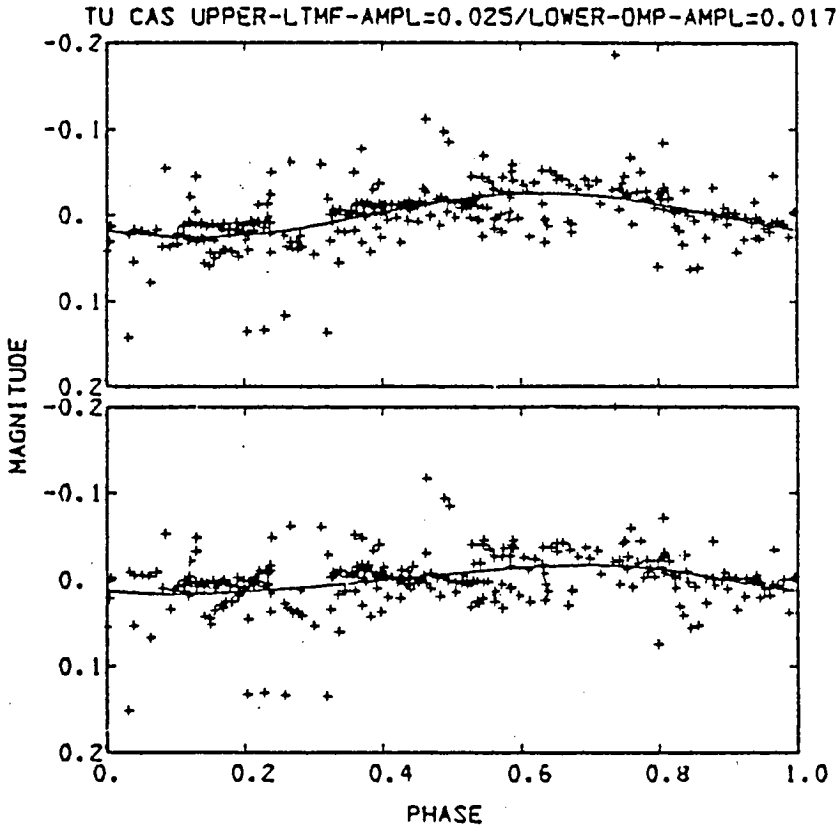

Fig. 5. The upper panel shows the Π_2 single frequency variation of the 290 point Faulkner triple-mode fit and the points obtained by prewhitening by all the Π_0 and Π_1 terms of his fit. The lower panel gives the variation of the residuals of a double-mode fit with the proposed Π_2 phase together with a spline fit through the points.

fit, it interacts in varying degrees with the other natural modes, resulting in a substantial amplitude for this mode. Hence, one cannot reliably determine the significance of a variation by its amplitude size given by multimode fitting.

In searching for amplitude changes in TU Cas, we selected the longest time base possible with the hope of revealing the more conspicuous variations in modal amplitude. A summary of our results is given in Table 3.

The 1911-12 epoch by van Biesbroeck and Casteels was converted from a visual estimates system to V magnitudes. Initially, our

TABLE 3

MODE AMPLITUDES OF TU CASSIOPIAE*

Epoch	No. of Observations	A_0	A_1	σ	A_1/A_0
1911-12†	192	.70	.45	.13	.64
1911-12††	192	.72	.54	.19	.74
1911-12†††	192	.86	.53	.14	.62
1946-1977	390	.71	.27	.04	.38
1946-1959	279	.71	.29	.03	.41
1962-1977	111	.67	.24	.03	.35

* Third order double-mode Fourier Series fit

† Adopted magnitudes by Van Biesbroeck and Casteels

†† Revised magnitudes from HD catalog

††† UBV magnitudes by Henden (private communication, 1978)

primary uncertainty in converting these observations resulted from the absence of any recorded UBV measurements of the six comparison stars used for this study. Van Biesbroeck and Casteels estimated these magnitudes from a relative scale used to determine the variable's changing magnitude. We attempted to improve on these magnitudes using the best revised estimates from the HD catalog (as suggested by Bidelman, private communication). Eventually we were able to obtain UBV magnitudes for the six comparison stars from Arne Henden at Indiana University (private communication, 1978)

The ratio of first overtone to fundamental mode amplitude (A_1/A_0) for this earliest epoch averages ~ 0.67 and is appreciably higher than for the 1946-1977 era (~ 0.38). To check this last ratio

we split the modern era into two ~ 15 year intervals to determine if this trend still persisted. The decrease of the ratio from 0.41 to 0.35 is suggestive, but probably within the range of uncertianty.

Due to the relatively larger uncertainty of the 1911-12 data, we are unable to conclude that the first overtone mode really decayed substantially since 1911. However, observations after 1945 span nearly 32 years and comprise a long time base of quality UBV measures. With the inclusion of new observations the decrease of A_1/A_0 within the modern epoch may possibly be confirmed.

Our conclusions are that TU Cas is not a triple-mode pulsator, and that maybe the first overtone pulsations have decayed since 1911.

We wish to thank R. F. Stellingwerf for locating the van Biesbroeck and Casteels data and providing it to us.

REFERENCES

Cogan, B. C. 1978, Ap. J., 221, 635.

Cox, A. N., King, D. S., and Hodson, S. W. 1978, Ap. J., 224, 000.

Faulkner, D. J. 1977, Ap. J., 218, 209.

Gordon, K. C. and Kron, G. E. 1947, Ap. J., 106, 318.

Hodson, S. W. and Cox, A. N. 1976, in Proceedings of the Los Alamos Solar and Stellar Pulsation Conference, eds. A. N. Cox and R. G. Deupree, p.202.

Kwee, K. K. and Braun, L. D. 1967, BAN Suppl., 2, 77.

Oosterhoff, P. Th. 1957, BAN, 13, 320.

Oosterhoff, P. Th. 1960, BAN, 15, 199.

Pel, J. W. and Lub, J. 1978, in IAU Symposium 86, The H-R Diagram, eds. Philip and Hayes (Reidel Dordrecht).

Rodgers, A. W. and Gingold, R. A. 1973, MNRAS, 161, 23.

Schmidt, E. G. 1972, MNRAS, 167, 613.

Stellingwerf, R. F. 1975, Ap. J., 199, 705.

Stobie, R. S. 1977, MNRAS, 180, 631.

Takase, B. 1969, Tokyo Ast. Bull., Sec. Series, 191.

van Biesbroeck, G. and Casteels, L. 1914, Ann. Obs. Royal Belgique, New Series 13, 184.

Weaver, H., Steinnetz, D., and Mitchell, R. 1960, Lowell Obs. Bull., 5, 30.

Williams, J. A. 1966, A. J., 71, 615.

Worley, C. E. and Eggen, O. J. 1957, A. J., 62, 104.

Stephen W. Hodson and Arthur N. Cox, Mail Stop 288, Los Alamos Scientific Laboratory, P. O. Box 1663, Los Alamos, New Mexico 87545.

Discussion

Wesselink: How do you identify a mode? How do you know whether it is the fundamental or an overtone?

Hodson: Hopefully, the one with the longest period with largest amplitude is the fundamental. Sometimes that turns out to be the 1st or 2nd overtone. But that's the nomenclature I use.

J. Cox: In 1977, I think, Stobie pointed out that there was no observational evidence for amplitude changes over at least a 50-year time span. Do you think this is because no one has looked, or is there more substantial evidence?

Hodson: The evidence we have suggests that this might be happening. We have 32 years of observations in the "modern" era. We need quite a few more "modern" observations to resolve the problem.

THE RADII OF SU CAS AND TU CAS

Gordon D. Niva
and
Edward G. Schmidt

Behlen Observatory
Department of Physics and Astronomy
University of Nebraska
Lincoln, NE 68588

It is possible to obtain the masses of Cepheid variables by several methods involving the pulsation theory. However, these masses are frequently smaller than those indicated by the theory of stellar evolution. The cause of this discrepancy is not fully understood although a number of possibilities have been suggested. Since the pulsation theory indicates that there is a relation among the mass, the radius and the period, the discrepancy also manifests itself in the radii of these stars (Cogan 1978). With this in mind, we have undertaken radius determinations for two Cepheids which are of special interest in connection with pulsation theory.

It has been suggested that the short period Cepheid SU Cas is pulsating in the first overtone mode (Iben and Tuggle 1975, Gieren 1976). If this is correct the radius should be larger than a fundamental pulsator of the same period. Thus, the radius can be used to test the pulsation mode. Since Stellingwerf (1975) found from pulsational calculations that the hottest short period Cepheids should be overtone pulsators, this provides an opportunity to test a prediction of the theory.

TU Cas is a beat Cepheid with a fundamental period of 2.14 days. Several investigators (Schmidt 1972c, Petersen 1973, King et al. 1975, Stobie 1977) have shown that it is possible to determine the radii and masses of such stars from the periods which are observed. The beat masses so determined are only a little greater than half the evolutionary mass and the radii are much smaller than those calculated from the period-Luminosity-color

relation. On the other hand, the PLC relation radii are consistent with evolutionary masses. Thus, an independent determination of the radius will help decide if the beat mass discrepancy is due to the pulsation theory or the evolution theory.

We have employed a modified version of the Wesselink method proposed by Barnes et al. (1977) in which surface brightnesses are determined from the (V-R) color. This has the advantage, especially in the analysis of TU Cas, of allowing a radius to be determined without complete light and velocity curves. There are a number of problems connected with the application of any version of the Wesselink method. The phase matching between the velocity and light curves must be very good. In the case of a beat Cepheid, where the curves do not repeat, simultaneous observations are necessary. We have obtained these by the use of the coudé feed telescope and one of the 0.9 meter telescopes at Kitt Peak National Observatory. A further difficulty is that any version of the Wesselink method is sensitive to small photometric errors. We have dealt with this by using two comparison stars for each variable and observing the variable and comparison stars repeatedly. The standard deviations in the photometry averaged $0^{m}.004$ for both V and (V-R). Finally radii determined in this fashion are subject to a variety of systematic errors. By adopting the method of Barnes et al. we can compare our stars directly with the stars they have analyzed. Thus, we can determine how the radii of SU Cas and TU Cas compare with other Cepheids even in the presence of systematic errors.

The data were obtained over a period of 11 days in September 1977. Figure 1 shows the data for TU Cas. The top two panels contain the magnitudes and colors while the radial velocities are in panel c. A third order Fourier fit was made to the velocities following the methods described by Faulkner (1977). Using a systemic velocity of -14.5 km/sec and a foreshortening factor of 24/17, this fitted curve was integrated to produce the displacement curve shown in the lower panel. It can be seen that the gaps which occur in the observations during each day have produced apparently spurious bumps in the fitted curve. Without more velocity measurements, we can not improve this situation. For SU Cas we have combined the velocity measurements of Abt (1959) and Gieren (1976) with our own to produce the velocity curve. Their data were adjusted in phase and zero point to fit ours.

In Figure 2 we plot the relative radius, R/R_0, determined from the photometry against the displacement, $R-R_0$, obtained from the velocity integration. The value R_0 refers to an arbitrarily chosen initial epoch. The slope of the relation in this diagram determines the value of R_0 and a suitable constant is added to this to convert it to the mean radius. The sensitivity of this method to photometric errors can be seen from the error bars in the upper left corners of the diagrams. These represent the effect of an error of $0^m.01$ in (V-R). The scatter can be seen to be consistent with small photometric errors. In the lower panel the data for TU Cas are plotted with a different symbol for each of the nights on which it was observed. Significant shifts are

evident from night to night. We attribute these to our inability to define the velocity curve continuously over the entire interval. We have therefore determined the radius of TU Cas on each night and have averaged over all the nights.

The measured radii for SU Cas and TU Cas are listed in the fourth column of Table 1. The radii in the fifth column were calculated from the luminosities obtained from the period-luminosity-color relation. For SU Cas we have done the calculation under assumptions of fundamental and first overtone pulsation. The radii in column six are from a period-radius relation which is a straight line fit to the radii listed by Barnes et al. These were derived in the same fashion as the present radii and should be directly comparable. For TU Cas we also list the radius determined from the period ratios (King et al. 1975). The effective temperatures listed in the last column are the averages of temperatures determined for these stars from continuum scans and Hα profiles (Schmidt 1972a, 1972b, 1972c).

Looking first at the results for SU Cas we see that the present radius agrees with that obtained from the PLC relation if we assume fundamental pulsation. However, the radii determined by Barnes et al. are much smaller than the PLC radii at these short periods. Whether this reflects an error in the calibration of the PLC relation or some systematic effect in the radii, it is clear that the present value should be compared with the Barnes et al. values. Figure 3 shows a plot of the Barnes et al. radii and the present determinations against period. From the diagram

it is clear that the radius of SU Cas is too large if it assumed to be pulsating in the fundamental. However, for overtone pulsation the present radius in only slightly more than one standard error larger than the value indicated by the period-radius line. This evidence therefore supports the previous contention that this star is an overtone pulsator.

The original suggestion that SU Cas pulsates in the first overtone was made by Iben and Tuggle (1975) on the basis of a distance modulus determined by Racine (1968). Racine had noted that the field around SU Cas contains several stars which illuminate reflection nebulae as does the Cepheid. He then obtained spectroscopic parallaxes for the field stars. Within the accuracy of these parallaxes it appeared that the field stars defined a group at a true distance modulus of 7.5. He took this to be the distance of SU Cas. Because spectroscopic parallaxes are relatively inaccurate the distance moduli of the stars in this region have been redetermined using uvbyβ photometry (Schmidt 1978). Two of the stars are at a distance modulus of 7.2 while a third is at 8.2. If SU Cas is at the nearer distance, the implied radius is 19.1 $R_\odot$. Referring to Table 1 we see that the smaller value is consistent with the radius for overtone pulsation if the Barnes et al. relation is correct while the larger value is consistent if the PLC relation is valid. Neither agrees with fundamental pulsation under any assumption. While this gives some indication that SU Cas is an overtone pulsator, it should be viewed with caution. There are field stars at three distinct distances

in this region which are associated with reflection nebulae. It is possible that SU Cas is associated with none of them. Its pulsation mode must ultimately be decided on other grounds.

A further point which bears on the pulsation mode of SU Cas is its temperature. Stellingwerf (1970) studied the mode behavior of a model representing U TrA. He found that models between T_{eff} = 6350K and 6675K should be unstable in the first overtone only while those between 6200K and 6350K should be unstable both to the fundamental and the first overtone. At cooler temperatures there is a region with only fundamental pulsation which extends to 5840K. The temperature given in Table 1 for SU Cas clearly places it in the first overtone region. Thus, there are three pieces of evidence favoring the identification of SU Cas as an overtone pulsator and the observational data support Stellingwerf's calculations.

Turning now to TU Cas we see that the present radius is much smaller than the PLC radius. However, the agreement with the period-radius relation and the beat radius is good. As stated above, our determination should be consistent with the period-radius relation and we thus conclude that TU Cas has a radius appropriate to its fundamental period. Also, the agreement between the Wesselink radii and the beat radius suggests that the beat radius is correct and that the PLC radius is too large.

We note that the temperature for TU Cas given in the table is at the edge of the range Stellingwerf predicted for stars unstable in both the fundamental and the first overtone. This

suggests that while SU Cas is an overtone pulsator due to its high temperature, TU Cas is switching from one mode to the other at the present time.

We conclude, because of the agreement between the present radius and the beat radius of TU Cas, that the pulsation theory is giving us correct information about the radii of beat Cepheids. This implies that the luminosities of short period Cepheids have been overestimated. It further implies that the masses are significantly less than evolutionary masses. Thus, the solution to the mass discrepancy should perhaps be sought in the theory of stellar evolution or in the possibility of mass loss.

Table 1

RADII OF SU CAS AND TU CAS

		$R/R_\odot$					T_{eff}
		P_o	Wess.	PLC	P - R	Beat	
SU Cas	F	1.95	25.2±4	24.1	14.5	--	6530
	1H	2.75	25.2±4	30.7	19.9	--	6530
TU Cas		2.14	17.4±4	25.6	15.8	15.7	6360

REFERENCES

Abt, H. A. 1959, Ap. J., 130, 1021.

Barnes, T. G., Dominy, J. F., Evans, D. S., Kelton, P. W., Parsons, S. B., Stover, R. J. 1977, M.N.R.A.S. 178, 661.

Cogan, B.C. 1978, Ap. J., 221, 635.

Faulkner, D. J. 1977, Ap. J., 218, 209.

Gieren, W. 1976, Astron. & Astrophys. 47, 211.

Ibe, I., Tuggle, R.S. 1975, Ap. J., 197, 39.

King, D.S., Hansen, C. J., Ross, R. R., Cos, J. P. 1975, Ap. J., 195, 467.

Petersen, J. D. 1973, Astron. & Astrophys. 27, 89.

Racine, R. 1968, A. J., 73, 588.

Schmidt, E.G. 1972a, Ap. J., 174, 595.

Schmidt, E.G. 1972b, Ap. J. 174, 605.

Schmidt, E.G. 1972c, Ap. J. 176, 165.

Schmidt, E.G. 1978, A. J., (in press).

Stellingwerf, R. F. 1975, Ap. J., 199, 705.

Stobie, R. S. 1977, M.N.R.A.S., 180, 631.

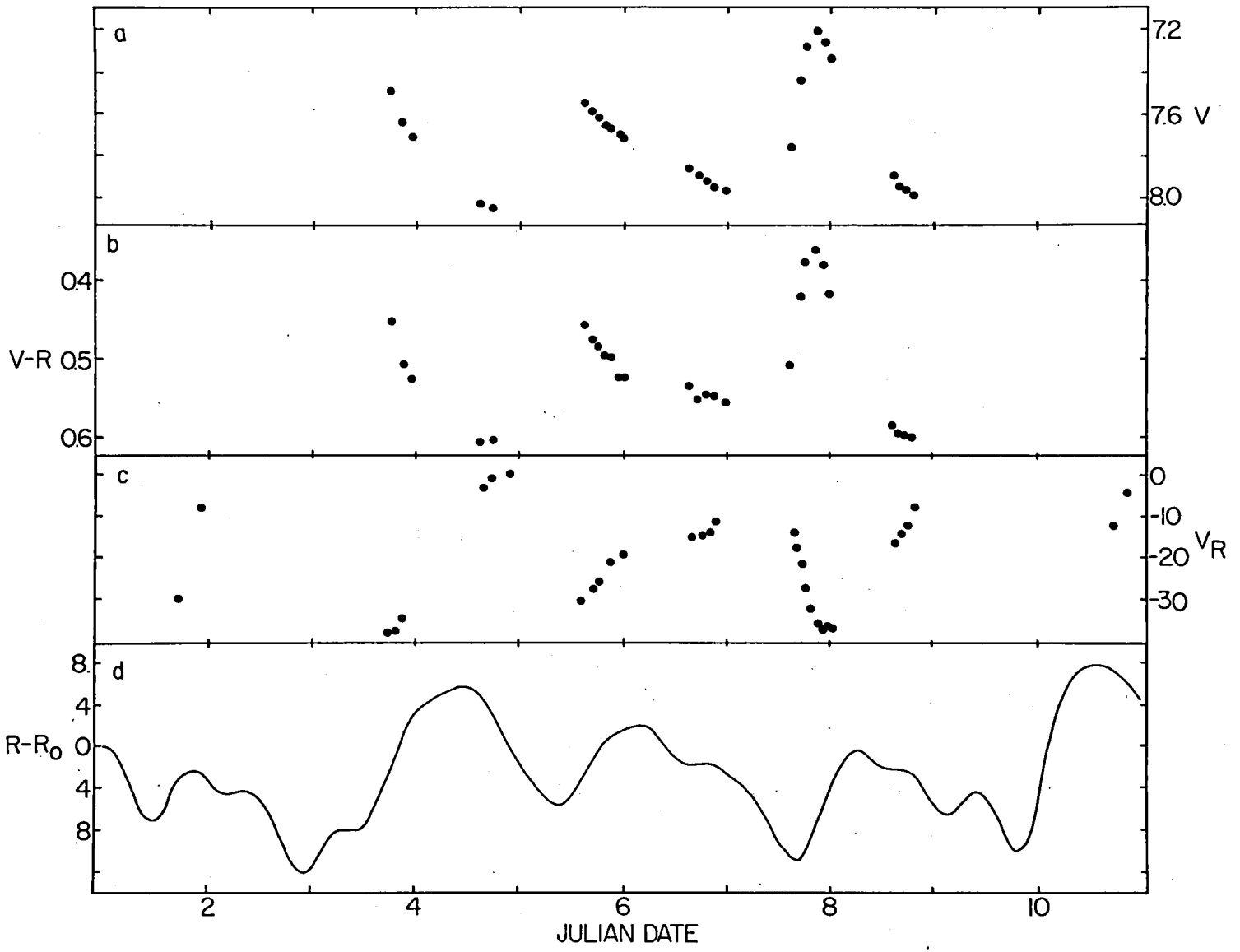

Figure 1. The observational data for TU Cas. The Julian Date -2443400 is plotted as the abscissa. a). V magnitudes. b) V-R colors. c) radial velocity in km/sec. d) a radius displacement curve generated from a third order fit to the velocities.

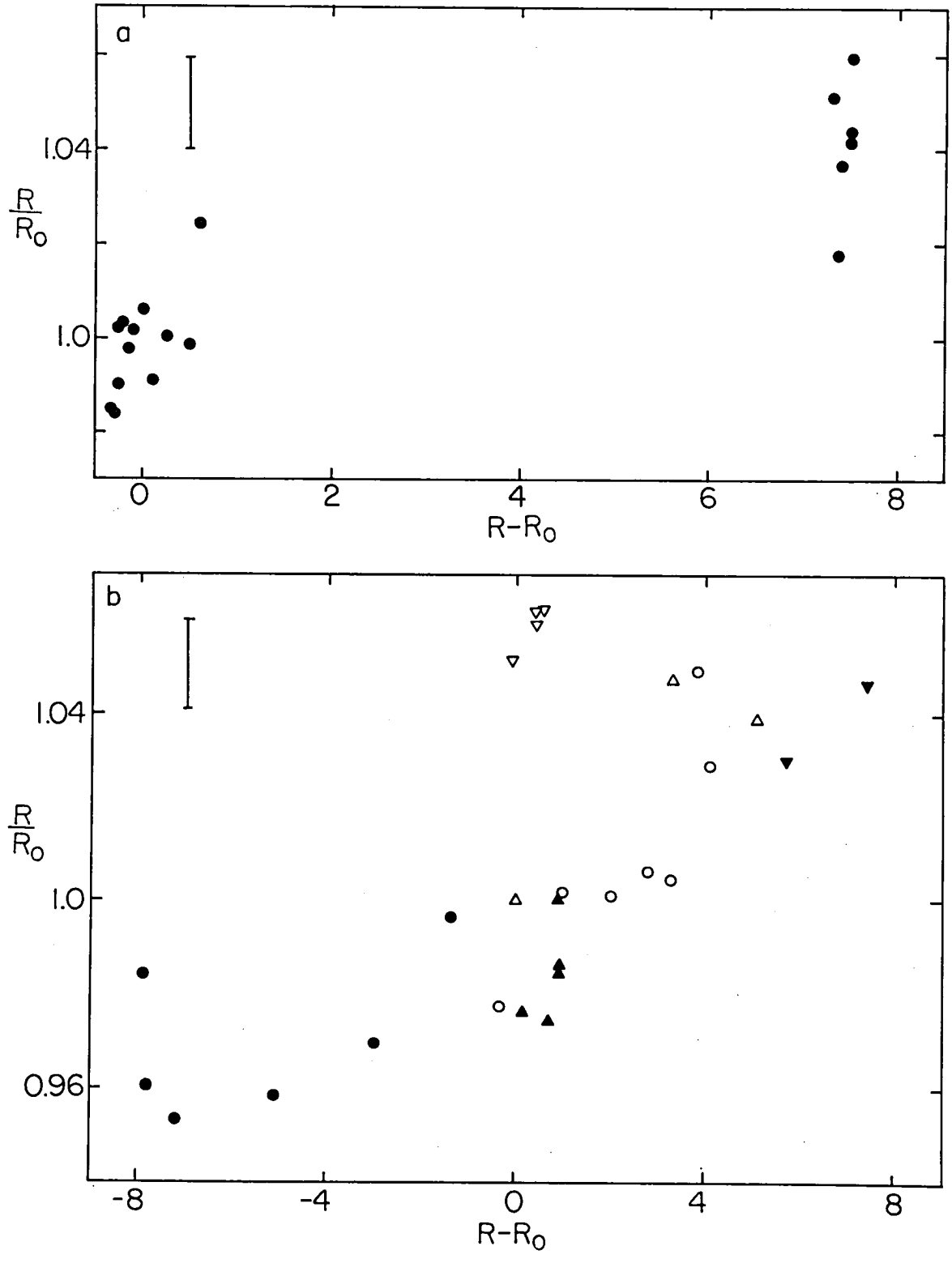

Figure 2. A plot of relative radius versus displacement. The radius displacement is in units of 10^5km. a) SU Cas. b) TU Cas. Different symbols denote different nights.

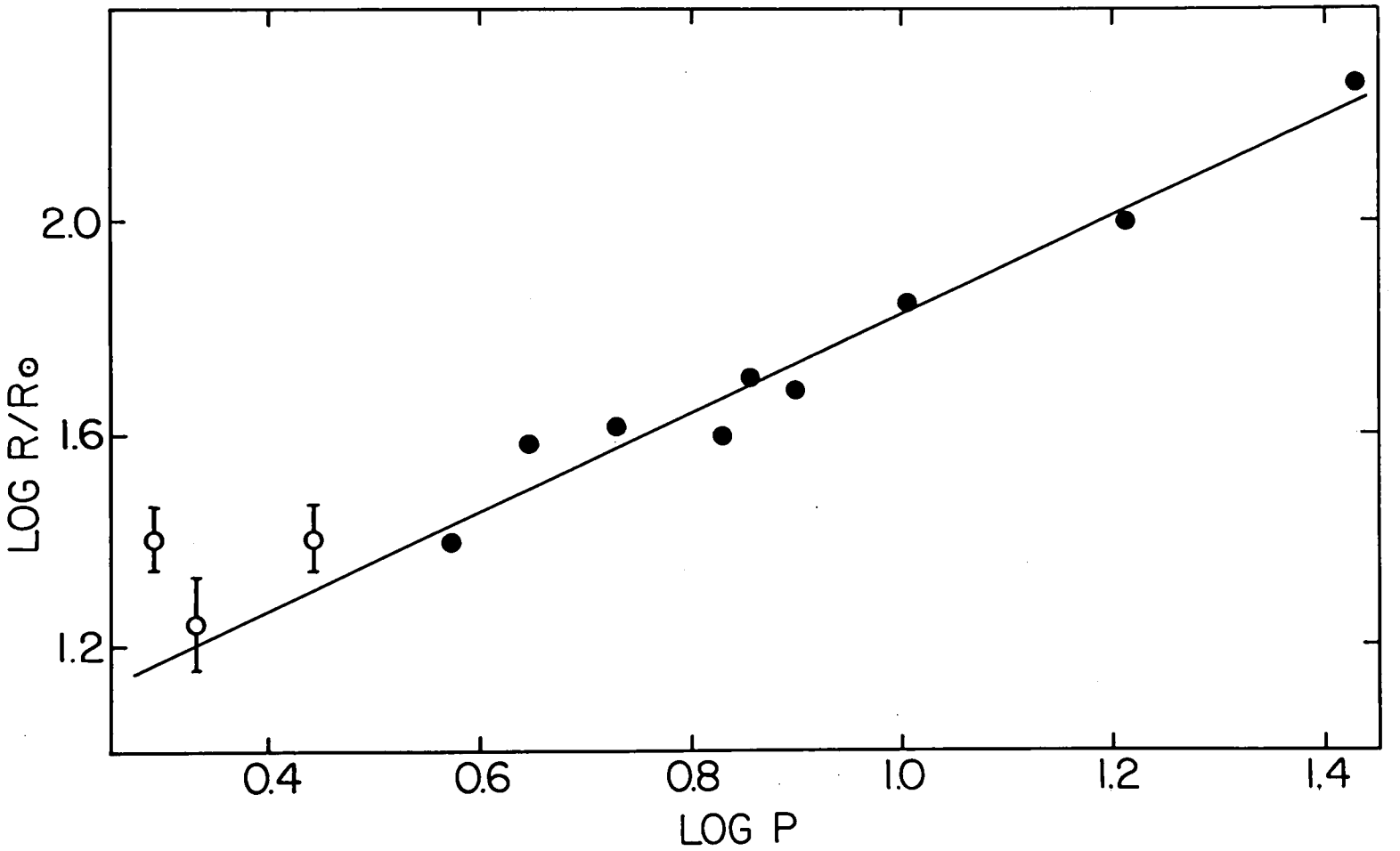

Figure 3. The radius-period relation. The filled circles represent radii obtained by Barnes et al. and the solid line is fitted to them. The two open circles with error bars at log R/R_θ= 1.4 represent the present radius for SU Cas assuming fundamental and first overtone pulsation. The lower circle with error bars is the radius of TU Cas.

Discussion

A. Cox: It seems to me Opolski had observations of TU Cas which were reported at the Budapest meeting, but I haven't seen the proceedings yet.

Rosendhal: We earlier saw divergent temperature scales. How sensitive are the results you obtained to the use of different temperature scales?

Schmidt: The various temperature scales are reasonably consistent at the hot end of the range. This star is quite hot so it doesn't matter which scale is used. I used my own scale.

89 Her: A Cepheid Outside the Instability Strip?

J. D. Fernie

David Dunlap Observatory

University of Toronto

UBVRI photometry and some radial velocities of the interesting high-latitude F2 Ia supergiant 89 Herculis are presented. The photometry confirms Worley's discovery that the star is a low-amplitude (about 0.1 mag in V) variable of period close to 70 days. On the basis of such characteristics as amplitude versus wavelength the variability strongly suggests pulsation, and the cepheid period-luminosity relation gives an absolute magnitude close to that found spectroscopically.

The radial velocities are as yet insufficient to confirm the pulsation hypothesis, although they would be difficult to interpret on any alternative theory, such as ellipsoidal binary motion.

The color indices of the star are entirely normal for its spectral type after allowance for $E_{B-V} \simeq 0.05$ mag, a value not inconsistent with the high galactic latitude. These colors and the rather well-determined absolute magnitude place the star several tenths of a magnitude to the blue of the cepheid instability strip in the H-R diagram, despite the apparent cepheid-like pulsation. It may be further noted that a previous spectroscopic study by Searle, Sargent, and Jugaku showed the star to have entirely normal Population I abundances.

Further photometry and radial velocity observations are being obtained.

Discussion

Van Horn: Would it be useful to plot your last diagram as $\dot{P}$ vs P rather than $\dot{P}$ vs effective temperature? Would that make it easier to compare theory with the observations?

Fernie: It might well be. It hadn't occurred to me to do that. It would be worth a try.

Van Horn: It would be exciting to see that sort of comparison.

ZEEMAN OBSERVATIONS OF W SGR*

H. J. Wood, W. W. Weiss, and H. Jenkner

University Observatory, Vienna, Austria

Footnote *Based on observations obtained at the European Southern Observatory, La Silla, Chile.

Abstract A new precise method for measuring magnetic fields on Zeeman plates of the southern cepheid W Sgr is reviewed. Ten plates over the $7^{d}.6$ period of pulsation show two extrema in the measured values of the effective magnetic field. The method has a precision of ±0.4μ in the Zeeman shift corresponding to ±50 gauss (g). A negative "spike" of -220g occurred at the time of arrival of the compressional wave of pulsation at the stellar surface. A positive field of +270g occurred at the phase of most rapid contraction near the temperature minimum of the pulsation cycle.

I. INTRODUCTION

In his classic compilation of observational results on stellar magnetic fields, H. W. Babcock (1958) includes observations of a number of pulsating variables. Most of the fields measured were small and observationally uncertain. However, RR Lyr (No. 68 in the catalogue) showed stronger fields of as high as H_e = -1580±115g on plate Pc2294 and +1170±112g on plate Ce10149. For FF Aql, plate Ce7035 gave a field of -250±38g and on plate Pb1008ηAql gave H_e = -85±85g. A number of Zeeman plates were obtained by Preston on δ Cep but measurements of those plates have not appeared in the literature. Kraft (1967), however, mentioned that the plates showed a field reaching a maximum as high as -500g at minimum light (and zero field at maximum light).

Line crowding and asymmetric profiles make conventional Zeeman measurements extremely difficult for these stars with F - G spectral types.

II. RESULTS OF A NEW TECHNIQUE

A southern sky survey for magnetic fields was begun in 1970 at the European Southern Observatory by HJW (Wood & Campusano, 1975). The ten plates discussed here have 3.3Å/mm reciprocal dispersion. Details of the observations are given in a recent paper by Wood et al. (1977) and are shown in Figure 1. The curve is Jacobsen's (1974) "1923 standard" radial velocity curve calculated on:

$$JD(\text{vis max}) = 2434587^{d}.26 + 7^{d}.594812E$$

From a discussion of a large body of observations spanning more than 50y, Jacobsen found that the 1923 and 1973 RV curves were nearly identical

but that large distortions in the hump near phase 0.36 occur with a period of about 17y.

We have found that a small shift of 0.057 in phase was necessary to fit our RV observations (Wood et al., 1977, op. cit., Fig. 1) onto Jacobsen's curve. This correction has also been applied to the magnetic observations shown in Figure 1 of this paper. Jacobsen found that similar small phase and velocity shifts were necessary to fit all his observations together.

The measurements were obtained from the conventional coudé Zeeman plates in a new way. The spectrograms are first digitized using a computer-controlled digital microdensitometer described by Albrecht et al. (1977). Then, in a separate data handling program, sections of the o- and e-ray are shifted with respect to each other in a manner analagous to that used in the photoelectric radial-velocity spectrometer.

We have found that the correlation curve (sum of the squares of the channel-by-channel differences of the two spectra) reaches a sharp minimum when the best-fit Zeeman shift between the two spectra is achieved. In the case of W Sgr, we use a 116Å band centered on λ4262Å in which we have counted approximately 130 lines. We recall that the z-values are different for each line. However, since the lines are sharp in this supergiant and the measured field is expected to be small, it is gratifying to see how smooth and symmetric are the correlation curves for the 10 plates of W Sgr: they are easily fit by parabolas to aid in the precise determination of the Zeeman shifts.

After removal of the projected slit tilt using the Fe comparison spectra (typically $\sim$ 1μ), the residual relative shift between the two spectra is a measure of the mean Zeeman shift of all 130 lines in the 116Å region used. The technique is described in detail in Weiss et al. (1978) where an error discussion is also included.

A detailed line-identification study of this spectral region centered on λ4262Å was carried out for the spectrum of Canopus by Rakos et al. (1977). The study showed that the mean z-value for the region is $\sim$ 1.3. We have applied this value in order to set the ordinate in Figure 1 in gauss. The maximum Zeeman shifts measured are of the order of 2μ (270g) which are five times the precision of the method (±0.4μ).

III. DISCUSSION

On the assumption that these observations, taken over 190 cycles (1445d) form a pattern which repeats in the $7^d.6$ pulsation period, let us consider the physical behavior of the stellar atmosphere and the related magnetic field changes. At phase 0, we have maximum light, but maximum radius occurs much later, in the variable hump area of the RV curve at phase $\sim$ 0.5. Thus maximum light is caused by a considerable temperature increase of the photosphere as the compressional wave hits these layers. Just before phase zero, the field reaches -220g at RV minimum where the photosphere is expanding most rapidly.

It is at the time when the compressional wave of pulsation encounters the atmospheric layers observed that we might expect lines of force "frozen" into the material to be compressed yielding a momentarily higher-valued

field. This negative-field spike at RV minimum is followed immediately by an overshoot to positive field values of ∿ 100g. These two positive field points (phases between 0.0 and 0.1) come from two plates taken in quick succession on the same night during maximum light.

Maximum radius (∿ phase 0.5) shows a measured value of ∿ -120g at phase 0.4. However, near minimum light when the photosphere is at its greatest velocity of contraction (phase 0.75) the opposite positive field extreme has occurred (+270g at phase 0.63). Why, when the photosphere is contracting fastest and cooling, should we see an increase in the effective field? Perhaps, if the temperature is as large as in β Dor: 1550°K (Estes & Wood, 1970), a change in the continuous opacity might be sufficient to move line-formation regions into layers which have higher-valued (positive) fields.

IV. CONCLUSION

Observations of the $7^{d}.6$ cepheid W Sgr have been described on the assumption that the phase plot of Figure 1 holds true for every cycle. A negative-field spike of -220g at the phase of maximum light may be related to the sudden compression of the photosphere at the time of arrival of the pulsational wave from the interior. Another less strong negative-field minimum occurs at the phase of the hump. Christy (1966) suggests that the hump represents the arrival of a pulse reflected off the stellar core ∿ 1.4 cycles later. Thus one would expect a negative spike at the hump phase for the same reasons that one finds the negative spike at the phase of arrival of the main pulse.

The positive field maximum, on the other hand, is observed at the time of contraction and cooling. The surface reaches its highest velocity at this

time. The cooling may be sufficient for a significant continuum opacity change so that layers with stronger fields are seen.

REFERENCES

Albrecht, R., Jenkner, H., Weiss, W. W., and Wood, H. J., 1977, Astron. Astrophys., 58, 93

Babcock, H. W., 1958, Ap. J. Suppl., 3, 141, No. 30

Christy, R. F., 1966, Stellar Evolution, ed. by Stein & Cameron, Plenum Press, New York

Estes, J. K., and Wood, H. J., 1970, Astron. J., 75, 999

Jacobsen, T. S., 1974, Ap. J., 191, 691

Kraft, R. P., 1967, Aerodynamic Phenomena in Stellar Atmospheres, ed. by R. N. Thomas, Academic Press, London & New York, p. 227

Rakos, K. D., Schermann, A., Weiss, W. W., and Wood, H. J., 1977, Astron. Astrophys., 56, 453

Weiss, W. W., Jenkner, H., and Wood, H. J., 1978, Astron. Astrophys., 63, 247

Wood, H. J., and Campusano, L. B., 1975, Astron. Astrophys. 45, 303

_____, Weiss, W. W., and Jenkner, H., 1977, Astron. Astrophys., 61, 181

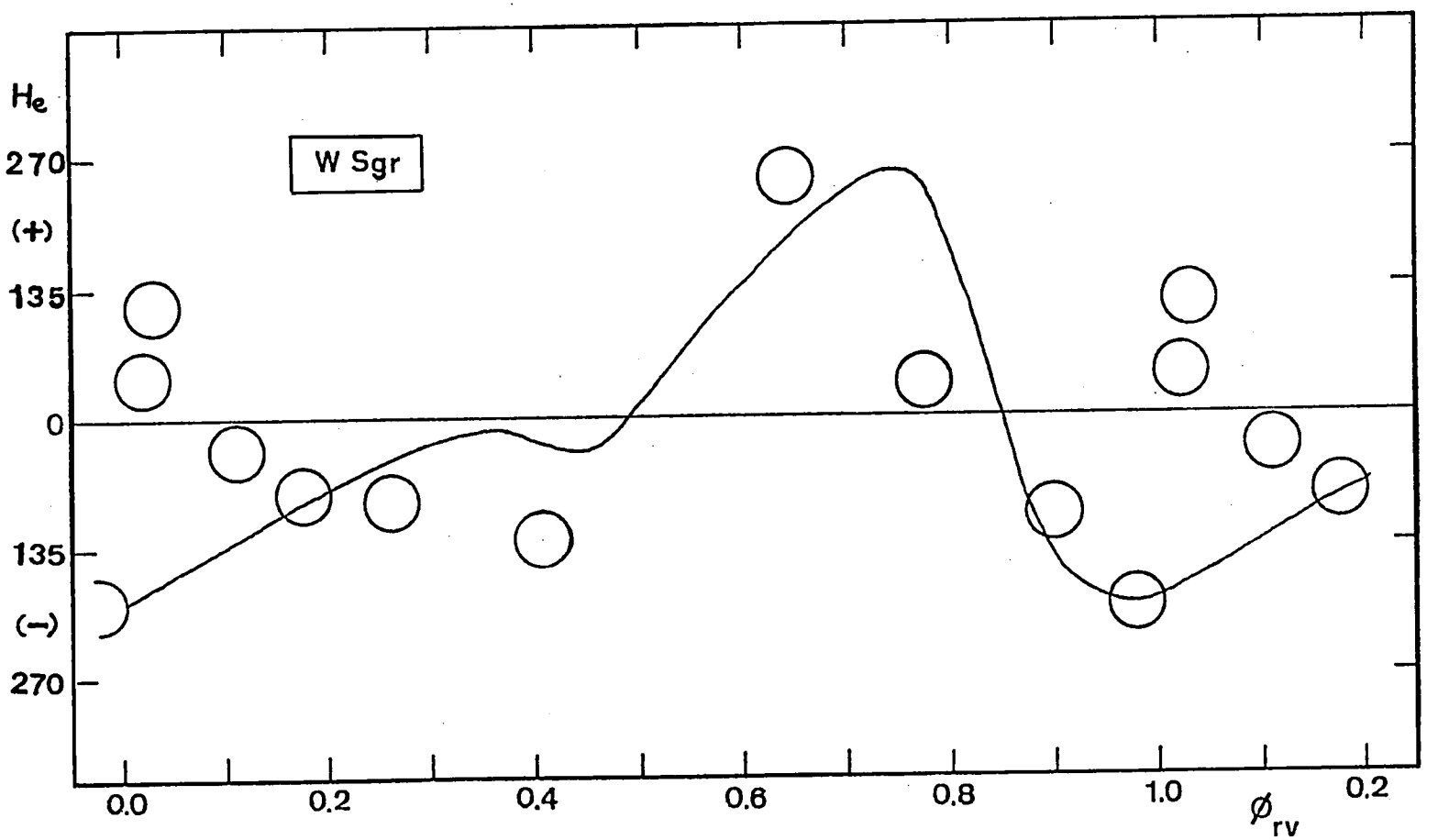

Figure 1. Effective magnetic fields for W Sgr plotted on the 7.d6 period of pulsation. The curve is Jacobsen's "1923 standard" radial velocity curve. The γ-velocity and zero-field axes coincide.

Discussion

Mullan: Sometimes during the oscillation of a Cepheid there is emission in the K line. Do you find any correlation between your measurements of the field, and emission in the K line core?

J. Wood: My plates were not exposed well enough to see the K line core, since I was looking at the continuum around 4300 and exposing for those metallic lines. So I really can't say anything about that.

Mullan: I think that would be an extremely crucial observation.

J. Wood: Yes. I might mention that we found a magnetic field for Canopus, which has a K2 width that doesn't fit on the Wilson-Bappu relation. And Bappu himself has said that he finds this to be the case on the Sun: whenever there are strong magnetic regions, the K2 width does not correspond to the average K2 width for the Sun.

Michalitsianos: Have there been attempts to measure the circular polarization?

J. Wood: This is circular. That is, we have two spectrograms which are analyzed for right-hand and left-hand circular polarization. Do you mean, in the integrated light?

Michalitsianos: I thought you said the transverse component.

J. Wood: No, these are only longitudinal Zeeman effect, which means circular polarization.

Stellingwerf: You mentioned a 17-year cycle of the radial velocity curve. That sounds suspiciously like some kind of a star spot cycle. I wonder if you

could comment on whether we might be able to pick up magnetic field effects on that.

J. Wood: That's an interesting question. The only people I know who have looked into this are Sidney Wolff, Preston, and others who have looked at 73 Dra and other stars that are spectrum variables. They have been observed over long periods of time, and there was really no evidence of long-term changes in the magnetic field. But this, of course, was not a Cepheid. You might expect spots if there are magnetic fields, although these fields are weak compared to those in the Ap stars.

Stellingwerf: I believe it was suggested by Detre and Szeidl that the Blazhko long-term variations of RR Lyrae (two-year period) might be due to a stellar cycle effect. He explains the discrepancy between Babcock's measurements on RR Lyrae and Preston's lack of positive detection of a field in this way.

J. Wood: I've played around a lot with Detre and Szeidl's observations, trying to get some sense out of Babcock's many magnetic observations of RR Lyrae. But there is no way to fit those observations into any of the periods that Detre and Szeidl found. I could not find any "solar cycle".

A DISCUSSION OF CEPHEID MASSES

Arthur N. Cox
Theoretical Division
Los Alamos Scientific Laboratory
University of California

ABSTRACT

Masses and compositions of Cepheids are essential to map the places in the Hertzsprung-Russell diagram where various radial pulsation modes occur. Luminosity observations and stellar evolution theory give masses for Cepheids which range from 10 percent to a factor of four more than those given by pulsation theory. Combining the evolution and pulsation theories, a theoretical mass can be determined using only the period and an approximate surface effective temperature, T_e. The ratio of the theoretical to evolutionary masses averages 0.99 ± 0.07 for 16 Cepheids with good data. A pulsation mass can be calculated using an observed period, luminosity, and T_e. The ratio of pulsation to evolutionary masses averages 0.70 with the old distance scale for the Hyades cluster and the older T_e values, 0.84 ± 0.17 with the accepted 13 percent distance increase of the Hyades cluster and presumably all the clusters with Cepheids, 0.97 ± 0.25 with the new distance scale and improved interstellar reddening corrections giving cooler T_e values, and 1.07 ± 0.27 using in addition surface helium enriched envelope models. These inhomogeneous models allow theoretical predictions of the correct phase of light and velocity curve bumps for evolutionary theory mass Cepheids with periods between 5.5 and 13 days. They also give the proper observed period ratios for double-mode Cepheids with evolution theory masses. Using radii measured by the Wesselink method, the ratio of this mass to the evolutionary mass is

0.93 with homogeneous and 1.02 with inhomogeneous models. Above about 10-20 days a mass loss of 20-30 percent is indicated for stars in their early B star evolution with originally 15 or more solar masses. Six Cepheids with at least four different mass determinations show that for periods below 10 days there are no longer any Cepheid mass anomalies.

A long term goal in understanding the pulsation of the classical Cepheids is to theoretically map their pulsation instability strip in the Hertzsprung-Russell diagram. Several previous attempts have been made starting with J. P. Cox (1963) and including Christy (1966), Stobie (1969ab), Iben(1971), Iben and Tuggle (1972ab, 1975), and Stellingwerf (1975), and the Los Alamos centered group who have published the papers Cox, et al. (1966), King, Cox, and Eilers (1966), King, et al. (1973), Cox, King, and Tabor (1973), and King, et al. (1975). It has been shown that instability strip blue edges are well understood, and now Deupree is completing a discussion of the Cepheid red edge. What remains to learn is what pulsation modes occur and where they are in the instability strip.

The masses and compositions of the Cepheids are essential if this further mapping in the H-R diagram is attempted. Even the blue and red edges depend on the mass and composition, but their lesser dependence has resulted in the current reasonably satisfactory agreement between theory and observation. See Cox and Hodson (1978). The persistent uncertain Cepheid masses and compositions has led Christy (1966) to what I consider a very misleading relation between luminosity and transition period for the fundamental mode:

$$\Pi_{tr} = 0.057\ (L/L_{\odot})^{0.6}\ \text{days.}$$

Stobie (1969b) in discussing modal behavior proposed an incorrect rule that if the pulsation period was between 2 and 7 days, it was a first overtone pulsator, and if less than 2 days a second overtone pulsator. Stellingwerf (1975), searching for double-mode conditions got it (wrongly we now think) at the red side of the instability strip or maybe beyond the red edge. All these studies used atrocious masses and compositions, oblivious of the results of stellar evolution theory.

Starting with Cogan (1970) several others like Rodgers (1970), Fricke, Stobie, and Strittmatter (1973), and Petersen (1973), found that masses based on observations and pulsation theory were anywhere from 10 percent to a factor of four lower than those infered from observed luminosities and evolution theory.

Iben and several of his collaborators have tried to reconcile pulsation and evolution theories and both of these with observations. Various schemes for solving the Cepheid mass anomalies have been proposed. Iben and Tuggle (1972a) wanted to move the period-luminosity calibrating Cepheids further away by 15 percent making them intrinsically brighter, bigger and more nearly the mass given by evolution theory. King, et al. (1975) proposed they were really cooler and larger than the current $(B-V)_0$ - log T_e relation gives. Both these effects have now been realized with the best distance scale to the galactic clusters containing Cepheids increased by 13 percent and a new concept that the interstellar reddening was overestimated making Cepheid surface temperatures now 100 K or so cooler with the same $(B-V)_0$ - log T_e scale.

However, the phase of the bumps in Cepheids between 5.5 and 13 days and the period ratio of the dozen or two double-mode Cepheids still indicate low masses. These bump and beat masses are independent of the distance and temperature scales. Simon and Schmidt (1976) have now showed that the bump phase was related to the ratio Π_2/Π_0, making both these classes double-mode Cepheids.

Our proposal after considerable discussion, much of it already published by Cox, et al (1977) and Cox, Michaud, and Hodson (1978), is that the Cepheids have helium enriched envelopes, caused by a helium deficient Cepheid wind, which changes their internal structure enough to change Π_1/Π_0 and Π_2/Π_0 without appreciably changing Π_0. I now believe that the masses of all Cepheids are given correctly by evolution theory. Most are in blue loops, but at the shortest periods, as for the only triple-mode Cepheid AC And, and for the masses above 13 $M_\odot$, the star is having its first instability strip crossing. Can we prove that evolution and pulsation masses are now equal?

Let me first dispose of a very poor way to get Cepheid masses - use of photometric multicolor measurements interpreted in terms of log g and T_e. If

$$g = G\frac{M}{R^2}$$

$$\left(\frac{Q}{\Pi}\right)^2 = \frac{M}{R^3}$$

and $$Q_1 = Q_1\ (M,R,L,T_e \text{ composition}) \qquad (1)$$

using the Faulkner (1977) form for Q_1, then

$$g \sim \frac{M}{R^2} \text{ and } \frac{1}{\Pi^{1.38}} \sim \frac{M}{R^{2.44}}$$

$$\text{or } M \sim g^{5.6} \text{ for Cepheids.}$$

Thus a factor of two error in g, which apparently can be improved for earlier type stars, is nevertheless disastrous for getting Cepheid masses.

The latest evolutionary tracks for Cepheids are given by Becker, Iben, and Tuggle (1977). As noted many times before, the rather tight relation between mass and blue loop luminosity allows a determination of the evolutionary mass for Cepheids with known luminosities. The relation

$$\begin{aligned} \log L/L_\odot &= 0.46 - 41(Z - 0.02) + 6.6(Y - 0.28) \\ &+ [3.68 + 21(Z - 0.02) - 4.5(Y - 0.28)] \log M/M_\odot \end{aligned} \tag{2}$$

suggested by Becker, Iben, and Tuggle applying to an evolution time weighted mean of the first, second, and third crossing is used here.

Let me describe the method of determining what I call theoretical masses. We use the four equations

$$L = 4\pi R^2 \sigma T_e^4 \tag{3}$$

$$Q_0 = \Pi_0 \sqrt{\frac{M/M_\odot}{(R/R_\odot)^3}} \tag{4}$$

together with Equations (1) and (2) above to relate four unknowns M, R, L, and Q_0. Here we know Π_0, the fundamental pulsation period, very well, and we know T_e to usually better than 10 percent. If we assume Y = 0.28 and Z = 0.02, an iterative method of solution gives

a theoretical mass, radius, luminosity, and a Q_0.

Table 1 gives 20 Cepheid evolutionary, theoretical, and pulsation masses, where the pulsation masses, discussed first by Cogan (1970), need an observed period, luminosity, and color. For these pulsation masses the color gives T_e which together with the luminosity gives a radius, which further, with the period, gives a mass. The Q_0 for this table comes from the Cox, King, and Stellingwerf (1972).

TABLE 1

CALIBRATION CEPHEIDS
REVISED HYADES DISTANCE
SANDAGE AND TAMMANN OR VAN DEN BERGH PERIODS AND COLORS

Cepheid	Π_0(d)	log $L/L_\odot$	$M_{ev}/M_\odot$	T_e(K)	$R/R_\odot$	Q_Q(d)	$M_Q/M_\odot$	Q_T(d)	$M_T/M_\odot$
SU Cas	1.95	2.98	4.8	6599	23.8	.0355	4.5	.0353	4.9
EV Sct	3.09	3.06	5.1	6113	30.5	.0371	4.1	.0362	5.4
CEb Cas	4.48	3.30	5.9	6138	39.8	.0381	4.6	.0369	6.3
CF Cas	4.87	3.26	5.8	5895	41.3	.0386	4.4	.0372	6.2
CEa Cas	5.14	3.34	6.1	5943	44.5	.0384	4.9	.0373	6.4
UY Per	5.36	3.40	6.3	6088	45.4	.0386	4.8	.0373	6.8
CV Mon	5.38	3.37	6.2	5943	46.1	.0385	5.0	.0374	6.6
VY Per	5.53	3.45	6.5	6162	47.0	.0386	5.0	.0373	7.0
CS Vel	5.90	3.25	5.7	5895	40.8	.0410	3.3	.0377	6.7
V367 Sct	6.29	3.54	6.8	6313	49.7	.0394	4.8	.0375	7.6
U Sgr	6.74	3.59	7.1	6162	55.2	.0390	5.6	.0378	7.6
DL Cas	8.00	3.57	7.0	5801	60.9	.0398	5.6	.0385	7.5
S Nor	9.75	3.65	7.4	5731	68.4	.0409	5.6	.0391	8.0
TW Nor	10.79	3.46	6.5	5572	58.1	.0448	3.4	.0396	8.0
VX Per	10.89	3.77	7.9	5943	73.0	.0415	5.6	.0392	8.8
SZ Cas	13.62	3.93	8.8	6015	85.7	.0424	6.1	.0398	9.8
VY Car	18.93	4.05	9.5	5309	126.3	.0416	9.7	.0418	9.4
T Mon	27.02	4.27	10.8	5224	168.1	.0426	11.8	.0433	10.6
RS Pup	41.38	4.35	11.4	5373	174.2	.0495	7.6	.0449	13.0
SV Vul	45.04	4.48	12.4	5018	232.0	.0457	12.8	.0461	12.2

All these Cepheids which are listed by Sandage and Tammann (1969) or van den Bergh (1977) are in galactic clusters or have their distance known by some other method. At least all the cluster Cepheids need their distance modulus increased by $0^m.26$, and, not knowing what to do for the other six, they also have been assumed more luminous. The six not in galactic clusters are: SU Cas in front of a reflection nebula, UY Per, VY Per, VX Per, SZ Cas, in the dubious h + χ Perseus association and RS Pup discussed recently by Eggen. While the h + χ Perseus cluster may not exist, Turner (1977) now proposes that at least one of the questionable Cepheids, UY Per, may be in one of the clusters King 4 or Czernik 8. A glance at the table shows that the pulsation masses are still anomalously low even with most of the Iben suggested distance increase. Evolution and theoretical masses always agree well.

But I don't want you to dwell much on this table, because there is a further necessary change in the T_e values. Dean, Warren and Cousins (1978), in a still unpublished paper, list newly determined color excesses for 16 of these 20 Cepheids. Unfortunately, the four not listed by DWC, CEb Cas, CEa Cas, CS Vel, and V367 Sct, are all in clusters. Anyway these new color excesses, based on fitting tracks in the B-V, V-I, and B-V, R-I planes for each pulsating variable are significantly less than those older ones determined by Kraft based on photometry of the G band. Therefore, the intrinsic colors are redder and the Cepheids are cooler. Figure 1 gives these 16 Cepheid mass ratios M_T/M_{ev} with both the improved distance and T_e values. Actually, the T_e used for U Sgr and S Nor is given by Pel (1978) who obtained them by his multicolor photometry. I have also used for the Q_0 values

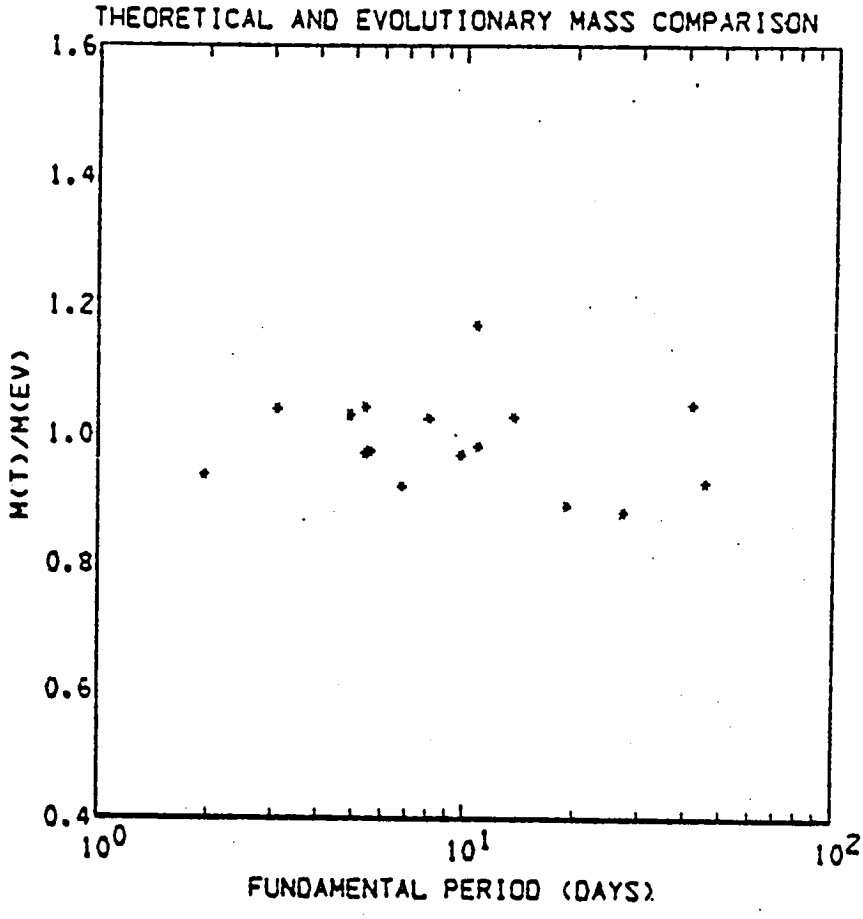

Fig. 1. Theoretical to evolutionary mass ratio versus fundamental period for 16 Cepheids. The new distance, temperature, and Q_0 values are used.

those from helium enriched models which I have advocated. One now sees again that the theoretical masses are very close to the evolutionary masses, the mean ratio being 0.99 ± 0.07.

An important point here is that one can get a theoretical mass, based on only Π_0 and an approximate T_e value, for any Cepheid if one believes the theoretical evolution mass-luminosity law and the theoretical pulsation constants. Later we will use these theoretical masses for Cepheids not in clusters to compare with masses from other methods.

Figure 2 on the same scale plots the ratio of pulsation to evolution masses for 16 Cepheids with the new observational data, but with homogeneous (not helium enriched) envelope Q_0 values. The Cogan mass anomaly has disappeared as predicted by Iben and Tuggle and Fricke, Stobie, and Strittmatter. The mean ratio M_Q/M_{ev} was 0.70 according to Stobie (1974), and it becomes 0.84 ± 0.17 if the new distance scale is used alone and here 0.97 ± 0.25 when both the new distances and T_e values are used.

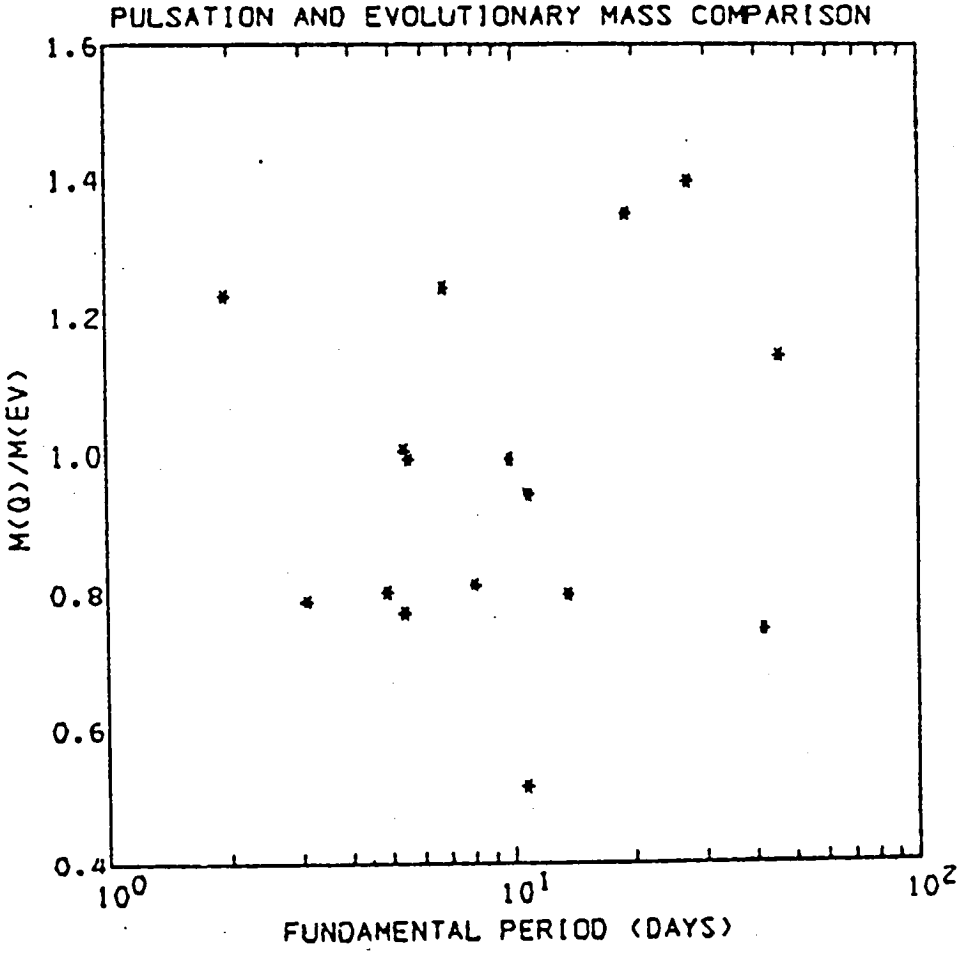

Fig. 2. Pulsation to evolutionary mass ratio versus fundamental period for 16 Cepheids. The new distances and temperatures, but homogeneous Q_0 values are used.

We must consider what happens if the inhomogeneous model Q_0 values are used, because if they solve the bump and beat mass anomalies they must not be excluded for these 16 calibrating Cepheids. Indeed, 5 of these 16 Cepheids have bumps in their light and velocity curves. The ratio M_Q/M_{ev} is given in Figure 3, and the mean ratio is 1.07 ± 0.27. Inclusion of the surface helium enriched model Q_0 values here actually reverses the pulsation mass anomaly, but maybe Schmidt's (1978) new cluster distances, based on Hβ photometry of the B stars will now decrease distances to these calibrating Cepheid clusters.

Let me briefly discuss the problem of converting mean colors to T_e. The latest word by Bell and Parsons (1974) seems to be that the venerable Kraft relation

$$\log T_e = 3.886 - 0.175\ (B-V)$$

is still to be used. Therefore, that is the origin of T_e from unreddened DWC colors for the theoretical and pulsation masses. Note in Figure 4, however, the problem is still not solved. We plot the unreddened DWC colors versus the Pel (1978) log T_e for 44 Cepheids where both values are known. The discrepancy has been claimed by DWC to indicate that Pel has determined too little reddening from his multicolor work and obtained temperatures too low by a few percent or about 150 K. Cogan tells me that the points in this slide are better fit with the Flower (1977) formula, but it really seems that Pel's reddenings are too small by 0.05 - 0.08 in B-V. I don't worry too much about this, though we still need refinement of T_e values.

Bump masses, discussed mostly by Fricke, Stobie, and Strittmatter (1972), are based on the phase of the light curve bump for those Cepheids with periods between 5.5 and 13 days. Christy, and parti-

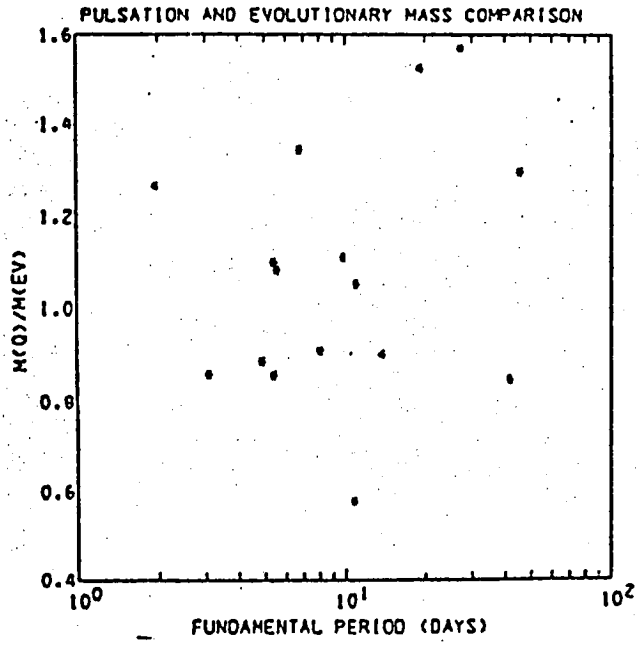

Fig. 3. Pulsation and evolutionary mass ratio versus fundamental period for 16 Cepheids. New distances, temperatures, and Q_0 values are used.

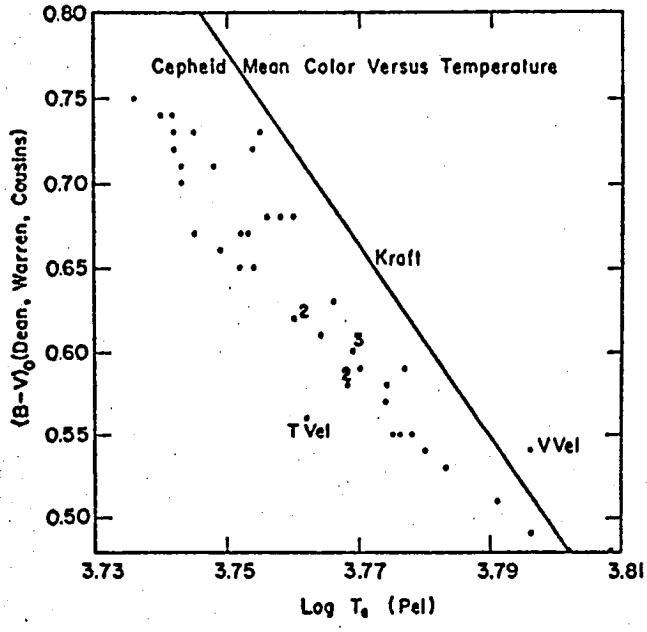

Fig. 4. Dean, Warren and Cousins unreddened colors are plotted versus Pel's log T_e values for 44 Cepheids. The Kraft relation is shown.

cularly Stobie, found that the bumps were at a phase way too late and often invisible for a 10 day Cepheid unless the mass was only like 4-5 $M_\odot$. This is about 70 percent of that given by evolution theory, and is the basis for Stobie's (1969b) different, anomalous mass luminosity law.

Fricke, Stobie, and Strittmatter (1972) related the period times the bump phase to the equilibrium radius by using Stobie's theoretical models. The radius can then be put into the period - mean density formula to get the mass. Masses averaged 0.75 the evolution masses.

Simon and Schmidt (1976) discovered that the bump phase correlated with Π_2/Π_0. If we use linear theory for Π_2/Π_0 and evaluate the sound echo time for the models we get the lines in Figure 5. Echo time is like bump phase, because if the echo time is long (in the equilibrium model) then the bump generated by nonlinear mechanisms,

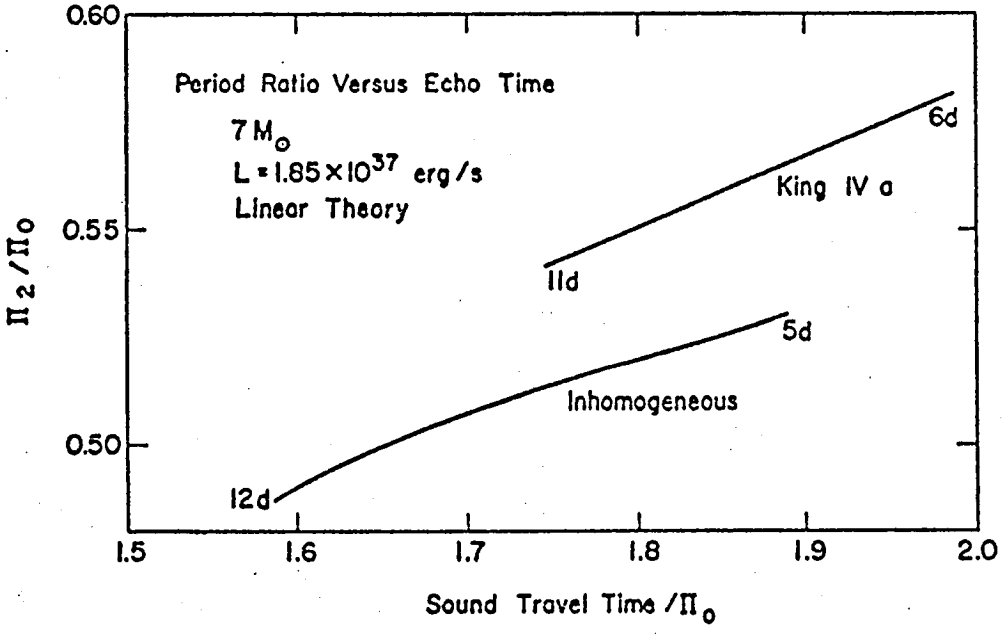

Fig. 5. Period ratio Π_2/Π_0 versus echo time from linear theory for 7 $M_\odot$ with evolution theory luminosity. Both homogeneous and inhomogeneous models are shown.

at minimum radius, will also be late in a full amplitude pulsating model. This figure shows that there is not a universal relation between echo time and Π_2/Π_0, but the relation is much as Simon and Schmidt discovered using Stobie's nonlinear models. Note that the inhomogeneous models give earlier echo times even though these linear theory times are still too late.

Figure 6 gives some results I spoke about in IAU Symposium 80. Here Π_2/Π_0 is plotted against Π_0. First look at the homogeneous King IVa 7 $M_\odot$ models at evolution luminosities. The region of Π_2/Π_0 between 0.46 and 0.53 is never reached for these linear theory models. Note the blue B, and red R edges. If we retain the luminosity but reduce the mass to 5 $M_\odot$, then bumps appear nearer the correct phase, where the Π_2/Π_0 ratio equals 0.50 at 10 days with the bump near the velocity and light curve peaks. The unpublished Carson C312 opacities give improve-

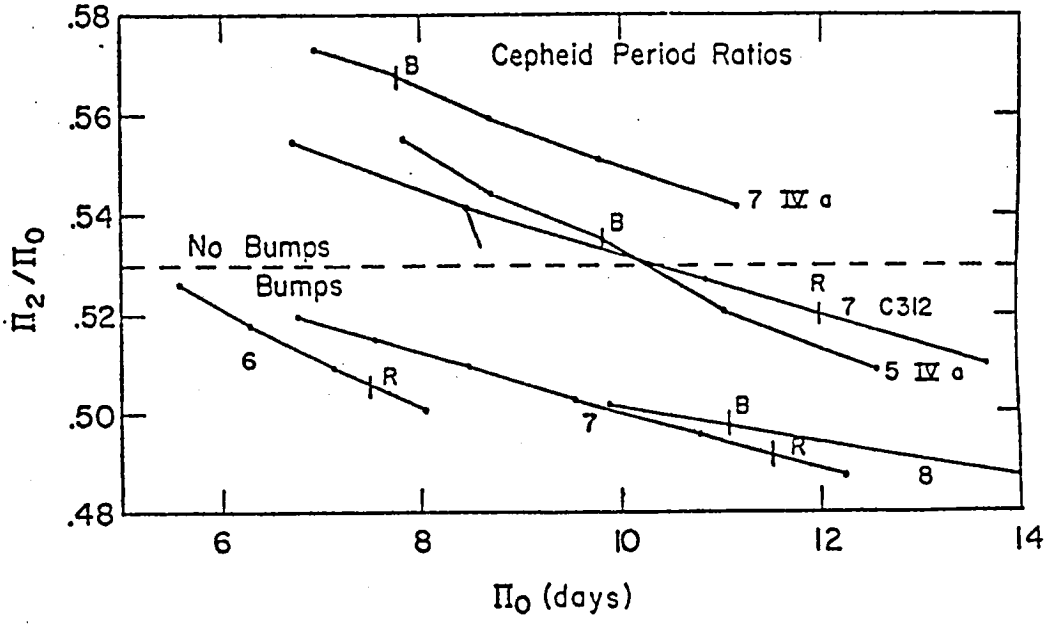

Fig. 6. The period ratio Π_2/Π_0 versus Π_0 for Cepheid models in the instability strip. Approximate blue (B) and red (R) edges are indicated. Inhomogeneous models at 6.0, 7.0, and 8.0 $M_\odot$ show the appropriate Hertzsprung relation.

ment for homogeneous compositions, but really not enough. These opacities are considered very uncertain. Finally, Y = 0.75 surface layers give the proper Π_2/Π_0 progression - that is the Hertzsprung progression - with fundamental mode period.

Above 8 or 9 $M_\odot$ there is not enough time in Cepheid blue loop evolution to have a Cepheid wind enrich the surface layers. Bumps then might be expected at long periods for these homogeneous variables, and some are actually seen. For example, bumps are on light curves for RU Sct (19.7d), UZ Pup (23.2d), and on X Pup (26.0d). If there is mass loss way back when the star is a B star, we might have a case, such as studied by Sreenivasan and Wilson (1977) of a luminosity for a 10-15 $M_\odot$ Cepheid with a mass of perhaps 25 percent less. In that case the Π_2/Π_0 would always be less than 0.46, and no bumps would occur.

Let me turn now to the double-mode Cepheids whose masses have been studied theoretically by Petersen (1973), King, et al. (1975) and by Cox, King and Hodson (1977) and more observationally by Rodgers (1970), Fitch and Szeidl (1976), and Schmidt (1972, 1974). With only the ratio Π_1/Π_0, and we are sure that these periods have been correctly identified, the mass of a variable like U Tr A can be determined.

Figure 7 has the whole story for this Cepheid at Π_0 = 2.568 days. The homogeneous King IVa composition mass is like 1.2 $M_\odot$, but the several ways of getting enriched surface layers give larger masses. A thin layer with Y = 0.75 down to 70,000 K and the Population I King IVa composition interior gives 4 $M_\odot$. This slide has been expanded

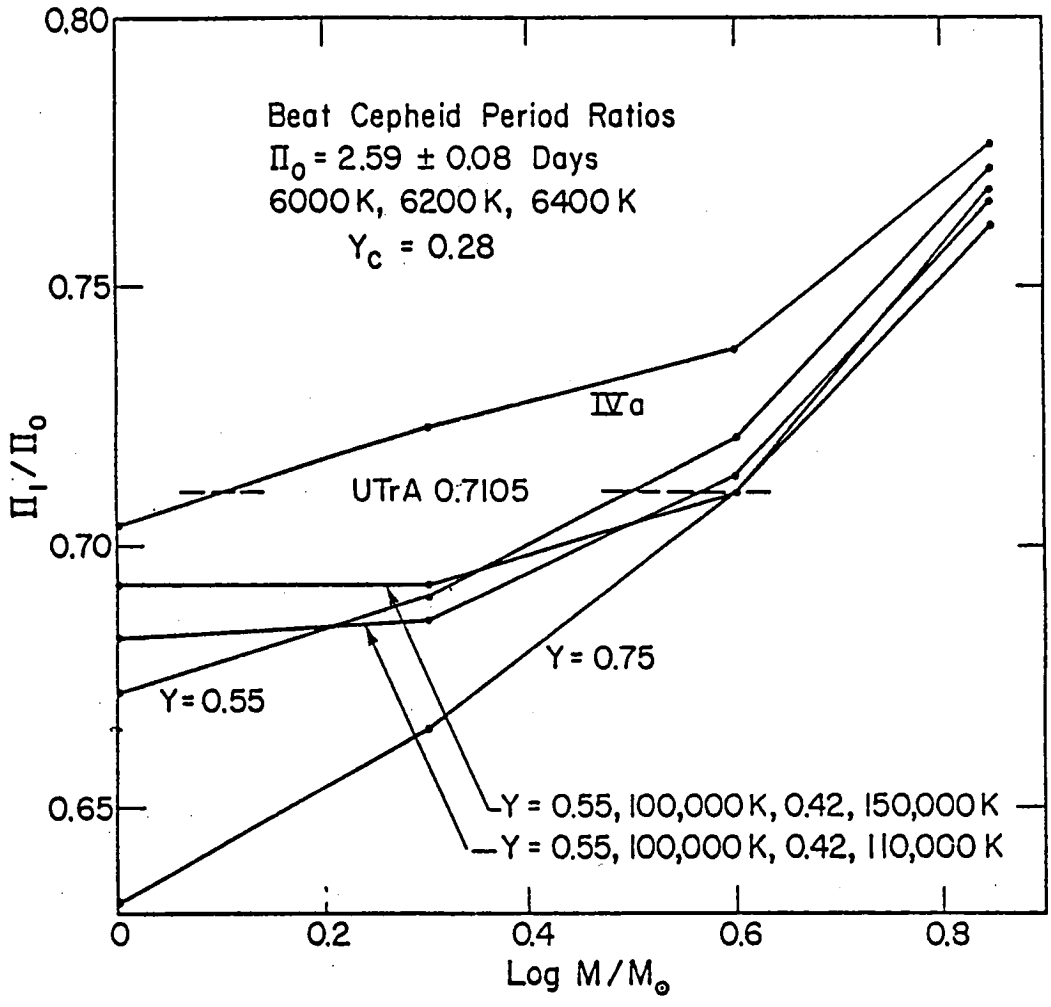

Fig. 7. The period ratio Π_1/Π_0 versus mass is shown for U Tr A models at T_e of 6000 K, 6200 K, and 6400 K. The dashed line gives the observed period ratio which indicates masses like 4 $M_\odot$ for surface Y between 0.55 and 0.75.

since I showed it at the IAU Symposium 80. I now believe that a surface Y of 0.55 is large enough if one allows the inverted μ gradient instability to mix some helium down to deeper levels like 100,000 K. These enrichments are all possible according to Cox, Michaud, and Hodson (1978) considering the age of the Cepheid and the same wind and wind composition per surface area as for the sun.

Our newest mass results are those given by Wesselink radius measurements. Balona (1977) sent me his recent tabulation, and that together with the Evans (1976) and Scarfe (1976) data, allow

69 mass determinations. The idea is simple - plug the radius and period into the period mean density relation with known Q_0 to get the mass.

Figure 8 gives the ratios of the Wesselink radius masses to theoretical masses for Q_0 values applicable for homogeneous models. The ratio is 0.93 for periods less than 10 days and 0.60 above. The tremendous scatter was not expected by me because Balona advertises errors of less than 10 percent in the radius. The Wesselink radius masses go like $R^{2.44}$. Better radii, accurate to 10 or less percent, are needed

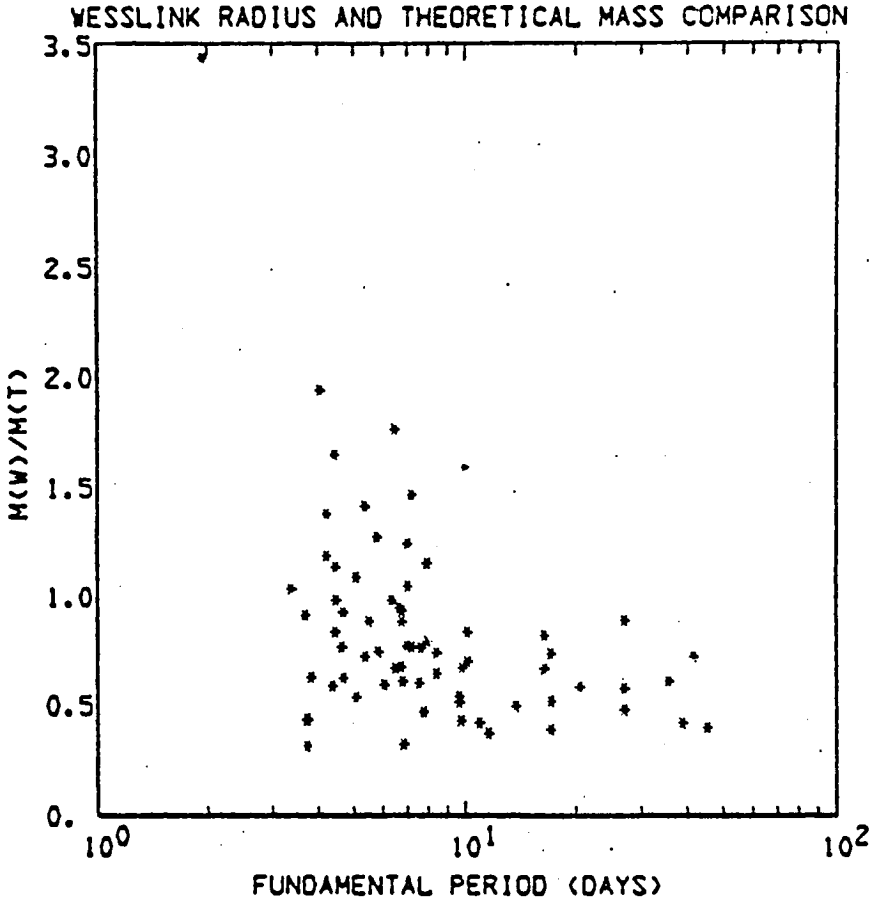

Fig. 8. The ratio of the Wesselink radius mass to theoretical mass is plotted versus period for 69 cases. Evolutionary masses use X = 0.70 and Y = 0.28, and Q_0 values are based on the homogeneous composition X = 0.602, Y = 0.354.

Figure 9 shows that the anomalous masses are partially cured with the Q_0 values for the inhomogeneous models. For these, Q_0 is up by 5-10 percent. For shorter periods, the ratio M_W/M_T is 1.02. The longer period Cepheids show a mass anomaly (ratio equal 0.70) which is not new - see Schmidt (1976) for example. I speculate that these Cepheids have had mass loss in the B star stage which does not affect their luminosity as much as their mass.

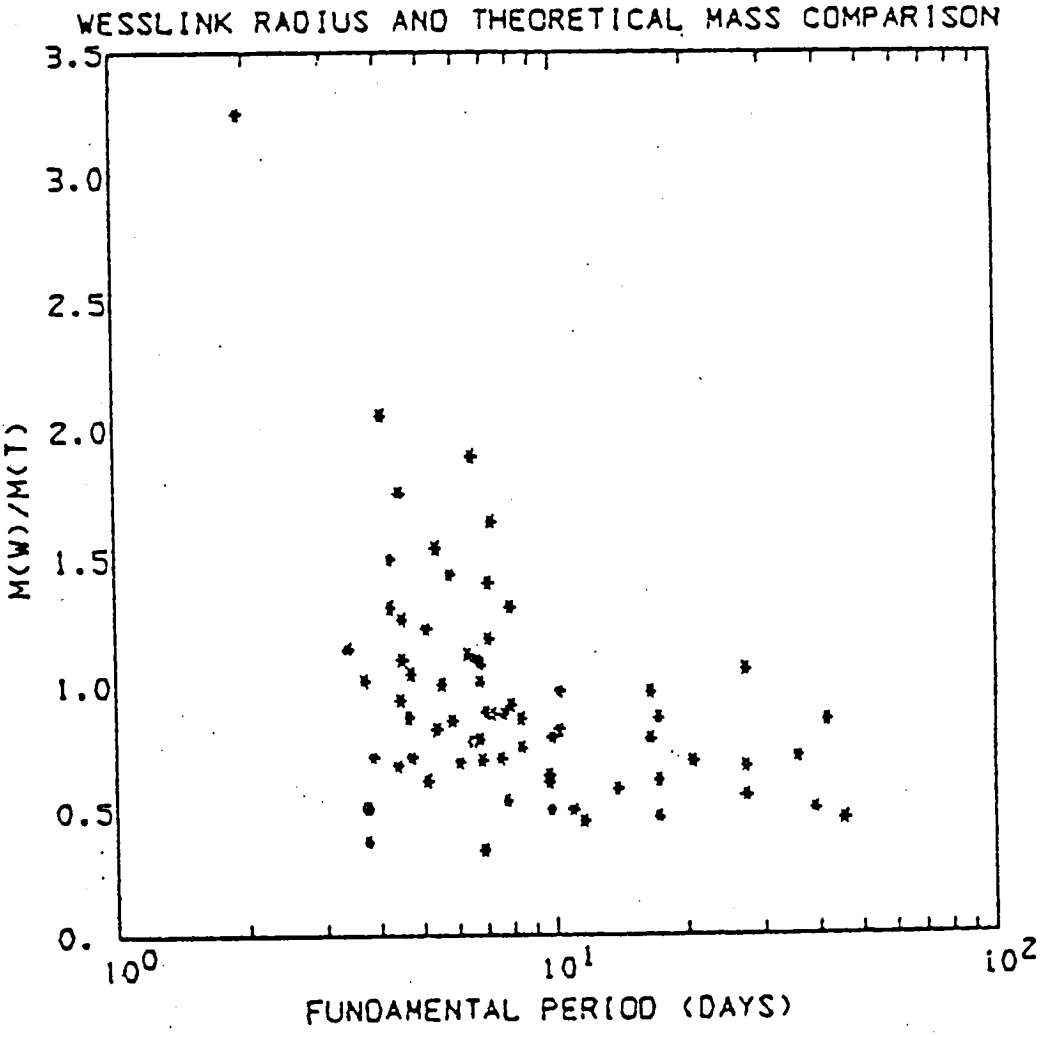

Fig. 9. The ratio of the Wesselink radius mass to theoretical mass is plotted versus period for 69 cases. Evolutionary masses use X = 0.70 and Y = 0.28, and the Q_0 values come from the inhomogeneous models with Y_S = 0.75.

Earlier I pointed out that use of a photometrically measured gravity cannot get an accurate mass. But the preceeding theoretical and evolutionary masses can give good log g values which can be compared to Pel's measurements. The difference

$$\log g_P - \left(\frac{\log g_T + \log g_W}{2}\right)$$

is + 0.02 ± 0.20 for the homogeneous models and - 0.02 ± 0.20 for the inhomogeneous models, where P, T, and W are the Pel, theoretical, and Wesselink radius values of g. The very close agreement is not unexpected since

$$\frac{M_W}{R_W^2} \sim \frac{R_W^{0.44}}{\Pi_0^{1.38}} \qquad \frac{M_T}{R_T^2} \sim \frac{T_e^{0.28}}{\Pi_0^{1.06}}$$

Evidently the comparison of log g values with theory cannot indicate whether the inhomogeneous enriched helium envelopes are more realistic than the homogeneous ones.

My Wesselink radius mass paper (Cox 1979) has more, for example the possibility of overtone pulsation and the use of the Barnes et al. radii, which I will not cover here.

As a final point let me compare the masses of U Sgr, S Nor, and V367 Sct, all cluster Cepheids which are determined by at least four ways. Table 2 gives the usual low values for the Fricke, Stobie, and Strittmatter bump, and Cox, et al. beat masses, using homogeneous models. Also in the table I have masses for T Mon, RS Pup, and SV Vul showing the Wesselink radius mass anomaly for all but RS Pup.

My conclusion is that all previous mass anomalies can be considered solved by distance, temperature, and inhomogeneous model improvements. Wesselink radii urgently need improvement. If there is no systematic radius error due to strange limb darkening effects, etc., there is a

TABLE 2

CEPHEID MASSES

Cepheid	M_{ev}	M_T	M_Q	M_ϕ	M_B	M_W
U Sgr*	7.1	6.5	9.5	4.0	-	6.6
S Nor*	7.4	7.2	8.2	3.8	-	3.6
V367 Sct**	6.9	7.3	5.6	-	2.3	-
T Mon	10.8	9.6	17.0	-	-	5.3 - 10.2
RS Pup	11.4	12.0	9.6	-	-	10.3
SV Vul	12.4	11.5	16.0	-	-	5.3

* The bump masses are given by FSS.

** The V367 Sct theoretical and pulsation masses are based on the van den Bergh T_e and not the new T_e from Dean, Warren, and Cousins unreddened colors. The homogeneous model beat mass is from Cox, et al.

persistent mass anomaly for the longer period Cepheids that may really indicate early mass loss. More observations are suggested for galactic cluster distances, to improve pulsation masses, for Wesselink radii, to improve Wesselink radius masses, and for Cepheid spectra and even for the solar wind, to confirm if inhomogeneous models with surface helium enrichment really exist.

REFERENCES

Balona, L. A. 1977, Mon. Not. R.A.S., 178, 231.

Becker, S. A., Iben, I., and Tuggle, R. S. 1977, Ap. J., 218, 633.

Bell, R. A. and Parsons, S. B. 1974, Mon. Not. R.A.S., 169, 71.

Christy, R. F. 1966, Ann. Rev. Astr. Ap., 4, 353.

Cogan, B. C. 1970, Ap. J., 162, 139.

Cox, A. N. 1979, Ap. J. (in press).

Cox, A. N., Deupree, R. G., King, D. S., and Hodson, S. W. 1977, Ap. J. Lett., 214, L127.

Cox, A. N. and Hodson, S. W. 1978, Proc. IAU Symposium 80.

Cox, A. N., King, D. S., and Hodson, S. W. 1977, Ap. J., 212, 451.

Cox, A. N., King, D. S., and Tabor, J. E. 1973, Ap. J., 184, 201.

Cox, A. N., Michaud, G., and Hodson, S. W. 1978, Ap. J., 222, 621.

Cox, J. P. 1963, Ap. J., 138, 487.

Cox, J. P., Cox, A. N., Olsen, K. H., King, D. S., and Eilers, D. D. 1966, Ap. J., 144, 1038.

Cox, J. P., King, D. S., and Stellingwerf, R. F. 1972, Ap. J., 171, 93.

Dean, J. F., Warren, P. R., and Cousins, A. W. J. 1978, preprint.

Evans, N. R. 1976, Ap. J., 209, 135.

Faulkner, D. J. 1977, Ap. J., 218, 209.

Fitch, W. S. and Szeidl, B. 1976, Ap. J., 203, 616.

Flower, P. J. 1977, Astr. and Ap., 54, 31.

Fricke, K., Stobie, R. S., and Strittmatter, P. A. 1972, Ap. J., 171, 593.

Iben, I. 1971, Ap. J., 168, 225.

Iben, I. and Tuggle, R. S. 1972a, Ap. J., 173, 135.

Iben, I. and Tuggle, R. S. 1972b, Ap. J., 178, 441.

Iben, I. and Tuggle, R. S. 1975, Ap. J., 197, 39.

King, D. S., Cox, J. P., and Eilers, D. D. 1966, Ap. J., 144, 1069.

King, D. S., Cox, J. P., Eilers, D. D., and Davey, W. R. 1973, Ap. J., 182, 859.

King, D. S., Hansen, C. J., Ross, R. R., and Cox, J. P. 1975, Ap. J., 195, 467.

Pel, J. W. 1978, Astr. and Ap. Suppl., 31, 489.

Petersen, J. O. 1973, Astr. and Ap., 27, 89.

Rodgers, A. W. 1970, Mon. Not. R.A.S., 151, 133.

Sandage, A. R. and Tammann, G. A. 1969, Ap. J., 157, 683.

Scarfe, C. D. 1976, Ap. J., 209, 141.

Schmidt, E. G. 1972, Ap. J., 176, 165.

Schmidt, E. G. 1974, Mon. Not. R.A.S., 167, 613.

Schmidt, E. G. 1976, Ap. J., 203, 466.

Schmidt, E. G. 1978, Ap. J. Lett. (in press).

Simon, N. R. and Schmidt, E. G. 1976, Ap. J., 205, 162.

Sreenavasen, S. R. and Wilson, W. J. F. 1977, Astr. and Space Sci., 53, 193.

Stellingwerf, R. F. 1975, Ap. J., 199, 705.

Stobie, R. S. 1969a, Mon. Not. R.A.S., 144, 485.

--------1969b, Mon. Not. R.A.S., 144, 511.

Stobie, R. S. 1974, in IAU Symposium 59, Stellar Instability and Evolution.

Turner, P. G. 1977, Pub. ASP, 89, 1977.

van den Bergh, S. 1977, in IAU Colloq. 37, Decalages vers le Rouge et Expansion de l'Univers.

Discussion

Wesselink: Would there be any mass loss in the evolution of a Cepheid, and would this affect your conclusions?

A. Cox: The standard answer to that question as given by stellar evolution people is that there may be mass loss while the star is a B star, but if it loses more than 10% of its mass in the yellow giant and red giant stage, it will not go through a blue loop. This was a very amazing result that came out about 1970 by Refsdal, Roth and Weigart, and they stick to it. Even recent results for a 15 $M_\odot$ star by Sreenivasan and Wilson indicate the same thing. You might have a little bit of mass loss from the red giant as it comes back through the blue loop, but not enough to explain any of these anomalies. You can get 10%, but that's all.

Hillendahl: On the basis of believing in models (cf. PASP 82, 1231, 1970) you would predict that any time a star evolves across any instability strip in the H-R diagram -- not just the Cepheid instability strip -- there would be mass loss and helium enrichment in the atmosphere. I wonder if there is any possibility of testing that with the data?

A. Cox: There are two or three ways. You don't see the mass loss itself because it is very low, about 10^{-10} $M_\odot$/yr, and there is no way of easily measuring that low a mass loss. But there is a possibility of looking at the spectra to see if this enriched helium really exists. But it turns out that it's very hard to find helium in a yellow star, like the Sun or a Cepheid. The other thing to do is to study the solar wind to see if we

understand what is happening. The solar wind is deficient in helium, so the solar atmosphere is probably being enriched. But you don't notice it because the solar atmosphere is very deep, comprising about 1% of the mass of the Sun. So it mixes in and you never notice the enrichment. For the Cepheids, we need to enrich about 10^{-4} or 10^{-5} of the mass, which is the mass of the convection zone.

J. Cox: Do you know if there is any observational evidence for a Cepheid wind?

A. Cox: No. The only reason you know about the solar wind is that you are sitting here in it. But if you take the relative size of the Cepheid and the Sun and let the solar wind blow from the Cepheid (which we call a Cepheid wind), you can enrich that very thin layer in the lifetime of the blue loops.

Scuflaire: If the external layers of the star are enriched with helium, do you get an instability?

A. Cox: Yes. Unfortunately, there is a problem, because if you have an inverted μ -gradient it is very likely to be unstable. We are working on that problem also in a two-dimensional hydrodynamical calculation to see what will happen. We fully expect that at first the layer will mix and not persist. If that is really true, there will be no explanation for the bump and the beat Cepheids. So at the moment we are trying to see if there is some way of stabilizing that layer, perhaps by pulsation or by the flow of hydrogen through that layer. Your question could be unanswered for the next 50 years. It is a question of whether you believe the period of Cepheids, indicating a helium enriched layer, or whether you believe from linear theory that the layer will mix.

Keller: You showed a diagram that put beat Cepheids and bump Cepheids in the same class by looking at the period ratio, and that all you had to do was get below a certain period ratio to get bumps. There are several ways of doing this. One is mass loss, another enrichment. It seems to me that something we should do if we don't like these two is to look for any other means for adjusting the structure of the star to get below that period ratio. Have you thought of any other scheme that might be done?

A. Cox: There are two or three points on that. Faulkner in his article in 1977 proposed that when these stars have two modes at once, the period ratio is not correctly given by linear theory. In other words, what we measure is not what we think we measure. But there hasn't been any further pursuit of that. Cogan proposed that a very deep helium convection zone changes the period. But that doesn't seem to work. In a recent letter from Cogan, he stated that he doesn't believe it will work now. Castor, in a private conversation, suggested that the opacities are wrong. After all, you can always change your opacities in astrophysics to solve your problems. That seems out of the question, because we have two widely disparate chemical compositions giving opacities which give similar results. (Dave King will talk about that.) It seems that the only thing that will significantly change the structure is a change in the equation of state.

Connolly: You said higher mass stars could experience mass loss. Could you give a range in Cepheid periods over which this might occur?

A. Cox: Sreenivasan and Wilson have done a study that shows that higher mass stars can lose 25-30% of their mass as B stars; and when they become yellow and red giants, they are undermassive. If they were to lose another

10%, then they would not blue loop. The same lack of blue loops holds for the lower mass stars that do not experience the early mass loss. The answer to your question is that there might be 25% undermassive stars for masses > 10 or 12 $M_{\odot}$, periods above 10 or 15 days.

TRIPLE MODE CEPHEID MASSES

David S. King

Department of Physics and Astronomy, The University of New Mexico

Arthur N. Cox and Stephen W. Hodson

Los Alamos Scientific Laboratory, University of California

I. INTRODUCTION

In the preceding paper (Cox 1978) we have heard about the general problem of Cepheid masses. Large mass anomalies for beat (double-mode) Cepheids (2-6 days) have been discussed by Petersen (1973), King, et al. (1975), and Cox, King, Hodson, and Henden (1977). Ratios of these masses to evolution masses were previously found to be as little as one quarter.

The possibility that nonlinear coupling between the two principal modes in double-mode Cepheids might lead to period ratios which are sufficiently different from those predicted by linear theory as suggested by Faulkner (1977a) does not seem to solve the problem (Cox, Hodson, and King, 1977). Large amplitude mixed mode models lead to period ratios which agree with the linear values to within 0.4 percent, whereas the change required to yield masses close to the evolution value is of the order of 3.0 percent. This result is in agreement with that found by Stellingwerf (1975) in his investigation of a mixed mode model with characteristics similar to those of an RR Lyrae variable.

The suggestion that convection might change the structure in such a way as to alter the period ratios by the required amount, as suggested by Cogan (1977), has been investigated by Deupree (1977a) and by Cox, King, Hodson,

and Henden (1977). It was found that for reasonable values of the ratio of mixing length to pressure scale height, convection played a very small role and was not able, in the absence of other changes, to produce the desired effect.

A possible reconciliation of low Cepheid masses obtained by using linear theory periods with the larger ones obtained by stellar evolution theory has been suggested by Cox, Deupree, King, and Hodson (1977) and Cox, Michaud, and Hodson (1978). The convection zones, presumably enriched in helium by a helium deficient Cepheid wind, change the structure of yellow giants to give the Π_1/Π_0 for double-mode Cepheids consistent with observations.

Until quite recently there were thought to be two cases of triple mode Cepheids. The star AC Andromedae has been discussed by Fitch and Szeidl (1976) who obtained periods of Π_0 = 0.711d, Π_1 = 0.525d and Π_2 = 0.421d. It should be noted that this star is outside of the range of periods previously indicated for the double-mode Cepheids, and there may still be some question as to whether this star is a Population II RR Lyrae star, which would be consistent with its period, or a very short period Population I Cepheid, more consistent with its spectrum.

Faulkner (1977b) has recently reported a third period for the variable TU Cassiopeiae. With periods of Π_0 = 2.14d, Π_1 = 1.52d, and Π_2 = 1.25d, this star does have fundamental and first overtone periods which place it among the other double-mode Cepheids. We have heard Hodson and Cox (1978) report in an earlier paper in this conference that the third period (Π_2) does not appear to be real. Prior to learning this models were studied in an attempt to explain the three periods. We will discuss this in Section III.

The models previously suggested had homogeneous (Y = 0.50 to 0.75) convection zones which extend to 60,000 K or 70,000 K, counting the pulsation and overshooting excursions, and then a deeper 10,000 K wide buffer zone with half the surface helium enrichment. There are now at least two difficulties with those models. Possibly the large helium abundance in the atmosphere conflicts with spectral observations of the metal to hydrogen ratio for Cepheids. This difficulty must await detailed calculations of synthetic spectra to see if high helium can be tolerated. The second difficulty is that possibly the helium rich layer is very unstable due to the inverted μ gradient, and it may quickly mix by a process described by Kippenhahn (1974). Previously, the period ratios of triple-mode Cepheids AC And and TU Cas could not be correctly predicted by very thin enriched layer structures as reported by King, Cox, and Hodson (1977). Deeper enriched layers are now indicated.

It appears that the period ratios of AC And indicate that Cepheid wind enrichment from the surface and the instability mixing below the convection zones compete to give much deeper large Y homogeneous and transition layers than previously thought. The time spent as a yellow giant and the mass loss due to the wind, inferred from the solar wind and the relative size of the sun and the Cepheid, allow a mass fraction of perhaps 2×10^{-4} to be enriched to maybe Y = 0.75. If this layer is unstable and is mixed deeper, the Y will be somewhat smaller and the temperature at the bottom will be hotter. We show that if the enrichment goes to 250,000 K ($1-q = 2 \times 10^{-4}$) with a transition zone to 300,000 K ($1-q = 5 \times 10^{-4}$) for AC And, its periods can be explained. For TU Cas a very unlikely model is required to give the three periods reported by Faulkner (1977b).

The observations of AC And are reviewed in Section II. A discussion of the periods of TU Cas has been given by Hodson and Cox (1978) and need not

be repeated here. Section III gives our theoretical model data and derived masses. Conclusions are given in Section IV.

II. AC ANDROMEDAE PERIODS

The data of Fitch and Szeidl (1976) has been analyzed by a method adapted from Lafler and Kinman (1965) and described by Cox, Hodson, and King (1977). We here, however, have adopted the Fitch and Szeidl periods with no attempt at refining them. The original data, kindly supplied by Fitch, was grouped by averaging all points in magnitude and time within 0.0142d starting at the first data point used by Fitch and Szeidl. The differing weight of these average points has been ignored in our period analysis. Component fundamental (F), first overtone (1H), and second overtone (2H) light curves are given in Figure 1. Three other periods that are found are the nonlinear coupling beats between F and 1H, F and 2H, and 1H and 2H. These final component light curves were obtained after iteratively prewhitening the mean data points with all the other 5 periods. Clearly, the second overtone is present as Fitch and Szeidl found.

The standard error of the amplitudes is 0.06 mag, much larger than obtained by Fitch and Szeidl. The reason seems to be that we have not prewhitened with so many additional periods. It may be necessary to include periods to more exactly define the distorted light curves of the three basic variations. Our curves in Figure 1 and our three nonlinear beat variations then probably do not show the exact shape of each component, but the analysis is good enough to give rather accurate amplitudes.

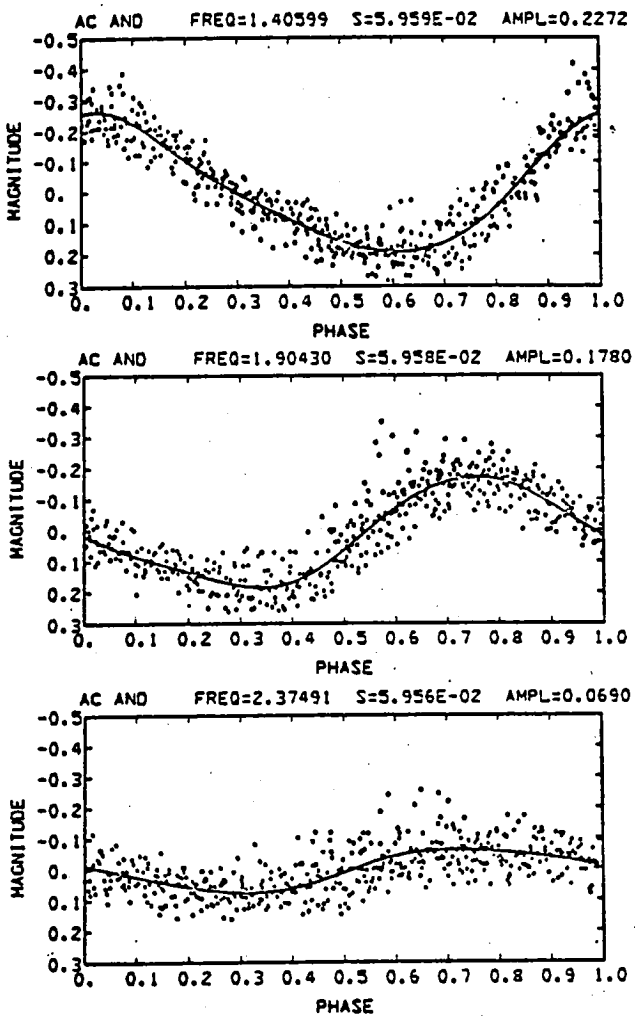

Fig. 1. Component light curves for the three periods of AC Andromedae using the data of Fitch and Szeidl. Their periods have been used. Our three amplitudes are 0.227, 0.178, and 0.069 magnitude with the standard deviation of 0.060 for all three.

III. TRIPLE MODE CEPHEID MASSES

Numerous models have been constructed and analyzed for periods and growth rates using a linear nonadiabatic program originally developed by Castor (1971). Convection with varying ℓ/H_p (Deupree 1977b) is allowed, but ℓ/H_p is

limited to unity. The previous structures, which can explain the bump and double-mode Cepheids with evolutionary theory masses, were modified in ways that did not destroy their Π_1/Π_0 and Π_2/Π_0 period ratios. Thus the new revised bump and double-mode Cepheid masses remain unchanged.

One problem with the surface helium enrichment is that the structure is not stable. Helium will leak downward at a, as yet undetermined, rate. If one assumes some downward mixing to a mass level with only about 5×10^{-4} of the stellar mass above, there is still time to enrich it by a Cepheid wind to a large Y in the few million years during a 3 $M_\odot$ first evolutionary crossing of the pulsation instability strip. Thus our AC And model is enriched to Y = 0.48 from the surface to 250,000 K to Y = 0.38 between there and 300,000 K, and finally with Y = 0.28, or a normal value, deeper all the way to the nuclear burning core.

Figure 2 gives a plot of Π_2/Π_1, Π_1/Π_0, and Π_2/Π_0 versus mass for this structure with the fundamental period for all models within a few percent of that for AC And. The observed period ratios indicate approximately 3 $M_\odot$; a more definitive value would need unknown details of the internal composition structure.

This value of 3 $M_\odot$ is the same as that suggested by Fitch and Szeidl (1976), but we do not completely agree with their techniques of getting the mass. The best data available to them was from the Cogan (1970) grid of models which was coarse and probably the models included too much convection. Fits to the pulsation constant Q_i for various M and R values may not give period ratios Π_{i+1}/Π_i to the accuracy of one part or less per thousand that observations merit. The error in the Fitch and Szeidl mass value was perhaps

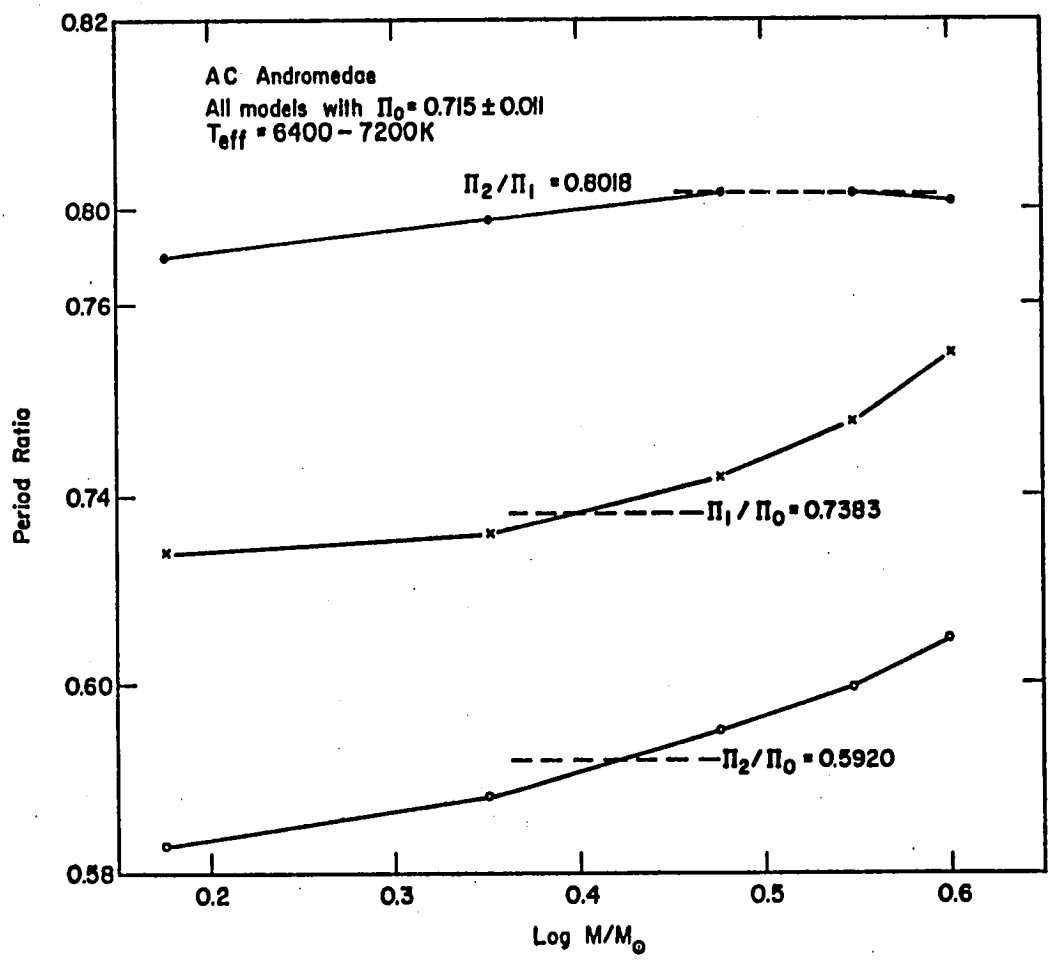

Fig. 2. Period ratios for the fundamental and first two overtones for our inhomogeneous models for AC Andromedae plotted versus log $M/M_\odot$. Luminosities range from 100-300 $L_\odot$.

30 percent or more whereas ours, using specially calculated models, is considerably smaller, assuming of course our unconventional composition structure.

As pointed out by Cox, Deupree, King, and Hodson (1977), the primary effect which leads to the correct period ratios in the inhomogeneous case is the change in the density structure of the outer envelope.

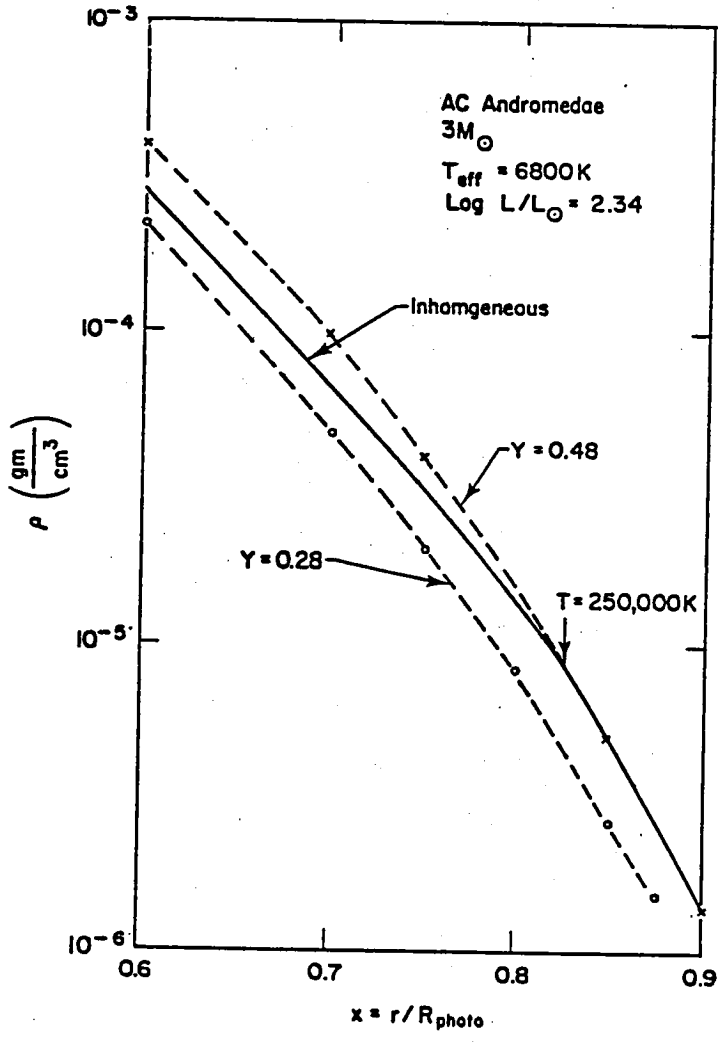

Fig. 3. Density versus fractional radius in three models for AC Andromedae. The two homogeneous models have parallel density structures and similar periods for the first three radial modes. In the inhomogeneous case, the fundamental mode feels the shallower density gradient more than the higher modes and has a larger period than for the two homogeneous cases.

Figure 3 shows the density as a function of fractional radius for a three solar mass model of AC And. This is near the derived mass as can be seen in Figure 2. Three cases are shown; two homogeneous models and the adopted inhomogeneous case. In the outer region of the star where $T \lesssim 250{,}000$ K, the density in the case for Y = 0.28 is about a factor of two less than in the helium enriched inhomogeneous model. As one approaches the base of the envelope the densities become more nearly equal, i.e. the magnitude of the density gradient is less steep in the inhomogeneous case. Since the total mass and radius of the models is the same, this leads to a less centrally condensed model and hence to a longer fundamental period. By allowing the envelope to be helium enriched into a depth of 250,000 K the periods of the first and second overtones are little affected since their eigenfunctions are large only in regions exterior to this and see roughly a homogeneous model. Table 1 confirms this for these cases. The lengthening of the fundamental period is about four percent whereas the first overtone and second overtone periods are increased by slightly more than one tenth of one percent.

TABLE 1

Ac And Models at 3 $M_\odot$, 217 $L_\odot$, T_e = 6800 K

Model Y	Π_0	Π_1	Π_2	Π_1/Π_0	Π_2/Π_0	Π_2/Π_1
.48	0.6834	0.5336	0.4287	0.781	0.627	0.804
Inhomo-geneous	0.7106	0.5277	0.4232	0.743	0.596	0.802
.28	0.6841	0.5270	0.4226	0.770	0.618	0.802

It is of some interest to briefly discuss the models that were necessary when we were attempting to explain the reported third period of TU Cas. The ratio Π_2/Π_1 would be 0.8249 whereas for most models this ratio is about 0.80, as for AC And. The only model we were able to find which would give the Faulkner(1977b) Π_2/Π_1 had normal helium (in our case actually Y = 0.35) from the surface to 80,000K, Y = 0.70 between 80,000K and 150,000K, and then Y = 0.28 to the nuclear burning region. Using this model a mass of about $4M_\odot$ was derived. This type of structure is not needed to explain any of the other Cepheids and led us to doubt the reality of the second overtone. In the absence of the third period there is no difficulty in explaining TU Cas as just another double-mode Cepheid with the high gravity of Schmidt (1974), explained by the large surface helium abundance.

IV. CONCLUSIONS

Unconventional composition structures are proposed to explain the periods of the triple mode Cepheid AC And. A strong Cepheid wind appears to enrich helium in the convection zones down to about 60,000 K or 70,000K. Then some downward partial mixing occurs to the bottom of a layer with about $1-q = 5 \times 10^{-4}$ of the stellar mass.

Petersen (1978b) has suggested that AC And may be a c-type RR Lyrae variable pulsating only in the first, second, and third overtones. Fitch and Szeidl indicate, however, a Population I composition. We have two major objections to the Petersen models. First, we find that if nonadiabatic periods are calculated instead of his adiabatic ones, the period ratios are too small by as much as 4 percent for Π_2/Π_1 and somewhat less for Π_3/Π_1 and Π_3/Π_2. This leads to an unacceptable solution for the masses given by Petersen.

Second, we find that the second and third overtones for either a Population I or II mixture are stable at all surface effective temperatures for these low masses. The rapid kinetic energy decay rates, like 25 percent per period, give the few percent difference between the adiabatic and nonadiabatic periods. At 0.6 and 1.0 $M_\odot$ the first overtone is sometimes pulsationally unstable, but not at the T_e value of 7100 K suggested by Jakate (1978). For our inhomogeneous models with more surface helium, the fundamental and first two overtones are all naturally unstable for T_e between 6400 and 7000 K.

We note that AC And is not unlike the anomalous Cepheids recently discussed by Zinn and Searle (1976) and Deupree and Hodson (1977). Masses of between one and two solar masses are suggested, however, and the population is more likely type II.

It is worthwhile noting that the double-mode Cepheids, such as U Tr A, can still be explained with our proposed enrichment below the homogeneous convection zones. A case where Y is 0.50 from the surface to 150,000 K ($1-q = 2 \times 10^{-4}$), 0.39 from there to 200,000 K, and then 0.28 to the nuclear burning core gives the proper $\Pi_1/\Pi_0 = 0.7105$ for the double-mode Cepheid U Tr A (2.57d) at about 4 $M_\odot$. Thus we do not destroy the explanation for any of the double-mode Cepheids.

The bump Cepheids, however, cannot have enrichment below the convection zones or the ratio Π_2/Π_0 and its variation [also the Hertzsprung (1926) light curve bump variation] with phase will be upset. Note that in this case the mass level of about 10^{-4} of the stellar mass is right at the bottom of the lower He II convection zone.

We finally note that some of the B stars also have helium enrichment, according to Osmer and Peterson (1973), which has been discussed by S. Vauclair (1977). The problem of stabilizing a helium enriched layer, established in B stars by downward diffusion in the presence of a stellar wind, and in Cepheids by a Cepheid wind, seems to be an important problem to be solved.

We wish to acknowledge many discussions with R. G. Deupree, A. M. Heiser, G. Michaud, and R. F. Stellingwerf.

This work was performed under the auspices of the DOE and supported in part by NSF grant AST-76-15445.

REFERENCES

Castor, J. I. 1971, Ap. J., 166, 109.

Cogan, B. C. 1970, Ap. J., 162, 139.

----------1977, Ap. J., 211, 890.

Cox, A. N. 1978 (This Conference).

Cox, A. N., Deupree, R. G., King, D. S., and Hodson, S. W. 1977, Ap. J., 214, L127.

Cox, A. N., Hodson, S. W., and King, D. S. 1978, Ap. J., 220, 000.

Cox, A. N., King, D. S., Hodson, S. W., and Henden, A. A. 1977, Ap. J., 212, 451.

Cox, A. N., Michaud, G., and Hodson, S. W. 1978, Ap. J., 222, 000.

Deupree, R. G. 1977a, Ap. J., 215, 232.

----------1977b, Ap. J., 215, 620.

Deupree, R. G. and Hodson, S. W. 1977, Ap. J., 218, 654.

Faulkner, D. J. 1977a, Ap. J., 216, 49.

---------- 1977b, Ap. J., 218, 209.

Fitch, W. S. and Szeidl, B. 1976, Ap. J., 203, 616.

Hertzsprung, E. 1926, BAN, 3, 115.

Hodson, S. W. and Cox, A. N. 1978 (This Conference).

Jakate, S. 1978, preprint.

King, D. S., Cox, A. N., and Hodson, S. W. 1977, BAAS, 9, 360.

King, D. S., Hansen, C. J., Ross, R. R., and Cox, J. P. 1975, Ap. J., 195, 467.

Kippenhahn, R. 1974, in IAU Symposium No. 66, Late Stages of Stellar Evolution, ed. R. J. Tayler (Dordrecht: Reidel), p. 20.

Lafler, J. and Kinman, T. D. 1965, Ap. J. Suppl., 11, 216.

Osmer, P. S. and Peterson, D. M. 1973, Ap. J., 187, 117.

Petersen, J. O. 1973, Astr. and Ap., 27, 84.

--------1978a, preprint.

--------1978b, preprint.

Schmidt, E. G. 1974, M.N.R.A.S., 167, 613.

Stellingwerf, R. F. 1975, Ap. J., 199, 705.

Vauclair, S. 1975, Astr. and Ap., 45, 233.

Zinn, R. and Searle, L. 1976, Ap. J., 209, 734.

Discussion

J. Wood: Could the instability be caused by a magnetic field?

King: I've no idea.

J. Wood: What's the status on magnetic fields in models? Can they be neglected?

King: They have been neglected, but whether they can be is questionable. If they are really as large as indicated, perhaps they should be included.

A. Cox: Georges Michaud, who has worked with me on helium enrichment, has great hope for magnetic fields, but I don't. However, they would have to be stronger that what you [J. Wood] measured. That's why I don't believe they will be effective.

Mullan: How do you estimate the ammount of mass loss?

King: We take the solar value scaled by the ratio of the surface areas. We don't know anything more than that. It may exceed that value.

Mullan: There was some discussion here at an IAU Colloquium on stellar winds arising in chromospheres. Wouldn't those be better values? If the supersonic point moves down into the chromosphere, large mass loss rates can occur.

King: I forget the exact values, but if you have too high a rate and lose a large amount, it is unnecessary to use inhomogeneous models to explain the anomalies.

Mullan: It amounts to not more than 10%.

King: Ten percent is not enough to explain the anomalies.

A. Cox: Let me just remark, we have no idea what the Cepheid wind is like. But it has been pointed out that if it is too strong, it will carry away the helium also. We need to have helium left.

Dependence of Red Edge on Eddy Viscosity Model Parameters

Robert G. Deupree*
Peter W. Cole

Boston University
Boston, Massachusetts

ABSTRACT

The dependence of the red edge location on the two fundamental free parameters in the eddy viscosity treatment has been extensively studied. It is found that the convective flux is rather insenitive to any reasonable or allowed value of the two free parameters of the treatment. This must be due in part to the fact that the convective flux is determined more by the properties of the hydrogen ionization region than by differences in convective structure. The changes in the effective temperature of the red edge of the RR Lyrae gap resulting from these parameter variations is quite small ($\sim$150K). This is true both because the parameter variation causes only small changes and because large changes in the convective flux are required to produce any significant change in red edge location. The possible changes found are substantially less than the $\sim$600 K required to change the predicted helium abundance mass fraction from 0.3 to 0.2.

*Consultant to Los Alamos Scientific Laboratory

INTRODUCTION

Recently, Deupree (1977b) calculated the location of the red edge for RR Lyrae variables and concluded that the color width of the instability strip was a sensitive function of the helium abundance. This property is emphasized by the fact that the color width appears to be virtually independent of any other property: mass, luminosity, opacity, and metal abundance (at least for normal Population I or II compositions). Comparison with the observed color width of the RR Lyrae gap in a number of globular clusters indicates that $Y \sim 0.3$ with little, if any, variation from cluster to cluster.

This result has come into conflict with the helium abundance implied ($Y \sim 0.15$) by the horizontal branch semiconvective models of Sweigart and Gross (1976) when used in comparing the number ratio of red giants to horizontal branch stars.

We have calculated models varying the parameters of the eddy viscosity approach in an effort to discern the limitations of the method and the resulting accuracy of the helium abundance determination. We shall discuss first the basis of the eddy viscosity concept and then the results of the parameter study.

THE EDDY VISCOSITY MODEL

Convection in stars is expected to be highly turbulent because of large length scales and low viscosities. A simplified picture is that "large scale" convective cells form and break up into progressively smaller cells until the size reaches a scale at which

the kinetic energy of the cell can be converted into heat. Our model assumes that this conversion is the sole function of suitably small scale elements. They may thus be considered to act as an effective (or eddy) viscosity on the large scale elements. Clearly, the accuracy of this assumption should depend on the dividing line between large and small scales.

The adaption of an eddy viscosity and the restriction to two spatial dimensions effectively "define" the theory of convection. As one of our colleagues has pointed out, the theory of convection is the Navier-Stokes equations. Making the calculation two-dimensional understandably results in a great savings of computer time at the expense of some degree of physical reality. Since full scale three-dimensional calculations are quite rare, it is difficult to develope a feeling for how erroneous this approximation might be in any given situation. Since even people with enormous (by astronomical standards) amounts of computer time use two-dimensional codes, one can draw conclusions about 1) the great difficulty and computer requirements of the three-dimensional problem and 2) the relative success of the two-dimensional codes in obtaining meaningful results. The mood regarding two-dimensional results of most workers in this area may perhaps be defined as cautious optimism.

Our eddy viscosity model is about the simplest possible - a one parameter model. Much more sophisiticated models have been derived, but usually at the expense of physical logic and with only mixed numerical success. The one parameter is the eddy viscosity. One other parameter that is usually included in our approach is the width of the convective cell. If the mesh is fine enough to allow the convection to chose its own width (Deupree 1975),

the resulting ratio of width to depth is always about the classical value of three to one (Spiegel 1960; Schwarzschild 1975). This is generally regarded as a artifact of the two dimensional restriction.

PARAMETER STUDY

Because of the uncertainty regarding the convective cell width selected by two-dimensional calculations, we regard both the cell width and the eddy viscosity as free parameters. For the eddy viscosity model to make sense, only roughly a factor of ten variation in the eddy viscosity coefficient (defined in Deupree [1977a]) is allowed. We have computed convective steady state models covering this range for a model with the properties of the Goddard model except that $M=6M_{\odot}$. The largest fraction of the energy transported by convection is given for various viscosity coefficients in Table 1. There is hardly any dependence of the convective flux on the eddy viscosity coefficient.

Table 1 - Eddy Viscosity Coefficient Effects

Eddy Viscosity Coefficient	Peak Convective Flux Fraction
0.5×10^{-5}	.21
1.5	.21
5.0	.17

The variation of convective flux as a function of horizontal cell width is examined in Table 2 for the 6500K RR Lyrae model discussed by Deupree (1977c). There is more variation in the convective flux with this variable, but the amount is not enormous. One might conclude that the red edge is $\lesssim$ 150K cooler than originally found if the cell width to depth ratio departs significantly from three to one. This would correspond to a decrease in the Y deduced of about 0.03.

Table 2 - Cell Width Effects

Cell Width to Depth Ratio	Peak Convective Flux Fraction
0.9	.08
3.0	.13
9.0	.09

DISCUSSION

The parameter study indicates that the variations of convective flux with eddy viscosity coefficient are small. This is not always true in other applications and probably results from the lack of boundary layers in the astrophysical problem. The variations with cell width are larger, but the change in location of the red edge can be expected to remain small as large changes in convective flux near the red edge produce only small changes in the effective temperature of the red edge. We would estimate that $Y \gtrsim .27$ in the RR Lyrae envelopes and that, with the results of Deupree *et al.* (1978) probably $Y \gtrsim .25$ for the main sequence stars in globular clusters.

REFERENCES

Deupree, R.G. 1975, Ap.J., 201, 183.

----- 1977a, Ap.J., 211, 509.

----- 1977b, Ap.J., 214, 502.

----- 1977c, Ap.J., 215, 620.

Deupree, R.G. Eoll, J.G., Hodson, S.W. and Whiteker, R.W. 1978, Publ. Astron. Soc. Pacific, 90, 53.

Schwarzschild, M. 1975, Ap.J., 195, 137.

Spiegel, E. 1960, Ap.J., 132, 716.

Sweigart, A.V. and Gross, P.G. 1976, Ap.J. Suppl., 32, 367.

Discussion

Sweigart: The value of 0.15 that you quoted for the helium abundance when semiconvection is taken into account assumes that the ratio R of horizontal-branch to red-giant-branch stars is about 1. Renzini has recently reanalyzed the observed number counts and has found R to be typically about 1.6. This larger value for R increases the helium abundance that you obtain with semiconvection to approximately 0.22 with an uncertainty of 0.04. Such a helium abundance is in agreement with the lower limit you indicated.

Cole: Yes, when this [calculation] was done the abundance was taken from Iben's formal equations, which yield the 0.15.

Sweigart: The original Iben work gave 0.3 for R = 1. When the effects of semiconvection are included in the simplest way, i.e., by just doubling the horizontal-branch lifetime, the helium abundance is reduced to roughly 0.15.

Pel: Could you comment briefly on the observed fact that the red edge seems to move toward lower temperatures as you go to higher luminosity? In other words, the instability strip seems to get wider at the longer periods.

Cole: In our calculations, the width does not depend on the luminosity. From very well determined red and blue edges of globular clusters in the galaxy, a helium abundance of 0.3 is obtained. For other places with other helium abundances, our calculations do not have any real relevance.

J. Cox: I think it is very nice that your results for the fraction of the flux carried by convection are so insensitive to the coefficient of eddy

viscosity. Are there any other parameters to which the results are insensitive?

Deupree: Essentially, there are five things that we input. Cole talked about two of them; the other three are essentially equivalent. One is the usual coefficient of artificial viscosity, and the other two are stability parameters which have the same effect as the artificial viscosity coefficient. So you do what you always do, turn them as low as you possibly can. You make them high enough to keep your program glued together, but otherwise you make them small. As long as you have them "small," then the results are insensitive to them. The two Cole talked about are the only ones in which you have any leeway at all. The fact that there are no boundary layers in the classical convection sense, really determines the fact that the results are insensitive to the eddy viscosity coefficient.

THERMAL FLICKERS: A SEMI-ANALYTICAL APPROACH

J. Perdang[†]
Institut d'Astrophysique, Université de Liège
Cointe-Ougrée, Belgium, B-4200

and

J. Robert Buchler[††]
Department of Physics and Astronomy
University of Florida, Gainesville, FL 32611

Abstract

With the purpose of enhancing our physical insight into the nature of thermal oscillations arising from a thin helium burning shell we analyze the behaviour in its "phase-plane" of a simple two-zone model which, however, contains all the relevant physics. This simple model very naturally reproduces thermal flickers and is relatively insensitive to all but two parameters.

[†]Chercheur Qualifié du FNRS

[††]Supported in part by the National Science Foundation

It has been known since the pioneering work of Schwarzschild and Härm [1] that thin helium burning shells can give rise to thermal oscillations which have been studied by a number of authors [1 - 9]. A systematic exploration of this and similar evolutionary phases has been hampered by the enormous amount of computing time which is required to follow but a few of the thermal cycles. At the same time the interplay between the zones responsible for the thermal throbs is somewhat obscured by the complexity of the evolution codes. In order to enhance our understanding of the mechanism of the oscillations we have constructed a simple two-zone model appropriate for shell helium burning and radiation conduction with a Thomson opacity. The remainder of the star merely acts to impose boundary conditions. The behaviour of this model can readily be analyzed in the two-dimensional "phase-plane" of the temperatures and one is not limited as in a multi-zone model to a linear analysis of the neighbourhood of the equilibrium point. In fact, in our model, a linear stability analysis yields two real (unstable) roots while nevertheless a stable limit cycle can exist.

The simplest stellar configuration in which thermal oscillations have been reported is that of helium stars [3] in which energy generation takes place in a narrow shell. In order to mimick this situation we consider therefore a star with an inner, inert core, a narrow, energy generating first zone (shell), a second buffer zone on top of the shell and an outer region, e.g. the atmosphere; subscripts c, 1, 2, and a refer to these various regions. The equations governing the evolution can then be written in the form (see [11] for details) if we assume radiative energy transport:

$$\frac{dT_1}{dt} = \frac{1}{c_{p1}} \{\varepsilon(T_1) - \frac{1}{\Delta m_1} [K_1 (T_1^4 - T_2^4) - K_c (T_c^4 - T_1^4)]\} \equiv F_1(T_1,T_2) \quad (1a)$$

$$\frac{dT_2}{dt} = \frac{1}{c_{p2}} \left[-\frac{T_2}{T_{2h}}\right] \frac{1}{\Delta m_2} \left[K_1(T_1^4 - T_2^4) - K_2(T_2^4 - T_a^4)\right] \equiv F_2(T_1,T_2) \qquad (1b)$$

where the coefficients $K_i = (4\pi R_i^2)^2 \, ac/(3\kappa(T)\Delta m_i)$ are connected with the radiation transport and where $\kappa(T)$ is the opacity. The other symbols have their usual meaning. The first coefficient in square brackets, $-T_2/T_{h2}$ is a hydrostatic adjustment factor:

$$T_h = (.1 \text{ to } 1.) \times \frac{GM}{Rc_p} \frac{M}{\Delta m} \qquad (2)$$

For the buffer zone $T_{h2} = 10^6 - 10^7$ K $< T_2$, whereas for the shell, in view of the smallness of $\Delta m_1/M$, we have $T_{h1} >> T_1$ and hydrostatic adjustment can be neglected. For the energy generation the expression appropriate for the triple-alpha reaction is given by

$$\varepsilon(T) = \zeta T^{-3} e^{-Q/T} \equiv \zeta T^{\nu(T)} \qquad (3)$$

where ζ and Q are constants. At the temperatures and densities of interest the opacity is due to Thomson scattering and is constant (in contrast to the model of [10]). In this simplified model the radii are assumed time-independent, so that the K_i become constants. The buffer zone is energetically inert and can only act as a reservoir of heat fed by radiation conduction. The effect of the core appears through its temperature T_c, assumed constant, and similarly the atmosphere is held at a constant temperature T_a. (It turns out that the model is highly insensitive to the values of T_c and T_a.)

We now analyze the conditions under which these equations (1) allow a limit cycle (LC) oscillation. The equilibrium curves (EC), $F_1(T_1,T_2) = 0$ for the shell (EC1) and $F_2(T_1,T_2) = 0$ for the buffer zone (EC2) are exhibited in the figure. If the EC1 has an S-shape as shown, it is clear that the fold points A and B are points of exchange of stability; if the function F_1 is positive to the right of EC1, as it turns out to be, the lower and upper branches are both stable, whereas the arc AB is unstable. The criterion for

the existence of a fold point (A) is (similarly to [1]) that

$$(T_1^4 - T_2^4) \,/\, T_1^4 > 4/\nu(T_1) \qquad (4)$$

while a second fold point (B) exists provided that $\nu(T_1)$ drops below 4 at higher T_1. These two conditions then guarantee the existence of an S-shaped EC. The EC for the second zone is monotonic. The hydrostatic adjustment factor is vital in making it unstable (F_2 is positive to the right of EC2). We assume now that EC1 and EC2 intersect at a point P located on the unstable branch AB of EC1, which point P is therefore an unstable equilibrium point.

Turning to a discussion of the existence of a stable oscillation, we first assume for the sake of argument that the ratio χ of the order of magnitudes of F_1 and F_2 is very large. A stable LC then occurs when the following two conditions are satisfied: First, both F_1 and F_2 are positive to the right of their respective EC, and P is on the unstable arc AB; only for this one among four sign combinations can there exist a stable LC; secondly, there is no other equilibrium point (like Q on the figure) inside the curve AB'BA'. This curve then represents the resulting relaxation oscillation. For arbitrary values of χ, no simple criterion for the existence of a stable LC can be formulated, but it is obvious that a LC still exists under condition (1) provided the other possible equilibrium points (like Q) are sufficiently far from the fold points.

It is interesting to note that a linear stability analysis in the neighbourhood of the equilibrium point P yields purely real eigen-values

$$\lambda_1 = \frac{4K_1}{c_{p1}\Delta m_1} \, S \, T_1^3 \quad + O(\chi^{-1}) \qquad (5a)$$

$$\lambda_2 = \frac{4K_1}{c_{p2}\Delta m_2} \quad T_2^3 \; \frac{T_2}{T_{h2}} \; (1 + \gamma + \frac{1}{\zeta}) \; + O(\chi^{-1})$$

where $\zeta = \frac{\nu}{4} \frac{T_1^4 - T_2^4}{T_1^4} - 1$, (5b)

and where we have neglected the small contributions of K_c and T_a.

Equations (5) of course also show that P is an unstable node point (λ_1 and $\lambda_2 > 0$). As the parameter $\gamma \equiv K_2/K_1$ is lowered, the point P moves south beyond A, becoming first a saddle point ($\lambda_1 < 0$, $\lambda_2 > 0$) and soon afterwards a stable node (λ_1 and $\lambda_2 < 0$).

The existence of an oscillation is in this model clearly the result of non-linearity. This can nicely be exhibited by an inspection of the "velocity" field $\underline{v} \equiv (\frac{dT_1}{dt}, \frac{dT_2}{dt}) = (F_1, F_2)$ in the two-dimensional "phase-plane" (T_1, T_2).

In the figure we show the trajectory of the oscillation in the temperature "phase-plane". The physical parameters have been chosen to be: $Q = 26$ (hence all temperatures in units of 1.66×10^8K), $T_c = 6$, $T_a = 0.5$, $K_c/K_1 = 10^{-4}$, $\Delta m_2 c_{p2} T_{h2} = 1$, $\zeta \Delta m_1/K_1 = 10^7$, $\gamma = 4$ and $\chi \equiv K_1/(c_{p1}\Delta m_1) =$ 50 and 500. The point P falls on the unstable branch AB and oscillations exist for values of γ in the range (1,8). The innermost cycle (AA'BB') corresponds to a relaxation oscillation ($\chi >> 1$). The middle and outer cycles correspond to $\chi = 500$ and $\chi = 50$ respectively. For smaller values of χ, e.g. $\chi = 5$ already, this limit cycle disappears because of the influence of the saddle point located at Q. For large χ, $\lambda_2 << \lambda_1$ and the order of magnitude of the period of the relaxation oscillation is given by $1/\lambda_2$. As χ is lowered the excursion into the nonlinear regime increases and the period lengthens. The profiles of the temperatures as a function of time are very similar to those found by Rose

Schwarzschild and Harm [2] have attributed the thermal oscillations to the interaction between the shell and the underlying zone; they reach this conclusion on the basis of a linear stability analysis in which the entropy eigen-functions exhibit a 90° phase difference between the shell and the

zones below. Their argument, however, does not hold in general even for linear oscillations (except e.g. for mechanical oscillators when represented by the velocity and position). This criticism does not exclude, though, the possibility of such an interplay between shell and underlying zones; we, however, have not succeeded in reproducing such oscillations with a two-zone model unless we include additional physical effects, like neutrino losses, in the bottom zone and the model becomes rather contrived.

In conclusion one has a fair amount of confidence that our model, because of both its insensitivity to most of the parameters involved and its physical simplicity, is representative of the thermal oscillations as reported in helium burning shells; in addition, the physical parameters of the model, needed to obtain the oscillations, take on quite reasonable values. Our geometric approach of representing the oscillators in a phase-portrait is quite general and one hopes that it may prove useful in the search for similar oscillatory phases in different burning stages.

We gratefully acknowledge the support of the National Science Foundation (grant numbers AST 75-05012 and AST 77-17572). One of us (JRB) also thanks the Government of Luxembourg for a grant and the other of us (JP) the Belgian FNRS for travel support.

References

1) Schwarzschild, M. and Härm, R., 1965, Ap. J. 142, 855; 1967, Ap. J. 150, 961.

2) Härm, R. and Schwarzschild, M., 1972, Ap. J. 172, 403.

3) Rose, W. K., 1966, Ap. J. 146, 838.

4) Weigert, A., 1966, Zs. 7. Ap., 64, 395.

5) Sweigart, A. V., 1971, Ap. J. 168, 79; 1973, Ad Ap 24, 459.

6) Faulkner, D. J. and Wood, P. R., 1972, Ap. J. 178, 207.

7) Christy-Sackmann, I. J. and Paczynski, B. E., 1975, Mém. Soc. Roy. Sci. Liége, 6e sér., 8, 335.

8) Iben, I., Jr., 1975, Ap. J. 196, 525, and 549; 1976, Ap. J. 208, 165.

9) Sugimoto, D. and Nomoto, K., 1975, Publ. Astron. Soc. Jap. 27, 197.

10) Defouw, R. J., 1973, Ap. J. 183, 215.

11) Buchler, J. R. and Perdang, J., 1978, "Thermal Relaxation Oscillations in a Two Zone Model", Ap. J. (submitted).

12) Henyey, L. G. and Ulrich, R. K., 1972, Ap. J. 173, 109.

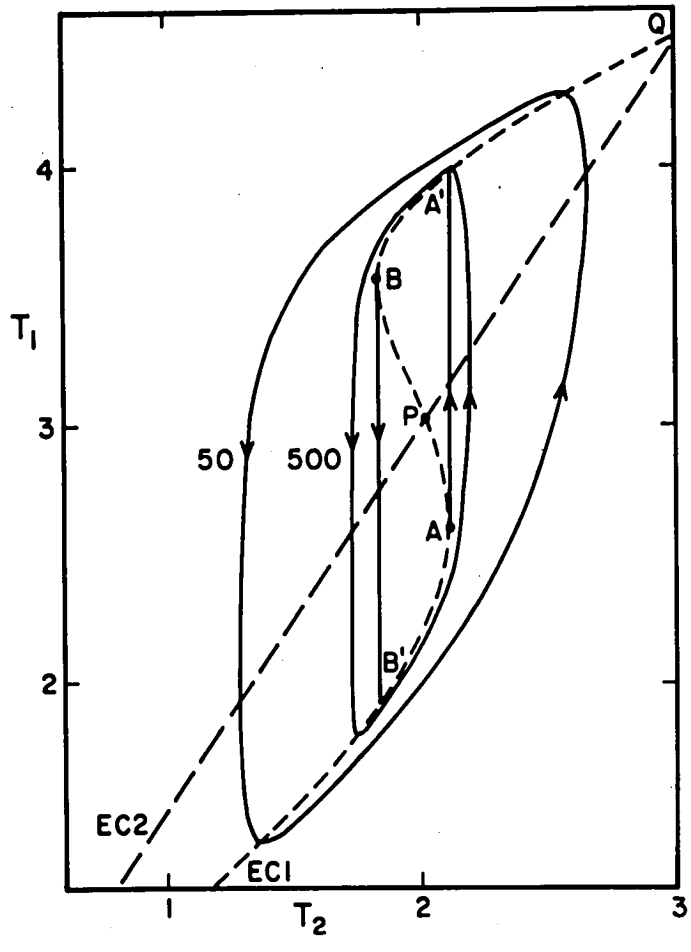

Equilibrium curves (dashed lines) for the two zones in the temperature phase plane and trajectories of the oscillation for various values of χ: inner curve, relaxation oscillation, $\chi \gg 1$, middle curve, $\chi=500$ and outer curve, $\chi=50$.

Discussion

Adams: Can you relate the time between the pulses to the shell parameters?

Buchler: The numerical quantities we used were all scaled. It is difficult to relate them to actual physical numbers unless one determines what masses and radii to put in. It is uncertain what to use for the buffer zone mass.

Sweigart: Have you made any attempt to look at the stability of the hydrogen-burning shell in the subgiant branch phase of globular cluster stars?

Buchler: We have not applied it to anything like that.

Baker: Do you find the oscillations to be strictly periodic for all values of the parameters which you used?

Buchler: The abundances don't change, so it has to be periodic.

Baker: Could it be an aperiodic oscillator?

Buchler: We have not found any evidence of that. The relaxation oscillation is certainly strictly periodic. The three we have considered here are periodic. Rose, who only considered the helium burning shell, found very periodic oscillations. Schwarzschild and Harm found that the oscillation decayed, disappeared, and returned later. We're speculating on what may happen. Some of the parameters we kept constant may vary, so we need a three- or four-zone model because it is really the coupling of two different types of oscillations. So a zone may expand and relax, which is a regime of oscillation.

Rotation, Convection, and Cepheid Mass Determinations

Robert G. Deupree
Boston University
Boston, Massachusetts

ABSTRACT

Solid body rotation has been included in a two-dimenstional hydrodynamic code to study its effects on periods and period ratios in pulsating stars. Both the fundamental and first overtone pulsation periods are slightly increased by reasonable rotation rates. The ratio of the first overtone to fundamental period increases very slightly with the addition of rotation. It does not appear possible to change either the "pulsation" mass on the "double mode" mass to any significant extent using rotation.

Several nonlinear models using the Deupree (1977a) two dimensional approach to convection were compared with the same models computed omitting convection in an effort to assess the effects of convection on the bumps in Cepheid velocity curves. The results indicate that convection plays little role in enhancing the production, or altering, of bumps in the velocity curve.

ROTATION

Solid body rotation has been included in pulsation calculations using a two-dimensional hydrodynamics code developed some time ago by Deupree (1974). The initial model was taken to be an n=3 rotating polytrope (equatorial surface rotational velocities up to 10 km/s) whose structure was taken from the functions

tabulated by Chandrasekhar and Lebovitz (1962). The initial velocity distribution is taken from the linear eigenfunction for a nonrotating polytrope. We assume a γ law gas equation of state and include twenty angular zones in the calculation. The fundamental mode period increases approximately linearly with surface equatorial velocity, as predicted by linear theory (Clement 1965). The first overtone period, however, also increases in such a way that the period ratio Π_1/Π_0 appears to increase by about 0.25% per 5 km/s of rotation. While this number is quite uncertain, there is no reason to believe that rotation can produce the approximately factor of ten larger percentage change (in the other direction) required to remove the very low masses predicted for double mode Cepheids.

CONVECTION

We have computed several Cepheid models in which bumps occur in the velocity curve twice: once allowing only (diffusion approximation) radiation as the sole mode of energy transport and once in which convection is allowed according to the two dimensional approach outlined by Deupree (1976, 1977a). One result is that convection penetrates no more deeply in a Cepheid envelope than it did in an RR Lyrae envelope. Hence, based on the results of Deupree (1977b), one should not expect the inclusion of convection in Cepheid models to alter their period ratios appreciably.

By comparing the models that include convection with those that do not, we can gauge the effects of convection on the existence and location of the bump on the velocity curve. The models considered

had the parameters of the Goddard model except that we considered masses of $4.8M_\odot$ and $5.5M_\odot$, as well as the traditional $4.0M_\odot$. There was some evidence in these models that convection slightly enhanced the bump, but not to any great extent. It did not appear to produce bumps when the radiative models did not show them, nor did it change the bump phase.

DISCUSSION

From these two-dimensional calculations we find it very difficult to expect either rotation or convection to change periods, period ratios, or other characteristics of classical Cepheids to remove any of the mass determination difficulties. It is possible that the small number of models we considered could affect this result. For rotation, this would be hard to accept because the effects were so small. The convective models are somewhat less general, and one must admit that there may be cases in which convection may play some role. However, one should probably not expect convection to be much assistance in the general problem of bump masses.

REFERENCES

Chandrasekhar, S. and Lebovitz, N.R. 1962, Ap.J., 136, 1082.

Clement, M.J. 1965, Ap.J., 141, 210.

Deupree, R.G. 1974, Ap.J., 194, 393.

------ 1976, Los Alamos Scientific Laboratory Report, LA-6383.

------ 1977a, Ap.J., 211, 509.

----- 1977b, Ap.J., 215, 232.

Discussion

A. Cox: Do you have any evidence that the Cepheid red edge is related to the helium content?

Deupree: At the moment, the answer is no, because I've only done a few models. I have done some steady-state models using different helium abundances, and it looks like the effect is going to be there in the sense that as you put in more helium, you change the convective flux a little bit. One expects that the red edge probably won't change very much and the blue edge will. It will then work basically the same way as the RR Lyrae stars did.

Recent Theoretical Work on Cepheids and Other Types of Variables

John P. Cox

Joint Institute for Laboratory Astrophysics
University of Colorado and National Bureau of Standards

ABSTRACT

Some important problems in the theory of Cepheids and of other types of variables are pointed out. Three of these are: (1) large-amplitude mode behavior, (2) convection, and (3) Cepheid masses, which must essentially always be inferred indirectly. Of the several types of indirect mass which can be defined, the inferred masses of the "beat (or double-mode) Cepheids," seem to be smaller than one expects, for this period range, by factors of 2-3. For the nonbeat Cepheids, the indirect masses also appear to be low, as compared with conventional stellar evolution theory, but by a smaller amount, say some 20-40 percent. Some conceivable ways of explaining these mass discrepancies are discussed. In particular, if the beat Cepheid masses, as usually inferred, are spuriously low (as appears likely), then two kinds of resolution appear possible: (1) accept pulsation theory, but question the assumed stellar envelope structure; (2) accept the conventional envelope structure, but question pulsation theory. In line with (2), we ask: is it possible that the apparently predominantly radial pulsations of the beat Cepheids could be contaminated with a small admixture of nonradial pulsations, so that the use of purely radial pulsation theory may not be applicable to the beat Cepheids? Some other conjectures which may bear on ordinary or beat Cepheids are offered.

I. INTRODUCTION

Despite the title, this paper will be a review of recent theoretical work on, primarily, classical Cepheids, although some things that are said may apply to related types of variables, such as RR Lyrae variables. We shall not discuss in detail the "line profile variable B stars" (Smith 1977), for which the obvious unsolved problem is the cause of the observed variations; the variable DA white dwarfs (the "ZZ Ceti stars," e.g., McGraw, 1977; Robinson, Nather, and McGraw 1976); nor the oscillations observed at some phases in the cataclysmic variables (e.g., Patterson, Robinson, and Nather 1977).

The observational properties of classical Cepheids have been well summarized in the past, and so will not be dealt with in detail here (see, e.g., Cox 1974; Pel 1978; and the excellent summary paper in this conference by Pel). Suffice it to say here that they are relatively cool (effective temperatures ~5000-7000°K), luminous (a few hundred to 10^4-10^5 solar luminosities) stars whose light output varies periodically with periods $\sim 1^d$ to 50^d or 100^d.

The classical Cepheids are believed to be predominantly radial pulsators. The mechanism of excitation of the pulsations is now also reasonably well understood as due to "envelope ionization mechanisms" (especially He^+). These stars are thought to be in the core helium burning phase, on a "blue loop" just after core helium ignition in the red giant

phase. This "blue loop" has intersected the "Cepheid instability strip," so that these stars will be Cepheids as long as they are in the instability strip. The blue edge of the instability strip is well defined theoretically, and agrees reasonably well with observations (e.g., Iben and Tuggle 1975). The red edge, being determined, most likely, by convection, is more of a problem theoretically, and will be discussed in more detail in §II.

In recent years a few (eleven, according to Stobie 1977) "beat Cepheids," with two or more periods (the longer period lying between about 1 and 7 days) superposed, have been discovered. Since the longer period is only 1 to 7 days, the beat Cepheids would occupy the lower portions of the instability strip. As Stobie (1977), Petersen (1973, 1978), and others have pointed out, these variables provide us with a new way of determining Cepheid masses. These mass values as determined in this way present us with further problems which will be discussed in §III.

As seen by this reviewer, there are at least three remaining outstanding theoretical problems of Cepheids. These problems are: (1) the large-amplitude mode behavior, (2) convective transfer, and (3) Cepheid masses.

These problems, as well as perhaps others, will be discussed in §II. In §III we shall review what is perhaps the most controversial and most talked-about difficulty, that of Cepheid masses. We shall present some conjectures in §IV. The purpose of these conjectures is to offer possible clues to the eventual solution or alleviation of some of the above problems.

II. SOME IMPORTANT PROBLEMS IN CEPHEID THEORY

The three main problems in Cepheid theory (in the opinion of this reviewer) referred to in §I, i.e., (1) the large-amplitude mode behavior, (2) convection, and (3) Cepheid masses, will be discussed in turn in the following subsections.

A. Large-Amplitude Mode Behavior

It would be desirable to know the answer to the following question: Suppose a star or stellar model is found by means of a linear theory to be unstable in two or more pulsation modes. Then, at large amplitudes, where nonlinear effects are important, which one (or ones) of the above unstable modes will be present? Thus, for example, in the case of the beat Cepheids, are the two periods that are observed (representing, presumably, two pulsation modes) a permanent feature of these stars, or are they in the process of switching modes?

Opinions seem to be divided on this point. Thus, according to Stobie (1977), there has been no evidence for a change in amplitude observed for the beat Cepheids over at least a 50-year time span. Theoretical evidence derived by Stellingwerf (1975a) indicates a switching time of some 80 years. In fact, Faulkner (1977a) suggests that any amplitude changes, if they exist, should be detectable within a few more years. On the other hand, Takeuti (1973) has suggested that the beat Cepheids may be in the process of mode switching (a view also espoused by Stobie 1970 and Rodgers 1970; see also Cox, Hodson, and Davey 1976).

In the early days of nonlinear calculations of pulsating stars (e.g., Christy 1964, 1966a,b; Cox, Brownlee, and Eilers 1966; Cox, Cox, Olsen, King, and Eilers 1966) the first question posed above was answered

(hopefully!) by the "brute force" method of long computer runs, in which the model is followed in time from given initial values through hundreds or thousands of pulsation periods. This method is obviously inelegant, and it is also possibly subject to accumulation of rounding errors and other numerical problems.

Attempts to improve on the above method were initiated by Baker and collaborators (e.g., Baker 1970, 1973; Baker and von Sengbusch 1969). They sought periodic solutions of the nonlinear equations of hydrodynamics and heat flow. Their method was reasonably successful, and also yielded information on the modal stability, i.e., on the stability of a given nonlinear mode against switching to some other mode.

A new method was originated by Stellingwerf (1974a,b), in which the above initial-value techniques and the seeking of periodic solutions of the nonlinear equations were combined. This method also appeared to be successful, and was applied to the problems of the modal behavior of RR Lyrae variables, with applications to beat Cepheids (Stellingwerf 1975a,b). The method was subsequently adapted to and applied to another hydrodynamic pulsation code by Cox, Hodson, and Davey (1976). Again, modal stability information was obtained.

However, the modal stability information as obtained above does not seem to agree, at least in the several cases that have been investigated, with the results of extended nonlinear, initial-value calculations (e.g., King, Cox, Eilers, and Cox 1975; Cox and Cox 1976; Hodson and Cox 1976). For example, one model studied by Stellingwerf (1975a) (his model 2.6) showed, according to the modal stability analysis, instability of the fundamental mode to a switch-over to the first overtone, and at the same time instability of the first overtone mode to a switch-over to the

fundamental mode. (However, in a subsequent calculation different stability results were obtained; see Stellingwerf 1976). Double-mode behavior, i.e., a fairly permanent mixture of these two pulsation modes, seems to be implied by these results. Yet this same model (or at least a slightly different numerical version of it) showed only pure fundamental or pure first overtone mode behavior when examined by initial-value techniques (Cox, Hodson, and King 1978), in apparent disagreement with Stellingwerf (1975a).

As another example, consider the $6\ M_\odot$ ($M_\odot$ = solar mass) Cepheid model which was computed using the initial-value techniques by King, Cox, Eilers, and Davey (1973). This model was found by the above authors to be slowly switching modes from the fundamental to the first overtone. This model was further investigated by Cox, Hodson, and King (1978), who found, also using initial-value techniques, that it eventually actually switched to the first overtone. Yet the modal stability analysis, when applied to this model, showed the fundamental mode to be stable against switch-over to the first overtone mode! The above stability analysis also yielded the periodic fundamental mode, whose amplitude was considerably larger than the amplitude of the corresponding mode in the initial-value calculations of King, Cox, Eilers, and Davey (1973). This apparent discrepancy between the results of the modal stability analysis technique and those of the initial-value technique were, in fact, attributed by Cox, Hodson, and King (1978) to this difference in amplitude. Presumably, a larger-amplitude fundamental mode would have been found, using the initial-value approach, to remain more or less permanently in this mode in this model.

Why does this discrepancy exist? More importantly, why has it not been possible to get multiple mode behavior in initial-value type pulsation calculations, in spite of the fact that this kind of behavior may occur

in real stars? It appears to this reviewer that these questions have not yet been satisfactorily answered, at least in the published literature.

B. Convection

Here we shall once again repeat the oft-made statement that what is desperately needed for the theoretical study of pulsating stars, is a reliable and (hopefully!) usable time-dependent theory of convective transfer. Considerable efforts have been made, and some tangible results obtained, about stellar convection in general, by Toomre, Spiegel, and collaborators (Latour, Spiegel, Toomre, and Zahn 1976; Toomre, Zahn, Latour, and Spiegel 1976).

An attempt to come to grips with the problems of convective transfer in pulsating stars has recently been made by Deupree in a series of papers (Deupree 1975a,b; 1976a,b,c; 1977a,b,c,d). This work represents perhaps the most ambitious attempt so far in this direction, and has given us, for the first time, perhaps some idea as to how pulsation is "throttled" by convection at the red edge of the instability strip (see below). Although these calculations are almost certainly not definitive, and although questions may legimately be raised about some of Deupree's assumptions, and also about how well his results actually mimic convection in real stars, still it must be admitted that his results are suggestive, and perhaps even, essentially, physically correct. They are certainly the most far-reaching obtained so far.

Deupree actually solved the equations of mass, momentum, and energy conservation in time and in two spatial dimensions in a convectively unstable region. Because of computer time limitations, he could follow only the motion of the largest "eddies." He treated the break-up of these

large eddies into smaller ones and the subsequent turbulent cascade which eventually shows up as heat, by the introduction of an "eddy viscosity" coefficient. Perhaps the most serious of Deupree's assumptions is that convection can be adequately treated with two (as compared to three in nature) spatial dimensions. While his results may nevertheless be qualitatively correct, this may still be a serious assumption.

However, if we accept Deupree's results at face value, we have a theoretical calculation of the red edge of the instability strip, at least for RR Lyrae variables, and presumably also for Cepheids, not based on any kind of phenomenological theory such as a mixing-length theory of convection (however, Baker and Gough 1967 computed a red edge on the basis of the quasiadiabatic approximation in linear theory and of a variant of mixing-length theory). Moreover, Deupree's calculated red edge is in reasonable agreement with observations. The dependence of this red edge on various factors, such as luminosity, composition, and overtone pulsations, has been examined by Deupree (1977a,b,c).

From the above work the following physical picture emerges as to how convection may "throttle" instability at the red edge of the instability strip. Deupree finds that the convective heat flux is greatest at about the instant of maximum compression (near minimum stellar radius) of the convective regions. Thus, convection causes the energy which has been "dammed up" by the operation of the kappa and gamma mechanisms in the He^+ ionization zone, to "leak out" at this phase. Thus, the driving effects of the ionization zone(s) are essentially "undone" by the convection. According to Deupree, only a small amount of convection in the relevant regions (say with the convective flux amounting to only a few percent of the total flux) is needed effectively to "throttle" pulsations on the red side of the instability strip.

This picture certainly seems plausible, and, as Deupree (1977a) points out essentially on grounds of overall reasonableness, the picture is not likely to be fundamentally incorrect in any important respect. Nevertheless, one must bear in mind that the picture is based on a much simplified, two-dimensional treatment of convection, although the computational complications are still horrendous. Whether this picture will be modified appreciably by a more elaborate treatment of convection remains an open question, to be answered (presumably) in the future.

C. Cepheid Masses

As this subject will be discussed in some detail in §III, we simply refer the interested reader to that section.

III. CEPHEID MASSES

It is well known that no Cepheid is a member of a binary system whose stars are close enough together to admit of a reliable mass determination (the relevant empirical information has been summarized by Latyshev 1969 and Abt 1959). Therefore, one is forced to resort to indirect methods of mass determination for the Cepheids. (However, it is pointed out by Pel 1978 that perhaps a fourth of all Cepheids are members of binaries, and that the companions are usually unseen. He correctly states that this frequent binary membership might have a significant effect on some of these indirect methods of mass determination.) These we shall discuss in this section.

These indirect methods of Cepheid mass determination have been discussed very thoroughly in the paper at this conference by A. N. Cox

(see also Cox 1978b). We shall therefore only summarize some of this information, together with some brief discussion, in §IIIA. Then, we shall discuss these results further in §IIIB.

A. Types of Masses

As stated by A. Cox (see also Cox, Deupree, King, and Hodson 1977), there are (at least) some six kinds of these indirect masses, denoted by M_{evol}, M_T, M_Q, M_W, M_{bump}, and M_{beat}. These are defined as follows.

M_{evol}: This is the mass, for given mean or equilibrium luminosity L, while the star is in the Cepheid region of the Hertzsprung-Russell diagram, as computed from conventional stellar evolution theory. One generally assumes that the observed Cepheids are undergoing the second crossing of the instability strip after having left the main sequence, on a "blue loop." This second crossing is normally considerably slower than any other crossing, because the star derives most of its energy in this phase from core helium burning (but there is also a hydrogen-burning shell in this phase; see, e.g., Iben 1967), and is thus nearly in thermal equilibrium. The relation between mass M and L during this core-helium burning phase is given as ($L_\odot$ and $M_\odot$ denote solar luminosity and mass, respectively)

$$\log(L/L_\odot) = 3.48 \log(M/M_\odot) + 0.68 \qquad (1)$$

(King, Hansen, Ross, and Cox 1975) or as

$$\log(L/L_\odot) = 3.1 + 4[\log(M/M_\odot) - 0.7] - 4(X - 0.7) - 12(Z - 0.02) \qquad (2)$$

(Iben 1974), where X and Z are, respectively, the mass fractions of hydrogen and "metals." Equation (1) is purportedly accurate to within a

factor of about two in $L/L_\odot$ (King, Cox, Eilers, and Davey 1973). This uncertainty includes uncertainties in chemical composition, which crossing of the instability strip is involved, etc. For $X = 0.7$ and $Z = 0.02$, equations (1) and (2) agree in $(L/L_\odot)$ to within better than a factor of two for $2 \lesssim (M/M_\odot) \lesssim 15$. The formula given by Becker, Iben, and Tuggle (1977) agrees with equation (2) to about the same accuracy for X and Z close to the above values.

Despite the above formulae, one should bear in mind that these "evolutionary masses," for given luminosity, are themselves rather uncertain, perhaps by some 20-30 percent. The main reason is that they depend on the rather poorly known composition (mostly helium). Also, one should realize that these stars are in a rather advanced (beyond the main sequence) evolutionary phase, and that the uncertainties in computations of stellar evolution increase with increasing evolution away from the main sequence. In particular, the exact causes of the occurrence of the loops are not really known. These loops have been discussed at some length in the literature (e.g., Hofmeister 1967; Schlesinger 1969; Hallgren and Cox 1970; Paczyński 1970; Robertson 1971a,b, 1972; Lauterborn, Refsdal, and Roth 1971; Lauterborn, Refsdal, and Weigert 1971; Lauterborn, Refsdel, and Stabell 1972; Fricke and Strittmatter 1972; Lauterborn and Siquig 1974a,b,c, 1976; Flower 1976; Durand, Eoll, and Schlesinger 1976; Schlesinger 1977), and they are generally thought to show some correlation with the details of the hydrogen abundance profile in the shell-burning region. These precautionary remarks are perhaps even more worth bearing in mind, since it is not so certain that even the sun is well understood -- witness the "solar neutrino problem" (e.g., Bahcall 1977 and references therein). Also, one should beware of certain complicating factors, such as secular

instabilities during these relatively late evolutionary phases (see Hansen 1978 and references therein), and possibly also differential rotation (Wiita 1978).

M_T: This mass was defined by Cox, Deupree, King, and Hodson (1977), and is obtained as follows. One assumes an L-M relation, such as in equations (1) or (2), based on conventional stellar evolution theory; a period-mean density relation which is a relation involving mostly Π (period), M, and R (radius), for a given assumed mode of pulsation; and the defining relation connecting L, R, and T_e (effective temperature). With five quantitites, i.e., L, M, R, Π, and T_e; and three relations; specification of some <u>two</u> will then determine the rest. Cox, Deupree, King, and Hodson (1977) use an empirical value of Π for a given star, and <u>assume</u> a value of T_e such that the star is in the instability strip. Thus, the remaining parameters are determined. Masses obtained in this way are called "theoretical masses," and are denoted by M_T. This mass should be close to M_{evol}, because the underlying assumptions are essentially the same; the near equality of these two kinds of mass has, in fact, been shown by Cox (1978b).

A mass somewhat similar to M_T may be inferred from Cogan's (1978) work. He assumes the above relations, plus an additional one, namely the relation among, say, L, M, and R along the center of the instability strip or its blue edge. With one additional relation among the same five quantities, only one quantity, for example, the observed period Π, need be specified. Thus, the mass introduced by Cogan (1978) differs from M_T only in that the T_e as used in Cogan's mass is such that the star is <u>guaranteed</u> to be in the instability strip, whereas in M_T the value of T_e is chosen in such a way that the star <u>should</u> be in the instability strip.

In the following we shall not distinguish between M_{evol} and M_T, and shall only speak of M_{evol}.

M_Q: This mass, sometimes called the "pulsation mass," is obtained as follows. One somehow obtains the average absolute visual magnitude, say $\langle V \rangle$, and the average color, say $\langle B \rangle - \langle V \rangle$, for the star, where both quantities are assumed to have been corrected for reddening and extinction. For example, for the thirteen Cepheids in galactic clusters (see, e.g., Cogan 1970), one gets these quantities fairly directly. Otherwise, say for "field" Cepheids, one may use a "period-luminosity-color" (PLC) relation (e.g., Sandage and Tamman 1969, 1971). At any rate, given $\langle V \rangle$ and $\langle B \rangle - \langle V \rangle$, one may then apply a bolometric correction to get the mean luminosity L, and an adopted color-effective temperature (T_e) relation to get a corresponding mean value of T_e. The mean radius R then follows from the defining relation connecting L, R, and T_e ($L \propto R^2 T_e^4$).

One then assumes a certain (radial) pulsation mode. As shown by Cogan (1970) and by Cox, King, and Stellingwerf (1972), the pulsation period Π of a star in a given mode is determined mostly by M and R. Hence, given Π from observations as determined, for example, above, one can now compute, for a given assumed pulsation mode, M, the "pulsation mass" (denoted above as M_Q). Results as found by Cogan (1970) yielded $M_Q/M_{evol} \approx 0.7 - 0.8$ (similar results were reported by Stobie 1974).

However, as pointed out by Cox, King, and Stellingwerf (1972) and others, M_Q is quite sensitive to R (roughly, $M_Q \propto R^3$). Thus, a 10 percent uncertainty in R, for example, will appear as approximately a 30 percent uncertainty in M_Q. The value of R is, in turn, fairly sensitive to the assumed color-effective temperature relation, the distance scale, and the reddenings adopted. As shown by King, Hansen, Ross, and Cox (1975),

the color-effective temperature relation needed to make $M_Q \approx M_{evol}$ results in lower effective temperatures, for given color, by some 300°K to 600°K, than are given by the relation of Schmidt (1972). This needed relation is close to others that have been proposed (e.g., Böhm-Vitense 1972; van Paradijs 1973; Flower 1977). It is interesting to note that the solution favored by Iben and Tuggle (1972a,b) is based on an increase in the above value of R by virtue of an assumed slightly increased distance, and hence luminosity L (corresponding to a 0.3 magnitude increase in L) of the Cepheids (since, for given color [T_e], $L \propto R^2$).

It has been pointed out by A. Cox (1978b) that the new Hanson (1975, 1977) Hyades distance scale (implying an increase in stellar luminosities by $\sim 0^m.27$) and the lower effective temperatures inferred from the data of Pel (1978) both conspire to yield larger radii than previously thought. A. Cox (1978b) points out that with these larger values of R, the ratio M_Q/M_{evol} is now sometimes larger, sometimes smaller, than unity and that this ratio differs from unity by only some 10-20 percent or less.

M_W: This mass, the "Wesselink mass," discussed extensively by A. Cox (1978b), is obtained as follows. One first obtains the "Wesselink radius," which we shall denote simply by R. As is well known, the method originally devised by Baade (1926) and Wesselink (1946, 1947) is based on the assumption that the total radiant power, say L_ν, emitted by a star in a given spectral region depends only on the color of the star and on its radius (in particular, $L_\nu \propto R^2$). Thus, measurements of L_ν at two phases of equal color give a measure of the ratio of the radii of the star at these two phases. Measurements of the radial velocity of the star at these two phases, and integration of the velocity curve, give one also the difference in radii at these two phases. From the ratio and the difference of the two

radii, one can thus solve for the actual radius values at these two phases. Repeating this procedure around a pulsation cycle, and averaging over the cycle, gives one a value of R. Some of the difficulties in getting R in this manner have been discussed by, for example, Parsons (1972), Karp (1975), Cox and Davis (1975), and Evans (1976).

Once R is known, the procedure for obtaining M_W is exactly the same as in obtaining M_Q from R, as explained above. This procedure involves assuming a certain pulsation mode for the star. Also, just as in the case of M_Q, any uncertainty in R is magnified quite considerably in M_W. As pointed out by A. Cox (see also Cox 1978b), the results show a rather large scatter for M_W. Nevertheless, straight averages give M_W/M_{evol} close to 0.7 - 0.8. The possible significance of these results will be discussed in §IIIB below.

M_{bump}: As indicated originally by Christy (1966b) and Stobie (1969), M_{bump} is the mass required for the nonlinear pulsation calculations to yield a secondary bump on the descending portion of the velocity curve in the period range $\sim 7^d$-10^d, where a corresponding secondary bump usually shows up on the descending portion of observed light curves of Cepheids (the "Hertzsprung relation"; see, e.g., Payne-Gaposchkin 1951, 1961; Payne-Gaposchkin and Gaposchkin 1966; Cox 1974). (It is usually assumed that the phasings of the secondary bump on the relatively easily observed light curve and on the relatively reliably computed velocity curve are the same. This assumption has been discussed by Stobie 1976, who presents empirical results for six Cepheids. He finds that the phasing of the secondary bump on the descending portion of the velocity curve is always about $1^d.3$ later than on the descending portion of the light curve.) Results found by Christy (1966b) and by Stobie (1969) gave

$M_{bump}/M_{evol} \sim 0.4 - 0.6$ (see also Stobie 1974). Similar results have been found by other workers (summarized in Fischel and Sparks 1974).

However, these results are based, for the most part, on a comparison of two different things -- observed light curves and computed velocity curves. It seems to this reviewer that only a comparison of similar things, for example, observed and computed light curves, will yield really reliable and trustworthy results regarding M_{bump}/M_{evol}.

Computations of Cepheid light curves are greatly facilitated by the new non-Lagrangian, moving-mesh kind of calculation originated by J. Castor and presently being pursued by Adams, Davison, Davis, and others (see, e.g., Castor, Davis, and Davison 1977; Davis and Davison 1978). Results of this kind of calculation should be forthcoming soon, and some of them may in fact be reported at this conference (see paper by Adams, Castor, and Davis). Preliminary results of Davis and Davison (1978) (also Adams 1978) suggest that $M_{bump} < M_{evol}$, and perhaps $M_{bump}/M_{evol} \approx 2/3$, at least for one Cepheid model (the "Goddard model").

We note that it has been suggested by Simon and Schmidt (1976) that the above bumps on the theoretical velocity curves of Christy (1966b) and Stobie (1969) correspond to stars for which a reasonance exists between the fundamental and the second overtone, such that the ratio of the second overtone period Π_2 to the fundamental period Π_0 is close to 0.50. If this interpretation is correct, it suggests that the value $M_{bump}/M_{evol} \approx 0.5$ may apply at least to radiative Cepheid models (see §III).

M_{beat}: As stated in §I, M_{beat} applies only to Cepheids for which (usually) two distinct periods may be derived. These stars have been discussed by Fitch (1970), Stobie (1970, 1972, 1976, 1977), Stobie and Harwardin (1972), Rodgers and Gingold (1973), Schmidt (1974), and others.

It was originally suggested by Petersen (1973) that, since two periods (say radial fundamental and first overtone) were available for each such star, and in view of Cogan's (1970) result that the period is determined mostly by mass M and radius R, both M and R should be obtainable for each star. Such an analysis yielded $1 \lesssim M/M_\odot \lesssim 2$; the luminosities of these stars are, according to the available information, probably a few hundred solar luminosities. The mass determined by this kind of analysis is usually called M_{beat}. Note that $M_{beat}/M_{evol} \approx 1/3 - 1/2$. This discrepancy with respect to the evolutionary masses is perhaps even worse than for the other types of masses, and has generated a great deal of discussion in the literature (e.g., Petersen 1973, 1974, 1978; King, Hansen, Ross, and Cox 1975; Takeuti 1973; Stobie 1976, 1977; Cox, Hodson, and Davey 1976; King, Cox, and Hodson 1976; Cox and Cox 1976; Hodson and Cox 1976; Henden and Cox 1976; Cogan 1977; Cox, King, Hodson, and Henden 1977; Faulkner 1977a,b; Cox, Deupree, King, and Hodson 1977; Saio, Kobayashi, and Takeuti 1977; Cox 1978a,b; Cox, King, and Hodson 1978). Other investigators, making similar (and conventional) assumptions, have obtained results in general agreement with those of Petersen (1973) (however, see Cox, Deupree, King and Hodson 1977).

Some of the above results have been summarized in Table 1, and a general discussion will be given in §§IIIB and IV.

We note that Cogan (1978) has chosen to compare theory and observations in regard to pulsation theory and Cepheid variables not by a comparison of some inferred mass based on pulsation theory and the evolutionary mass, but as follows. As explained above in relation to M_T, the five quantities L, M, R, T_e, and Π may be related by the following four relations: a mass-luminosity relation, involving mostly L and M, based on

Table 1

Cepheid Masses

Type of Mass	M/M_{evol}
M_{evol}	-----
M_Q	0.7 - 1.3
M_W	0.7 - 0.8
M_{bump}	0.4 - 0.7 (?)
M_{beat}	1/2 - 1/3

conventional stellar evolution theory; a period-mean density relation (for a given assumed mode of pulsation), involving mostly Π, M, and R; a relation defining the location of the instability strip, involving mostly L, M, and T_e; and the defining relation among L, R, and T_e ($L \propto R^2 T_e^4$). Consequently, any one of these quantities may be expresed as a function of only one other of them, say the directly (and accurately!) observed period, Π, which is the independent parameter that Cogan (1978) has chosen. One of these expressions is a period-radius relation. Cogan (1978) has compared radii, for a given period, based on this expression, with radii inferred directly from the observations. He has obtained "empirical" radii for over 100 Cepheids, and refers to work by Balona (1977) in which the empirical radii of some 50 Cepheids have been obtained. He finds that different methods give somewhat different results (differing by up to, say, 20-30 percent) regarding radii of Cepheids. However, to this reviewer the overall agreement between theory and observation, when looked at this way, appears fairly satisfactory; i.e., there seem to be no glaring discrepancies between theory and observation.

B. Is There a Mass Discrepancy?

The above question may seem superfluous and unnecessary, in view of the above remarks. However, it appears to this reviewer that only in the case of M_{beat} is there incontrovertible evidence for a real mass discrepancy. Some conjectures regarding M_{beat} will be presented in §IV. We have tried to point out above some of the many uncertainties involved in obtaining the above indirect estimates of Cepheid masses. Except in the case of M_{beat}, the uncertainties in the above estimates are, for the most part, in the general range of 20-40 percent or less. As pointed out in the excellent and very thorough discussions of Fricke, Stobie, and Strittmatter (1971, 1972), it is impossible to exclude uncertainties of this order, due to various factors, both observational and theoretical.

Nevertheless, the weight of the evidence does seem to suggest that these estimates of Cepheid masses (again excluding M_{beat}) do seem to be somewhat less than conventional evolutionary masses. If this is a correct statement, then it appears to this reviewer that at least two general routes are open.

First, one may regard these conventional evolutionary masses as essentially correct, and then try to account for the discrepancy. The implication would then be that there is something wrong with pulsation theory, the way in which this theory is being applied to stellar envelopes, or the envelopes themselves. In line with the last two of these possibilities, it has been argued by Carson and Stothers (1976) that larger opacities can increase M_{bump}, and so remove at least part of the discrepancy. However, this explanation is not agreed upon by all workers (e.g., Cox, Deupree, King, and Hodson 1977).

Proceeding along the lines of seeking a modification of the envelope structure, Cox, Deupree, King, and Hodson (1977) have pointed out that a chemically inhomogeneous envelope, in particular one with a helium-enriched layer near the surface (having a helium mass fraction of at least 0.5 for temperatures less than 10^5°K), can increase M_Q (although this theory was originally conceived in relation to M_{beat}). Assuming that the Simon and Schmidt (1976) resonance-effect explanation of bumps on the nonlinear velocity curves is correct, the authors conclude that helium enrichment of the outer layers will also probably increase M_{bump}.

The existence of such a helium-enriched layer near the stellar surface raises new questions, which of course do not invalidate this possibility. Thus, it is known that such an "inverted μ-gradient" is unstable against slow mixing of the helium-enriched material down to the hydrogen-rich material below (e.g. Ulrich 1972; Kippenhahn 1974), as has been admitted by Cox, King, and Hodson (1978). Such a helium-enriched outer layer must therefore be continuously maintained, in order to offset this tendency to mix with the underlying material. It is suggested by A. Cox (1978a) that such a maintenance might be effected by radiation pressure acting on the helium atoms in the outer stellar layers, or perhaps by means of a "Cepheid wind" that is rich in hydrogen and that thus leaves the helium behind. (This last possibility has also been suggested by Cox, King, and Hodson 1978).

Second, one could assume that pulsation theory and the way it is being applied to stellar envelopes are essentially correct, and question the evolutionary calculations, and hence M_{evol}. This is perhaps a somewhat unpopular approach, but the precautionary remarks made earlier should be kept in mind, in particular as regards the relative lateness of those evolutionary phases relevant to the Cepheid question. For example, could

mass loss have occurred before the Cepheid stage, perhaps while the star was a red giant? It is true that Lauterborn, Refsdal, and Weigert (1971) have shown that a loss of mass of more than about 10 percent or less than some 80 percent will prevent a Cepheid model from executing a loop. However, considering the many uncertainties involved in calculations of blue loops, and our apparent lack of understanding of what causes them, this reviewer wonders about the universality of such a conclusion. Thus, could such a conclusion conceivably be code-dependent? To the best of our knowledge, a similar conclusion, obtained with a different stellar evolution code by an entirely independent group, has not appeared in the published literature.[1] (Iben 1974 also acknowledges the possibility of mass loss prior to the Cepheid phase.) Such a conclusion would seem to be sufficiently important and far-reaching that it should be checked in as independent a way as possible.

We are here only making a plea that we not be too complacent, and that we not put too much weight on conclusions that have been reached in the recent past. For example, in the course of this reviewer's lifetime the value of the Hubble constant has changed by about a factor of ten, despite statements occasionally made that the value of this constant is known at any given time to within 15 or 20 percent! Hopefully, Cepheid masses are not as difficult to obtain as the value of the Hubble constant, but the principle is the same. Also, it is a bit sobering to realize that an error of a factor of 4 in Cepheid luminosities persisted among astronomers for some 40 years prior to the early 1950's (the zero point of the Cepheid period-luminosity relation, the history of which has been described so beautifully by Fernie (1969)! These examples will, hopefully, encourage us to be very cautious in our acceptance of at least some quantitave results.

[1]Recently, it has been shown by Sreenivaran and Wilson (1978) that a loss of 10% of the mass in the red giant phase of a 15 $M_\odot$ stellar model will suppress a blue loop.

IV. SOME CONJECTURES ABOUT BEAT CEPHEIDS

As we have pointed out before, it seems difficult to avoid the conclusion that the masses of the beat Cepheids (M_{beat} in §III), as usually computed, are significantly less (by a factor of 1/3 to 1/2) than conventional evolutionary masses, say (3-4) $M_\odot$ for Cepheids in this period range (1^d to 7^d for the longer period). This discrepancy apparently exists even if we do not accept a mass discrepancy for the other kinds of mass considered in §III.

Apparently, one can adopt the view that these stars really have the low masses found as described in §III, and that these stars thus represent a new kind of stellar object. This was the opinion expressed by King, Hansen, Ross, and Cox (1975). However, as pointed out by Stobie (1977), this view runs into the difficulty that the existence of such objects is hard to understand within the context of stellar evolution theory.

The alternative view is that the above small mass values are for some reason illusory, and that the beat Cepheids really have normal Cepheid masses for their periods. We have, according to this standpoint, for some reason been led astray as regards the masses of these stars. The present reviewer is now somewhat inclined to this viewpoint.

Assuming that there is a mass discrepancy, and that the masses as given by the usual kind of analysis are for some reason too low, we seem to have available at least two alternative sets of assumptions: (1) Pulsation theory (assumed purely radial) is correct, but the stellar envelope structure normally assumed in the calculation is incorrect. Or, (2) the conventional envelope structure is correct, but pulsation theory, as it is usually assumed and used, is incorrect.

In keeping with the set of assumptions (1), Cogan (1977) pointed out that the presence of convection in the envelope, with a rather large value of the ratio α of mixing length to pressure scale height, say $\alpha \approx 1.5$ or 2.0, could sufficiently modify the envelope structure so as to result in considerably larger masses than for purely radiative envelope models. This modification is, as might be expected, more and more pronounced, the lower is the effective temperature T_e. The way in which the presence of convection in the envelope works, is as follows: It is known (e.g., Table 27.3 of Cox and Giuli 1968) that lowering the relative mass concentration of a star lowers the value Π_1/Π_0 of the ratio of radial first overtone to fundamental periods. Now, it is known observationally (see, e.g., Cogan 1977) that the beat Cepheids have $\Pi_1/\Pi_0 = 0.70\text{-}0.71$ compared to the value $\Pi_1/\Pi_0 = 0.74\text{-}0.75$ found for purely radiative models having expected masses of, say, (3-4) $M_\odot$ (e.g., Henden and Cox 1976; Cox, King, Hodson, and Henden 1977). Essentially, the lower mass concentration increases Π_0 more than Π_1. With a smaller mass concentration produced by the presence of convection, Cogan (1977) found that the observed period ratio Π_1/Π_0 could be obtained with "normal" Cepheid masses for the relevant period range.

More specifically, Cogan (1977) assumed that the fundamental and first overtone periods were, respectively, $\Pi_0 = 2^d.5684$ and $\Pi_1 = 1^d.8248$ ($\Pi_1/\Pi_0 = 0.7105$) for U TrA. He then constructed a series of model envelopes, in which convection was included according to the mixing-length formalism with a given value α of the ratio of mixing length to pressure scale height. The equilibrium or average luminosity L was the parameter in this series. Since $L \propto R^2 T_e^4$ and since both Π_0 and Π_1 are functions of L, M (mass), and T_e, then specification of L, Π_0, and Π_1 leads to

values of M, R, and T_e. For values of L corresponding to rather low values of T_e (near the red edge of the instability strip) and for $\alpha \gtrsim 1.5 - 2.0$, Cogan (1977) found that $M \approx 4\ M_\odot$, about the expected value, for this star.

However, Cogan's (1977) conclusion has been criticized by Henden and Cox (1976); Cox, Deupree, King, and Hodson (1977); and Deupree (1977c), who come to quantitatively different conclusions. It is found by these other investigators that the presence of convection, as usually modelled, has very little influence on derived masses of beat Cepheids.

In a recent study by Saio, Kobayashi, and Takeuti (1977), the influence of convection, again with use of the mixing-length formalism, on the periods of beat Cepheids was reexamined. Conclusions qualitatively similar to those of Cogan (1977), and not greatly different quantitatively, were reached by these investigators: namely, that with (mixing-length) convection included in the static model, if the beat Cepheids are fairly cool, then the observed periods can be obtained with "normal," or expected, masses. Saio, Kobayashi, and Takeuti (1977) attributed the (rather small) quantitative differences from the results of Cogan (1977) to differences in the formulation of mixing length theory, in particular to differences in convective efficiency.

Saio, Kobayashi, and Takeuti (1977) also examined the effect of (mixing-length) convection with $\alpha = 1.5$ on the ratio Π_2/Π_0 of second-overtone period to fundamental period. They found that this ratio achieved the approximate value of 0.50 appropriate to the Simon-Schmidt (1976) resonance interpretation of the bumps on certain Cepheid velocity curves (see earlier) for a mass of $M/M_\odot = 4.7$ for the bump Cepheid S Nor. With the value $\log(L/L_\odot) = 3.518$ adopted by Saio, Kobayashi, and Takeuti (1977)

and equations (1) or (2), we obtain $M_{evol}/M_{\odot} = 6.5$. If the above value of $M = 4.7\ M_{\odot}$ can be equated to M_{bump}, we obtain $M_{bump}/M_{evol} \approx 0.72$. This ratio is comparable to the value given above as obtained by Davis and Davison (1978), but larger than the value suggested by Christy (1966b), Stobie (1969), Fischel and Sparks (1974), and others. (The value given by Cox 1978b for S Nor is $\log[L/L_{\odot}] = 3.7$; the corresponding value of M_{evol} is $M_{evol}/M_{\odot} \approx 7.4$, and $M_{bump}/M_{evol} \approx 0.64$.)

Once again, this reviewer would like to urge exteme caution in our acceptance of at least certain kinds of quantitative information. After all, convection is one of the most poorly understood phenomena in astrophysics, and its effects may be much more important than our current thinking indicates. So the possibility suggested by Cogan (1977) should not, in this reviewer's opinion, be excluded out of hand.

The proposal made by Cox, Deupree, King, and Hodson (1977) regarding helium enrichment of the outer stellar layers, is also along the lines of the set of assumptions (1), i.e., keep (radial) pulsation theory but modify the envelope structure. The helium-rich outer layers serve to decrease the mass concentration of the star. Physically, the helium-enriched material compresses the outer stellar layers, and leaves the inner regions nearly unaffected. The net result is, just as in the case of a significant amount of convection in the envelope, that the observed first overtone-to-fundamental period ratio for the beat Cepheids can be obtained with "normal" masses of about (3-4) $M_{\odot}$.

However, as an alternative viewpoint, this reviewer has recently begun wondering if perhaps we ought not to look more carefully at the set of assumptions (2), i.e., accept currently assumed envelope structures but question pulsation theory as it is usually used. It is well known that

the derived masses (and radii) of beat Cepheids are very sensitive to the details of the theory of pulsation, as has been emphasized by Stobie (1977). So far, all work on the question of beat Cepheid masses has assumed purely radial pulsations. Suppose that the actual pulsations were mostly radial, but that there was a small admixture of nonradial pulsations. Then, if the nonradial component were sufficiently small, the usual interpretation of single-mode variables as radial pulsators would not be appreciably affected. However, this small admixture of nonradial pulsations might conceivably alter the period ratios just enough to imply (assuming strictly radial pulsations) anomalously small masses for the beat Cepheids.

After all, it has recently been shown by Osaki (1977) and Dziembowski (1977) that stars in the Cepheid instability strip are unstable against not only radial pulsations, but also certain nonradial pulsations. These nonradial pulsations are excited by the same envelope-ionization mechanisms that excite radial pulsations, and the growth rates of these nonradial pulsations are found to be comparable to those for radial pulsations. In particular, nonradial acoustic modes having values of the index $\ell \gtrsim 4$ in the spherical harmonic $Y_\ell^m(\theta,\phi)$ are found to be excited. (The index ℓ in $Y_\ell^m[\theta,\phi]$ is equal to the number of "node lines" in the star.) Osaki (1977) finds that p_1 modes are excited for $\ell \geq 4$ in a $7\ M_\odot$ Cepheid model, whereas Dziembowski finds that p_1 modes are excited for $\ell \geq 6$ for approximately $0.6\ M_\odot$ RR Lyrae models.

An inspection of the properties of nonradial oscillations (e.g., Cox 1976) shows that the periods of these acoustic modes decrease as ℓ increases. Moreover, the periods of those p_1 modes found by Osaki to be overstable (i.e., those with $\ell \geq 4$) for his $7\ M_\odot$ model, when divided by the fundamental radial period, give values of the period ratio $\lesssim 0.6$. If

the presence of a small amount of nonradial pulsation would have the effect of lowering the period ratio, then the presence of only a small amount of nonradial pulsation might therefore be sufficient to lower the period ratio to the observed value of 0.70-0.71.

It is also of some interest that, according to numerous investigations (e.g., Dziembowski 1977), the number of modes that may be excited increases as one descends the instability strip. And, as was pointed out earlier, the beat Cepheids occupy just the lower portions of the instability strip. Very low down on the instability strip are the Delta Scuti variables, in which, as Dziembowski (1975, 1977) has suggested, many different modes, both radial and nonradial, may be excited, thus possibly accounting for the complex observed behavior of these stars. (The Delta Scuti variables in the lower part of the instability strip.) Perhaps at the very bottom of the instability strip are the variable DA white dwarfs (the ZZ Ceti stars) which, as McGraw (1977) has suggested, may be pulsating exclusively in nonradial g modes.

The proposal that the pulsations of the beat Cepheids may involve a small amount of nonradial pulsation raises a number of questions, which will not be answered here. For example, would a mixture of predominantly radial pulsations with a small amount of nonradial pulsations produce a lowering of the observed period ratio? Would the relevant nonradial modes be excited in a star that was already executing radial pulsations? (The models assumed by Osaki 1977 and Dziembowski 1977 were static models.)

It is likely that this conjecture does not make life any simpler for the theorist in seeking an interpretation of the beat Cepheids. The combination of (mostly) radial and nonradial pulsations is a complicated phenomenon indeed. However, no one has ever guaranteed us that life would

be simple in nature. The main point of this conjecture is that purely radial pulsation theory may not be strictly applicable to the beat Cepheids.

Below are a few other conjectures which may bear either specifically on the beat Cepheids or on the problem of Cepheid masses in general. We do not necessarily expect these conjectures to be taken seriously, but we hope that they will at least provide some "food for thought."

The possibility of some kind of mass loss prior to the Cepheid stage should not be rejected until or unless more work has been done. This statement applies even in spite of the work of Lauterborn, Refsdal, and Weigert (1971) which suggests that mass loss, except for a very little bit or a lot, will prevent a star from making a blue loop, and thus becoming a Cepheid. As stated in §III, our knowledge of the causes of the loops, and what they are affected by, is still extremely rudimentary.

The use of the linear theory may not really be adequate, as Dziembowski and Koslowski (1974) have pointed out. It is true that the work of Stellingwerf (1975b) and of Cox, Hodson, and King (1978) make it appear very likely that the linear theory can be relied upon to give a good interpretation of observed periods of Cepheids. In the case of single-mode pulsators, linear theory periods are almost certainly adequate. However, in beat Cepheids, as also was pointed out above, even a slight change in the periods can make a big difference in the inferred masses. In Cox, Hodson, and King (1978) the linear and nonlinear periods were compared, and found to be nearly identical, in the case of a decaying mode and a growing mode. However, in a beat Cepheid it may be that <u>both</u> modes are excited, and it is well known that an oscillator that is either excited or damped will have a slightly different period from that of a constant-amplitude oscillator. Perhaps the question of the strict applicability of a linear theory cannot

really be answered until we can calculate true double- (or multiple-) mode behavior!

It is also possible that the existence of finite-amplitude pulsations in a star could affect its evolution, so that the conventional theory of evolution, applicable to nonpulsating stars, may not be appropriate for Cepheids. It has, in fact, been shown by Buchler (1978) that for large enough pulsation amplitudes in a star there can indeed be a feedback, so that the pulsations can affect the evolution of the star. Simon (1974) had suggested earlier that such a feedback may exist in a pulsating star.

V. SUMMARY AND CONCLUSIONS

We have reviewed most of the recent theoretical work on Cepheids and RR Lyrae variables, and have indicated what appear to this reviewer to be the main remaining problems. These are (1) the large-amplitude mode behavior, (2) convection, and (3) Cepheid masses.

It is pointed out, with respect to the large-amplitude mode behavior, that not only do two methods of calculating it seem to yield contradictory results, but also true double- (or multiple-) mode behavior in model stars has apparently not yet been calculated to everyone's satisfaction. With respect to convection, we are still apparently without a really workable and entirely satisfactory theory of time-dependent convection, in spite of the beautiful and pioneering work of Deupree on two-dimensional convection (see §II).

Cepheid masses are still a problem. Except in the case of the beat Cepheids, the inferred masses may be low by some 20-40 percent as compared to conventional evolutionary calculations. Whether this discrepancy is

serious, is apparently a matter on which opinions differ. To this reviewer, this discrepancy, while it is somewhat disturbing, is not necessarily alarming, in view of the many uncertainties involved, both observational and theoretical.

It is only in the case of the beat Cepheids, in our opinion, that the very low inferred masses are cause for genuine and/or serious concern. As pointed out in §IV, one can retain conventional (strictly radial) pulsation theory, and attempt to resolve the beat Cepheid mass problem by assuming an alteration of the envelope structure. Evidently, a lowering of the mass concentration can resolve the mass problem. Attempts in this direction have called upon convection in the static model, as suggested by Cogan (1977) and Saio, Kobayashi, and Takeuti (1977); or the assumption of a helium-enriched outer layer, as suggested by Cox, Deupree, King, and Hodson (1977).

Alternatively, one can retain presently computed static envelope models, but question the applicability of strictly radial pulsation theory to the beat Cepheids. This reviewer wonders if a small admixture of nonradial pulsations would not be sufficient to invalidate the use of a theory of strictly radial pulsations for these stars. It is pointed out that Cepheid models have recently been shown by Osaki (1977) and Dziembowski (1977) to be unstable to certain nonradial modes, with growth rates comparable to those of the radial modes. Moreover, the simultaneous excitation of several pulsation modes is more likely in the lower parts of the instability strip, where the beat Cepheids are, than in the upper parts (Dziembowski 1975, 1977). It looks as if we have problems enough in attempting to understand Cepheids, to keep us busy for some time!

We would like to acknowledge helpful conversations with T. Adams, C. Chiosi, A. N. Cox, C. G. Davis, P. Flower and C. Keller. We also wish to thank R. Buchler, B. Cogan, A. N. Cox, W. Dziembowski, Y. Osaki, H. Saio, N. Simon, R. Stellingwerf, E. Kobayashi, M. Takeuti, and P. Wiita for sending preprints and/or reprints of their work. This work was supported in part by National Science Foundation Grant No. AST72-05039 A04 through the University of Colorado.

References

Abt, H. A. 1959, Ap. J., 130, 769.

Adams, T. 1978, private communication.

Baade, W. 1926, Astr. Nachr., 228, 359.

Bahcall, J. N. 1977, Ap. J., 216, L115.

Baker, N. H. 1970, Bull. A. A. S., 2, 181.

Baker, N. H. 1973, in Stellar Evolution, eds. H.-Y. Chiu and A. Murial (Cambridge, Mass.: MIT Press).

Baker, N. H., and Gough, D. O. 1967, A. J., 72, 784.

Baker, N. H., and von Sengbusch, K. 1969, "Mitteilungen der Astronomischen Gesellschaft," No. 27, p. 162.

Balona, L. A. 1977, M.N.R.A.S., 178, 231.

Becker, S. A., Iben, I., Jr., and Tuggle, R. S. 1977, Ap. J., 218, 633.

Böhm-Vitense, E. 1972, Astron. and Astrophys., 17, 335.

Buchler, R. J. 1978, Ap. J., 220, 629.

Carson, T. R., and Stothers, R. 1976, Ap. J., 204, 461.

Castor, J. I., Davis, C. G., and Davison, D. K. 1977, Los Alamos Rept. LA-6664.

Christy, R. F. 1964, Rev. Mod. Phys., 36, 555

Christy, R. F. 1966a, Ann. Rev. Astron. and Astrophys., 4, 353.

Christy, R. F. 1966b, Ap. J., 145, 340.

Cogan, B. C. 1970, Ap. J., 162, 139.

Cogan, B. C. 1977, Ap. J., 211, 890.

Cogan, B. C. 1978, Ap. J., 221, 635.

Cox, A. N. 1978a, Sky and Telescope, 55, 115 (February, 1978).

Cox, A. N. 1978b, preprint (submitted to Ap. J.).

Cox, A. N., Brownlee, R. R., and Eilers, D. D. 1966, Ap. J., 144, 1024.

Cox, A. N., and Cox, J. P. 1976, in Multiple Periodic Variable Stars (IAU Colloq. No. 29), ed. W. S. Fitch (Dordrecht: Reidel), p. 115.

Cox, A. N., and Davis, C. G. 1975, Dudley Obs. Rept., 9, 297.

Cox, A. N., Deupree, R. G., King, D. S., and Hodson, S. W. 1977, Ap. J., 214, L127.

Cox, A. N., Hodson, S. W., and Davey, W. R. 1976, in Proc. Los Alamos Solar and Stellar Pulsation Conference, eds. A. N. Cox and R. G. Deupree, p. 188.

Cox, A. N., Hodson, S. W., and King, D. S. 1978, Ap. J., 220, 996.

Cox, A. N., King, D. S., and Hodson, S. W. 1978, preprint (submitted to Ap. J.).

Cox, A. N., King, D. S. Hodson, S. W., and Hendon, A. A. 1977, Ap. J., 212, 451.

Cox, J. P. 1974, Rep. Progr. Physics, 37, 563.

Cox, J. P. 1976, Ann. Rev. Astron. and Astrophys., 14, 247.

Cox, J. P., Cox, A. N., Olsen, K. H., King, D. S., and Eilers, D. D. 1966, Ap. J., 144, 1038.

Cox, J. P., and Giuli, R. T. 1968, Principles of Stellar Structure (New York: Gordon and Breach).

Cox, J. P., King, D. S., and Stellingwerf, R. S. 1972, Ap. J., 171, 93.

Davis, C. G., and Davison, D. K. 1978, Ap. J., 221. 929.

Deupree, R. G. 1975a, Ap. J., 198, 419.

Deupree, R. G. 1975b, Ap. J., 201, 183.

Deupree, R. G. 1976a, Ap. J., 205, 286.

Deupree, R. G. 1976b, in Proc. Los Alamos Solar and Stellar Pulsation Conference, eds., A. N. Cox and R. G. Deupree, p. 222.

Deupree, R. G. 1976c, in Proc. Los Alamos Solar and Stellar Pulsation Conference, eds., A. N. Cox and R. G. Deupree, p. 229.

Deupree, R. G. 1977a, Ap. J., 211, 509.

Deupree, R. G. 1977b, Ap. J., 214, 502.

Deupree, R. G. 1977c, Ap. J., 215, 232.

Deupree, R. G. 1977d, Ap. J., 215, 620.

Durand, R. A., Eoll, J. G., and Schlesinger, B. M. 1976, M.N.R.A.S., 174, 641.

Dziembowski, W. 1975, Mem. Soc. Roy. Sci. Liège, 6^{e} Ser., VIII, 287.

Dziembowski, W. 1977, Acta Astron. 27, 95.

Dziembowski, W., and Kozlowski, M. 1974, Acta Astron., 24, 245.

Evans, N. R. 1976, Ap. J., 209, 135.

Faulkner, D. J. 1977a, Ap. J., 216, 49.

Faulkner, D. J. 1977b, Ap. J., 218, 209.

Fernie, J. D. 1969, Publ. A. S. P., 81, 707.

Fischel, D., and Sparks, W. M. 1974, eds., Cepheid Modelling (NASA Rept. NASA-SP-383).

Fitch, W. D. 1970, Ap. J., 161, 669.

Flower, P. J. 1976, Ph.D. dissertation, University of Washington, Seattle, Washington.

Flower, P. J. 1977, Astron. and Astrophys., 54, 31.

Fricke, K. J., Stobie, R. S., and Strittmatter, P. A. 1971, M.N.R.A.S., 154, 23.

Fricke, K. J., Stobie, R. S., and Strittmatter, P. A. 1972, Ap. J., 171, 593.

Fricke, K. J., and Strittmatter, P. A. 1972, M.N.R.A.S., 156, 129.

Hallgren, E. L., and Cox, J. P. 1970, Ap. J., 162, 933.

Hansen, C. J. 1978, Ann. Rev. Astron. and Astrophys., 16 (in press).

Hanson, R. B. 1975, A. J., 80, 379.

Hanson, R. B. 1977, in The H-R Diagram (IAU Symp. No. 80), eds. A. G. D. Philip and D. Hayes.

Henden, A. A., and Cox, A. N. 1976, in Proc. Los Alamos Solar and Stellar Pulsation Conference, eds. A. N. Cox and R. G. Deupree, p. 167.

Hodson, S. W., and Cox, A. N. 1976, in Proc. Los Alamos Solar and Stellar Pulsation Conference, eds. A. N. Cox and R. G. Deupree, p. 202.

Hofmeister, E. 1967, Z. Ap., 65, 194.

Iben, I., Jr. 1967, Ann. Rev. Astron. and Astrophys., 5, 571.

Iben, I., Jr. 1974, Ann. Rev. Astron. and Astrophys., 12, 215.

Iben, I., Jr., and Tuggle, R. S. 1972a, Ap. J., 173, 135.

Iben, I., Jr., and Tuggle, R. S. 1972b, Ap. J., 178, 441.

Iben, I., Jr., and Tuggle, R. S. 1975, Ap. J., 197, 39.

Karp, A. H. 1975, Ap. J., 201, 641.

King, D. S., Cox, A. N., Eilers, D. D., and Cox, J. P. 1975, Bull. A. A. S., 7, 251.

King, D. S., Cox, J. P., Eilers, D. D., and Davey, W. R. 1973, Ap. J., 182, 859.

King, D. S., Cox, A. N., and Hodson, S. W. 1976, in Proc. Los Alamos Solar and Stellar Pulsation Conference, eds., A. N. Cox and R. G. Deupree, p. 157.

King, D. S., Hansen, C. J., Ross, R. R., and Cox, J. P. 1975, Ap. J., 195, 467.

Kippenhahn, R. 1974, in Late States of Stellar Evolution (IAU Symp. No. 66), ed. R. J. Tayler (Dordrecht: Reidel).

Latour, J., Speigel, E. A., Toomre, J., and Zahn, J.-P. 1976, Ap. J., 207, 233.

Latyschev, I. N. 1969, Astrofizika, 5, 331.

Lauterborn, D., Refsdal, S., and Roth, M. L. 1971, Astron. and Astrophys., 13, 119.

Lauterborn, D., Refsdal, S., and Stabell, R. 1972, Astron. and Astrophys. 17, 113.

Lauterborn, D., Refsdal, S., and Weigert, A. 1971, Astron. and Astrophys., 10, 97.

Lauterborn, D., and Siquig, R. A. 1974a, Astron. and Astrophys., 30, 385.

Lauterborn, D., and Siquig, R. A. 1974b, Ap. J., 187, 299,

Lauterborn, D., and Siquig, R. A. 1974c, Ap. J., 191, 589.

Lauterborn, D., and Siquig, R. A. 1976, Astron. and Astrophys., 49, 285.

McGraw, J. T. 1977, Ph. D. dissertation, University of Texas.

Osaki, Y. 1977, Publ. A. S. Japan, 29, 235.

Pacyński, B. 1970, Acta Astron., 20, 195.

Parsons, S. B. 1972, Ap. J., 174, 57.

Patterson, J., Robinson, E. L., and Nather, R. E. 1977, Ap. J., 214, 144.

Payne-Gaposchkin, C. 1951, in Astrophysics: A Topical Symposium, ed. J. A. Hynek (New York: McGraw-Hill), Chap. 12.

Payne-Gaposchkin, C. 1961, Vistas in Astron., 4, 184.

Payne-Gaposchkin, C., and Gaposchkin, S. 1966, Vistas in Astron., 8, 191.

Pel, J. W. 1978, Astron. and Astrophys., 62, 75.

Petersen, J. O. 1973, Astron. and Astrophys., 27, 89.

Petersen, J. O. 1974, Astron. and Astrophys., 34, 309.

Petersen, J. O. 1978, Astron. and Astrophys., 62, 205.

Robertson, J. W. 1971a, Ap. J., 164, L105.

Robertson, J. W. 1971b, Ap. J., 170, 353.

Robertson, J. W. 1972, Ap. J., 173, 631.

Robinson, E. L., Nather, R. E., and McGraw, J. T. 1976, Ap. J., 210, 211.

Rodgers, A. W. 1970, M.N.R.A.S., 151, 133.

Rodgers, A. W., and Gingold, R. A. 1973, M.N.R.A.S., 161, 23.

Saio, H., Kobayashi, E., and Takeuti, M. 1977, Sci. Rep. Tôhoku University, 51, 144.

Sandage, A., and Tamman, G. A. 1969, Ap. J., 157, 683.

Sandage, A., and Tamman, G. A. 1971, Ap. J., 167, 293.

Schlesinger, B. M. 1969, Ap. J., 158, 1059.

Schlesinger, B. M. 1977, Ap. J., 212, 507.

Schmidt, E. G. 1972, Ap. J., 174, 605.

Schmidt, E. G. 1974, M.N.R.A.S., 167, 613.

Simon, N. R. 1974, B. A. A. S., 6, 469.

Simon, N. R., and Schmidt, E. G. 1976, Ap. J., 205, 162.

Smith, M. A. 1977, Ap. J., 215, 574.

Sreenivaran, S. R. and Wilson, J. F. 1978, Astrophys & Space Sci, 53, 193.

Stellingwerf, R. F. 1974a, Ph.D. dissertation, University of Colorado

Stellingwerf, R. F. 1974a, Ap. J., 192, 139.

Stellingwerf, R. F. 1975a, Ap. J., 195, 441.

Stellingwerf, R. F. 1975b, Ap. J., 199, 705.

Stellingwerf, R. F. 1976, private communication.

Stobie, R. S. 1969, M.N.R.A.S., 144, 485.

Stobie, R. S. 1970, Observatory, 90, 20.

Stobie, R. S. 1972, M.N.R.A.S., 157, 167.

Stobie, R. S. 1974, in Stellar Instability and Evolution (IAU Symp. No. 59), eds. P. Ledoux, A. Noels, and A. W. Rodgers (Dordrecht: Reidel), p. 49.

Stobie, R. S. 1976, in Multiple Periodic Variable Stars (IAU Colloquium, No. 29), ed. W. S. Fitch (Dordrecht: Reidel), p. 87.

Stobie, R. S. 1977, M.N.R.A.S., 189, 631.

Stobie, R. S., and Hawardin, T. 1972, M.N.R.A.S., 157, 157.

Takeuti, M. 1973, Pub. A. S. Japan, 25, 567.

Toomre, J., Zahn, J.-P. Latour, J., and Spiegel, E. A. 1976, Ap. J., 207, 545.

Ulrich, R. K. 1972, Ap. J., 172, 165.

van Paradijs, J. 1973, Astron. and Astrophys., 23, 369.

Wesselink, A. J. 1946, B. A. N., 10, 91.

Wesselink, A. J. 1947, B. A. N., 10, 252.

Wiita, P. J. 1978, preprint.

Discussion

Hillendahl: On your last slide, you showed various ways of getting the mass, and all of them relied rather heavily on theoretical interpretations. But if you look at the models various people have made for classical Cepheids, one thing that seems to be rather universal is that the atmospheres appear to be in gravitational collapse between phases 0.5 and 0.7, so the photosphere stays essentially in the same mass zone. Now if you use only that idea, you can get an actual physical displacement in centimeters by measuring the displacement of the Fe II lines at those phases; and from the fact that the atmosphere is moving linearly with time, you can get the gravity. Thus you have g and R, and from them you can deduce values of M around 0.6 of the evolutionary mass, using very little theory.

J. Cox: Is that related to the method described by Art Cox this morning, involving gravities?

Hillendahl: I don't think so. I first tried this method using some data from a 1937 paper by A. H. Joy (Ap. J. 86, 363). He did a velocity survey, and I noticed that if you plotted the rate of change of velocity during that period, you got straight lines from which you would deduce g. You plot this versus period and at zero period you get a gravity of around 4. As you go to longer periods, the gravity becomes less - it's a very nice relationship. I think that if you could combine this with something that requires less theoretical interpretation, it might give you guidance as to which one of these masses might be nearer the truth.

A. Cox: What is the ℓ value for these high nonradial modes?

J. Cox: About 4 to 6.

A. Cox: Is that observable with so many bumps on the star?

J. Cox: I think that's a very good question - how do you detect this? I can't answer that, but maybe somebody else can.

Aizenman: I think the question of how you tell whether a higher mode is present has been addressed by Dziembowski in 1977, in a paper in Acta Astronomica. He described general observational characteristics of nonradial pulsation. If you take the ratio of the observed radial velocity, integrated over the disk of the star, to the change in the bolometric magnitude, this is independent of the angle of inclination. If you know the radius of the star and assume a limb darkening law, you can get a very strong criterion for the value of ℓ ($\ell = 0,1,2,\ldots$).

Deupree: Would you expect these modes to have $m = 0$ or $m \neq 0$, and does it matter? Do these nonradial modes show the oscillations in the interior that were found in Dzienbowski's 1972 paper? As you may remember, there were oscillations in the eigenfunctions, and instead of going smoothly to zero, as you went into the deep interior, there was coupling of the g-modes.

J. Cox: The modes that are excited are the p_1-modes, and their amplitudes become rather small in the interior. So the answer to your second question is that the essential parts are not excited at large amplitude. With regard to your first question about the m value, it doesn't matter, as long as there are no perturbing influences. If you have rotation or a magnetic field, then the

m value does matter. I must say that I don't have a very specific picture of these nonradial modes, except to say that that possibility might exist. It raises more questions than it answers. For example, if there were nonradial modes present, would the period ratio go in the right direction? Is a star that is already executing radial oscillations stable against nonradial oscillations? The models studied by Osaki and Dziembowski were static models -- now we are asking about nonstatic models. So there are many questions to be asked.

LIGHT CURVES FOR "BUMP CEPHEIDS" COMPUTED WITH A DYNAMICALLY ZONED PULSATION CODE

T. F. Adams
Group J-15, MS 420
University of California, Los Alamos Scientific Laboratory
Los Alamos, NM 87545

J. I. Castor*
JILA, University of Colorado
Boulder, CO 80309

C. G. Davis
Group J-15, MS 420
University of California, Los Alamos Scientific Laboratory
Los Alamos, NM 87545

ABSTRACT

The dynamically zoned pulsation code developed by Castor, Davis, and Davison has been used to recalculate the Goddard model and to calculate three other Cepheid models with the same period (9.8 days). This family of models shows how the bumps and other features of the light and velocity curves change as the mass is varied at constant period. This study, with a code that is capable of producing reliable light curves, shows again that the light and velocity curves for 9.8-day Cepheid models with standard homogeneous compositions do not show bumps like those that are observed unless the mass is significantly lower than the "evolutionary mass." The light and velocity curves for the Goddard model presented here are similar to those computed independently by Fischel, Sparks, and Karp. They should be useful as standards for future investigators.

*Also Los Alamos Scientific Laboratory Consultant.

I. INTRODUCTION

Cepheids with periods around ten days are known to show secondary bumps in their light curves around the time of maximum light (Cox 1974). Until recently, however, theoretical light curves for Cepheids have been unsatisfactory because of contamination by spurious "zoning bumps" (Keller and Mutschlecner 1971). The new dynamically zoned stellar pulsation code developed by Castor, Davis, and Davison (1977) is capable of producing reliable light curves without these artifacts. We have used a somewhat improved version of this code to recalculate the Goddard model and to calculate three other 9.8-day Cepheid models. We will discuss here the systematic trends that appear in the light and velocity curves for this family of models.

II. THE MODELS

The family of models represents a one-parameter sequence with mass as the independent variable, subject to the constraints that: 1) the period is fixed at 9.8 days, and 2) the models lie along a line in the HR Diagram near the center of and roughly parallel to the instability strip. The characteristics of the models are given in Table 1. The actual masses of the models range from 62 to 99 percent of their respective "evolutionary masses" (corresponding to their luminosities with a standard mass-luminosity relation; see Table 1). The light and velocity curves for the four models are shown in Figures 1 and 2.

TABLE 1

MODEL PARAMETERS

Mass ($M_\odot$)	4.0	5.0	6.0	7.4
Luminosity ($L_\odot$)	3187.	3849.	4421.	5210.
Effective Temperature (K)	5700	5690	5687	5682
Evolutionary Mass ($M_\odot$)*	6.46	6.82	7.10	7.44
Zones in Model (Opt. Thin)	65(12)	72(15)	73(12)	74(10)
Artificial Viscosity Coeff.†	1.0	2.0	2.0	2.0
Fractional Core Radius	0.12	0.12	0.13	0.11
Period (days)	9.79	9.78	9.79	9.78
Peak KE (10^{42} ergs, Expanding)	1.78	3.30	5.30	9.70
Periods Calculated‡	46	52	37	51
Time Steps per Period	1670	1170	1160	1230
Periods per Minute (CDC 7600)	0.54	0.67	0.64	0.67
Comments	Goddard Model			Evolutionary Mass Model

*Log [M(evolutionary)/$M_\odot$] = 0.287 log ($L/L_\odot$) - 0.195.

†Stellingwerf (1975) cutoff at 0.1.

‡Includes periods of amplification.

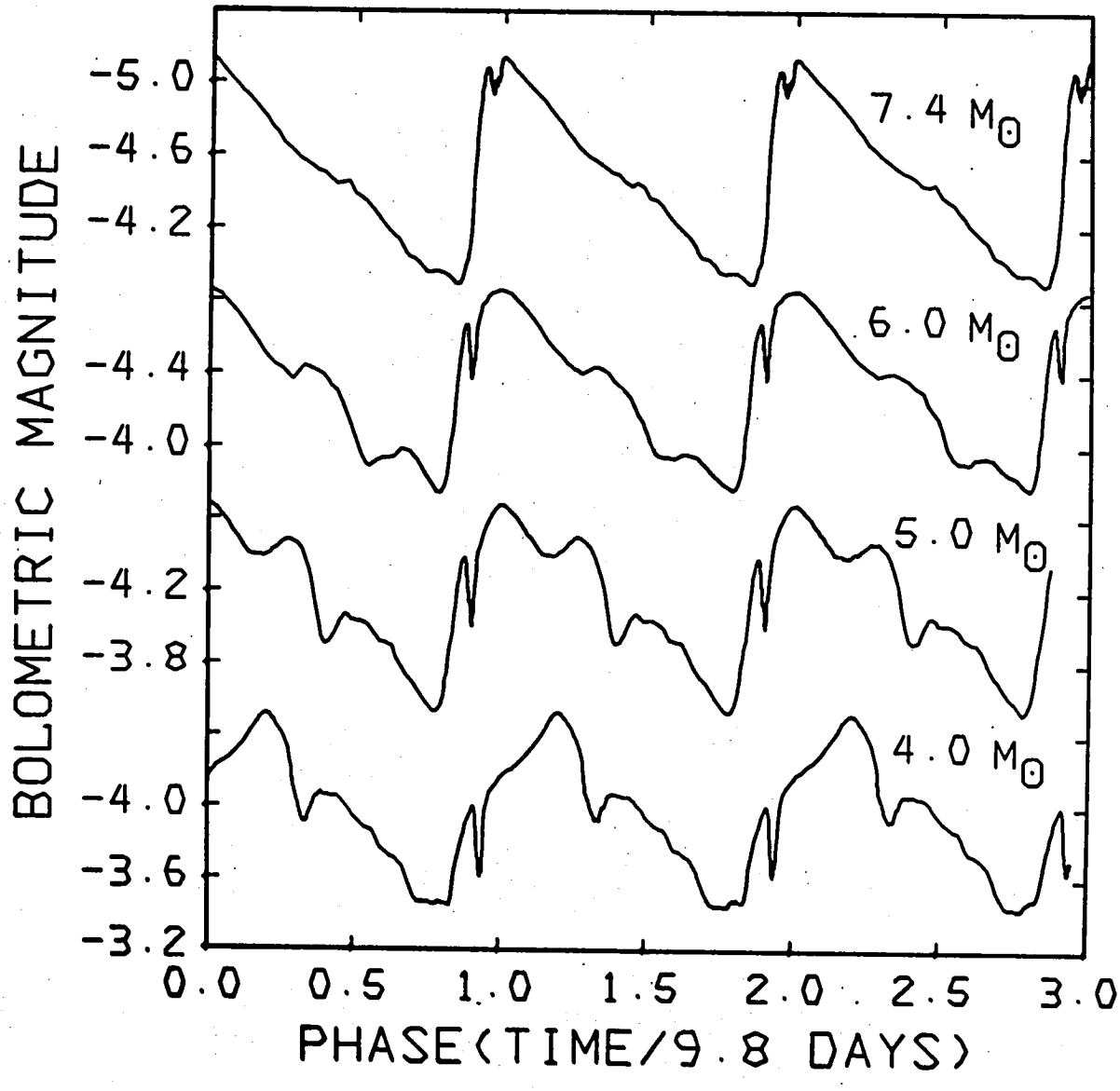

Fig. 1. Bolometric light curves for four 9.8-day Cepheids. Zero phase is at maximum light, except for the 4.0 $M_{\odot}$ (Goddard) model, where zero phase was shifted 0.2 units earlier for easier comparison. The model parameters are given in Table 1.

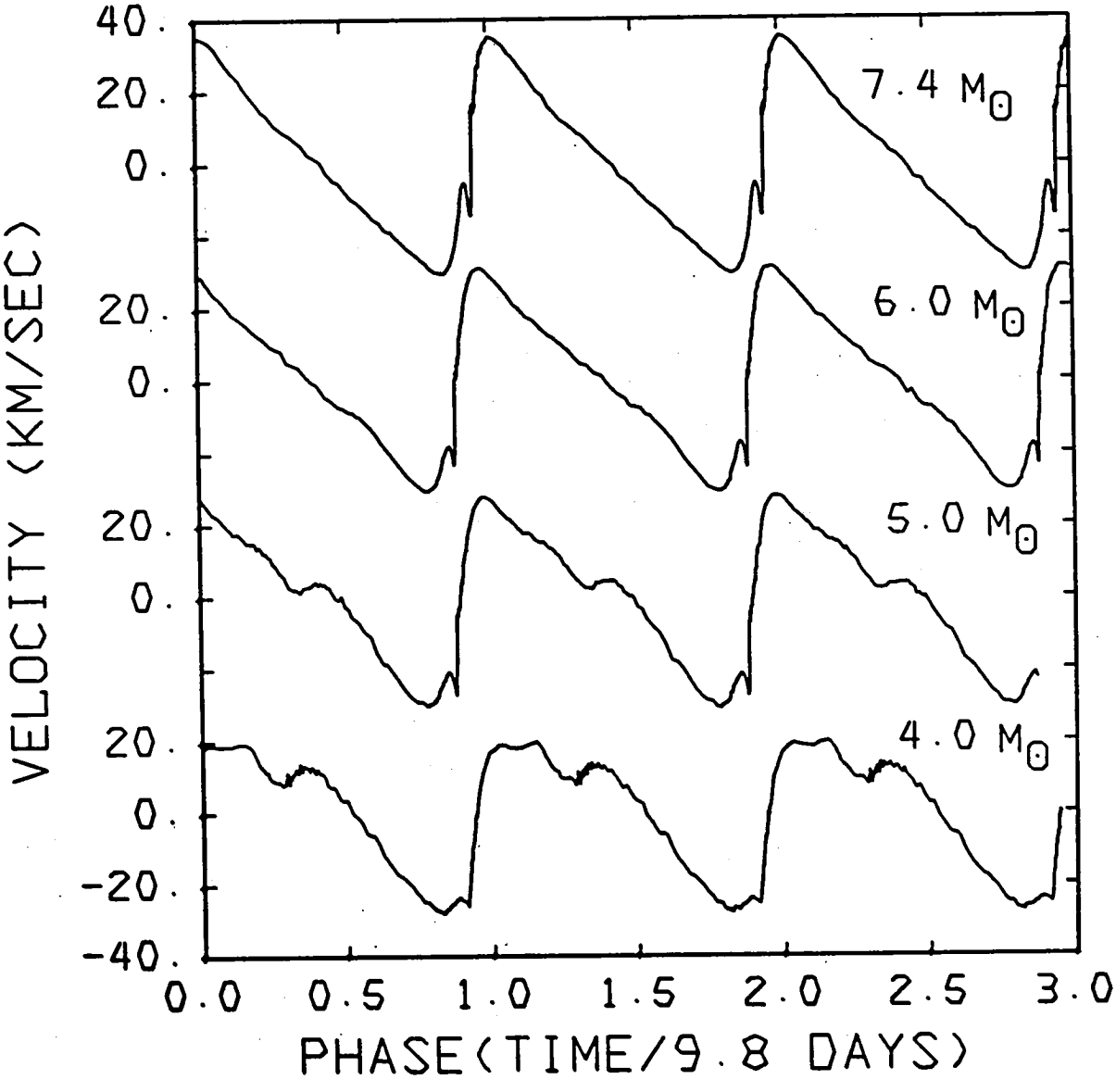

Fig. 2. Velocity curves for four 9.8-day Cepheids. The velocities (positive for radial expansion) are interpolated values that show the motion of the matter at optical depth two-thirds. The phase convention is as in Fig. 1. The model parameters are given in Table 1.

The original version of the code, used by Castor, Davis, and Davison (in Deupree 1976; see also Davis and Davison 1978) to calculate their Goddard model, incorporated an exponential artificial viscosity cutoff. The principal change in the code since then has been to go to the standard Stellingwerf (1975) cutoff. In addition, the value of the cutoff has been increased from one to ten per cent of the isothermal sound speed. These changes account for the higher limiting amplitude and the slightly different appearance of the light and velocity curves for the present Goddard model compared with the earlier one (their model II).

The light and velocity curves for the Goddard model in Figures 1 and 2 should be useful as reference light and velocity curves for the Goddard model. They are quite similar to those presented by Fischel, Sparks, and Karp (in Deupree 1976). It is comforting that there is now reasonable agreement between the light and velocity curves calculated by (at least two) independent investigators for the same model.

III. DISCUSSION OF THE LIGHT AND VELOCITY CURVES

Let us first discuss the features in the light and velocity curves for the Goddard model. Starting at minimum light, we see the phase of rapidly rising light, interrupted by the so-called "artificial viscosity dip." The dip is associated with the compression wave that stops the infall of the envelope. The artificial viscosity plays a role in that it spreads out the compression wave in the mesh. However, the dip itself may not be entirely artificial, since the compression wave undoubtedly raises the effective gravity briefly and can thus cause the light output to drop.

In this model, peak light is preceded by a shoulder in the light curve. There is a broad maximum in the velocity curve that begins at the phase of the shoulder and lasts through the light maximum. The light curve near maximum seems to be governed by changes in the effective gravity at optical depth two-thirds, as there is an increase in the gravity between the shoulder and the peak and a gravity minimum at the peak itself. However, the physical origin of the shoulder is not yet clear.

After maximum light, there is a dip and then the "Christy bump," which is associated with the reflection of a compression wave off the core. The bump in the velocity curve actually agrees in phase with the dip preceding the bump in the light curve. Therefore, in agreement with previous investigators, we identify the feature in the light curve as a "Christy dip," due to the compression that occurs when the reflected wave reaches the surface. Although the light and velocity curves are similar, they differ in detail. This raises some questions about the practice of comparing observed light curves with calculated velocity curves.

We now discuss how these features change as the mass is increased. In general, the Christy bump or dip moves down the descending branch. At the same time, it becomes less prominent, especially in the velocity curve. In fact, there is no bump in the evolutionary mass (7.4 $M_{\odot}$) model. This confirms the conclusion that, with a standard homogeneous composition, the mass must be less than the evolutionary mass to show bumps like those that are observed.

Another interesting change that occurs as the mass is increased involves the light curve near maximum. In the 5.0 $M_\odot$ model, what was the shoulder in the Goddard model has become the peak, while the peak in the Goddard model has evolved into a bump following maximum light. This bump then moves down the descending branch and becomes less prominent as the mass is further increased.

The ascending branch also changes with increasing mass. It becomes steeper and the "artificial viscosity dip" moves up the ascending branch until it nearly coincides with the peak in the evolutionary mass model. The compression wave associated with the dip increases greatly in strength as this happens. It should be emphasized, though, that this phenomenon is probably amplitude-dependent, and that the limiting amplitude, which also increases with mass (cf. Table 1), may depend on subtle physical or numerical effects in the calculation.

Another interesting phenomenon occurred in the 4.0 and 5.0 $M_\odot$ models, although it is not apparent in the light or velocity curves. In these models, at the phase of rapid expansion, when the hydrogen ionization front is racing inward, a shock forms on the neutral side following the front. This can be understood as a transition in the nature of the ionization front from D to R type (Kahn 1954, Castor 1966). Conditions change too rapidly for a steady-state R-type front to develop, and the front soon returns to its usual D-type behavior. This transition occurs about the time of the Christy dip in the Goddard model, and about the time of the dip just after maximum light in the 5.0 $M_\odot$ model. The front is near optical depth unity at this time, so there should not be any major changes in the emergent spectrum or energy distribution. However,

the following shock may be connected with the weak redshifted Ca II emission features that appear just after maximum light in Beta Doradus (Gratton 1953). The ionization front transition will be discussed in detail elsewhere (Adams and Castor, in preparation).

IV. CONCLUSIONS AND FUTURE PLANS

We have calculated a family of 9.8-day Cepheid models with a code that can produce reliable theoretical light curves. We find that only if the mass is significantly less than the "evolutionary mass" do the bumps in the light and velocity curves occur near maximum light, where they are observed to occur in real ten-day Cepheids (Cox 1974). However, only models with homogeneous population I compositions were calculated. It thus appears that we require either reduced masses, inhomogeneous compositions, or some change in the physics in order to match the observed light curves of ten-day Cepheids.

We plan to continue this program by calculating families of models at other periods to see how the light and velocity curves vary with period. Our goals will be to learn more about the mechanisms that produce bumps in the light and velocity curves and, in general, to see if the Hertzsprung sequence (variation of bump location with period) can be reproduced theoretically. We would also like to calculate some inhomogeneous models to study Art Cox's proposed solution to the "mass anomaly."

Finally, we conclude that there is now a consensus standard Goddard model that can be used as a benchmark for any new pulsation code. It is entirely fitting that this consensus should be reported here at the

Goddard Space Flight Center only two conferences after the idea of a standard Goddard model was originated.

ACKNOWLEDGEMENTS

This work was supported under the Los Alamos Scientific Laboratory New Research Incentives Program. The authors would like to thank S. S. Bunker, A. N. Cox, J. P. Cox, D. K. Davison, R. G. Deupree, C. F. Keller, and D. S. King for their helpful comments and suggestions.

REFERENCES

Castor, J. I. 1966, "Atmospheric Dynamics in a Model RR Lyrae Star," Ph. D. Thesis, California Institute of Technology, Pasadena.

Castor, J. I., Davis, C. G., and Davison, D. K. 1977, "Dynamical Zoning Within a Lagrangian Mesh by Use of DYN, a Stellar Pulsation Code," Los Alamos Scientific Laboratory Report LA-6664.

Cox, J. P. 1974, Rept. Progr. Phys., 37, 563.

Davis, C. G., and Davison, D. K. 1978, Ap. J., 221, 929.

Deupree, R. G. 1976, in "Proceedings of the Solar and Stellar Pulsation Conference," A. N. Cox and R. G. Deupree, eds., Los Alamos Scientific Laboratory Conference Proceeding LA-6544-C, pp.243-270.

Gratton, L. 1953, Ap. J., 118, 570.

Kahn, F. D. 1954, Bull. Astr. Soc. Netherlands, 22, 187.

Keller, C. F., and Mutschlecner, J. P. 1971, Ap. J., 167, 127.

Stellingwerf, R. F. 1975, Ap. J., 195, 441.

Discussion

J. Wood: Do you have a temperature range for this β Dor Goddard model? From the G-band, I found about 1500° over the cycle, but Rogers and Bell found about 450° from Hα profiles. Sidney Parsons found about 900° from UBV work.

Adams: First of all, I didn't make any attempt to match a particular star. This was simply a theoretical sequence, so the parameters may not be correct for a particular star. The temperature data are available, and could be used to plot loops in the color-color diagram. However, there's a larger question that has to do with limiting amplitudes. The light amplitude shown here was rather large for a Cepheid; therefore, any behavior that depends on the limiting amplitude is questionable. But I don't know whether the temperature range depends on the limiting amplitude.

Wesselink: Have you made any comparison between your light curves and observed light curves?

Adams: I've just taken a cursory look at the observed light curves. I can't claim that I can match any observed light curve. The most important conclusion is that we can calculate good light curves, and they still show the traditional mass anomaly with the bumps. Let me add that even the features seen in the superb light curves produced by Pel and Lub still leave a little freedom for the theoretician to imagine various things happening. It's an extremely difficult problem to get sufficient data.

Connolly: What is causing that sharp dip at rising light and is it a dip, not actually a bump?

Adams: It is a dip. In the theoretical calculations it is due to the fact that when the envelope is falling in, it is stopped by a compression wave or shock wave. The intense compression for a short period of time steals some luminosity and puts it into ionization or compression. Therefore there is a sharp drop in the luminosity as the shock passes through the photosphere at $\tau = 2/3$.

Wesselink: I know one observed light curve -- VZ Her -- which resembles one of yours. It has a dip on the rising light.

Adams: That is interesting. However, I would not go so far as to say that the dip has to exist theoretically, even though it shows up in the models. I think that it is difficult to find any observer who has a well-documented dip in the rising light because that's a very hard thing to see. It looks a lot like a cloud going by, lasting only a very short time.

Pel: But they exist for longer period stars, with 15-30 day periods. There is a "standstill."

Adams: That feature may be a bump, related to the bumps that define the Hertzsprung progression.

TIME DOMAIN PERIOD DETERMINATION TECHNIQUES

R. F. Stellingwerf
Department of Physics and Astronomy
Rutgers University

Abstract

Two simple period determination schemes are discussed. They are well suited to problems involving non-sinusoidal periodic phenomena sampled at a few irregularly spaced points. Statistical properties are discussed. The techniques are applied to the double-mode Cepheids BK Cen and TU CAS as test cases.

Introduction

Fourier techniques offer the "best possible" methods of spectral analysis in a number of respects, but they are not well suited to cases with strongly non-sinusoidal variation, or cases in which only a few scattered data points are available. Unfortunately, this is exactly the situation in many physical problems, including variable stars. I will discuss two classical techniques that do treat these cases efficiently in cases involving several discrete frequencies.

When departing from Fourier methods, invariably some type of sacrifice must be made. In this case "ghosts" appear at subharmonic frequencies of a strong spectral line. An important point in the analysis is to show that the unwanted subharmonics can be minimized and can be distinguished from the real frequency. Once understood, these "ghosts" can be used to good advantage as indications of the presence or absence of high frequency components.

A more complete description of these techniques will appear in Stellingwerf (1978).

I. THE PDM METHOD

A discrete set of observations can be represented by two vectors, $\underset{\sim}{x}$, and the observation times $\underset{\sim}{t}$, where the i^{th} observation is given by (x_i,t_i) and there are N points in all (i = 1,N). Let σ^2 be the variance of $\underset{\sim}{x}$, given by

$$\sigma^2 = \frac{\Sigma(x_i-\bar{x})^2}{N-1} \qquad (1)$$

where $\bar{x}$ is the mean, $\bar{x} = \Sigma x_i/N$. For any subset of x_i's we define the sample variance, s^2, exactly as in equation (1). Suppose we have chosen M distinct samples, having variances s_j^2 (j = 1,M) and containing n_j data points. The overall variance for all the samples is then given by

$$s^2 = \frac{\Sigma(n_j-1)s_j^2}{\Sigma n_j - M} \qquad (2)$$

as a consequence of equation (1).

We wish to minimize the variance of the data with respect to the mean light curve. Let Π be a trial period, compute a phase vector $\underset{\sim}{\phi}$: $\phi_i = t_i/\Pi - [t_i/\Pi]$; brackets indicate integer part. Equivalently, $\underset{\sim}{\phi} = \underset{\sim}{t} \bmod (\Pi)$. We now pick M samples from $\underset{\sim}{x}$ using the criterion that all the members of sample j have similar ϕ_i. Usually the full phase interval (0,1) is divided into fixed bins, but the samples may be chosen in any way that satisfies the criterion. All points need not be picked, or, alternatively, a point can belong to many samples. The variance of these samples gives a measure of the scatter around the mean light curve defined by the means of the x_i in each sample, considered as a function of ϕ. We define the statistic

$$\theta = \frac{s^2}{\sigma^2} \qquad (3)$$

where s^2 is given by equation (2) and σ^2 is given by equation (1). If Π is not a true period, then $s^2 \approx \sigma^2$ and $\theta \approx 1$, whereas if Π is a correct period θ will reach a local minimum compared with neighboring periods, hopefully near zero.

Since this technique seeks to minimize the dispersion of the data at constant phase, we will refer to it as "phase dispersion minimization", or PDM for short. Mathematically, this is a least-squares fitting technique, but rather than fitting to a given curve (such as a Fourier component), the fit is relative to the mean curve as defined by the means of each bin. We simultaneously obtain the best least-squares light curve and the best period. The PDM technique is thus a "Fouriergram" method [as discussed by Faulkner (1977)] of infinite order, since all harmonics are included in the fitted function. The Fourier series technique, a least squares fit to a truncated series with variable amplitudes and phase, often requires additional constraints and rather high orders for nonsinusoidal variations (Lucy, 1976).

Although the individual samples may be chosen in many ways, it is convenient to define a standard bin structure. We divide the unit interval into N_b bins of length $1/N_b$, and take N_c "covers" of N_b bins, each cover offset in phase by $1/(N_bN_c)$ from the previous cover, using

periodic conditions on the unit interval to obtain a uniform covering. We thus obtain $M = N_b N_c$ bins, each of length $1/N_b$, and whose midpoints are uniformly spaced along the unit interval at distance of $1/(N_b N_c)$. Clearly, each data point will fall in exactly N_c bins. Denote a given bin structure by (N_b, N_c).

To compute Θ, we take the ratio of variances of the two subsets of $\underset{\sim}{X}$, that of the actual observations, $\underset{\sim}{x}$, and that of the bins. Θ therefore has a probability density given by an F distribution with $\Sigma n_j - M$ and $N-1$ degrees of freedom. It is convenient to define F as a number greater than unity, so $F \equiv \Theta^{-1}$. The probability, P, that a given value of Θ is due to random fluctuations (also called the "significance") is twice the area of the F distribution above Θ^{-1} (two-sided test). This probability approaches unity as $\Theta \to 1$. Thus, for significance P, we compute

$$F_{(P/2, N_{1f}, N_{2f})} = 1/\Theta, \quad N_{1f} = N-1, \quad N_{2f} = \Sigma n_j - M. \tag{4}$$

P may then be obtained by reference to an F table, or using an approximation to $P(F, N_{1f}, N_{2f})$, see Abramowitz and Segun (1965), § 26.

If N is large (> 100), we may take $\sigma^2(\underset{\sim}{x}) \approx \sigma^2(\underset{\sim}{X})$. In this case we may use the somewhat simpler χ^2 test,

$$\chi^2_{(P/2, N_f)} = N_f \Theta , \quad N_f = \Sigma n_j - M. \tag{5}$$

Here P is twice the area of the χ^2 distribution below $N_f\Theta$.

II. THE WR METHOD

An interesting related method is discussed by Whittaker and Robinson (1926, "WR") in which one seeks the maximum variance of the bin means (as opposed to the mean of the bin variances). If s_m^2 is the variance of the bin means, define $\Theta_{WR} = 1 - s_m^2/\sigma^2$ for comparison purposes. In general Θ_{WR} will vary between 0 and $1 - \langle 1/n_j \rangle$, where $\langle n_j \rangle$ is the mean number of points per bin. At a true period $s_m^2 \approx \sigma^2$ and $\Theta_{WR} = 0$. Here we seek periods at which the amplitude of the mean curve is a maximum, which in most cases will correspond to minimum phase dispersion. The calculation of σ_m^2 is easier than s^2 (equation 2), but the number of degrees of freedom is much lower, suggesting less sensitivity (see § III). We will show below that in most cases this supposition is true, although for one range of parameters the WR technique may be preferrable. The WR method is discussed in detail by Chapman and Bartels (1940) under the title "persistence analysis".

A statistical criterion may also be derived for the WR technique. The distribution of bin means is normal if M is large with $\sigma_m^2 = \sigma^2/n_j$. Since M is generally not large, however, a t distribution with M-1 degrees of freedom will actually be obtained, with $\sigma_m^2 \approx (M-1)/(M-3)\ \sigma^2/n_j$. We may always select bins with $n_j = N/N_b$, for all j. Note that normal constant-phase bins will produce binomially distributed n_j and increase σ_m^2 since a harmonic mean of n_j appears in σ_m^2. We wish to test whether the observed s_m^2 is significantly bigger than σ_m^2. Evidently s_m^2/σ_m^2 follows an F distribution with M-1 and N-1 degrees of freedom. Using the definition of Θ_{WR}, we have

$$F_{(M-1,N-1)} \approx \frac{(M-3)}{(M-1)} \frac{N}{N_b} (1-\Theta_{WR}). \qquad (6)$$

III. APPLICATIONS

Here I will briefly describe the practical aspects of these methods; for details see Stellingwerf (1978).

Typical transforms are illustrated by Figure 1, which shows the computed Θ-transforms for a sine wave [sin(2πft)], panel A, and a

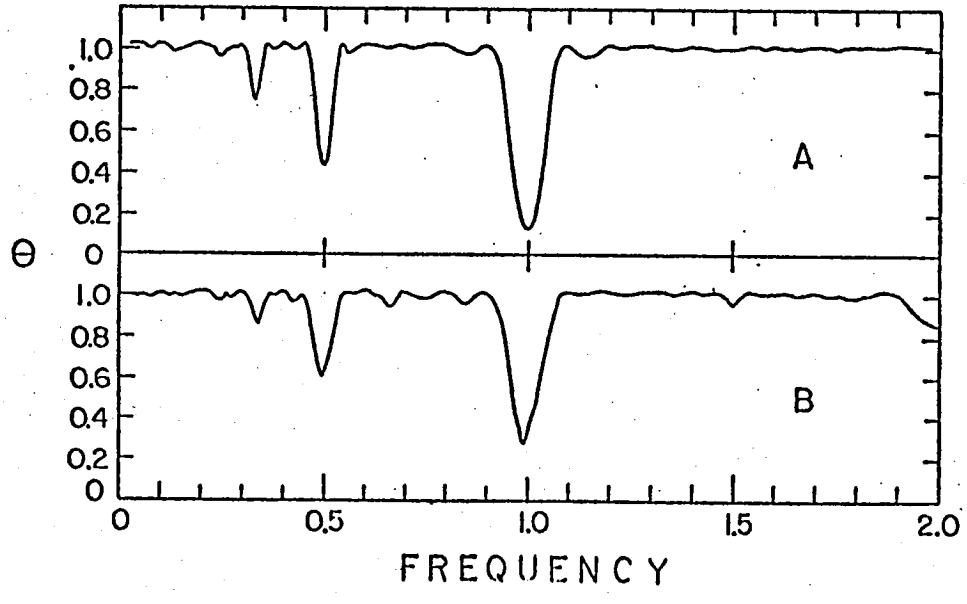

Fig. 1: Θ statistic versus frequency for the two test cases described in the text. Panel A: sine-wave transform; Panel B: sawtooth function transform.

"saw-tooth" function (fractional part of ft), panel B. These functions have been selected because they represent the two extremes found in variable star light curves. In each case x consisted of 201 data points evenly distributed over ten periods with f = 1, T = 10. A bin structure of $(N_b,N_c) = (5,2)$ was used. The main line at f = 1 is virtually identical to the Fourier power spectrum line shape $[(\sin(x)/x)^2]$. Two subharmonics are present (the third, just visible at f = 1/4 is below the cutoff $n = N_b \approx 3$, and is not significantly different from 1). The great similarity of the two curves shown in Figure 1 is, of course, the strong point of the PDM technique: highly nonsinusoidal variations are handled just as efficiently as a sine wave. The presence of subharmonic response could be a disadvantage if oscillations with widely spaced frequencies are present. In practice, however, subharmonics can be distinguished in at least three ways: 1) light curve shape, 2) narrow line widths, 3) reduced significance with increasing bin size. If initial scans of the full frequency range use broad bin sizes [(5,2), say], subharmonics should pose no problems.

It is important to know the number of observations required to achieve a given significance with these methods. This quantity ("N") is plotted in Figures 2 and 3 as a function of the signal-to-noise ratio, $\varepsilon = \sigma/\sigma_{Noise}$. A variety of bin structures are shown. It is seen that coarse bins and multiple covers are needed for small N and ε. Clearly, the PDM technique is superior at small N, while the WR technique seems preferable in noisy cases ($\varepsilon < 0$) if N is large enough. Accuracy is lost if bins are too wide, and multiple covers will not help if many bins contain the same points. In general (5,2) structure works very well. To obtain mean curves for prewhitening, bins should be made as fine as possible.

IV. MULTIPLE PERIODS OF BK CEN

To illustrate the use of these methods, we briefly present an analysis of the light variation of the double-mode Cepheid BK Centauri. For this purpose we will use only the 49 photoelectric measurements made by C. J. van Houten in 1965 for which Leotta-Janin (1967) has published the ΔV values. This author comments that "their number is too small to allow a reliable determination of the beat period" and so uses 25 years of plate estimates as well as knowledge of other Cepheid period ratios to obtain $\Pi_0 = 3^d.17389$, $\Pi_1 = 2^d.2366$. We have found that the photoelectric points alone unambiguously confirm these results, and provide information on mode interaction as well.

The 49 measures span 137 days. Line widths will therefore be about 0.007 in frequency, so the frequency step size was taken to be .0015 for moderate resolution. Twelve nights have two observations, providing minimal alias discrimination. Although the measurements are quite accurate, we nonetheless estimate $\varepsilon \approx 1.5$ due to the secondary oscillation. Figures 2 and 3 indicate that the PDM and the WR techniques should be about equally good for this case, provided $N_b<10$. We choose a (5,2) bin structure to maintain about 10 points per bin.

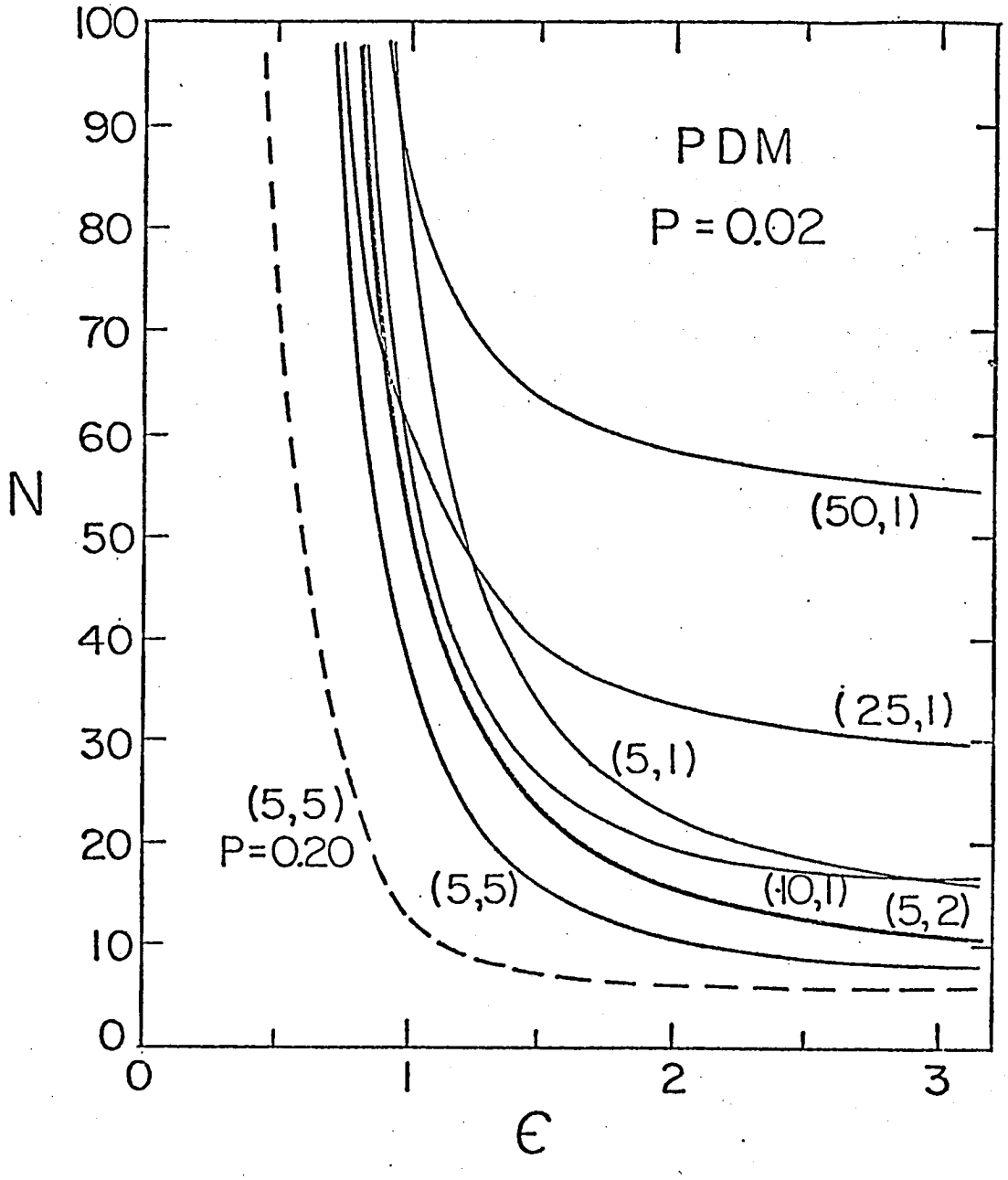

Fig. 2: Statistical characteristics of the PDM method. Notation as in text with various bin structures (N_b, N_c) as indicated. Solid lines refer to P = 0.02, dashed line is P = 0.20.

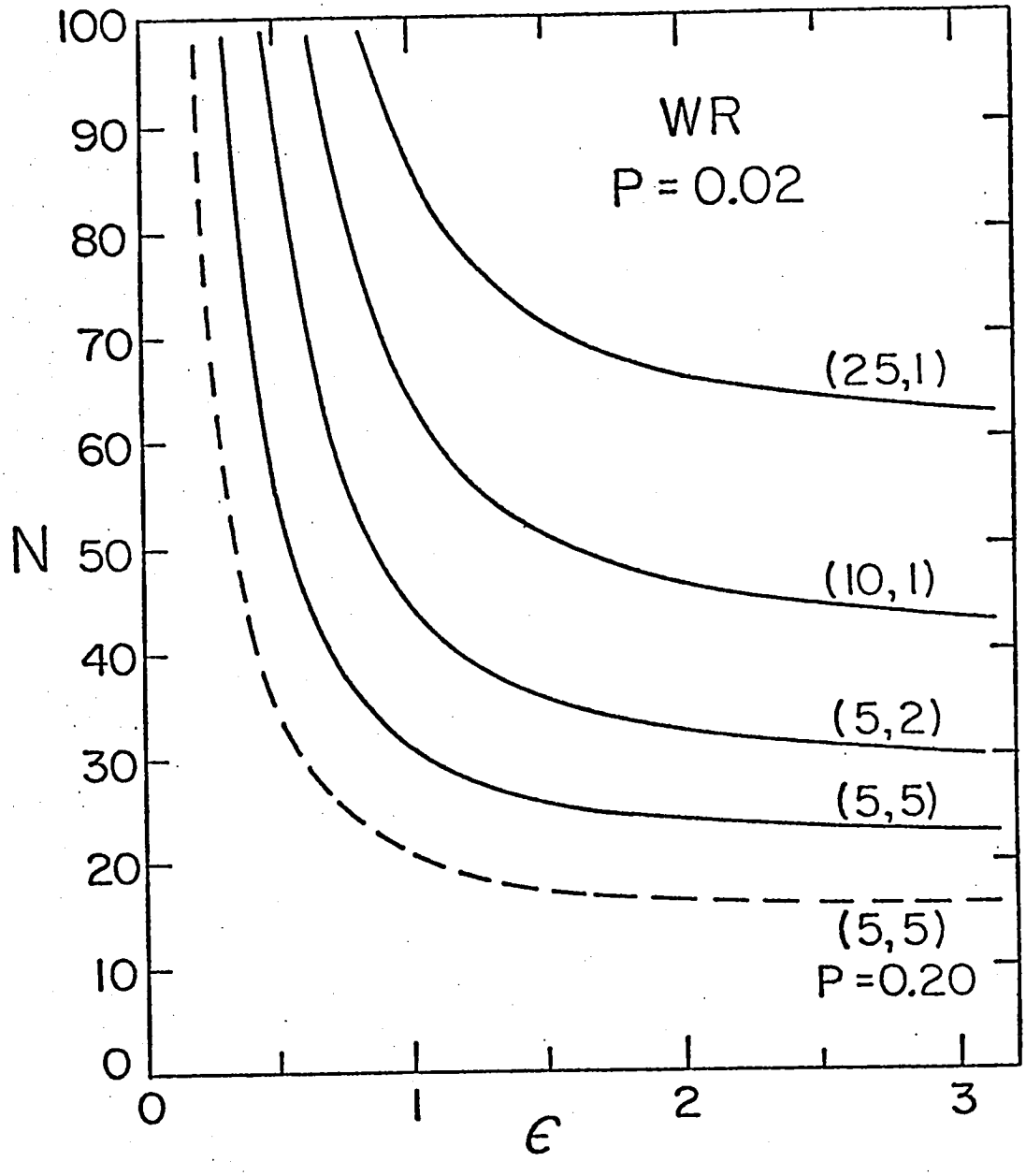

Fig. 3: Statistical characteristics of the WR method. Notation as in Fig. 2.

Figure 4, panel A shows the Θ transform of the raw data. The primary period is clearly evident (minimum e), with minima a and b forming the standard subharmonic sequence found in Figure 1. Minimum f is narrow and showed a two-cycle mean curve, it is therefore the

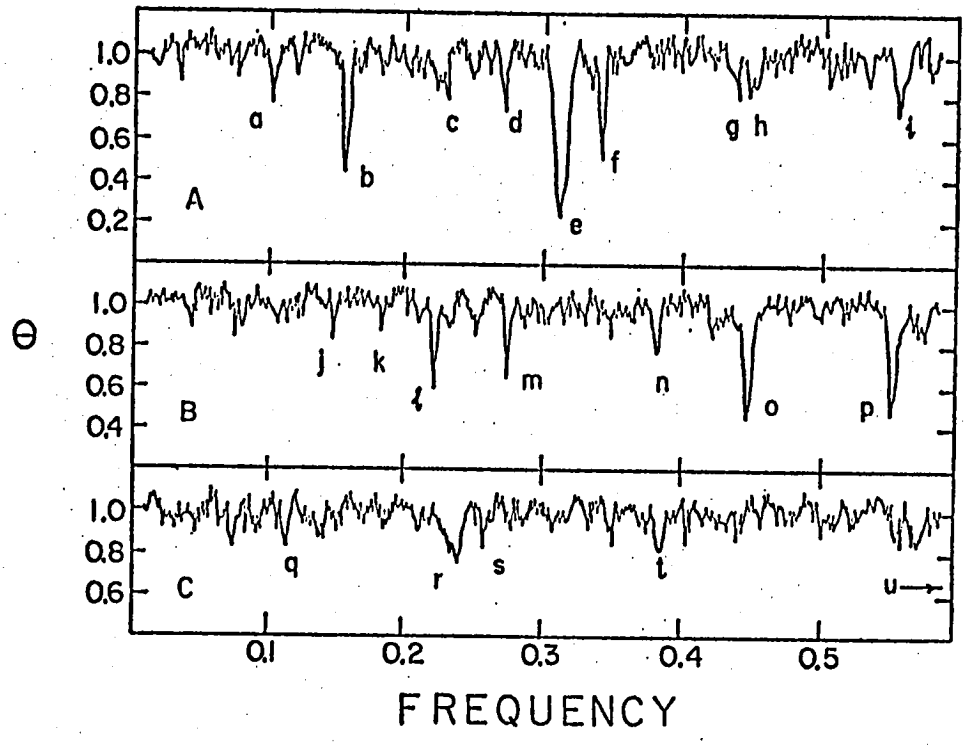

Figure 4: Θ transforms of the BK Cen data, plotted versus frequency in cycles/day. Panel A: transform of the raw data. Panel B: transform of the data after removal of the fundamental oscillation. Panel C: transform of the data after removal of the fundamental and first overtone oscillations. Labeled minima are identified in Table 1.

first subharmonic of a sizeable minimum off the scale, at $f \approx 0.7$. This is the main alias of e, occuring at $1-f_0$. Comparison of the subharmonics b and f indicates that e is the principal frequency. The identifications of the minima, together with their approximate frequencies and significances, are given in Table 1. Among the barely significant group, we identify g as the second subharmonic of the second alias of e, at $1+f_0$, while d, h and i are first overtone features.

We see here a distinct advantage of the subharmonic response of this method: any other major frequency in the range .6<f<1.2 would show a subharmonic on Figure 1(A) comparable to b or f. Any minimum in the range 1.2<f<1.8 would show a second subharmonic comparable to

TABLE 1

Identification of Features in Figure 4

Feature	Identification	Frequency (d^{-1})	Significance
a	$f_0/3$	.105	0.13
b	$f_0/2$	.158	0.00
c	$(1-f_0)/3$	.226	0.39
d	$(1-f_1)/2$	.276	0.09
e	f_0	.316	0.00
f	$(1-f_0)/2$	.344	0.00
g	$(1+f_0)/3$	.439	0.24
h	f_1	.447	0.27
i	$1-f_1$	.553	0.05
j	$f_1/3$	.148	0.50
k	$(1-f_1)/3$	.183	0.55
l	$f_1/2$	.224	0.04
m	$(1-f_1)/2$	.276	0.08
n	$(f_0+f_1)/2$	.385	0.33
o	f_1	.447	0.00
p	$1-f_1$	.553	0.00
q	$(1-(f_0+f_1))/2$	.116	0.60
r	$1-(f_0+f_1)$	.235	0.27
s	$(f_0+f_1)/3$	.253	0.55
t	$(f_0+f_1)/2$	.383	0.43
u	f_0+f_1	.764	0.11

a or g. Since all features have been identified, no high frequency components exist. This "look-ahead" feature can be extended by increasing N_b, at the expense of further complicating the spectrum.

Having identified the principal frequency (f_0), this component was then removed from the data (using linear interpolation between bin means). The transform of the reduced data is shown in panel B of Figure 1. Here j, l, o are due to the first overtone, while k, m, p represent the aliases. Note that each alias feature is slightly less significant than the corresponding "real" feature. A mode interaction feature, n, has also appeared. We can again conclude that no more significant modes exist to f = 1.8, since no subharmonics appear.

Panel C shows the transform of the doubly-reduced data. No significant feature appears, but many marginal features are related to the mode interaction term f_0+f_1. An extension of the transform to higher frequencies showed that this mode did indeed appear at the P = 0.11 level. This is the only remaining significant mode. This particular interaction term (f_0+f_1) has also been found to be excited in several other studies of similar objects (Fitch 1976, Henden 1976, Faulkner 1977a,b, Fitch et.al. 1978). In particular, this term invariably dominates the beat frequency (f_1-f_0) component. At present the

meaning of this is not clear.

The periods and amplitudes of the three components were determined using a finer frequency scan, and are given in Table 2. Allowing for the bin size, the actual amplitudes should be about 20% larger, this is

TABLE 2

Summary of Principal Components

Mode	Frequency (d^{-1})	Period (d)	Amplitude	Adjusted Amplitude	Phase*
f_0	0.3153	3.172	$0^m.544$	$0^m.648$	0.40
f_1	0.4473	2.236	$0^m.222$	$0^m.264$	0.56
f_0+f_1	0.7662	1.302	$0^m.151$	$0^m.180$	0.16

*Phase = $(t_{max}-t_1)/\Pi_0$, t_1 = JD2,438,813.48

shown in the "corrected amplitudes". The sum of these estimates is $1^m.1$, in agreement with the range of the photoelectric measures. The standard deviation of the residuals (triply-reduced data) was $0^m.048$.

The frequency labeled f_0+f_1 in Table 2 is listed as derived and differs from the sum of the principal components. The discrepancy may not be real, since it amounts to about 1/T -- suggesting a side lobe problem.

This research is supported by NSF grant AST 77-26993 through Rutgers University.

References

Abramowitz, M., and Segun, I. A., 1965, Handbook of Mathematical Functions, (Dover, N. Y.).

Brault, J. W., and White, O. R. 1971, Astr. and Ap., 13, 169.

Chapman, S. and Bartels, J. 1940, Geomagnetism, (Oxford, London), Volume 2, p. 545.

Cox, A. N., Hodson, S. W., and King, D. S. 1978, Ap. J., in press.

Faulkner, D. J. 1977a, Ap. J., 216, 49.

Faulkner, D. J. 1977b, Ap. J., 218, 209.

Fitch, W. S., 1967, Ap. J., 148, 481.

Fitch, W. S. and Szeidl, 1976, Ap. J., 203, 616.

Henden, A. A. 1976, Proc. of the Los Alamos Solar and Stellar Pulsation Conf., ed. A. N. Cox and R. G. Deupree, Los Alamos Report LA-6544-C, p. 202.

Hesser, J. E., Ostriker, J. P., and Lawrence, G. M. 1969, Ap. J., 155, 919.

Lafler, J., and Kinman, T. D. 1965, Ap. J. Supp., 11, 216, "LK".

Lucy, L. B. 1976, Ap. J., 206, 499.

Ostriker, J. P., and Hesser, J. E. 1968, Ap. J., 153, L151.

Stellingwerf, R. F. 1975, Ap. J., 199, 705.

Stellingwerf, R. F. 1978, Ap. J., in press, (Sept. 15).

Stobie, R. S. 1977, M.N.R.A.S., 180, 631.

Stobie, R. S. 1972, M.N.R.A.S., 157, 167.

Stobie, R. S., and Hawarden, T. 1972, M.N.R.A.S., 157, 157.

Wehlau, W., and Leung, K. 1964, Ap. J. 139, 843.

Whittaker, E. T., and Robinson, G. 1926, The Calculus of Observations, (Blackie and Son, London), "WR".

Discussion

A. Cox: What is the σ of the data after you've taken the periods out?

Stellingwerf: The residual σ following the triple reduction was $\sigma \approx 0.05$ magnitudes.

OPTICAL OBSERVABLES IN STARS WITH NON-STATIONARY ATMOSPHERES

R. W. Hillendahl
Science Applications, Inc.
2680 Hanover Street
Palo Alto, California

ABSTRACT

Experience gained by use of cepheid modeling codes to predict the dimensional and photometric behavior of nuclear fireballs is used as a means of validating various computational techniques used in the cepheid codes. Predicted results from cepheid models are compared with observations of the continuum and lines in an effort to demonstrate that the atmospheric phenomena in cepheids are quite complex but that they can be quantitatively modeled. It is hoped that the discussion may provide guidance for cepheid observers.

INTRODUCTION

The application of the artificial viscosity technique (Von Neumann and Richtmyer, 1950) to the explicit hydrodynamic modeling of spherical systems (Brode, 1955) represents a fundamental milestone in computer modeling. Subsequently, Brode combined radiative diffusion with the hydrodynamic motion (Brode, 1956-1957), having incorporated the implicit Henyey method (Henyey, Le Levier, Levee, Böhm, and Wilets, 1959) with the assistance of Le Levier. He then produced the first radiation-hydrodynamic models of the fireball which results from a nuclear explosion in the atmosphere (Brode, 1958, 1959a, 1959b). Christy (Christy, 1964, 1967) later modified the Brode technique and applied it to his pulsation studies of stellar envelopes and thus laid the foundation for many subsequent investigations.

During the period where Brode was producing his models of fireballs, the present author was engaged in making astrophysical and photgraphic observations of fireballs (Hillendahl, 1959). This afforded an opportunity for the quantitative comparison of Brode's modeling techniques with observational data having a much higher degree of precision than is possible from stellar observations. The results of such comparisons validated the hydrodynamic and radiative diffusion techniques used by Brode, but identified the need for an improved treatment of the radiative transport in the observable atmospheric layers. As a student of Henyey, the author developed a radiation-hydrodynamics technique designed to treat all regions of the star (Hillendahl, 1962,

1964) which was used both for cepheid modeling and in a relaxation technique (Hillendahl, 1965a) for the study of stable Henyey models. This "SUPER NOVA" code was later adapted for use in an extensive study of fireballs (Hillendahl, 1965b, 1966).

This presentation provides a brief review of selected numerical and interpretational techniques which have a proven usefullness, and a description of some physical processes which the computer models predict to occur in stellar atmospheres.

It is well established that some features of stellar models are sensitive to particular details of the computational technique. For example, the behavior of a cepheid model employing the artificial viscosity technique may be dependent upon the formulation used. One approach to resolving such difficulties is a careful comparison against data. Another approach is for a number of modelers to use their codes to model a well defined test case so that differences due to computational techniques can be identified. Both techniques have been used extensively by the fireball modelers (Brode, 1965). Much of this material is no longer subject to government security restrictions. The brief exposition given here is intended to allow the stellar modeling community to benefit from these findings and to reduce the number of uncertainties in their models.

Brode (1965) compared "standard model" calculations performed by a number of investigators. He demonstrated conclusively the importance of an accurate equation of state which includes the relevant dissociation and ionization processes. He also demonstrated that equation of state must maintain the correct relationship between the pressure P and internal energy E if predicted hydrodynamic phenomena are to correspond to the experimental observations. Thus if curve fits or data tables are used in the computational model, care must be taken to see that the correct relationship between P and E is reproduced. False hydrodynamic signals may otherwise be produced.

The artificial viscosity technique is a useful device in the treatment of shock discontinuities. The literature abounds with various versions referred to as "linear", "quadratic", "quartic"; various versions formulated in terms of velocity gradients and/or compression ratios; and various recommended values for the damping constant. Many of these have proven to be applicable over limited ranges of the variables or only under limited circumstances. The formulation discussed by Richtmyer (Richtmyer and Morton, 1967, page 319) has been shown (Hillendahl, 1965b) to accurately (±2%) reproduce, without adjustment, the shock front properties in a nuclear fireball while the shock pressure changes some six orders of magnitude. Furthermore, the shock structure produced by the model satisfies the Rankine-Hugeniot conditions to a high degree of accuracy. One has no reason to expect that the Richtmyer formulation would not perform equally well in stellar calculations.

A useful technique for locating shock fronts and related phenomena at a given epoch is a listing of the quantity Q/P as a function of mass or radius, where Q is the artificial pressure and P is the gas pressure. Non-zero values, which indicate a compression of the gas, are then easily identified. The largest value of Q/P occurs as the shock front is in the process of transversing a given zone. This behavior has been employed as a shock locator (Simpson, 1973) and as a print control to cause the radial structure to be displayed at the instant the shock compression of a given zone is complete.

In a model using the artificial viscosity technique, the Rankine-Hugeniot conditions are satisfied on a time averaged basis, but not always on an instantaneous basis. Use of the Simpson technique automatically selects epochs when these conditions are satisfied and make the data analysis process simpler.

In the interest of conserving computer time, most modern codes employ continuously variable time steps chosen to satisfy various hydrodynamic, radiative, or energetic criteria. With this capability available, the last time step during compression of the zone can be chosen so as to cause a print-out precisely at the end of the compression of the zone in question. The effects of finite zoning upon the time history of the shock location and the shock properties are then minimized.

Use of the artificial viscosity technique results in a compression of the material ahead of the true shock front. This compression results also in a false temperature rise. At temperatures lower than about $15,000^{\circ}K$, the absorption coefficient of the gas is very temperature dependent ($\sim T^{9}$) and the artificial compression can thus result in the creation of false optical properties ahead of the shock. Under conditions where the pre-shock gas would be transparent, and the post-shock gas opaque, an artificial photosphere will will be created having a temperature lower than the post-shock temperature. The emergent flux is then depressed. Thus a sudden depression in the computed light output of a cepheid model may be associated with the emergence of a shock wave.

Two aspects of this distortion of the temperature profile by the artificial viscosity are of interest. Simpson (1973) conducted numerical experiments on fireball shock waves in which he artificially increased the opacity by a factor of 10^6. When the post-shock temperature was below $10^{4\circ}$K, he found that this opacity increase had a negligible effect upon the temperature and density profiles because the radiative transfer could not compete with the hydrodynamics at lower temperatures. It is clear, however, that the false compression due to the artificial viscosity does affect the radial heat flow, but only in a transient manner. By separately printing out the hydrodynamic and radiative terms of the energy equation, one can assess their relative importance and also to determine whether a particular configuration exists long enough to result in a distortion of the temperature profile. This type of distortion has not proven to be important if the zone structure if fine enough to meet the other requirements of good modeling.

If one desires to obtain high quality optical output as a shock wave emerges through the photosphere, it may be necessary to correct the distorted regions of the temperature, density, and velocity profiles. The quantity Q/P described above is very useful in controlling this process. When the artificial pressure is small compared to the gas pressure, no correction is needed. When corrections are needed, the "distorted" values are temporarily stored so that they can be

recovered in order to proceed with the pulsation model. Substitute values are then used to compute the observable properties at the epoch in question. Some investigators, e.g., C. G. Davis (LASL), prefer not to interrupt the main calculation. They store the configuration at epochs of interst for later "snap-shot" light output calculations.

The estimation of these corrected values is relatively easy in fireball modeling as the profiles ahead of the shock are usually known. Two techniques have been used in cepheid modeling: space extrapolation and time extrapolation. In both techniques data prior to the artificial viscosity distortion are used to predict the needed substitute values. The choice between the two methods is made on the basis of the slowest rate of change of the zone properties in either time or space.

The appearance of a region where Q/P is greater than zero may not indicate the presence of a shock front. If the disturbance moves toward a region of lower pressure it is likely to be a shock wave. If the disturbance moves toward a region of higher pressure, it may be an unloading or rarefaction wave. The optical properties of various waves are discussed below.

Because of the demonstrated inability of radiative diffusion techniques to adequately reproduce the optical observables from nuclear fireballs, it is to be expected that such techniques would also have similar deficiencies when applied to the atmospheres pulsating stars. Here one is faced with the classical problem of radiative

transfer, i.e., the equation of transfer of radiation describes change in the intensity for a given radiation frequency and along a given direction in space. To obtain the radiative flux divergence it is necessary to integrate over both the frequency and over all directions in space. One approach is to use a large number of rays at various angles and a large number of radiation frequencies. One fireball code employing this approach used about 250 hours of machine time to model the equivalent of one period of a star. The SUPER NOVA technique (Hillendahl, 1964, 1965) produced virtually indistinguishable results and utilized only about 1 hour of machine time (about 5 minutes equivalent CDC 7600 time). In this technique, the source function is expanded in a Taylor series, in terms of optical distance, centered on each zone boundary. An integral formulation of the equation of transfer is applied to the finite zone configuration in an equivalent ray approximation. This results in direct and chord transmission terms, and in a series of emission terms. In the optically thin extreme, the zero order emission term reproduces the Planck approximation. In the optically thick extreme, the first order term reproduces the Rosseland approximation. Higher order terms are truncated. The formulation leads to a novel technique for spectral averaging that is a finite zone equivalent of the Chandrasekhar or flux weighted mean.

An important feature of this formulation is that it provides a reasonably high order solution to the well known problem in cepheid modeling in which the opacity increases very rapidly at the photosphere causing one zone to be very optically thick and the next exterior

zone to be nearly transparent. This difficulty arises when a Rosseland mean or equivalent opacity approximation is used in which the opacity of a zone depends only upon the local temperature. The zone exterior to the photosphere has a low temperature and thus a low opacity. It cannot absorb radiation and must depend upon hydrodynamic compression to heat it sufficiently to increase its opacity so that the absorption of outward flowing radiation can begin. The SUPER NOVA formulation employs transmission functions for the outwardly directed radiation which are of the form

$$T = \frac{\int_{\lambda} B_{\lambda}(T_s)\ \exp(-\mu_{\lambda}\ell)d\lambda}{\int_{\lambda} B_{\lambda}(T_s)\ d\lambda}$$

wehre T is the outward transmission

ℓ is the zone thickness along the characteristic ray

T_s is the temperature of the next interior zone

B_{λ} is the Planck function

λ is the wavelength

μ_{λ} is the local spectral absorption coefficient and is a function of the local gas density and temperature.

In common with the Planck and Rosseland means, the transmission function depends upon the local temperature and density of the gas. But it also depends upon the zone thickness and temperature of the "source" zone. It is therefore a function of four variables instead of two.

In practice these functions are computed in great detail in a preliminary calculation from detailed spectral absorption coefficient codes. Because of the existence of absorption edges, and because the Planck distribution is a function of λT, it is convenient to index these precomputed data in terms of T_s and λ_z, where T_s is a property of the source zone and λ_z depends only on the properties of the zone whose transmission is desired. This affords a reduction in complexity which makes the method workable.

Other investigators have used the Rosseland approximation in the interior and a finite number of spectral bands in and exterior to the photosphere. Both of these methods provide for the non-gray radiative heating of the gas prior to shock compression which cannot be accounted for with an unmodified diffusion approximation. With the great increase in computer capabilities since the SUPER NOVA technique was developed, the later technique is probably to be preferred because less effort is involved when the chemical composition is changed.

ATMOSPHERIC OBSERVABLES

The fireball from a nuclear explosion is a relatively simple object in the astrophysical sense. If one considers only relatively high energy explosions, then the nuclear device simply causes the formation of a hot isothermal sphere of air and exerts no significant influence on the subsequent hydrodynamic and radiative development which follows. Even so, this relatively simple object exhibits a great deal of structure involving periods of radiative growth, the formation of shocks, hydrodynamic growth, rarefaction waves, radiative cooling waves, dissociation fronts that mimic H II regions, absorption shells, and similar phenomena.

Pulsating stars are much more complex objects than fireballs because the gas ahead of the expanding shock front is not of uniform density. One would, therefore, expect that the atmospheric phenomena might be even more complex than in the fireball.

In the case of the fireball, the author (Hillendahl 1966) demonstrated the capability of the SUPER NOVA cepheid modeling code (as modified for air) to quantitatively model the atmospheric phenomena which occur in fireballs. Both the hydrodynamic and radiative phenomena predicted by the code are verified by photographic and photometric measurements. If the same modeling techniques are used on a cepheid, what type of atmospheric phenomena are predicted? Can any or all of these phenomena be confirmed by observation?

In an attempt to answer these questions, a number of models of a 7.6 day cepheid were computed and analyzed using analysis techniques developed from fireball experience. The model consisted of a periodic envelope model supplied by Christy (1968) to which an extended atmosphere was appended. The augmented models remain periodic in the denser envelope regions, but never reach a completely repetitive behavior in the extreme outer layers where mass loss is predicted to occur (Hillendahl 1970). The physical phenomena discussed below are not dependent upon the precise periodic behavior of the star.

Figure 1 shows the radius-time history of every fifth mass point in the computed model. Although several shock fronts (S1, S2, S3) have been labeled, it is clear that little, if any, detailed information can be obtained or illustrated on such a radius-time display. Figure 2 shows the same model displayed in a different fashion. Various shock fronts and rarefaction waves which have been identified are labeled S and R, respectively. The photosphere (τ=1) has been indicated by the continuous line.

For a shock front to be observable in continuum light, it must occupy the photospheric region of the star. In the model shown, the thickness of the photosphere is from 1 to 2 mass zones throughout the cycle. Thus, the model predicts that shock waves, including the very strong shock S2 which "drives" the pulsation, will occupy the photosphere only for very brief intervals in time, i.e., of the order of 1-3 hours in a 7-day cepheid.

Since the cepheid light curve rises over a time interval of several days, it is clear that the light being observed is not being emitted by the shock front itself.

In the nuclear fireball, the rapid rise in the light curve, which follows after the expanding shock becomes transparent, results from the rapid density decrease on the back side of the shock front. Interior to the shock front, the density decreases rapidly in the inward direction, while the temperature rises rapidly so as to maintain a nearly constant pressure behind the shock. Just after shock transparency, the photosphere resides in a layer of gas just behind the shock front. As the whole system expands radially, the density at every point on the back of the shock decreases with time in order to conserve mass. This decrease in density lowers the opacity of the photospheric layer and causes the photosphere to progress inward in terms of mass and toward regions of higher temperature. Since the opacity depends strongly on the temperature and weakly on the density, only a slight increase in temperature is needed to compensate for the density decrease. Thus, the photosphere moves inward relatively slowly in terms of the mass coordinate, and actually moves outward in terms of radius.

During rising light in the fireball, the radius of the photosphere increases by about a factor of two, while the light output may increase a factor of 50 or more. It is clearly the increase in temperature which is responsible for most of the light increase. This being the case, one expects, and observes, a larger

amplitude for wavelengths to the short wavelength side of the maximum of the Planck function, i.e., the amplitude is larger in blue light just as in the cepheid.

The model calculations predict that the same mechanism operates during the rising light phases in a cepheid. During these phases, the models predict an abrupt spatial density decrease on the back side of the shock front. If one follows a given shock as it emerges from deep in the star, it is found that the density profile behind the shock changes rapidly with radius. In most regions of the star, the density minimum behind the shock is only about 30% below the shock front density. However, when the gas undergoes thermal ionization as it crosses the shock, the density minimum is as much as a factor of 10 lower than the shock front density. This phenomenon is easily explained. The ionization increases the number of particles and hence the gas pressure. The increased pressure forces the gas to expand thus lowering its density.

Clearly then, the amplitude of the light curve depends upon the magnitude of the density decrease behind the shock, which in turn depends upon the shock compression to dissociate or ionize the gas. One would, therefore, expect pulsating stars to be highly visible if an ionization or dissociation zone happens to occur near the photospheric layers. Estimates of the light amplitude caused by shock emergence when ionization is not present are of the order of 0.1 mag. (Hillendahl 1969).

Because of the real possibility that considerations such as these might contribute to an observational selection bias, further investigation seems to be indicated.

Maximum light (phase 0.0) in the cepheid apparently occurs when the photosphere has progressed down the back side of the shock density profile and arrives at the density minimum. The previously discussed process responsible for rising light is then interrupted. The model calculations then indicate an unloading or rarefaction wave then dominates the atmospheric phenomena (Hillendahl 1969, 1970). Figure 3 shows the density and temperature profiles at phase 0.103 during the rarefaction wave R2 (see Fig. 2). The density spike shown is not the shock wave, which has traversed the atmosphere, but is a residual structure resulting from the previously described series of events. The density minimum has a value of 5×10^{-10} gm cm^{-3}. The dashed box labeled "54" is a graphical device for denoting the mass zone in which the photosphere occurs. Its width is that of the mass zone and its height is a factor of 6. Graphs similar to Figure 3 have been used to construct a 16 mm movie which shows the atmospheric structure throughout the entire period.

The strange atmospheric profiles shown in Figure 3 provided the nucleus for an idea for the construction of "dynamic" model atmospheres (Hillendahl 1968) for cepheids. The temperature external to the photosphere is practically uniform, while the density profile is slab-like in appearance. Since the absorption

coefficient depends strongly on the temperature and weakly on the density, the profile was approximated by a slab of uniform temperature and density overlying a blackbody photosphere.

Using a very detailed code for computing the spectral absorption coefficients, simple models were constructed using the photospheric temperature T_b and the slab temperature T_a, density ρ_a, and thickness Δ_x as variable parameters (Hillendahl 1968). Table 1 shows the results obtained using the "dynamic" model technique to match the spectral scanner data (Oke 1961) for Eta Aquilae. Outside the Balmer line blanketed region, the agreement is relatively good at all but a few wavelengths. The same technique was applied indiscriminately at all phases with the results shown in Table 2. At 14 of the 20 phases, the results are quite good.

Figure 4 shows the density of the semi-transparent slab as a function of phase and also the densities obtained by Fe line analysis (Schwarzschild, et al, 1948). Note the relatively good agreement and also the amount of detail. The shock and rarefaction labels correspond to those on the model results in Figure 2. One would expect to see a transient density increase after each shock wave emerges. Figure 4 appears to confirm this expectation.

The dynamic atmosphere technique also yields the relative radius as a function of phase. An absolute normalization of the radius can be obtained by two methods (Hillendahl 1968). The results of this analysis are

Table 1: Example of a Dynamic Atmosphere (Phase 0.10)

Wavelength Å	$B(T_b)$	Abs. Coeff.	$B(T_a)$	Calc. F	Obs. F	Calc. F/Obs. F	
10309	40.74	7.168(-12)	14.92	21.479	21.479	1.000	
7194	52.13	8.148(-12)	13.85	22.056	22.285	0.999	
5714	53.64	7.088(-12)	10.60	21.680	21.678	1.000	
5128	51.89	6.638(-12)	8.65	20.693	20.702	1.000	
5000	51.24	6.544(-12)	8.19	20.372	20.324	1.002	
4901	50.66	6.474(-12)	7.82	20.095	19.953	1.007	
4784	49.88	6.393(-12)	7.38	19.727	19.055	1.035	**
4673	49.04	6.319(-12)	6.94	19.334	19.589	0.987	
4566	48.14	6.252(-12)	6.53	18.920	19.055	0.993	
4464	47.19	6.192(-12)	6.12	18.484	18.031	1.025	**
4367	46.20	6.140(-12)	5.74	18.209	17.702	1.018	
4255	44.96	6.087(-12)	5.30	17.460	17.539	0.995	
4166	43.90	6.051(-12)	4.95	16.969	17.219	0.985	
4081	42.80	6.022(-12)	4.62	16.463	16.293	1.010	
4032	42.14	6.009(-12)	4.43	16.154	15.417	1.048	***
3906	40.34	5.986(-12)	3.95	15.311	13.677	1.119	***
3846	39.44	5.981(-12)	3.73	14.881	12.942	1.150	***
3774	38.29	5.618(-12)	3.46	15.060	10.578	1.425	***
3703	37.14	5.622(-12)	3.21	14.504	6.792	2.136	***
3636	35.99	1.437(-11)	2.98	5.549	5.495	1.010	
3571	34.85	1.396(-11)	2.76	5.421	5.346	1.014	
3508	33.71	1.359(-11)	2.55	5.293	5.297	0.999	
3448	32.58	1.325(-11)	2.36	5.163	5.754	0.897	**

$T_b = 8400^\circ K$ $T_a = 5500^\circ K$ RR = 0.9829

$U_s = 3.56\ (+06)$ $\Delta X = 1.247\ (+11)$ $U_a = 2.00\ (+06)$

** Difference greater than 2 percent, reason unknown

*** Balmer line effect

Units for Planck functions and fluxes are arbitrary scale.

Table 2: Dynamic Model Atmosphere Parameters for Eta Aquilae

Phase	T_b (^oK)	T_a (^oK)	ρ_a (gm cm^{-3})	ΔX (cm)	Relative Radius	Velocity	Quality of Result
0.55	11000	5300	1.20(-9)	4.41(11)	1.052	25.2	good
0.60	10800	5200	1.00(-9)	6.71(11)	1.051	16.9	good
0.65	12800	5300	8.37(-10)	8.75(11)	1.024	----	good
0.70	16600	5300	8.37(-10)	1.05(12)	1.020	----	good
0.75	11900	5300	1.44(-9)	3.78(11)	0.979	----	good
0.80	11000	5500	2.48(-9)	1.02(11)	0.966	-1.57	good
0.85	9600	5900	1.72(-9)	6.36(10)	0.908	7.92	good
0.90	9000	5700	2.48(-9)	3.40(10)	0.932	25.8	poor
0.95	8300	5800	1.43(-9)	3.20(10)	0.890	36.4	excellent
0.00	8700	5400	5.78(-10)	3.67(11)	0.929	43.5	poor
0.05	8050	5700	8.37(-10)	5.70(10)	0.930	37.1	poor
0.10	8400	5500	1.00(-9)	1.24(11)	0.983	35.7	good
0.15	8400	5900	2.07(-9)	2.53(10)	0.959	31.3	poor
0.20	9600	5800	3.00(-9)	3.02(10)	1.009	32.6	poor
0.25	11000	5900	3.00(-9)	3.24(10)	1.002	36.5	poor
0.30	10600	5900	2.50(-9)	4.09(10)	1.001	31.9	good
0.35	10000	5800	2.07(-9)	5.92(10)	1.015	26.4	good
0.40	9600	5600	1.20(-9)	2.00(11)	1.049	23.5	good
0.45	9400	5300	1.20(-9)	3.27(11)	1.056	21.1	good
0.50	10000	5400	1.44(-9)	2.45(11)	1.038	23.1	good

compared with other results (Whitney 1955) for Eta Aquilae in Figure 5.

The method of dynamic atmospheres should not be interpreted as a theoretical modeling technique, but rather as a means of interpreting observations of the stellar continuum. The agreement obtained for Eta Aquilae apparently occurs since hydrodynamic motion is responsible for the creation of the atmospheric profiles. Numerous attempts to fit the observed continuum from cepheids with radiative equilibrium model atmospheres have not proven successful over the entire width of the observed spectrum.

The cepheid models computed with the SUPER NOVA code also predict some interesting results relative to the line spectra from cepheids. During the first half of the period, when rarefaction waves dominate the atmosphere (Fig. 2), the atmospheres exhibit a large velocity gradient in which the particle velocity within the unloading region increases almost linearly with radius. Such a velocity gradient should have an observable effect on the shapes of spectral lines formed in this region of the star.

Line profiles have been computed (Hillendahl 1969) from the atmospheric profiles produced by the SUPER NOVA code. Figure 6 shows the computed profile for the λ 4508 Å line of Fe II and is labeled V=F(R). Other profiles shown were obtained by numerical experimentation in which the velocity was set to various constant values throughout the atmosphere.

In the computed profile, the velocity distribution is seen to produce an asymmetry in the line and to approximately double the equivalent width. A satellite line is obtained at approximately twice the Doppler shift of the main line. This results from velocity doubling in the unloading wave (Hillendahl 1970) and is similar to features often seen in stars above the main sequence - whether or not they are "pulsating".

Figure 7 shows computed lines for the H_β and Ca II K lines. The noticeable feature of the H_β line is the depression of the continuum over a broad region of the spectrum. Balmer line blanketing is thus predicted by the models and is apparently confirmed by the results of Table 1. The Ca II K line is quite broad and shows a weak red shifted emission core. This emission core results from the slight temperature inversion in the outermost region of the model (Fig. 3). The dashed line shows the change in the K line profile when this outer shell in the model is arbitrarily removed during the line profile calculation. The blue shifted profile with a red shifted core seems to be in agreement with the observations of Jacobsen (1956).

The SUPER NOVA model calculations also achieve some success in predicting the complex behavior which occurs when the cepheid atmosphere collapses. Figure 8 shows the predicted structure of the atmosphere for a 7.6 day cepheid at several phases. The heavy lines indicate various shock fronts and the photosphere. The finer lines are radius-vs-time trajectories for various mass

zones in the model. The numerical values indicate the local particle velocities in various regions.

Figure 9 shows the observed H_α profile for SV Vul as observed by Grenfell and Wallerstein (1969). The doppler shift measured from FeI lines is indicated by the arrow. (Note that the observed radial velocities would be approximately 17/24 of the particle velocities predicted by the model. However, the velocity applitude of SV Vμl is approximately 24/17 that of the 7.6 day model, so that the two effects tend to compensate).

At phase 0.84, the model predicts three distinct layers of material having velocities corresponding very well with the doppler shifts of the observed line cores.

The author's purpose in this presentation has been to demonstrate that relatively complex phenomena occurring in cepheid atmospheres. It is hoped that this discussion might provide guidance to cepheid observers in planning their programs and in limiting the duration of their observations so that they isolate in time the various features predicted by the models.

REFERENCES

Brode, H. L. 1955, J. Appl. Phys. 26, 766.

Brode, H. L. 1956, RM-1824-AEC.

Brode, H. L. 1957, RM-1825-AEC.

Brode, H. L. 1958, RM-2247.

Brode, H. L. 1959a, RM-2248.

Brode, H. L. 1959b, RM-2249.

Brode, H. L. ed., 1965, "Reliability of Current Nuclear Blast Calculations", Proceeding, of the DASA Conference on Nuclear Weapons Effects and Re-Entry Vehicles, DASA Report 1651 (Classified)

Christy, R. F. 1964, "Rev. Mod. Phys. 36," 555.

Christy, R. F. 1967, "Computational Methods in Stellar Pulsation", in Vol. 7 of "Methods in Computational Physics" ed. B. Alder. Academic Press, New York.

Christy, R. F. 1968, Private Communication.

Grenfell, T. C., and Wallerstein, G. 1969, P.A.S.P. 81, 732.

Henyey, L. G., LeLevier, R., Levee, R. D., Böhm, K. H., and Wilets, L. 1959, Astrophys. J. 129, 628.

Hillendahl, R. W. 1959, "Characteristics of the Thermal Radiation from Nuclear Detonations" AFSWP 902, Vols. I, II, III.

Hillendahl, R. W. 1962, Appendix B of "The Spectral Absorption Coefficient of Heated Air", DASA 1348, Unclassified.

Hillendahl, R. W. 1964, "Approximation Techniques for Radiation - Hydrodynamics Calculations", DASA 1522, Unclassified.

Hillendahl, R. W. 1965a, Proceedings of the Workshop on the Interdisciplinary Aspects of Radiative Transfer, J.I.L.A., ed. R. Goulard.

Hillendahl, R. W. 1965b, "Theoretical Models for Nuclear Fireballs" Part A, Lockheed Palo Alto Research Laboratories, DASA 1589 - LMSC BOO 6750, Unclassified.

Hillendahl, R. W. 1966, "Theoretical Models for Nuclear Fireballs (U)", DASA report 1589, Part B in 40 volumes, (Classified).

Hillendahl, R. W. 1968, "Atmospheric Phenomena in Classical Cepheids", dissertation, University of California at Berkeley.

Hillendahl, R. W. 1969, NBS Special Publication 332, "Spectrum Formation in Stars With Steady-State Extended Atmospheres".

Hillendahl, R. W. 1970, P.A.S.P. 82, 1231.

Jacobsen, T. S. 1956, Pub. Dom. Ap. Obs. Victoria, 10, 145.

Oke, J. B. 1961, Ap.J. 133, 90.

Richtmyer, R. D., and Von Neumann, J. 1950, J. Appl. Phys. 21, 232.

Richtmyer, R. D. and Morton, K. W. 1967, "Difference Methods for Initial Valve Problems", Second Ed., Interscience Publishers, New York.

Simpson. E. 1973, Science Applications, Inc., Palo Alto, California - Private Communication.

Schwarzschild, M., Schwarzschild, B., and Adams, W. S. 1948, Ap.J. 108, 207.

Von Neumann, J., and Richtmyer, R. D. 1950, J. Appl. Phys. 21, 232.

Whitney, C. 1955, Ap.J. 121, 682.

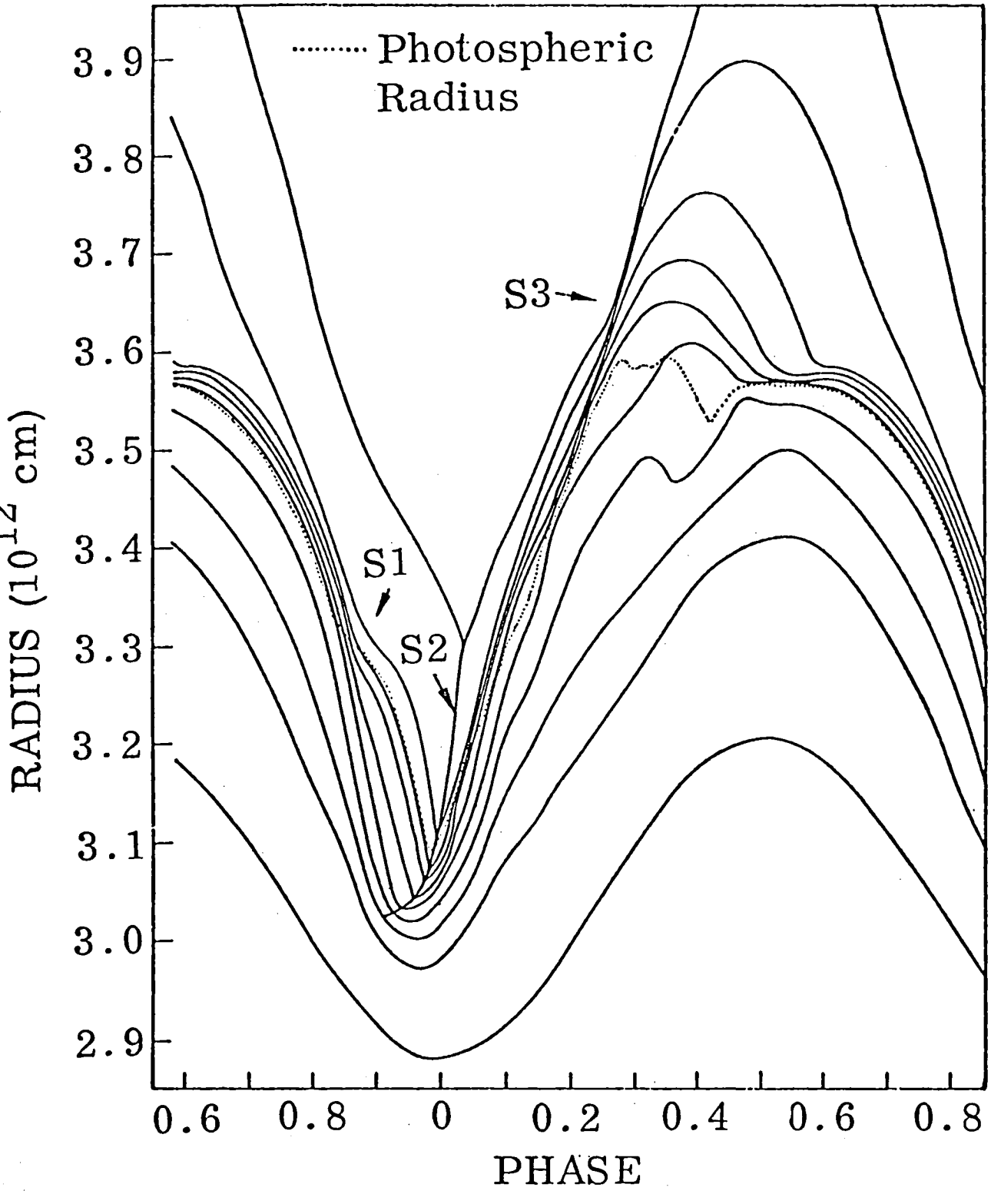

Figure 1. Radius-versus-Phase for a Cepheid Model

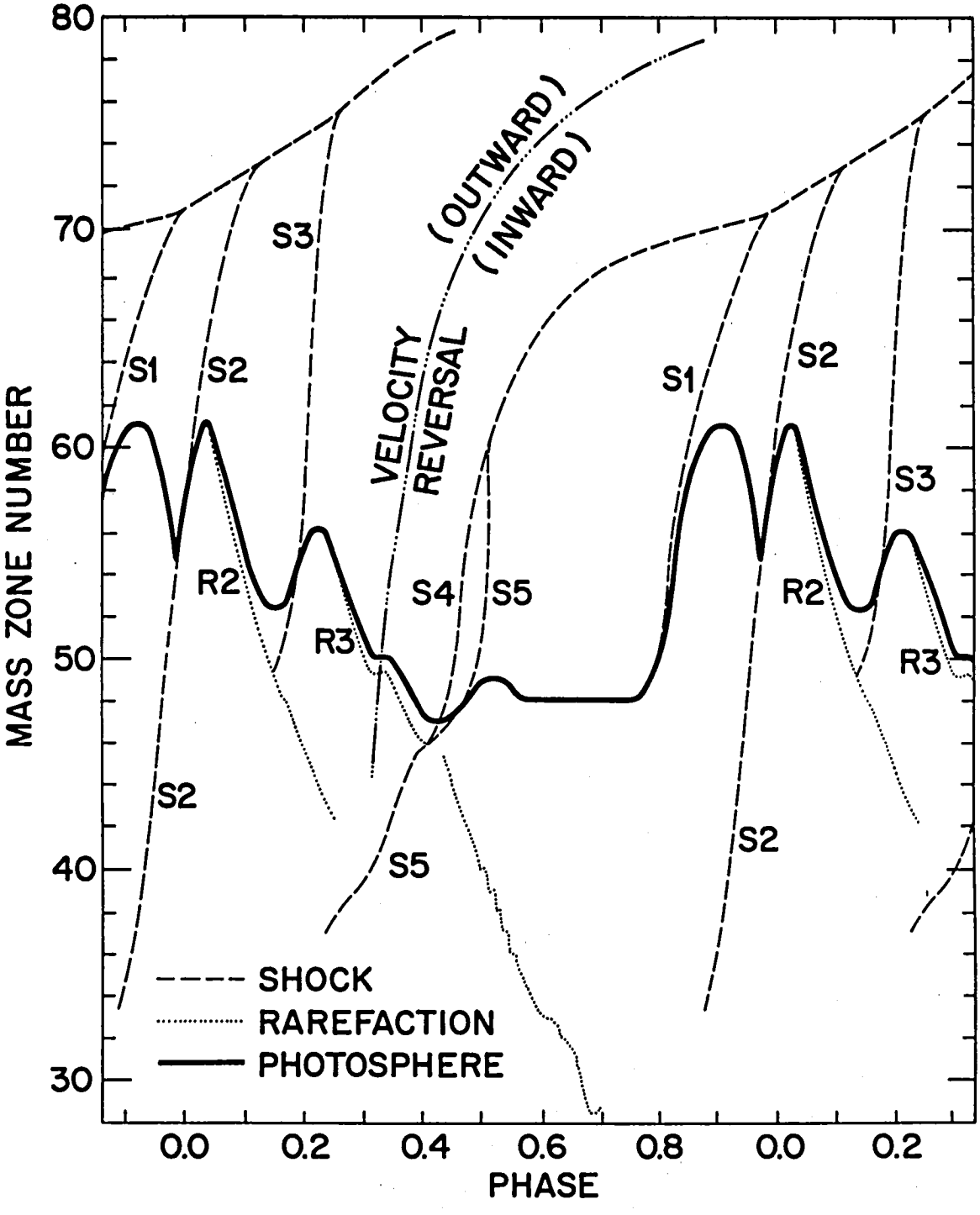

Figure 2. Diagnostic Diagram for a Cepheid Model

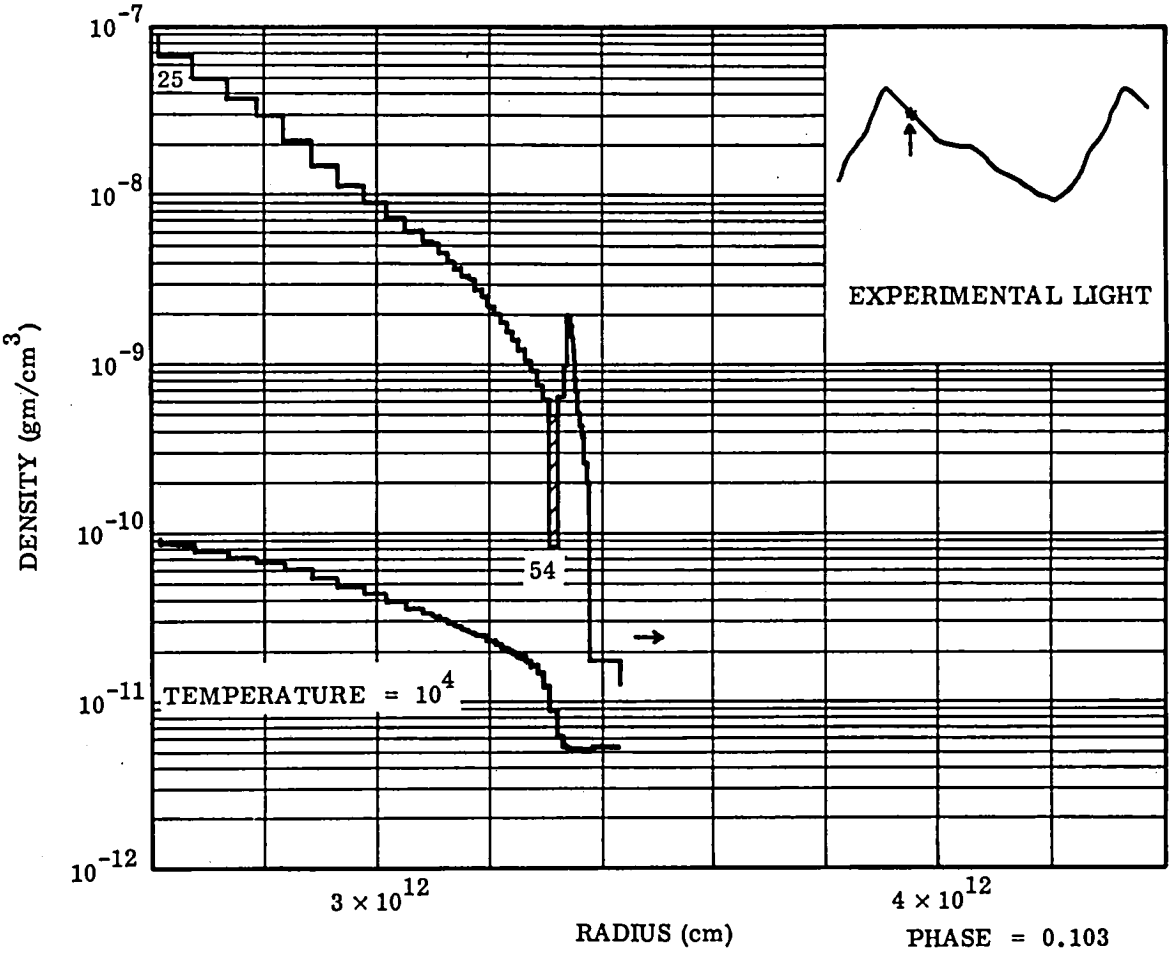

Figure 3. Atmospheric Profiles at Phase 0.103

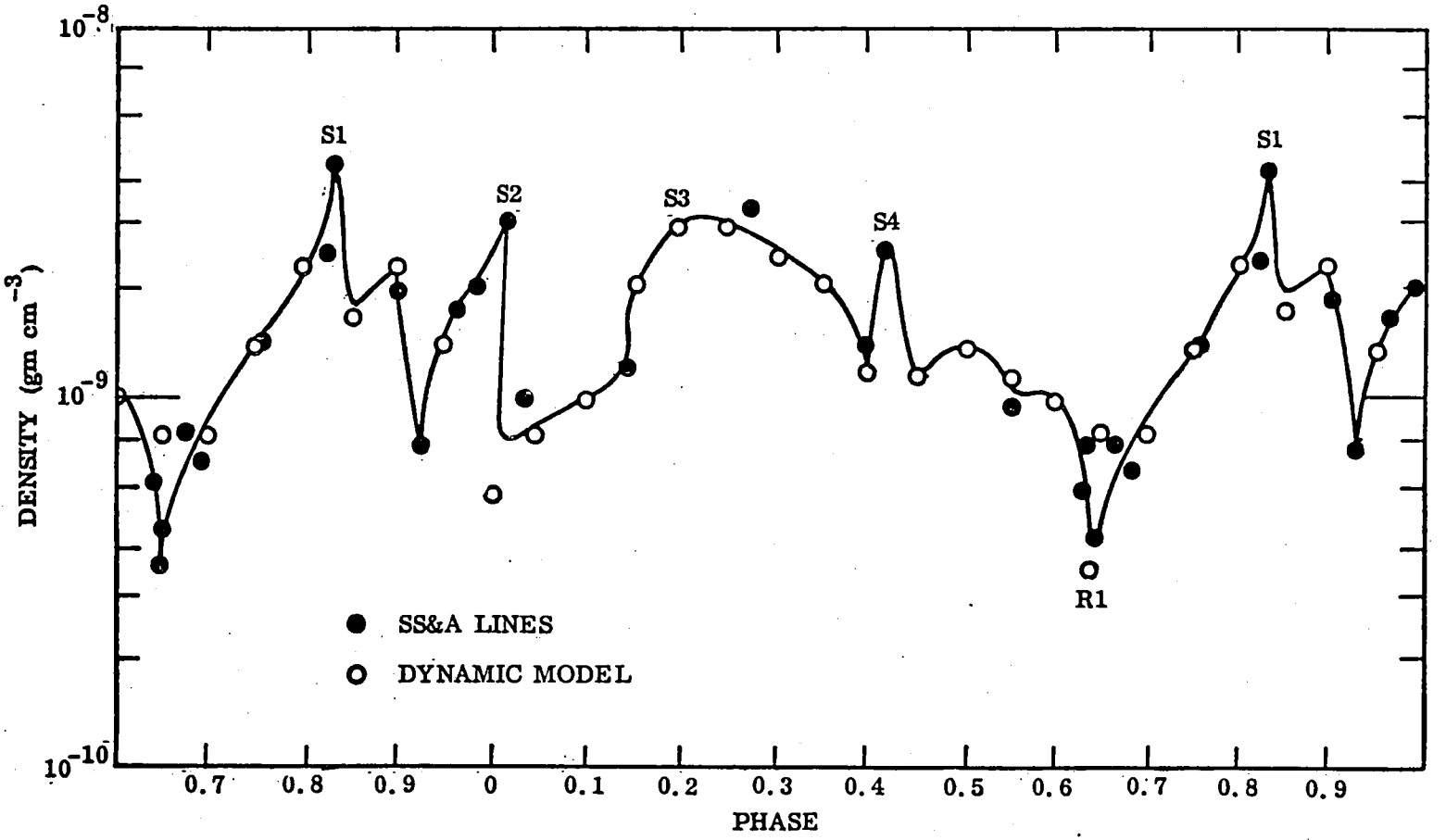

Figure 4. Density-versus-Phase for Eta Aquilae as Deduced from Two Types of Observations

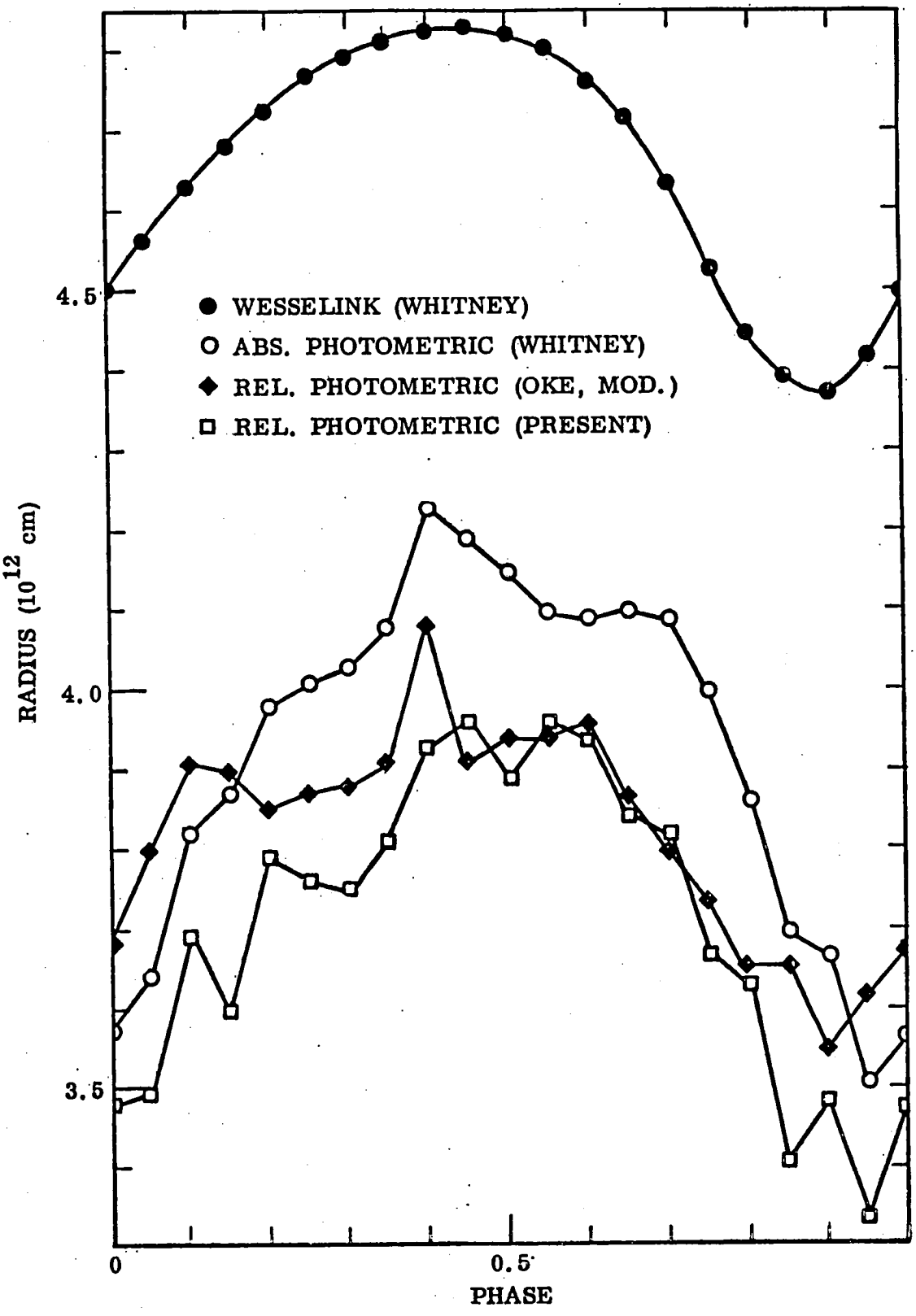

Figure 5. Radius-versus-Phase for Eta Aquilae

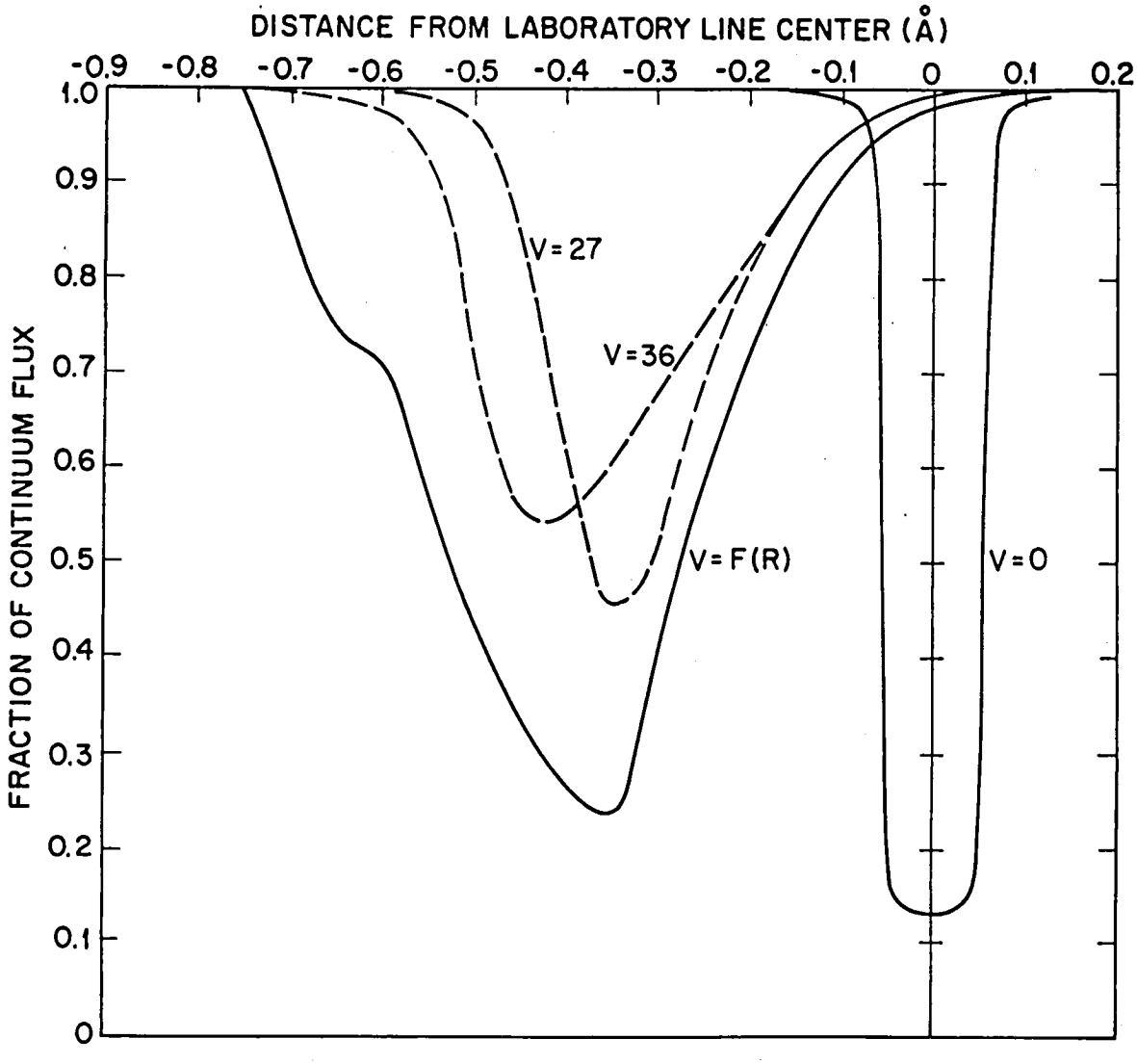

Figure 6. Computed Line Profiles for λ4508Å Fe I

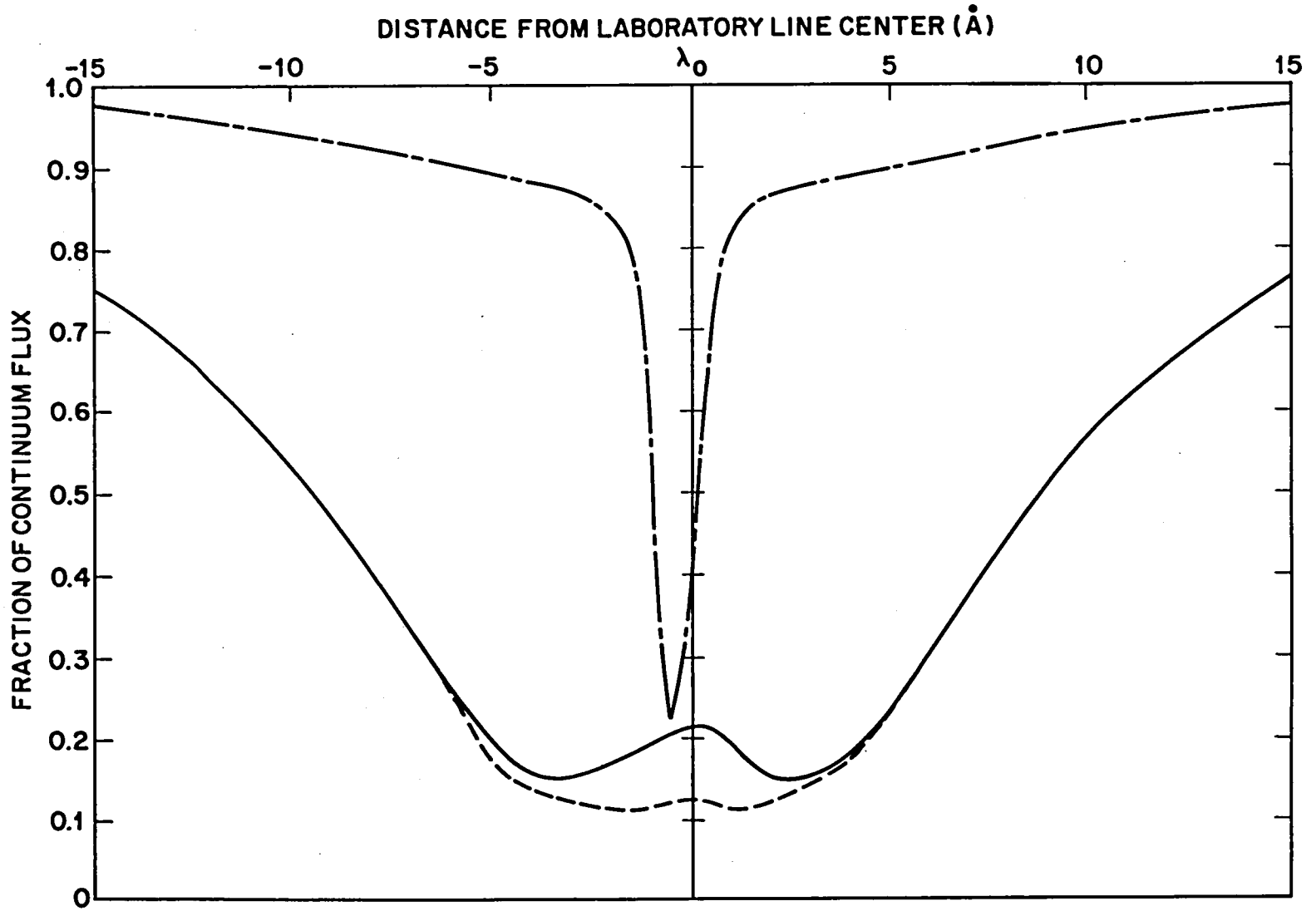

Figure 7. Computed Line Profiles for Hβ and Ca II K

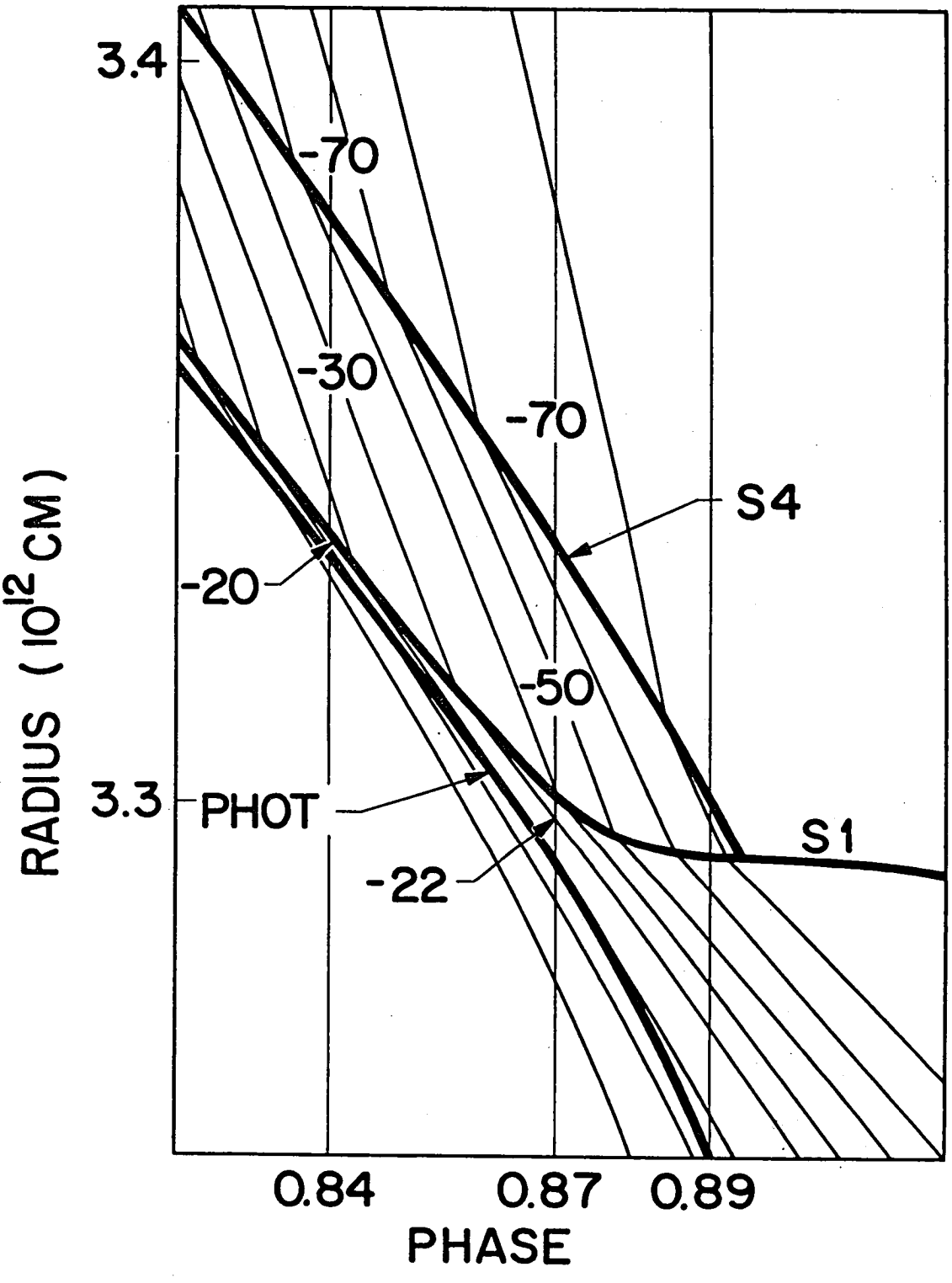

Figure 8. Atmospheric Structure During Collapse

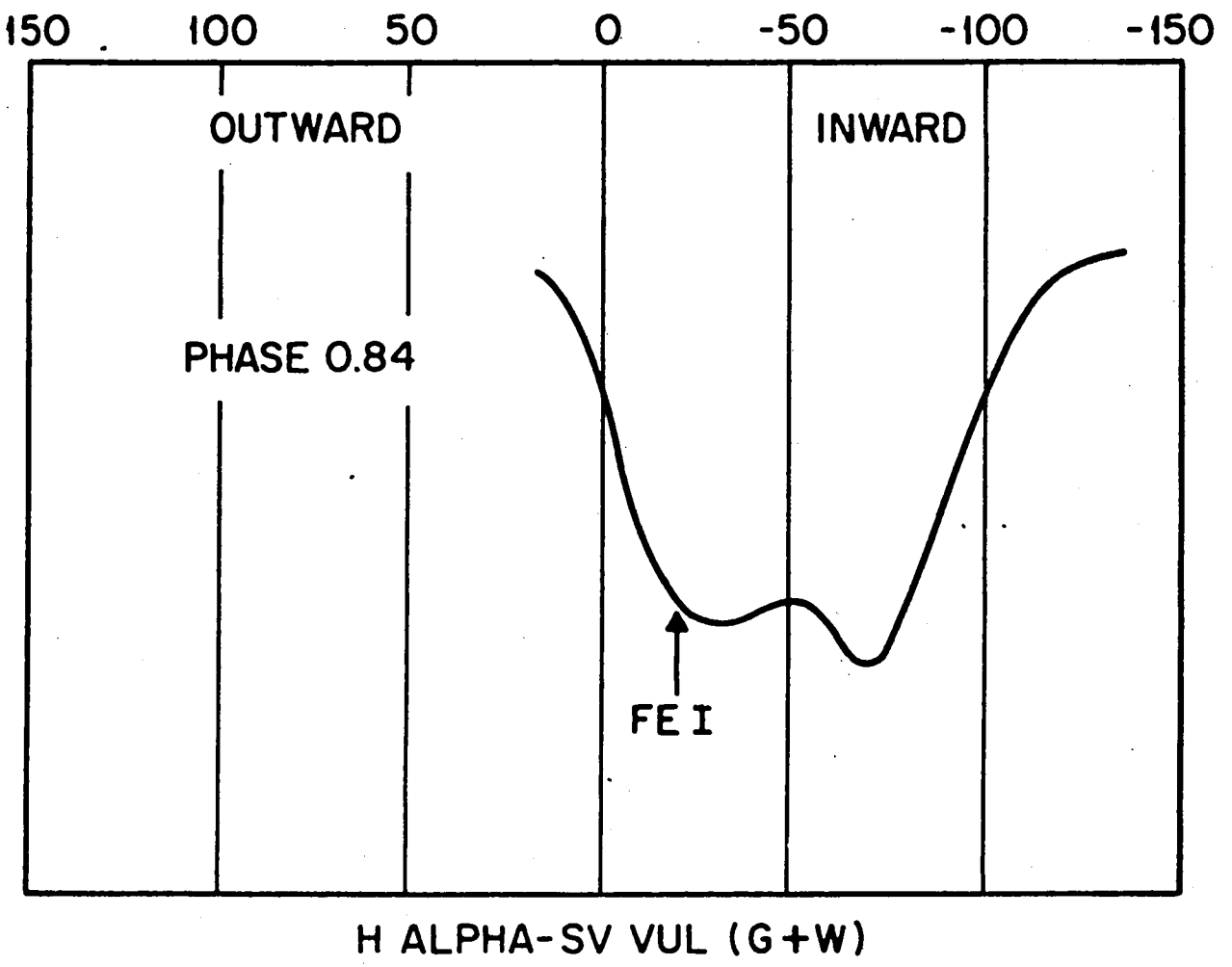

Figure 9. Observed Line Profiles SV Vul

Discussion

Adams: Do you have anything to say about the mass anomally?

Hillendahl: I'm prejudiced. I used the low Christy mass. I did a paper in 1955 that says the masses are about one half of what they should be. This technique I've talked about -- trying to use the maximum possible observational data with the minimum possible theoretical interpretation -- leads to the same sort of result. What you are doing is taking lines that you hope are in the photosphere and following them for a particular part of the phase, and if you integrate the velocity over that time, you get the absolute displacement of that part of the cycle. If you differentiate the velocity you get g. The problem is then that you have absolute displacement over part of the cycle but you don't have radius, so you have to go to some other technique to get the relative radius. If you do this, you end up with masses that are too small compared to the evolutionary mass.

Pel: At the last Goddard conference in this series, Hutchinson, Hill and Lilly presented some observational data for β Dor from the OAO-2 satellite. They thought they saw sharp blue peaks on the rising branch of this 10-day Cepheid, which they interpreted as evidence for shock waves. Together with J. Lub and J. Van Paradijs, I observed this star with the ANS satellite. I think we have much better data and we do not see these blue peaks. On the other hand, we have problems fitting the whole rising branch of the light curve with the Kurucz models. I don't find a satisfactory equilibrium model that fits the energy distribution from 5500Å to 1800Å. So there is some evidence for non-equilibrium radiation.

Hillendahl: Well, it's a question of whether it's non-equilibrium radiation in the Dick Thomas sense or LTE radiation from a moving gas.

Pel: We can't distinguish between those two things. What we can say is that there don't seem to be pronounced short-lived peaks on the light curve there, but the energy distribution cannot be represented well by a hydrostatic equilibrium model atmosphere.

Hillendahl: No. In all deference to Stromgren, I think he was wrong. I think Karl Schwarzschild was right. In 1905, his two-stream method was for convective atmospheres, not for radiative ones. At the time I did this work, the OAO-2 information on Cepheids was just beginning to come down. I think they did see a little blip at 0.95, which is about where I would expect to see the shock. One of the things you must be careful of in a model calculation is the zoning. Simply because your code says there is a shock wave, it doesn't necessarily mean you can see it. In a fireball model where your zoning is a 1 meter scale, these effects are on a scale of 0.1 mm. There is a radiative structure in which the gas dynamic discontinuity is embedded. There is a paper by J. Zinn and R. C. Anderson (Phys. Fl. 16, Nov. 10, 1973), in which they have done the modeling of a radiative shock front. Shock fronts don't always have that great brightness you might expect them to have. Only under certain relationships between the density of the gas and the radiative mean free path will you see the shock front itself. The rest of the time it's going to be embedded in radiative precursors. So my guess is that your ability to see shock waves is going to be very limited. Just a little bump on the curve. Most of the gross features that you see that last for days and

days are caused by the progression of the photosphere inward due to hydrodynamic expansion of the gases behind the front, and sometimes rarefaction waves. I think you can show this quite easily.

J. Wood: In your fireball graph you mentioned a Christy reflection. What's it reflecting off of?

Hillendahl: A fireball is quite different from a star. A star has a very dense center. A fireball is essentially evacuated in the center, but nonetheless, the shock wave does reflect off the center. It makes a difference (sort of a coefficient of restitution) what sort of materials and structure you use. Particularly in the outer layers, it has been shown by comparison with experiment that the equation of state is absolutely sacred.

MICROTURBULENCE AND WESSELINK RADII

Nancy Remage Evans
Department of Astronomy
University of Toronto, Canada

ABSTRACT

Using the calibration of Bell and Parsons (1974), the effects of changes in microturbulence and surface gravity throughout the cycles of δ Cephei and η Aquilae are estimated. After the changes in microturbulence have been taken into consideration, Wesselink radii for these stars are reduced 20%.

I. INTRODUCTION

Because the Wesselink technique allows the radius for a pulsating star to be determined without the use of reddening, or a temperature or luminosity scale, it can be used as a valuable check on such calibrations. Wesselink radii have recently been discussed in connection with the Cepheid mass problem (Cox, 1978; Cogan, 1978). Both these papers point out discrepancies among various methods of radius determination. In addition some techniques similar to Wesselink's method (Balona, 1977; Budding , 1977) give results which disagree with the Wesselink radii. Finally, there are indications of internal inconsistencies within the Wesselink technique itself (Evans, 1976; Gieren, 1976).

The assumption in Wesselink's method which appears the most likely to cause errors is that points of equal color are points of equal temperature. The calibrations of Bell and Parsons (1974) of B-V, which is used in most Wesselink radius determinations, allows one to check the effect of two

possible causes of deviation from this equal colour--equal temperature condition. From their Table II, it is possible to estimate the effect on B-V of variations of effective gravity and microturbulence throughout a Cepheid cycle. This paper is a discussion of these effects for two stars, δ Cephei and η Aquilae. These stars were chosen because surface gravities and microturbulent velocities are available for many phases of these stars.

II. SURFACE GRAVITIES

Surface gravity curves of Cepheids reported in different studies show dissimilarities. Pel (1978) has provided data for 170 Cepheids using the Walraven photoelectric system and Kurucz (1975) model atmospheres. Parsons (1971) has similarly derived surface gravities for 48 Cepheids using 6 color photometry and his atmospheres. Only a few stars are common to both studies, but a detailed comparison of the data for η Aquilæ show disagreements in the shapes of the curves. Pel's curve is quite flat from phases ϕ = .0 to .6, with a sharp peak near ϕ = .8. This is in agreement with dynamical surface gravity curves which are determined primarily by the acceleration of the atmosphere. Parsons' curve, on the other hand has a gradually downward sloping branch from ϕ = .0 to .7, and a peak at maximum light.

Figure 8 in Lub and Pel (1977) makes it clear that taking account of the variation in microturbulence as a function of phase is critical in interpreting the photometric colors in terms of surface gravity. Though this is not done in Pel's curves, rough estimates of the effects, based on the microturbulence curves in the next section show that the change in microturbulence will leave the basic form of the curve unchanged but

smooth out the dip in the surface gravities at $\phi = .6$, and increase the maximum of this curve.

The purpose of this section is to estimate the effect on B-V of differences in surface gravities at points of equal color. The results from the spectral synthesis of Bell and Parsons (1974) were combined with gravity differences for various B-V colors for η Aquilae. Both estimates of surface gravity curve, Parsons' and Pel's, were used for the test. Instead of Pel's curve, the curve computed by Parsons (1971) from the acceleration and radius variation tabulated by Schwarzschild,Schwarzschild,and Adams (1948) was used. This curve and Pel's are similar in shape but Pel's curve has a smaller amplitude. For both types of surface gravity curve, the effect on B-V was only a few thousandths of a magnitude. Thus these two rather different cases both show that the distortion to B-V is inconsequential, as has been previously suggested by Woolley and Carter (1973).

For δ Cephei the surface gravity curve found by Parsons (1971) from the 6 color data also yielded negligible effect.

III. MICROTURBULENCE

Variations in microturbulence throughout Cepheid cycles have been observed, but for only a few stars have enough points been observed to give more than a suggestion of the phase dependence of this parameter. Table I summarizes the available data. The variation in microturbulent velocity has been estimated from the results of various curve of growth studies. In general the trend mentioned by Schmidt (1971a) of higher microturbulence during the steep branch of the radial velocity curve is confirmed, while nearly all stars have a small constant microturbulent velocity during the gradual branch of the radial velocity curve.

TABLE I

	Period (days)	Minimum & Maximum Microturbulent Velocity (km/sec)	Comments (v = microturbulent velocity)	Reference
TU Cas	2.14	--	v = 10 km/sec, 3 plates	(1)
SZ Tau	3.15	4.0 - 6.4	4 plates	(1)
RT Aur	3.73	3.5 - 5.0	11 plates, good phase coverage	(2)
α UMi	3.97	--	v = 5.9, 1 plate ϕ = .46	(1)
δ Cep	5.37	3.8 - 5.5	9 plates, good phase coverage	(3)
U Sgr	6.74	4.2 - 7.5*		(4)
η Aql	7.18	4.0 - 5.8		(5)
		4.7 - 9.0*		(4)
S Nor	9.75	5.0 - 10.0* or 9.0		(4)
β Dor	9.84	5.5 - 6.0		(6)
RX Aur	11.62	5.4 - 7.6	5 plates	(7)
X Cyg	16.39	6.2 - 7.6	2 plates	(7)
Y Oph	17.12	7.5 - 10.0*		(4)
T Mon	27.02	--	v = 9.0 km/sec, 3 plates	(7)
ℓ Car	35.54	6.0 - 7.9	no plates from ϕ = .69 to .94	(8)
SV Vul	45.10	7.6 - 9.9	4 plates	(9)

*high velocities from Schmidt's plates taken without an image tube, which give systematically higher microturbulent velocities than those with an image tube.

References

(1) Schmidt, 1974

(2) Bappu and Raghavan, 1969

(3) van Paradijs, 1971

(4) Schmidt, 1971a

(5) van Hoof and Deurinck, 1952

(6) Bell and Rodgers, 1964

(7) Schmidt, et al, 1974

(8) Rodgers and Bell, 1968

(9) Kraft, et al, 1959

Schmidt points out that his data are somewhat puzzling. His plates taken with an image tube give smaller values than those taken without, and it is not clear whether some of the large values in Table I are accurate. Most entries in Table I indicate an amplitude of microturbulence of about 2 km/sec. There is no indication that the amplitude increases with period, though the mean values do. Because no attempt has been made to adjust the data for variations on technique, such as different oscillator strengths or temperature fitting procedures, this trend should be only taken as suggestive.

It is clear that it is very important to consider variations of microturbulence in interpreting colors in terms of physical parameters (Pel, 1978; Relyea and Kurucz, 1978) and that the amplitudes of Table I will have an appreciable effect on the colors. In the next section, the results of this effect on Wesselink radii will be discussed.

IV. WESSELINK RADII

In order to assess the effect of changes in microturbulence, the results of Bell and Parsons (1974) have again been used, together with the microturbulence data from van Paradijs (1971) for δ Cephei, and van Hoof and Deurinck (1952) for η Aquilae. The corrections to the color curves resulted in a 20% decrease in the Wesselink radius in both cases.

In the case of δ Cephei, there was a further interesting result. The following internal inconsistency has been noted in Wesselink's method. If the ratios of the radii at different colors are plotted as a function of the differences of radii from the radial velocity curve, the result should be a line which passes through the point (0,1). In many, though not all cases (Evans, 1976; Gieren, 1977), the points in fact lie on a loop

as the colors go from blue to red. This loop appears too large to be explained by observational errors. In the case of δ Cephei when the corrections for microturbulence were made, the loop was reduced considerably and the internal standard error of the mean radius was reduced from 4.3 solar radii to 2.5 solar radii. For η Aquilæ the reduction was less, from 4.8 solar radii to 3.8 solar radii.

V. DISCUSSION

The inclusion of the correction for microturbulence, based on the results of Bell and Parsons is important in determining Wesselink radii, though the current information on the variation of surface gravity indicates that a correction for it is not. A small surface gravity correction may be necessary for cooler stars, in the opposite sense to the microturbulence correction.

Schmidt (1971b) has made an extensive study of four Cepheids, including their line blocking. His conclusions are somewhat different from those of this paper, partly because he finds variations in gravity which are different in amplitude and phase from those used here. However, his measurements of the line blocking in B-V indicate that blocking increases when microturbulence increases. In his Figure 2b,c,d, points with high microturbulence sit above those with low-microturbulence.

Variations to Wesselink's method such as that used by Balona (1977) or Thompson's (1975) method for deriving the slope of the surface brightness-color relation should be affected by differences in microturbulence, but because the effect on B-V is a few hundredths of a magnitude, the results will be little changed. In Thompson's Figure 2, the variation of surface brightness as a function of color, there is a suggestion that the red end

of the relation for several stars has more scatter than the blue end. If a check of the data reveals that the scatter is phase dependent at the red end, then it is probably due to changes in microturbulence. A range of slopes for the surface brightness--color relation from roughly 2.0 to 2.2 is possible from the graph of η Aquilae. These values are extremes, but they may explain some of the scatter in the values of the slopes from different stars. In addition if the Wesselink radii used are approximately 20% too large, the slopes will be systematically about 5% too small.

The analyses in sections II and III above indicate that a method such as Balona's (1977) will be affected by changes in microturbulence or effective gravity for less than half the period. In particular, if only the descending branch of the light curve is used, the results will be altered by these changes very little. The fact that Balona's radii are in general smaller than those of Evans (1976) confirms the results of this paper. (This is true even after the Evans radii are multiplied by 1.31/1.41, to use the current foreshortening-limb darkening correction.)

Because of the importance of uniform, detailed information about microturbulence in Cepheids, an observational program is being undertaken, but from the current information it seems that Wesselink radii of these short period stars must be reduced.

I would like to thank Alan Irwin for several stimulating discussions, and my husband for comments on the writing. This work was carried out with the financial support of Operating Grant A 5419 from the National Research Council of Canada to Dr. J. R. Percy.

REFERENCES

Balona, L.A. 1977, M.N.R.A.S., 178, 231.

Bappu, M.K. and Raghavan, N. 1969, M.N.R.A.S., 142, 295.

Bell, R.A. and Parsons, S.B. 1974, M.N.R.A.S., 169, 71.

Bell, R.A. and Rodgers, A.W. 1964, M.N.R.A.S., 128, 365.

Budding, E. 1977, Ap. and Space Sci., 48, 249.

Cogan, B.C. 1978, Ap.J., 221, 635.

Cox, A.N., 1978, preprint.

Evans, N.R. 1976, Ap.J., 209, 135.

Gieren, W.P. 1976, Astr. and Ap., 47, 211.

Hoof, A.van and Deurinck, R. 1952, Ap.J., 115, 166.

Kraft, R.P., Camp, D.C., Fernie, J.D., Fujita, C., and Hughes, W.T. 1959, Ap.J., 129, 50.

Kurucz, R.L. 1975, Dudley Obs. Rep., 9, 271.

Relyea, L.J. and Kurucz, R.L. 1978, preprint.

Lub, J., and Pel, J.W. 1977, Astr. and Ap. 54, 137.

Paradijs, J.A. van 1971, Astr. and Ap. 11, 299.

Parsons, S.B. 1971, M.N.R.A.S., 152, 121.

Pel, J.W. 1978, Astr. and Ap., 62, 75.

Rodgers, A.W. and Bell, R.A. 1968, M.N.R.A.S., 138, 23.

Schmidt, E.G. 1971a, Ap.J., 170, 109.

——— 1971b, ibid. 165, 335.

——— 1974, M.N.R.A.S., 167, 613.

Schmidt, E.G., Rosendhal, J.D., and Jewsbury, C.P. 1974, Ap.J., 189, 293.

Schwarzschild, M., Schwarzschild, B., and Adams, W.S. 1948, Ap.J., 108, 207.

Thompson, R.J. 1975, M.N.R.A.S., 172, 455.

Woolley, R. and Carter, B. 1973, M.N.R.A.S., 162, 379.

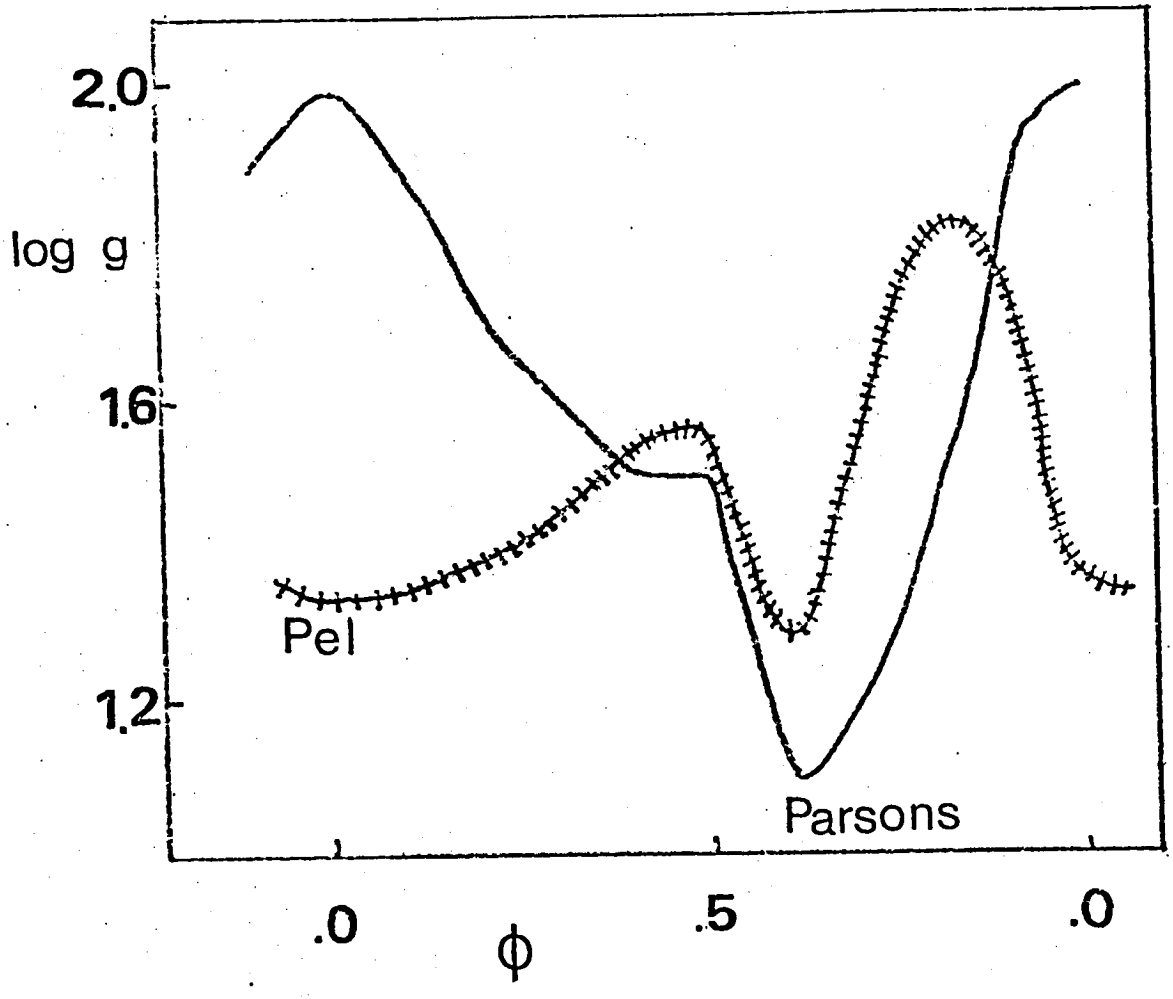

Figure 1. Gravity curves from Parsons (1971) and Pel (1978) (schematic) for η Aquilae

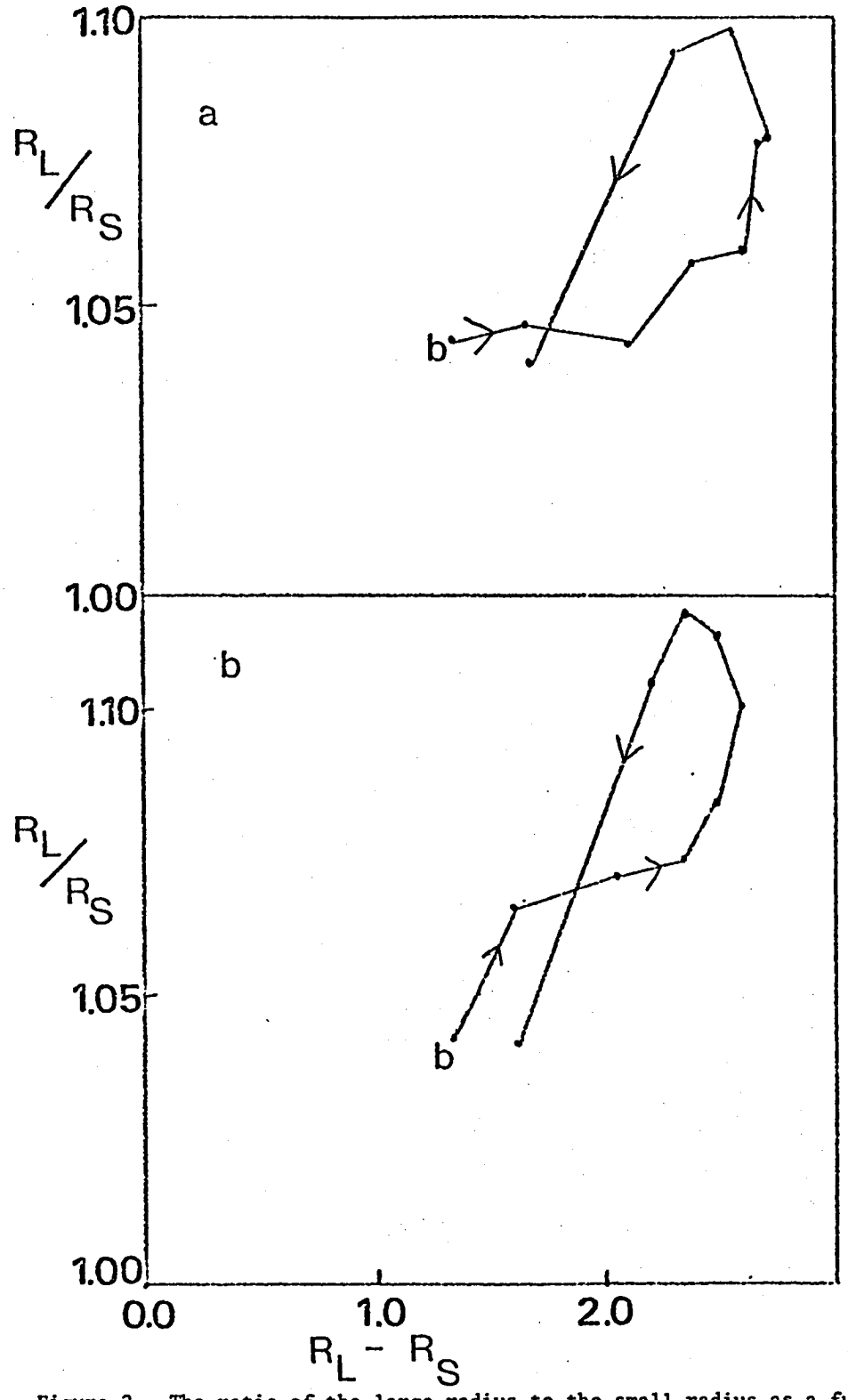

Figure 2. The ratio of the large radius to the small radius as a function of the difference in radii for δ Cephei, a) before correction for microturbulence; b) after correction. The b near the end of the curve indicates the bluest point.

POPULATION OF THE LOWER PART OF THE INSTABILITY STRIP: DELTA SCUTI STARS AND DWARF CEPHEIDS (or AI VELORUM)

by

AUVERGNE, M., BAGLIN, A., LE CONTEL, J.-M., VALTIER, J.-C.

Observatoire de NICE - France

ABSTRACT

In the last five years, more than 30 new δ Scuti stars have been discovered. As inferred from the statistics of dwarfs and evolved stars and also from observational bias (i.e. duration of a good sequence of photometric measurements compared to the period) most of the newly discovered stars are dwarf δ Scuti stars with periods less than 0.1 day and small amplitudes. A very luminous one has been detected around $M_V = 0$.

The problem of period determination has not yet been completely settled and the stars can still be divided into two groups: stars with apparently no stable period (almost all the dwarfs and some low amplitude giants) and stars with stable combination of period and repetitive light curve (giants with large amplitude and/or binaries). The last class resemble the AI Velorum in this respect.

Some properties of the atmospheric variations in δ Scuti stars are emphasized. The amplitude and the shape of both light curves and radial velocity curves are small and rapidly variable in the case of dwarf δ Scuti stars; for the evolved stars the situation is more complex. Rapid rotators have small amplitudes while slow rotators have larger ones. Moreover the shapes of the light curves are more regular. Recent work on spectrographic data points out some bumps in the radial velocity curves and in the core of strong line profiles. These phenomena appear qualitatively very similar to those observed in Cepheids and described by Karp in his hydrodynamical model of a 10 day Cepheid.

The relation between variables and non-variables, and also the results on abundances in the atmospheres of these stars has already given some insight of the hydrodynamics of their envelopes. However, if diffusion theory explains qualitatively the abundances anomalies of the Am stars, a quantitative agreement has not been reached yet. This microscopic diffusion prevents the vibrational instability when it is at work. The mechanism which prevents diffusion is still associated to rotation, but no complete hydrodynamical model exists.

The coexistence of abundances anomalies and variability among giants has been strongly confirmed, and on the main sequence two variables seem to be mild Am. This fact poses a new problem to the diffusion theory, as it is difficult to understand how diffusion could be strong enough to produce abundances anomalies and at the same time turbulence strong enough to mix the helium. Attempts have been made to relate the variability to the hydrogen ionization zone in an envelope deprived from helium. But the comparison with observations is not very good. A better description of the hydrodynamics in these envelopes is badly needed.

The AI Velorum stars are treated separately because the main problem under discussion is the question of their population. This group has been defined by their pulsation characteristics: short period, larger amplitude and regularity of the light curves. Contrary to RR Lyrae or δ Scuti stars their evolutionary status is not known. The existence of RR Lyrae stars in globular cluster and of δ Scuti stars in open clusters allow to infer that RR Lyrae belong to population II or intermediate population I and that the δ Scuti are typical population I stars. In the case of the AI Velorum stars the problem is less clear. Observationally the values of the metal content, period and velocities calculated from proper motions show a large dispersion. From pulsational models it is possible to obtain the observed period with high masses (2 $M_\odot$) and normal metal content, but also with low metal content and low mass (0.5 $M_\odot$). So that we conjecture that the AI Velorum stars do not form a homogeneous group from the population point of view.

I. Introduction

In the population of the lower part of the instability strip (from the main sequence up to $M_V = 0$) one can distinguish different groups: δ Scuti stars (as defined in Baglin et al. (1973)), metallic line stars (as defined for example by Conti (1970)), and AI Velorum stars for which a definition is given in Section V. Since Breger (1969) the normal A stars are considered as low amplitude pulsators; i.e., δ Scuti stars. The main properties of δ Scuti and AI Velorum stars have been reviewed by Baglin et al. (1973) and then complemented by review papers of Fitch (1976), Petersen (1976), and Baglin (1976) at the IAU Colloquium 29 in Budapest. The properties of AI Velorum stars have been more recently studied and discussed extensively by Breger (1976). The extension of the Am domain and the variation of the Am character is being extensively looked at (see for example Burkhart (1978)).

We do not want here to give an extended review of all the works which have been done on the subject but rather emphasize the problems raised by these stars. We first review the newly discovered variables (Section II), then discuss new results on the atmospheric properties of their pulsation (Section III). The coexistence of variables and non-variables related to abundances anomalies is discussed. Emphasis is made on the questions raised concerning the physical processes at work in the envelopes of these stars (Section IV). Recent works on the properties of AI Velorum stars confirm the fact that the lower part of the instability strip probably contains variables of different populations, and that the definition of the two groups, AI Velorum and δ Scuti, do not represent this difference (Section V).

II. General Statistical Properties: Discovery of New Variables

A. Discovery of New Variables

During the last five year some thirty new δ Scuti variables have been detected. Most of them are of luminosity classes V and IV with short periods between 0.05 day and 0.1 day and small amplitude, i.e., dwarf δ Scuti stars.

They are listed in Table I, which can be considered as an addition to the catalogue of Baglin et al. (1973). It has to be noticed that the mean duration of excellent sequences of photometric measurements favor evidently the discovery of stars with periods less than 0.1 day. γ Bootis, which our group has recently classified as a δ Scuti variable, is a good example of the difficulties to observe stars with periods longer than 0.2 day. In addition the dwarfs are the most numerous due to their longer evolutionary time scale. However, the discovery of HR 2557 by Kurtz (1977) extends the δ Scuti domain to very high luminosities ($M_v \simeq 0$). These results definitely confirm that the δ Scuti and AI Velorum domains overlap (see Section V).

B. Periods

The problems of the stability of the variations in δ Scuti stars has not yet been solved. The complexity of the light curves needs long photometric sequences to make a serios period analysis. Nevertheless, from the few stars studied up to now, some conclusions can be drawn.

It seems that the CC And is the only star in which tidal modulation is responsible of the complexity of the light curve (Fitch, 1967). In the case of 14 Aur (Morguleff et al., 1976; Fitch, 1976) or Y Cam (Broglia and Marin, 1974) for instance, the binary nature does not appear in the mixture of periods. Except the particular case of CC And, all the objects which have been studied extensively up to now can be separated into two groups:

- The evolved large amplitude δ Scuti stars seem to have several stable periods and repetitive light curves as for example 14 Aur (Morguleff et al., 1976) or 1 Mon (Shobbrook et al., 1974). This stability in the period spectrum seems to exist also in small amplitude giants as 38 Cnc for instance (Guerrero, 1978) or 4 CVn (Shaw, 1977).
- The dwarf δ Scuti stars, which have generally (but not always) small amplitude of variations, non stable periodicities and non repetitive

light curves, as for instance, Θ Tuc (Stobie et al., 1976), HR 4684 (Guerrero, 1978), HR 8006 (Le Contel et al., 1974), or HR 812 (Fesen, 1973). However, this "classification" is only tentative and needs more studies to be confirmed.

III. Properties of the Atmospheric Variations in Delta Scuti Stars

The amplitudes of radial velocity curves are low and generally variable (as in photometry), generally lower than 40 km/s. The correlation between large amplitudes and low projected rotational velocity (V_R sin i) which has been claimed by different authors has still to be confirmed.

Light and radial velocity curves are roughly in opposition: Breger et al. (1976) studying seven stars showed that minimum velocity and maximum light are shifted by 0.09 period which means that the phase lag is less than in Cepheids. They proposed that the reason for this is the reduced H-ionization zone of δ Scuti stars which is located very high in the atmosphere of these stars. However, in Cepheids, when a secondary bump is present in both light and radial velocity curves, Stobie (1976) pointed out that the two curves are not mirror images so that the observed phase lag is not exactly 90°. The observed shift in δ Scuti stars may be due to the same reason, at least for evolved ones (Auvergne et al., 1978, on γ Boo; Valtier et al., 1978b, on HR 432 and HR 515) in which bumps are present at the minimum and maximum of the radial velocity curves. In the case of HR 515 simultaneous observations of the continuum allow us to see that a bump is also present around maximum light (fig. 1). These irregularities are related to line profile variations of the strong lines (Balmer lines and Ca II K line). In particular a line splitting of the K line is observed at the end of the radial velocity bump. Dravins et al. (1977) have observed the same phenomenon in ρ Pup.

Such perturbations of light and radial velocity curves associated with line profile splitting are similar to what is observed in Cepheids. The same kind

of phenomena have been obtained by Karp (1975) in his hydrodynamical models of a 12 day Cepheid: the critical period of the atmosphere and the period of the envelope are very similar so that resonance phenomena may appear. As the envelope is still expanding the atmosphere starts to slow down. A pressure wave is generated which propagates both inward and outward and heats the gas. The observed line splitting could be produced by this temperature uprising when it is strong enough at small optical depths. However we have to explain how it is possible to observe such splittings (with a characteristic length of 60 km/s) in the core of lines in such rapid rotators as γ Boo (145 km/s) or HR 515 (200 km/s). In the case of a velocity field, it has to be concentrated on some parts of the disk. A possibility could be looked for with non radial oscillations.

IV. Properties of the Envelopes: Coexistence of Variables and Non Variables

We will discuss in this section the atmospheric abundances of the variables and of the non variables in the same domain. These abundances are built at the bottom of the convective zone, down in the envelope and will give information on the hydrodynamical behaviour of these deep layers.

A. Observational Results

1. On the main sequence the exclusion metallicism-pulsation is generally confirmed. Since the discussion by Baglin (1976), 32 Vir has been recognized as a binary star with one Am and one δ Scuti star (Kurtz et al., 1976). However, two stars on the main sequence HR 4594 and HR 8210 have been discovered as variable by Kurtz (1978); they are classified as mild Am. The classification mild Am is dubious - for example 28 Andr has been classified mild Am with the same spectral type as HR 8210 but the detailed analysis has shown that it has normal abundances. So, as no detailed analysis of abundances is available for these two stars one has to be careful before claiming the coexistence of anomalies and variablity on the

main sequence. In addition it is not completely settled that no companion exists (as in the case of 32 Vir), as the stars rotate quite fast.

2. Outside the main sequence the situation is more complicated.

a) The evolution of the Am character towards the giant domain has been studies in more detail. Smith has defined abundances of "evolved Am" from an analysis of several stars lying one or two magnitudes above the main sequence (HR 1103, 1248, 3752, 6559, 7653 cited by Kurtz, 1976). But Burkhart (1978) analysed the hot evolved Am 22 Boo and α Cnc and found that they look like classical Am stars. Kurtz (1976) studied stars classified as δ Del (Bidelman, 1965) which are generally quite cool and found that some of them have abundance anomalies compariable to the "evolved Am" as defined by Smith though some of them do not show any abundance anomalies.

So that the evolution of the abundance anomalies toward the giants seem to present important variations from one star to another and no clear correlation with either temperature or gravity has been established (Table 2 and figure 2).

b) The giants variables have peculiar pulsation characteristics (See section III).

Some abundances analyses are available. Kurtz (1976) obtained a homogeneous set of results on seven known variables. In some cases they are comparable to the Smith "evolved Am" while in other cases [Fe/H] is enhanced and the relative abundances with respect to iron are normal. However, the coexistence of variability and abundance anomalies can be considered as proven. Up to now, no statistics can be made because only a few stars have been tested. Some work is in progress in that domain, and in particular testing variability of giant Am is badly needed.

B. Theoretical Interpretation

These properties -variability and abundance anomalies - give us some insight on the structure of the envelope of these stars down to the bottom of their convective envelope.

1. Variability is due - at least on the main sequence - to the helium ionization zone and is present only when the concentration of helium is larger than 0.15 More stability analysis have been done recently which defines the blue border of the strip for normal population I composition (Percy, 1977; Valtier et al., 1978a; Stellingwerf, 1978). As for Cepheids the theoretical blue border is too red (figure 3). Fundamental and first harmonic are unstable almost for the same conditions, depending a little bit of the outside boundary conditions.

2. Abundance anomalies are qualitatively explained by the microscopic diffusion in stable medium (Michaud et al., 1976). But a quantitative agreement is not yet reached. Vauclair et al. (1978) propose to add some turbulent diffusion due either to overshooting or shear instability due to meridional circulation which would prevent the concentration to become too high. They tried to estimate an "ad hoc" coefficient and show that the observed abundances of some of the elements can well be explained but that the rare earths abundances are still too low by a large amount. Microscopic diffusion deprives also the envelope from helium. Within 10^6 years no helium is left down to 0.1 R_* in a stable envelope of an A star. Turbulent diffusion as proposed by Vauclair et al. (1978) is not large enought to prevent this sorting.

3. Exclusion between metallicism and pulsation

As it is the same mechanism which is responsible for abundance anomalies and vibrational stability the exclusion between metallicism and pulsation can be understood. In a variable, it does not take place because some mixing process is at work which prevents diffusion. As from observations one knows that statistically slow rotators are Am and fast rotators are variables, the mechanism which prevents diffusion is probably due to rotation. Several works have proposed the shear flow due to the meridional circulation as the agent of mixing (Baglin, 1972; Vauclair, 1976, 1977) but no satisfactory picture exists now, and the crude

treatment of the hydrodynamical behaviour of these envelopes has to be improved. As we have seen the coexistence of metallicism and pulsation is well established for giants and could also be present among some dwarfs. Helium is so easily sorted that it is difficult to understand how an envelope could be quiet enough to allow diffusion to produce abundance anomalies and turbulent enough to prevent the sorting of helium.

Valtier et al. (1978a) propose that the variability is due to another vibrational instability seated in the hydrogen ionization zone, which grows when the gravity decreases instead of the helium ionization zone. They have computed the instability of such hydrogen envelope models and can find an instability but quite marginal and in a very small domain (figure 3). A lot of work has to be done on this intriguing question which will bring some insight on the hydrodynamic of the envelopes.

V. Are AI Velorum and δ Scuti Stars the Same Group of Objects?

From the pulsational properties (period less than 0.2 d, amplitude greater than 0.3 m and regularity of light curves) and AI Velorum stars belong to a well defined group. They are distinct from δ Scuti stars by their amplitude and the shape of their light curves, and from RR Lyrae stars by their period. There are some objects for which the classification is not so clear: for instance DE Lac (P_o = 0.254 d) or δ Sct itself (amplitude = 0.29 m), but the existence of these three groups defined with pulsational characteristics is not doubtful. We have listed in Table 3 the main characteristics of the best known AI Velorum stars. However, since several years the question has been raised of the physical nature of the AI Velorum stars which occupy approximately the same domain of the HR diagram as the δ Sct stars. Detailed reviews of the subject have been given by Fitch (1976) and Petersen (1976) and also by Breger (1976). Breger, considering that only a detailed study of individual objects would bring some

light on the subject, observed AD CMi (Breger, 1975), VX Hydr (Breger, 1977a) and AI Velorum (Breger, 1977b). He found that metallic index and the mean gravity indicate that these stars are high masses population I objects. Previously some stars like AI Vel were considered to belong to population II stars on the basis of very imprecise parallaxes or observed period ratios. Petersen (1976) has shown that in the domain covered by the dwarf cepheids the P_1/P_o ratio is not a good indicator of the mass and the metal content. But Stellingwerf (1978) indicates that the same P_1/P_o ratio can be obtained for models of low mass $M = 0.4M_\odot$ and low metal content $Z = .005$, and for models fo high mass $M = 3\text{-}4\ M_\odot$ and high metal content $Z = 0.02$. He also emphasized the difficulty of determining the mass, as many modes are unstable. Using a higher mass leads to accepting a higher mode. The ambiguity could be restricted only if the luminosity was known, which implies the knowledge of the parallax!

A new dwarf Cepheid has been discovered with a particularly short period (0.039 d) by Berg and Duthie (1977) and spectra have been obtained by McNamara and Feltz (1978). These authors conclude that the star (GD 428), though metal poor, is evolving off a metal poor main sequence and is still in its hydrogen shell burning stage.

From the period luminosity-color relation Breger and Bregman (1975) found SX Phe above the population I locus in the absolute magnitude-period diagram. As the longer period population II stars are also above the population I Cepheids they conclude that SX Phe probably belongs to the population II.

At the present time it seems confirmed that the AI Velorum stars, as defined by their pulsational properties do not form a homogeneous group. Most of them are the same kind of objects as δ Scuti stars. But some stars as SX Phe or GD 428 seem to be definitely metal poor, and some others like DY Peg or CY Aqr have high log g and intermediate δm_1 (see table 3). If we accept the idea that most of the AI Velorum stars are not different from

δ Scuti stars, it is necessary to explain why the amplitude of these stars is so large and the light curve so regular. Evidently the problem of explaining the amplitudes leads to a non linear hydrodynamical treatment of the pulsation. In the case of AI Velorum stars the growth rate is so small that different techniques like non-linear relaxation (Stellingwerf, 1974) are needed.

By the presence of two main excited modes with quite large amplitude they look like the double mode Cepheids. Stellingwerf (1975) has predicted a double mode pulsation for one of his models representing a dwarf Cepheid. However other investigators like Hodson and Cox (1976) have failed to reproduce the results. Simon (1978) proposes that these stable double mode pulsations can be explained by a resonance. It explains the small range of P_1/P_o, but the population I hypothesis has to be excluded.

From this short review it appears that both from the observational and theoretical points of view the situation is still confused.

REFERENCES

Auvergne, M., Le Contel, J.-M., Baglin, A. 1978, to be published.

Baglin, A. 1972, Astron. Astrophys. 19, 45.

Baglin, A., Breger, M., Chevalier, C., Hauck, B., Le Contel, J.-M., Sareyan, J.-P., Valtier, J.-C. 1973, Astron. Astrophys. 23, 221.

Baglin, A. 1976, in "Multiple Periodic Variable Stars", I.A.U. Col. 29 Budapest, ed. Fitch.

Berg, R.Q., Duthier, J.G. 1977, Astrophys. J. Lett. 215 L25.

Bidelman, W.P. 1965, Vistas in Astronomy 8, 53.

Breger, M. 1969, Astrophys. J. Suppl. 19, 79.

Breger, M. 1975, Astrophys. J. 192, 75.

Breger, M. 1976, Proceedings of the Solar and Stellar Pulsation Conference, ed. A.N. Cox, R.G. Deupree, Los Alamos.

Breger, M. 1977a, Publ. Astron. Soc. Pacific 89, 55.

Breger, M. 1977b, Publ. Astron. Soc. Pacific 89, 339.

Breger, M., Bregman, J.N. 1975, Astrophys. J. 200, 343.

Breger, M., Hutchins, J., Kuhi, L.V. 1976, Astrophys. J. 210, 163.

Broglia, P., Marin, F. 1974, Astron. Astrophys. 34, 89.

Burkhart, C. 1978, Thesis, Lyon University, to be published.

Conti, P. 1970, Publ. Astron. Soc. Pacific 82, 781.

Dravins, D., Lind, J., Särg, K. 1977, Astron. Astrophys. 54, 381.

Fesen, R.A. 1973, Publ. Astron. Soc. Pacific 85, 732.

Fitch, W.S. 1967, Astrophys. J. 148, 481.

Fitch, W.S. 1976, in "Multiple Periodic Variable Stars", I.A.U. Col. 29 Budapest, ed. Fitch.

Guerrero, G. 1978, private communication.

Hodson, S.W., Cox, A.N. 1976, Proceedings of the Solar and Stellar Pulsation Conf., ed. A.N. Cox, R.G. Deupree, LASL LA 6544 C, p. 202.

Karp, A.H. 1975, Astrophys. J. 201, 641.

Kurtz, D.W. 1976, Astrophys. J. Suppl. 32, 651.

Kurtz, D.W. 1977, Publ. Astron. Soc. Pacific 89, 941.

Kurtz, D.W. 1978, Astrophys. J. 221, 869.

Kurtz, D.W., Breger, M., Evans, S.W. 1976, Astrophys. J. 207, 181.

Le Contel, J.-M., Valtier, J.-C., Sareyan, J.-P., Baglin, A., Zribi, G. 1974, Astron. Astrophys. Suppl. 15, 115.

McNamara, D.H., Feltz, K.A. 1978, tc appear in Publ. Astron. Soc. Pacific.

Michaud, G., Carland, Y., Vauclair, S., Vauclair, G. 1976, Astrophys. J. 210, 447.

Morguleff, N., Rutily, B., Terzan, A. 1976, Astron. Astrophys. Suppl. 23, 429.

Percy, J.R. 1977, Mon. Not. R. Astron. Soc, 181, 563.

Petersen, J.O. 1976, in "Multiple Periodic Variable Stars", I.A.U. Col. 29 Budapest, ed. Fitch.

Shaw, S. 1977, Astron. J. 81, 661.

Shobbrook, R.R., Stobie, R.S. 1974, Mon. Not. R. Astron. Soc. 169, 643.

Simon, N. 1978, preprint.

Stellingwerf, R.F. 1974, Astrophys. J. 192, 739.

Stellingwerf, R.F. 1975, Astrophys. J. 195, 441.

Stellingwerf, R.F. 1978, preprint.

Stobie, R.S. 1976 in "Multiple Periodic Variable Stars", I.A.U. Col. 29 Budapest, ed. Fitch.

Stobie, R.S. 1977, Mon. Not. R. Astron. Soc. 180, 631.

Stobie, R.S., Shobbrook, R.R. 1976, Mon. Not. R. Astron. Soc. 174, 40.

Valtier, J.-C., Baglin, A., Auvergne, M. 1978a, to be published

Valtier, J.-C., Le Contel, J.-M., Ducatel, D., Auvergne, M., Sareyan, J.-P, 1978b, to be published.

Vauclair, G. 1976, Astron. Astrophys. 50, 435.

Vauclair, G. 1977, Astron. Astrophys. 55, 147.

Vauclair, G., Vauclair, S., Michaud, G. 1978, Astrophys. J. in press.

Table 1

New δ Scuti variables

HD	HR	S T	Name	Periods	Amplitudes	V	M_V	Log T_{eff}	Ref
4490	214	A 5	59 Psc	0.104	0.04	6.01	1.19	3.88	1
4818	238	F 6		0.136	0.025	6.39	2.29	3.87	2
4849	239	F		0.055	0.15	6.47			3
11285		F 0	l	0.08	0.02	6.8			18
14940		F 0		0.21	0.005	6.6			18
15165-4		A 3		0.100	0.07	6.71			19
28319	1412	A 7 III	78 Tau	0.07	0.03	3.41			9
30020	1505	F 2 III	55 Eri			6.75	2.23	3.85	11
50420	2557	F 0				5.98	0.	3.87	16
71496	3329	A 5	28 Cnc	0.096	0.02	6.05	1.21	3.89	13
71935	3350	F 3		0.07		5.10	1.05	3.87	11
75747	3524	A 5	RS CHa	0.08		6.04			4
74439	3662	A 5 V	18 UMa	0.125	0.03	4.82	2.07	3.91	13
85040	3889	A 8	20 Leo	0.082	0.04	5.92	1.54	3.89	8
104513	4594	A m	67 UMa	0.08		5.00	2.48	3.88	15
108506	4746	A 8 n		0.05		6.23	1.59	3.81	11
110377	4824	A 5	27 Vir	0.05	0.02	6.30	1.83	3.89	7
127986	5441	F 5		0.13	0.02	6.38	2.94	3.79	5
153747		A 1		0.05	0.02	7.41			6
199603	8024	A 3		0.12	0.1	6.02	1.52	3.89	10
201707	8102	F 0		0.097	0.1	6.48	1.27	3.88	10[a,b]
204188	8210	A m		0.04		6.03	2.83	3.90	15
215874	8676	F 0	70 Aqr	0.086	0.025	6.15	1.35	3.89	3
223781	9039	A 3	82 Peg	0.06	0.005	5.29	1.36	3.91	14

Table 1
(end)

HD	HR	S T	Name	Periods	Amplitudes	V	M_V	Log T_{eff}	Ref
		A 7 V	Y Cam	0.063	0.04	10.45			12
BD + 48°894		F 0 IV		0.037	0.012	9.14	2.8		17
BD + 48°905		A 8 V		0.03	0.014	8.98	2.8		17
BD + 47°842		A 6 Vn		0.08	0.022	8.78	2.4		17

M_V and log T_{eff} from Dunley Observatory Report.
V and Sp type from H.R. Catalogue, except for the three last stars see 17.

1 Gupta, S.K., Bhatnagar, A.K., I.A.U. Bull. Com. 27 n° 751.

2 Gupta, S.K., Bhatnagar, A.K., I.A.U. Bull. Com. 27 n° 778.

3 Weiss, W.W., I.A.U. Bull. Com. 27 n° 1364.

4 McInally, C.J., Austin, R.D., I.A.U. Bull. Com. 27 n° 1334.

5 Auvergne, M., Le Contel, J.-M., Sareyan, J.-P., Valtier, J.-C., Daguillon, J., I.A.U. Bull. Com. 27 n° 1365.

6 McInally, C.J., McKay, B.J., I.A.U. Bull. Com. 27 n° 1257.

7 Bartolini, C., Piccioni, A., Silveri, P., I.A.U. Bull. Com. 27 n° 981.

8 Elliott, J.E., 1974, A.J. 79, 1082.

9 Horan, S., I.A.U. Bull. Com. 27 n° 1232.

10a Kilambi, G.C., I.A.U. Bull. Com. 27 n° 1024.

10b Kilambi, G.C., Dupuy, L.D. 1978, P.A.S.P. 90, 194.

11 Eggen, O.J., I.A.U. Bull. Com. 27 n° 935.

12 Broglia, P., I.A.U. Bull. Com. 27 n° 823.

13 Horan, S.J., Michael, J.L., Seeds, M.A., I.A.U. Bull. Com. 27 n° 896.

14 Le Contel, J.-M., Valtier, J.-C., Sareyan, J.-P., Baglin, A., Zribi, G. 1974 Astron. Astrophys. Suppl. 15, 115.

15 Kurtz, D.W. 1978, Astrophys. J. 221, 869.

16 Kurtz, D.W. 1977, P.A.S.P. ___, 941.

17 Slovak, M.H. 1978, Ap. J. 223, 192.

18 Weiss, W.W., I.A.U. Bull. Com. 27 n° 1400

19 SEEDS, M.A., Horan, S. 1976, P.A.S.P. 88, 251.

Table 2

Abundances relative to the Sun of a "classical Am" 63 Tau, 3 evolved Am (15 Vul, 22 Boo and α Cnc) and two δ Delphini stars (δ Del and ρ Pup).

	63 Tau	15 Vul	22 Boo	α Cnc	δ Del	ρ Pup
log Te	7650	7650	7750	8400	7320	7100
log g	4.4	3.5	3.5	3.8	3.25	3.25
Ca	-0.7	-0.3	-0.4		-0.08	.6
Sc	-0.45	-0.35	-0.5	-0.8	-0.40	.2
Cr	1	-0.1	-0.1	-0.3	-0.20	.1
Mn	0.5	-0.3	0		+0.06	.5
Fe	0.8	0	0.1	0	0	:54
Ni	1.2	0.4	0.7		0	.7
Zr	0.5	0.65	0.8		0.3	.6
Ba	15				0.7	.2
Y		1.1	0.8	1.1		
Eu	1.6	0.55	1.2	1.1	0.8	1.3

(1) 63 Tau is from Provost et al. (1969).

(1) 15 Vul is from Faraggia et al. (1973).

(2) 22 Boo and α Cnc are from Burkhart (1978).

(3) δ Del and ρ Pup are from Kurtz (1976).

Table 3

Characteristics of the best known A I Velorum Stars.

Star	P_o	P_1	ΔV	T_{eff}	<log g>	$<m_1>$	M_V c,T /c,1	δm_1
SS Psc	0.288		0.43	7300 °K	3.29	0.178	0.7/0.3	+ 0.01
BS Aqr	0.198		0.51	7200	3.60	0.177	0.8/1.0	+ 0.002
VZ Cnc	0.178	0.143	0.29	7100	3.62	0.181	1.3/1.1	- 0.004
DE Lac	0.254		0.31	6960	3.57	0.180		
SX Phe	0.055	0.042	0.51	7850	4.20	0.135	2.9	0.135
CY Aqr	0.061	0.045	0.73	7930	4.13	0.146	2.8	0.059
AE Uma	0.086	0.66						
RV Ari	0.093	0.072	0.7					
DP Peq	0.109	0.084	0.4					
AI Vel	0.111	0.086	0.67	7620	3.98	0.176	1.1/1.7	0.018
V703 Leo	0.149	0.115	0.50					
VX Hya	0.223	0.173	0.1-0.68	6940-7040	3.49-3.46	0.180	0.1/1.1	+ 0.006
AD Cnc	0.123		0.32	7580	3.94	0.181	0.9/1.6	0.009
GD 428	0.039			8050	4.18	0.08	4.4	0.125
DY Peg	0.073		0.54	7800	4.0	0.141	2.7	0.062
EH Lib	0.088		0.50	7930	4.12	0.175	1.3	0.028
YZ Boo	0.104		0.40	7650	3.97	0.175	1.8/1.1	0.021
SZ Lyn	0.120		0.48	7540	3.88	0.189	1.3/1.6	0.001
RS Gru	0.147		0.56	7600	3.83	0.158	0.7/1.3	0.035
DY Her	0.148			7130	3.66	0.188	1.8/1.3	- 0.012

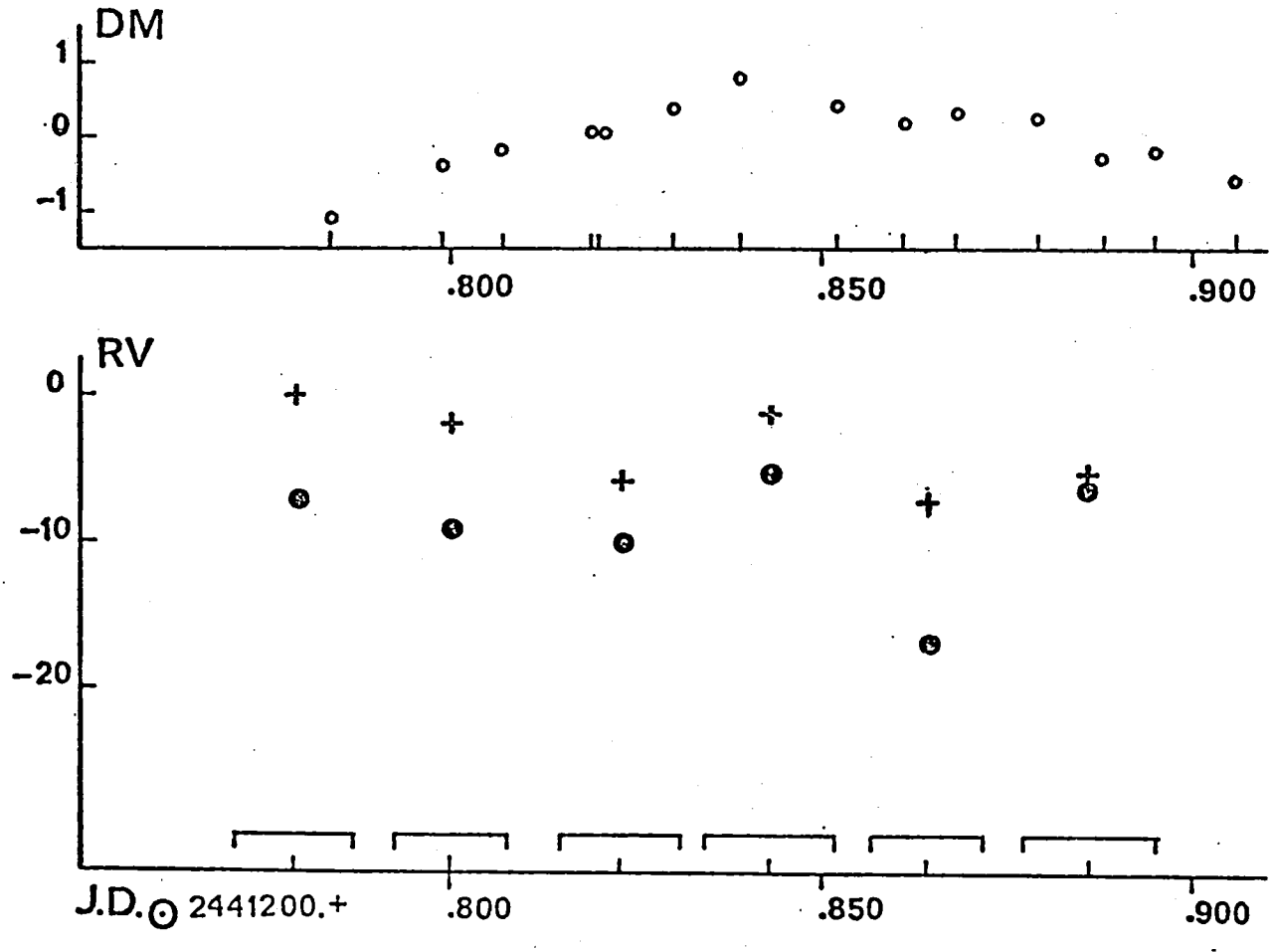

Figure 1. HR 515

Fig. 1 Simultaneous light (circles pannel) and RV curves (low pannel) of the giant Delta Scuti star HR 515.
Crosses : K line.
Dots : H lines.

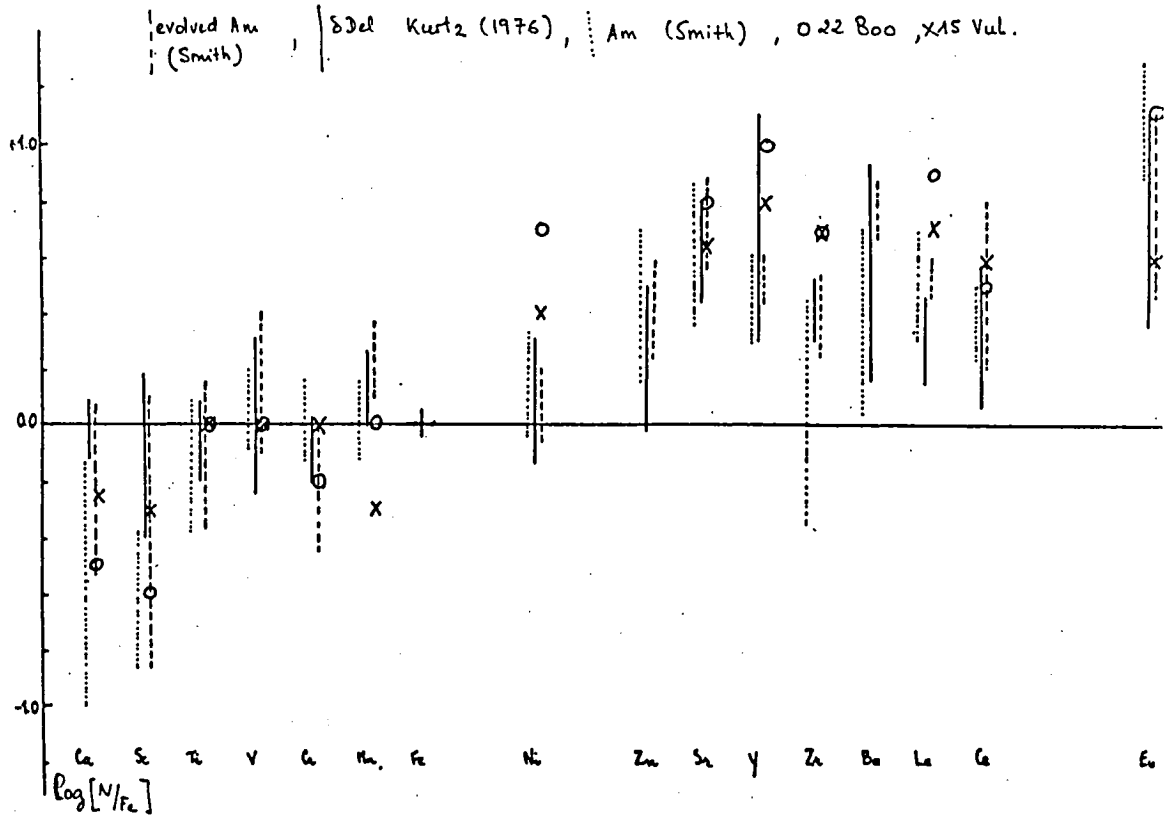

Figure 2. Compared relative abundances of classical evolved Am Delta Del stars from Kurtz (1976) 15 Vul and 22 Boo from Burkhart (1978).

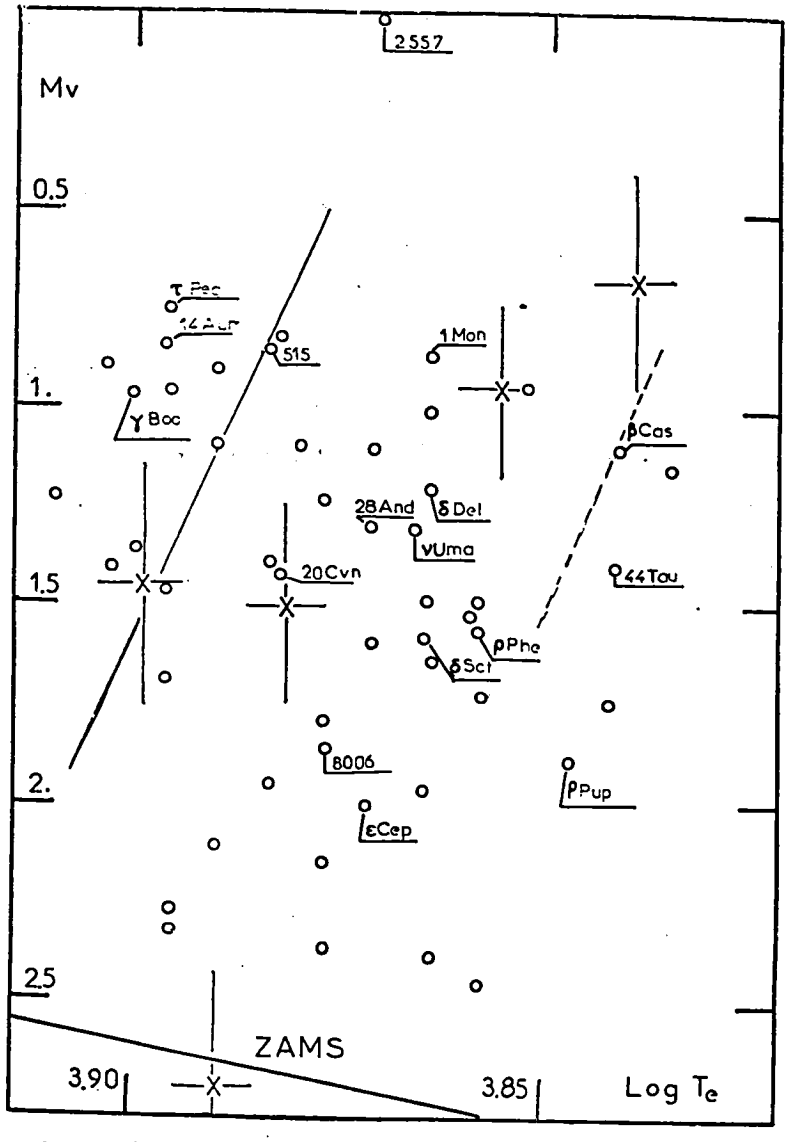

Figure 3. HR diagram showing the position of

o - some dwarf Delta Scuti stars

o - all the known giant Delta Scuti variables

x - several A I Velorum stars for which Stromgren photometry is available with the estimated errors bars.

- the theoretical blue edge of models of normal compsition

- the theoretical blue edge due to the hydrogen ionization zone (dotted line)

- some well studied Am or Delta Del stars.

ON THE ORIGIN OF PERIOD CHANGES IN RR LYRAE STARS

A. RENZINI

Osservatorio Astronomico, Bologna, Italy

and

A. V. SWEIGART

Laboratory for Astronomy and Solar Physics

NASA Goddard Space Flight Center, USA

To appear in the proceedings of the Los Alamos/Goddard Conference on "Current Problems In Stellar Pulsation Instabilities", June, 1978.

I. INTRODUCTION

Since the work of Martin (1938, 1942), it has been known that the pulsation periods of many RR Lyrae stars vary at a typical rate of a few parts in 10^5 every 100 yrs. It was originally hoped that the observed period changes would provide information about the rate and direction of the evolution of RR Lyrae stars in the HR diagram and thus of horizontal-branch stars in general, particularly those in globular clusters. However, the comparison of the observed rates of period change with the rates predicted from evolutionary models did not substantiate this expectation in two major respects: i) in several globular clusters increasing and decreasing periods occur with nearly equal frequency, while the models generally spend much of their horizontal-branch lifetime evolving in one direction, and ii) the observed rates of period change typically exceed the evolutionary ones by roughly an order of magnitude (cf. Iben and Rood 1970). For these reasons many authors have suggested that most period changes are due to some sort of "noise" or random fluctuations superimposed on the mean evolutionary changes in the stellar structure (Ledoux and Walraven 1958; Iben and Rood 1970; Schwarzschild 1970, 1973; Szeidl 1975). A fundamental problem therefore is to determine the origin of this noise.

The available observational material on period changes sets several constraints on the characteristics of the noise. First, the typical size of the period changes requires that the noise should be able to produce variations in the stellar radius of a few parts in 10^5 in both directions. Second, such fluctuations should occur approximately every 100 yrs. Third, the noise should produce both relatively slow and fast changes in the stellar radius, since both continuous and abrupt period changes apparently occur in RR Lyrae stars.

The last point is somewhat controversial and deserves a little more attention. In most cases, phase-shift diagrams can be fitted both with parabolas (implying a continuous period change) or with straight lines (implying an abrupt period change) as shown, for instance, by Goranskij, Kukarkin and Samus (1973). It is worth emphasizing that the terms "slow" (continuous) and "fast" (abrupt) are relative to the time interval spanned by the observations Δt_{obs}, which is typically around 50 to 75 yrs. A fluctuation in the stellar structure is characterized by its time duration τ. If $\tau \geq \Delta t_{obs}$, a "continuous" period change is produced, while if $\tau << \Delta t_{obs}$, one has an "abrupt" period change. Among the best observed cases (Szeidl 1975), RR Leo has a "continuous" period change, implying $\tau \geq \sim 60$ yrs, while RR Gem has suffered an "abrupt" period change. Only an upper limit, $\tau < \sim 4$ yrs, can be set for the duration of the period change in RR Gem because of the limited time resolution of the observations. From the existing observations it is difficult to decide whether "continuous" and "abrupt" period changes are two entirely different kinds of phenomena or whether there is a continuous spectrum of τ values from, say, a few years to a few decades. In the following discussion we will assume the second point of view.

Some period changes may be related to the Blazhko effect (variable pulsation amplitude generally suspected to originate from some sort of modal interference). RR Lyrae stars exhibiting the Blazhko effect have on average larger period changes than non-Blazhko variables. For instance, RR Gem passed through a Blazhko phase just around the epoch of its abrupt period change (Szeidl 1975). In a non-linear oscillating system the period marginally depends on the amplitude of the oscillation. This dependence is a second order effect and is shown, for example, by the ordinary pendulum. Consequently amplitude fluctuations in RR Lyrae stars might also lead to

period fluctuations whose cumulative effects might produce observable period changes. A quantitative check of this possibility is extremely difficult. In principle, one could look at the behavior of the period during the growth to full amplitude pulsation of non-linear models, but, since we are looking for an effect in the fifth decimal place, such models are currently far from being sufficiently accurate. However, it is unlikely that the Blazhko effect can account for the bulk of the observed period changes. RR Lyrae stars with the Blazhko effect are normally excluded when deriving period changes for the variables in a globular cluster. We must thus look elsewhere for the main source of the required noise.

The most obviously "noisy" process occurring in the stellar interior is convection, and in this respect RR Lyrae stars present quite a complex picture: i) RR Lyrae stars possess a convective helium-burning core, ii) they have a convective zone just below the photosphere due to hydrogen and helium ionization, and, finally, iii) around the fully convective core most RR Lyrae stars have a semiconvective zone (SCZ) (Castellani, Giannone and Renzini 1971a,b; Renzini 1977). Although semiconvection has been included here under the general category of convection, we emphasize that there are fundamental differences between semiconvection and ordinary convection. For example, the composition within a SCZ is not uniform. Furthermore, the mass motions needed to maintain the proper composition distribution within a SCZ are always assumed to carry a negligible amount of the outward flux.

There is no doubt that the structure of a convective region can fluctuate in time because of the inherent nature of the convective process. Such fluctuations can be described in terms of a statistical fluctuation in the number of "convective elements" present at a given time in the

convective region or in terms of a fluctuation in the convective pattern, i.e., in the geometry of the convective cells, columns, currents and so on. Variations of this kind might be reasonably expected to produce slight variations in the convective efficiency and therefore in the average temperature gradient. This in turn would affect the structure of the convective zone and hence of the whole star. In the framework of the mixing-length theory a fluctuation in the convective efficiency can be treated as a fluctuation in the mixing length, but the mixing-length theory itself can say nothing about the magnitude or the characteristic time scale of such fluctuations. However, in spite of these limitations, both the convective core and the outer convective zone can be ruled out as the region where the noise causing the observed period changes originates.

Convection within the core is so efficient (Schwarzschild 1958) that even a huge fluctuation in the mixing length does not significantly perturb the stellar structure. In other words, varying the mixing length within a range much wider than the "canonical" one (which is between 1/2 and 2 pressure-scale heights) has a completely negligible effect on the actual temperature gradient within the convective core. Since the actual temperature gradient always remains very close to the adiabatic-temperature gradient, it would be difficult to understand how core convection could generate the required noise.

This kind of argument does not, however, apply to the outer convective zone, where sizable departures from the adiabatic-temperature gradient can occur and where fluctuations in the convective efficiency might therefore affect the stellar radius. Such fluctuations in the convective efficiency could, in principle, produce period changes. However, the characteristic time scale of convection in the outer layers is only a few hours, and consequently it is not clear how slow changes in the period could be produced.

As we have seen, period changes with a duration on the order of several decades or more are observed. Furthermore, the structure (thickness, degree of superadiabaticity, etc.) of the outer convective zone in RR Lyrae stars changes dramatically in going from the blue to the red edge of the instability strip. If the observed period changes were due to fluctuations in the outer convective zone, the typical period change should increase dramatically from the blue to the red edge, i.e., with decreasing effective temperature or increasing period. This trend is not in fact observed. There is no obvious correlation between the period changes and the location of the RR Lyrae stars within the instability strip. For these reasons the outer convective zone would also seem to be an unlikely source of the required noise.

There remains the possibility that the noise is associated with the SCZ surrounding the fully convective core. We have analyzed this possibility in detail (Sweigart and Renzini 1978, hereafter SR), and in the following section we will summarize the most important concepts and results.

II. SEMICONVECTION AND PERIOD CHANGES

During the initial horizontal-branch evolution the convective core grows in mass as a result of convective overshooting. (Castellani et al. 1971a; Renzini 1977). Once the helium abundance Y_c within the convective core falls below $\sim$0.7 (Sweigart and Gross 1974, 1976), a SCZ develops around the convective core in order to maintain convective neutrality (i.e., equality of the radiative- and adiabatic-temperature gradients) at the convective-core edge (Castellani et al. 1971b). By definition a SCZ is a region where the chemical composition varies from point to point in a way that ensures convective neutrality. As a horizontal-branch star

evolves, the SCZ becomes more extensive until it typically contains ~0.1 $M_\odot$ shortly before the end of core-helium burning. Some mixing process is therefore necessary in order to adjust properly the abundances of helium, carbon and oxygen throughout the SCZ at each stage of the evolution.

It is universally known that stellar convection still awaits a physically satisfactory treatment, and the case of semiconvection is even worse. Most efforts in this field pertain either to the formulation of algorithms suitable for treating SCZ's in stellar-model calculations (Robertson and Faulkner 1972) or to the proper definition of "convective neutrality", i.e., whether the Schwarzschild or Ledoux criterion is more appropriate. There is unfortunately very little theoretical understanding of how a SCZ actually manages to maintain convective neutrality. However, the composition distribution within a SCZ would not be expected to change continuously during the evolution. Rather, the composition changes probably result from many discrete mixing events occurring randomly throughout the SCZ (see SR). The typical size of such mixing events would have to be substantially smaller than the whole SCZ. Otherwise a large part of the SCZ would be mixed up, and the composition gradient would disappear, thus leading to a major departure from convective neutrality. During the evolution one would expect small parts of the SCZ to become occasionally unstable due to the changes in the interior structure caused by the central helium burning. The resulting convection within these small parts of the SCZ would persist until the composition distribution has been changed sufficiently to restore convective neutrality. These considerations suggest that the SCZ manages to remain close to neutrality through a series of relatively small mixing events, each of which perturbs the interior structure by slightly altering the composition distribution. Semiconvection should therefore be an inherently noisy phenomenon.

The mixing events can be characterized by their size ΔM_r, duration τ_{ME} and the time interval Δt_{ME} between them. In principle, a spectrum of ΔM_r, τ_{ME} and Δt_{ME} values would be expected. The typical values of these quantities may vary during the evolution and thus may depend on Y_c. Without a theory of the semiconvective process there is no way to predict these typical values. However, one can use the observed properties of the period changes to obtain some insight into the characteristics of the mixing events and hence into the nature of the semiconvective process itself. The period changes could thus be one of the few available tools for probing the stellar interior.

By imposing canonical semiconvection (i.e., the requirement of convective neutrality both at the convective-core edge and within the SCZ), one can compute horizontal-branch sequences without a detailed knowledge of how the composition redistribution actually takes place within the SCZ. In these sequences the composition redistribution is usually treated as a continuous process, not as the result of discrete mixing events (Robertson and Faulkner 1972). However, the computed evolution is not significantly affected as long as neutrality is maintained on average throughout the SCZ. Sequences obtained in this manner provide information on the mean evolution of horizontal-branch stars and determine the average rate at which the composition distribution within the core is changing.

The composition redistribution within the core leads to the mixing of a substantial amount of helium (and therefore carbon and oxygen) through the SCZ and between the SCZ and the convective core. This mixing probably takes place in the following manner. As the helium burning gradually reduces Y_c, the opacity and hence the radiative-temperature gradient increase within the convective core (Castellani et al. 1971a). The resulting superadiabaticity at the convective-core edge leads to convective overshooting. Each overshooting event captures a small amount of helium from the inner layers of

the SCZ. In this way the convective core is able to restore convective neutrality at its edge. However, the carbon and oxygen which have been deposited into the inner layers of the SCZ cause these layers to become convectively unstable, and consequently the whole SCZ must then readjust. This readjustment is probably accomplished through a series of mixing events which have the cumulative effect of transferring the excess carbon and oxygen outward through the SCZ or, equivalently, of bringing additional helium into the SCZ. Castellani et al. (1971b) have referred to this process as "induced semiconvection" to emphasize how overshooting at the convective-core edge fundamentally drives the development of the SCZ. Each mixing event produces an irreversible change in the stellar structure, since helium is always carried inward and carbon and oxygen are always carried outward. During the horizontal-branch lifetime ($\sim 10^8$ yrs), approximately 0.1 $M_\odot$ of helium are transferred inward through the SCZ and into the convective core. Therefore the number of mixing events of a given size that a star can have during its entire core-helium-burning phase is prescribed by standard horizontal-branch sequences if canonical semiconvection is on average fulfilled.

In view of this description of the mixing process we can distinguish three different types of mixing events, hereafter denoted as types A, B and C (see Fig. 4 of SR). An overshooting event at the convective-core edge will be referred to as a type A event. Mixing events confined to the SCZ will be labeled type B, while those responsible for bringing helium from the outer radiative region into the top of the SCZ will be termed type C.

The change in the composition distribution caused by a mixing event forces a readjustment in both the hydrostatic and thermal structure of a star. The hydrostatic readjustment, occurring on a dynamical time scale, leads to a concomitant change in the radius and hence to a change in the

pulsation period. However, the thermal readjustment proceeds on the much longer Kelvin time scale and hence would be unlikely to cause a detectable period change.

Along an evolutionary sequence the interior composition distribution changes as a result of i) the various types of mixing events and ii) the nuclear burning in the convective core and in the hydrogen shell. Each of these separate effects would by itself alter the pulsation period. According to our previous discussion, the period changes associated with the mixing events occur discretely in time. Whether or not these period changes appear to be continuous or abrupt depends on how τ_{ME} compares with Δt_{obs}. Between mixing events the nuclear burning gradually alters the interior composition, an effect that can only give rise to a continuous period change. In general, the evolutionary period change ΔP_{ev} between two consecutive horizontal-branch models can be written in terms of four components

$$\Delta P_{ev} = \Delta P_n + \Delta P_A + \Delta P_B + \Delta P_C \qquad (1)$$

where ΔP_n is the period change due to the nuclear burning alone and ΔP_A, ΔP_B and ΔP_C are, respectively, the cumulative period changes due to the type A, B and C mixing events.

In evolutionary sequences constructed according to canonical semi-convection the composition redistribution due to the mixing events is assumed to be tightly coupled to the composition changes due to the nuclear burning. Over long time intervals such a coupling must on average exist, since it is the nuclear composition changes which basically determine the growth of the SCZ. However, this coupling need not necessarily hold at every moment. In actual stars one might expect to observe the individual

period changes resulting from the separate mixing events and from the nuclear burning, provided that these individual period changes are large enough to be detected. If these individual period changes do not all have the same sign, then the sum $|\Delta P|$ of all period changes observable over a time interval, as given by

$$|\Delta P| = |\Delta P_n| + |\Delta P_A| + |\Delta P_B| + |\Delta P_C| \quad , \tag{2}$$

will exceed $|\Delta P_{ev}|$. Because of this decoupling between the mixing events and the nuclear burning, one could have relatively large fluctuations in the period superimposed on the small evolutionary period changes. The only requirement is that the individual period changes must on average combine to give ΔP_{ev}.

Using a stellar-evolution program, we have artificially imposed mixing events of types A, B and C on the composition profile of several suitably selected horizontal-branch models and in this way have determined how the period changes depend on the mixing events (see SR for details). It turns out that type A events produce negative period changes while type B and C events produce positive period changes. For the representative sequence studied by SR the net period change ΔP_{ME} ($= \Delta P_A + \Delta P_B + \Delta P_C$) due to all types of mixing events differs in sign from ΔP_{ev} during much of the evolution. According to Equation (1), ΔP_{ME} must then also differ in sign from ΔP_n. The observational requirement that both positive and negative period changes be produced is therefore satisfied.

The results of SR show that only small mixing events are needed to produce a typical period change $|\Delta P/P|$ of 3×10^{-5}. At $Y_c = 0.37$, for example, a type A event involving overshooting by only 0.008 $M_\odot$ in ΔM_r and 0.02 in Δlog pressure is sufficient to cause this period change. The

amount of helium captured by the convective core during such an event is only 5×10^{-6} $M_\odot$. As Y_c decreases, the pulsation period becomes appreciably more sensitive to the type A events. For the type B events the required width of the mixed region is also about 0.008 $M_\odot$ in ΔM_r and 0.02 in $\Delta \log$ pressure over a wide range in Y_c. Since the SCZ contains $\sim$0.1 $M_\odot$, the condition that the type B events be small compared with the SCZ is amply fulfilled. The type C events turn out to be relatively unimportant. The sensitivity of the period changes to the mixing events can vary by a factor of 2, depending on the horizontal-branch parameters (i.e., the mass and composition).

The frequency of a typical period change $|\Delta P/P|$ of 3×10^{-5} can be obtained from the following procedure. The period-change testing of horizontal-branch models outlined above determines the amount of helium mixed inward during a typical mixing event. At each point along an evolutionary sequence the average rate at which helium is mixed through the SCZ and into the convective core can be derived from the change in the composition distribution between consecutive models. Knowing this rate and the amount of helium involved in a single mixing event, one can compute the frequency of each type of mixing event and hence the period changes ΔP_A, ΔP_B and ΔP_C. The evolutionary period change ΔP_{ev} can be readily obtained from the models. The value of ΔP_n then follows from Equation (1). We find that the mixing events and the nuclear burning make roughly equal contributions to the observed period changes. The results for the sequence studied by SR indicate that a typical period change should occur roughly every 300 yrs while the observed value is roughly 100 yrs. In view of the sensitivity of the period changes to the model parameters and in view of the substantial theoretical and observational uncertainties, we consider the agreement between the present theory and the observations to be quite

satisfactory. For a more detailed discussion, see SR.

III. CONCLUSIONS

Our proposed explanation for the observed period changes is based on the behavior of the SCZ within the core of an RR Lyrae star. General physical considerations suggest that the composition changes occurring within the SCZ during the horizontal-branch evolution result from many small mixing events, each of which slightly perturbs the pulsation period. Between mixing events the interior structure of an RR Lyrae star gradually changes because of the nuclear burning, and this effect should also contribute substantially to the observed period changes. A more detailed examination of this theory would require an improved theoretical understanding of the semiconvective process as well as the availability of better observational data on the sizes and frequencies of the period changes.

Our main conclusions may be summarized as follows:

1. Small mixing events within the core of an RR Lyrae star can produce changes in the pulsation period comparable with those typically observed.

2. These mixing events together with the nuclear burning between them can produce period changes of both signs.

3. The theoretically predicted frequency of the period changes is in satisfactory agreement with the observed value, although the uncertainties involved are substantial.

We gratefully acknowledge helpful discussions with J. Lub and A. Wesselink.

Castellani, V., Giannone, P., Renzini, A.: 1971a, Astrophys. Space Sci. 10, 340

Castellani, V., Giannone, P., Renzini, A.: 1971b, Astrophys. Space Sci. 10, 355

Goranskij, V. P., Kukarkin, B. V., Samus, N. N.: 1973, in Variable Stars in Globular Clusters and in Related Systems, IAU Colloquium No. 21, Ed. J. D. Fernie, D. Reidel, Dordrecht, p. 101

Iben, I., Jr., Rood, R. T.: 1970, Astrophys. J. 161, 587

Ledoux, P., Walraven, Th.: 1958, in Handbuch der Physik, Ed. S. Flügge, Springer Verlag, Berlin, 51, p. 353

Martin, W. C.: 1938, Ann. Sterrew. Leiden 17, Part 2

Martin, W. C.: 1942, Astrophys. J. 95, 314

Renzini, A.: 1977, in Advanced Stages in Stellar Evolution, Proc. Seventh Advanced Course of the Swiss Society of Astronomy and Astrophysics, Eds. P. Bouvier, A. Maeder, Geneva Observatory, Sauverny, p. 149

Robertson, J. W., Faulkner, D. J.: 1972, Astrophys. J. 171, 309

Schwarzschild, M.: 1958, Structure and Evolution of the Stars, Princeton University Press, Princeton

Schwarzschild, M.: 1970, Quart. J. Roy. Astron. Soc. 11, 12

Schwarzschild, M.: 1973, in Variable Stars in Globular Clusters and in Related Systems, IAU Colloquium No. 21, Ed. J. D. Fernie, D. Reidel, Dordrecht, p. 228

Sweigart, A. V., Gross, P. G.: 1974, Astrophys. J. 190, 101

Sweigart, A. V., Gross, P. G.: 1976, Astrophys. J. Suppl. 32, 367

Sweigart, A. V., Renzini, A.: 1978, Astron. Astrophys., in press

Szeidl, B.: 1975, in Variable Stars and Stellar Evolution, IAU Symposium No. 67, Eds. V. E. Sherwood, L. Plaut, D. Reidel, Dordrecht, p. 545

Discussion

Stellingwerf: If you look at calculations of linear pulsation analysis, you find that the period is very insensitive to actual conditions deep in the model.

Sweigart: That was the initial suspicion that one would have.

Stellingwerf: The period changes must reflect an overall redistribution in the structure of the model. Would this then produce a change in the luminosity or effective temperature?

Sweigart: That is basically what happens. When you change the interior composition by a small amount, you cause a small fluctuation in the location of the model in the H-R diagram and hence a small change in the radius. The result is a change in the period.

Stellingwerf: Can you see that?

Sweigart: No, you are talking about changes of a few parts in 10^5.

Belserene: How quickly does the event take place?

Sweigart: That's an important question, because it relates to the question of whether or not the period changes are continuous or abrupt. There is unfortunately little theoretical understanding of how the semiconvection zone actually readjusts during the horizontal-branch evolution.

Belserene: Does your scenario give you some feeling for it?

Sweigart: We impose the mixing events on the models without assuming a time scale for these events, so we cannot say. Nevertheless, from the general requirement of convective neutrality within the semiconvective zone, we do know the overall extent of the composition redistribution that occurs within the core during the evolution. Since our calculations provide an estimate for the size of a typical mixing event, we can therefore predict the frequency of these events. However, the duration of a particular mixing event cannot be theoretically predicted at the present time. One might speculate offhand that, since a mixing event involves convective motions, the time scale of a mixing event might be relatively short, thus leading to an abrupt period change. However, the composition changes due to the nuclear burning between the mixing events are also very important in producing period changes, and these composition changes would only lead to continuous period changes. So, it may in fact be possible to produce both abrupt and continuous period changes, as are observed among the field RR Lyrae stars.

Aizenman: Wouldn't you expect that those changes are happening where some are giving positive and some negative contributions, such that the net effect comes back to the change in evolution?

Sweigart: That is a basic condition. When you construct an evolutionary sequence, you are simultaneously changing both the composition distribution and the total amount of helium in the core. Standard model computations only determine the net effect on the stellar structure and hence only determine the small evolutionary changes in the period. What we are trying to do here is to separate the effects of the composition redistribution due to the mixing events from the effects of the composition changes due to the nuclear burning.

These separate effects can each produce relatively large period changes, even though they add up to a small evolutionary rate of period change. Essentially we have examined the question of how does a horizontal-branch star actually evolve from one point to another along an evolutionary sequence. We are suggesting that this evolution is inherently noisy because of the basic characteristics of the semiconvective process and that the observed period changes are in fact a measure of this noise.

Sreenivasan: What kind of numerical mixing scheme do you use? And is there a difference whether you use the Schwarzschild criterion or the Ledoux criterion?

Sweigart: All of our models have been computed with the Schwarzschild criterion. The numerical technique for treating semiconvection was that described by Robertson and Faulkner (1972, Ap. J., 171, 309). When studying the effects of the individual mixing events, we first mixed small regions of the semiconvective zone and then computed the resulting change in the stellar structure and hence in the period.

Sreenivasan: Would you see a difference if you used a diffusive type of mixing?

Sweigart: We have not investigated different numerical techniques for determining the structure of the semiconvective zone. If exact neutrality is assumed to exist within the semiconvective zone, one would not expect the structure of the semiconvective zone to depend on the adopted numerical technique, once the stability criterion is specified.

Sreenivasan: We found that the type of mixing would make a change in the fluctuations.

Sweigart: The thing which is of basic importance as far as our calculations are concerned is how extensive the semiconvective zone becomes or, equivalently, how much helium flows through it.

Baker: I have several comments. First, whether a process like this takes place or not is something that has to do with the hydrodynamics. It is not sufficient to do it in a completely local way. It is a global question, and you have to see what the eigenfunctions look like throughout the whole star. Second, if you look at the observations of RR Lyrae stars, what you see is not only changes in period, but also changes in amplitude and almost discontinuous changes in phase. Certainly phase changes occur, as well as period changes. Nonperiodic behavior is also seen in Population II Cepheids. It would be helpful to have more observations of such objects. The third point is that it is not at all clear that it is necessary to invoke major changes in the structure of the star in order to find abrupt changes in period or phase. It is pervasive characteristic of coupled nonlinear oscillators or other nonlinear systems with enough degrees of freedom, that in certain regions of the parameter space, it is quite easy to find nonperiodic behavior -- sudden changes in amplitude, jumps in period, changes in phase, and so on. These things deserve to be looked into in efforts to explain these stars.

Wesselink: I have a question with regard to the period changes in the RR Lyrae stars in ω Cen. There are a large number of them, and a dominance of one sign -- more positive changes than negative changes. Does that agree with your theory?

Sweigart: Our theory would predict that the mean rate of period change for the RR Lyrae stars in a globular cluster should correspond to the average evolutionary period change. The fact that the mean period change in ω Cen is positive would therefore indicate that the RR Lyrae stars in ω Cen are on average evolving redward in the H-R diagram.

Wesselink: It seems to me that the mean value should be determined rather well. Does that agree with your theory?

Sweigart: It depends upon precisely where the RR Lyrae stars in ω Cen are located along their horizontal-branch tracks. If they are returning to the asymptotic branch following the end of the horizontal-branch phase, the rate of evolution could be relatively rapid. The evolution could then produce a relatively large positive period change, as observed.

Wesselink: Inversely, you may be able to identify what position the RR Lyrae's are in.

Sweigart: There is a consistency check which one can make: does the morphology of the horizontal branch agree with the mean rate of period change one observes? If the morphology is such that you have a predominance of blue horizontal-branch stars, then you would expect to see, if anything, a positive mean rate of period change. That is in fact the case in ω Cen.

A. Cox: I want to drop a name. What seems to happen is, you want the period to change, but as Norman says, the period isn't going to change right away because the bell rings for a while in its original frequency.

Sweigart: There will be a hydrostatic readjustment of the star immediately following the adjustment of the composition.

A. Cox: But that will create a pulsation itself. The name I wanted to drop is the Blazhko effect. Maybe this is a beating of the period it had before, with the period it wants to go to. What do you think?

Sweigart: You are the expert on that! [Laughter] Normally, when people report changes in period, they try to exclude variables showing the Blazhko effect. If the Blazhko effect results from a beating between two periods, I would suspect that the required difference between these periods would considerable exceed the period change associated with a typical mixing event.

THEORETICAL MEAN COLORS FOR RR LYRAE VARIABLES

C. G. Davis and A. N. Cox
Los Alamos Scientific Laboratory
University of California

ABSTRACT

A hydrodynamically pulsating 0.6 $M_\odot$ model of a typical RR Lyrae variable has been studied with a radiation transport-hydrodynamic computer program to predict theoretical T_e and colors at many phases and to find the proper methods for getting mean colors and the consequent mean effective temperatures. The variable Eddington radiation approximation method was used with gray and with multifrequency absorption coefficients to represent the radiation flow in the outer optically thin layers. Comparison between observed and computed B-V colors indicate that these low Z Population II models are reasonably accurate using King 1A composition opacities. The well known Oke, Giver, and Searle relation between B-V and T_e is reproduced. Mean colors are found by four different averaging methods. The method that gives a mean color and the mean T_e closest to the nonpulsating model was the separate intensity means of B and V, just as the case for previous studies of classical Cepheids. The best mean for T_e, which is known for all pulsation phases from four color observations of real RR Lyrae variables or from the calculated model, is a time average of T_e without any weighting function.

I. INTRODUCTION

The problem of obtaining the mean color of RR Lyrae stars, in order to get the correct non-pulsating temperature, is similar to that for Cepheids (Cox and Davis 1975). In our nonlinear dynamic models we know the original nonpulsating temperature, and by using a multi-frequency snapshot approach with the appropriate filter responses, in this case for the UBV filters, we can study various ways to obtain mean colors. In this paper we study a model using nonlinear gray and multifrequency hydrodynamic transport calculations and Population II (Y = .299, Z = .001) King 1A mixture opacities. The discussion concerns the taking of color averages as well as the question, if we know the effective temperature at many phases, how best to obtain an average for the non-pulsating temperature of the model.

II. METHOD

The radiation flow for our RR Lyrae model is treated by a non-equilibrium diffusion approximation where the radiation field is not directly coupled to the material energy field as in the equilibrium diffusion approximation. The method limits to equilibrium gray diffusion in optically thick zones and to streaming in optically thin zones. The forward peaking of the radiation field is correctly described using variable Eddington factors. In our model we use a plane geometry characteristic ray calculation for the Eddington factors at each time step and for each frequency group. The multifrequency calculation is carried out for 13 frequency groups selected so that ionization edges and the Planck function emission are well resolved (Davis 1971). Some attempt has been made to include effects due to line radiation as perceived to be important by Mihalas (1969). This effect is included using a formulation proposed by Cassinelli and described in Davis (1978).

Effects on colors due to shock waves transiting the atmosphere are approximated using a number of optically thin zones outside the photosphere and the Richtmeyer-Von Neuman method of pseudoviscosity. The phase of shock transiting occurs between 0.4 and 0.5, where phase 0.5 is approximately the phase of peak luminosity. There is some evidence that a UV excess occurs during this phase to affect the continuum colors (Davis 1975). Conditions for hydrogen line emission and Ca line doubling do exist during this phase (Hill 1972).

III. MODEL

The selected mass is 0.6 $M_\odot$, and luminosity ($\log L/L_\odot = 1.6$) is equivalent to an $M_{bol} = 0.72$ where $M_{bol\odot} = 4.72$. This is in reasonable agreement with Oke, Giver, and Searle (1962) estimate for SU Dra. A $T_{eff} = 6840$ K ($\log T_e = 3.835$) then gives a fundamental period of 0.44 days. The inner radius of the model is less than 10% of the photospheric radius. No convection is allowed as appropriate for this T_e value (Deupree 1977). A zero pressure hydrodynamic boundary condition is applied.

In our structure calculations we have found that 72 zones with 5-10 zones in the optically thin atmosphere are sufficient to resolve the luminosity curve. Some noise still remains near light minimum when the ionization front has approached to 1 or 2 zones from the star's surface. The shock escaping during the phase near light minimum through light maximum results in the observation of H_γ line emission. In our models we have not resolved the detailed atmospheric structure during this phase (Hill 1972). The effects therefore of line emissions

during the phase of light minimum to rising light are not treated exactly but the effects on the colors are expected to be small.

Spectra using the calculated structures at many phases and 30 different frequency groups are convolved with the B and V filters. Raw colors b, v are corrected for their relative transparency by the formula

$$B - V = b - v + 0.65$$

as for the classical Cepheids considered previously by Cox and Davis (1975).

Figure 1 shows the calculated M_{bol} for the model where the variation is $> 1.8^m$. This is larger than the usual observed range of V for RR Lyrae stars ($\sim 1^m$). Figure 2 shows the variations of T_{eff} versus phase which go from approximately 5600 to 8700 K. In Figs. 3 and 4 we show the radius and velocity variations as calculated. The variation in radius is like 10-15% around a value of 4.5 $R_\odot$. The observed range in velocity is 62 km/s. The lower line is the velocity calculated at $\lambda = 4404$ Å at an optical depth of 0.10 (the location of the metal lines).

IV. RESULTS

The transformation formula for the conversion from B-V colors to T_{eff}, as derived by Oke, Giver and Searle (1962) for SU Dra with the assumption that the star is unreddened is $\theta = 0.62 + 0.51\ (B-V)$ where $T_{eff} = 5040/\theta$. We use this formula for our comparisons. In Figs. 5 and 6 we plot the OGS relationship against the calculation for the gray and multifrequency structures, respectively. There is

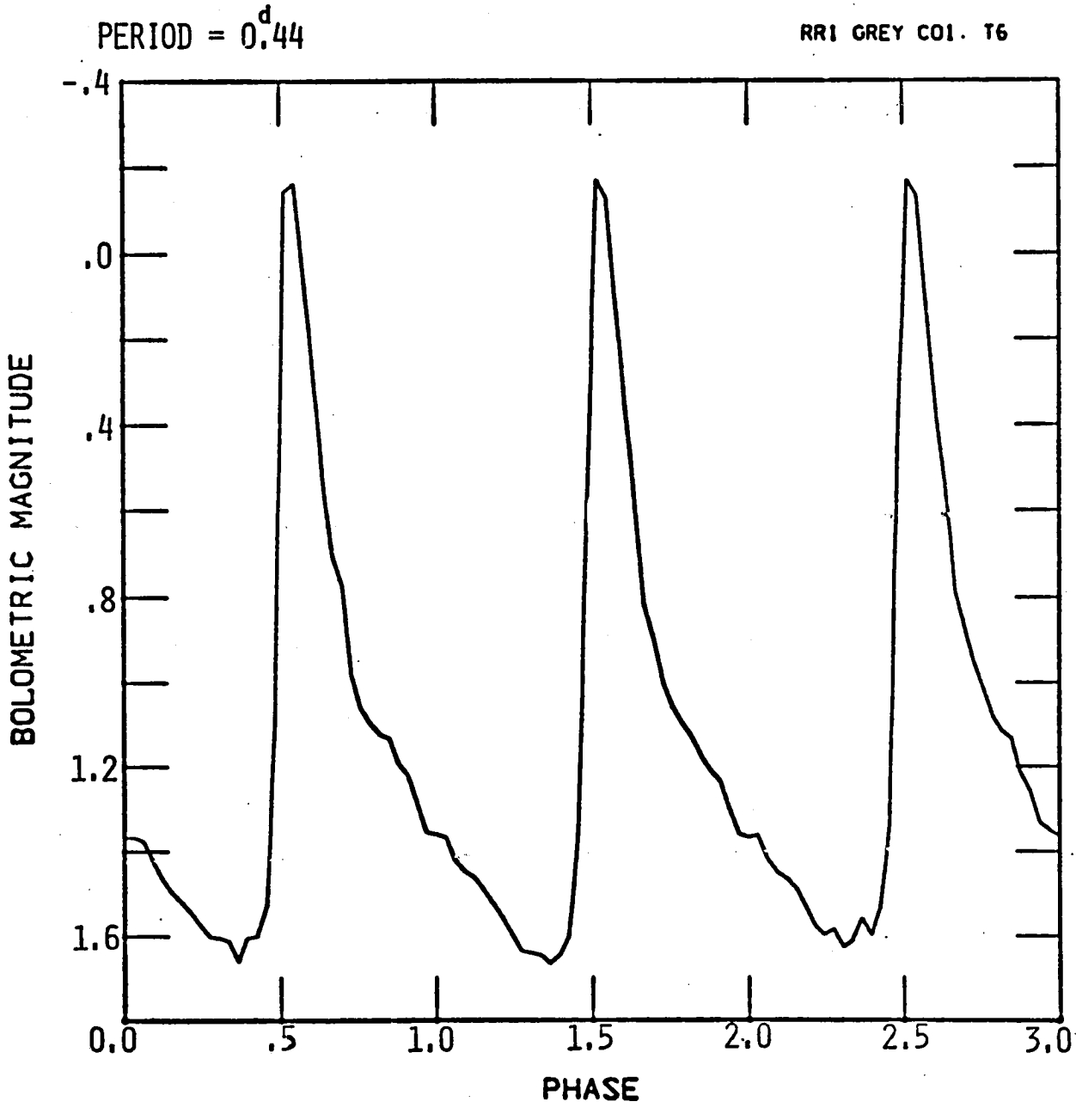

Fig. 1. Calculated bolometric magnitude for three periods (P = $0^d.44$). Note wiggles near light minimum (see text).

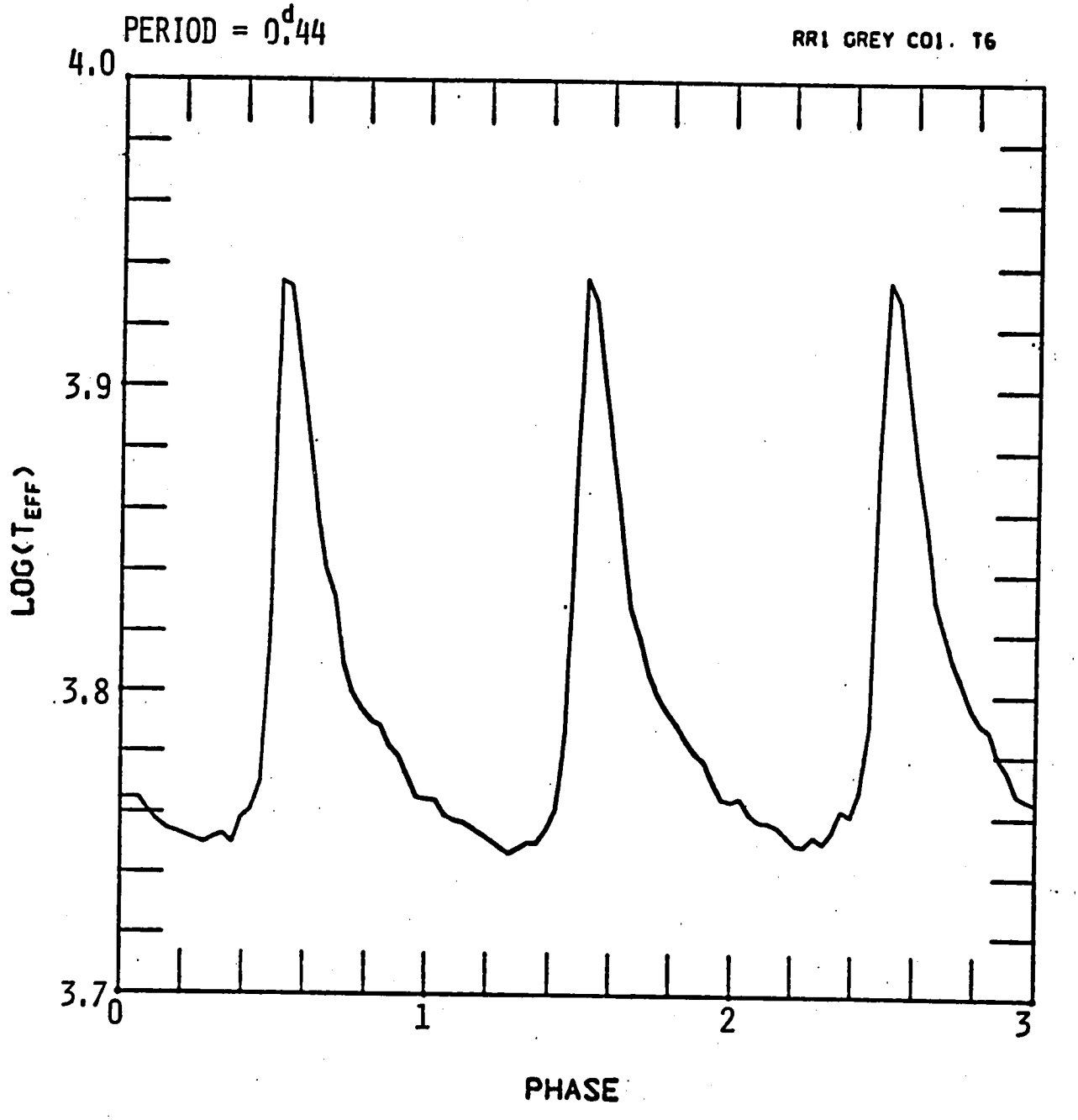

Fig. 2. Log T_{eff} versus phase with variations in T_{eff} calculated as 5600 - 8700 K.

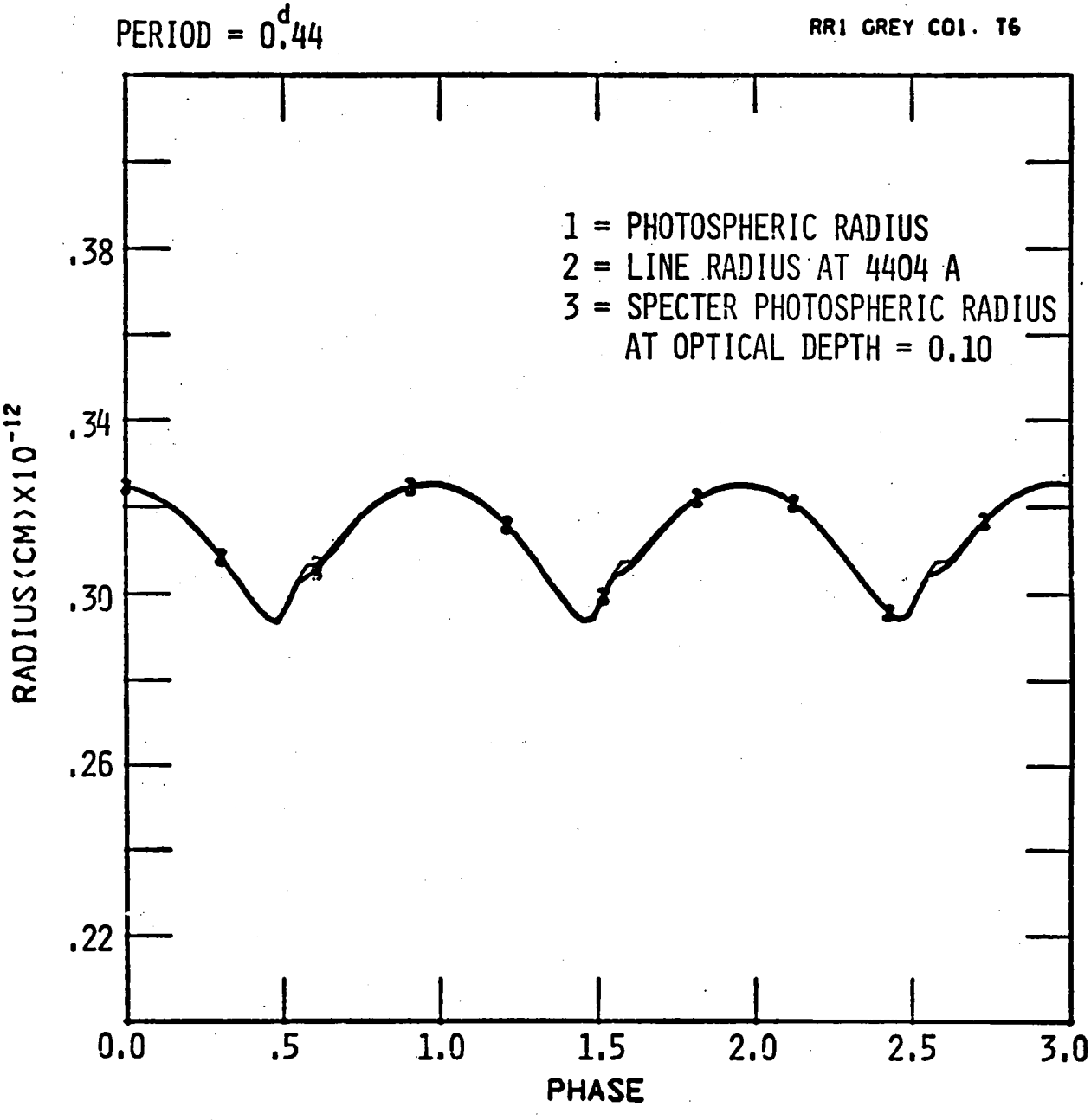

Fig. 3. Calculated photospheric radius ($R_{eq} \cong 4.5\ R_{\odot}$).

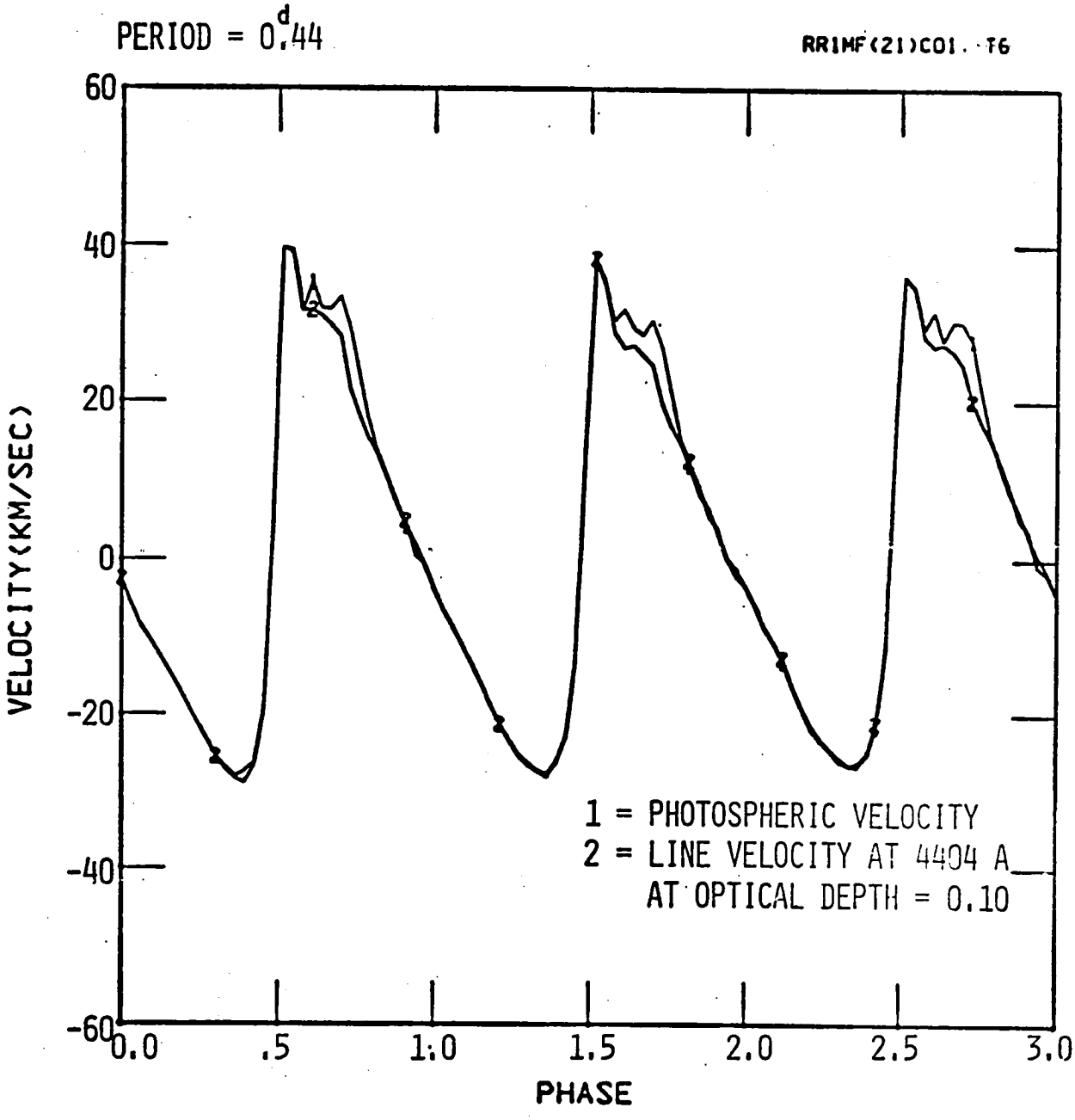

Fig. 4. Calculated velocity at $\tau = 2/3$. 2 = line velocity at 4404 Å, $\tau = 0.10$.

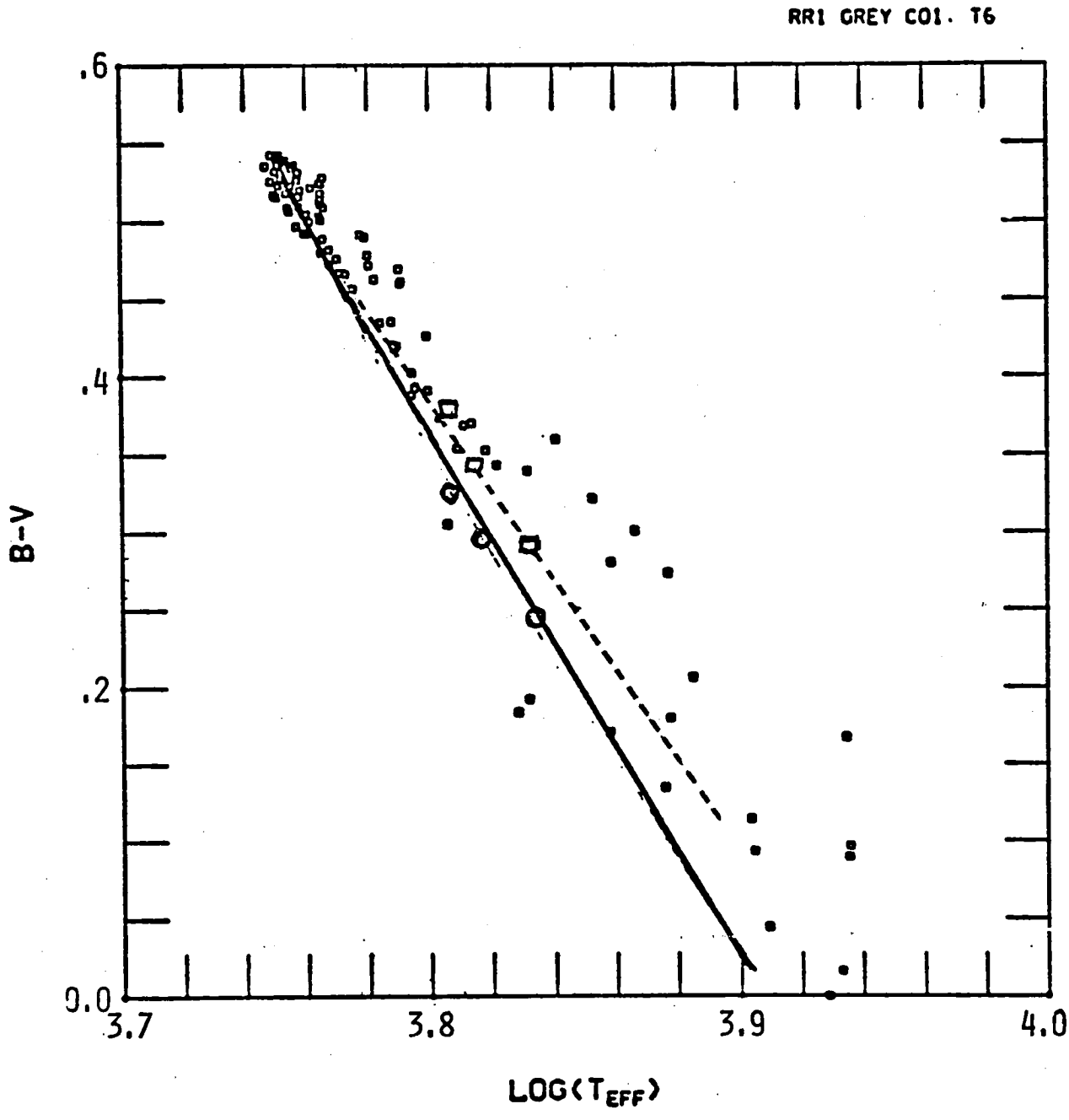

Fig. 5. B-V versus log T_{eff} calculated using gray transport structure. Solid line shows Oke, Giver, and Searle relation. Calibration values (O) for static models at L = 38 $L_\odot$ and T_{eff} = 6800, 6500 and 6350 K are plotted. Squares (□) are calibration values with convection. Dashed line is fitted to Kurutcz's latest results (unpublished).

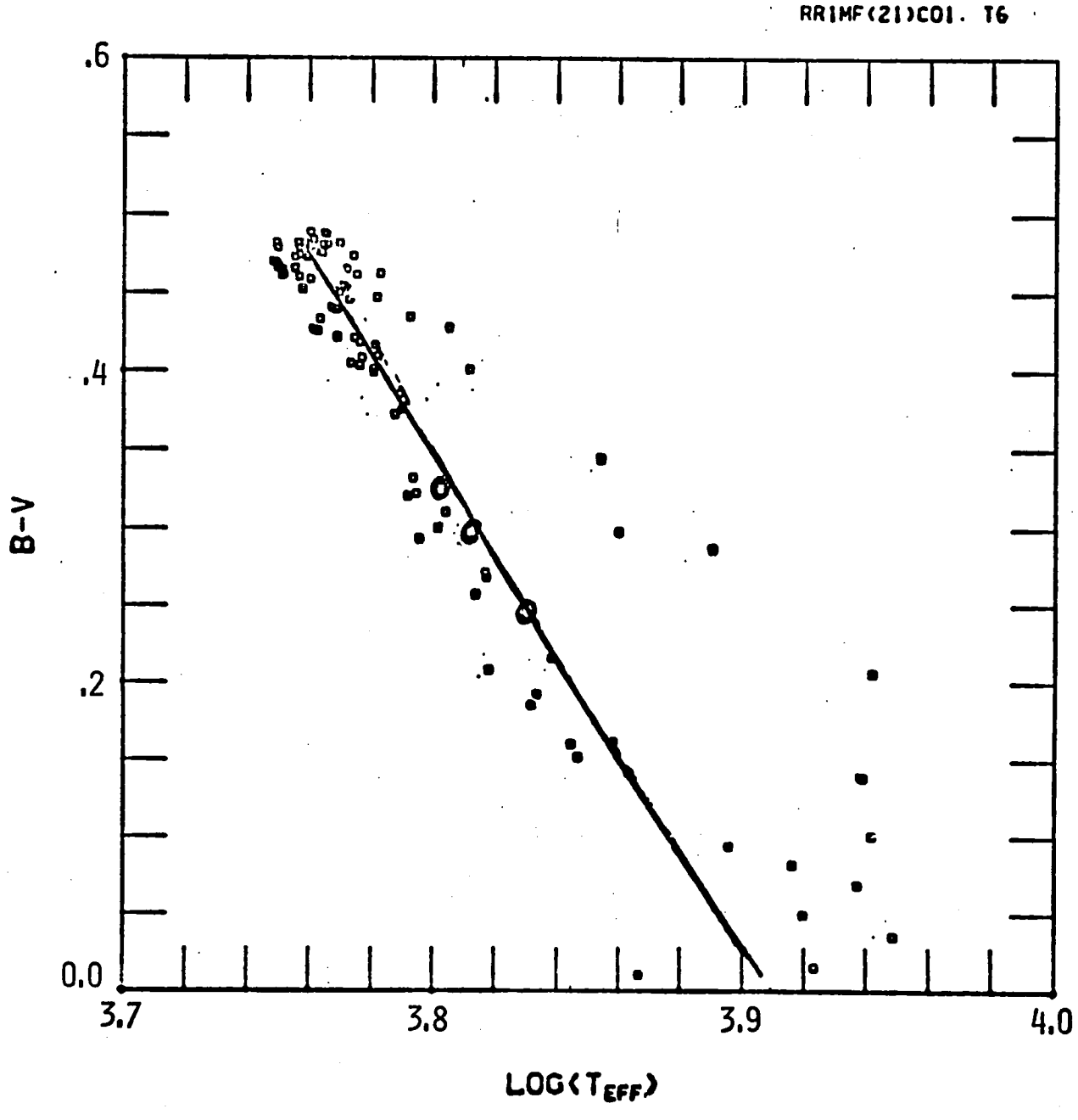

Fig. 6. B-V versus log T_{eff} calculated using MF/G transport structure. Solid line shows the Oke, Giver, and Searle relation. Calibration values (0) for static models at L = 38 $L_{\odot}$ and T_{eff} = 6800, 6500, and 6350 K are plotted.

an improvement in slope for the multifrequency structure as anticipated by Cox and Davis (1975).

The various averages of B-V that we obtained are shown in Table 1. Averages over the three periods, for the intensity means $\langle B \rangle_{int} - \langle V \rangle_{int}$, for the gray structure which is essentially the same for the multifrequency structure is 0.264. The average T_{eff} calculated from the OGS relation is 6678 K within 162 K of the model T_{eff} (6840 K). The other means are at least 600 K low. The static fine zoned radiative model gives a (B-V) of .244 and an OGS T_{eff} of 6770. In Fig. 6 we also plot calibration points for static models with L = 38 $L_\odot$, and 6800, 6500 and 6350 K effective temperatures.

Direct averages of T_{eff} were obtained using 100 phases over three periods for a more reasonable amplitude variation of RR Lyrae ($\sim 1.1^m$) and for our King 1A large amplitude model (1.8^m). T_{eff} is determined from the relationship:

$$L = 4\pi R_*^2 T_{eff}^4$$

where L is the multifrequency transport calculated luminosity and R_* the photospheric radius determined at $\tau = 2/3$. The weightings used were none, direct weighting on L and a weighting similar to that used by Lub (1977), i.e.,

$$\theta_{eff}^{eq} = [(L/\langle L \rangle)^{1/2} \theta_{eff}^2]^{1/2} .$$

The results for the 1.1^m model (Fig. 7), averaged over three periods are: T_{eff} = 6800, 7115, and 6670 K, respectively. Only the direct luminosity weighting is well out of line, being high by 300 K, but

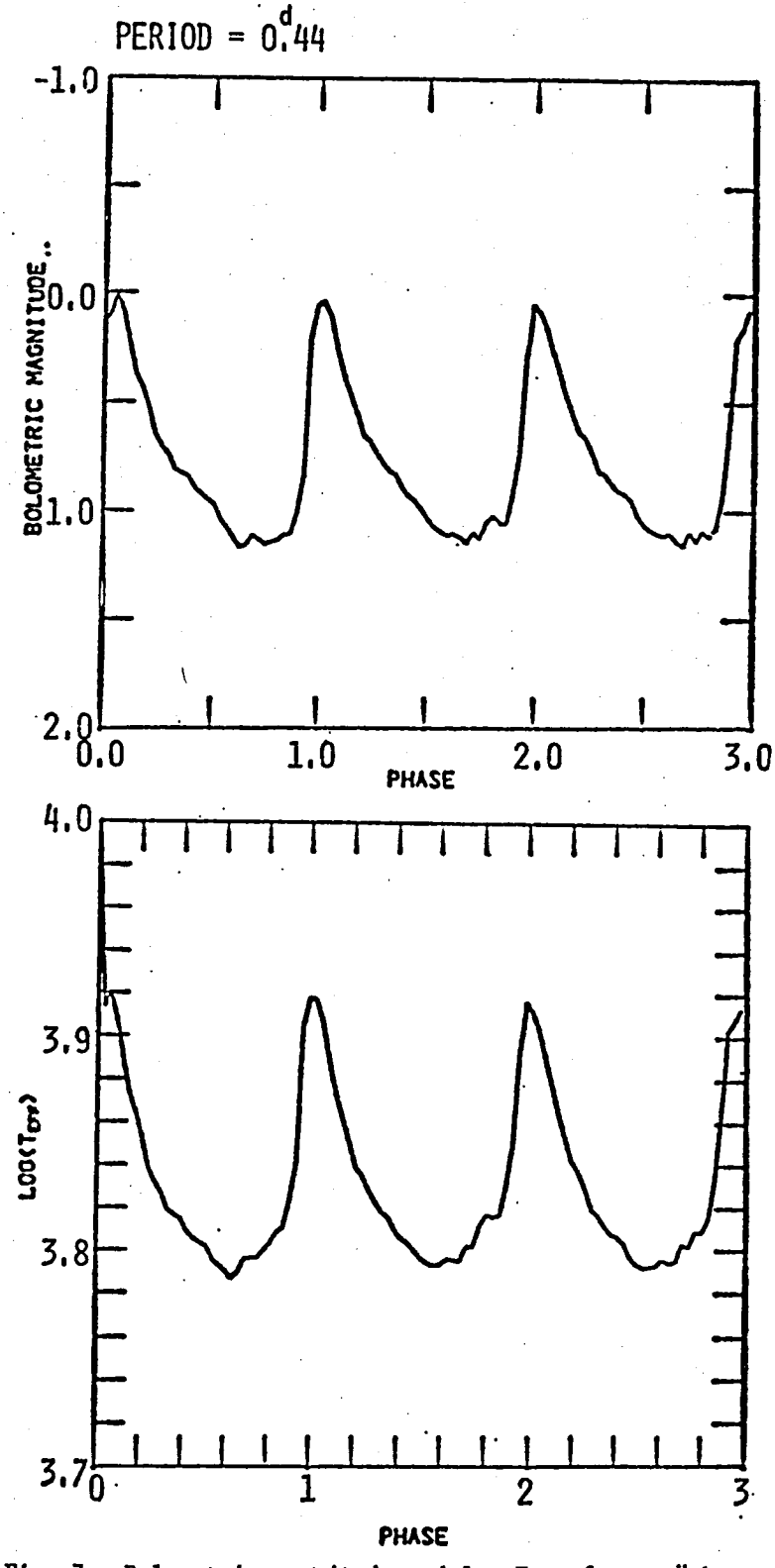

Fig. 7. Bolometric magnitude and log T_{eff} for an "observed amplitude" RR Lyrae used to obtain averages of T_{eff} over phase. (This model used opacities that we believe are too high).

TABLE 1

	B-V	T_{eff}(K)	T_{eff}(K)
$\langle B-V \rangle_{mag}$	.3907	6151	-689
$\langle B \rangle_{int} - \langle V \rangle_{int}$	.2640	6678	-162
$\langle B-V \rangle_{int}$	.4018	6108	-732
$-\langle V-B \rangle_{int}$	.4532	5925	-915

using the Oke, Giver, and Searle relation

$\theta_e = 0.62 + 0.51(B-V)$ where $T_{eff} = 5040/\theta_e$

the unweighted mean is the best. For our larger amplitude King 1A model the direct T_{eff} average is 500 K low and the Lub average was not attempted.

V. CONCLUSIONS

The slope of our (B-V), log T_e relation is close to that given by Oke, Giver, and Searle if one uses a full transport solution for the atmospheric structure. It appears that an intensity mean on B and V is the most appropriate mean to use for RR Lyrae stars as for Cepheids. From $\langle B \rangle_{int} - \langle V \rangle_{int}$ we obtain a calculated T_{eff} within about 160 K of the known nonpulsating T_{eff}. A model calculated that agrees in amplitude variations with RR Lyrae implies that a direct time average of T_e is preferable to any other weighting.

REFERENCES

Cox, A. N. and Davis, C. G. 1975, Memoires Societe, Royale des Sciences de Liege, 6^{e} Serie Tome VIII, p.209.

Davis, C. G. 1971, J.S.Q.R.T. 11, 647.

Davis, C. G. 1975, Proceedings of the IAU Colloquium #29, Budapest.

Davis, C. G. 1978, Ap. J. 221, 929.

Deupree, R. G. 1977, Ap. J. 211, 509.

Hill, S. 1972, Ap. J. 178, 793.

Lub, J. 1977, Thesis, University of Leiden.

Mihalas, D. 1969, Ap. J. 157, 1363.

Oke, J. B., Giver, L. P., and Searle, L. 1962, Ap. J. 136, 393.

Discussion

Baker: Can you say anything in a general way about how the Cox-Davis opacities compare to the Cox-Stewart opacities?

Davis: They seem to about double the opacities in the region below 5000°K, and we're not ready to say what the reasons are. But it appears to be a difference in the treatment of the line wings from that used in the original Cox-Stewart opacities. The Cox-Davis opacities are a great improvement because molecules are included, so that the line blanketing treatment for Cepheids is improved. We found good agreement, where we didn't without the Cox-Davis opacity, in Cepheids. Here for RR Lyrae stars we didn't expect it to make much difference, and it made a big difference, so we were surprised. We're studying the question of what really went into the Cox-Davis opacities.

Spangenberg: That opacity effect might be subject to the effect of zoning when you're doing the low photoshere. Your temperature structure could be quite a bit different if you had significantly more zones in one case than in the other. But if you kept the number of zones the same, then you would lose resolution in the one case, but the opacity would be adding a lot of temperature-dependent features which would get lost in the zones. If you changed the atmospheric zoning, you would understand these opacity effects better.

Davis: The zoning was done in the same manner as for the Goddard Cepheid model -- we used 72 zones with a 10% inner radius. Art has looked at the opacities in this region and there is a difference of a factor of two. Your point is well taken concerning the position of these effects.

Spangenberg: When you're trying to estimate the optical depth in order to get T_{eff}, it could be quite zone-dependent.

A. Cox: You're right, Bill, but unfortunately we seem to have gotten into a glitch and we hope it will be straightened out soon.

Davis: The new opacities did improve the amplitude . . . I wish we could keep those opacities.

A. Cox: Do you think your amplitudes will decrease if you use a non-zero boundary pressure?

Davis: No. It just disturbs my light curve. I did not try the Castor boundary condition.

A. Cox: I'd like to elicit something from Pel about criticisms we have on how you take your temperature means.

Pel: What we did is very simple. As soon as you have the temperature and radius variation, it is clear how you have to average. If you assume the luminosity mean over the cycle is exactly the time average over the luminosity curve, and the radius mean is approximately the time average over the radius curve, then the Stefan-Boltzmann relation tells you what the temperature mean is. Where we may come out with different results is that our definition of the mean radius is not exactly where the equilibrium radius was. I think that's all the play there is in the definitions, and I'm a bit surprised that there is a difference of about 190°K for the RR Lyrae stars. Did I hear that correctly?

Davis: 170°K cooler than T_{eff}.

A. Cox: He took three means. One was the time average, one weighted with the luminosity (which weights the higher temperatures more), and then your technique.

Pel: You would prefer the intensity time average of the individual bands and we would prefer the average, not in the colors, but in the temperature and gravity curves, working back to see what that meant in the colors. That is a little bit closer to the straight time average of the color itself.

A. Cox: I should tell the audience that he [Pel] is talking about Cepheids, whereas Davis was talking about RR Lyrae stars.

Pel: Yes, but this recipe works for both.

ULTRAVIOLET LIGHT CURVES OF RR LYRAE

by

Chi-Chao Wu

Computer Sciences Corporation
Silver Spring, Maryland

RR Lyrae was observed with the University of Groningen ultraviolet experiment on board the ANS satellite. The observations were made in October 1974, April and October of 1975 and April of 1976. The Groningen instrument consists of a 22-cm Cassegrain telescope followed by a five-channel spectrophotometer with central wavelengths and full widths (in parentheses) at 1550 (150), 1800 (150), 2200 (200), 2500 (150) and 3300 (100)Å (van Duinen et al. 1975). The ANS instrument sensitivity change was small and was well monitored by daily observations of standard stars ϵ and ν Dor (Aalders and Wesselius 1976). The sensitivity varied by 18 percent at 1550Å and 3 percent at the other four channels during the period covered by the RR Lyr observations. The ANS count rates are corrected for the sensitivity change and converted into absolute fluxes by means of laboratory absolute calibration (Aalders et al. 1975). Magnitudes are obtained by adopting $M_\lambda = 0^m.00$ at $f_\lambda = 3.64 \times 10^{-9}$ erg cm^{-2}s^{-1}Å^{-1} (Oke and Schild 1970).

The ultraviolet light curves of RR Lyrae are shown in Figure 1. The phase is calculated with the ephemeris of Detre and Szeidl (1973) for the visual medium brightness

$$C(\bar{V}) = \text{JD2414856.487} + 0^d.56683957 \times E.$$

RR Lyrae is rather faint at 1550Å, only those observations with signal-to-noise ratio of 1 to 12 are plotted. The error bars are typically $0^m.08$ at 1800Å and $\lesssim 0.02$ at 2200, 2500 and 3300Å. The amplitude of

the variations is 3.5, 3.2, 1.7, 1.5 and 0.8 magnitudes respectively at 1550, 1800, 2200, 2500 and 3300Å. There are structures in the light curves at phases 0.53 and 0.88. These may be caused by shock wave heating in the atmosphere of pulsating stars (see e.g. Hutchinson, Hill and Lillie 1977).

Figure 2 gives the $m_{1800} - m_{3300}$ color as a function of brightness at 3300Å. It is obvious that the star is bluest when it is brightest. Another interesting feature is the cluster of points near $m_{3300} \approx 8.7$, they are bluer than the main curve. These points lie between phases 0.51 and 0.66, when the pulsational cycle is at the maximum rate of contraction. This probably is the result of shock heating during the rapid infalling of the atmosphere.

I thank Drs. J. W. G. Aalders, K. S. de Boer, R. J. van Duinen, D. Kester and P. R. Wesselius for help in obtaining the observations. The ANS project was sponsored by the Dutch Committee for Geophysics and Space Research of the Royal Netherlands Academy of Sciences.

REFERENCES

Aalders, J. W. G., van Duinen, R. J., Luinge, W. and Wildeman, K. J. 1975, Space Science Instrumentation, 1, 343.

Aalders, J. W. G. and Wesselius, P. R. 1976, Internal ROG Note 76-24.

Detre, L. and Szeidl, B. 1973, Variable Stars in Globular Clusters and in Related Systems, ed. J. D. Fernie (Dordrecht - D. Reidel), p. 31.

van Duinen, R. J., Aalders, J. W. G., Wesselius, P. R., Wildeman, K. J., Wu, C.-C, Luinge, W., Snel, D. 1975 Astr. Ap. 39, 159.

Hutchinson, J. L., Hill, S. J. and Lillie, C. F. 1977, Ap. J., 211, 207.

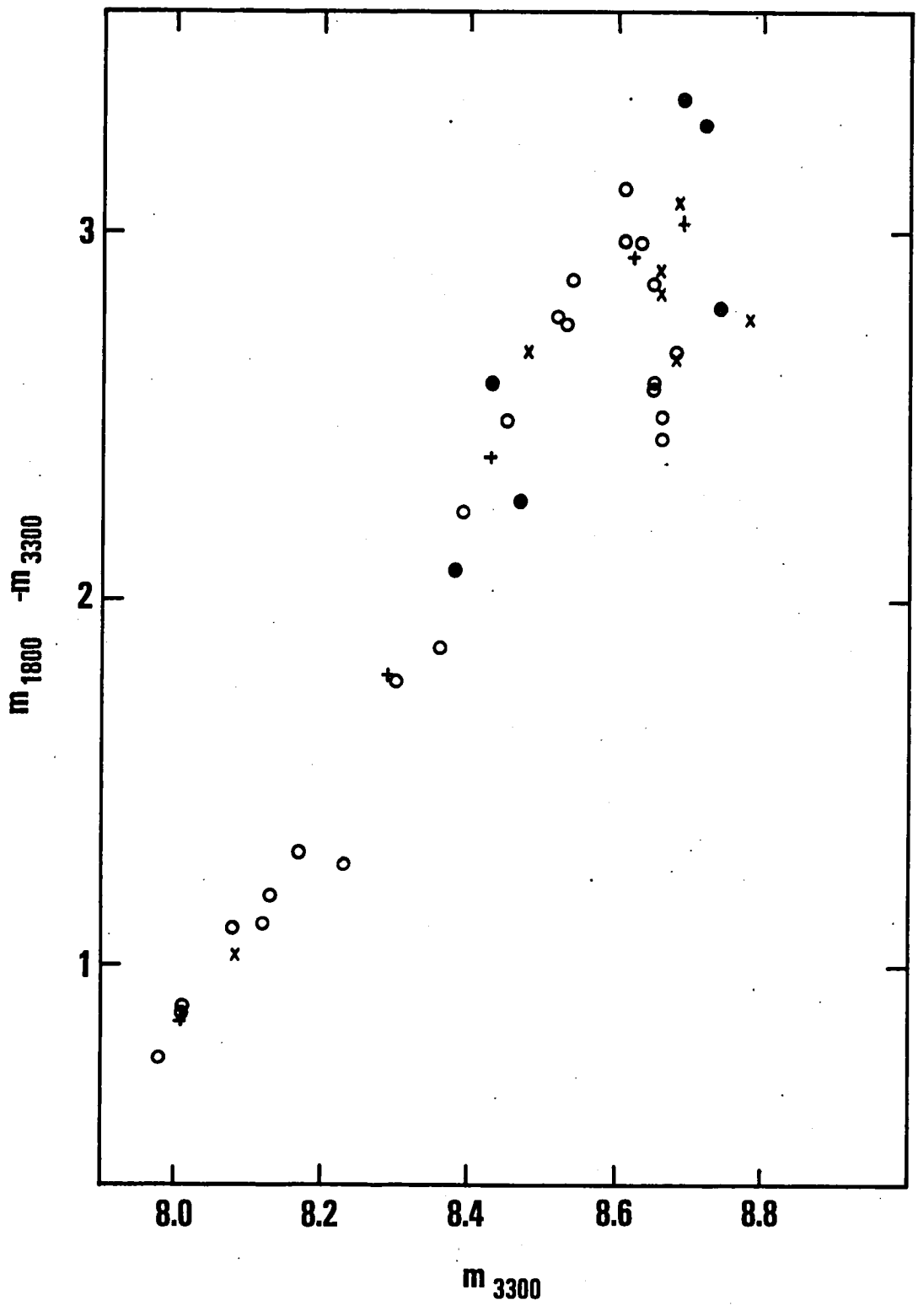

Figure 1. Five-channel light curves of RR Lyrae. Different symbols indicates the epochs when the observations were made: ● Oct. 1974, x Apr. 1975, ● Oct. 1975, + Apr. 1976.

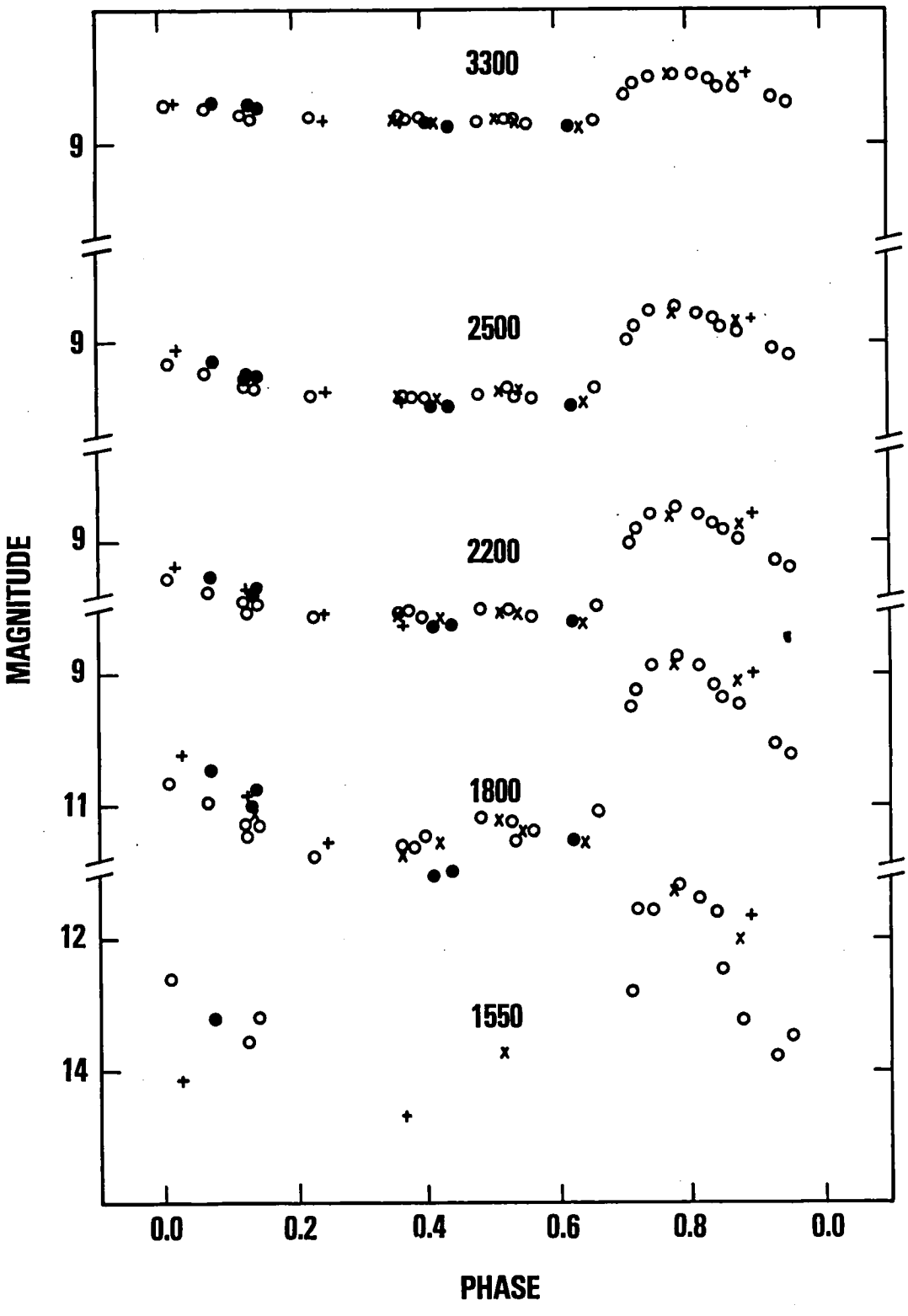

Figure 2. Color versus Brightness diagram of RR Lyrae. Symbols have the same meaning as those in Figure 1.

Discussion

Pel: Have you made any comparisons with theoretical energy distributions?

Wu: No, I haven't.

A. Cox: Have you compared with visual observations? You know that Lub has done many RR Lyrae stars and has found bumps in the bottom of the visual light curve. Is that also the case for RR Lyr itself?

Wu: I haven't had a chance to make comparisons with ground-based observations.

A. Cox: Let me ask Dr. Wesselink a question: Is that true for all RR Lyrae stars?

Wesselink: No. About 30% show the bump at the bottom of the light curve.

The Evolutionary Stage of an RRs Star SX Phe

Hideyuki Saio and Mine Takeuti

Astronomical Institute, Tôhoku University

Sendai 980 Japan

Abstract

The evolutionary stage for a short period variable SX Phe is investigated. It is supposed that SX Phe is a mixed star with low metal abundance, in which the material was mixed after the star evolved off the main sequence, and is in the second hydrogen burning stage. To examine the validity of this hypothesis we constructed two evolutionary sequences with $(X,Z,M/M_{\odot}) = (0.5,0.004,0.75)$ and $(0.5,0.001,0.70)$ in the hydrogen burning phase and computed the pulsation period. Agreement between theoretical results and observational data is sufficient for us to conclude that the mixed model is actually adequate for SX Phe. The applicability of this model to other RRs stars is briefly discussed.

1. Introduction

A group of short period variable stars characterized by their relatively large amplitude and extremely short period, called as RRs stars or dwarf Cepheids, has not yet been elucidated on the basis of pulsation theory. The RRs stars occupy the same range of period with short period δ Scuti stars which are the Population I pulsating stars. In the usual classification, the RRs stars were distinguished from δ Scuti stars mainly by their large amplitude of light variation ($\Delta m_v \geq 0.3$) and the difference of the shape of light curve. SX Phe is an outstanding object of these stars.

On the classification of these stars, there are some controversial problems (see review papers by Baglin et al. 1973 and Petersen 1976). Recent investigations mainly based on the intermediate band photometry (Breger 1975, 1977a, b, McNamara and Feltz 1976) suggest that RRs stars are not different from δ Scuti stars. On the other hand, there exist some evidences suggesting that at least SX Phe is significantly different from δ Scuti stars. As pointed out by Breger and Bregman (1975), since the trigonometric parallax of SX Phe yields the luminosity which is less than that of Population I zero age main sequence, we cannot suppose that SX Phe is a δ Scuti type star, because a star with Population I composition cannot pass the observed position of SX Phe during the main sequence or post main sequence evolution as δ Scuti stars. Moreover, according to the theoretical investigation by Petersen and Jørgensen (1972), low metal abundance is necessary to explain its high period ratio of first harmonic to fundamental modes.

In this paper, after discussing some possibilities of its evolutionary phase, we suppose that SX Phe is a mixed star whose material was stirred up at a phase after main sequence evolution. It will be shown that this model is in good agreement with the observed position in H-R diagram and the period. Finally we discuss the applicability of this model to other RRs stars.

2. Evolutionary Stage of SX Phe

To explain that the luminosity of SX Phe obtained from trigonometric parallax is less than that of Population I zero age main sequence (ZAMS), some possibilities on its evolutionary stage have been considered, as reviewed in detail by Petersen (1976). Here, we discuss some of those, i.e. (a) stars of mass M = 0.20-0.25 $M_{\odot}$ contracting towards the white dwarf

stage, (b) main sequence or immediately post main sequence stage, and (c) post red giant stage of mass $M \sim 0.5\ M_{\odot}$.

(a) Dziembowski and Kozłowski (1974) constructed the model which is constituted from a degenerate helium core, very thin hydrogen burning shell, and an extended envelope. They concluded that its fundamental period and the position in H-R diagram can be explained by this model, however the period ratio of the model $P_1/P_0 \sim 0.75$ is significantly less than the observed value 0.778 for SX Phe. Therefore, this model may not be appropriate for this star.

(b) To pass the position of SX Phe on H-R diagram during the main sequence evolution it is necessary that a star have a smaller metal abundance or larger helium content than those of normal Population I stars. The low metallicity is adequate to explain the observed large period ratio as indicated by Petersen and Jørgensen (1972) and was confirmed by a spectroscopic analysis by Bessell (1969). Petersen (1976) concluded that main sequence model with (X,Z) = (0.7,0.004) would be in agreement with the observed position in H-R diagram and periods of SX Phe. However, the mass of his model is 1.1 $M_{\odot}$ and its allowable maximum age is 3×10^9 yr. Existence of a star which has a metal abundance of $\sim 1/4\ Z_{\odot}$ and is younger than the Sun conflicts with the recent conception of the chemical evolution of the Galaxy. This contradiction also appears in color of SX Phe (B-V) = 0.22 mag, i.e., its mean color is bluer than the turnoff color $(B-V)_o$ = 0.59 mag of old open cluster NGC188 and than the bluest color (Sandage 1969) of the subdwarfs $(B-V)_o$ = 0.36 mag. Therefore, above model seems also to be inappropriate to the model for SX Phe.

(c) Combining the gravity obtained from the spectroscopic analysis, Bessell (1969) estimated a mass $M/M_\theta = 0.5\pm0.3$ for SX Phe. This value of mass is significantly less than that of main sequence stars in the neighbor of this star in H-R diagram. He concluded that the RRs stars are in the post red giant stage. The result suggesting low mass have been derived also by Fitch (1970). The low mass is convenient to explain the large amplitude of SX Phe, because according to Kippenhahn (1965) the pulsation of low mass model is excited more strongly than that of the model with a main sequence mass in the considering region of H-R diagram.

The large value of P_1/P_0 requires that the metal abundance of SX Phe is less than that of Population I as mentioned item (b). To explain that a metal-poor star which evolves in post red giant phase is observed in the neighbor of main sequence, we consider that the material in the star was mixed by stirring and homogenized after the star evolved off the main sequence, likely at the phase of helium flash. The helium-rich homogeneous star formed as above should reach its "second" main sequence stage. The star evolves now in "second" main or immediate post "second" main sequence phase with large helium abundance in the envelope.

Supposing the above evolutionary history on SX Phe, in the following section we have constructed the evolutionary sequences in the hydrogen burning phase with helium and low metal abundances, and computed the adiabatic linear pulsation period for these models.

3. Results

According to the discussion of Petersen (1976), we adopted the position of SX Phe in H-R diagram as $M_{bol} = 4.0$ (+0.7,-0.9) mag and $\log T_{eff} = 3.88\pm0.01$,

which are based on the trigonometric parallax, and Bessell's (1969) spectroscopic analysis and intermediate band photometry by Jones (1973), respectively. The position of SX Phe is shown in Figure 1 with the Population I ZAMS which is based on the relation between M_v and (B-V) by Morton and Adams (1968) and between (B-V), T_{eff}, and B.C. by Code et al. (1976). Evolutionary sequences with $(X,Z,M/M_\odot) = (0.5,0.004,0.75)$ and $(0.5,0.001,0.70)$ were constructed from the homogeneous main sequence stage to the thick-shell hydrogen burning phase. Opacities were interpolated from the tables of Cox and Stewart (1969, 1970). In the convection zone in the envelope, the ratio of mixing length to pressure scale height was taken as $\ell/H = 1.5$. These evolutionary tracks are illustrated in Figure 1. These tracks pass near the position of SX Phe. The period of fundamental and first harmonic modes was calculated for these models. Obtained periods and period-ratios are plotted in Figure 2, with the observed period P = 0.0550 days and the period ratio $P_1/P_0 = 0.778$ for SX Phe. As indicated by Takeuti and Saio (1978), the period ratio is largest when the star is at the homogeneous stage and decreases rapidly as the central concentration of matter increases. However, after the exhaustion of hydrogen in the central region, period ratio hardly changes during the evolution, while the period continues to increase. As shown in Figures 1 and 2, the model of mixed star well reproduce the observed position in H-R diagram, the period, and the period ratio of SX Phe.

The large helium abundance in the envelope of the model as well as its low mass is a factor of increasing the excitation of pulsation. These two factors may be supposed to cause the observed large amplitude of SX Phe. The adapted mass of the model is less than that of a star at the turnoff point ($\simeq 0.8\ M_\odot$) of the globular clusters with Z = 0.004-0.001. This difference of mass is common to that between the masses of horizontal branch

stars and a star at turnoff point of globular clusters, and it may be a consequence of mass loss in the red giant phase or at the phase of helium flash.

4. Discussion

The model considered in this paper is in agreement with Breger and Bregman's (1975) suggestion that SX Phe is a member of the "true" dwarf Cepheids which have the characteristic of Population II stars. We shall discuss other RRs stars on the consequence of the present model for SX Phe. The double periodicity has been observed for some of RRs stars (see, e.g. Fitch 1970). For most cases the period ratio is larger than 0.77. Two periods of these stars are usually recognized as those of fundamental mode and first overtone. According to Petersen and Jørgensen (1972), the period ratio between the fundamental and first harmonic oscillations cannot be greater than 0.75 for Population I chemical composition. If it is true, it is natural to think that at least the RRs stars with double periodicity belong to the same group of SX Phe or "true" dwarf Cepheids in Breger and Bregman's terminology. These should be distinguished from Population I stars. Moreover, the mixed star model discussed in this paper may be appropriate for also these stars. In this case, all of these stars are not necessarily less luminous than Population I ZAMS, because mixed star evolves and becomes luminous from its "second" main sequence.

According to the statistical investigation by Okazaki (1978), the binary frequency of RRs stars is as small as that for Population II stars, while the fraction of δ Scuti stars in binary system is similar to that of main sequence stars. This supports the classical grouping in short period Cepheids.

On the other hand, recent investigations based on intermediate band photometry already mentioned suggest that there is no significant difference between RRs stars and δ Scuti stars. Atmospheric features of these stars are determined mainly by surface gravity and the metal to hydrogen ratio Z/X. Since the mixed star has a small X, the observed metal-poorness may not be so conspicuous as for the normal Population I stars. Moreover, the metal abundance of SX Phe may be the smallest in other stars of which the evolutionary history is the same as SX Phe, because the period ratio of the former is the largest in RRs stars. It is possible that the difference of photometric features between RRs stars and δ Scuti stars may not be evident.

In conclusion, there is no fatal contradiction between observational evidences and the mixed star model presented here for SX Phe. Further investigations are necessary to confirm that present model is adequate for many other RRs stars.

One of the authors (M.T.) is indebted to Dr. J. Otzen Petersen for valuable discussions.

References

Baglin, A., Breger, M., Chevalier, C., Hauck, B., Le Contel, J.M., Sareyan, J.P., and Valtier, J.C. 1973, Astron. Astrophys., 23, 221.

Bessell, M. S . 1969, Astrophys.J.Suppl., 18, 195.

Breger, M. 1975, Astrophys.J., 201, 653.

Breger, M. 1977a, Publ.Astron.Soc.Pacific, 89, 55.

Breger, M. 1977b, ibid., 89, 339.

Breger, M. and Bregman, J.N. 1975, Astrophys.J., 200, 343.

Code, A.D., Davis, J., Bless, R.C., and Brown, R.H. 1976, ibid., 203, 417.

Cox, A.N. and Stewart, J.N. 1969, Nauch.Inf.Akad.Nauk S.S.S.R., 15, 3.

Cox, A.N. and Stewart, J.N. 1970, Astrophys.J.Suppl., 19, 261.

Dziembowski, W. and Kozłowski, M. 1974, Acta Astron., 24, 245.

Fitch, W.S. 1970, Astrophys.J., 161, 669.

Jones, D.H.P. 1973, Astrophys.J.Suppl., 25, 487.

Kippenhahn, R. 1965, IAU 3rd Colloquium on Variable Stars, Bamberg, 7.

McNamara, D.H. and Feltz, K.A. 1976, Publ.Astron.Soc.Pacific, 88, 510.

Morton, D.C. and Adams, T.F. 1968, Astrophys.J., 151, 611.

Okazaki, A. 1978, private communication.

Petersen, J.O. 1976, Multiple Periodic Variable Stars, IAU Colloquium No. 29, ed. W.S. Fitch (D. Reidel Publ., Dordrecht-Holland), 195.

Petersen, J.O. and Jørgensen, H.E. 1972, Astron.Astrophys. 17, 367.

Sandage, A. 1969, Astrophys.J., 157, 515.

Takeuti, M. and Saio, H. 1978, in preparation.

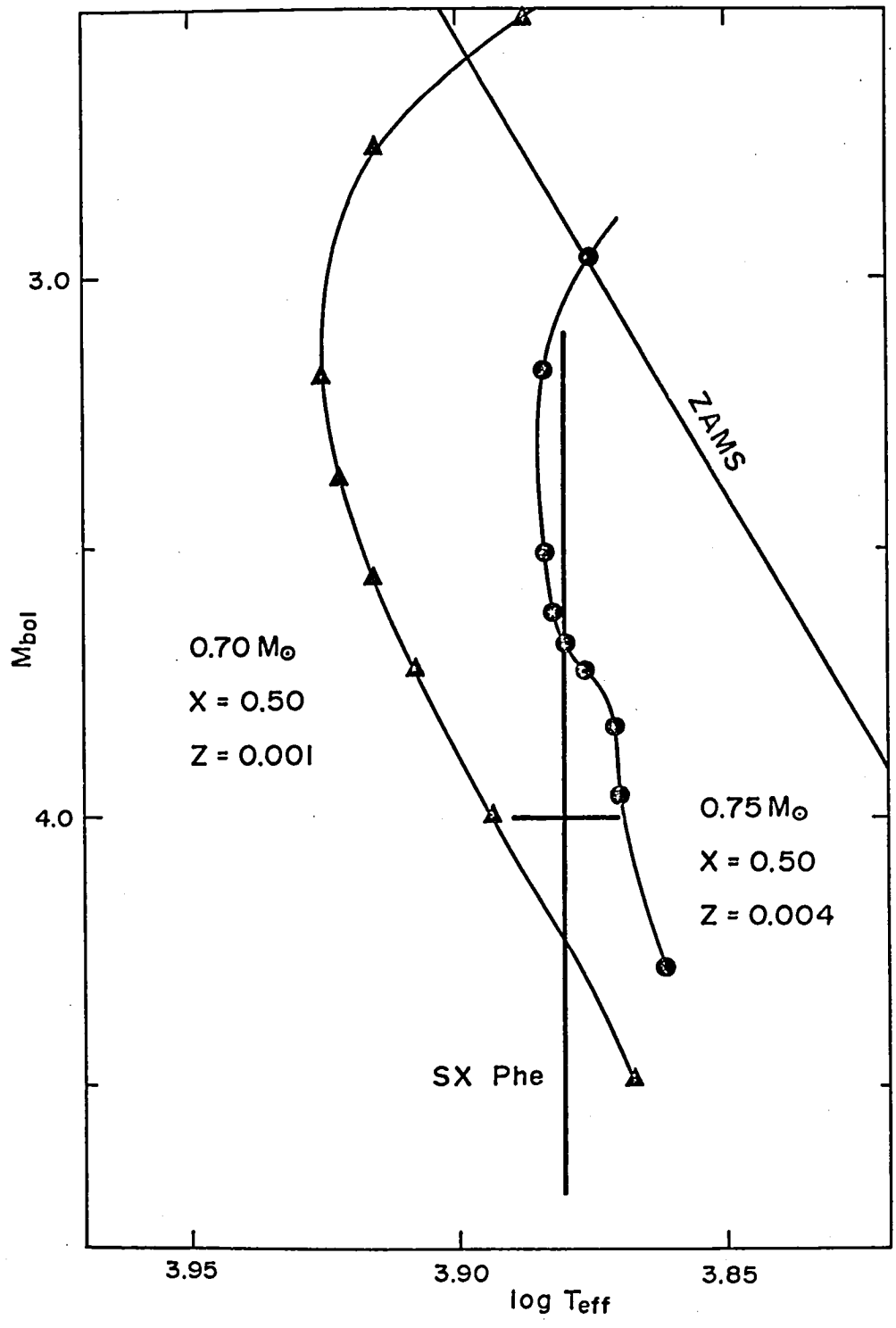

Figure 1. Computed evolutionary models with $(X,Z,M/M_\odot)$ = (0.5,0.004,0.75) and (0.5,0.001,0.70) are indicated in H-R diagram. Positions of models for which pulsation periods were calculated are marked on their paths. Observed data for SX Phe are also shown.

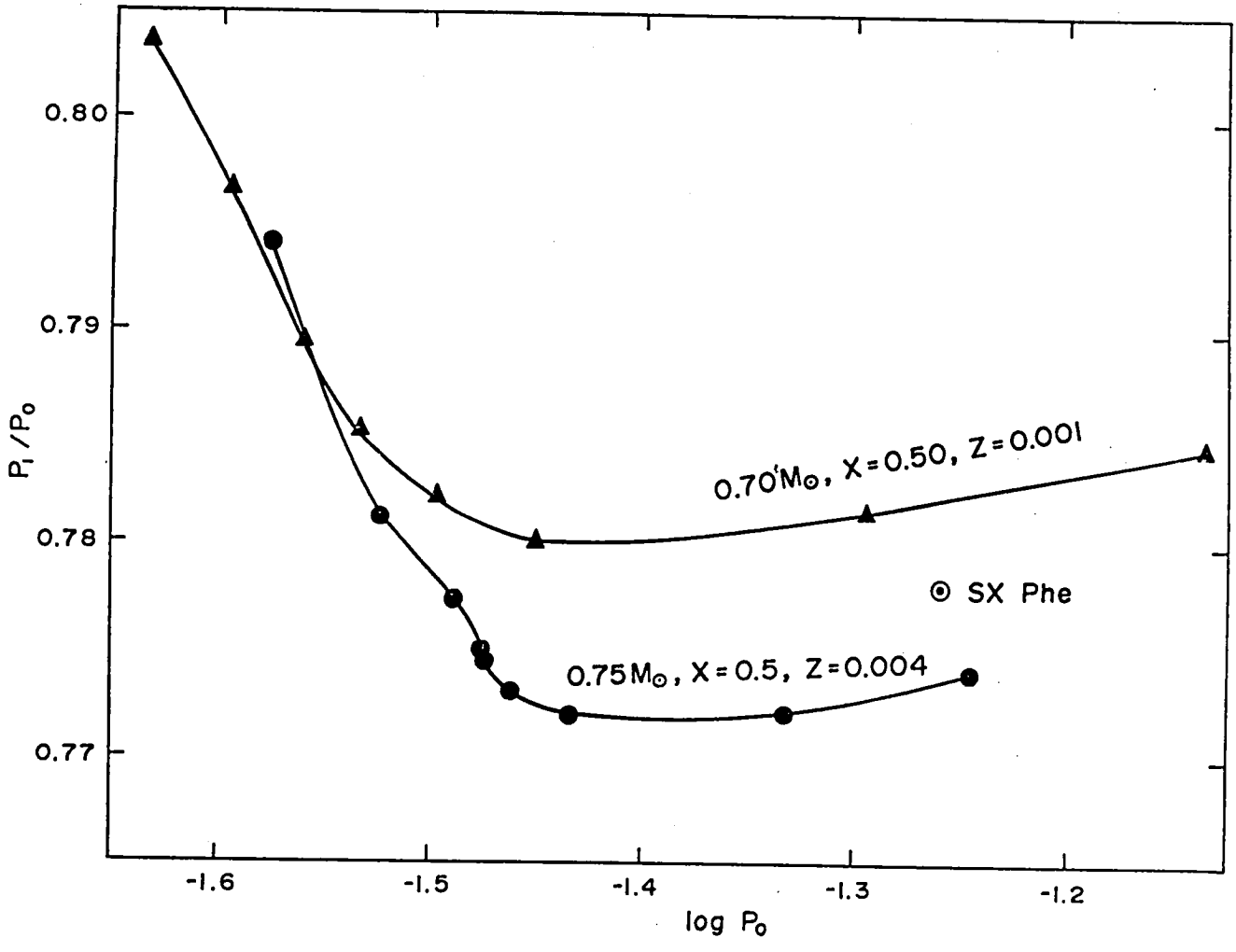

Figure 2. The period to period-ratio diagram for SX Phe and models indicated in Figure 1. Symbols are common to both diagrams.

Discussion

J. Wood: I have a comment about the monumental work by Jurgen Stock from Tololo. He tried to apply the Wesselink method and it just didn't work.

A. Cox: I am aware that Jorgensen has done the Wesselink radius method on this star also, and has been frustrated.

J. Wood:, In the latest A and A there is a second paper on this star by a group from Munich, who are also kind of throwing up their hands on this. They investigated whether it was a binary and concluded it wasn't.

A. Cox: Didn't someone get an orbital period for it?

J. Wood: Yes, obviously Kozar must disagree with Schmidt.

A. Cox: Evidently, he believes he has a correct orbital period. [Laughter] The idea here is that you have a star evolved well off the main sequence which you mix up and it comes back to the main sequence. I think that's rather unusual.

The Period Change of SV Vul.

J.D. Fernie
David Dunlap Observatory
University of Toronto

ABSTRACT

New UBVRI photometry and a few concurrent radial velocities have been obtained for the 45-day classical cepheid, SV Vul. It is found that these data, when combined with earlier data covering sixty years, show the star to have a linearly decreasing period with $\dot{P}$=-254±10 sec/year.

This value is compared with that predicted by theoretical models of Flower, assuming the period change to be caused by evolution across the H-R diagram. Although excellent agreement is found, this is in part fortuitous because the models are sensitive to such parameters as mass, chemical composition, and ℓ/H. Precisely because of this, however, it is suggested that a search for significant $\dot{P}$ values in long period cepheids generally might afford useful constraints on theoretical models.

Discussion

A. Cox: Don, you've really vexed us for years, finding non-variables in the instability strip. We thought we might get at you by moving blue edges around and changing the helium content. Maybe we'll have to do the same thing if you vex us the other way by finding variable stars where you're not supposed to. We'll have to work on that.

J. Cox: I expected you to mention the period-mean density relationship.

Fernie: Something I didn't say in support of the pulsation hypothesis is that if you simply take a period-luminosity relation, a period of 67 days gives an absolute luminosity of -6.8, which is what it is. I didn't use a period-mean density relationship because I'm still trying to convince myself that it's a pulsation, before worrying about that.

A. Cox: Let me ask the question in another way. If you take an evolutionary track through there, what's the mass?

Fernie: I haven't done that either.

MODE IDENTIFICATION IN BETA CEPHEI STARS

By

Morris L. Aizenman

Division of Astronomical Sciences

National Science Foundation

Washington, D. C. 20550

and

Janet Rountree Lesh*

Laboratory for Astronomy and Solar Physics

NASA/Goddard Space Flight Center

Greenbelt, Maryland 20771

*NAS-NRC Senior Resident Research Associate

I. Introduction

The Beta Cephei stars are unique among well-known variable stars in that we still have no idea why they pulsate. Cepheids, RR Lyrae stars, Mira variables and Delta Scuti variables are now reasonably well understood; while there are still problems with discrepencies of evolutionary and pulsational masses for some of these stars, the basic physics controlling the instability seems to be known. We do not know why the Beta Cephei stars pulsate -- in fact there is still some question as to whether these stars are radial or nonradial oscillators -- and it is because such questions still are unresolved that the subject of mode identification is of high interest and significance. It is the fervent hope among workers in this field that if the pulsation mode of the Beta Cephei stars is definitely established, it will provide a clue to the instability mechanism.

II. Observational Characteristics Related to Mode Identification

The Beta Cephei stars are short-period, small-amplitude variables of early spectral type (generally BO.5-B2). The first member of this group was discovered by Frost in 1902 (see Frost 1902, 1906). Their observational properties have been extensively reviewed and discussed, most recently by Lesh and Aizenman (1978). Here we shall summarize only the essential characteristics, which may be of importance in attempts to identify the pulsation mode:

1. Both light and velocity amplitudes in these stars are small, typically less than 0.1 mag in blue light and 50 km/sec in radial velocity. However, the light amplitudes are greater at ultra-violet wavelengths.

2. Typical periods in both light and radial velocity are 4 to 7 hours. However, about half of the stars in the Beta Cephei group exhibit more than one period. This effect is often detected as a long-period modulation of the amplitude of the principal variation, usually interpreted as an interference between two nearly equal short periods. This is known as the "beat phenomenon". It was discovered by Meyer (1934).

3. In contrast to the classical Cepheids and RR Lyrae stars, the light curve for Beta Cephei stars lags approximately 90 degrees (one-quarter period) behind the radial velocity curve. Thus if the star is pulsating radially, maximum brightness occurs at minimum radius. De Jager (1953) showed that this relationship holds for <u>each</u> set of light and radial velocity curves in multiperiodic stars.

4. In many Beta Cephei stars, the radial velocity curves derived from different elements are not quite in phase: the phase derived from the hydrogen lines lags behind the helium-line phase, which in turn lags behind the phase derived from the metallic lines. This is called the "van Hoof effect".

5. Although both light and radial velocity curves are usually sinusoidal for these stars, the radial velocity curve sometimes exhibits a "stillstand" -- a phase of apparently constant velocity -- on the descending branch. In extreme cases, the velocity curve may even appear discontinuous. Occasionally the light curve exhibits a stillstand as well.

6. Finally, the line profiles of many Beta Cephei stars show very complex variations when observed at high dispersion. Changes in line width,

strong asymmetry, the appearance of secondary components, and even complete splitting appear in the spectral lines of various members of this class. In multiperiodic stars, the line profiles vary with only one of the two short periods. The great detail with which this phenomenon has been observed makes it a prime candidate for the detection of potentially small differences between neighboring pulsation modes.

III. Early Work Related to the Beat Phenomenon

It was undoubtedly the apparent presence of two oscillation frequencies in the Beta Cephei stars that generated most of the initial interest on the part of theoreticians; it led to a number of hypotheses as to their possible interpretation. Let us state at the outset that in most of these analyses, there was no attempt to identify the instability mechanism. Rather, the interest was in providing an explanation and interpretation of the two periods. Woltjer (1935, 1937, 1943, 1946) considered the case of nonlinear oscillations and analyzed the behavior of a system containing two radial frequencies σ_1 and σ_2 with $\sigma_1 \simeq 2\sigma_2$. Such a situation can lead to resonance, with one of the resonance frequencies being $\sigma = \sigma_1 - \sigma_0 \simeq \sigma_0$. It was thought that what we observe in the Beta Cephei stars is the original frequency plus the difference frequency, but the objection has been raised that it is difficult to see how this frequency could be associated with the broadening of the lines. We cannot go to into the many aspects in this review but the point to be noted here is that the beat phenomenon is interpreted as being due to a resonance existing between two frequencies, one being the double of the other. In principle, one should also expect to find the phenomenon at the frequency $2\sigma_0 = \sigma_1$.

Struve (1955) and Odgers (1956) also tried to account for the observed splitting of the lines and van Hoof effect. They assumed radial pulsations,

and hypothesized that a thin layer of the atmosphere is ejected at regular intervals with a period P_0. The layer falls back under gravity, and if the time of fall is smaller than P_0, there is a stillstand on the velocity curve. If the time is slightly larger than P_0 the interfering motions that arise between the layer and the rest of the star could give rise to a beat phenomenon.

Here we have the introduction of an underlying radial oscillation plus an atmosphere free-fall oscillation time. However, the objection has been raised by Ledoux (1958) that it is practically impossible for this free-fall period to be fixed to such an extent that regular beats could be observed over very long periods of time. Another suggestion along these lines has been that there is a strictly atmospheric oscillation, but here the difficulty is one of making this atmospheric period independent of the interior. The atmosphere would eventually experience a forced oscillation under the influence of the interior, and if nonlinear coupling were taken into account, a beat phenomenon might result. The question has never been thoroughly investigated.

With regard to all of these theories, it should be noted that Huang points out that the equivalent widths of the lines remain constant during the doubling stages. Hence the phenomenon cannot be due to superposed layers but must be due to different parts of the stellar surface. Another question is whether the broadening of some lines is simply a case of unresolved doubling.

Ledoux (1951) has also suggested that the two periods may be related to the fact that if one assumes that one is observing nonradial oscillations, then a splitting of the frequencies is possibly due to rotation, and the

amount of splitting is proportional to the rotational velocity. The interference of one of the travelling waves with the stationary oscillation would give rise to a beat frequency proportional to the angular velocity. In this theory, the broadening of the lines is attributed to the differential velocities on the surface of the star, resulting from the combination of rotation and the components of the travelling wave. The major problem is that if one of the travelling waves is chosen, the other remains unexcited. It was believed that this may be connected with the cause of the oscillation itself, possibly due to the interaction of a close companion. But this is physically unrealistic. The period of the companion would have to be almost the same as the pulsation period, which would put the companion inside the other star. Also, line duplicity and the van Hoof effect are not explained.

Other explanations of the beat phenomenon were made by Chandrasekhar and Lebovitz (1962). They criticized the Ledoux hypothesis because they felt it was unlikely that purely nonradial oscillations would be excited in preference to radial ones. Their argument was that the nonradial modes would be highly damped relative to the radial oscillation. Instead, they presented an alternative explanation of the beat phenomenon. The theory was based on the assumption that the ratio of specific heats for these stars is such that degeneracy occurs between the fundamental characteristic frequencies of the radial and the $\ell = 2$ modes of oscillation. They showed that rotation would remove this degeneracy and lead to two normal modes characterized by slightly different frequencies. The advantage of this theory over the Ledoux theory was that a separate mechanism would not be required for the excitation of the nonradial mode. In their schema, rotation coupled the radial mode to the nonradial mode to produce two distinct normal modes, which were both nonradial.

There was an objection to this, however. On the basis of this theory, the rotational velocities that were required to give the observed beat periods were larger by factors of 3 to 4 than those observed. Clement (1965) showed that this splitting could be increased for centrally condensed models. He proceeded to make a calculation of the effects of nonradial oscillations in terms of radial velocities, variations in brightness, and periods. His calculations included broadening due to macroscopic motions and the velocity of the center of the line profile. He concluded that when beats are observed in a particular star, the angle of inclination of the rotation axis would normally have to be at an intermediate angle. At either extreme (pole-on or line-of-sight in the equatorial plane) one velocity amplitude would be much greater than the other. Clement also calculated line broadening, motion of the center of the line profile, the mean radial velocity as a function of the equatorial velocity, the angle of inclination, the ratio of the angular rotation to the oscillation frequency, and the amplitudes of the two radial velocity components. He considered the effect of the area changes and changes of magnitude with time. He found that even for polytropes with n = 3.0-3.5, the rotation velocities required to produce the beat phenomenon were considerably reduced (from $\sim$ 200 km/sec to 140 km/sec), but were still too high to match the observations. The only exception was β Canis Majoris, which has an observed Ω R sin Θ of about 60 km/sec and a very small period splitting ($\frac{\Delta P}{P_o} = \frac{P_1 - P_2}{P_o} = 0.006$). Clement also calculated the broadening and radial velocity curves for three stars: β Canis Majoris, 12 Lacetae, and BW Vulpeculae. His results implied that β Canis Majoris was being viewed from a small angle of inclination (almost pole-on), and that the observed variation in broadening would vary with the longer of the two short periods.

In order to explain the observation that the line profiles of 12 Lacetae change with the shorter period, it was necessary to postulate that this star was being observed from a large angle of inclination. His final example, involving BW Vulpeculae, does predict the existence of a stillstand on the velocity curve for the profile center.

Thus, on the basis of this theory, β Canis Majoris and σ Scorpii have small angles of inclination with respect to the line of sight. Other stars exhibiting the beat phenomenon require a large angle of inclination.

Another observational point should be made. On the descending branch of the radial velocity curve of BW Vulpeculae, it is found that the absorption lines actually become double; this coincides with the phases of maximum broadening. At the points of minimum broadening, the lines are single. The theory of Clement, assuming that the line broadening arises only from the macroscopic motions of the nonradial oscillations, shows that although the profiles are asymmetrical, there is no indication of doubling.

A major problem with Clement's solution was the fact that the rotation required to produce the splitting of the modes was 3 to 4 times larger than observed. Clement (1967) considered the case of differentially rotating polytropes, with the choice of a suitable rotation law, which would be consistent with stability against local perturbations. He adapted Stockly's (1965) rotation law to polytropes. He found that with this law of rotation, the observed splitting could be produced with a considerable reduction in the equatorial velocity, and the required velocities were in agreement with observations. The subject has not been pursued beyond this point, primarily because there has been little further interest in exploring polytropic types of models. Nevertheless, this area should be examined further.

We have spent some time on this subject because it leads us naturally into the title of our review paper -- mode identification. We have discussed two types of theories: 1) Ledoux's theory, which involves nonradial modes in the presence of rotation, has the advantage that it can explain line doubling. 2) The Chandrasekhar and Lebovitz scheme, as elaborated by Clement, requires coupling of a radial mode to a nonradial mode, and leads to two distinct modes, both of which are nonradial. But this model does not seem to explain all of the variations in line widths. There is no real preference between the two schemes because the excitation mechanism is not known.

IV. Simple Observational Quantities Interpreted as Mode Indicators

Before approaching the question of detailed line profile variations and their theoretical interpretation, we shall review in this Section some simple, easily observed quantities that have been proposed by various authors as indicators of the pulsation mode either in individual Beta Cephei stars or in the group as a whole.

As we noted in Section II, both the light and radial velocity amplitudes of Beta Cephei stars are quite small. Leung (1968) pointed out that the ratio of these quantities

$$\frac{\Delta m \text{ (blue)}}{2K} = 0.0021 \text{ mag/km s}^{-1}$$

is also extremely small in Beta Cephei stars, compared to other types of variables that are assumed to be radial pulsators (classical Cepheids, RR Lyrae stars, and Delta Scuti stars). Leung suggested that this might indicate that Beta Cephei stars are nonradial oscillators.

However, Watson (1971) correctly pointed out that the small visible light change in Beta Cephei stars is mainly a consequence of their high temperatures, which result in most of the energy being emitted in the ultraviolet. (It has since been confirmed by satellite observations that the light amplitude of these stars does increase greatly with decreasing wavelength). Watson showed that the physically more meaningful quantity

$$\frac{(\Delta R/R)}{\Delta M_{bol}} = \frac{24\ P}{17\ 2\ \Pi\ R} \frac{2K}{(\Delta M_v + \Delta BC)}$$

has a characteristic value of 0.12 for Beta Cephei stars; this does not differ greatly from the value computed for other types of variables.

Lesh (1976) measured values of $(\Delta R/R)/\Delta M_{bol}$ for several Beta Cephei stars using ultraviolet data, and suggested that a comparison of the observed values of this ratio with theoretically predicted ones might serve to discriminate between radial and nonradial modes. But Stamford and Watson (1977) felt that the physical significance of $(\Delta R/R)/\Delta M_{bol}$ would be unclear in the case of nonradial oscillations. They suggested using instead the ratio of light range to color range $\Delta V/\Delta$ (U-B) (where the latter, of course, is indicative of temperature range), in conjunction with $\Delta V/2K$. Their results were ambiguous, for they found that the observed $\Delta V/\Delta$ (U-B) suggested the presence of both radial and nonradial oscillations in the Beta Cephei stars.

Dziembowski (1977) also rejected the quantity $(\Delta R/R)/\Delta M_{bol}$ because his theoretical calculations showed that it is insensitive to the index ℓ (in the spherical harmonic Y^{ℓ}_{m}). Dziembowski carried out a general analysis of the light and radial velocity variations in a nonradially oscillating star. He computed the radial velocity averaged over the visible stellar disk, as well

as variations in the bolometric magnitude. He found that the ratio of the mean radial velocity to the magnitude variation $V_{rad}/\Delta M_{bol}$ is independent of the angle of inclination of the rotation axis. Consequently, a straightforward generalization of the Baade-Wesselink formula for stellar radius is possible. On this basis, if radius of the star is known, it is possible in principle to determine in which spherical harmonic the star is oscillating (i.e., whether the pulsation is radial or nonradial). The quantity $(V_{rad}/\Delta M_{bol})$ was found to have a strong dependence on ℓ for models appropriate to Delta Scuti stars (with a mass of $2M_\odot$). Dziembowski did not perform this calculation for the more massive models corresponding to Beta Cephei stars ($10 - 15M_\odot$). But it would be of great interest to do so, for the method appears to hold out great promise.

A more "classical" approach was taken by Lesh and Aizenman (1974). They constructed period-luminosity diagrams for Beta Cephei stars in the $(\log P, M_{bol})$ plane, using 10 and $15M_\odot$ models. On such a diagram (shown in Figure 1), the Beta Cephei "instability strip" maps into a discrete, relatively narrow band for a given radial pulsation mode. When the observed variable stars are plotted on this diagram most of them fall in the region appropriate to the second harmonic radial mode (but for a different assumed chemical composition, the first harmonic would be preferred). A similar diagram for nonradial pulsation modes (shown in Figure 2, where only the right-hand edge of this band for each mode is drawn) has most of the observed stars falling in the region appropriate to the P_2 and P_1 ($\ell = 2$) nonradial modes. These conclusions are reinforced by the study of the pulsation constant $Q = P\sqrt{\bar{\rho}}$. The mean value for the observed Beta Cephei stars is found to be 0.025, a value appropriate for the first harmonic

radial mode or the P_1 nonradial mode. On the basis of these data, the fundamental radial mode and nonradial f- and g- modes seem less likely than the radial harmonics and nonradial p-modes as candidates for the observed oscillation mode in Beta Cephei stars. But this method is not able to distinguish between radial and nonradial pulsation as such.

Schafgans and Tinbergen (1978) attempted to detect time variations in the linear polarization of β Cephei; if present, such variations might be interpreted as due to the time-varying anisotropy of the scattering geometry in nonradial pulsation. However, the authors did not detect any such variations to their level of accuracy ($4X10^{-4}$ r.m.s. in 4 minutes).

Finally, in approaching the study of the spectral lines themselves A. Karp and M. Smith (private communication) have suggested the simple criterion that if the change in line width is greater than the change in radial velocity, the pulsation is probably nonradial, and in the opposite case the pulsation is more likely to be radial. However, Karp (1978) has shown that the van Hoof effect is more strongly dependent on the ionization balance than on the velocity field in the stellar atmosphere, and hence is not a good diagnostic tool.

V. The Study of Line Profile Variations

By far the greatest emphasis in current work on Beta Cephei variables is on the detailed observation of the spectral line profiles, and their theoretical interpretation.

The observations have been greatly facilitated in recent years by the use of new types of detectors, which permit high time resolution and high spectral

resolution to be achieved simultaneously. One of the first such investigations was a study of β Cephei by Goldberg, Walker, and Odgers (1974) using image isocon and silicon diode vidicon television cameras as detectors, giving effective exposure times of 7-10 minutes. They observed SI III 4568 Å and 4553 Å, and found that the lines had an extended wing to the blue when the radial velocity was positive, indicating contraction of the star. When the radial velocity was negative, there was an extended wing to the red.

In a study of BW Vul, Goldberg, Walker and Odgers (1976) obtained a spectral resolution of 0.6 Å over a bandpass of about 140 Å with a refrigerated image isocon. The region studied included the lines He I 4471 Å, Mg II 4481 Å and Si III 4553, 4568, and 4575 Å. The effective exposure time was about 2 minutes. BW Vul has the largest light and radial velocity amplitude of any known Beta Cephei star, has a "stillstand" on the descending branch of its radial velocity curve, and exhibits dramatic line profile variations. The lines are sharpest, deepest, and essentially symmetric on the ascending branch of the velocity curve. As the cycle progresses through maximum radial velocity, they become shallower, broader, and somewhat asymmetric, with an extended wing to the red. The lines become double just before the radial velocity stillstand, are fairly sharp and deep during stillstand, and are highly asymmetric during the blueshift following the stillstand. A very detailed picture of this doubling on the descending branch of the radial velocity curve was obtained because of the high time resolution.

Similarly detailed observations of Si III 4553 Å and 4568 Å in 12 Lac were made by Allison, Glaspey and Fahlman (1977). This star also has strong,

deep, essentially symmetric lines on the rising branch of the velocity curve, and asymmetry and line splitting on the descending branch.

The U1 scanner on the Copernicus satellite was used by Lesh and Karp (1977) to obtain profiles of Si III 1294.5 Å in a number of Beta Cephei variables, with a spectral resolution of 0.05Å and an "effective exposure time" of about 20 min. The results for ν Eri and σ Sco are shown in Figures 3 and 4, respectively. There are two important points to be noted here: 1) in ν Eri, the phase of maximum asymmetry occurs on the descending branch of the radial velocity curve, as in the stars described above, but in σ Sco the greatest asymmetry occurs on the ascending branch (around phase 0.75, in the notation of Lesh and Karp); 2) in both ν Eri and σ Sco, the asymmetry is always in the sense of a depressed blue wing - depressed red wings do not occur.

The interpretation of the line profiles of β Cephei in terms of a radial oscillation - i.e., an atmosphere that alternately expands and contracts -- has been based on the early work of Wilson (1935) for uniform expansion, and Abhyankar (1965) for differential expansion following an exponential velocity law. Figure 5 shows some typical profiles for these two cases. Upon comparing their observations of β Cephei with these profiles, Goldberg, Walker and Odgers (1974) concluded that this star undergoes purely radial pulsation. However, Kubiak (1978) points out that stationary nonradial modes ($m = 0$) produce very similar profile variations.

The modelling of line profile variations in terms of nonradial oscillations was pioneered by Osaki (1971). He considered the case of quadrupole oscillations taking place in a rotating star, and, in order to calculate the line profiles, assumed that the line broadening was produced by the Doppler shift due to the mass motion of the surface elements. He assumed

that variations in surface area and brightness due to the oscillation are negligible. The equivalent widths of the lines would then remain constant throughout the oscillation, but the detailed structure of the line profiles would be affected by brightness variations due to the oscillation itself. His calculations included the effects of both rotation and the oscillation itself. The visible hemisphere was divided into about 5000 surface elements, and their radial velocities were computed and added to construct the line profiles.

In the case of the mode m = -2 (i.e. a wave travelling in the same direction as the rotation and symmetric with respect to the equator) he found that such a wave produced a discontinuous radial velocity curve, very sharp lines on the ascending branch of the radial velocity curve, and very diffuse lines around phase $\phi = 0.75$. This is characteristic of Beta Cephei stars such as BW Vulpeculae, σ Scorpii and 12 Lacertae. It appears, as first noted by Christy (1966) that a wave travelling in the same direction as rotation would explain such variations. Osaki thus proceeds to identify Struve's P_2 oscillation (the one associated with variable line broadening,) as the P^2_2 mode of oscillation.

The original calculation was made assuming an inclination of 90°. There appears to be little difference in the radial velocity curves for inclinations varying from 45° - 90°, but there were large deviations for i = 30°.

It should be noted that a wave travelling in the opposite direction to rotation (m = + 2) has the same characteristics as m = - 2, but the sign of the radial velocity is reversed. Thus for a wave with m = + 2 the sharpest lines occur on the descending branch of the radial velocity curve and the

lines become diffuse on the ascending branch. But the observations contradict this, and so Osaki believes that this can probably be excluded.

Osaki believes that waves that are antisymmetric with respect to the equator (m = + 1) should not be excluded because there is simply no basis for doing so. In the case of m = -.1, he finds that the shape of the velocity curves depends very strongly on the inclination. Nevertheless the actual shape of the line profile is very similar to that of the m = - 2 curve if viewed from near i = 45°. In fact, the cases m = - 2 or m = - 1 cannot really be separated. Nevertheless, Osaki believes that m = - 2 should be identified as being the main oscillation mode. He feels that it is unlikely that the mode m = - 1 will be excited in preference to the symmetric mode m = - 2. Furthermore, the profiles agree only when i ≃ 45°. It is possible that m = - 1 corresponds to one of the secondary oscillations.

The case where m = 0 is the case of a mode which is axisymmetric, and so it does not couple with rotation. The period of variation in line broadening is half that of the radial velocity curve and this is clearly contradicted by the observations. This is the mode that Chandrasekhar and Lebovitz consider, and Osaki feels that this mode is clearly not as successful in matching the observations as the m = - 2 mode.

Osaki also considers the possibility of identifying the separate modes which give rise to the beat phenomenon. The Struve P_2 oscillation associated with the variation in the line profiles generally has a shorter period and a larger velocity amplitude than the P_1 oscillation. The exception is β Canis Majoris where the opposite applies. Osaki identifies P_2 with m = - 2 (as do Ledoux and Christy). What about P_1? We can have m = + 2, + 1, 0, and - 1. We can exclude m = - 1 because a superposition does not give the beat phe-

nomenon where we have a long term amplitude modulation. Rather we get a long term modulation of the gamma velocity. Some Beta Cephei stars do exhibit such a variation (σ Scorpii). This variation has also been interpreted as being due to an orbital motion. Nevertheless, the alternate possibility should not be excluded. Also, a superposition of $m = -2$ and 0 can bring about a beat in which the amplitude of the radial velocity curve is modulated. Osaki thus identifies the P_2 wave as having $m = -2$ (travelling in the same direction as rotation) and the P_1 oscillation as a standing oscillation. He also considers $m = -1$ and $m = -2$ and finds that beats can occur. So this case is not totally excluded although the observed beat periods imply rotational velocities that are twice as large as those required for $m = 0$. Osaki speculates that $m = -2$ is preferably excited compared with other modes and so the excitation mechanism may be closely related to the rotation.

Some of the line profiles computed by Osaki (for $\ell = 2$, $m = -2$) are shown in Figure 6. Similar computations have been performed by Stamford and Watson (1976) and by Kubiak (1978).

The line profiles predicted for the various nonradial modes with $\ell = 2$ bear a strong resemblence to the type of profile encountered in the Beta Cephei stars that were originally noted for their large line-width variations. However, there are still some discrepancies. For instance, it is difficult to produce an outright splitting of the components with a nonradial oscillation alone. More importantly, all forms of nonradial pulsation (as well as radial pulsation) necessarily produce profile variations in which the direction of asymmetry is equally distributed between red and blue. In other words, if a certain asymmetric profile occurs at a given phase, its mirror image must

necessarily occur at another phase. Situations in which the asymmetry is always to the blue, as observed by Lesh and Karp (1977) for ν Eri and σ Sco, cannot be explained by either a radial or nonradial oscillation alone.

For this reason, Lesh and Karp proposed that an accelerating velocity gradient in the stellar atmosphere (indicating the presence of a "stellar wind") is superimposed on the underlying radial or nonradial oscillation. This would mean that at least some Beta Cephei stars are losing mass to their surroundings. Lesh and Karp succeeded in producing consistently blueward asymmetries with a velocity field of the form $v = -\alpha \log \tau + v_c$, where α (the acceleration term) = 40 km/sec and v_c (the radial pulsation amplitude) = 50 km/sec. Some of their profiles are shown in Figure 7. But the mass loss rate implied was of the order of 10^{-5} $M_\odot$/yr, which is contradicted by the observations (these stars show no emission pines, P Cygni profiles, etc). Lesh and Karp suggested that the combination of a nonradial pulsation and a smaller velocity gradient might produce the desired asymmetry without requiring an unacceptably high mass loss rate.

Nonradial pulsation theory also can be used to predict the form of the radial velocity curve, which can then be compared with the observations. Thus far, such comparisons have not been very successful, partly because of the difficulty of measuring the radial velocity consistently when several components are present in the line profile, and partly because of the lack of a full hydrodynamic theory.

VI. Conclusion

On the whole, then, the problem of mode identification in Beta Cephei stars cannot be said to have progressed to a state where it is a useful

indicator of the instability mechanism. Most simple, easily measured physical quantities are ambiguous in their interpretation - at best, they may serve to distinguish between radial and nonradial pulsation in general, or between fundamental modes and harmonics. The study of the line profiles holds out great promise for the identification of the actual pulsation mode, but more theoretical work and more observations are needed. The theoretical work should include a study of the effect of temperature and geometric changes in the stellar surface due to the nonradial oscillation, and especially a study of the effect of the depth-dependent velocity field on the structure of the stellar atmosphere. On the observational side, high time and spectral resolution investigation of profile variations in additional Beta Cephei stars should be made, and the observations already made should be repeated to check for the reproducibility of the profiles at identical phases. The simultaneous observation of strong and weak lines in the same multiplets and of lines from neighboring ionization stages would help to disentangle the various effects in the atmosphere.

Bibliography

Abhyankar, K. D. 1967, Ap.J. 141, 1056.

Allison, A. M., Glaspey, J. W., and Fahlman, G. G. 1977, A.J., 82, 283.

Chandrasekhar, S. and Lebovitz, N. R. 1962, Ap.J. 136, 1105.

Christy, R. F. 1966, A. J. 72, 293.

Clement, M. J. 1965, Ap.J. 141, 210.

Clement, M. J. 1967, Ap.J. 150, 589.

Dziembowski, W. 1977, Acta Astron. 27, 203.

Frost, E. B. 1902, Ap. J. 15, 340.

Frost, E. B. 1906, Ap. J. 24, 259.

Goldberg, B. A., Walker, G. A. H., and Odgers, G. J. 1974, Astron. Astrophys. 32, 355.

Goldberg, B. A., Walker, G. A. H., and Odgers, G. J. 1976, A.J. 81, 433.

Karp, A. 1978, Ap.J. 222, 578.

Jager, C. de 1953, BAN 12, 82,88,91.

Kubiak, M. 1978, Acta Astron. 28, in press.

Ledoux, P. 1951, Ap.J. 114, 373.

Ledoux, P. 1958, Hd. d. Astrophys. 51, 579.

Lesh, J. R. 1976, Ap.J. 208, 135.

Lesh, J. R., and Aizenman, M. L. 1974, Astron. Astrophys. 34, 203.

Lesh, J. R., and Aizenman, M. L. 1978, Ann. Rev. Astron. Astrophys. 16, 215.

Lesh, J. R., and Karp, A. H. 1977, Veroeff. Remeis Sternw. Bamberg 11, No. 121, p. 625.

Leung, K. C. 1968, Astrophys. Space Sci. 2, 302.

Meyer, W. F. 1934, PASP 46, 202.

Odgers, G. J. 1956, PDAO 10, 215.

Schafgans, J. J., and Tinbergen, J. 1978, preprint.

Stoeckly, R. 1965, Ap.J. 142, 208.

Struve, O. 1955, PASP 67, 135.

Stamford, P. A., and Watson, R. D. 1976, Proc. Ast. Soc. Australia 3, 75.

Stamford, P. A., and Watson, R. D. 1977, MNRAS 180, 551.

Watson, R. D. 1971, Ap.J. 170, 345.

Wilson, O. C. 1935, Ap.J. 82, 233.

Woltjer, L. 1935, MNRAS 95, 260.

Woltjer, L. 1937, BAN 8, 193.

Woltjer, L. 1943, BAN 9, 435, 441.

Woltjer, L. 1946, BAN 10, 125, 130, 135.

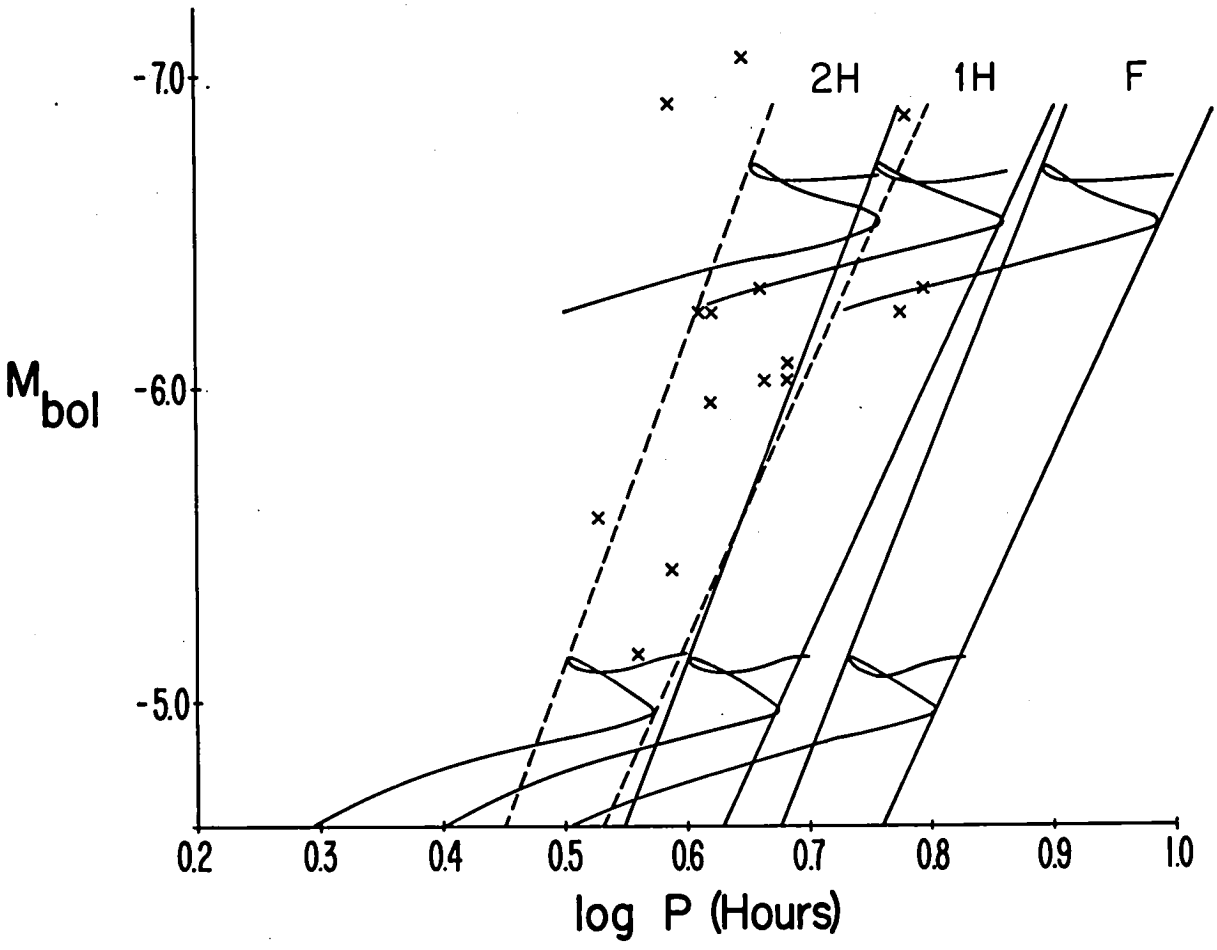

Figure 1. Period-luminosity diagram for observed Beta Cephei stars (crosses), and the "instability strips" calculated for the fundamental (F), first harmonic(1H), and second harmonic (2H) radial models (after Lesh and Aizenman 1974).

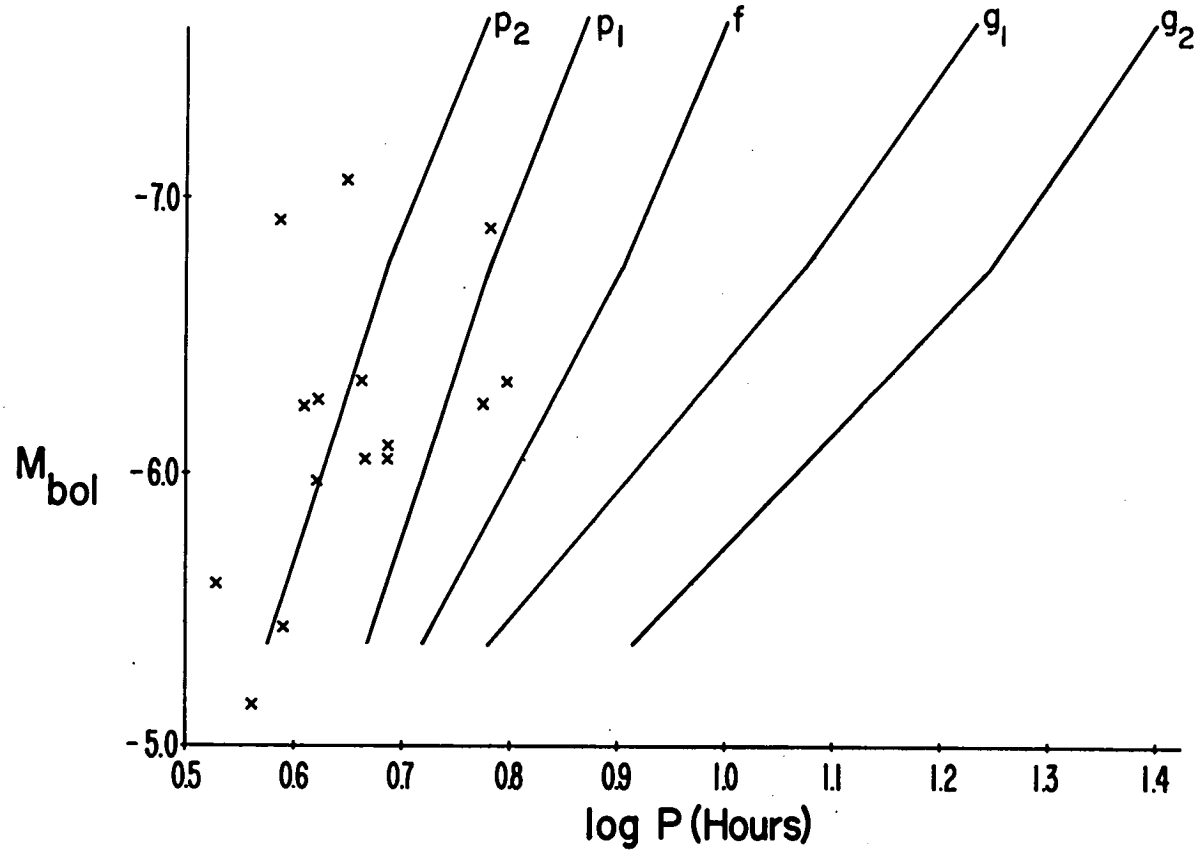

Figure 2. Period-luminosity diagram for observed Beta Cephei stars (crosses), and the right-hand edge of the predicted instability strips for nonradial p-, f-, and g-modes (after Lesh and Aizenman 1974).

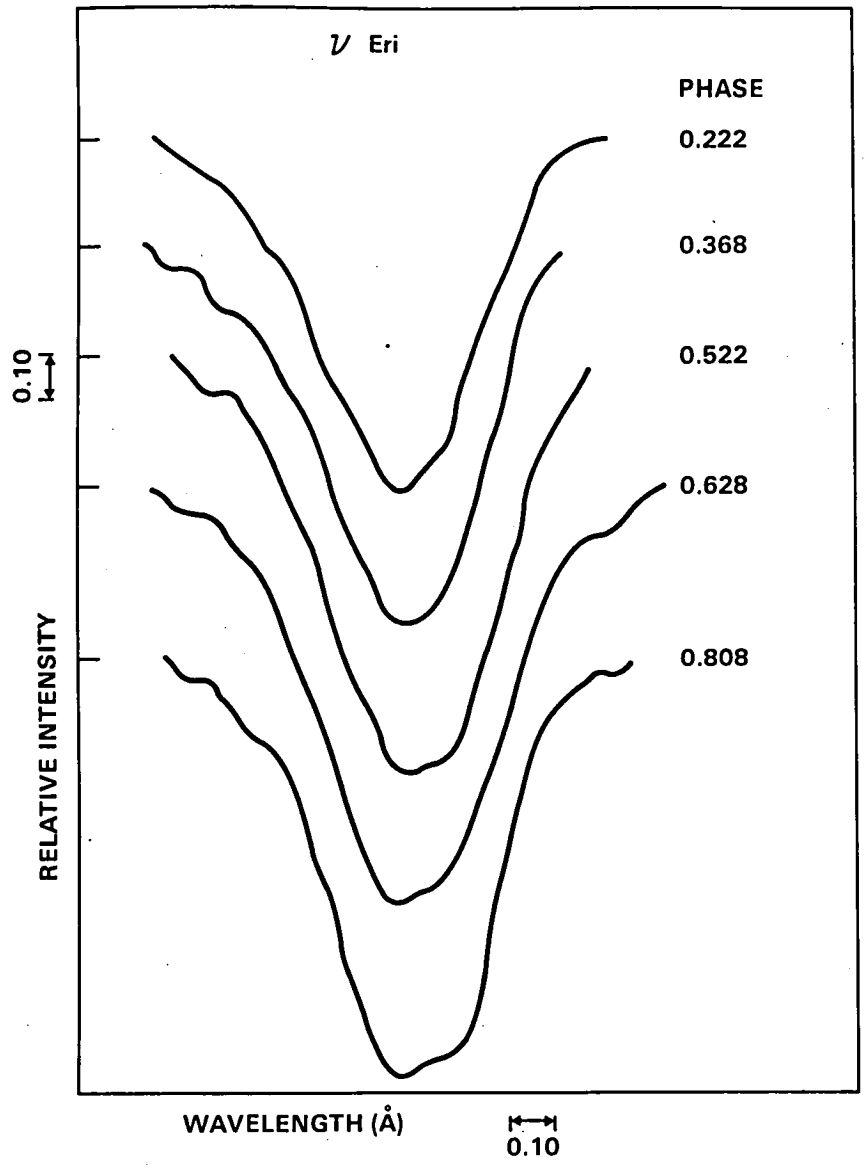

Figure 3. Profiles of the Si III 1294.5Å line in ν Eri, obtained with the Copernicus U1 scanner (after Lesh and Karp 1977).

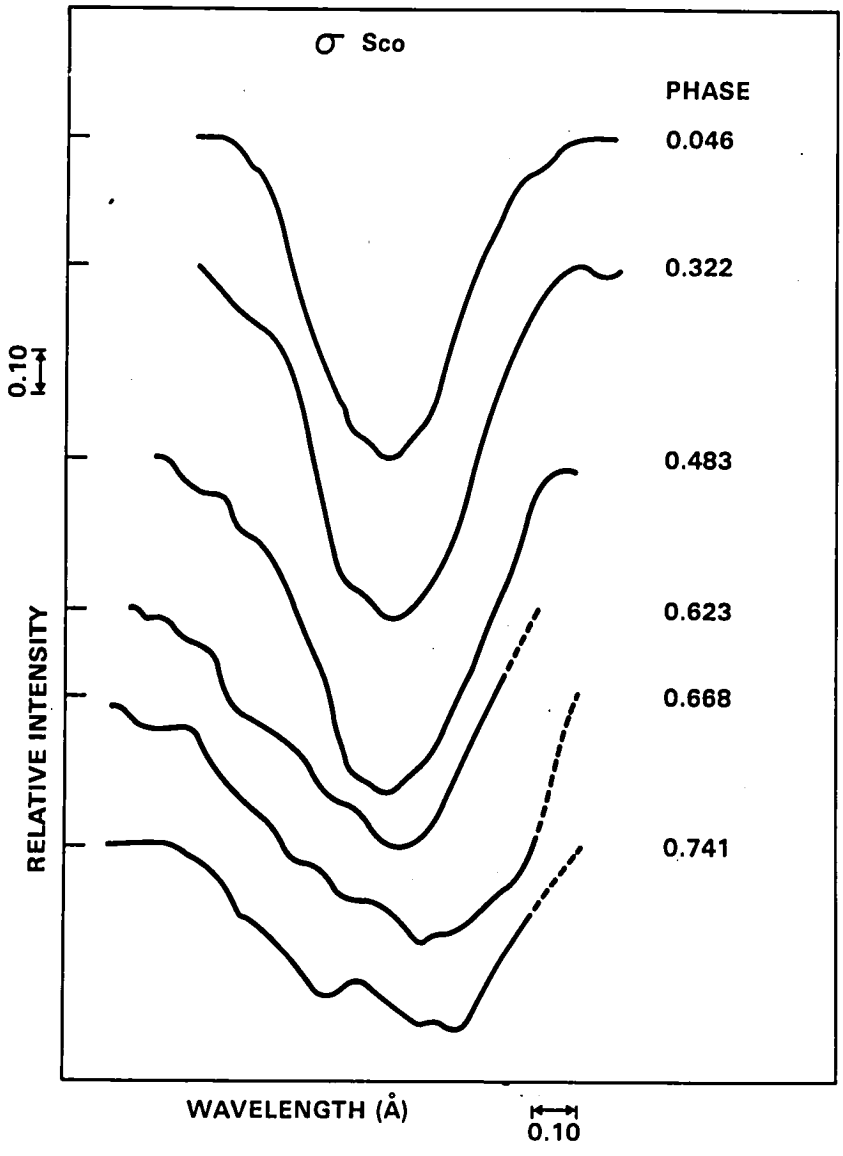

Figure 4. Profiles of the Si III 1294.5 Å line in σ Sco, obtained with the Copernicus U1 scanner (after Lesh and Karp 1977).

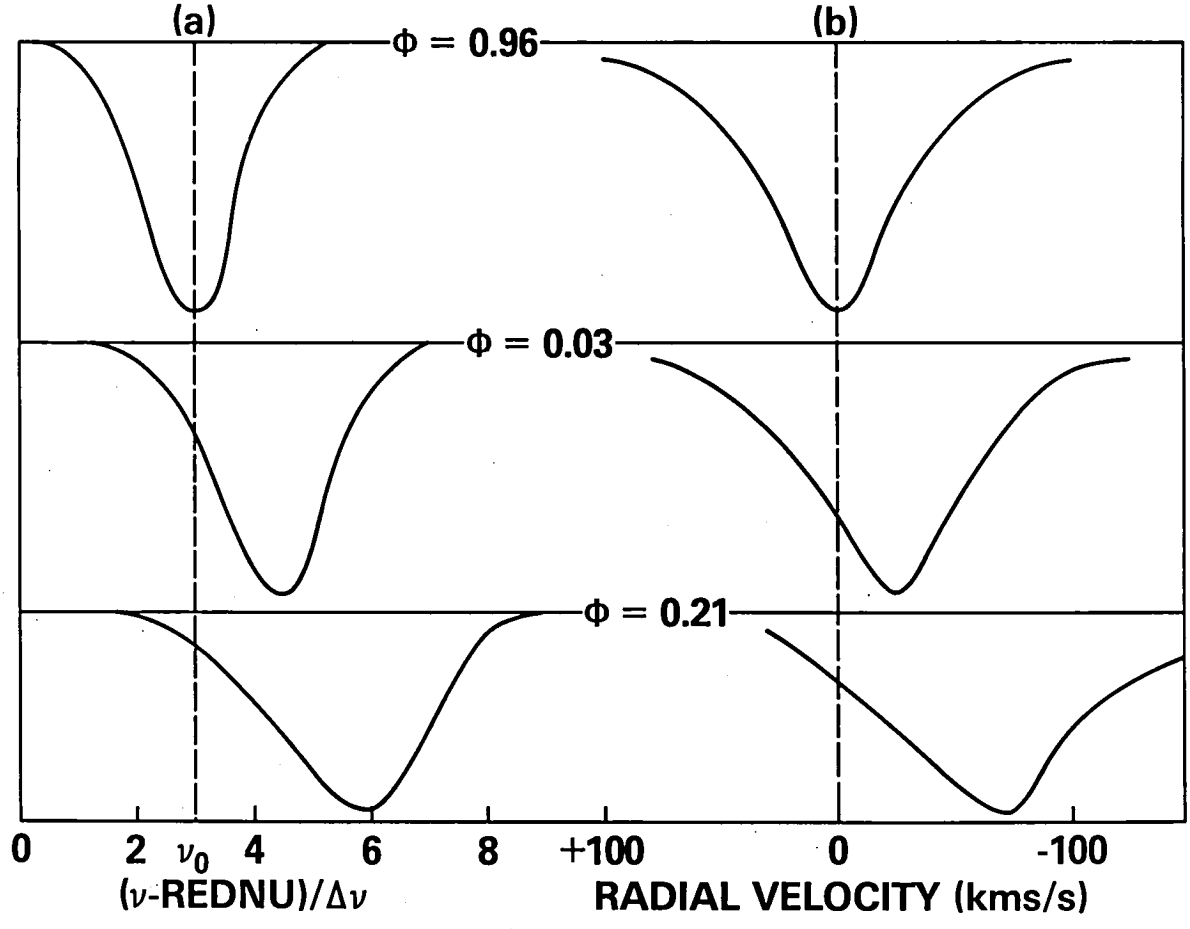

Figure 5. Synthertic line profiles for a star undergoing radial pulsation, with (a) differential expansion and (b) uniform expansion (after Goldberg, Walker and Odgers 1974).

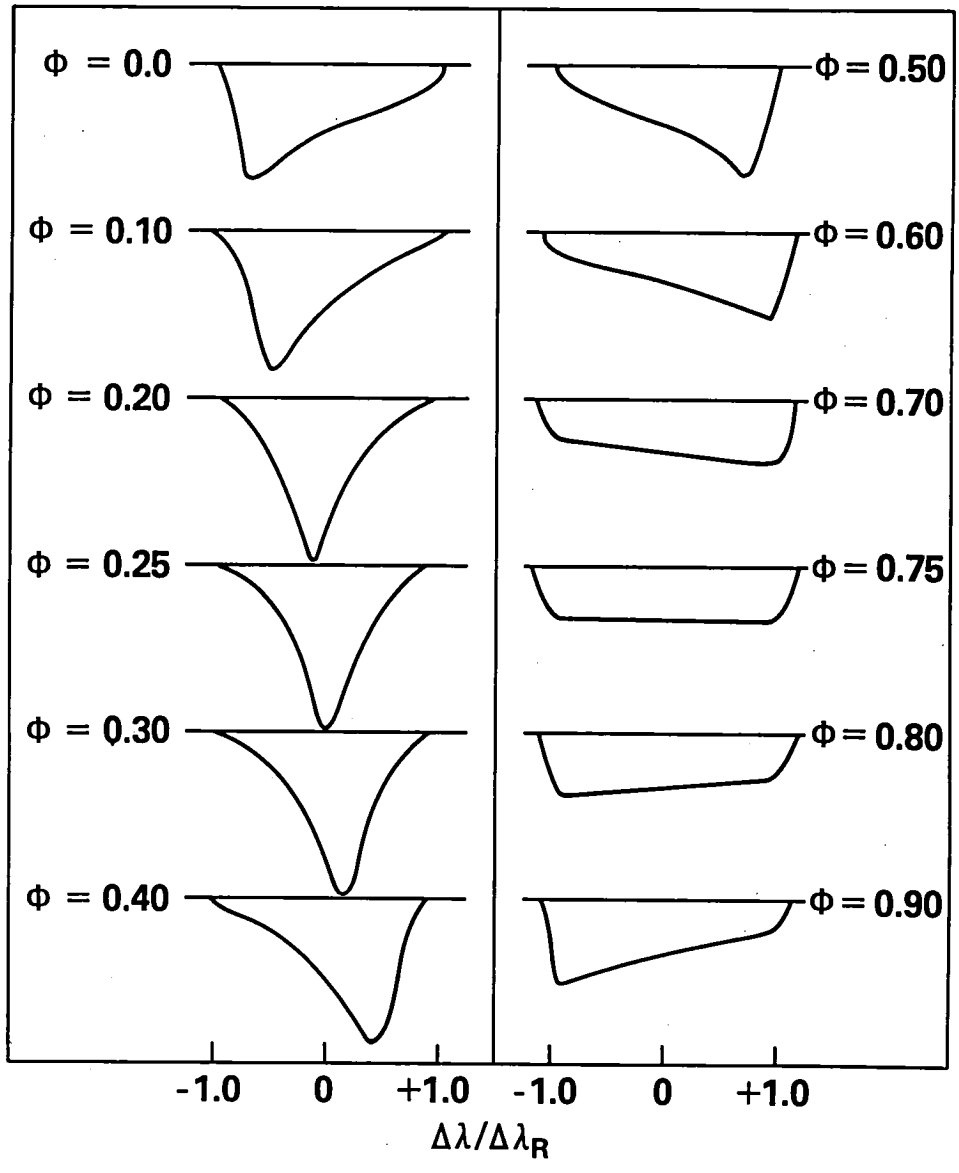

Figure 6. Synthetic line profiles for a rotating star undergoing nonradial pulsation in the $\ell = 2$, $m = -2$ mode (after Osaki 1971).

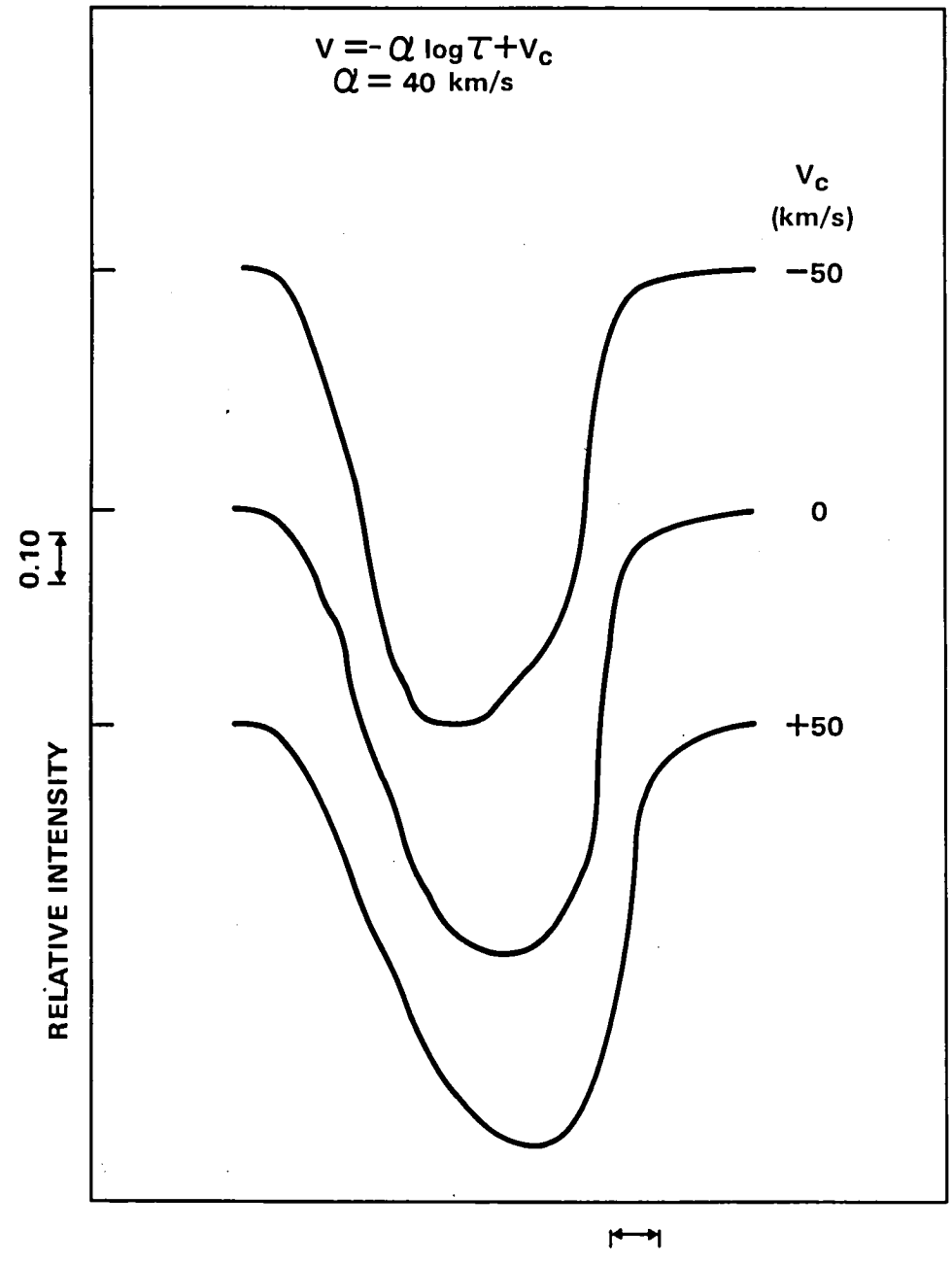

Figure 7. Synthetic line profiles for a star undergoing radial pulsation, with a superimposed stellar wind. The velocity field in the stellar atmosphere is of the form $v = -\alpha \log \tau + v_c$ (after Lesh and Karp 1977).

Discussion

M. Smith: I would like to second what you said about a shell in σ Sco. I would like to show you privately a little later some Reticon spectra of σ Sco that I observed which show emission P Cygni-type profiles at one particular phase in the star.

Lesh: That's very interesting. Of course, P Cygni profiles occur in stars where you have velocity gradients and mass loss, so perhaps we are finding evidence of the same phenomena.

Van Horn: To what extent is the symmetry in Osaki's theoretical profiles, which you showed, conditioned by an assumed symmetry of the underlying mode? In other words, could you get away from the comparable red and blue wings by going to a different order of spherical harmonics?

Lesh: I believe that Osaki considered only cases with $\ell = 2$ in his paper, and he found this type of symmetry for all values of m. I don't know what would happen for $\ell = 1$, for example, or whether Osaki has considered this case. Do you know, Myron?

M. Smith: Yes, I have modeled various profile sequences from $\ell = 1$ up to $\ell = 4$, and you find the same symmetry. It comes out of the spherical harmonic functions, which themselves have symmetrical properties. And this is true for intermediate inclinations as well.

Van Horn: Even the odd spherical harmonics?

M. Smith: Yes.

Shipman: Do all of the line profiles vary in the same way or are the variations different from one line to another?

Lesh: Normally, they all vary in the same way, with the occasional exception of hydrogen and helium. The Balmer lines tend to behave somewhat differently, and they are the only lines in which equivalent width variations are normally detected. But this is believed to be due to incipient emission at some phases, which causes the equivalent width apparently to decrease when, in fact, the line is simply being filled in. In stars in which the helium lines are very strong, the helium lines sometimes behave like the hydrogen lines, rather than like the metallic lines. But all of the metallic lines generally behave the same way.

A. Cox: What about abundance anomalies?

Lesh: As far as been observed, there are no abundance anomalies in these stars. People have done classical high-dispersion studies and have always found abundances in these stars that are comparable to those in other B stars. I myself have looked at the spectra of all these stars at classification dispersion and have never found any classification anomalies in them at all. So it would be nice to believe in the "helium fairy" [Laughter] who would increase the helium abundance in these stars quite a bit, because I am told that this is a possibility for creating an instability. But I would have to say, as an observer, that there is no evidence of very anomalous helium abundance or any other kind of abundance anomalies in these stars.

A. Cox: I am slightly worried that your lines may arise too high in the atmosphere. Have you tried to look at the variation in the weak lines which

come from very deep in the photosphere? In answer to another question, you said all lines behaved the same. Is that true of the weakest lines too?

Lesh: The lines that are observed in the visible are certainly weaker than the ones in the ultraviolet. The lines that we pick up in the ultraviolet tend to be very strong. Some people have tried to interpret the van Hoof effect as a means of measuring the velocity difference in different parts of the atmosphere, because there you are dealing with very gross effects -- hydrogen vs. helium vs. metals. However, Alan Karp has shown that the van Hoof effect is produced more by the ionization balance in the atmosphere than by the velocity field. In order to disentangle the velocity field from the ionization balance, you really have to observe a fairly large number of lines simultaneously. This hasn't been done yet, as far as I know, but it is something I am planning to do with IUE, if possible.

Hillendahl: I would just like to point out that the evidence for an outward velocity gradient increasing with radius doesn't necessarily mean that you have mass loss. This is an ordinary consequence of post-shock rarefaction waves. But you do get profiles like the ones that I showed in my paper. You do get outward flowing material, but it doesn't necessarily lead to mass loss. You have got to reach escape velocity for that.

Lesh: Yes, I agree with that, of course.

Hillendahl: Very elementary theory predicts that if you have pulsating stars with shock waves, you are likely to get a phenomenon called velocity doubling. That is, at various times you get apparent line cores that differ by a factor of two. I think it would be nice if people would indicate on their graphs a

Doppler shift corresponding to a factor of two, so you can see if this sort of thing is present. That will be one way of identifying a particular type of wave.

Lesh: Thank you. I will keep your suggestion in mind.

Baker: Have you tried to take the line shape change out of the radial velocity curve? What should we believe about the radial velocity curve, when there are these changes in line shape?

Lesh: I haven't done this myself. But it has been done by various people. If you are very careful about how you measure the radial velocity, curves which are apparently discontinuous -- like the one for BW Vul -- in fact, turn out to be continuous. The discontinuity can be fully explained by the change in the line shape or by the splitting into components. However, I suppose I should mention that BW Vul also shows a stillstand in its light curve which can't be explained away in the same way, and is probably due, in fact, to a shock wave in the atmosphere.

NASA/GODDARD AND LOS ALAMOS CONFERENCE ON STELLAR PULSATION INSTABILITIES

1978 June 1-2.

Some Evolutionary Considerations of β Cephei Stars

S.R. Sreenivasan and W.J.F. Wilson

Department of Physics, The University of Calgary

Calgary, Alberta, Canada

ABSTRACT

It is pointed out that the evolutionary characteristics of massive population I stellar models undergoing mass-loss and angular momentum loss do not favour an interpretation of the β Cephei phenomenon related to semi-convection or to the non-radial oscillations connected with semi-convection. They are not contradictory, however, to the interpretation that the phenomenon can be understood as a manifestation of Kelvin-Helmholtz instability arising from the differential rotation due to a faster rotating interior and an external layer or surface that has lost most of its angular momentum.

I. INTRODUCTION

In a clear and comprehensive review article Lesh and Aizenman (1978) have pointed out that "an apparently ordinary class of early type stars like the β Cephei objects defies physical explanation despite three quarters of a century after their discovery." It appears that some of the observational features such as rotation, the mode of pulsation etc. are still subject to either uncertainties or controversy. Although a number of such objects have been discovered and studied, clear cut statements about the nature of their pulsation also appear to be difficult from a theoretical point of view. The theoretical aspects of these objects have been also comprehensively reviewed recently by Cox (1976) and Kato (1976). Thus Lesh and Aizenman (1978) conclude that "if a reasonable instability mechanism could be found that applied only to a certain evolutionary state and to one or two pulsation modes, most of the controversy concerning the interpretation of the observations would be quickly removed." We refer the reader to the excellent review articles by Lesh and Aizenman, Cox and Kato for an observational and theoretical picture of these objects. However, we would like to stress that the theoretical interpretation of these objects relied in the past on evolutionary models which did not take into account either semi-convection or mass-loss satisfactorily. Although it cannot be said at the present time that this shortcoming has been rectified fully to everyone's satisfaction, new models of evolutionary sequences of massive population I stars have been published recently by several groups which take into account semi-convection and mass and angular momentum losses as best as one can at the present time. (Chiosi, Nasi & Sreenivasan, 1978; de Loore et al, 1977; Dearborn et al, 1978; Sreenivasan & Wilson 1978a; and

Sreenivasan & Wilson, 1978b, 1978c and 1978d). Further observational studies are also available that have not been included in the review by Lesh and Aizenman, e.g. Smith and McCall (1978) and a theoretical study of the non-radial oscillations of rotating stars that has a bearing on the problem of β Cephei stars has also been reported recently by Papaloizou and Pringle (1978). In the light of these developments it seems pertinent to ask what evolutionary constraints are placed on the interpretation of the β Cephei objects.

II. EVOLUTIONARY ASPECTS

We have recently completed a series of studies on the evolutionary aspects of massive population I stars and compared our results with those published by the Belgian group of de Loore and others. We have treated semi-convection in two different ways, and included mass-loss both in the early as well as later spectral stages. We have also taken the effect of rotation into account recently and studied the time evolution of angular momentum of these models, and further discussed the effect of differential rotation due to the faster rotating interiors and slowed-down surface layers. For details we again refer the reader to the papers mentioned in section 1. The results are summarised in the accompanying diagrams.

Figure 1 shows the evolutionary tracks of models of 15, 20 and 30 solar masses. The 15 and 30 $M_\odot$ tracks employed Paczynski's code as modified for our purposes. The 20 $M_\odot$ track used the code developed by Hofmeister et al and modified to take account of semi-convection and mass-loss by Chiosi. Chiosi treats semi-convection as described by Chiosi and Summa (1970). The mixing is treated mechanically until a stability criterion is satisfied. We

have treated semi-convective mixing as a diffusive process and described our procedure in Sreenivasan and Ziebarth (1974) and Sreenivasan and Wilson (1978a). Thus semi-convection has been treated in three different ways and except for minor quantitative differences the principal conclusion is that semi-convection almost disappears in models that are losing mass in the early spectral stages. This result has been clarified by different procedures for calculating the amount of mass lost by the models (Chiosi & Nasi, 1974, Chiosi et al, 1978 and Sreenivasan & Wilson 1978 a-d). Chiosi, Sreenivasan and Wilson therefore came to the conclusion that the β Cephei phenomenon cannot be attributed to the presence of semi-convection or to the non-radial oscillations that have been suggested to cause semi-convection (Gabriel et al 1976). Any possible uncertainties about either the nature of the phenomenon of semi-convection (see Spiegel for a review of this aspect: 1971, 1972) or reservations about dealing with it (Lamb et al 1976) therefore need not concern us on this account.

If these β Cephei objects are found to be slow rotators, and if the evidence for separate rising and falling shells and evidence for mass-loss found by Smith and McCall (1978) is a general feature of these objects, we might then ask whether this is in agreement with the evolutionary picture of stars in the mass range 15-30 $M_{\odot}$ undergoing mass-loss and angular momentum-loss. We have shown that most of the angular momentum of stars in this mass range in the outer layers is lost well before core hydrogen has been exhausted. This is more so if you take an averaged k^2 for the calculation of the moment of inertia $I = M k^2 R^2$, where M is the mass and R the radius of the star. It is also true if you include macroturbulent pressure due to differential rotation. We would like to emphasize that the actual mass-loss

rates used may be subject to uncertainties by an order of magnitude but that does not change the qualitative result that the outer layers spin down before hydrogen has been fully converted into helium in the core.

Smith and McCall (1978) suggest that the β Cephei star γ Pegasi is a slow rotator and that the spectral variations in this star are produced by radial pulsation. They also cite evidence for weak mass loss.

We have plotted the observed β Cephei stars given in the review article of Lesh and Aizenman on the same diagram as the one depicting the evolutionary tracks. One star happens to lie on the S-bend suggested by Lesh and Aizenman (1973,4). Three stars lie below the tracks of the 15 $M_\odot$ model on the main sequence. All the stars in their Table 2 lie in the field occupied by the 15 and 30 $M_\odot$ tracks except for the three mentioned above. Nine of these stars are very close to tracks that are made by models with initial masses 16 and 17 $M_\odot$. The three stars below the 15 $M_\odot$ track are probably in the mass range 10-12 $M_\odot$ and could be reached by evolutionary models showing very low mass-loss rates, lower than the threshhold of observations by Copernicus. On the other hand, the minimum mass at which semi-convection appears unambiguously is in the neighbourhood of 14 $M_\odot$ (Sreenivasan and Ziebarth 1974) or 13 $M_\odot$ (Barbaro et al 1972). One can therefore argue that if the stars showing β Cephei phenomenon are in the mass range 10-12 $M_\odot$, they would not probably possess semi-convective regions but may have very feeble mass-loss rates that do not affect drastically their evolutionary patterns. Taken together, the stars less massive than about 15 $M_\odot$ which do not have appreciable mass-loss and the stars more massive than 15 $M_\odot$ and in the mass range 15-30 $M_\odot$ which do have appreciable mass-loss rates, and hence no semi-convective regions, would

suggest that the β Cephei phenomenon may not be linked to either semi-convection or effects associated with semi-convection such as non-radial oscillations. Kato (1976) argues that a number of other mechanisms proposed do not appear to be probable either.

The only suggestion that does not conflict with evolutionary constraints is then that of Papaloizou and Pringel who suggest that the β Cephei phenomenon is a manifestation of Kelvin-Helmholtz instability arising from the differential rotation of the interior with respect to the surface layers. We have not examined any of our models for radial pulsation but are aware of the work of Davey (1973) which sugqests that these stars are stable for radial pulsations.

It is tempting to visualize a scenario which depicts β Cephei stars which are in the early spectral range BO - B2 as stars which have lost a significant amount of rotation in the surface layers, subject to Kelvin-Helmholtz instability and showing the spectral variation they do, subsequently ejecting a shell or losing mass in sufficient amount to cause shell formation. In such a picture β Cephei objects would be the precursors of the shell stars. But clearly more work is needed both from the evolutionary point of view as well as pulsational to clarify this interesting type of sequences of evolutionary models with initial masses 16 and 17 $M_{\odot}$ on the main sequence to cover the centre of gravity of the observed group of confirmed β Cephei objects in Lesh and Aizenman's Table 2. It would be equally interesting and worthwhile to investigate in greater detail the consequences of Kelvin-Helmholtz instability in these objects.

III. CONCLUSION

Stars in the mass range 10-12 $M_\odot$ probably do not exhibit semi-convection. Stars more massive than 15 $M_\odot$ in the range 15-30 $M_\odot$ which undergo mass-loss do not exhibit semi-convection either. If the observation that the β Cephei objects are all slow rotators and subject to mass-loss is substantiated, then evolutionary constraints are consistent with the interpretation that the β Cephei phenomenon is a manifestion of Kelvin-Helmholtz instability. But more work is required and an examination of the evolutionary features as well as a detailed study of the instability are needed to clarify the nature of these fascinating objects.

IV. ACKNOWLEDGEMENTS

The work reported in this paper was supported in part by a research grant from the National Research Council of Canada to S.R. Sreenivasan. The argument concerning the role of semi-convection in the β Cephei stars was initiated in joint discussions with Dr. C. Chiosi during his stay in Calgary.

V. REFERENCES

Barbaro, G., Chiosi, C. and Nobili, L: 1972 A and A 18, 187.

Chiosi, C., and Nasi, E: 1974 A and A 34, 355.

Chiosi and Summa, C: 1970 Ap. Space Sci. 8, 478.

Chiosi, Nasi and Sreenivasan: 1978 A and A 63, 103.

Cox, J.P., 1976, Proc. Los Alamos/Goddard Conference on Stellar Pulsation Instabilities, p. 127 ed. A.N. Cox and R. Deupree, LA-6544-C.

Davey, W.R.: 1973 Ap. J. 179, 235.

Dearborn, D.S.P., Blake, J.B., Hainebach, K.L. and Schramm, D.N., Ap. J. in the press.

Gabriel, M. and Noels, A: 1976 A and A 53, 149.

Kato, S., 1976, Multiple periodic Variable Stars ed. W. Fitch, Reidel, Dordrecht, p. 33.

Lamb, S.A., Howard and Iben: 1976 Ap. J. 207, 209.

Lesh and Aizenman, 1973 A and A 22, 229; 26, 1.

Lesh and Aizenman, 1974 A and A 34, 203.

Lesh and Aizenman, 1978 Annual Reviews Astr. Ap. in the press.

de Loore, de Greve and Lamers: 1977 A and A 61, 254.

Papaloizou and Pringel, 1978, MN 182, 423.

Smith, M.A. and McCall, M.L. 1978, Ap. J. 221, 861.

Spiegel, E.A., 1971, Ann. Rev. Astr. Ap. 9, 323.

Spiegel, E.A., 1972, Ann. Rev. Astr. Ap. 10, 261.

Sreenivasan and Wilson, 1978a Ap. Space Sci., 53, 193.

Sreenivasan and Wilson, 1978b A and A in the press.

Sreenivasan and Wilson, 1978c IAU Symposium No. 83 on Mass-loss and Evolution of O-type Stars. ed. P.S. Conti (Reidel, Dordrecht).

Sreenivasan and Wilson, 1978d Bull. AAS in the press.

Sreenivasan and Ziebarth 1974 Ap. Space Sci. 30, 57.

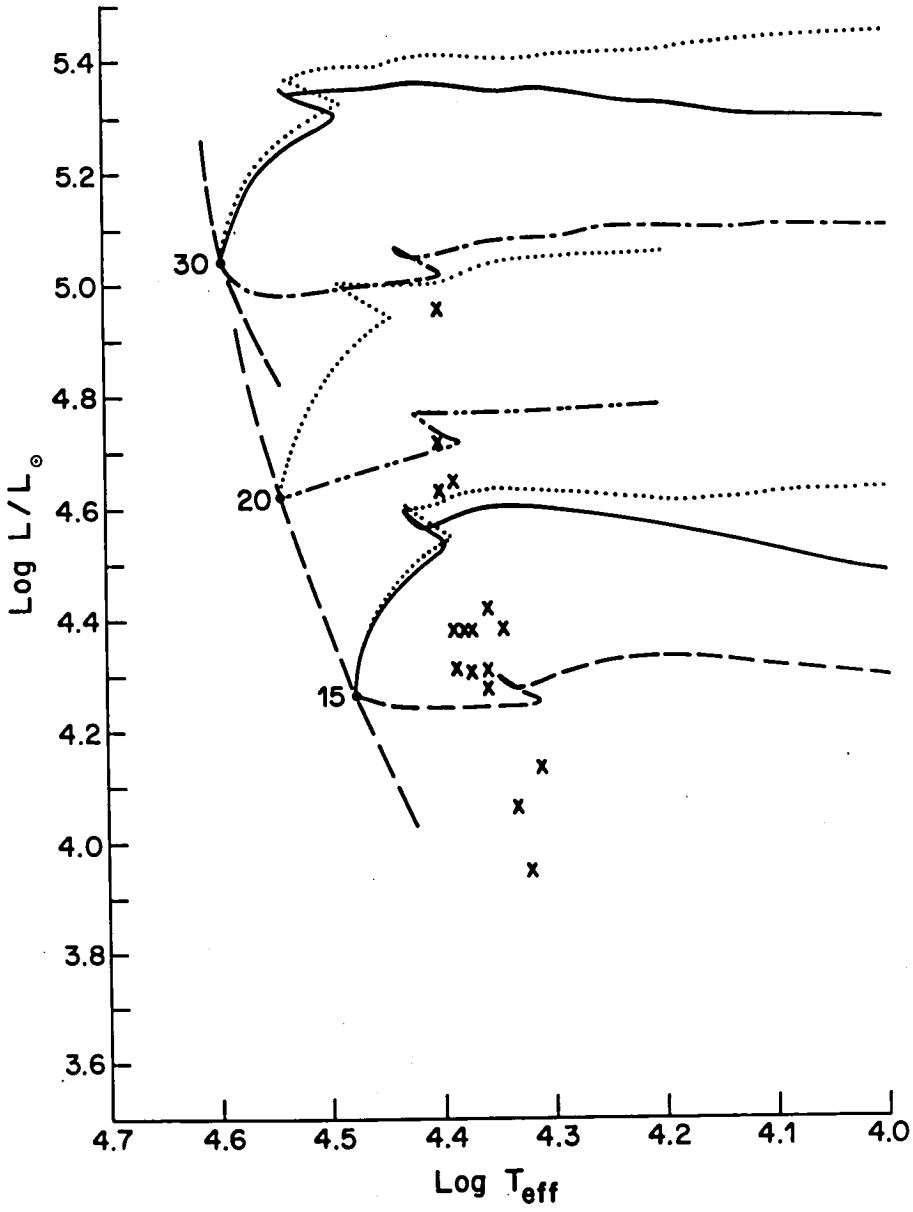

Figure 1. Evolutionary tracks for 30, 20, and 15 $M_{\odot}$ sequences near the main sequence. Solid line: evolution without mass-loss or semi-convection (sc); dotted line: without mass-loss but with sc; dashed line: with sc, and mass-loss including conservation of angular momentum; dot-dash line: with sc, and mass-loss including conservation of angular momentum; dot-to-dash line: with sc, but with mass-loss excluding rotation. The dashed line joining all sequences represents the zero age mass sequence. Crosses denote the β Cephei stars from Lesh and Aizenman (1978).

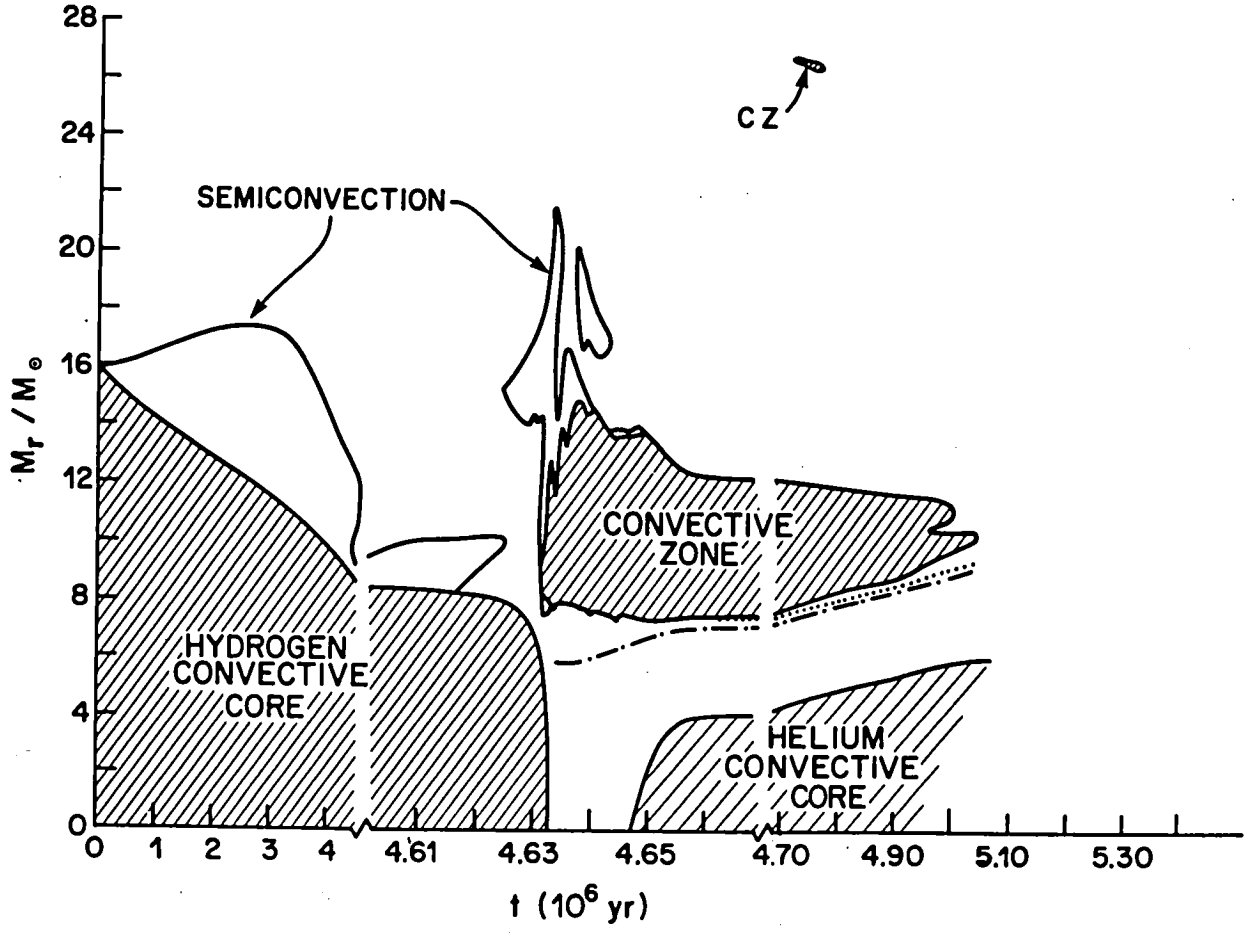

Figure 2. Location of the boundaries of fully convective zones (cz) and semi-convective zones for the 30 $M_\odot$ sequence without mass loss. The shell source maximum (dotted line) and the outer boundary of the helium-rich core (dash-dot line) are also shown.

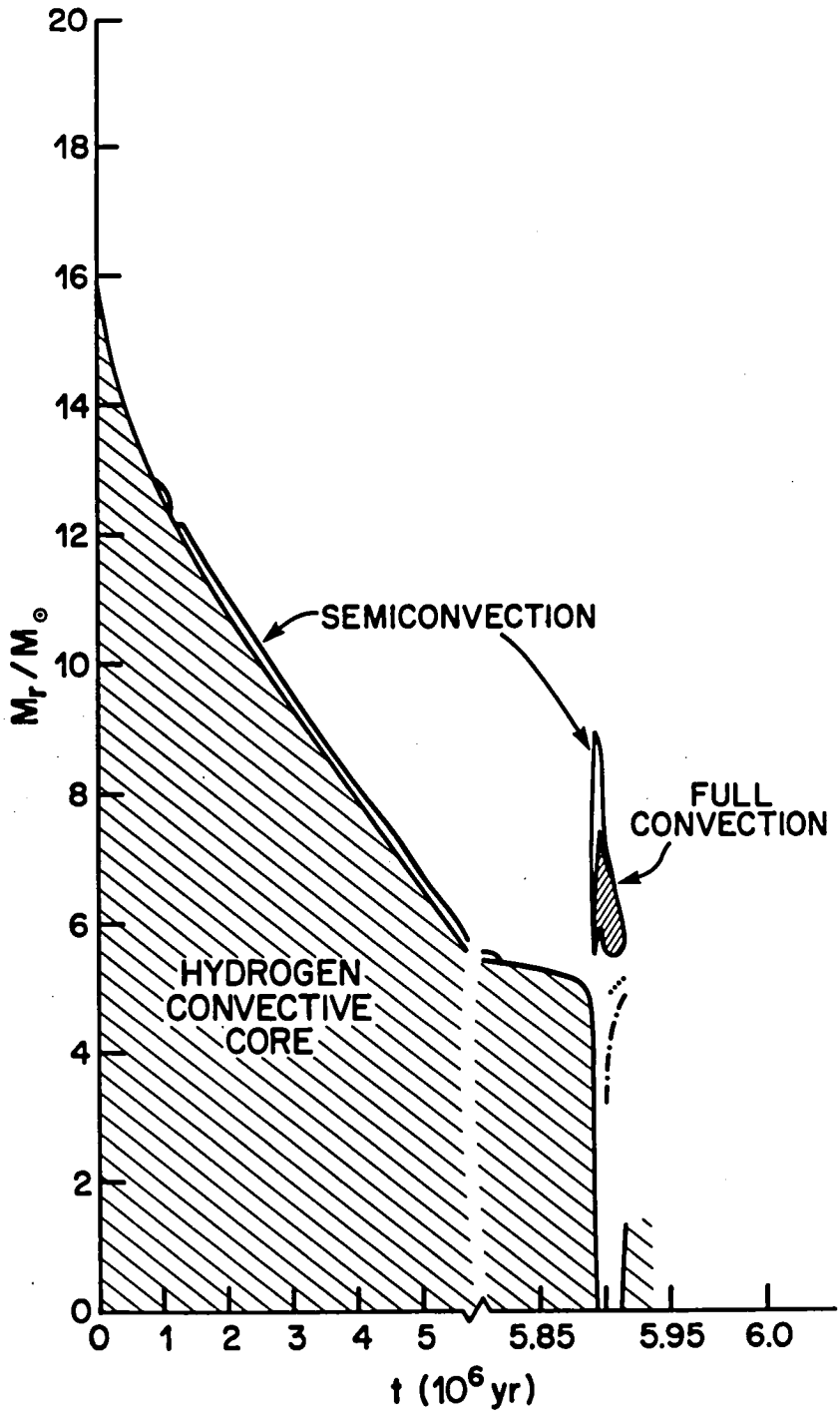

Figure 3. Boundaries of convective regions in the 30 $M_\odot$ sequence with mass-loss including turbulence and conservation of energy and angular momentum.

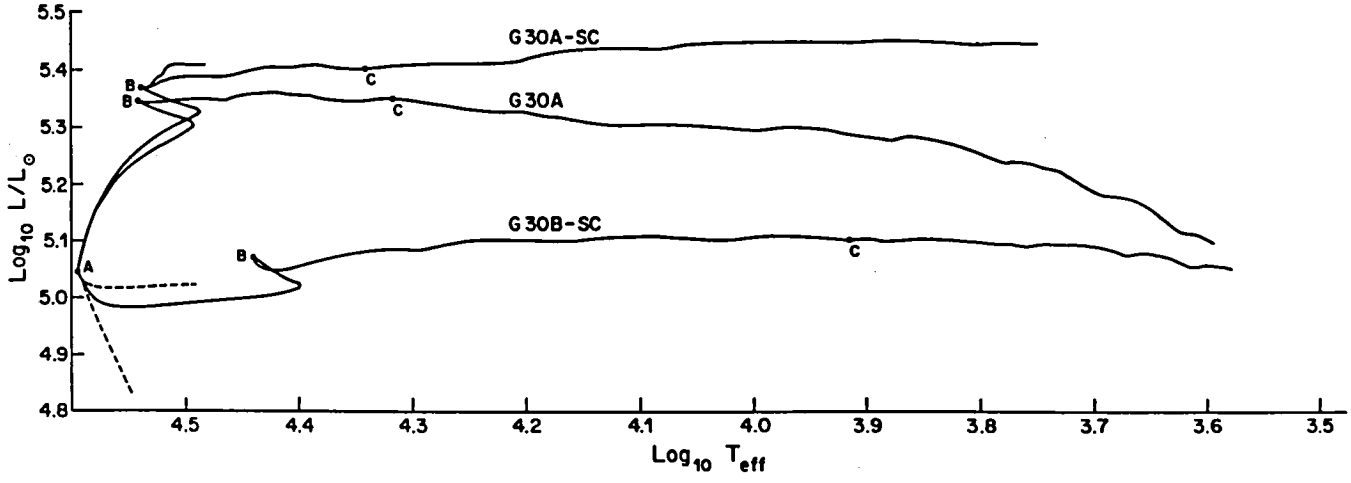

Figure 4. Evolutionary tracks for 30 $M_\odot$ models. 30 A-sc: evolution without mass-loss but with semi-convection. 30 A: evolution without mass-loss or semi-convection. 30 B-sc: evolution with semi-convection, and mass-loss including turbulence and conservation of energy and angular momentum.

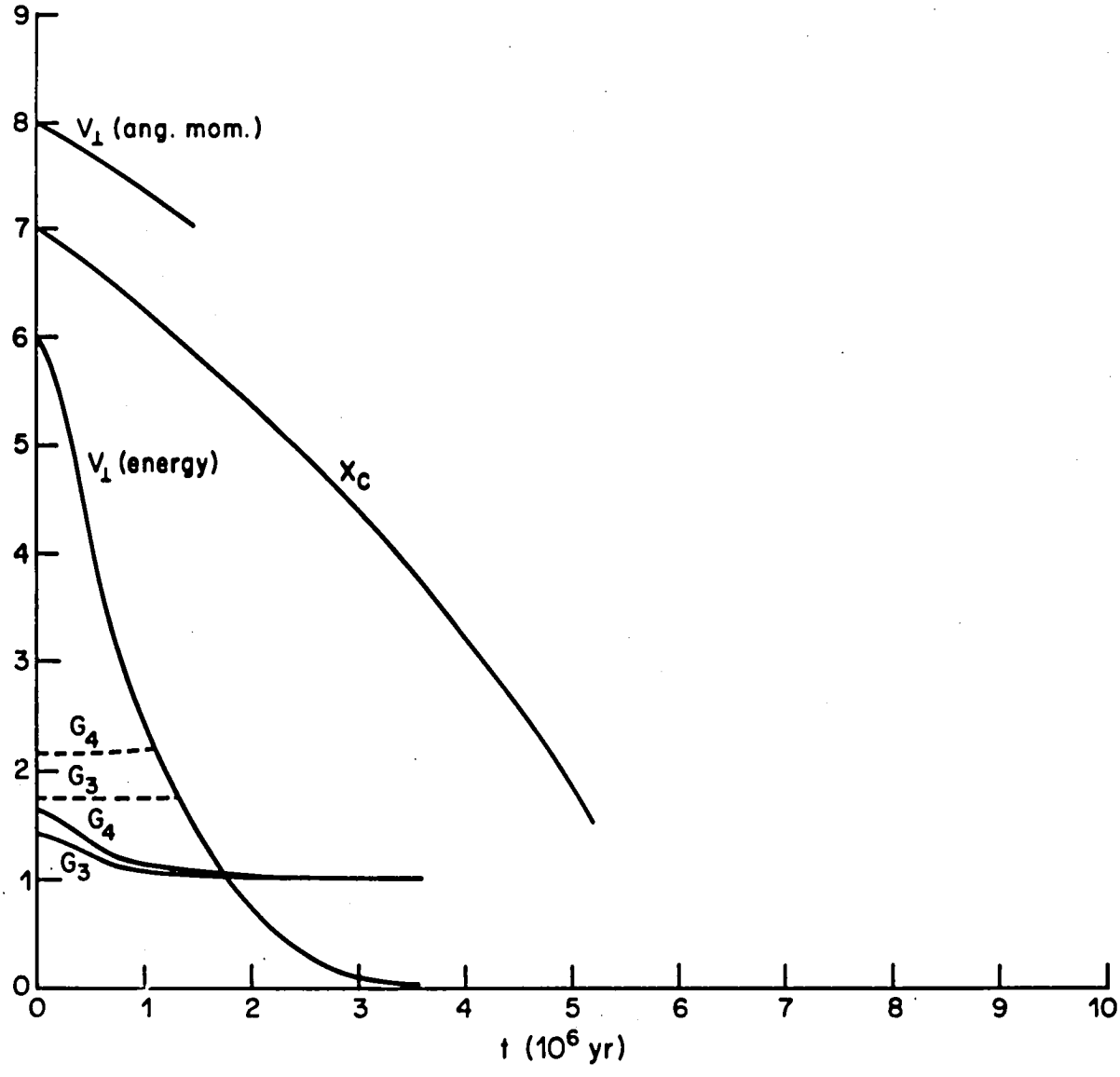

Figure 5. Plot of rotational velocity versus time for conservation of energy and angular momentum (labelled energy) for 30 $M_\odot$, in units of 100 km/sec. G3 and G4 shown for the energy and angular momentum case (solid lines) and angular momentum case (dashed lines), in units of 1.0, where $\dot{M}_4 = G4 \cdot \dot{M}$, and $\dot{M}_3 = G3 \cdot \dot{M}_2$. The central hydrogen content, X_c, is also shown for reference, in units of 0.1.

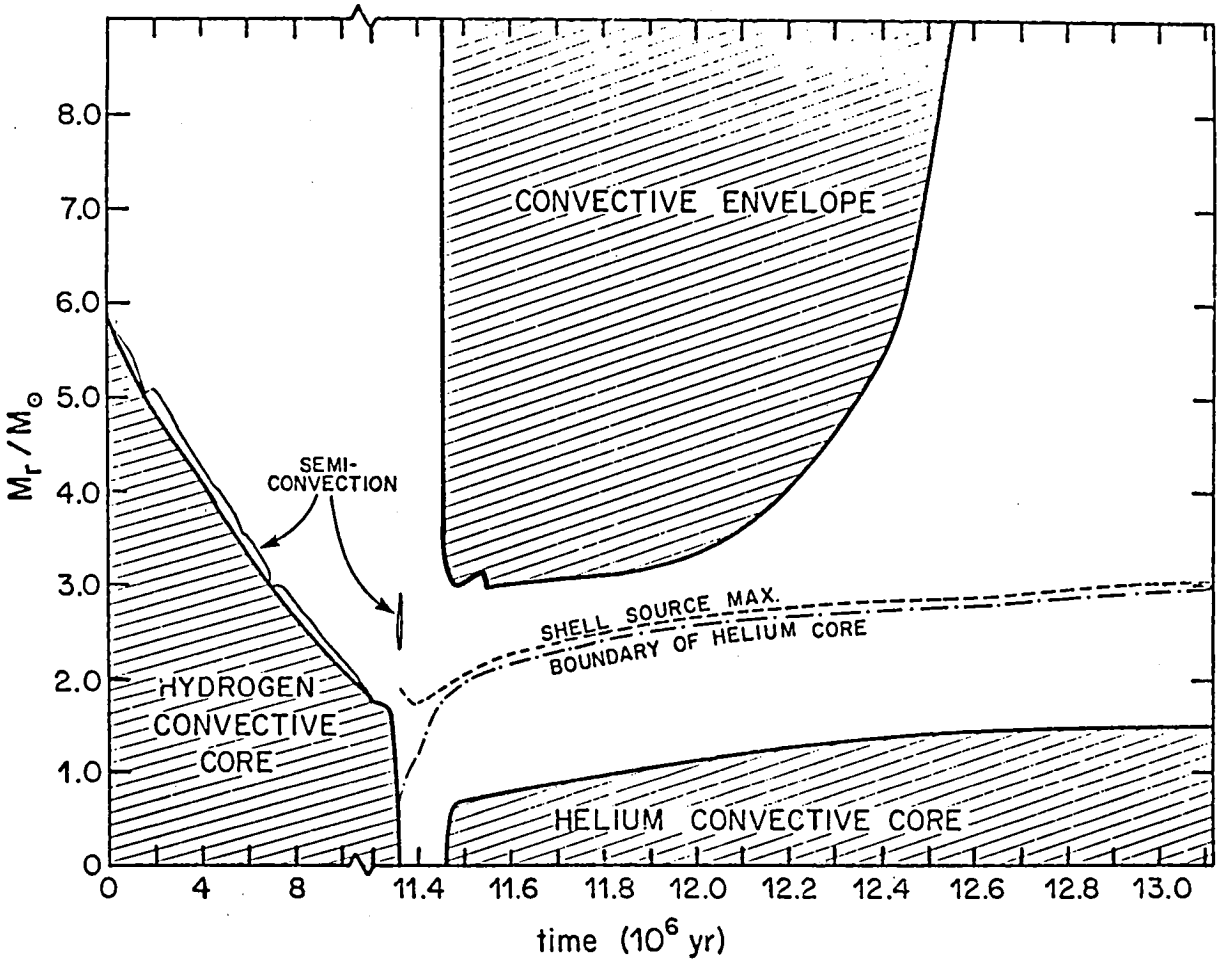

Figure 6. Locations of the boundaries of convective regions in the 15 $M_\odot$ sequence, with mass-loss including conservation of angular momentum.

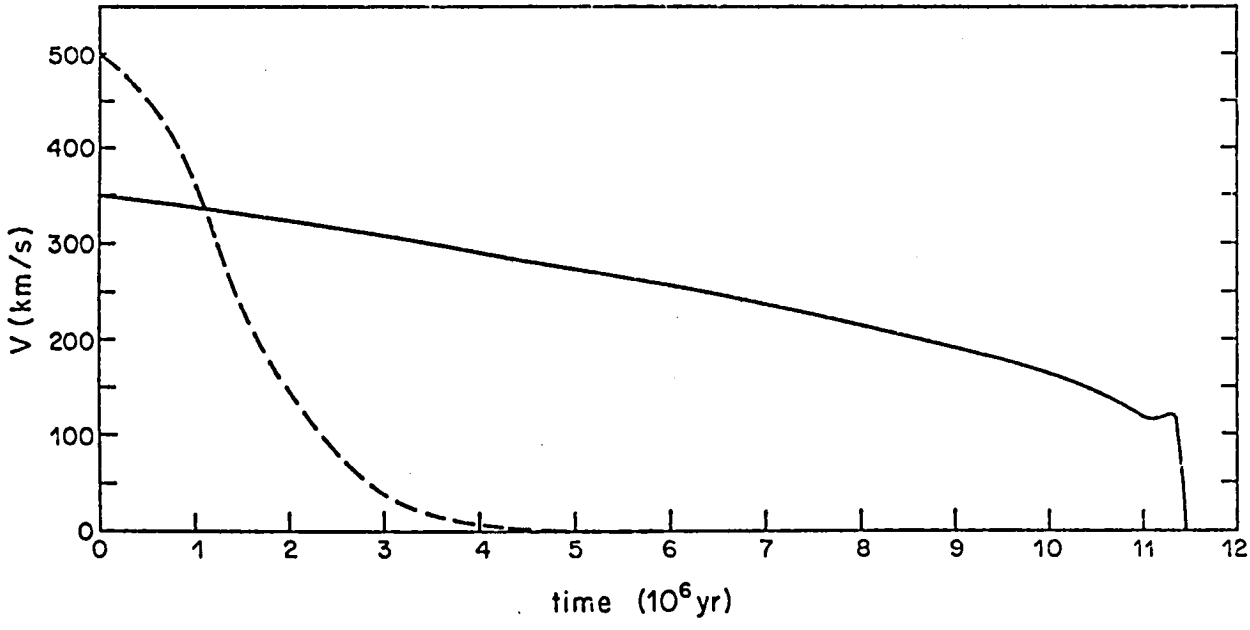

Figure 7. Plot of rotational velocity versus time for the 15 $M_\odot$ sequence, for mass-loss including conservation of angular momentum (solid line) and including both angular momentum and energy (dashed line). Central hydrogen exhaustion coincides with the secondary maximum in the solid line on the right hand side of the diagram.

Discussion

Baker: Didn't Smak get a rather secure mass estimate of about 10 $M_\odot$ for one of these stars -- α Vir? (Note added in proof: The actual number he got was 9 ± 1 $M_\odot$. See Acta Astro. 20, 75, 1970.)

Sreenivasan: Possibly. If it is 10 $M_\odot$, then there is no semiconvection in these objects. That is all I was saying. I was not claiming that the mass should be a certain value, but if it started on the main sequence as a 10 $M_\odot$ star, and then if there is any mass-loss, it will be too low to affect any evolutionary considerations.

Baker: I was just wondering what the actual tracks are.

Sreenivasan: I think 10 to 15 $M_\odot$ is the mass range that is quoted. On the other hand, if the star is losing a significant amount of mass, it may have started higher on the zero-age main sequence and come down to this region. A 30 M. star can lose about 40% of its mass by the time it exhausts hydrogen, and a 15 $M_\odot$ star loses 2 or 3 $M_\odot$.

Lesh: I think the measurement Dr. Baker is talking about was made not by Smak but by Hanbury-Brown and his coworkers in Australia, using the intensity interferometer. Their result for α Vir was 11 ± 1 $M_\odot$. I think that this error estimate is a bit optimistic, and the star may actually be a little more massive than that. But in general, the range of masses attributed to β Cephei stars in 10 - 15 $M_\odot$.

J. Cox: Can you say that it takes a significant amount of mass-loss to get rid of the semiconvection zone? Have you had a chance to investigate this relation?

Sreenivasan: Yes. We have investigated the 15 $M_\odot$ and 20 $M_\odot$ objects, as I showed you. The mass-loss on the main sequence is of the order of 10^{-7} $M_\odot$ per year for a 15 $M_\odot$ star. And if it has rotation, there is a centrifugal force with reduction of gravity, so that increases the mass-loss. It could be several times 10^{-7} $M_\odot$ per year, but it is certainly less than 10^{-6} $M_\odot$ per year. On the other hand, for a 30 $M_\odot$ star, it is of the order of 10^{-6} $M_\odot$ per year, and these figures are well within the observational limits imposed by the Copernicus satellite measurements. I think this is consistent with the observational information we now have from Copernicus. So even a few times 10^{-7} $M_\odot$ removes semiconvection in a 15 $M_\odot$ star. In other words, the type of mass-loss that is allowed by the theory of Castor et al., with proper α and K values, takes away semiconvection. This is a very interesting result, because many people are not quite sure what kind of a "beast" semiconvection is, and how to treat it; so if it disappears, that solves one of the problems. And the fact that it disappears is borne out by everybody who has looked at this problem. So we don't have to worry about what it is, but all we can say is that you can't blame the β Cephei phenomenon on semiconvection.

Aizenman: The mention of differential rotation is also interesting because the original Chandrasekhar and Lebovitz mechanism, which Janet mentioned earlier, was examined by Maurice Clement as a possible explanation of the beat phenomenon. Clement ran into problems explaining the phenomenon by

this mechanism because of the very large rotation velocities required to match the observed beat periods. In 1967, he wrote a paper assuming a Stokely differential rotation law, and he found that in that case, he could match the observations on this type of phenomenon. While no mechanism was involved, this type of differential rotation law did allow one to obtain the observed beat periods.

Sreenivasan: In fact, Papaloizou and Pringel invoked differential rotation as well. We have looked at two models of a 15 $M_\odot$ star starting out at 500 km/s on the main sequence, which has a ratio of centrifugal force to gravity of about 2/3, and at 350 km/s. From observations of angular momentum alone, all this surface rotation is gone by the time hydrogen is exhausted in the core; but if you take energy conservation into account as well as angular momentum conservation, the surface rotation is gone in about 5.5 million years. But of course, if it is differential rotation, the interior layers will be rotating faster, and this is consistent with what Papaloizou and Pringel said. All I'm saying is that if there is mass-loss, there is angular momentum loss, and thus differential rotation is enhanced. Semiconvection disappears, so you can't blame it on semiconvection, but you could blame it on differential rotation and a Kelvin-Helmholz instability. We have not investigated this Kelvin-Helmholz instability in detail, but we hope to.

THE VARIABILITY OF 53 PISCIUM AND THE EXTENSION OF THE β CMa INSTABILITY DOMAIN

SAREYAN J.-P.

LE CONTEL J.-M.

VALTIER J.-C.

DUCATEL D.

Observatoire de NICE

We have performed at the ESO (Chile) photometric and spectrographic observations on the B3V star 53 Piscium. Figures 1, 2, 3 show respectively the obtained light and radial velocity curves and the line profile variations. All the data are now in press (Sareyan et al., 1978). We classify 53 Psc as a new confirmed β CMa star on the basis of the short period variations characteristics of this group.

We are not able to say whether the 0.25 P shift between light and R.V. maxima exists because on the single night when the observations have been simultaneous, the photometric data are poor. However we can say that the scattering on the photometric data for that night is reduced when we superimpose on them the radial velocity curve with the 0.25 P phase shift.

53 Psc had been detected variable by Williams (1954), but Percy (1971) observed it constant, i.e. under his actual 0.005 magnitude detection threshold. These previous results are not contradictory with ours as the observed amplitudes remain small and probably variable.

However its spectral type and luminosity classification (B 3 V) locate it outside the so-called classical "instability box" of the β CMa variables.

This "instability box" is 0.3 magnitude wide, lays 1.5 magnitude above the zero age main sequence and is roughly parallel to it, in the BO - B2 and luminosity class IV to II ranges. Its lower corner is at $M_V = -3$ (Percy, 1970, 1971; Percy, Madore, 1972). This box contains the 18 first discovered β CMa stars. Its limits are approximately defined by the position of 16 Lac, γ Peg, α Lup and β Cru (fig. 4).

These 18 first stars have been discovered by the RV measurements which at the time selected bright stars with sharp-lined spectra. Later, due to the increase of photometric precision, new stars have been added to the group (Hill, 1967; Shobbrook and Lomb, 1972; Jerzykiewicz, 1975; Balona, 1977).

Some of these new variables have been immediately classified β CMa stars even when they had broad lines (K and λ Sco for instance) owing to the fact that they lay in the good region of the HR diagram, i.e. in the instability box. The other stars have been classified as "suspected" β CMa.

An example of such studies is given by the recent detection work by Sterken and Jerzykiewicz (1977). These authors restricted their search for new variables to the stars already located in the classical box of the HR diagram. If they had found a lot of new β CMa stars in that region, one could have concluded once more that the instability box had even steeper limits.

But there is anyway an increasing number of variables with β CMa variation characteristics outside the box (fig. 4) due particularly to different detection works by Balona, Jerzykiewicz, . . .

We think that simultaneous observations of short period variability in light and RV curves, with a 0.25 P shift, on a single night, would be sufficient to prove the β CMa character of the suspected β CMa stars. So new observations of suspected β CMa stars are badly needed.

Anyway the confirmed case of 53 Psc by our group puts (temporarily?) a new lower limit to spectral type and luminosity of the β CMa phenomenon.

If a large number of suspected β CMa variables belongs to a more extended region of the HR diagram reaching the main sequence (i.e. from O9 to B3 and luminosity classes V to II), the instability can no longer be assigned to a restricted evolutionary stage of the interior of the star (end of central core Hydrogen burning phase, subsequent gravitational contraction phase, beginning of Hydrogen shell burning phase). It then should probably be related to the envelope properties of these stars.

Bibliography

Balona, L.A. 1977, Mem. Roy. Astron. Soc. 84, 101.

Hill, G. 1967, Ap. J. Suppl. 14, 263.

Jerzykiewicz, M. 1975, Acta Astronomica 25, 81.

Percy, J.R. 1970, Ap. J. 159, 177.

Percy, J.R. 1971, Astron. J. 76, 1105.

Percy, J.R., Madore, K. 1972, Astron. J. 77, 381.

Sareyan, J.-P, Le Contel, J.-M., Ducatel, D., Valtier, J.-C. 1978, Astron. Astrophys., in press.

Shobbrook, R.R., Lomb, N.R. 1972, M.N.R.A.S. 156, 181.

Sterken, C., Jerzykiewicz, M. 1977, ESO Messenger 11, 5.

Williams, A. D. 1954, P.A.S.P. 66, 25 and 66, 88.

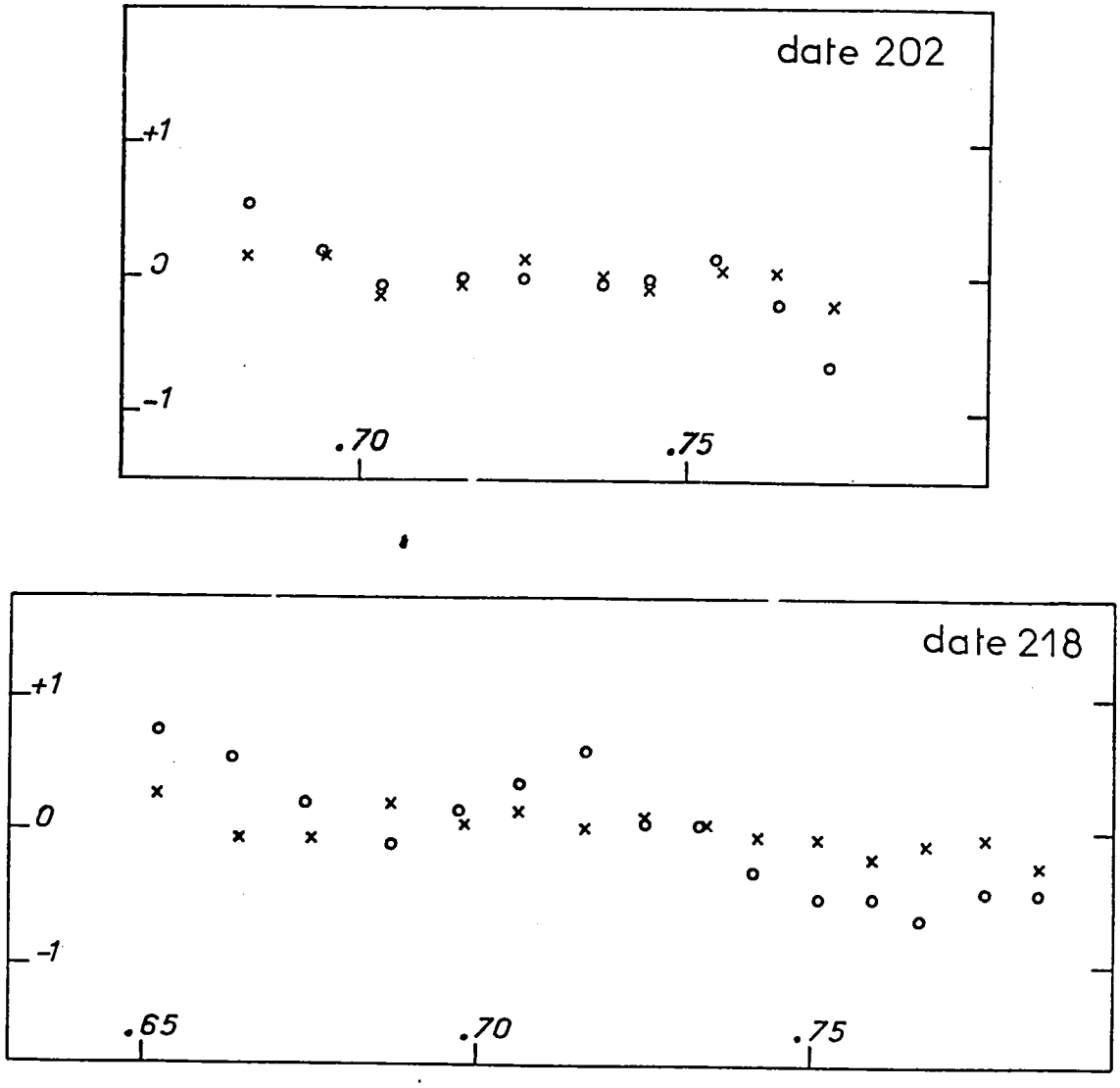

Figure 1. Light variations Δm (34 Psc- 53 Psc) in hundredths of magnitude versus fraction of heliocentric julian day on JD 2441202 and 218
Circles: UV filter Crosses: Blue filter

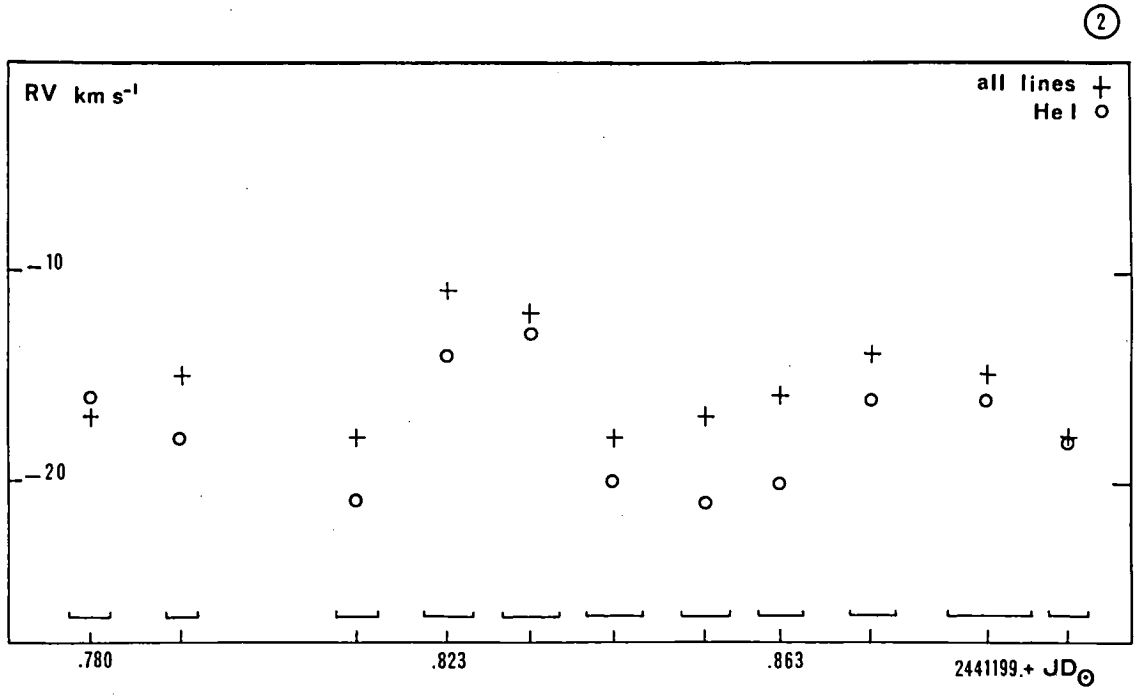

Figure 2. Radial velocity measurements. Brackets indicate the integration time for each plate.

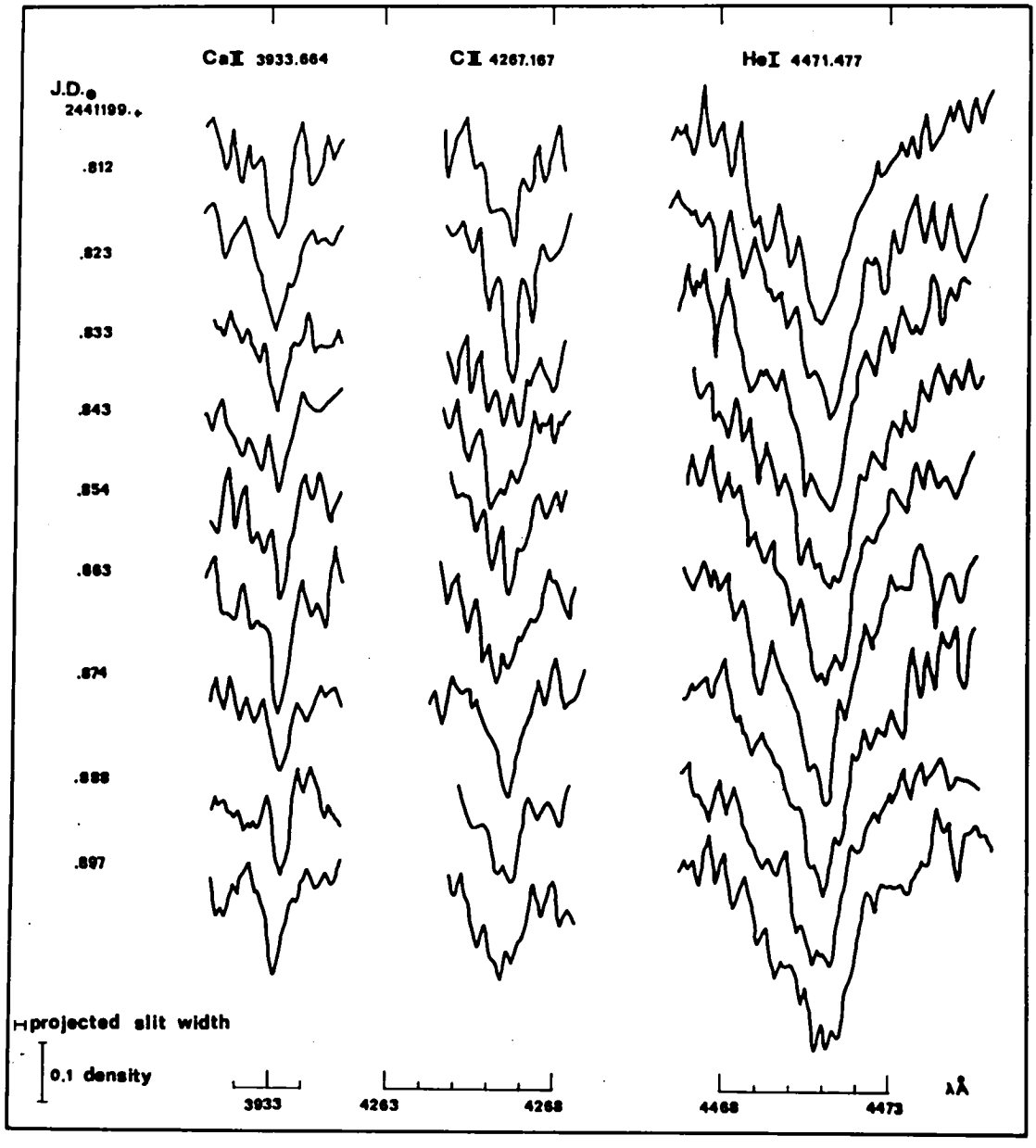

Figure 3. Tracings of K, C II doublets and He I (4471 Å) lines showing the variations of the shapes of the lines.

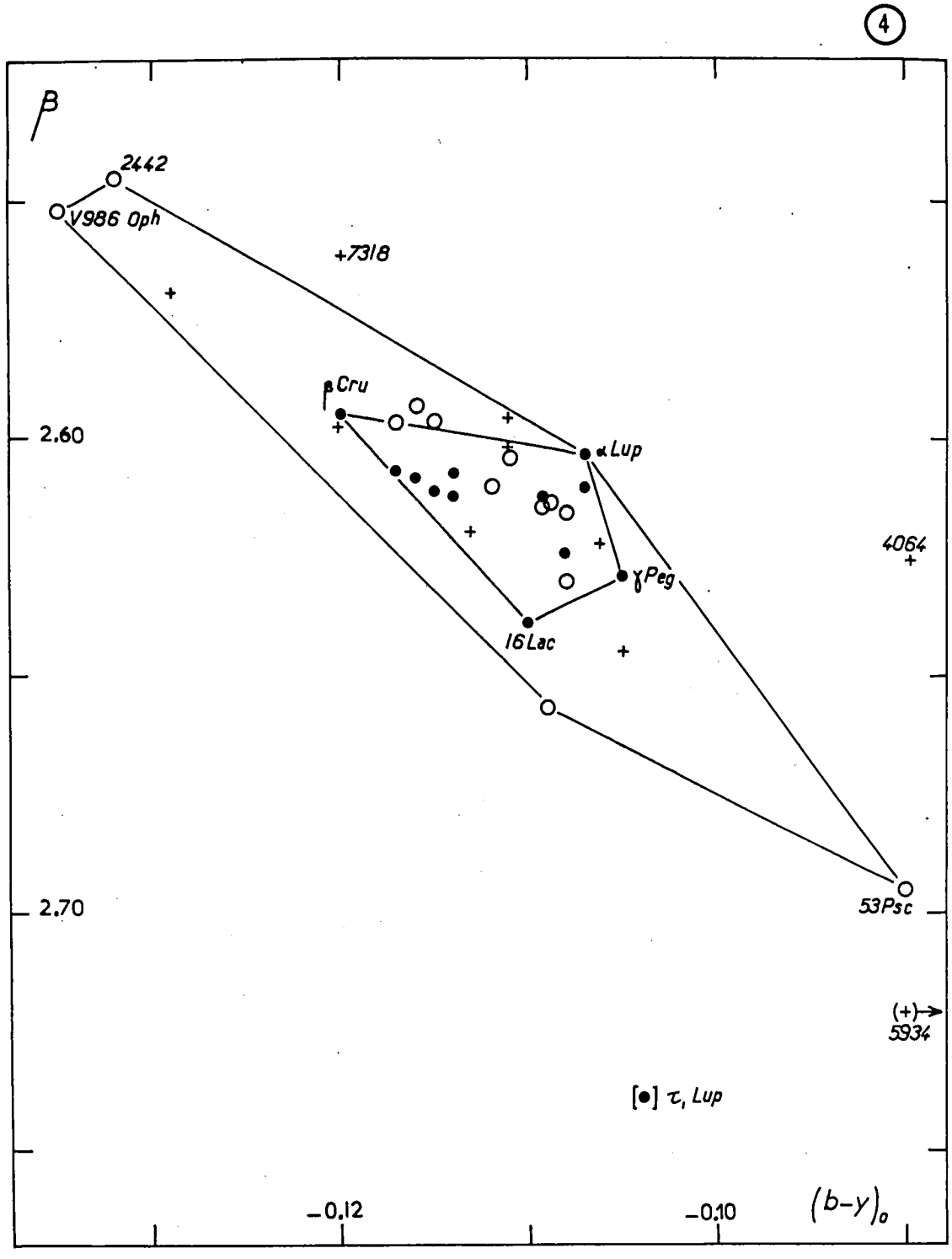

Figure 4. Positions of the β CMa stars in a β VS $(b-y)_o$ diagram; Dots are the classical β CMa stars, circles the more recent ones, and the crosses the suspected variables.

Discussion

Lesh: I have two comments. First of all, I didn't mean to be pedantic about the spectral type. The question is not whether it is a B2.5 or a B3, but whether or not it's on the main sequence. I believe that my classification is correct and that the star is not on the main sequence, but slightly above it. Although it is cooler than the stars that we normally call β Cephei or β Canis Majoris stars, this star does lie on the extension of the instability strip to lower temperatures.

Sareyan: From the uvby photometric classification, it seems that the star is really on the main sequence. [Ref. Fig. 4] On this diagram, I have plotted the previously known β Canis Majoris stars as dots, and the more recently discovered ones as circles. Here is the main sequence, here is class V and class III. 53 Psc is here.

Lesh: I have another question. Didn't Mike Jerzykiewicz also observe this star photometrically and find it to be constant in light?

Sareyan: Yes, but he didn't publish, for he didn't find any photometric variations.

Lesh: Exactly.

Sareyan: But he agreed with our photometric detection. We showed him our results and he said: "That's true. In your observations, it varies." The problem with β Canis Majoris stars is that the amplitude very often varies, so you can observe them for one or two nights and find no variations, and on another night, you find some.

Fernie: I didn't quite understand the scale on your first slide. What is the actual amplitude of the variation?

Sareyan: The actual amplitude in the ultraviolet, in a filter which is 100 Å wide and has an effective wavelength below the Balmer jump, is $0^m.01$ total amplitude on the night when we have good photometry. In the blue, the amplitude would be $0^m.002$ - $0^m.003$. Of course, this makes it very difficult to detect.

Aizenman: On this basis, would you definitely exclude an internal cause for the instability mechanism -- that is, one based on internal structure -- since you associate the instability with various phases of evolution?

Sareyan: The problem is that you and many other authors have tried to put some of these stars in a definite location in the H-R diagram, and we find β Cephei stars everywhere around the previous "box." So we have to find some mechanism which would not be connected with a particular evolutionary state.

THE LINE PROFILE VARIABLE B STARS

Myron A. Smith
Department of Astronomy and McDonald Observatory
The University of Texas at Austin, 78712

I. INTRODUCTION

I would like to summarize the observational status of a new and interesting group of stars which I have dubbed, not too imaginatively, the line profile variable B stars. These stars were apparently first recognized as a class by Petrie and Pearce (1962) in a survey of 570 B stars. In that study they called attention to "line width variations" in high dispersion photographic spectra of 14 early B stars. Since then there have been several reports of variability in studies of the spectra of 10 Lac, ζ Her, and 53 Pic (Grygar 1964, Chochol and Grygar 1974, 1976, Underhill 1966). However, given the low S/N and the low quantum efficiency of the photographic emulsion it has been difficult until recently to make quantitative statements about the profile activity.

The profile variables are of interest to the investigation of β Cephei variables because these B stars surround the β Cephei variables in the H-R diagram; many of the latter are themselves profile variables. I shall keep these two types of stars separate in this paper. It is an intriguing possibility that the β Cephei stars may actually represent only the most easily observed "tip of the iceberg" of a much larger class of variable stars.

II. RECENT HISTORY

My "rediscovery" of these variables dates from observations made in November of 1975 (Smith and Karp 1976) with the self scanned Digicon detector at the coudé focus of the 107-inch telescope at McDonald Observatory. The initial observations were made in two or three 100 Å-wide spectral regions. Each showed that lines of a number of different ions and elements showed the same changes in shape. Not surprisingly the variations are most visible in lines of heavy elements for which the thermal broadening is small.

The basic trait of these spectral variations is that the line profiles change their width and asymmetry with little accompanying change in radial velocity (line centroid).

In the last 1-1/2 years I have observed these variations with a resolution of 0.1 Å using two other spectroscopic instruments, the coudé scanner and, lately, (exclusively) the coudé Reticon. Both instruments give a resolution of 0.1 Å. I have also had varying degrees of success observing the variations with the 82-inch photographic coudé system, with the Copernicus satellite (U1 mode), and photometrically.

Figure 1 shows the known line profile variable stars and the distribution of "classical" β Cephei stars (Lesh

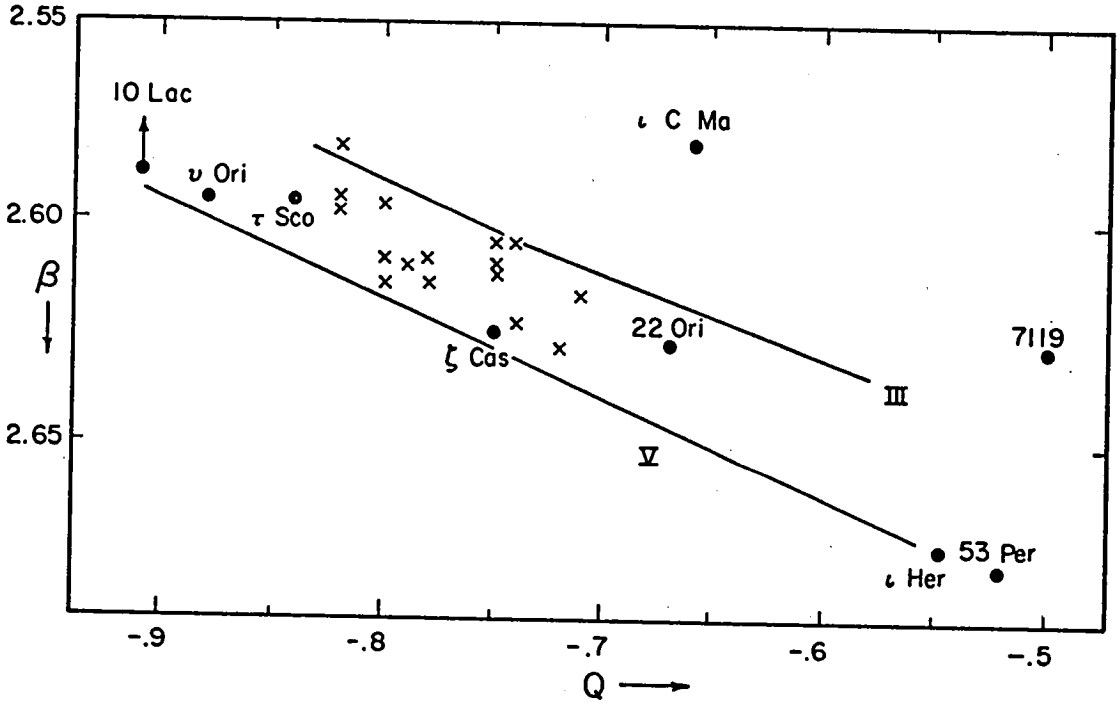

Figure 1: The β vs. Q photometric diagram for the bright, northern profile variables (except τ Sco). Crosses are known β Cephei stars.

and Aizenman 1973) in the narrow-band photometric β vs. Q diagram. The star λ Ori A may soon be added to the list, but this possibility needs to be confirmed carefully next season. All but two of the northern, sharp-lined (V_{rot} sin i < 50 km/sec) O8 to B5 stars, in luminosity classes V to II and brighter than m_v = 5 that I have investigated (Figure 1) show profile variations. The exceptions appear to be τ Sco and 3 Cen A. The latter is a Bp He-3 rich

star. So far the search has been restricted to the slow rotators because unless the amplitude of the profile changes were very large I could not detect them in rapid rotators.

Recently I searched for variability in the supergiants Rigel (B8 Ia) and Deneb (A2 Ia). So far it appears that any profile changes must be small if they are present. However, ρ Leo (B1 Ib) does appear to show variations.

III. EVOLUTIONARY STATUS

The masses of the profile variables appear to extend at least from 7 $M_\odot$ to 22 $M_\odot$ (Smith 1978) along the main sequence. Three of these stars, 10 Lac (Lac Ob Ib), 22 Ori (Ori Ia), and ν Ori (Ori Ic), are known members of clusters or young associations. Except for ν Ori, which is very young (Warren and Hesser 1978), even these stars are probably well evolved along the main sequence phase. On the other hand, at least four of the sample depicted in Figure 1 have photometric β indices typical of main sequence stars. Putting all these signs together certainly a reasonable statement is that profile variability occurs during both H core-burning and post H-exhaustion evolutionary phases.

IV. LINE PROFILE VARIATIONS

To observe the profile variations it is the usual procedure to monitor intermediate strength lines of a multiplet of a heavy ion for 1/2 to 1 hour. For B3 to B5 stars I observe the Si II $\lambda\lambda$4128, 4130 equal-strength doublet; for B0 to B2 stars, the Si III $\lambda\lambda$4552, 4567, 4574 triplet; for late O stars, the Si IV λ4654 line.

The accumulating data show that the profile variations are periodic and can be easily reproduced with models having traveling waves (nonradial pulsation). The observed periods are sufficiently long (5-15 hours) that they must be identified with g-modes, according to nonradial pulsation theory (e.g. Osaki 1975). Most if not all of the variables appear to change their pulsation amplitudes and periods on a timescale of a month or two. Such changes have probably been observed in progress three times thus far. Many periods have been observed to recur in individual stars, however, showing that period changes are not isolated events.

In order to produce profile variations without accompanying radial velocity changes one needs to vary a "macroturbulent" velocity field across the stellar disk in an ordered way. Struve (1955) first suggested rising and falling "prominences" on the surfaces of β Cephei stars.

Later Christy (1967) and Osaki (1971) showed that the spherical harmonic velocity distributions expected from the traveling wave modes of nonradial pulsation can produce large changes in line profiles. Smith (1977) showed that these velocity fields can actually be matched to observed profile changes in three β Cephei stars and to the largest changes in the profile variable B stars.

Figure 2 shows a progression of a modeled traveling wave cycle in terms of the distortion of the line profile.

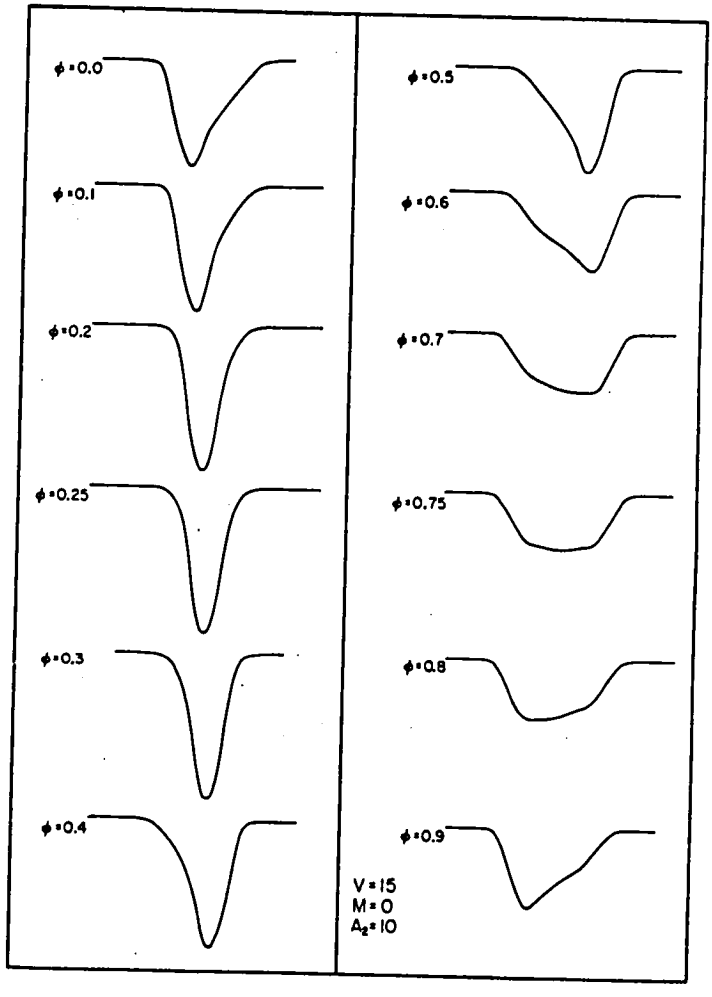

Figure 2: Progression of a model line profile with time through a traveling wave (ℓ = 2, m = -2) cycle.

A few clarifications about this diagram can be made:
1.) The profile distortions depend upon the interaction of the rotational and nonradial pulsational velocities. The distortions are always maximal when the two velocities are comparable.
2.) The retrograde modes (m > 0; traveling waves running azimuthally opposite to the sense of stellar rotation) can

be clearly distinguished from the direct modes. For retrograde modes the progression of phases depicted above runs backwards with time (cf. Figure 6, 22 Ori).
3.) The morphological changes shown are computed for a specific nonradial mode (ℓ = 2, m = -2). However, the changes often can be closely approximated by several other traveling wave modes of the same phase if one changes the velocity amplitude.
4.) If the profile variation is reasonably large a single observation fixes the phase. Therefore, unlike the case of radial velocity or light variability, a few profiles suffice to determine a period.

Statement 4 must be qualified by stating the important assumption that only one mode is visible at a time. In general I have invoked an "economy of assumptions" principle and fit the profiles to a single period if that is possible (it usually is). In the earliest data I often only had 5 to 7 observations per observing run in order to determine a pulsation period. The more typical recent figure is 12 to 18 observations, but this cannot always be maintained. As an experiment I have "withheld" a few profiles from the main data set. After determining a period and amplitude from this larger data set, one can predict model profiles for the withheld cases. The predicted profiles successfully match the "withheld" observed profiles (Smith 1978). This demonstrates the self-consistency of the periodic hypothesis. I have also deliberately switched two profiles in their time sequence and have then been unable to solve for a (false) period.

One can summarize the results from most of the profile modeling by stating that a direct, sectorial (m = -ℓ) mode seems to be required to fit the variations. Modes having $|m| < \ell$ produce radial velocity variations but negligible profile variations and are therefore unacceptable. The observed pulsational velocity amplitudes vary from a large (8 to 10 km/sec, 53 Per) to a small (3 to 4 km/sec) value, sometimes in a single star over a few months. For a typical S/N, spectral resolution, and number of profiles used in the observations (e.g. 200, 0.10 A, 12) the threshold pulsational amplitude is probably 2 to 3 km/sec. The phase resolution per observation, $\delta\phi$, is 0.03 to 0.05, depending on the data quality and velocity amplitude. Finally, I will add that in the best cases I might be able to discover a secondary mode but only if its amplitude were at least 1/3 that of the primary mode.

The observations are invariably fit best with traveling wave models in which local particles move primarily radially. This is surprising because nonradial theory predicts that material should move primarily horizontally in oscillations

of such long periods (Osaki 1971).

Examples --

Table 1 gives a summary of periods observed for six stars along with the numbers of observations used to derive them for several observing runs of 3 to 7 nights. The main point is that several periods are present at various times

TABLE 1

Summary of Useable Observations
on Several Line Profile Variables (May, 1978)

Star	Periods Observed (hrs.)	No. Runs/No. Profiles	Amplitude (km/sec)
53 Per	3.59*	1/5	8
	4.50:	1/3	12
	7.29(*)	2/4,5	9-12
	11.43	1/7	12
	14.6	2/8,8	7-10
		Total 6/35	
ι Her	4.92**	1/15	5
	9.92**	4/2,6,15,18	4-6
	13.92**	3/5,13,18	4
	15.4	1/17	4:
		Total 7/76	
10 Lac	4.88	4/4,5,15,5	4-10
	?	1/2	28
		Total 5/31	
22 Ori**	8.95**	3/8,4,11	5
	4.55**	2/5,11	
		Total 5/24	
η Ori	11.0	1/4 (1 cycle)	4
ζ Cas	21.5:	2/11,2	5
		Total 2/13	

GRAND TOTAL: 184 OBSERVATIONS

* Period once observed simultaneously with another.

** Mode observed changing to another mode.

but the most recently observed stars (ι Her, 10 Lac, 22 Ori) show frequently reoccurring periods. By far the most

recurrent period ratio is 2.0. Figures 3 through 8 show examples of profiles of the six profile variables modeled with a traveling wave solution (usually -m = ℓ = 2).

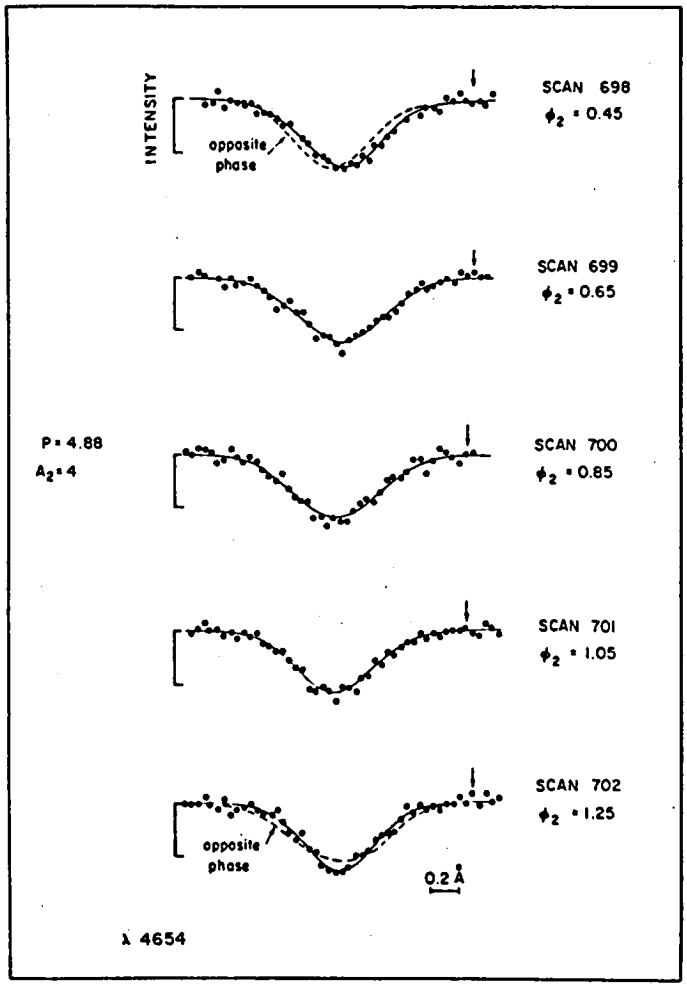

Figure 3: Contiguous observations of the λ4654 line of 10 Lac through a full pulsation cycle on Dec. 31, 1977. Solid and dotted lines indicate models of the nonradial pulsation profiles at the correct and opposite (for comparison) phases, resp. The indicated period and (small) amplitude are in hours and km/sec.

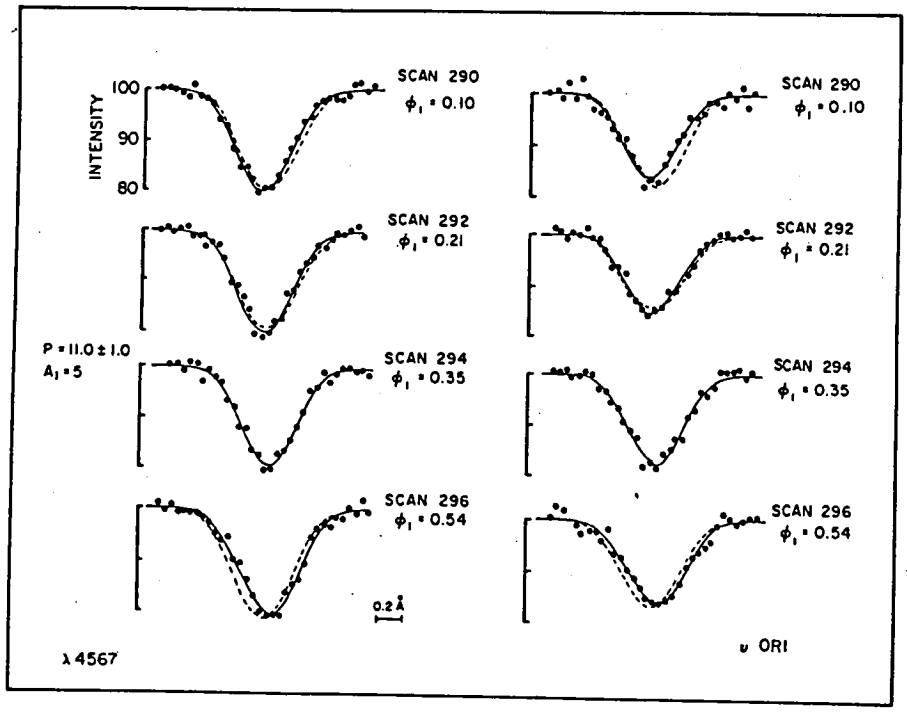

Figure 4: Observations of the 4552 and 4567 lines of the very young B0 star υ Ori during one night in December, 1976. On this and following diagrams the dashed line on selected profiles indicates the unperturbed profile that would occur if there were no pulsation.

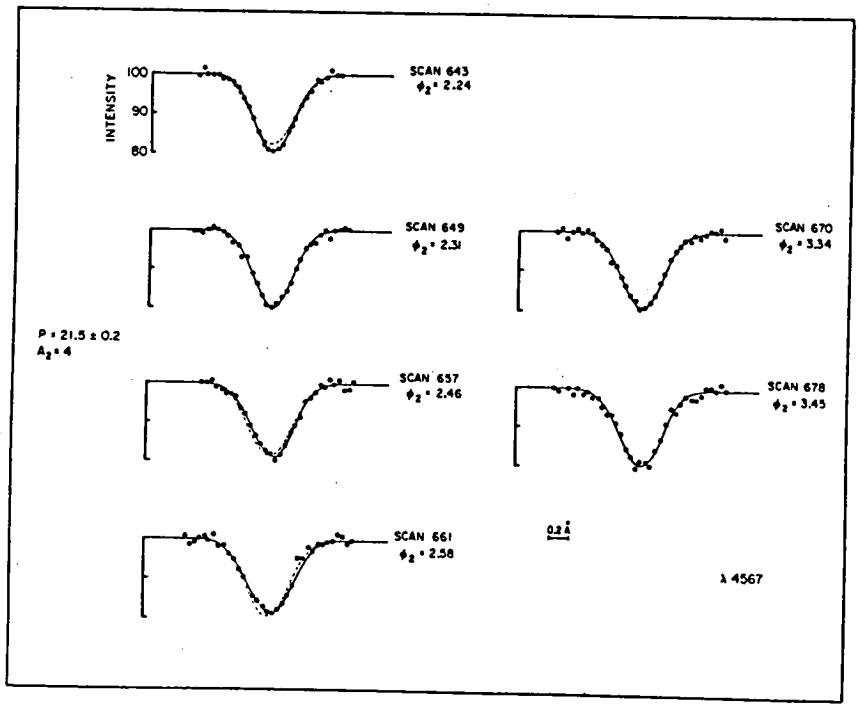

Figure 5: Observations and nonradial model fits to λ4567 of ζ Cas in August, 1977. Note the long period.

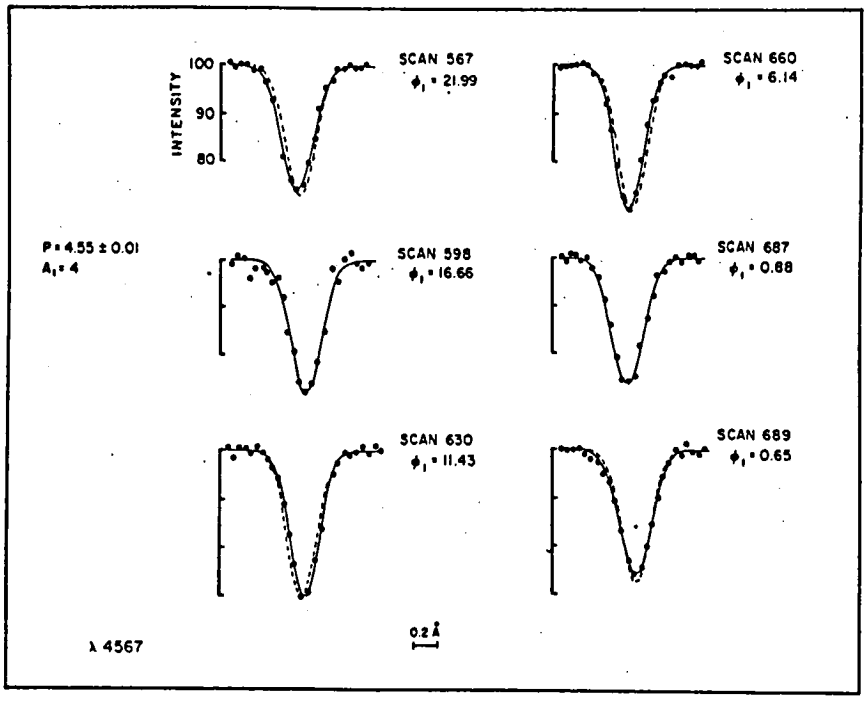

Figure 6: Observations and nonradial fits to λ4567 of 22 Ori in August, 1977. The reversed sequence of cycles indicates the presence of a retrograde mode.

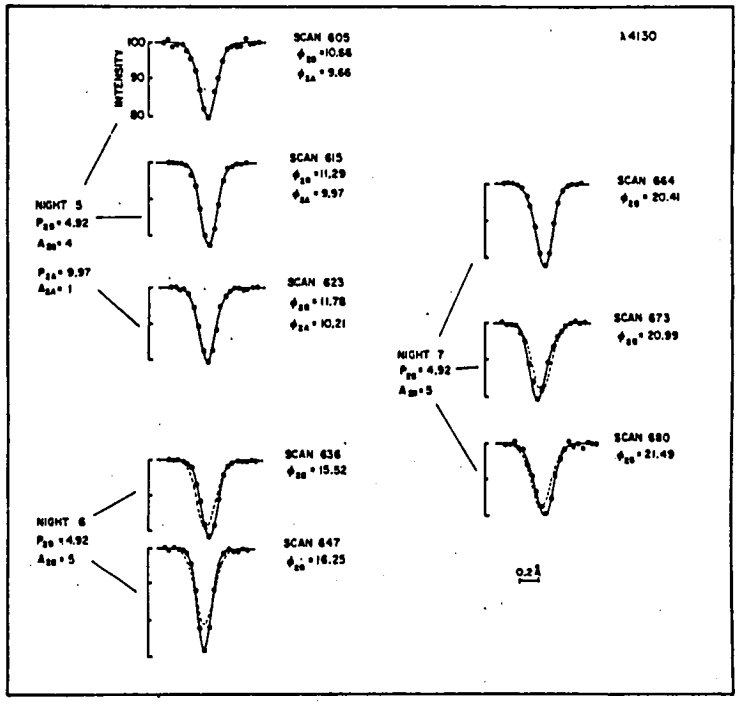

Figure 7: Observations and nonradial fits to 4130 of ζ Her during latter three nights of a run in August, 1977 (see Smith 1978).

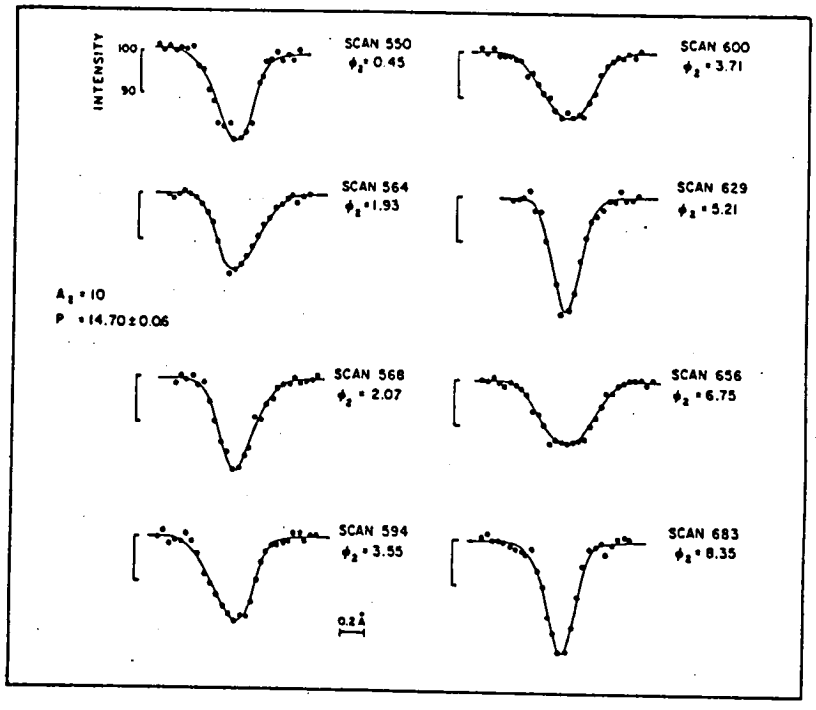

Figure 8: Observations and nonradial fits to λ4128 of the large amplitude variable 53 Per during August, 1977 (Smith and McCall 1978).

Estimates of the errors associated with the indicated periods and amplitudes can be found in Smith and McCall (1978) and Smith (1978). Two additional points of interest to note in these figures are the retrograde mode for 22 Ori (Figure 6) and the rather long period, 21 1/2 hrs., for ζ Cas (Figure 5).

V. LINE STRENGTH VARIATIONS

Because these stars are sharp-lined several of them, especially ι Her and 10 Lac, have been traditionally used as equivalent width standards in differential curve of growth analyses of other B stars. However, I wish to introduce a serious caution in their being put to this use. The metallic lines often vary in strength and this means the stars are not good standards. The amount by which they vary seems to be roughly proportional to the pulsational amplitude. The most extreme change found was a 100% variation in the strength of λ4654 in 10 Lac over two nights. Both 10 Lac and ι Her have occasionally shown 50% variations over a few nights. The variations during a particular cycle are certainly smaller, probably averaging 15 to 20% (assuming

line strengths of 50 to 70 mÅ (Smith 1978). Both the published and more recent unpublished data indicate that the strength variations correlate well with pulsation phase. The lines reach maximum and minimum strengths at phases near 0.65 and 0.15, respectively. Determining the detailed shape of the "line strength curve" in the future will be a worthwhile enterprise because it provides quasi-photometric information about the pulsation mode index ℓ that is complementary to what can be learned from the profile shapes. (This is because weak and strong line areas add linearly over the stellar disk, whereas opposite velocities occurring on different regions of the disk produce a smearing effect on the profile and do not cancel.)

Having also investigated the cause of the line strength variations, I have found (Smith 1978) that these changes cannot reasonably be caused by surface variations of temperature or gravity. At the same time, the strong lines do vary in strength proportionately more than the weak lines do. This is a clue that a "microturbulence" is present and that it increases at certain phases. Quantitatively, the required velocity is comparable to the atmospheric sound speed, if one assumes the $\ell = 2$ mode. Therefore, it is quite possible that we are witnessing the generation and propagation of shock waves at $\phi \sim 0.65$. Interestingly enough, this time corresponds to the phase during which atmospheric material in the wave is falling and compressing material below it.

VI. PHOTOMETRIC VARIATIONS

The question arises do the line profile variables also show light variations? Percy (1970) first showed that very small variations exist in a few of the Petrie-Pearce stars. However, he was unable to derive light curves or periods. Percy and Lane (1977) and Africano (1977) recently observed 53 Per for one and two nights, respectively. They each found peak to peak variations of 0.01 mag. Africano's obseryations were consistent with a 7.3 hr. period derived a few nights later from line profiles.

In an effort to add to our meager knowledge of the photometric behavior of these stars, Ron Buta observed 53 Per for several nights during November and December, 1977. As Figures 9 and 10 show, variations of several hundredths of a magnitude were the rule at these times. To complement this coverage I observed the λ4129 doublet photographically in this star on three nights in November (JD 2442466-8).

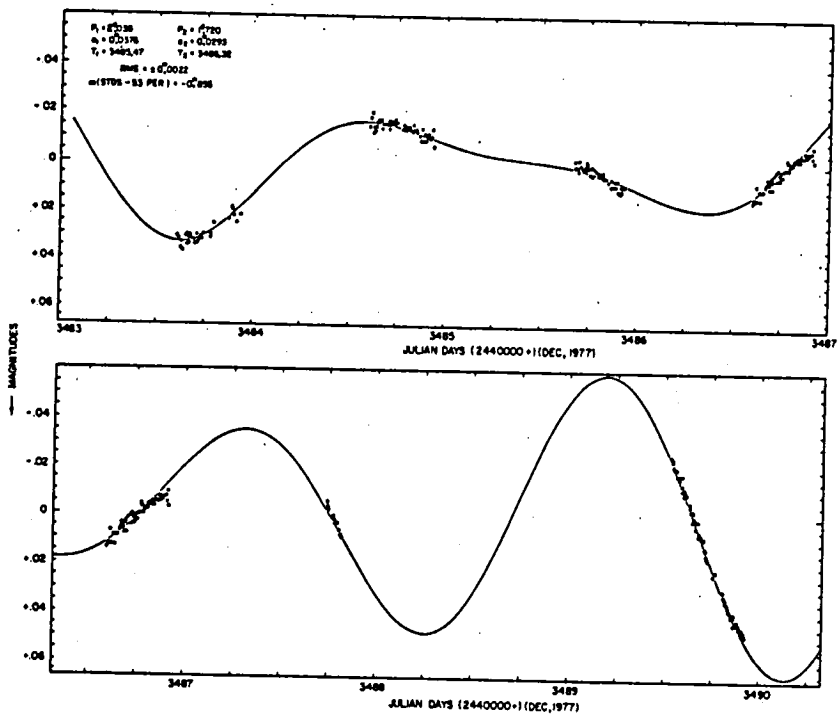

Figure 9: Light curve (Strömgren v-filter) of 53 Per obtained by Mr. Ron Buta in December, 1977. The solid line and indicated parameters apply to a two-sine curve fit to this data.

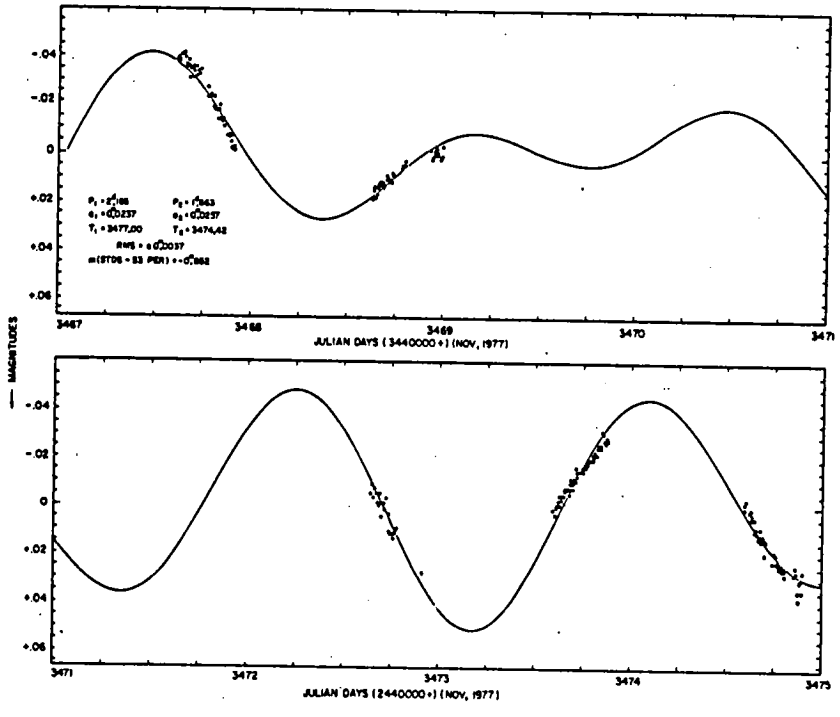

Figure 10: Buta's light curve for 53 Per in November, 1977.

These profiles and modeled fits are shown in Figure 11. Naturally the S/N is low here, but it seems to be sufficient

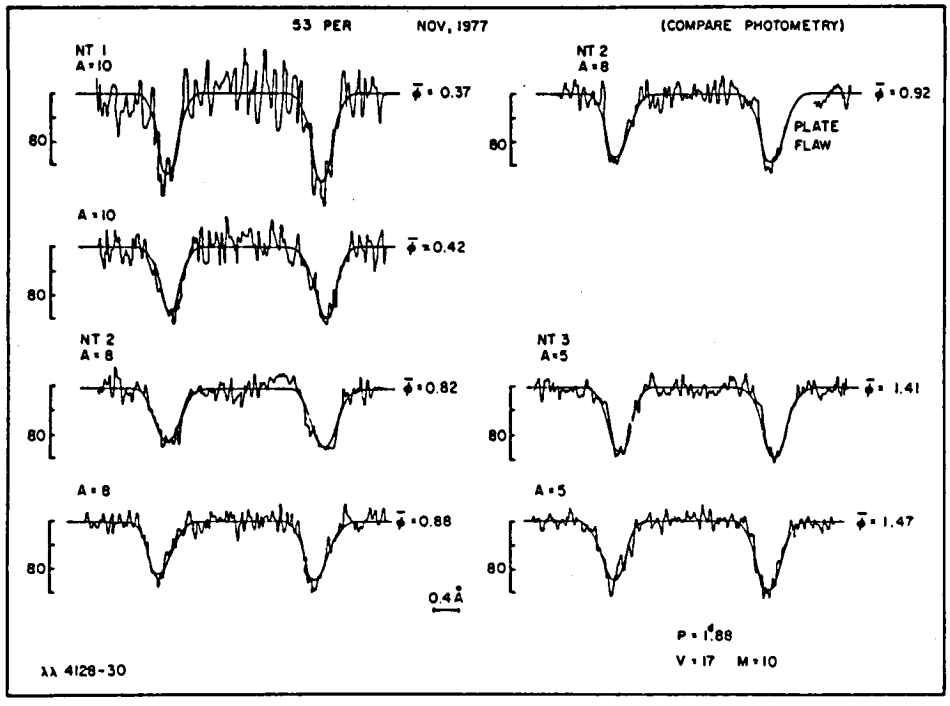

Figure 11: Photographic observations for the λλ4128-30 doublet in 53 Per obtained by the author on three nights in November, 1977. The latter two nights overlap with the first two nights of photometric coverage shown in Figure 10.

to show that a surprisingly long period of about 1.9 days was dominant at this time.

The modeling of Buta's photometric data on 53 Per has been investigated. Note first that phase reversals in both data sets occur near JD 2443469.5 and 2443485.3. Their appearance implies the interference of at least two modes. Therefore I have attempted to fit the photometric data sets independently with a minimum of two sine curves. The best solution in both cases is a pair of periods which average 1.87 ± 0.01 days. The two components are nearly of the same amplitude but differ in period by several percent. It should be added that I attempted to model the two data sets with many other pairs of periods, including those corresponding to "alias" peaks in the power spectra of the data. However, they did not allow a good solution.

The quality of the fit to the December data as shown in Figure 9 is remarkably good (r.m.s. is ±0.0022 mag.),

but it is wanting in the November observations (Figure 10). Perhaps a third mode is present in November. On the other hand the data span is so short that a truly credible solution is not possible. In fact, if it were not for the spectroscopic agreement in Figure 11 one could not be sure that either solution given in Figures 9 or 10 is even approximately correct. As it is the spectroscopy offers an important confirmation.

Two periods differing by a small amount have been observed in one other star, the white dwarf R548 (Robinson, Nather, and McGraw 1976). The existence of these periods has been convincingly ascribed by these authors to nonradial m-mode splitting. Such may be the case for 53 Per as well. If so, it would appear that a tesseral mode ($m < \ell$) can occur at least sometimes along with the sectorial mode.

Taken at face value, this 1.87 day period of 53 Per is interesting because it is about three times the 14.6 hour period observed at certain other times. (The multiples, 7.3 and 3.6 hour periods, have probably already been observed in 53 Per too.) This is intriguing because it is well known that subharmonics of $\omega/3$ occur commonly in nonlinearly oscillating systems. Perhaps there is an additional clue here that explains the period changes. For example, it may well be that like the large amplitude ZZ Ceti (DA) stars the line profile variable B stars are overdriven pulsators. Then their nonlinear character could serve as a starting point to build a description of the frequent period changes, especially those involving harmonic factors of two.

I wish to thank Fred Campos for his aid in the spectroscopic reductions and profile modeling. I am also indebted to Ron Buta and John Africano for permitting me to exhibit their superb photometric observations prior to their more complete description and publication. This work has been supported by N.S.F. Grant AST 77-06965 and N.A.S.A. Grant NSG-5167.

REFERENCES

Africano, J. 1977, I.A.U. Comm. 27 Info. Bull. Var. Stars, No. 1301.
Chochol, D., and Grygar, J. 1974, Bull. Astr. Inst. Czech., 25, 231.
_____. 1976, Bull. Astr. Inst. Czech., 27, 181.
Christy, R. F. 1967, A. J., 72, 293.
Grygar, J. 1964, Bull. Astr. Inst. Neth., 17, 305.
Lesh, J. R., and Aizenman, M. L. 1973, Astron. Astrophys., 22, 229.

Osaki, Y. 1971, Pub. A. S. J., 23, 485.
_____. 1975, Pub. A. S. J., 27, 237.
Percy, J. R. 1970, A. J., 75, 818.
Percy, J. R., and Lane, M. J. 1977, A. J., 82, 353.
Robinson, E. L., Nather, R. E., and McGraw, J. T. 1976, Ap. J., 210, 211.
Smith, M. A. 1977, Ap. J., 215, 574.
_____. 1978, Ap. J., 224, ---.
Smith, M. A., and McCall, M. L. 1978, Ap. J., 223, ---.
Smith, M. A., and Karp, A. H. 1976, Los Alamos Conf. on Solar and Stellar Pulsation, Aug. 3-5th, p. 289.
Struve, O. 1955, Ap. J., 122, 103.
Underhill, A. B. 1966, The Early Type Stars, (Dordrecht: D. Reidel Publ. Co.), pp. 258-9.
Warren, W. W., Jr., and Hesser, J. E. 1978, Ap. J. Suppl., 36, 497.

Discussion

J. Wood: Do you have any information on the wavelength dependence of the amplitude of the photometric variation, or was this all monochromatic? And what color was the light curve?

M. Smith: These were Stromgren v filter observations. We tried one or two quick tests on that which seemed to suggest it's almost flat, but it's too early to say yet. And according to nonradial theory, for this particular period, temperature-compression effects should dominate the two geometric effects. But we're going to go back and look into this a little more carefully this fall, to confirm or refute that tentative observational result.

J. Wood: So you wouldn't expect any depth dependence of maximum light?

M. Smith: No.

J. Cox: Can you determine a rational velocity from your period splitting?

M. Smith: If I do, the other Texas people, who do this work much more carefully, will laugh at me. It turns out the rotation velocity that I derive for 53 Per spectroscopically is 17 km/sec. And if you take the 13 days between the two phase reversals, you can infer a very accurate period difference. If you are foolhardy enough to play that game, you come up with surprisingly good agreement, and the implied inclination of the star is 60°. But you asked me -- I would never volunteer that otherwise.

Aizenman: Did you find any mode that you interpreted with m = + 2?

M. Smith: In one star, 22 Ori, there is always either a 9 or a 4.5 hour period. And in every case, the oscillation appears to be going backwards. Therefore, $m>0$, and probably $m \approx +\ell$, but that's all I can say. There also seems to be one β Cephei star which Struve discovered, that is doing this.

Aizenman: Then all the others would have negative values of m?

M. Smith: Exactly.

Shipman: Have you looked in this or any other star for a variation in the line ratios, like Si III/Si IV, to try to detect temprature changes over the cycle? I think you could do a pretty sensitive job on this.

M. Smith: I think so too, with this data. Some of the signal-to-noise ratios in this data, by the way, were as high as 700. So you certainly could do that. What I have found, are line strength changes that are correlated with the strengths of the lines, in the sense that a microturbulence would. Unfortunately, in the early B stars, lines of different ionizations are in different wavelength regions. And even though I'm getting 100Å coverage in an observation, that's not enough -- we'll have to wait for Bob Tull's "Octocon," with 800Å coverage.

PULSATION OF LATE B-TYPE STARS

W. R. Beardsley,* T. F. Worek,* and M. W. King*

Allegheny Observatory, Department of Physics and Astronomy,
University of Pittsburgh, Pittsburgh, PA

Three of the brightest stars in the Pleiades, Alcyone, Maia and Taygeta, were observed repeatedly for radial velocity throughout the course of one night, 25 October 1976. All three stars were discovered to be pulsating with periods of a few hours. Analysis of all published radial velocities for each star, covering more than 70 years and approximately 100,000 cycles, has established the value of the periods to eight decimal places, and demonstrated constancy of the periods. However, amplitudes of the radial velocity variations change over long time intervals, and changes in spectral line intensities are observed in phase with the pulsation. All three stars may also be members of binary systems.

INTRODUCTION

Three classes of short period variable stars have been intensively studied to date -- RR Lyrae stars, Beta Cephei stars and Delta Scuti stars. The existence of stars exhibiting short period variability but located on the H-R diagram between these classes seems virtually unknown.

Originally, Struve (1955) postulated an intermediate class of such stars which he designated as the Maia Sequence. This sequence was defined by Maia

*Visiting Astronomers, Kitt Peak National Observatory, which is operated by the Association of Universities for Research in Astronomy, Inc., under contract with the National Science Foundation.

(B7 III) at the bright end and by γ UMi (A3 II-III) at the faint end. No other stars were ever included in the sequence and Struve (Struve et al. 1957) later abandoned the sequence when he concluded that Maia did not show short period variability in either light or radial velocity. This investigation demonstrates that his conclusion is incorrect, at least with respect to radial velocity.

The existence of other stars quite similar to γ UMi such as Vega (Beardsley 1969) and θ Vir (Beardsley and Zizka 1977) suggests that the so-called Maia Sequence may not be invalid. Consequently, three bright member stars in the Pleiades were sampled by the authors at Kitt Peak National Observatory in a search for short period variation in radial velocity. The instrument used was the Coude' Feed (0.9m) telescope, dispersion 17 Å mm^{-1}. The Pleiades were chosen since it seemed likely that the suspect nature of Maia might properly implicate other Pleiades members as well. The three stars in the sample were Alcyone, Maia, and Taygeta.

All survey observations were obtained on the night of 25 October 1976. Baked 127 emulsion was employed together with suitable blocking filters. Since these stars are bright exposure times never exceeded 10 minutes and the spectra were all well exposed in the spectral region λλ3700 - 4400 Å. The plates were measured on a Grant engine with oscilloscopic display. Most lines, including hydrogen, displayed near Lorentzian profiles facilitating accurate setting. Every possible spectral line was measured except for obvious blends. Final velocities are based upon an average of about 20 stellar lines in the case of Maia, 15 in the case of Taygeta and 10 in the case of Alcyone. For each plate approximately 40 Fe-comparison lines were measured. The final radial velocity reduction employed a polynomial fit to

the comparison lines using a computer program entitled RSPEC (Worek 1977).

DETAILED SURVEY RESULTS

a) Alcyone, - Alcyone (25 Tauri, HD 23630) is the brightest member of the Pleiades cluster. Nothing of particular significance has been reported about this star. Radial-velocity observations show a scatter not considered unusual for a B-type star having fairly broad lines. The five radial velocities obtained on the survey night are plotted in Figure 1. The evidence suggests, though not convincingly, that a period of 0.27 day may exist. Early Allegheny Observatory observations (Beardsley 1969) were found to corroborate the 0.27-day period and it was possible to improve the period until all observations were included. The final period is 0.27118746 day,

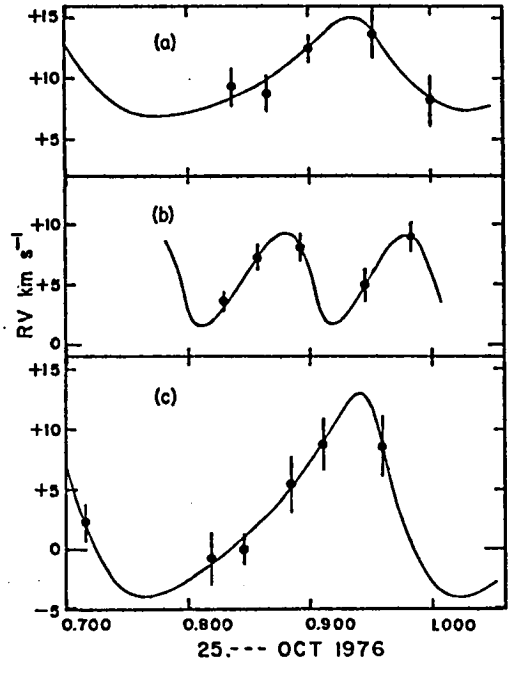

Fig. 1.--A plot of all the survey radial velocities obtained on the night of 25 October 1976. (a) denotes Alcyone, (b) denotes Maia, and (c) denotes Taygeta. Error bars represent standard error of the mean.

and Figure 2 represents a phase plot of all radial velocity observations since 1903 based upon this period. In forming this plot no systematic

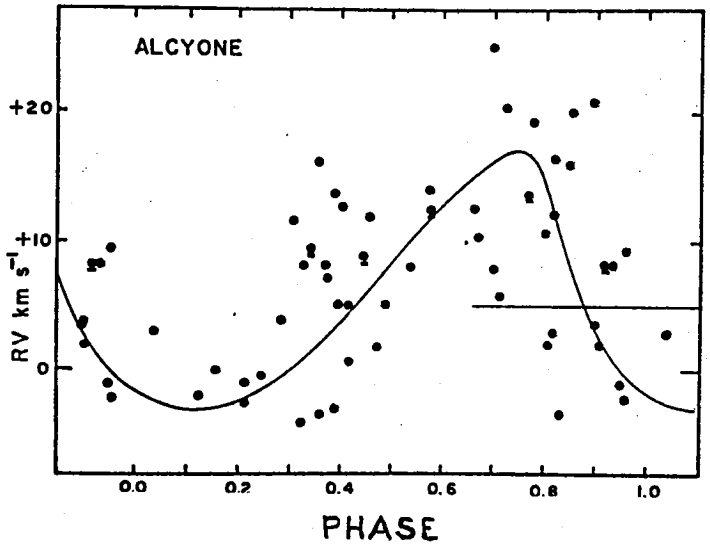

Fig. 2.--A phase plot of all published radial velocities since 1903 based upon a period of 0.27118746 day and beginning at JD2416418.475. Nearly 100,000 cycles are represented.

observatory corrections have been applied, obvious variations in amplitude over many years time have been neglected as well as possible variation of the systemic velocity due to binary motion with an as yet undetermined period. All act to introduce the observed scatter. Evidence of a possible standstill in the pulsation is suggested by the increased scatter at phase 0.4.

b) Maia, - Maia (20 Tauri, HD 23408), the fourth brightest cluster member, was originally suspected of pulsation-type radial velocity variation many years ago by Henroteau (1921) who suggested correctly that the period might be close to 2 hours. Radial velocity variation had previously been detected by Adams (1904) and studied intensively by Merrill (1914). Merrill was looking for binary motion but could reach no conclusion due to the unsuspected presence of the pulsation. Henroteau was searching for very

short-period binary motion and concluded that perhaps pulsation was present instead. Since each complicated the search for the other, it was not possible to define either. Struve et al. (1957) searched carefully for pulsation. Why it was not detected is unclear since the individual radial velocities remain unpublished. However, variations in the spectral line widths were detected which also suggested a period of about 2 hours.

Measurement of the six survey spectra obtained on the night of 25 October 1976 for radial velocity convincingly showed that pulsation was present with a period of about 0.10 day. These measures are also plotted in Figure 1. Figure 3 presents the observations of Henroteau for two of his five full-night series. Clearly apparent is the presence of the pulsation

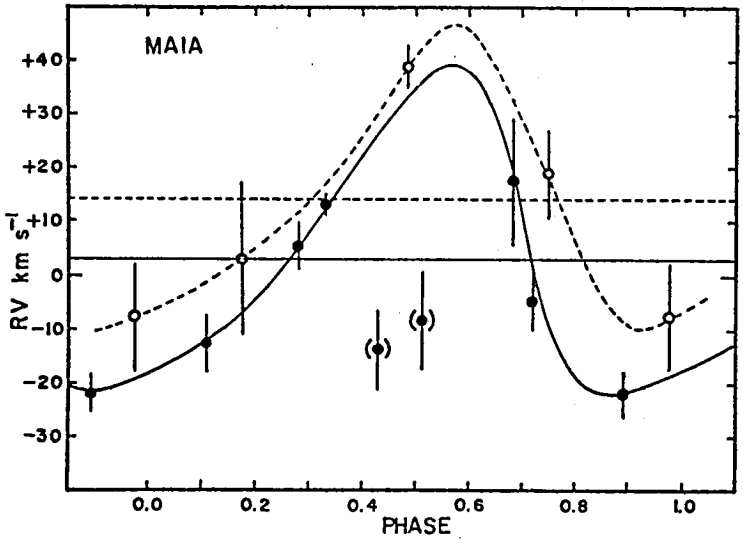

Fig. 3.--A phase plot of the published radial velocities by Henroteau obtained on two separate nights. Filled circles represent observations obtained on the night of 16 December 1919 and open circles the night of 16 August 1920. Note the strong shift in systemic velocity due to binary motion. The two rejected velocities at phases 0.4 and 0.5 are possibly the result of blending of separate shock wave component lines, one very positive and one very negative. A similar occurrence has been observed by the authors at about this phase for Taygeta.

and a variation in the systemic velocity as well, undoubtedly caused by binary motion. Note also the large variation in the pulsation amplitude between the 1919-20 and the 1976 epochs when compared with Figure 1. The period of pulsation has been determined to be 0.1032967 day. It has not been possible again to define the period of the binary motion. Consequently the velocities have not been combined into a single pulsation phase plot.

Changes in line widths have been noted in the Kitt Peak survey spectra as well as possible changes in excitation temperature. These changes vary in phase with the period with low excitation lines of FeII strong at times and high excitation lines of OII possibly present at other times. A quantitative study of this phenomenon is planned for a future time utilizing more suitable spectra obtained for this purpose.

c) Taygeta, - Taygeta (19 Tauri, HD 23338), the sixth brightest member of the cluster, has been utilized by Petrie (1953) as a standard star for a determination of B-star spectral-line wavelengths. Later, Abt (1965) suspected the presence of binary motion and presented tentative spectroscopic orbital elements but with expressed reservations. Six radial velocities were obtained for the survey night and a convincing pulsation variation was found to exist. These are also plotted in Figure 1 and indicate a period close to 0.27 day. A study of all published radial velocities suggests that the pulsation period is 0.2707795 day. A phase plot of the velocities based upon this period is presented in Figure 4. Again a variation in the systemic velocity due to apparent binary motion introduces scatter, and once again it is not possible to remove the binary motion until more reliable orbital elements can be obtained.

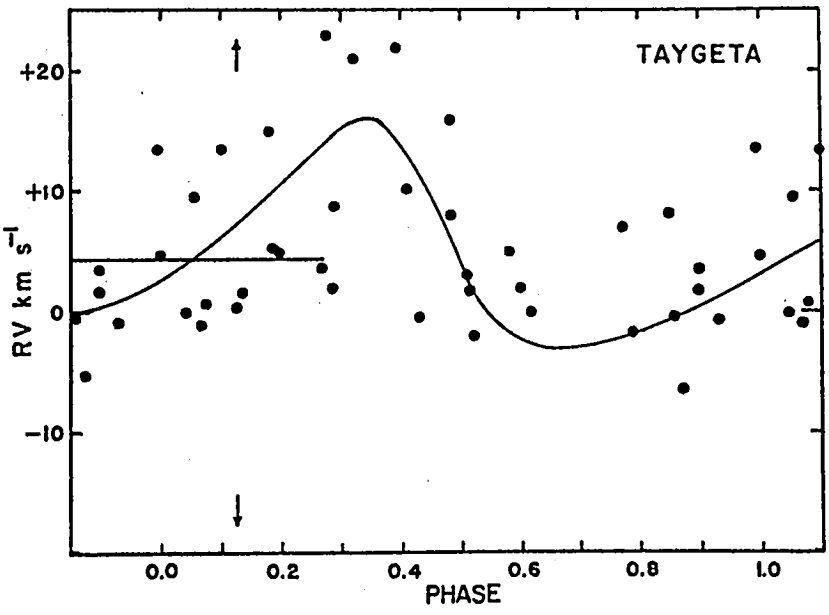

Fig. 4.--A phase plot of all published radial velocities of Taygeta since 1904 based on a period of 0.2707795 day beginning at JD2416503.475. The arrows refer to an observation obtained at the Allegheny on 12 October 1909. The lines on this plate appear double and possibly represent different shock wave components. The measured velocities are -49.6 km s^{-1} and 60.7 km s^{-1}.

Allegheny Observatory plate 3116 of this star, obtained on 12 October 1909 was originally measured for radial velocity by Stephen Thaw, and from this measurement a velocity of 40.5 km s^{-1} was derived (Beardsley 1969). Remeasurement of this plate by the authors revealed that the lines were in fact double, the velocities for which are presented in the figure caption above. The phase of this plate occurs at that point on the pulsation curve where a standstill might be suspected and the doubling may represent different shock wave components.

As in Maia, pronounced changes in line intensities and excitation temperature occur for this star in correlation with pulsation phase. These changes embody also the appearance and disappearance of low excitation Fe II

and high excitation O II lines and will be the subject of a future investigation.

CONCLUSION

The foregoing results, which are both new and unanticipated, suggest strongly that all three stars in the sample -- Alcyone, Maia and Taygeta, representing the brightest cluster members -- pulsate with well defined periods, constant over 100,000 cycles, and which have been determined to eight decimal places. The data also suggest that variations in velocity amplitude occur, and that spectral variations occur in phase with the velocity variation. Furthermore, these three stars are possible members of binary systems.

Note that in Figure 1 the peak velocity for both Alcyone and Taygeta occurs at nearly the same time. This coincidence raises a possibility that instrumental error has affected the velocities. During an observing run at Kitt Peak Observatory in March 1977 a strong series of Standard Velocity Star observations was obtained over the course of several nights. Results indicate that systematic differences in radial velocity were noted from night to night but that during each night these differences remained constant. This phenomenon will be investigated further but the authors are convinced that variation in velocity observed throughout the course of a single night may be considered real. Also the differing amplitude of velocity variation for each star serves to substantiate the non-instrumental nature of the results.

The implications of these results are many. For example: does the Pleiades cluster possess a very blue pulsation sequence, and if so does

there exist a cut-off position in the Cluster HR diagram or does this sequence blend into the δ Scuti region (see Breger 1975)? Do other clusters show this phenomenon as well and to what extent do early type field stars, excluding β Cepheids, also pulsate? Is this pulsation correlated with low rotation (most stars discussed here appear to have sharp lines) and is this pulsation correlated with cessation of hydrogen burning and recent evolution from the Main Sequence? Does the 25% helium content criterion for the onset of pulsation in the case of δ Scuti stars apply to these stars as well?

These are but a few possible questions these measures raise, but they suffice to indicate that the above pulsation discoveries point to an important new direction in observational astrophysics. Although no conclusive evidence is available as yet pro or con, it seems possible from the evidence presented that most, if not all, B-stars may be subject to pulsation. These observations will be continued.

The authors gratefully acknowledge the kind assistance and support of the staff of the Kitt Peak National Observatory, and also the support extended to one of us (WRB) by the Computer Center of the University of Pittsburgh.

REFERENCES

Abt, H. A., Barnes, R. C., Biggs, E. S. and Osmer, P. S. 1965. "The Frequency of Spectroscopic Binaries in the Pleiades," Ap. J., 142, 1604.

Adams, W. S. 1904. "The Radial Velocities of the Brighter Stars of the Pleiades," Ap. J., 19, 338.

Beardsley, W. R. 1969. "The Radial Velocities of 129 Stars in the Years 1906 to 1917," Pub. Allegheny O., 8, no. 7.

Beardsley, W. R. and Zizka, E. R. 1977. "Does the System Theta Virginus Represent a New Class of Pulsating Star?", Rev. Mexicana de Astron. y Astrof., 3, 109.

Breger, M. 1972. "Pulsating Variables in the Pleiades Cluster," Ap. J., 176, 367.

Henroteau, F. 1921. "A Spectrographic Study of Early Class B Stars," Pub. Dom. O., 5, 45.

Merrill, P. W. 1914. "The Radial Velocity of Maia," Pub. Univ. Michigan O., 1, 138.

Petrie, R. M. 1953. "Wavelength Standards for Radial-Velocity Determinations from B-Type Spectra," Pub. Dom. Ap. O., 9, 297.

Struve, O. 1955. "Some Unusual Short Period Variables," Sky and Telescope, 14, 461.

Struve, O., Sahada, J., Lynds, C. R. and Huang, S. S. 1957. "On the Spectrum and Brightness of Media (20c Tauri)," Ap. J., 125, 115.

Worek, T. F. 1977. "A Spectroscopic Orbit for the Subdwarf Mu Cassiopeia," M. S. Dissertation, Univ. of Pittsburgh.

Discussion

Schmidt: What are the spectral types of these stars?

Beardsley: Alcyone is a B6 giant, Maia is a B7 giant, and Taygeta is a B7 giant. Maia, of course, has a very sharp-lined spectrum and is very unusual, even for a giant.

A. Cox: Did you try to construct a periodogram to see if there were any other periods? I gather you based your period on your modern observations, and phased all the earlier observations. Did you try to see what other periods might exist?

Beardsley: No. These observations are much too embryonic to get involved in anything like that. We have to continue the observations. But obviously, we have a "standstill," so there must be something else involved.

Wesselink: I presume that all these stars are members of the Pleiades cluster, so you have a check on the gamma velocity of all your curves.

Beardsley: Yes, but one of the problems coming up at the next IAU meeting will be the question of standard velocity stars for B type stars. And I think the stars that ought to be proposed are the Pleiades stars. But to do so, we'll have to model out the pulsations and the binary motion, and then we can get very accurate radial velocities for the cluster itself.

Wesselink: In any case, the stars you have shown have the same gamma velocity.

Beardsley: Yes, very close. But I would say that right now our knowledge of the cluster velocity is very poor, on the basis of this work.

PULSATION OF SOME EARLY A-TYPE STARS

W.R.BEARDSLEY AND E.R.ZIZKA

Allegheny Observatory, Pittsburgh, Pennsylania, U.S.A.

Abstract. Analysis of the radial velocities of Alpha Lyrae, Theta Virginis, and Gamma Geminorum has shown that an ultrashort periodic variation is present. This variation can only be attributed to pulsation. These stars are of the earliest A-type and possess very sharp spectral lines.

A periodic variation of 0.19 day in the radial velocity of Alpha Lyrae was found by Belopolsky (Z.f. Astroph. 2, 245, 1931). This was emphatically disavowed by Neubauer (L.O.B. 17, 109, 193) even though some of his observations show abnormal scatter for such a sharp-line star. The scatter in the Allegheny series is considerable, but the observations clearly demonstrate that a periodic variation of 0.1903 day is present. The fact that the variation is still apparent after 370 cycles seems to be significant.

The radial velocity of Theta Virginis A has revealed that a periodic variation of 0.152360±0.000001 day is superimposed on an orbital variation with a period of approximately 13 years. The ultrashort variation seems to be constant for more than 29,000 cycles. A possible standstill is seen at the midpoint of the slow rise to maximum positive velocity and it occurs, as one would expect, at the maximum radius of the star.

Recently, Gamma Geminorum has been investigated for the possibility of possessing an ultrashort periodic variation. A remeasured set of Allegheny spectra over a very short time interval shows that a variation of 0.13 day is present. This star also has a well known orbital variation of 12.4 years.

THE PULSATING WHITE DWARFS

Edward L. Robinson
Department of Astronomy and McDonald Observatory
The University of Texas at Austin

The idea that white dwarfs could be pulsationally unstable is far from new. As early as 1949 Sauvenier-Goffin (1949) calculated pulsation periods of cold, non-relativistic white dwarfs. Between 1960 and 1970 a large number of theoretical investigations of white dwarf pulsations appeared in print using increasingly realistic and increasingly complicated models for the white dwarfs (c.f. Ostriker 1971). With very few exceptions (e.g. Harper and Rose 1970) these investigations, which were made in an observational vacuum, assumed that the most likely pulsations to be excited were radial pulsations. Thus, the calculated periods were quite short, typically 2-10 sec. The first of the pulsating white dwarfs to be discovered was HL Tau-76 (Landolt 1968). A portion of the light curve is shown in Figure 1. As so often happens, the universe refused to heed our preconceived ideas. The typical interval between successive pulses in the light curve is about 750 sec, not 2-10 sec. This gross discrepancy exists for all of the variable white dwarfs discovered since HL Tau-76, and raises a number of questions. Which white dwarfs are variable? Are the variables otherwise normal white dwarfs or are they pathological in other ways as well? Are the variations actually caused by pulsations, and if so, why are the periods so long? The observational data gives unequivocal answers to these questions. The variable white dwarfs are normal, single, DA white dwarfs.

The variations are caused by pulsations, but the pulsations are non-radial rather than radial pulsations. The purpose of this paper is to summarize the data which lead to these conclusions.

A total of 12 variable white dwarfs has now been found. They are listed in Table 1 along with their spectral types, UBV colors and magnitudes, and references to the discovery paper. The colors and magnitudes have been extracted from the series of papers by Eggen and Greenstein (Eggen 1968, 1969; Eggen and Greenstein 1965; Greenstein 1969). Three white dwarfs have been reported to be variable but are not included in Table 1. According to Richer and Ulrych (1974) G169-34 varies with a period of 465 sec. We have observed this star on several occasions, but it was always constant (McGraw and Robinson 1976). Either the star has changed its properties or the variations seen by Richer and Ulrych were spurious. Hesser et al. (1976b) have given a preliminary report of variations in LFT 1679. Since the data have not yet been published and since Hesser et al. suggest that the variations were caused by eclipses, we have temporarily

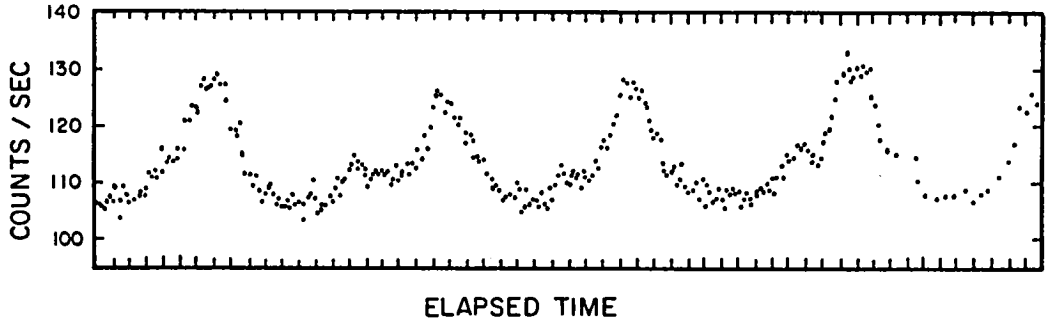

Figure 1. The light curve of HL Tau-76 on 1969 February 16 (from Warner and Nather 1970). Each point is the mean counting rate averaged over 10 seconds. The abscissa marks are minutes.

TABLE 1

THE VARIABLE WHITE DWARFS

STAR	Sp.	V	B-V	U-B	Ref.
BPM 30551	DA	15.26	+0.29	-0.58	1,2
R548	DA	14.10	+0.20	-0.54	3
BPM 31594	DA	15.03	+0.21	-0.66	4
HL Tau-76	DA	14.97	+0.20	-0.50	5
G38-29	DAs	15.63	+0.16	-0.53	6
GD 99	DA	14.55	+0.19	-0.59	7
G117 - B15A	DA	15.52	+0.20	-0.56	7,12
GD 154	DA	15.33	+0.18	-0.59	8
L19-2	DA	13.75	+0.25	-0.53	2,9
R808	DA	14.36	+0.17	-0.56	7
G207-9	DAn	14.64	+0.17	-0.60	10
G29-38	DA	13.10	+0.20	-0.65	11

REFERENCES

1) Hesser et al. (1976a)
2) McGraw (1977)
3) Lasker and Hesser (1971)
4) McGraw (1976)
5) Landolt (1968)
6) McGraw and Robinson (1975)
7) McGraw and Robinson (1976)
8) Robinson et al. (1978)
9) Hesser et al. (1977)
10) Robinson and McGraw (1976)
11) Shulov and Kopatskaya (1973)
12) Richer and Ulrych (1974)

excluded LFT 1679 from Table 1. G44-32 has been reported to be variable three times. In appendix A we give our reasons for believing that this star in fact is non-variable. Lists of non-variable white dwarfs are scattered throughout the literature. References to all of the published lists are given in Table 2.

TABLE 2

PUBLISHED LISTS OF NON-VARIABLE WHITE DWARFS

Hesser and Lasker 1971
Hesser and Lasker 1972
Hesser et al. 1969
Lawrence et al. 1967
McGraw 1976
McGraw 1977
Robinson and McGraw 1976
Robinson et al. 1978
Richer and Ulrych 1974

Two characteristics of the variable white dwarfs are immediately evident from Table 1: all are DA white dwarfs, and all have colors near B-V = +0.20. Figure 2 is the color-color diagram for all of the white dwarfs which have been examined for variability and have published colors. The filled triangles represent the variable white dwarfs, and the remaining symbols, which are explained in the figure caption, represent the non-variable white dwarfs. The variable white dwarfs occupy a narrow instability strip lying between B-V colors of +0.16 and +0.29. The restricted range of colors and spectral types of the variables cannot be attributed to selection effects. A total of 136 constant white dwarfs are listed in the references given in Table 2. Of the non-variables, 60 have colors outside the limits of the instability strip; 25 have spectral types other than DA; and 34 are white dwarfs with unknown spectral types. Two of the variables, GD 154 and BPM 31594, had unknown spectral types when their variability was first detected and only afterwards were found to have DA spectra. The DA spectral type shows that a white dwarf must have hydrogen in its atmosphere in order to be variable. The exact placement of the instability strip emphasizes the importance of hydrogen. The solid line in Figure 2 is the locus of the DA white dwarfs with log g = 8 (Terashita and Matsushima 1969). The dip in the line near B-V = +0.20 is caused by a maximum in the Balmer line and continuum absorption. The variable white dwarfs cluster near this region where the Balmer absorption is strongest.

A third characteristic of the variables is that, although only 12 are known, they must be considered to be very common. Among the DA white dwarfs which have been examined for variability, there are 12 variables and 37 non-variables within the instability strip. Thus, about 25 percent of the DA white dwarfs in the instability strip are variables. This must be a lower limit for two reasons. First, variations with

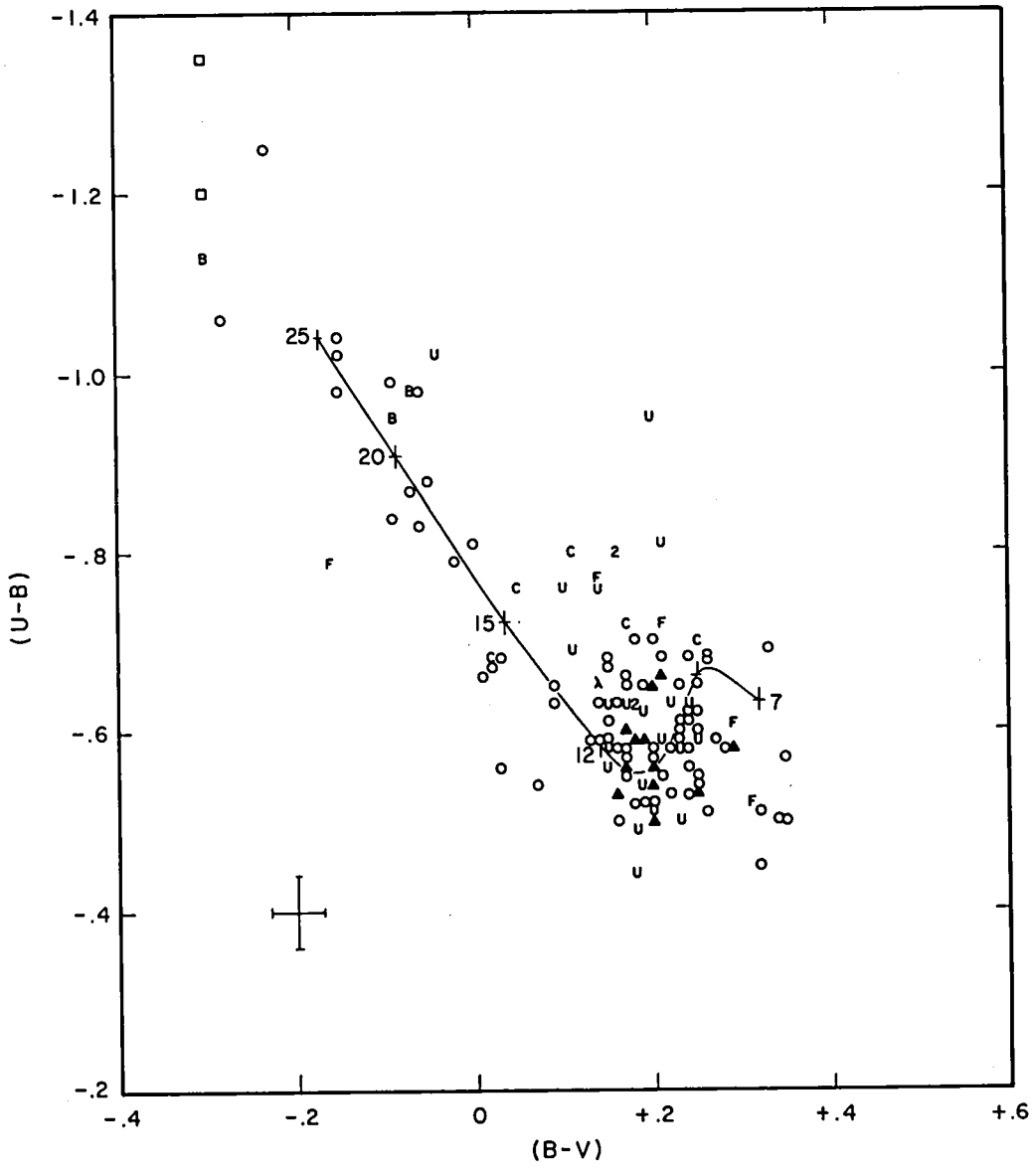

Figure 2. The Johnson two-color diagram for white dwarfs investigated for rapid luminosity variations. The variables are represented by filled triangles. The other symbols represent non-variable white dwarfs of different spectral types: DA stars are open circles; B is a DB star; C a DC star; 2 a C_2 star; λ a λ4671 star; F a DF star; DO stars are open boxes; U is a star with unknown spectral type. Typical uncertainties for the colors are shown by the crossed error bars. The solid curve is the locus of the DA sequence for Log g = 8 from Terashita and Matsushima (1969).

amplitudes less than 0.02 mag are difficult to detect in stars as faint as white dwarfs. Some of the non-variables could actually be low amplitude variables. Second, the measured width of the instability strip, 0.13 in B-V, is probably greater than the true width because the observational error in B-V is at least ± 0.03 mag. It is not possible to argue that all of the stars in the instability strip are variable, however. At least half, and possibly three quarters of the DA white dwarfs in the instability strip are non-variables. The solid line in Figure 2 is also the cooling sequence for DA white dwarfs. The cooling sequence passes through the instability strip. Since every DA white dwarf travels down the cooling sequence and must eventually traverse the instability strip, our statistics indicate that at least one quarter of <u>all</u> white dwarfs have been or will become variables. The ubiquity of the variables has an important impact on the

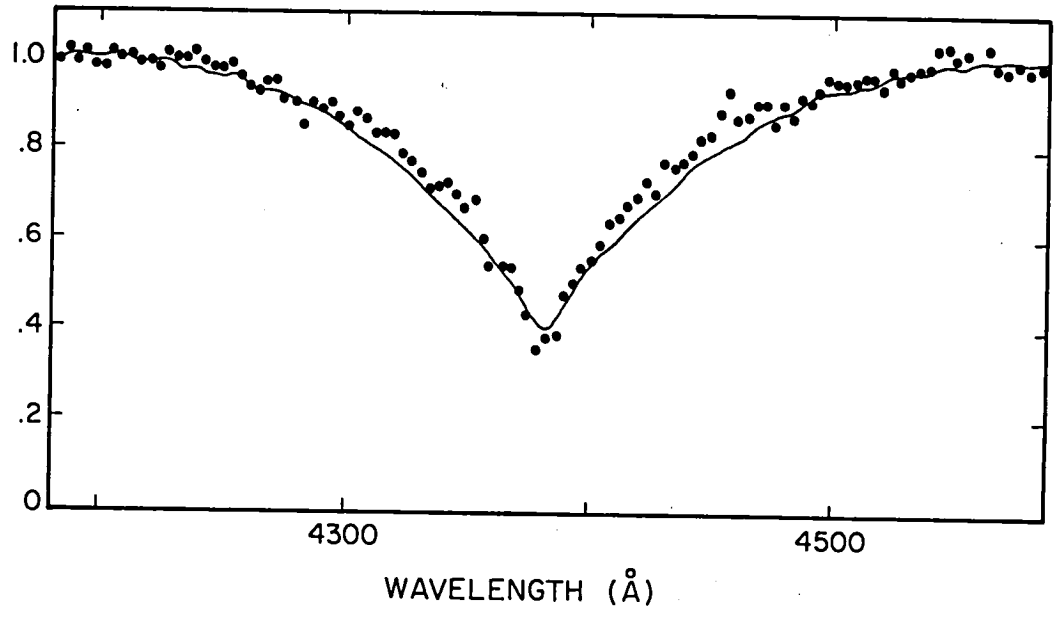

<u>Figure 3</u>. The Hγ line profiles of GD 154 and the DA white dwarf L47. That of GD 154 is shown by the dots, and that of L47 is shown by the solid line.

choice of physical mechanisms for producing the variations: it is inappropriate to invoke low probability or exceptional mechanisms of any kind.

A fourth characteristic of the variables is that, beyond the obvious fact of their variability, they are quite normal and completely indistinquishable from the non-variable white dwarfs. Figure 2 demonstrates that their colors are typical of DA white dwarfs. Figure 3 compares the Hγ line profile of GD 154 to that of L47, a non-variable DA white dwarf with B-V = +0.08. The spectra were obtained with the Tull Digicon spectrograph under identical conditions and may be directly compared. The line profile of GD 154 is slightly narrower and deeper than that of L47, but the difference is consistent with the slight difference in their colors. Thus, the spectrum of GD 154 is normal. Trigonometric parallaxes have been measured for 5 of the variables. They are listed in Table 3 along with the derived absolute visual magnitudes. The mean absolute magnitude of the group is 11.7 ± .2. A similar

TABLE 3

ABSOLUTE MAGNITUDES OF THE VARIABLE WHITE DWARFS

STAR	PARALLAX	ERROR	REFERENCE	M_V
R548	.014	.002	(1)	9.8 ± .3
G38-29	.013	.004	(2)	11.2 ± .8
R808	.034	.005	(2)	12.1 ± .3
G207-9	.030	.004	(3)	12.0 ± .3
G29-38	.071	.004	(4)	12.4 ± .2
			Weighted Average	11.7 ± .2

REFERENCES

1) Dahn et al. (1976)
2) Routly (1972)
3) Harrington et al. (1975)
4) Riddle (1970)

exercise for the non-variable DA white dwarfs with similar colors listed in the McCook and Sion catalogue (1977) yields $M_V = 12.5 \pm .2$. The variables seem to be slightly brighter than the non-variables, but since their mean magnitude is heavily biased by the unusual parallax of just one variable, R548, the difference is of only marginal significance. The most accurate way to estimate the effective temperatures and gravities of DA white dwarfs is by measuring their colors in the Strömgren uvby system. The Strömgren colors of 10 of the variable white dwarfs have been measured by McGraw and Wegner (McGraw 1978) and are listed in Table 4. The colors are time averages since the colors vary as the luminosity varies. The corresponding effective temperatures and gravities are also given in Table 4 and have been derived by comparing the colors to the theoretical colors of DA white dwarfs calculated by Wickramasinghe and Strittmatter (1972). The effective temperatures range from about 10,500°K to 13,500°K and log g ranges

TABLE 4

THE EFFECTIVE GRAVITIES AND TEMPERATURES
OF THE VARIABLE WHITE DWARFS

STAR	b-y	u-b	T_e	Log g
R548	.036	.686	12550±150	7.77±.02
HL Tau-76	.033	.634	13010±350	7.94±.02
G38-29	.063	.678	11900±1000	7.9 ±.4
GD99	.035	.587	13350±1000	8.1 ±.4
G117-B15A	.032	.556	13640±350	8.14±.05
R808	.078	.655	11730±250	7.98±.05
G29-38	.060	.614	12630±150	8.14±.02
BPM 30551	.122	.628	10315±400	7.79±.15
BPM 31594	.028	.665	12870±400	7.80±.25
L19-2	.071	.598	12520±400	8.24±.25

from about 7.8 to 8.1. None of these values is unusual for DA white dwarfs. The finite spread in the temperatures and gravities is real and not due to observational error. As a by-product of this study, McGraw was able to show that changes in the effective temperature are sufficient to account completely for the luminosity changes of the variables. This agrees with the earlier study by Warner and Nather (1972). Thus, the variables have normal colors, spectra, temperatures, and gravities. In addition, Angel (1978) was unable to detect any magnetic field in two of the variables, R548 and HL Tau-76; and Robinson and McGraw (1977) have shown that the space motions of the variables are undistinquished.

From their normality, we conclude that most of the variables are isolated, unperturbed white dwarfs. In particular, they are not all members of close binary systems. Any companion of the variables must be too faint to alter their absolute magnitudes or spectra. This is not possible unless the companion is either a similar DA white dwarf or is at least 2 magnitudes fainter than a white dwarf. In short, the companion must be invisible when next to a DA white dwarf. It is not impossible and perhaps even likely that a few of the variables have close, invisible companions (e.g. Fitch 1973). However, we have shown that the variables are very common. The probability that more than one quarter of all white dwarfs have invisible companions would appear vanishingly small.

We will now consider the variations themselves. McGraw will give a detailed account of the properties of the variations in an accompanying paper, so we will only give a short summary of the properties here. The light curve of each star has a characteristic peak-to-peak amplitude which ranges from about 0.02 mag to 0.34 mag among the known variables. The light curve of R548 in unfiltered light is shown in Figure 4. The amplitude of the variations is about 0.02 mag., the lowest

of the known variables, and the time scale of the variations is about 220 sec. Figure 5 shows power spectra of the light curve of R548 on three successive nights in 1975. At first sight two, but only two, periods are present in the light curve, one near 213 sec and one near 274 sec. Each period varies considerably in amplitude and slightly in period. A detailed analysis of the light curve demonstrates that there are four, not two, periods present (Robinson et al. 1976). Each of the two periods shown in Figure 5 is a pair of sinusoidal variations with periods so close that they are not resolved in the power spectra. Stover et al. (1978) find the periods to be

$$P_1 = 212.76840$$
$$P_2 = 213.13258$$
$$P_3 = 274.25081$$
$$P_4 = 274.77432,$$

with formal errors of about ± 2 in the least significant figure. The changes in the amplitudes and periods of the two spikes in the power spectra are due only to beating between the close pairs. These four periods reproduce the variations of R548 with an accuracy of ± 0.001 mag in amplitude and ± 10 sec in time for an interval of more than one year. The most

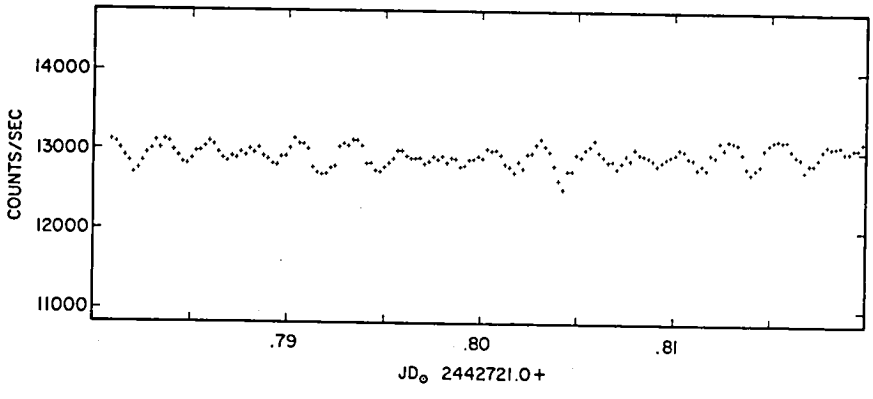

Figure 4. A portion of the light curve of R548. Each point is a 20 sec average of the photon counting rate.

notable feature of the light curve is the remarkable stability of the periods. Stover et al. (1978) give an upper limit of $|\dot{P}| < 10^{-11}$ for any period changes. For comparison, the rate of change of the period of the 71 sec variation of DQ Her is $|\dot{P}| \sim 10^{-12}$ (Patterson et al. 1978).

The light curves of G29-38 and G38-29 in unfiltered light are shown in Figure 6 and are typical of the light curves of the large amplitude variables. The peak-to-peak amplitude of the variations is about 0.21 mag in G38-29 and about 0.28 mag in G29-38. The individual pulses are highly variable in shape, but typically are asymmetric with a more rapid rise than decay. The mean interval between pulses is about 850 sec, but the

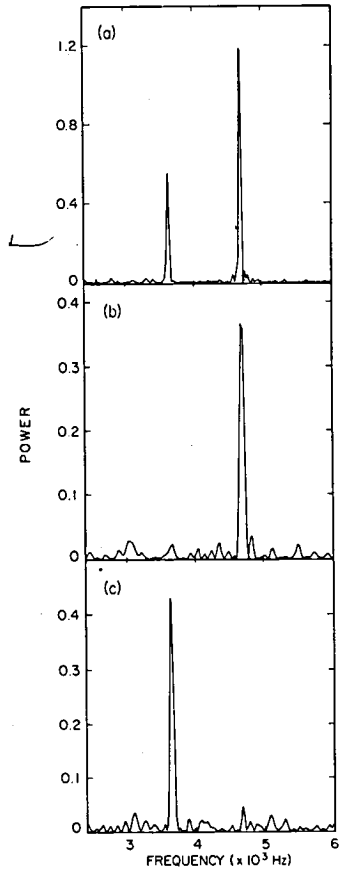

Figure 5. Power spectra of the light curve of R548 on UT dates (a) 1975 October 6, (b) 1975 October 7, and (c) 1975 October 8.

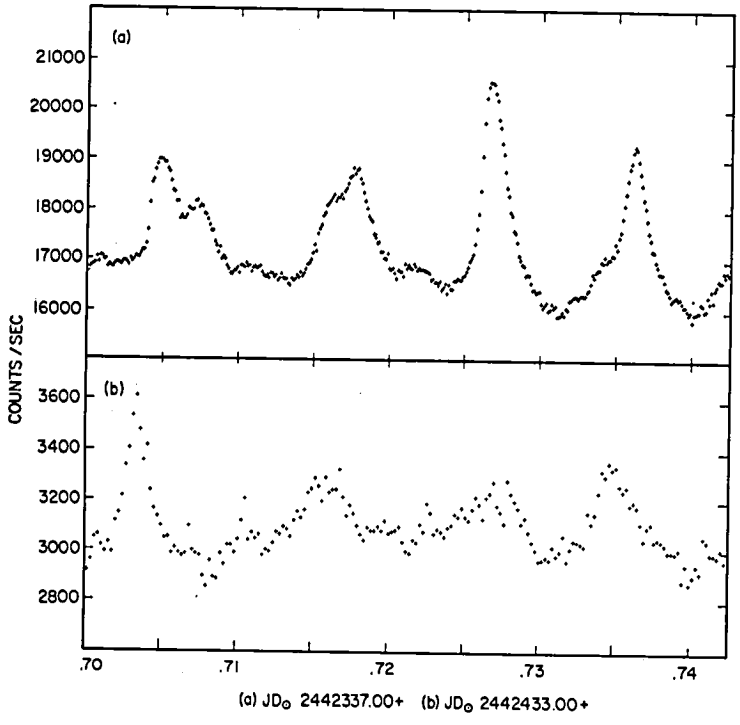

Figure 6. (a) A portion of the light curve of G29-38. The ordinate is expressed in detected photons per second in white light reduced to outside the atmosphere. (b) The same for G38-29.

light curve is very irregular. The times of arrival of the pulses are not predictable with any simple ephemeris. Figure 7 shows power spectra of the light curve of G29-38 on two successive nights. The power spectra are extremely complex. Literally scores of periods are simultaneously present, and the power spectra change from night to night so that neither the periods nor their amplitudes are constant. Although this complexity has prevented any detailed understanding of the light curve of G29-38, a few regularities can be found in the power spectra. Periods near 694 sec, 820 sec, and 930 sec usually are present in the spectra. Harmonics of the strongest periods usually are present, and are reflecting the non-sinusoidal appearance of the pulses. Cross frequencies between the strongest periods usually are present; if two strong periods with frequencies f_1 and f_2 are present in the power spectrum, $f_3 = nf_1 \pm mf_2$ is likely to be present also, where n and m are small integers.

The properties of the pulsations of all of the variables are summarized in Table 5. There are several important characteristics of the variations. The periods are all very long. Excluding harmonics and cross frequencies, the shortest period is 114 sec and the longest period is 1186 sec. Without exception every variable is multi-periodic. L19-2 has at least two periods, G117-B15A has at least three periods, and R548 has four periods. The remaining variables all have large numbers of periods. In the case of HL Tau-76, Desikachary and Tomaszewski (1975) were able to identify 25 periods, but they included only the periods with fairly large amplitudes, so this is a lower limit to the true number. The stability of the periods varies from extremely high in R548 to very low in G29-38. It should be noted, however, that the apparent

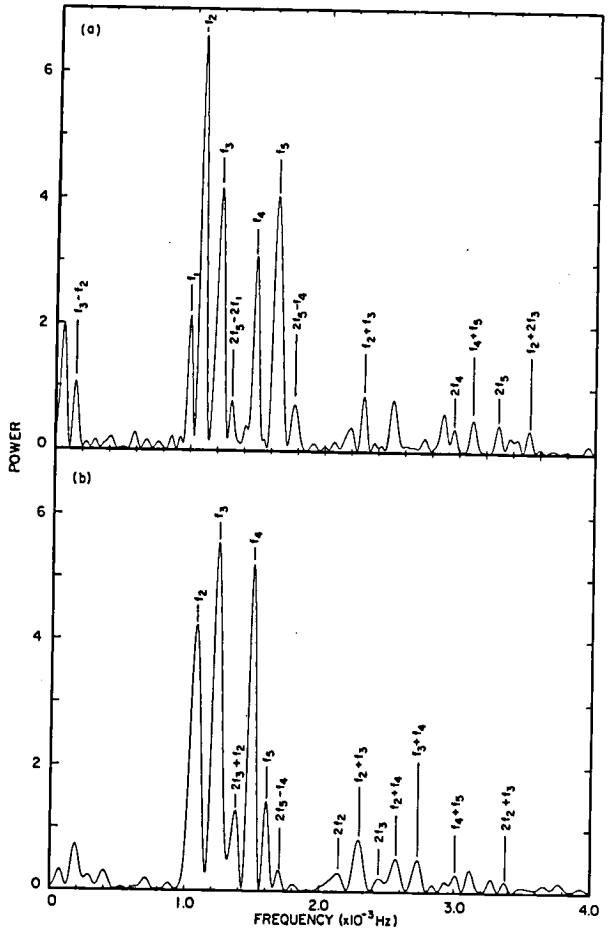

Figure 7. Two power spectra of the light curve of G29-38. Major frequencies and a few of the frequencies identified as harmonics and linear combinations of the major frequencies are indicated. (a) From 1974 October 16. (b) From 1974 October 17.

TABLE 5

PROPERTIES OF THE PULSATIONS

Star	Peak to Peak Amp(Mag)	Typical Pulse Interval (Sec)	Periods (Sec)	Period Stability	Ref.
R548	0.02	220	213 + 274	$\|\dot{P}\| < 10^{-11}$	(1,2,3)
L19-2	0.04	190	114 + 192	High	(4,5)
G117-B15A	0.06	215	216 + 272 + 308	High	(6)
G207-9	0.06	300	292 + 318 + 557 + 739	High?	(7)
GD 154	0.10	1200	780 + 1186 + Others	$\|\dot{P}\| < 10^{-8}$	(8)
GD 99	0.13	350	260 + 480 + 590 + Others	Moderate	(6)
R808	0.15	850	513 + 830 + Others	Low	(6)
BPM 30551	0.18	750	607 + 745 + 823 + Others	Moderate	(9,4)
BPM 31594	0.21	600	311 + 404 + 617 + Others	Moderate	(10)
G38-29	0.21	850	925 + 1020 + Others	Low	(11)
G29-38	0.28	850	694 + 820 + 930 + Others	Low	(11)
HL Tau-76	0.34	750	494 + 626 + 661 + 746 + Others	Low	(12,13, 14,15)

REFERENCES

1) Lasker and Hesser (1971)
2) Robinson et al. (1976)
3) Stover et al. (1978)
4) McGraw (1977)
5) Hesser et al. (1977)
6) McGraw and Robinson (1976)
7) Robinson and McGraw (1976)
8) Robinson et al. (1978)
9) Hesser et al. (1976a)
10) McGraw (1976)
11) McGraw and Robinson (1975)
12) Warner and Robinson (1972)
13) Page (1972)
14) Fitch (1973)
15) Desikachary and Tomaszewski (1975)

low stability of many of the variables may be due to incomplete data. Finally, there is a strong correlation between the amplitude of the variations and their remaining properties. The higher amplitude variables have more periods in their light curves and the periods are more unstable.

These last characteristics are sufficient to limit the physical mechanism for producing the variations to non-radial pulsations. Relatively few ways are known for producing periods as stable as those in R548. They are orbital motion, rotation, and pulsation. Only pulsations can produce multi-periodic variations with high stability. It is true that differential rotation can give multi-periodic variations, but the 213 sec and 274 sec sets of periods in R548 differ by about 30 percent. The shear across the surface of a star with differential rotation this large will destroy the period stability. We are left with pulsations, and thus we are left with the original discrepancy between the observed periods

and the periods expected for radially pulsating white dwarfs. The only way radial pulsations can have long periods is if the mass of the white dwarf is very low, but a low mass white dwarf will also have a low surface gravity which is inconsistent with the observed normal gravities. An easy and natural way out of this dilemma was suggested by Warner and Robinson (1972). Stars are not necessarily restricted to pulsations in purely radial modes, non-radial pulsations are also possible (c.f. the review by Cox 1976). Among the non-radial pulsations at least one group, the g^+ modes, can have periods long enough to match the observed periods. The non-radial modes also provide a natural framework in which to understand the large number of closely spaced periods in the light curves of the larger amplitude variables. Even if we consider only the low order non-radial pulsation modes, a very large number of modes, and thus periods, could conceivably be excited.

The g-mode interpretation has never been seriously challenged, although some interesting modifications of the g-mode model have appeared (e.g. Wolff 1977, Dziembowski 1977). It is also fair to say that the g-mode pulsation model has not been proven. Such a proof would require a demonstration that there is a detailed correspondance between the observed periods and the theoretical periods expected in a white dwarf. Such a demonstration has not been made for two reasons. The first reason is observational. Only one variable, R548, has had its period structure completely deciphered, and none of the variables have accurately known masses and chemical compositions. Without these data the comparison between observed and theoretical periods cannot be made. The second reason is theoretical. The theory of non-radial pulsations is still in its infancy. Only the results from the linear theory are available, and of these results, it is still true that no theoretical model of a white dwarf has been found to be pulsationally unstable. Thus, it is not possible to decide which pulsation modes are

most likely to appear. Nevertheless, there is an encouraging qualitative agreement between the observed and theoretical periods. The periods of R548 can be made to agree with Brickhill's (1975) periods of g-mode pulsations. One of the possible specific identifications of the excited modes is the 213 sec pair as the $\ell = 2$, $k = 1$ (= fundamental) mode; and the 274 sec pair as the $\ell = 2$, $k = 2$ (= first overtone) mode. The splitting of the modes into close pairs could be caused by slow rotation. A similar qualitative agreement between theoretical and observational periods has been found for HL Tau-76 (Desikachary and Tomaszewski 1975), BPM 30551 (McGraw 1977), G29-38, and G38-29 (McGraw and Robinson 1975). The agreement can only be called qualitative, however. The 1186 sec period in GD 154 requires the pulsation mode to be a very high overtone ($k \sim 10$-30) if the variations are caused by g-mode pulsations (Robinson et al. 1978). It is not clear that pulsations in such high overtone modes are acceptable. A more serious problem is that neither the mode assignments nor the basic pulsation model is uniquely specified by the data. McGraw (1977) and Hesser et al. (1976b) give completely different mode assignments to the periods of BPM 30551. Wolff (1977) suggests that the variations arise from the rotation of non-linearly coupled g-mode oscillations. In his model the period structure is determined by the rotation period of the white dwarf, not by the basic pulsation frequency. His model also agrees qualitatively with the observed periods.

The ultimate hope in studying the pulsating white dwarfs is that they will provide a direct observational test of models for the structure and evolution of white dwarfs. This hope has not yet been fulfilled. The reasons are not hard to find. Until the theoretical models can predict which pulsation modes should be excited and which should not, there are too many degrees of freedom available in comparing observation to theory. Van Horn will discuss the theoretical problems in dealing with white dwarfs, and we will not pursue this point. There is

also clear room for improvement of the observations. The period structure is known in detail for only one variable, R548. More are needed. The light curves of the low amplitude variables L19-2 and G117-B15A should be comparatively easy to decipher, but considerable effort will be needed to decipher the complex variations of the large amplitude variables. We have shown that at least one quarter of the white dwarfs with hydrogen rich envelopes that have temperatures near 12,000°K and gravities near log g = 8.0 are variable. It is equally true that three quarters of them are not variable or vary with undetectably low amplitudes. Apparently it is necessary to specify at least one more physical property of a white dwarf to insure that it is a variable. Since we have not been able to discover this additional parameter, it probably is some property that we have not yet measured. Two likely candidates are the exact hydrogen content of the atmosphere of the white dwarfs and the rotation period of the white dwarfs. Neither of these properties is easy to measure. A differential comparison of the variables to non-variables with similar colors might find differences in, if not actual values of, the rotation periods and hydrogen contents.

The research reported here could not have proceeded without the continued collaboration of J.T. McGraw and R.E. Nather. R.J. Stover helped with the spectra of GD 154 and L47. This work was supported in part by NSF grants AST 75-15124 and AST 76-23882.

APPENDIX A

G44-32 has been classified as a DC white dwarf by Greenstein (1970), although weak hydrogen absorption lines may be present so it could be a very weak lined DA white dwarf. Eggen and Greenstein (1965) give V = 16.5, B-V = +0.29, and U-B = -0.58 for its magnitude and colors. G44-32 has been reported to be variable three times, first by Giclas, Slaughter, and Burnham (1959), then by Lasker and Hesser (1969), and finally by Warner et al. (1970). Nevertheless, we believe that the evidence that G44-32 varies is not convincing and have not included it in Table 1. We give our reasons in this appendix.

G44-32 has been observed twice at McDonald Observatory, once in 1970 and once in 1973. Warner et al. (1970) discuss only the 1970 data. According to them, G44-32 displayed two types of variability during their observation. It showed low amplitude continuous variations, and it showed a flare with an amplitude of 0.61 mag which lasted for several minutes. We have re-examined the original data and the log book from 1970, and we have discussed the data with one of the original observers (GWvC). We find that the photometer used to acquire the data was definitely malfunctioning: high voltage was audibly arcing in the base of the photomultiplier tube during the observation. Therefore the 1970 data are unreliable and cannot be used to determine the properties of G44-32. The 1973 data consists of high speed photometry in unfiltered light taken with the 82-inch telescope. Conditions were good and the length of the light curve was 12,500 sec. Visual inspection of the light curve reveals no variability. The power spectrum of the light curve is shown in Figure A-1 and has several notable features. There are significant periodicities at 120 sec and 60 sec due to the periodic drive error in the 82-inch telescope. There are no other significant

periodicities between 40 sec and 30 min; the upper limit on the amplitude of any periodicity in this range is .002 mag. The mean power level increases at low frequencies. This increased power is not intrinsic to G44-32. Low frequency, or "red," noise is ubiquitous in nature and is always present in high speed photometry. The noise is introduced into light curves primarily by variations in sky background and atmospheric transparency. For an example of red noise in high speed photometry of a star known to be constant, see Figure 6 in Robinson (1973). In sum, G44-32 was constant during the 1973 observation.

Lasker and Hesser (1969) observed G44-32 on five nights in 1969. According to them, G44-32 varied at periods of 27.3 min, 13.7 min, and 10.0 min with amplitudes of 1.8, 1.2, and 1.5 percent respectively. However, only three of their light curves were long enough to be analyzed: runs 2, 4, and

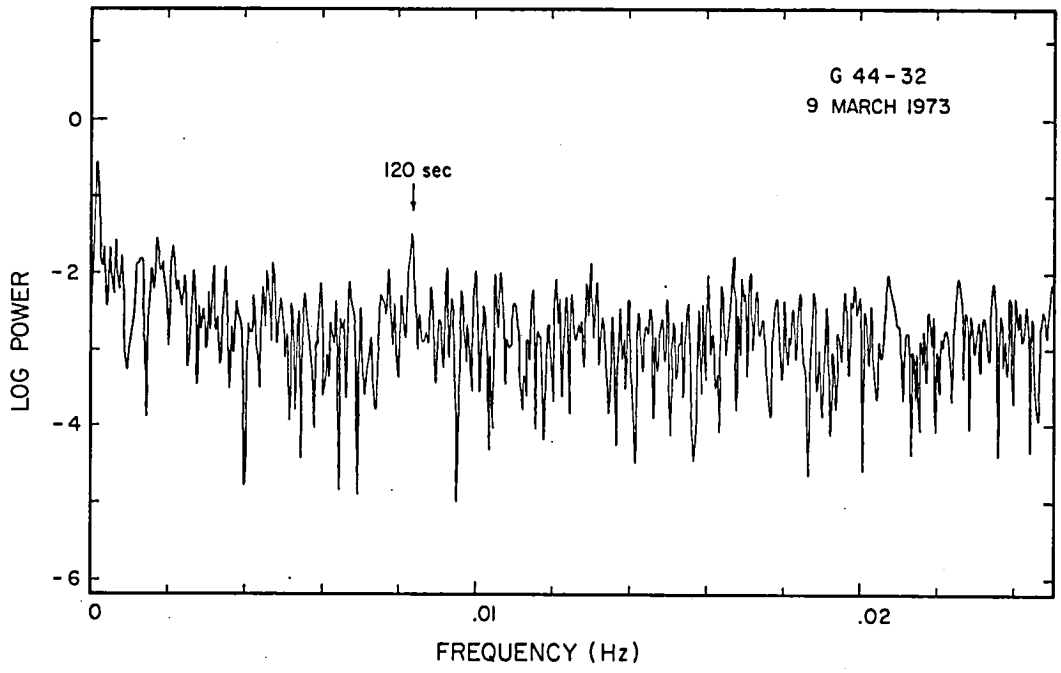

Figure A-1. The power spectrum of the light curve of G44-32 on 1973 March 9. The 120 sec periodicity is spurious and is caused by a periodic drive error in the telescope.

5. We assume here that what they call run 3 in the text must actually be run 2 in their Table 1. If not, their analysis is vitiated because the run from February 21-22 is far too short to be reliably analyzed for long periods. Lasker and Hesser themselves admit that G44-32 was constant during run 4, so the claim for periodic variability relies on runs 2 and 5 alone. The combined power spectrum for runs 2 and 5 is shown in their Figure 1. The spectrum does indeed have three high points at their three periods, but the real question is whether these points are significantly greater than the mean noise level in the power spectrum. In other words, are the three points just noise? Hesser and Lasker do not address this question and do not estimate the mean noise level. Suppose that two power spectra have been averaged together and that the mean level of noise in the averaged spectrum at frequency ν is P_o. The probability that a single measurement of the noise power at ν will give a value greater than P is $(1+2P/P_o)$ exp $(-2P/P_o)$. If N independent samples of the power are made at N independent frequencies, we expect $N(1+2P/P_o)$ exp $(-2P/P_o)$ of the samples to be greater than P. The mean noise level at low frequencies is very large in the spectrum shown by Lasker and Hesser since the spectrum clearly displays the red noise phenomenon. We estimate that in the frequency range of interest $N \sim 20$, and $P_o \sim (0.01 \text{ mag})^2$. Then for $P = (0.018 \text{ mag})^2$ we expect 0.23 high points; for $P = (0.015 \text{ mag})^2$ we expect 1.2 high points, and for $P = (0.012 \text{ mag})^2$ we expect 4.4 high points. Thus, there is a significant probability that the spectrum shown by Lasker and Hesser is caused by random noise rather than periodicities. Furthermore, the data has been pre-selected by the exclusion of run 4, so the probability that their spectrum is due to pure noise is yet higher. We note that even Lasker and Hesser characterize their results as "marginal and speculative."

Giclas, Slaughter, and Burnham (1959) observed G44-32 as part of the Lowell Observatory proper motion survey. Although they suspected that G44-32 varied, the data are photographic and the star is near the limiting magnitude of the survey. Non-intrinsic variability is common under these conditions.

REFERENCES

Angel, J.R.P. 1978, Private communication.

Brickhill, A.J. 1975, M.N.R.A.S., 170, 405.

Cox, J.P. 1976, Ann. Rev. Astr. and Ap., 14, 247.

Dahn, C.C., Harrington, R.S., Riepe, B.Y., Christy, J.W., Guetter, H.H., Behall, A.L., Walker, R.L., Hewitt, A.V., and Ables, H.D. 1976, Pub. U.S. Naval Obs., Second Series, 24, Part 3.

Desikachary, K., and Tomaszewski, L. 1975, IAU Colloquium No. 29, p. 283.

Dziembowski, W. 1977, Acta Astr., 27, 1.

Eggen, O.J. 1968, Ap.J. Suppl., 16, 97.

Eggen, O.J. 1969, Ap.J., 157, 287.

Eggen, O.J., and Greenstein, J.L. 1965, Ap.J., 141, 83.

Fitch, W.S. 1973, Ap.J., 181, L95.

Giclas, H.L., Slaughter, C.D., and Burnham, R. 1959, Lowell Obs. Bull., 4, 136.

Greenstein, J.L. 1969, Ap.J., 158, 281.

Greenstein, J.L. 1970, Ap.J. (Letters), 162, L55.

Harper, R.V.R., and Rose, W.K. 1970, Ap.J., 162, 963.

Harrington, R.S., Dahn, C.C., Behall, A.L., Priser, J.B., Christy, J.W., Riepe, B.Y., Ables, H.D., Guetter, H.H., Hewitt, A.V., and Walker, R.L. 1975, Pub. U.S. Naval Obs., Second Series, 24, Part 1.

Hesser, J.E., and Lasker, B.M. 1971, IAU Symposium No. 42, p.41.

Hesser, J.E., and Lasker, B.M. 1972, IAU Colloquium No. 15, p.160.

Hesser, J.E., Lasker, B.M., and Neupert, H.E. 1976a, Ap.J., 209, 853.

Hesser, J.E., Lasker, B.M., and Neupert, H.E. 1976b, IAU Circular No. 2990.

Hesser, J.E., Lasker, B.M., and Neupert, H.E. 1977, Ap.J.(Letters), 215, L75.

Hesser, J.E., Ostriker, J.P., and Lawrence, G.M. 1969, Ap.J., 155, 919.

Landolt, A.U. 1968, Ap.J., 153, 151.
Lasker, B.M., and Hesser, J.E. 1970, Ap.J. (Letters), 158, L171.
Lasker, B.M., and Hesser, J.E. 1971, Ap.J. (Letters), 163, L89.
Lawrence, G.M., Ostriker, J.P., and Hesser, J.E. 1967, Ap.J. (Letters), 148, L161.
McCook, G.P., and Sion, E.M. 1977, Villanova Univ. Obs. Contributions, No. 2.
McGraw, J.T. 1976, Ap.J. (Letters), 210, L35.
McGraw, J.T. 1977, Ap.J. (Letters), 214, L123.
McGraw, J.T. 1978, in preparation.
McGraw, J.T., and Robinson, E.L. 1975, Ap.J. (Letters), 200, L89.
McGraw, J.T., and Robinson, E.L. 1976, Ap.J. (Letters), 205, L155.
Ostriker, J.P. 1971, Ann. Rev. Astr. and Ap., 9, 353.
Page, C.G. 1972, M.N.R.A.S., 159, 25P.
Patterson, J., Robinson, E.L., and Nather, R.E. 1978, Ap.J., in press.
Richer, H.B., and Ulrych, T.J. 1974, Ap.J., 192, 719.
Riddle, R.K. 1970, Pub. U.S. Naval Obs., Second Series, 20, Part 3.
Robinson, E.L. 1973, Ap.J., 180, 121.
Robinson, E.L., and McGraw, J.T. 1976, Ap.J.(Letters), 207, L37.
Robinson, E.L., and McGraw, J.T. 1977, Proc. Los Alamos Conf. Solar and Stellar Pulsations, p.98.
Robinson, E.L., Nather, R.E., and McGraw, J.T. 1976, Ap.J., 210, 211.
Robinson, E.L., Stover, R.J., Nather, R.E., and McGraw, J.T. 1978, Ap.J., 220, 614.
Routly, P.M. 1972, Pub. U.S. Naval Obs., Second Series, 20, Part 6.
Sauvenier-Goffin, E. 1949, Ann.d'Ap., 12, 39.
Shulov, O.S., and Kopatskaya, E.N. 1973, Astrofizika (SSR), 10, 117.
Stover, R.J., Robinson, E.L., and Nather, R.E. 1978, P.A.S.P., 89, 912.
Terashita, Y., and Matsushima, S. 1969, Ap.J., 156, 203.
Warner, B., and Nather, R.E. 1970, M.N.R.A.S., 147, 21.
Warner, B., and Nather, R.E. 1972, M.N.R.A.S., 156, 1.

Warner, B., and Robinson, E.L. 1972, Nature Phys. Sci., 239, 2.
Warner, B., Van Citters, G.W., and Nather, R.E. 1970, Nature, 226, 67.
Wickramasinghe, D.T., and Strittmatter, P.A. 1972, M.N.R.A.S., 160, 421.
Wolff, C.L. 1977, Ap.J., 216, 784.

Discussion

Belserene: Have you looked for variability among the DA's?

Robinson: Yes, the width and the exact placement of the strip are not well defined. These stars are pretty faint, and the colors are only accurate to a couple of hundredths of a magnitude. So it's hard to know whether or not any individual star is actually in the strip. But I think it's fair to say that there are definitely non-variable DA white dwarfs in the strip. It's not sufficient just to pick out a DA white dwarf with the right color, in order to know that it's variable.

Belserene: Then there are no observable characteristics to distinguish them?

Robinson: Not that we have found so far.

A. Cox: You implied very strongly that the cause of the pulsation is the appearance of hydrogen.

Robinson: I was trying to state it a little less strongly than that. I said that you must have hydrogen in the atmosphere in order to see variability.

A. Cox: I was wondering whether that has any bearing on Wolff's theory, because if he's going to have these things rotate, it doesn't matter whether they have any hydrogen or not, or does it?

Wolff: You need something to drive the pulsations; otherwise, hydrogen content is irrelevant to my theory.

A. Cox: But you find that none of them pulsate unless they have hydrogen, is that right?

Robinson: That's right.

Wesselink: What is the period of the DA star in compound binary white dwarfs?

Robinson: Five to ten seconds.

Aizenman: Your Table V definitely implied a relationship between amplitude and number of periods. Have you got anything more specific than that -- some sort of curve?

Robinson: Yes, there is a very definite relationship between the amplitude and some of the other characteristics of the variables. As the amplitude goes up, you tend to see more periods in the light curve, and the light curve seems to get less stable. The canonical explanation -- at least in Texas -- is that the relationship between amplitude and the other properties is just caused by non-linearities. The low-amplitude ones are linear variables, and there's very little coupling between the modes. The variations are sinusoidal. As you drive up the amplitude, you're more likely to be coupling between modes, and to excite other modes, and so on.

Keeley: If you could look at the amplitude of an individual mode in a star with many modes, would you say that the amplitude of that individual mode is greater than it would be if it were the only mode? Is the higher total amplitude caused by the presence of many modes, or is the intrinsic amplitude of each mode higher?

Robinson: I can't answer that question. It's an interesting one.

Shipman: In terms of composition, the composition that Rob's talking about is the exterior composition.

Robinson: Oh, yes. It's just the photosphere.

Shipman: And the only thing that we know about the interior is that they're not hydrogen. [Laughter] We don't know what they are -- probably carbon. Now a question: how many (what fraction) of the helium white dwarfs have been searched for variability?

Robinson: I don't know the fraction. We've looked at a total of 136 stars which did not vary, of which I believe 25 were non-DA, and another 34 had no known spectral types -- but their colors and their proper motions placed them as white dwarfs. And among those, there are a fair number of DB's.

Nather: I think it's fair to say that the likelihood of a DB being variable is small, because among those that have been looked at, none has been known to vary.

Sion: Even though the variability seems to be unique to single white dwarfs, can you rule out the possibility that in certain close binaries where you have minimal interaction and no appreciable accretion disk, some of the optical variability could be due to a ZZ-Ceti type instability? So maybe it could operate in certain close binaries where the accretion rate is low.

Robinson: That's probably right. Also, I didn't want to rule out interacting binaries altogether. My main point was that a least some of the

ZZ-Ceti stars are single stars. So that the basic mechanism for exciting them is intrinsic to a single star. If you put in another star, you're going to modulate that, and it's going to get more complicated.

J. Cox: First a comment, and then a question. The comment is that it worries me a little when I see all these non-linearities. These are actually fairly small amplitudes, I think.

Robinson: Three tenths of a magnitude.

J. Cox: Anyway, there is evidence for non-linearity. The question is, is the $\dot{P}$ consistent with the cooling rate of these stars?

Robinson: It is consistent. There are various ways that you can change the period of a white dwarf. You can change the temperature, or the chemical composition. Temperature changes lead one to expect a $\dot{P}$ of the order of 10^{-15}, 10^{-16}, or 10^{-17}, depending on the chemical composition.

Theories of White Dwarf Oscillations

H.M. Van Horn

Department of Physics and Astronomy

and

C.E. Kenneth Mees Observatory

University of Rochester

Rochester, N.Y.

Abstract

The current status of theoretical understanding of the oscillations observed in the ZZ Ceti stars and cataclysmic variables is briefly reviewed. Non-radial g-mode oscillations appear to provide a satisfactory explanation for the low-amplitude variables such as R548, with periods in the range ~ 200-300 seconds, but for the longer-periods (800-1000 second) oscillators, the situation is still unclear. Rotation may play an important role in this problem, and the effects of both slow and fast rotation upon the mode structure are discussed. In the cataclysmic variables, both accretion and thermonuclear burning may act to excite oscillations of the white dwarf, and recent work on this problem is summarized also.

I. Introduction

The purpose of this review is to provide a summary of some of the recent developments in the theory of white dwarf oscillations. It is beyond the scope of this paper to provide a comprehensive review of all of the work in this area since the last LASL/GSFC pulsation conference. Instead I shall restrict myself to those subjects on which there has been recent activity or which appear to me to be particularly important, and I shall concentrate almost exclusively on theoretical research carried out within the past two or three years. Earlier work on white dwarf oscillations has already been summarized in a number of review papers to which reference is made below.

The general theory of non-radial oscillations of stars has recently been reviewed by Ledoux (1974) and by Cox (1976), both of whom include brief summaries of the work on white dwarf oscillations. A review devoted exclusively to white dwarfs has been presented by Van Horn (1976). The observational basis for the theoretical investigations are provided by the periodicities that have been detected in the ZZ Ceti stars (single, variable white dwarfs) and in the cataclysmic variables. The observed data on the ZZ Ceti stars were reviewed by Robinson and McGraw (1976) at the last LASL/GSFC pulsation conference, and an excellent, comprehensive discussion of the observed pulsational properties of these stars has recently been provided by McGraw (1977). The properties of the cataclysmic variable oscillators have been reviewed by Warner (1976a) and by Robinson (1976), and a comprehensive and detailed discussion of these systems has been given by Warner (1976b). The most recent survey of the observations of white dwarf oscillations has been provided by Robinson (1978) at this conference.

The plan of this paper is as follows. In § II some of the general problems associated with non-radial oscillations, but which have a special significance for white dwarfs, are reviewed. In § III research concerned primarily with oscillations of single white dwarfs is discussed, except for effects of rotation. Rotational modifications of the spectra of non-radial oscillations are considered separately in § IV, and this is followed in § V by a discussion of recent work on pulsational instabilities of high-luminosity degenerate stars, including those produced by thermonuclear burning. In § VI we conclude with recommendations concerning some problems for future study.

II. General Problems of Non-Radial Oscillations

a. ℓ=1 Modes

In the study of non-radial stellar oscillations, modes corresponding to spherical harmonics of degree ℓ=1 have generally been ignored. This is a result of the mistaken impression that such modes correspond to displacements of the center of mass, which of course cannot occur in isolated stars. For "stars" composed of homogeneous, incompressible fluids, this claim is true; however, real stars are neither homogeneous nor incompressible, and in such cases non-zero displacements at the center of the star need not correspond to a displacement of the center of mass. This was explicitly shown by Smeyers (1966) for adiabatic oscillations, and a more general proof has recently been given by Christensen-Dalsgaard (1975). Thus modes

corresponding to spherical harmonics of degree $\ell=1$ are physically realizable in stars. This is particularly important for the white dwarfs, because the $\ell=1$ modes have the longest periods of any of the g-modes, and because one of the most vexing problems connected with white dwarf oscillations has been the persistent inability of theory to identify low-order modes that have periods as long as those observed.

b. Connection between theory and observation

In contrast to radial oscillations, in which the relations between displacement, radial velocity, and luminosity variation are relatively straightforward, the connections of the radial and transverse displacements with the observed quantities are not simple in the case of non-radial oscillations. A pure eigenmode corresponding to the spherical harmonic $Y_{\ell m}(\theta,\phi)$, for example, has ℓ nodes in the colatitude interval $0 \leq \theta \leq \pi$, and the real part of the eigenfunction has m nodes equally spaced in azimuth between $0 \leq \phi \leq \pi$ (see Fig. 1). The observed light from a non-radially oscillating star will thus be a weighted integral over these angular functions. It is evident that the observed amplitude of a mode with ℓ or m even moderately large will be considerably reduced by cancellation. In addition, there will in general be mode-dependent phase shifts between the times of maximum radial velocity and maximum light. Dziembowski (1977a) has presented the general theory of the radial velocity and luminosity variations of non-radially oscillating stars. He has also evaluated the various integrals relating these quantities to the theoretical parameters for the case of an Eddington limb-darkening law, and he finds that the observed radial velocity amplitude is reduced to less than one-tenth of the maximum for $\ell \geq 4$. In a separate publication (Dziembowski 1977b) he has applied the theory specifically to evaluate the observed parameters

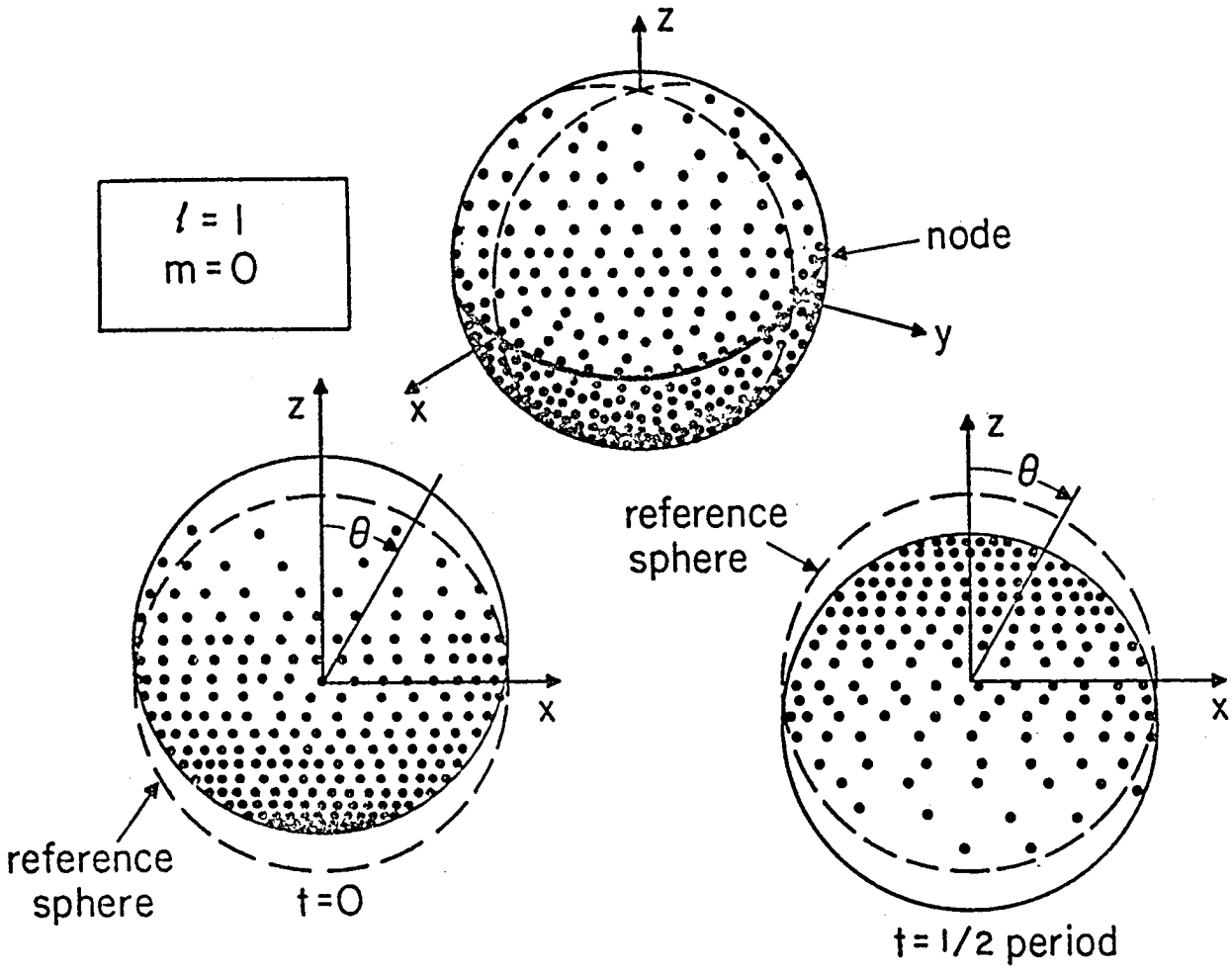

Fig. 1a - A pictorial representation of the luminosity variation corresponding to the spherical harmonic $Y_{1,0}(\theta,\phi)$. The upper figure gives a perspective view of the luminosity distribution projected onto a spherical surface. The figure at the lower left is a polar projection of the luminosity amplitude in the (x,z)-plane (ϕ=0) at the time of peak luminosity at θ=0. The distribution of luminosity amplitude in θ is given by the difference between the solid outline and the dashed curve representing the reference sphere. The figure at the lower left represents the luminosity distribution half a period later, when peak luminosity has shifted to θ=180°. This mode of oscillation corresponds to the alternate brightening and darkening of the upper (θ<90°) and lower (θ>90°) hemispheres of the star.

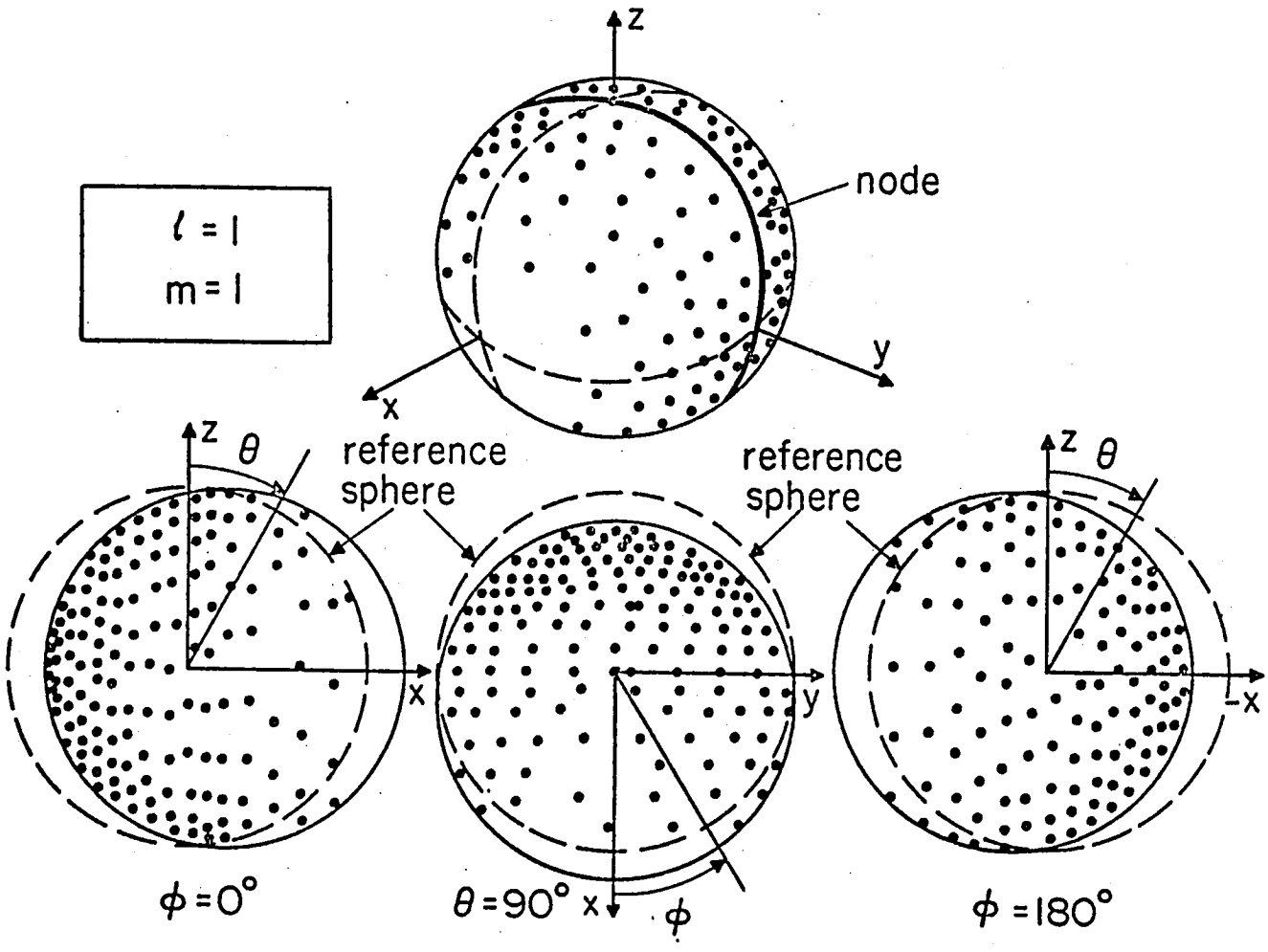

Fig. 1b - Similar to Fig. 1a, except for a different ℓ=1 mode. The actual mode shown is the standing wave corresponding to the combination $Y_{1,1}(\theta,\phi) + Y_{1,-1}(\theta,\phi)$. This mode represents the alternate brightening and darkening of the forward ($|\phi|<90°$) and backward ($|\phi|>90°$) hemispheres. The individual $m=\pm 1$ modes correspond to travelling waves in which the bright spot rotates in the direction of $\mp\phi$, making one revolution in the period of the oscillation. The figures at the lower left and right are polar projections of the luminosity variation at $\phi=0°$ and $\phi=180°$ (corresponding to the positions of maximum and minimum luminosity at $\theta=90°$). The central figure gives the luminosity distribution as a function of ϕ in the equatorial plane ($\theta=90°$).

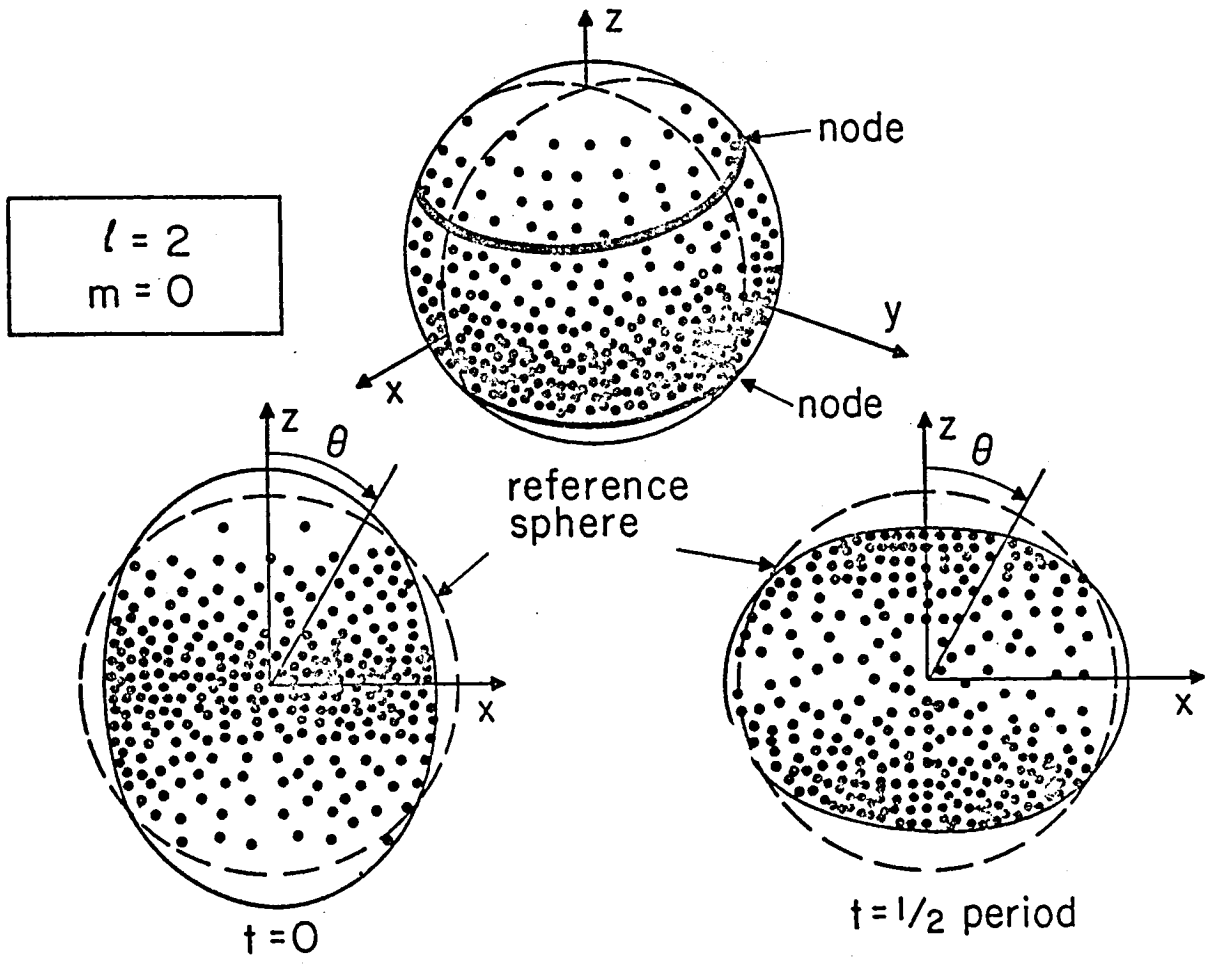

Fig. 1c - Similar to Fig. 1a, except for the mode $Y_{2,0}(\theta,\phi)$. In this mode both caps brighten and darken together, in anti-phase with the equatorial belt ($|\cos\theta|<1/\sqrt{3}$). The maximum luminosity amplitude at the equator is half that at the poles, as shown in the lower figure.

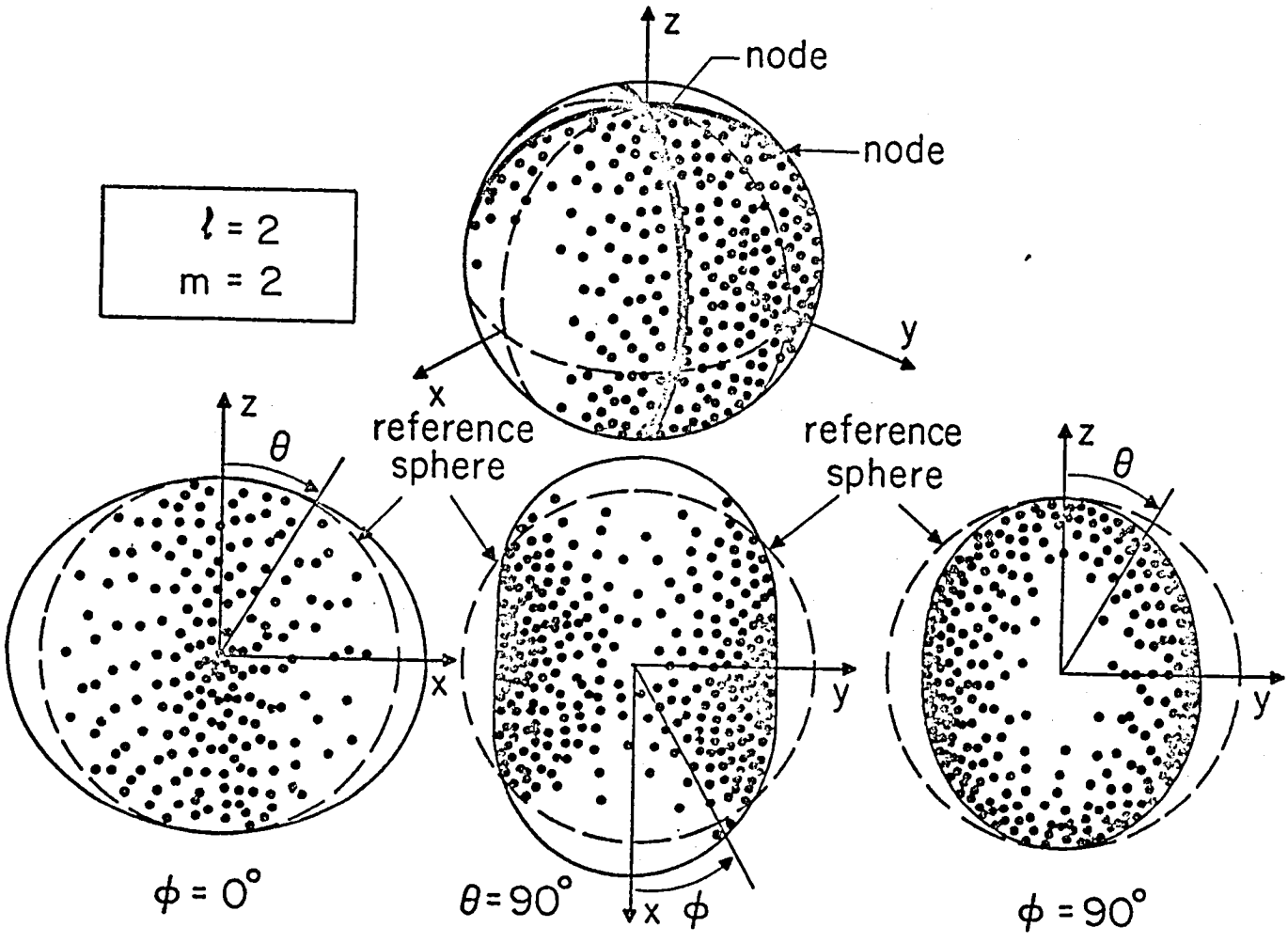

Fig. 1d - Similar to Fig. 1b, except for the standing wave $Y_{2,2}(\theta,\phi) + Y_{2,-2}(\theta,\phi)$. The individual $m = \pm 2$ modes correspond to traveling waves rotating in the $\mp\,\phi$ directions with the period of the oscillation.

corresponding to a variety of g-mode oscillations of $0.6M_\odot$ white dwarf models with $T_{eff} \approx 11{,}000°K$ and $12{,}000°K$. As expected, the observed luminosity amplitude decreases rapidly with ℓ; for the fundamental g-modes, he finds $\Delta M_{bol}(\ell=2)/\Delta M_{bol}(\ell=1) = 0.186$ at $11{,}000°K$ and 0.205 at $12{,}000°K$. Somewhat surprisingly, however, Dziembowski also finds that the observed luminosity amplitude increases with the radial wavenumber k (k is the number of radial nodes in the eigenfunction); for modes with $\ell=1$ or 2, $\Delta M_{bol}(k=10)/\Delta M_{bol}(k=1) \sim 20\text{-}30$. Thus if high radial overtones can be excited with amplitude $\delta r/r$ at the surface comparable to that of the lower k-modes, the high overtones will dominate the observed light variation. For the same reason, the observed oscillations must correspond to modes of moderately low values of ℓ and m.

c. Thermal imbalance

The problem of determining the pulsational stability of stars in thermal imbalance (i.e., evolving stars, in which $T\partial s/\partial t \neq 0$) has by now been studied quite extensively. It has been a subject of some controversy, and although some of the questions raised have now been resolved, it is not yet entirely clear (at least to this writer) that a complete understanding has been achieved. For the white dwarf stars this problem is of some importance, because, except perhaps in the cataclysmic variables, they have no thermonuclear energy sources; instead the luminosities of these stars are supplied by the cooling of the hot interiors, thus necessitating $T\partial s/\partial t \neq 0$.

A brief summary of recent work on this problem has been given by Cox (1976). In particular, Aizenman and Cox (1975), Demaret (1975), Simon (1977),

and Buchler (1978) have shown that the imaginary part of the complex pulsation eigenfrequency σ which gives exponential growth or decay of small-amplitude oscillations is necessarily different for the oscillation energy and the oscillation amplitude. In the linear, quasi-adiabatic case, they find

$$(\mathrm{Im}\sigma)_E = (\mathrm{Im}\sigma)_a - \frac{\dot{\omega}}{\omega} \quad , \tag{1}$$

where $\dot{\omega}$ is the time rate of change of the oscillation frequency $\omega = \mathrm{Re}\sigma$. This raises the interesting possibility that amplitude growth $[(\mathrm{Im}\sigma)_a > 0]$ may in some cases be associated with energy decay $[(\mathrm{Im}\sigma)_E < 0]$ and vice versa, and leads directly to the question of which complex eigenfrequency (if either!) is the more fundamental. This has been further discussed by Simon (1977), Buchler (1978), and Demaret and Predang (1978). An interesting example of amplitude growth coupled with energy decay has recently been found in a hydrogen shell-burning pre-nova model by Vemury (1978).

For our present purposes, it is sufficient to note that the thermal imbalance effects are appreciable only when the pulsation damping time $(\mathrm{Im}\sigma)^{-1}$ is comparable to or greater than the timescale of evolution of the unperturbed star, $\omega/\dot{\omega}$. For a cooling white dwarf, the latter is in the range 10^7 to 10^{10} years (cf. Lamb and Van Horn 1975; Sweeney 1976; Shaviv and Kovetz 1976). In the absence of gravitational radiation damping (Osaki and Hansen 1973), the damping times for the f- and p-modes are generally of this same order, indicating that thermal imbalance effects may be appreciable. However, for all of the g-modes, and —with gravitational radiation damping included— for the f- and p-modes as well, the damping times are sufficiently short that thermal imbalance is not significant.

III. Non-radial Oscillations of Single White Dwarfs

a. What are the modes of oscillation?

It has been pointed out repeatedly that the observed oscillation periods of the single white dwarfs (ZZ Ceti stars) are much too long to correspond to p- or f-modes, and must perforce belong to the class of g-mode oscillations. However, there still remains a multiple infinity of g-modes. The system of differential equations governing the non-radial oscillations of a spherical star contain the spherical harmonic order ℓ explicitly (cf. Ledoux and Walraven 1958, Cox 1974, Ledoux 1974, Van Horn 1976), so that the oscillation periods must depend on ℓ. For each ℓ-value, there are $2\ell+1$ independent angular modes of oscillation, corresponding to the different spherical harmonics $Y_{\ell m}(\theta,\phi)$, with $m = -\ell, -\ell+1, \ldots, 0, \ldots, \ell-1, \ell$. In the absence of rotation or magnetic fields, the oscillation periods corresponding to different m-values are all degenerate. (We shall defer discussion of the consequences of rotation to the following section). In addition, for given ℓ, it is possible to find eigensolutions of the set of differential equations plus boundary conditions which have $k \geq 1$ nodes in the radial eigenfunction. It is well-known that the periods of the high overtones increase without limit as $k \to \infty$ (Ledoux and Walraven 1958, Cox 1974, Ledoux 1974). These oscillatory modes are denoted as g_k^+ modes. If the star contains a convection zone (as is the case for all white dwarfs except DA stars with $T_{eff} \gtrsim 14{,}000°K$) an additional set of modes, which have a <u>real</u> exponential time dependence, becomes possible. These are termed g_k^- modes. We shall be mainly concerned with the oscillatory modes, however, and we shall therefore take "g-modes" to mean "g^+-modes" unless otherwise specified.

To investigate the nature of the oscillation modes observed in the ZZ Ceti stars, one may compare the observed periods with those computed for various theoretical models. This is shown in Fig. 2. The effective temperatures and the periods of the principal modes of the ZZ Ceti stars are taken from McGraw (1977), and theoretical values are taken from computations by Brickhill (1975) and Dziembowski (1977b), with the mode of oscillation identified. Several conclusions can be drawn from this immediately; most of them have been pointed out previously, especially by McGraw (1977) and references therein.

1. The observed region of instability for the white dwarfs lies in the range of effective temperatures $10{,}000°K \lesssim T_{eff} \lesssim 14{,}000°K$. Interestingly, this lies in precisely the region where the extrapolation of the Cepheid instability strip meets the white dwarfs (Fig. 3). This has prompted the suggestion by McGraw and Robinson (1976) that the same κ- and γ-mechanisms that operate in the hydrogen and helium ionization zones of the Cepheids are also responsible for exciting the oscillations in the ZZ Ceti stars. We shall return to this point again below.

2. The oscillations of the shortest period ZZ Ceti stars can be understood in terms of low overtones of $\ell=1$ or 2 g-modes. This point has been made previously by Brickhill (1975), by Robinson and McGraw (1976), and by Robinson, Nather and McGraw (1976), for the special case of R548.

3. The shortest period of oscillation changes abruptly from $\Pi \sim 200$ sec for stars with $\log T_{eff} \gtrsim 4.1$ to $\Pi \sim 800$-900 sec for those with $\log T_{eff} \lesssim 4.1$. The reason for this (if it is a real effect) is at present unknown.

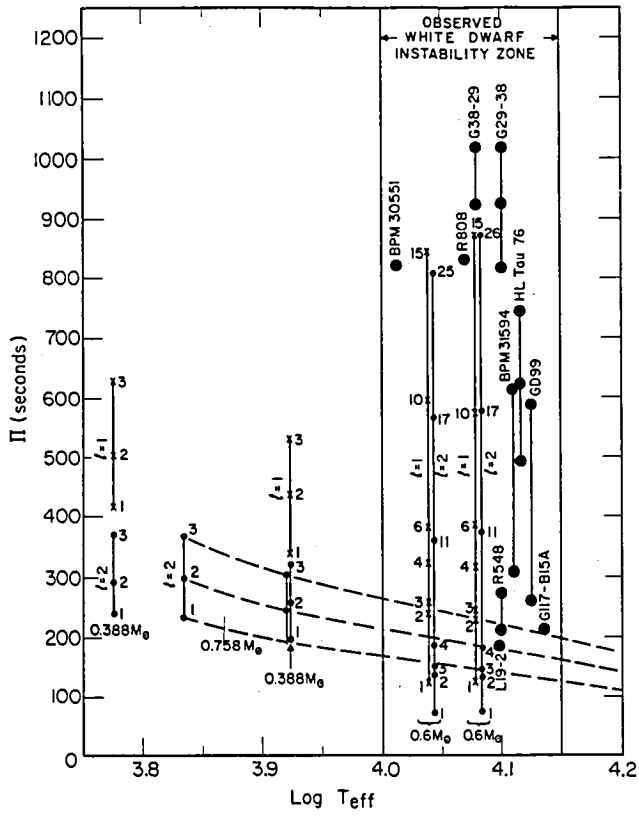

Figure 2. Observed periods of the ZZ Ceti stars from McGraw (1977) compared with theoretical g-mode periods calculated for different white dwarf models. For each star the various principal periods detected are plotted as large dots connected together and labelled with the star name. The effective temperatures are those tabulated by McGraw. The calculated periods for the $0.388M_{\odot}$ and $0.758M_{\odot}$ models are by Brickhill (1975); those for the $0.6M_{\odot}$ models are by Dziembowski (1977). The lowest few obertones of the $\ell=1$ and $\ell=2$ modes are shown (labelled by the values of k and ℓ) for the theoretical calculations. The shortest observed periods of the hotter ZZ Ceti stars ($\log T_{eff} \gtrsim 4.1$) are in the range of the low-order g-mode periods. The periods of the cooler ZZ Ceti stars ($\log T_{eff} \lesssim 4.1$) require rather high radial overtones ($k \gtrsim 15$-25) if these oscillations correspond to conventional g-modes.

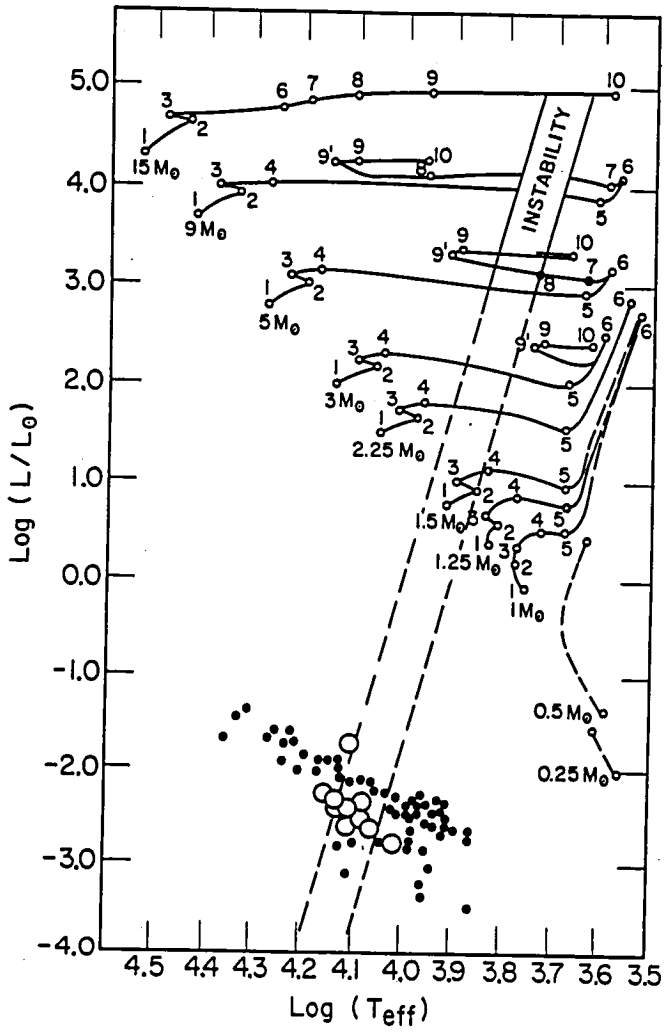

Figure 3. The instability strip in the H-R diagram. The upper portion of the figure showing the theoretical evolutionary tracks and the location of the Cepeheids is adapted from Figure 1 of Henden and Cox (1976). The instability strip has been extrapolated linearly along the dashed lines into the region occupied by the white dwarfs. The locations of the variable white dwarfs are shown by the large open circles.

4. In order to interpret the oscillations of the long-period ZZ Ceti stars in terms of modes which are presently understood, it is necessary to identify the observed oscillations as rather high overtones ($k \gtrsim 15$ for $\ell = 1$; $k \gtrsim 25$ for $\ell = 2$). Note that the high-order spectra belonging to various ℓ-values overlap, so that periods alone are insufficient to provide unique mode identifications in this range.

There are a few additional indications from the data which reinforce the interpretation of the long-period modes as high radial overtones. As pointed out by Robinson and McGraw (1976), there is a rough correlation of oscillation period with observed oscillation amplitude. This is shown in Fig. 4, where McGraw's (1977) periods and amplitudes are plotted. Note that the practice of assigning a single amplitude to the star is not really adequate for this purpose, as McGraw points out; a more detailed comparison with the theory can be made by using the observed amplitudes of the individual oscillation modes. Also shown in this figure are McGraw's estimates of the stability of the oscillations.

For a comparison we have also plotted in Fig. 4 Dziembowski's (1977b) bolometric magnitude variations, reduced by a factor of 10^{-3}, for the various radial overtones of the ℓ=1 and 2 g-modes computed for his $0.6M_{\odot}$, $T_{eff} \approx$ 11,000°K model; almost identical results are obtained for the $T_{eff} \approx$ 12,000°K model. This suggests the following conclusions:

1. The general trends of the observational data are broadly consistent with the theoretical curves. This is at least not in disagreement with the hypothesis that the long-period modes are high radial overtones.

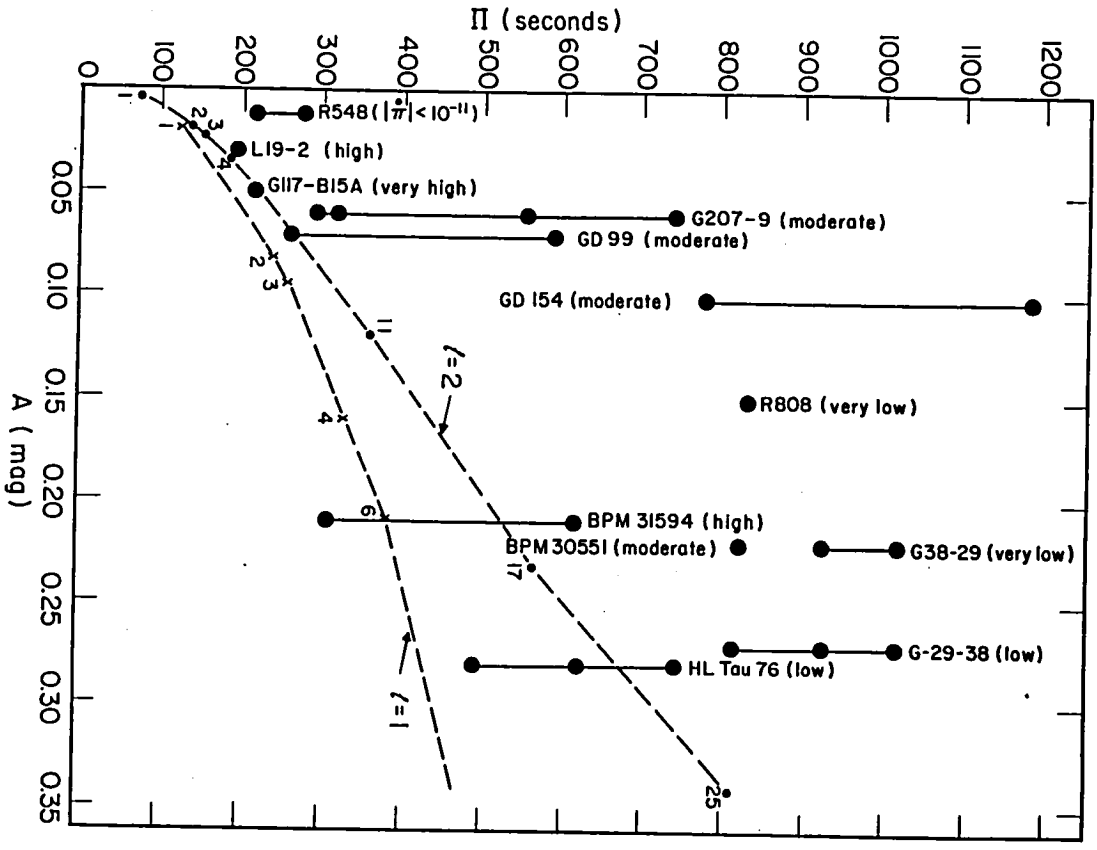

Figure 4. The correlation between period and amplitude of the oscillation for the ZZ Ceti stars. The observational data are taken from McGraw (1977), and his estimates of the stability of the oscillation modes are indicated in parentheses after the star name. Note that the "amplitude" plotted here is a "typical value" for each star; a more informative comparison is possible by making use of the amplitudes of the individual oscillation modes as determined from the power spectra. Also shown for comparison are the predicted bolometric magnitude variations for the various radial overtones for the ℓ=1 and 2 g-modes as calculated by Dziembowski (1977). The plotted points are labelled by the k and ℓ values of the modes. Dziembowski's tabulated values of ΔM_{bol} have been reduced by a factor of 10 for this graph, suggesting that the amplitudes of the radial oscillations are $\delta r/r \lesssim 10^{-3}$ for these stars.

2. The stability of the oscillations displays an interesting correlation with the periods. The shortest period oscillators display a very stable mode structure, while the longest period oscillators tend to be the least stable. This is also consistent with the suggested identification of the short periods with low-k modes and the long periods with high-k modes. Because the density of modes increases very rapidly with k in frequency space, the possibility of mode-coupling is enormously greater for the high-k modes than at low k. This may lead to beating or mode-switching that may be observed as apparent lack of stability of the oscillation. Precisely this type of interaction has been shown by Robinson, Nather, and McGraw (1976) to occur even in the most stable ZZ Ceti star, R548; when this is taken into account, the underlying mode structure of the star is found to have $|\dot{\Pi}| < 10^{-11}$.

3. The oscillation amplitudes as determined from the ratio of Dziembowski's calculations of ΔM_{bol} with the observed amplitude of variation A are quite small; $\delta r/r \lesssim 10^{-3}$ at the stellar surface.

As the previous discussion has been intended to show, great progress has been made in the past several years in understanding the nature of the oscillations in the ZZ Ceti stars. Despite this, the mode identifications, except perhaps in R548, are still unsettled. One reason for this is that theoretical models have yet to demonstrate pulsational instability in the modes suggested by the observations. A second reason is that additional oscillation modes may exist in white dwarfs which have not yet been studied adequately or that rotational modifications of existing g-modes may be important. We therefore turn next to considerations of these questions.

b. Excitation and non-linear mode-coupling

Only a few of the recent non-radial oscillation calculations have investigated the problem of excitation of the modes, and this has usually been restricted to the linear, quasi-adiabatic approximation. In their classic paper, Osaki and Hansen (1973) studied radiative, neutrino, and gravitational-radiation damping of non-radial oscillations. However, the pure ^{56}Fe white dwarf models they employed did not include a treatment of the ionization zones, and thus no pulsational instability was found. More recently, Hansen, Cox, and Van Horn (1977; see also Van Horn 1976) have studied the low-k, ℓ=1 and 2 non-radial oscillation modes of detailed models of pure ^{12}C white dwarfs. These models did include a careful treatment of the ionization/convection zone, and a hint of instability in the ℓ=2 g_1^+ and g_2^+ modes was found for a model with $T_{eff} \approx 58{,}000°K$. It is not clear that this is a real instability, however, because the result depends upon the assumed location of the "transition zone" (cf. Cox and Giuli 1967, ch. 27) where the quasi-adiabatic approximation breaks down. In any case, this "instability" is clearly irrelevant to the ZZ Ceti stars.

The only other theoretical study of the excitation mechanism in models for the ZZ Ceti stars of which this writer is aware is that by Dziembowski (1977b). In this important work, Dziembowski investigated the oscillations and stability of two $0.6M_\odot$ white dwarf models with $T_{eff} \approx$ 11,000°K and 12,000°K. These models, with element abundance distributions taken from the last model of Paczynski's (1971) planetary nebula sequence, did include hydrogen/helium envelopes with ionization zones. The results of Dziembowski's fully non-adiabatic calculations were: i) g-modes with $k \leq 15$-25 were found <u>not</u> to be self-excited, and ii) modes corresponding to very high orders ($\ell \sim 100$-400, $k \sim 15$-20) were driven violently unstable,

primarily by the HeII ionization zone, with growth timescales of days. However, the periods of these modes are much too short ($\Pi \sim 5$-20 sec), and the ℓ-value much too large for these modes to correspond to the observations. (For example, Dziembowski finds $\Delta M_{bol} \sim 10^{-2} - 10^{-5}$ for these high-ℓ modes as opposed to $\Delta M_{bol} \sim 200$ for the $\ell=2$ modes of comparable k-order).

Thus none of the theoretical calculations has yet succeeded in discovering pulsational instabilities in those modes which the observations indicate to be excited in the ZZ Ceti stars.

One possibility for resolving this problem was suggested by Dziembowski (1977b). He pointed out that non-linear interactions among the very high-ℓ modes which he finds to be excited may provide resonant excitation of the lower-order modes in the observed range of frequencies. (Vandakurov (1977) has subsequently considered non-linear driving of radial pulsations by these same unstable non-radial modes). This would be expected to lead to variability of the observed mode amplitudes, as is found in the long-period (800-1000 second) oscillators. It is difficult to accept this explanation for the short-period (~200-second) oscillators, however. In particular, the great stability of the oscillations in R458 strongly suggests that these modes are indeed correctly identified as low-ℓ, low-k oscillations that are self-excited. If this is correct, then there is an essential aspect of the non-radial excitation mechanism that we have yet understood.

Another, related, problem that may be important in the white dwarfs is the interaction between oscillations and convection. There are two aspects of this: the effect of convective flux variations upon the pulsational stability and the direct non-linear coupling between pulsational and convective motions. Work on the general problem of convection in pulsation theory has been briefly reviewed by Cox (1976). In the context

of white dwarfs, there has been no work on this problem, and time-variations in the convective flux have been entirely ignored in the pulsational stability analysis. From research on the effects of convection on other types of stars, however, it appears likely that this is inadequate. For example, in a series of papers concerned with the full hydrodynamic treatment of convection in Cepheids and RR Lyrae stars, Deupree (1976, pp. 222, 229, and references therein) has shown that convection becomes important at the red edge of the instability strip, where it dominates the damping of the oscillations. Is it too great an extrapolation to suppose that convection may play a similar role in the ZZ Ceti stars, perhaps even in determining the transition from stable 200-second oscillations to fluctuating 800-1000 second oscillations?

Unfortunately, Deupree's detailed numerical approach is ill-adapted for use in a survey of stability among non-radial modes, especially those of moderately high order. For this purpose one would prefer a simpler approximation that could be employed with linear theory. Two recent groups of papers are of interest in this regard. First, Gough (1977) has recently reviewed the time-dependent generalizations of mixing-length theory and has presented them in a form suitable for use in studies of radial pulsation. Second, Goldreich and Keeley (1977a,b) have presented a careful analysis of the interaction between convection and pulsation in connection with low-amplitude oscillations of the sun. They find (1977a) that turbulent dissipation renders unstable radial modes marginally stable. In their second paper (1977b) the treatment of convection/pulsation interactions is generalized to the case of non-radial oscillations, and they find that non-linear interactions lead to a tendency for equipartition of

pulsation modes which are close to resonance with convective eddies. In the white dwarfs, it has been pointed out before (Van Horn 1976) that convective timescales become comparable with g-mode periods for the cooler He-envelope white dwarfs with $M \sim 0.4\text{-}0.6M_{\odot}$. Clearly this problem needs further attention from the theorists.

c. New modes?

The difficulty of identifying the long-period oscillations of the ZZ Ceti stars with modes of low order has suggested to some the possibility of finding additional oscillation modes of the white dwarfs beyond the conventional p-,f-, and g-modes. Motivated in part by this, Van Horn and Savedoff (1976; see also Denis 1975) undertook a preliminary investigation of the effects of a solid core upon the oscillation spectrum of a white dwarf. Although their analysis has not yet been carried through for a complete stellar model, they were able to show that the ability of the solid core to sustain shearing motions permitted torsional oscillations of the core, just as in the case of the solid Earth. In addition, they found that the non-vanishing shear modulus produced modifications in the p- and g-mode oscillation periods; for the p-modes the change was only a few percent, while for the g-modes, the period ranged from the normal value in the case of small shear moduli, to that appropriate to the torsional oscillations. Since the torsional oscillation periods Π_t were estimated to be no more than 3 to 10 times longer than the p-mode periods, or $\Pi_t \sim$ 30-100 seconds, the effect of the solid core does not appear to be relevant to the problem of the long-period oscillations. In addition, while core crystallization begins near $T_{eff} \approx 13{,}000°K$ in a $1M_{\odot}$, ^{12}C white, it will not occur until considerably lower temperatures in stars of lower masses.

From McGraw's (1977) values of log g for the ZZ Ceti stars, the masses are expected to lie in the range of 0.5-0.7$M_\odot$; the values of T_{eff} at crystallization for these masses are so low that core crystallization will not begin until these stars have cooled well below the observed instability strip.

Another, as yet unexplored, possibility exists for introducing new modes into the white dwarfs, however. This has to do with the effect of composition discontinuities upon the mode structure of the star[1]. It is well-known that white dwarfs have undergone thermonuclear processing. They must initially have been more massive in order to have evolved off the main sequence and to have become white dwarfs; thus some of the hydrogen has been burnt into helium. In addition, the masses are larger than the minimum for helium burning; thus some of the helium has also been processed into carbon and oxygen. It is unlikely that the white dwarfs have undergone further nuclear processing, although this cannot yet be rigorously established. It is also well-known that the gravitational fields in white dwarfs are sufficiently high so that gravitational settling of the elements will have proceeded to its limit (cf. Schatzman 1958). Thus the compositional structure of a white dwarf is expected to consist of layers of virtually pure elements; hydrogen overlying helium overlying carbon and oxygen. Vauclair and Reisse (1977) and Koester (1976) describe the structure of the outer layers of such a star.

In cases with such layered structures, it is anticipated that additional modes of oscillation associated with the density discontinuities will appear. For the case of the heterogeneous incompressible sphere this has been

---

1. I am indebted to M.P. Savedoff for drawing my attention to this point.

confirmed within the past five years (cf. Ledoux 1974). The eigenfunctions associated with the additional modes peak near the density discontinuities; thus these modes can be regarded as "surface waves" associated with the discontinuities. The effect of the thickness of the various composition layers upon the oscillation spectrum of a white dwarf, however, has not yet been investigated. It is tempting to speculate that the location of the H/He composition boundary relative to the location of the HeII ionization zone may even be responsible for the existence of non-variables within the instability strip, just as Baglin (1976) has suggested in the region of the main sequence A stars.

IV. Effects of Rotation on Non-Radial Oscillations

a. Slow rotation

Up to this point we have ignored the effects of rotation upon the mode structure of a non-radially oscillating star. However, as we shall discuss in this section, rotation exerts a profound influence upon the periods of such oscillations. It is convenient to begin this discussion with the case of very slow rotation (rotation frequency $\Omega << \omega = 2\pi/\Pi$), both because it can be treated as a perturbation on the non-rotation case, and because it may be especially relevant to the ZZ Ceti stars we have been considering.

The theory of the leading (i.e., linear) corrections to the frequencies of non-radial oscillations due to uniform rotation has been well-established for some time now (cf. Ledoux 1951, Ledoux and Walraven 1958) and yields, in the inertial observer's frame,

$$\sigma_{k\ell m} = \sigma_{k\ell} - m\Omega(1 - C_{k\ell}). \qquad (2)$$

Here $\sigma_{k\ell m}$ is the (complex) eigenfrequency, $\sigma_{k\ell}$ is the value of $\sigma_{k\ell m}$ in the absence of rotation, m is the azimuthal spherical harmonic index ($m = -\ell, -\ell+1, \ldots, \ell$), and $C_{k\ell}$ is defined by

$$C_{k\ell} = \frac{\int \rho r^2 dr (2ab+b^2)}{\int \rho r^2 dr [a^2+\ell(\ell+1)b^2]}. \qquad (3)$$

In (3), the quantities a and b are, respectively, the amplitudes of the radial and tangential displacement eigenfunction, defined by

$$\underset{\sim}{\xi}_{k\ell m} = (\xi_r, \xi_\theta, \xi_\phi) = (\delta r, r\delta\theta, r\sin\theta\delta\phi) = [a(r)Y_{\ell m}, b(r)\frac{\partial Y_{\ell m}}{\partial\theta}, \frac{b(r)}{\sin\theta}\frac{\partial Y_{\ell m}}{\partial\phi}]. \qquad (4)$$

For moderately large k-values, $|a|$ is generally much smaller than $|b|$, and (4) reduces to

$$C_{k\ell} \approx \frac{1}{\ell(\ell+1)}. \qquad (4a)$$

Brickhill (1975) comments that (4a) is a good approximation for $k \gtrsim 4$, but he gives no quantitiative details beyond this.

Recently, Wolff (1977) has applied this formalism to interpret the multiperiodicities observed in the ZZ Ceti stars as beats produced by non-linear mode-coupling of rotationally-split g-mode oscillations. He argues (see Wolff 1974 for details) that g-modes with spherical harmonic index m and -m should be excited to comparable levels, and hence that the corresponding retrograde ($m > 0$) and prograde ($m < 0$) modes will combine to yield a not-quite-standing mode with azimuth and time dependence of the form (in the non-rotating inertial frame):

$$\cos\{|m|[\phi + \Omega(1-C_{k\ell})t]\}e^{i\sigma_{k\ell}t}. \qquad (5)$$

The rate of azimuthal drift of this wave pattern is thus given by

$$-\dot{\phi} = \Omega(1-C_{k\ell}) \equiv \Omega_{\ell} \ . \qquad (6)$$

In the case of uniform rotation and sufficiently large k, $C_{k\ell}$ assumes the simple form given by (4a), and the drift rate of the wave pattern then depends only upon ℓ and Ω, but not upon k or m.

Wolff then argues that it is the "slow" relative drift of groups of modes with comparable ℓ-values that dominates the observed variations. This leads him to consider the pattern frequencies given by (6) and (4a) together with simple differences of these frequencies as defining an oscillation spectrum depending only upon the stellar rotation rate Ω. A schematic illustration of this concept and its application to four of the ZZ Ceti variables are shown in Fig. 5, adapted from Wolff's paper. The coincidence of the theoretical spectrum with the observed power spectra is rather striking, despite some obvious differences. This, together with the fact that it yields potentially testable predictions of the rotation rates of the oscillating white dwarfs, makes Wolff's model of interest for further study.

In particular, the rotation rates Wolff predicts are in the range $2\pi/\Omega$ = 200 to 500 seconds. This would be consistent with the contraction of a star having approximately solar angular momentum from the main sequence

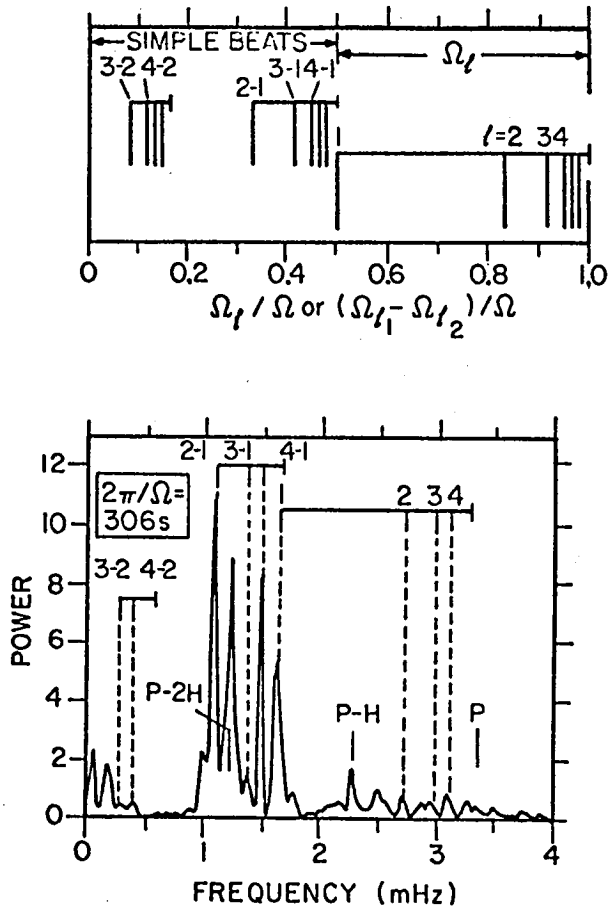

Fig. 5 - Wolff's theory for the oscillations of the ZZ Ceti stars. This figure is adapted from Wolff (1977). The right half of the upper panel shows schematically the azimuthal drift rates Ω_ℓ given by (6) for modes with ℓ = 1,2,3,4... in units of the stellar rotation frequency Ω. The left half of the same panel shows the beat frequencies $\Omega_{\ell=2} - \Omega_{\ell=1}$, ..., $\Omega_{\ell=4} - \Omega_{\ell=2}$, etc., also in units of Ω. The lower panel shows one example of a comparison of this theoretical spectrum with the observed oscillation spectrum of the ZZ Ceti star G29-38. The assumed stellar rotation period $2\pi/\Omega$ = 306 seconds has been chosen to provide the best match with this data. The frequencies labelled P, P-H, and P-2H have no theoretical foundation, but are introduced to correspond to other large peaks in the power spectrum. The frequency P is supposedly analogous to the so-called "prograde mode" identified in the sun while H is "the frequency of the highest maximum in the observed spectrum" (Wolff 1977).

to white dwarf dimensions without loss of angular momentum, but it is much faster than the rotation rates found so far in any other single white dwarf ($>10^3$-10^4 seconds in 14 DA white dwarfs: Greenstein and Peterson 1973, Greenstein et al. 1977; ~ 2.2 hours in Feige 7: Leibert et al. 1977; and 1.3 days in G195-19: Angel et al. 1972). A rotation period of ~ 200 seconds corresponds to an equatorial velocity of ~ 300 km s^{-1} and to a rotational Doppler broadening of ~ 4.5Å at H_γ. This is amply large enough to be measured, even in the presence of the very large pressure broadening in white dwarfs, and the results of such measurements are of very considerable interest. If such large rotation broadening is found, it will favor Wolff's theory and provide a new puzzle: why do the variable white dwarfs rotate so much faster than non-variables? If rapid rotation is not observed, the measurement will at least place useful limits on the rotation periods of the ZZ Ceti stars and reaffirm an existing puzzle: why and how are high-order g-modes excited?

Apart from its virtue of potential for observational test, there are a number of shortcomings of Wolff's model from the point of view of theory. Instead of developing his model from first principles, Wolff has introduced a number of ad hoc assumptions that should be checked. For example, he adopts the large-k limit for $C_{k\ell}$ for all of his modes; is this adequate? In part to address this question Hansen, Cox, and Van Horn (1977) have computed the rotational splitting of ℓ=2 g-modes in ^{56}Fe and ^{12}C white dwarf models in or near the observed white dwarf instability strip. For uniform rotation they find values of $C_{k\ell}$ ranging from -0.020 to 0.165, depending upon the stellar mass, T_{eff}, and the k-value of the mode; the result given by (4a) is $1/\ell(\ell+1) = 1/6 = 0.166$.

Hansen, Cox, and Van Horn have also carried out preliminary calculations of the effects of differential rotation in white dwarfs, assuming a "rotation law" of the form adopted by Ostriker and Bodenheimer (1968) in their study of massive differentially-rotating white dwarfs. For $1M_\odot$, ^{12}C white dwarf models, the calculations indicate a considerably different (and T_{eff}-sensitive) splitting of the $\ell=2$ g_1- and g_2-modes, although this result is rather model-dependent. (There is almost no difference in the g_1- and g_2-mode splittings for the much cruder ^{56}Fe white dwarf models in the T_{eff}-range of interest). This result is of interest in connection with the extremely careful and detailed analysis of the oscillations of R548 by Robinson, Nather, and McGraw (1976). They found that the power spectrum of this star consisted of two main peaks at periods of about 213s and 274s, and that these are each split into close pairs with very stable periods ($|\dot{\Pi}| < 10^{-11}$). The two close pairs, presumably split by rotation, each beat together to yield difference frequencies corresponding to periods of $\sim 1^d.44$ (for the 213s oscillations) and $\sim 1^d.66$ (for the 274s oscillations). From (2), these differences correspond to the quantity $2|m|\Omega(1-C_{k\ell})$, and the different splitting frequencies for the two modes thus require different values of $C_{k\ell}$. As the calculations of Hansen et al. show, this is not at all surprising for the low-order g-modes thought to be present in R548. Although it is premature to identify the precise mode and rotation period of R548 (other than that it appears to be of the order of a day or two) - much less to associate the observed splitting with differential rotation — the prospects for the future seem promising.

b. Rapid rotation and disk accretion

In contrast to the single white dwarfs, the white dwarfs in cataclysmic variables may exhibit rapid rotation as a byproduct of accretion.

In these systems, accretion onto the white dwarf must ultimately take place from the inner edge of the accretion disk, which rotates with the Keplerian circular velocity $v_K \sim (GM/R_*)^{1/2}$. For a white dwarf with mass $M = 1M_\odot$ and radius $R_* \sim 10^9$cm, this velocity is $v_K \sim 3000$ km s^{-1} which corresponds to an orbital period ~ 20 seconds. If such rapid rotation can be transferred efficiently to the white dwarf, the assumption of "slow" rotation, upon which the mode-splitting calculations are based, will be violated. For this reason, a number of recent papers have begun investigations of the effects of rapid rotation upon the oscillation spectra of stars.

A general formulation of the theory of non-radial oscillations of differentially rotating stars has been presented by Aizenman and Cox (1975; hereinafter denoted by AC). This approach was subsequently applied by Hansen, Aizenman, and Ross (1976) to a study of the non-radial oscillations of uniformly rotating isothermal cylinders. They found very peculiar behaviors of certain g-modes under rapid rotation and showed that some of the modes correspond to dynamically unstable spiral waves. This intriguing result stimulated Hansen and his collaborators to undertake further investigations of the effects of rotation upon the non-radial oscillation modes of stars. Hansen, Cox, and Carroll (1978) have accordingly adapted the theoretical formulation developed by AC to study this problem. In the limit of slow rotation (only correction terms to the eigenfunctions and eigenvalues that are linear in Ω are considered), they showed that the AC formalism recovers the conventional frequency-splitting constant C given by (3). However, Hansen et al. also extended their calculation to the quasi-adiabatic analysis of modal stability; they found the interesting

result that retrograde (m>0) modes are slightly more stable than prograde ones. Further, in a noteworthy appendix, Hansen, Cox, and Carroll studied the non-radial oscillations of rotating, cylindrical "white dwarfs" (the analogs of the rotating isothermal cylinders of Hansen, Aizenman, and Ross). In this work, which was not restricted to slow rotation, they found large effects on the g-mode periods even at rather moderate rotation rates ($\Pi \lesssim 500$ seconds for $\ell = 2$ g_1-modes). They also found substantial differences between the retrograde and prograde modes, as well as significant departures from the linear theory, even at periods as long as 1000 seconds. For this reason, they recommended a careful re-examination of Wolff's theory of the ZZ Ceti oscillations; if the mode splitting differs significantly from that given by (4a) with (2) and (6), the spectrum shown schematically in the top part of Fig. 5 will be modified, and it is not clear whether the degree of agreement with the observed oscillation spectra of the ZZ Ceti variables will be maintained.

An exciting new development in the theory of oscillations of rotating stars is contained in an important recent paper by Papaloizu and Pringle (1978). In this work, they pointed out the existence of a new class of modes which appear in rotating stars and which they have termed "r-modes" because of their similarity to Rossby waves. These modes have previously been missed by most workers because they belong to a completely different mode class (the toroidal modes) than do the spheroidal p-, f-, and g-modes, and because - for spherical stars - the toroidal modes are all degenerate at zero frequency.

The existence of the class of toroidal modes of stellar oscillation was noted in a group-theoretical paper by Perdang (1968; see also Chandrasekhar 1961). The nature of these modes was further clarified in an ex-

ceptionally careful study by Aizenmann and Smeyers (1977). They showed that the displacement fields $\rho\underset{\sim}{\xi}$ that correspond to oscillations of non-zero frequency have no toroidal component. In this case, they found that the displacement eigenfunction $\underset{\sim}{\xi}_{k\ell m}$ can be written in the familiar form (cf. equation [4])

$$\underset{\sim}{\xi}_{k\ell m} = (\xi_r, \xi_\theta, \xi_\phi) = [a(r)Y_{\ell m}, b(r)\frac{\partial Y_{\ell m}}{\partial \theta}, \frac{b(r)}{\sin\theta}\frac{\partial Y_{\ell m}}{\partial \phi}] \ . \tag{7a}$$

This separation of variables yields the spheroidal oscillation modes, for which Cowling (1941) introduced the subclassifications of p-, f-, and g-modes. Aizenman and Smeyers went on to show, however, that the modes which are degenerate at zero frequency in a spherical star consist of the f-mode belonging to $\ell=1$ and a new class of modes which have no radial component of the displacement. For the latter modes, the displacement eigenfunction can be written in the form (see also Van Horn and Savedoff 1976)

$$\underset{\sim}{\xi}_{k\ell m} = [0, \frac{c(r)}{\sin\theta}\frac{\partial Y_{\ell m}}{\partial \phi} \ , \ - c(r)\frac{\partial Y_{\ell m}}{\partial \theta}) \ , \tag{7b}$$

where $c(r)$ is a function of radius only. This separation of variables yields the toroidal oscillation modes.

In a rotating star, the equations governing the fluid motions contain additional terms not present in the spherical case. These correspond to the effects of the centrifugal and Coriolis forces, and they affect both the equilibrium configurations and the small-amplitude perturbations about equilibrium. These additional terms are the ones responsible for producing the mode-splitting that breaks the $(2\ell+1)$-fold degeneracy of the g-modes of

order ℓ that has been discussed previously (cf. equation [2]). However, as Papaloizu and Pringle (1978) show, the existing analysis of g-mode splitting (except for the very general formulation given by Aizenman and Cox 1975) is based upon the assumption of slow rotation of the star, and they argue that this is probably invalid for the white dwarfs in cataclysmic variables. Furthermore, as Papaloizu and Pringle also show (see also Perdang 1968), rotation breaks the degeneracy of the zero-frequency modes, producing in addition to the rotationally-modified g-modes a spectrum of toroidal modes with frequencies approximately given by (for uniform rotation)

$$\sigma_{k\ell m} \approx -m\Omega[1-\frac{2}{\ell(\ell+1)}], \quad \ell \neq 0. \tag{8}$$

These are the modes Papaloizu and Pringle have named r-modes. For the case $\ell=1$, (8) still yields zero frequency; in this case a slightly better approximation yields a non-zero result, which, however, is very small (cf. Papaloizu and Pringle 1978).

Papaloizu and Pringle go on to discuss some possible applications of their theory to the interpretation of observational data. In particular, they question whether the 20-30 second oscillations observed in some cataclysmic variables, usually in the post-maximum decline of the light curve, may be r-modes rather than g-modes as conventionally assumed (cf. Warner and Robinson 1972). There are three main points to their argument. First, they point out that although p- and f-modes generally have periods much shorter than 20-30 seconds in hot white dwarfs, the g-mode periods — although much shorter than the ~ 200 second periods found in models with T_{eff} ~

10,000°K — tend still to be longer than 20-30 seconds[2]. Secondly, they note that the timescales over which period changes are observed to occur in the cataclysmic variable stars (often $\lesssim$ 18 hours : cf. Warner 1976b) are enormously short compared to the characteristic e-folding (decay) timescales of the g-modes[2]. Third, they emphasize that the rotation expected in the cataclysmic variable white dwarfs is likely to be rapid enough to invalidate the slow-rotation approximation for g-mode splitting, and may be fast enough to permit the existence of r-modes with periods comparable to those observed.

In order to obtain decay timescales as short as the timescales of observed period changes in the cataclysmic variables, Papaloizu and Pringle argue that it is necessary to consider white dwarf models in which the mass involved in the oscillations is confined to the very outermost surface layers. To this end they have studied the properties of some ℓ=2 g-modes for models with a luminosity source embedded in the outermost $\sim 10^{-10} M_\odot$ of envelopes containing $\sim 10^{-6}$ to $10^{-7} M_\odot$ of hydrogen. These models are intended to simulate accretional heating of the surface layers, and the results indicate decay times as short as $\sim 10^4$ seconds for these highly surface-concentrated modes. For the low-k g-modes the periods are still too long for these models, however.

---

[2]However, see the discussion of accreting white dwarf models with nuclear burning in Section V below, especially the calculations by DeGregoria 1977 and by Sienkiewicz and Dziembowski 1978).

The interaction between the accretion disk and the surface layers of the white dwarf is further elaborated by Papaloizu and Pringle in Appendix 1 of their paper. Here they consider a simple model of the transition layer over which the angular velocity changes from the Keplerian value appropriate to the inner edge of the disk to the slower rotation rate of the star. They show that the perturbation equations for this flow lead to the analogs of Kelvin-Helmholtz instabilities, and they estimate conditions for the onset of instability. In the text of their paper they speculate that either this instability or the direct interaction of the accretion disk with the surface of the white dwarf may be responsible for the excitation of non-radial oscillations of the star, a concept already implicit in the work of Pringle (1977). This process, which is rather similar to the production of musical tones in a flute, represents an important new mechanism for the excitation of stellar oscillations and clearly merits considerably more detailed work. To date only a few papers have seriously considered the complex problems involved in this interaction region. In addition to those works already cited, we must add the fundamental paper of Lynden-Bell and Pringle (1974), the quasi-steady calculations of Durisen (1977), and the recent work by Kippenhahn and Thomas (1978). The latter authors in particular point out that the interface region in disk accretion differs drastically from that involved in spherical accretion flows.

V. Instabilities in Planetary Nucleus Stars and Nuclear-Burning White Dwarfs

To complete this survey of theoretical research on the oscillations of degenerate stars, mention must also be made of recent work on degenerate stars other than the ZZ Ceti variables and the cataclysmics. The two types of systems which have received attention are i) the central stars of planetary nebulae and ii) white dwarfs with H- or He-burning shells, usually thought of as resulting from accretion. To date, these theoretical models have only limited correspondence with the observational data, and for this reason my discussion of them will be brief.

a. Planetary nuclei

Research on the oscillations of planetary nuclei published within the past two or three years has been limited, to this writer's knowledge, to two short papers by Stothers (1977) and by Dziembowski (1978). Stothers' paper is another in his series of applications of T.R. Carson's new radiative opacities (cf. Carson 1976). In this newest work, Stothers finds that the fundamental model of radial pulsation (and in a few cases, the first overtone as well) is excited in very high luminosity degenerate stars by the κ-mechanism operating in the CNO ionization zone. This is a direct consequence of a large "bump" in the Carson CNO opacities that occurs over a wide temperature range aroung 10^6°K at low densities. The region of the H-R diagram in which pulsational instability is driven by this mechanism covers a range in luminosity given by $3.5 \lesssim \log L/L_\odot \lesssim 4$, with effective temperatures cooler than $\log T_{eff} \approx 5.0$, extending at least to the red of $\log T_{eff} \approx 4.65$ and possibly beyond. This is the same region occupied by the highest luminosity central stars of planetary nebulae, and Stothers suggests that this mechanism may perhaps explain some of the rapid vari-

ability that has been observed in some of the planetary nuclei. He quotes the observed timescales of variation as ranging from weeks to perhaps as short as seconds, while the theoretical models yield fundamental mode periods ranging from fractions of an hour to about a day.

Dziembowski's (1978) paper is concerned with short-period variability in FG Sge. Over the period from 1972 to 1975, during which time the spectral type changed from F6 to G2, observations quoted by Dziembowski indicate short-term variability with a period of 60 days in 1972 and 20 days in 1975. He has accordingly carried out calculations of the nonadiabatic pulsational instability of double (H- and He-) shell burning models in order to find the high-luminosity extension of the instability strip. For models with masses between $0.52M_\odot$ and $1M_\odot$ and with luminosities greater than about $10^3 L_\odot$, he finds that nonadiabatic effects are important, and by matching the models to the observed periods he is able to deduce the luminosity and mass of the star. He finds that a 60 day pulsation period can be fitted by a model with $L \approx 6300\ L_\odot$ and $M \approx 0.63\ M_\odot$, while a 20 day period requires $L \approx 1600 L_\odot$, which may be too low for the development of a He shell-flash.

b. Nuclear-burning white dwarfs

In a recent series of papers, Vila and Sion (1976), Sion and Vila (1976), Vila (1977), and DeGregoria (1977) have examined the pulsational and thermal stability of a number of static models of white dwarfs without accretion and with nuclear burning of a H/He envelope assumed to provide the entire luminosity of the star. Vila and Sion (1976) constructed static models with masses of 0.6 and $1.0M_\odot$ in which H shell-burning by pp and CNO reactions in an appropriately chosen envelope provided the only energy source. They found nuclear-energized instability of the fundamental radial (F) mode in the

luminosity interval $0 \leq \log L/L_\odot \leq 3$, with growth timescales of $\sim 10^6$-10^8 years. At $\log L/L_\odot$, the first radial overtone (H_1) mode was also excited, on a timescale of 10^8 years. In a closely related work, Sion and Vila (1976) found nuclear-energized pulsations of the F-mode alone in the range $0 \leq \log L/L_\odot \leq 3$ for models with He-burning shells near the surfaces. Vila (1977) subsequently undertook to examine the thermal stability of the H shell-burning models and came to the unexpected conclusion that the models were all thermally stable. A similar negative result was also found by Sion, Acierno, and Turnshek (1978), who discussed the thermal stability of models having masses $1.2 \leq M/M_\odot \leq 1.38$ and undergoing steady-state accretion with H-burning due to CNO reactions in the envelope as the only energy source. Unfortunately, from the brevity of the description given by these authors, it is unclear whether all of these calculations refer to models undergoing stationary accretion or whether that is only true of some of them. More seriously, it is not clear why the conclusions regarding the lack of thermal instabilities in these models differ from the conclusions for similar models based on the calculations of Sienkiewicz and Dziembowski, discussed below, and from the detailed, time-dependent shell-flash calculations carried out over the past several years, especially by Gallagher and Starrfield (1978), Sparks, Starrfield, and Truran (1977), and references therein. Until the differences are satisfactorily explained, these results must be used with caution.

Another recent paper dealing with nuclear-energized pulsations in white dwarfs is that of DeGregoria (1977), which follows up earlier, similar work by Cameron (1975). DeGregoria has investigated the radial and non-radial pulsational instability of static white dwarf models with masses between 0.6 and $1.4M_\odot$ and in which the sole energy source is

H-burning due to the CN reactions. His models have luminosities ranging from 10^{36} to 10^{38}ergs s^{-1}, and he finds instabilities in both radial and non-radial modes, the models with larger masses being consistently the more unstable. In most of DeGregoria's models, the fundamental radial (F) mode is unstable, with periods of a few seconds and growth times longer than about 10^4years. In models with lower luminosities and higher masses, radial overtones as high as H_3 may be excited, and in cases where the first overtone (H_1) mode is excited, it is found to be far more unstable than the F-mode. In all cases, the ℓ=2 g_1-mode (the only g-mode considered), with periods ~ 5-40 seconds was excited, with very short growth timescales, ranging from less than a week to some tens of years. The ℓ=2 Kelvin- (f-) mode and the p-modes were found always to be stable, however. The results of these calculations were discussed in the context of pulsating X-ray sources.

The final calculations to be discussed here are those of Sienkiewicz (1975) and Sienkiewicz and Dziembowski (1978). In the first of these papers, Sienkiewicz discussed the construction of white dwarf models of masses 1.0 and 1.39$M_\odot$, which are undergoing steady-state accretion with nuclear burning of the material at the same rate as it is accreted. Accretion rates between ~10^{-11} $M_\odot$ yr^{-1} and a few times 10^{-7} $M_\odot$ yr^{-1} were used, and the systematic behaviors of the H- and He- burning shells with accretion rate and stellar mass were studied. In the later paper, Sienkiewicz and Dziembowski (1978) investigated the thermal and vibrational stability of the 1 $M_\odot$ models from Sienkiewicz's accretion calculations. All of the models were found to be thermally unstable, in contrast to the conclusions of Vila (1977), with instability produced by the H-burning shell for $\dot{M} \lesssim 4 \times 10^{-8} M_\odot$ yr^{-1} and by the He-burning shell for $\dot{M} \gtrsim 3 \times 10^{-7} M_\odot$ yr^{-1}. Vibrational instability was

also found at all but the highest accretion rates, but the growth rate of the oscillations was slower than the thermal instabilities, except in the range $4 \times 10^{-8} M_\odot \text{ yr}^{-1} \lesssim \dot{M} \lesssim 3 \times 10^{-7} M_\odot \text{yr}^{-1}$. (see Fig. 6). Both radial and non-radial modes were found to be excited (similar multi-mode excitation has also been found in non-accreting nova and pre-nova models by Sastri and Simon 1973 and by Vemury (1978), although the growth rate of the most rapidly-excited g-modes was more than three orders of magnitude faster than that of the radial modes. The $\ell=1$ g_2-mode was found to be the most unstable, with growth rates of a few months in the range of $\dot{M}$ where pulsations develop more rapidly than thermal instabilities. The periods of these models are about 30 seconds, although a broad spectrum of g-modes corresponding to $\ell=1$-5 and with periods ranging from 10 to 50 seconds is excited simultaneously. Because of the high rates of accretion and nuclear burning in the pulsationally unstable models, the luminosities of these cases are quite large ($L \gtrsim 10^3 L_\odot$, $\log T_{eff} \gtrsim 5$), but because of the simultaneous excitation of many different modes, the pulsations may not be easy to detect observationally despite the high luminosities.

VI. Conclusions And Some Problems That Merit Further Work

Despite the real progress in clarifying the theoretical bases for an understanding of the observed oscillations of white dwarfs, some major problems remain to be resolved before a satisfactory comparison of theory and observation can be achieved. In particular, no theoretical calculation has yet succeeded in demonstrating pulsational instability in the oscillation modes which appear to be excited in these stars. On the positive side,

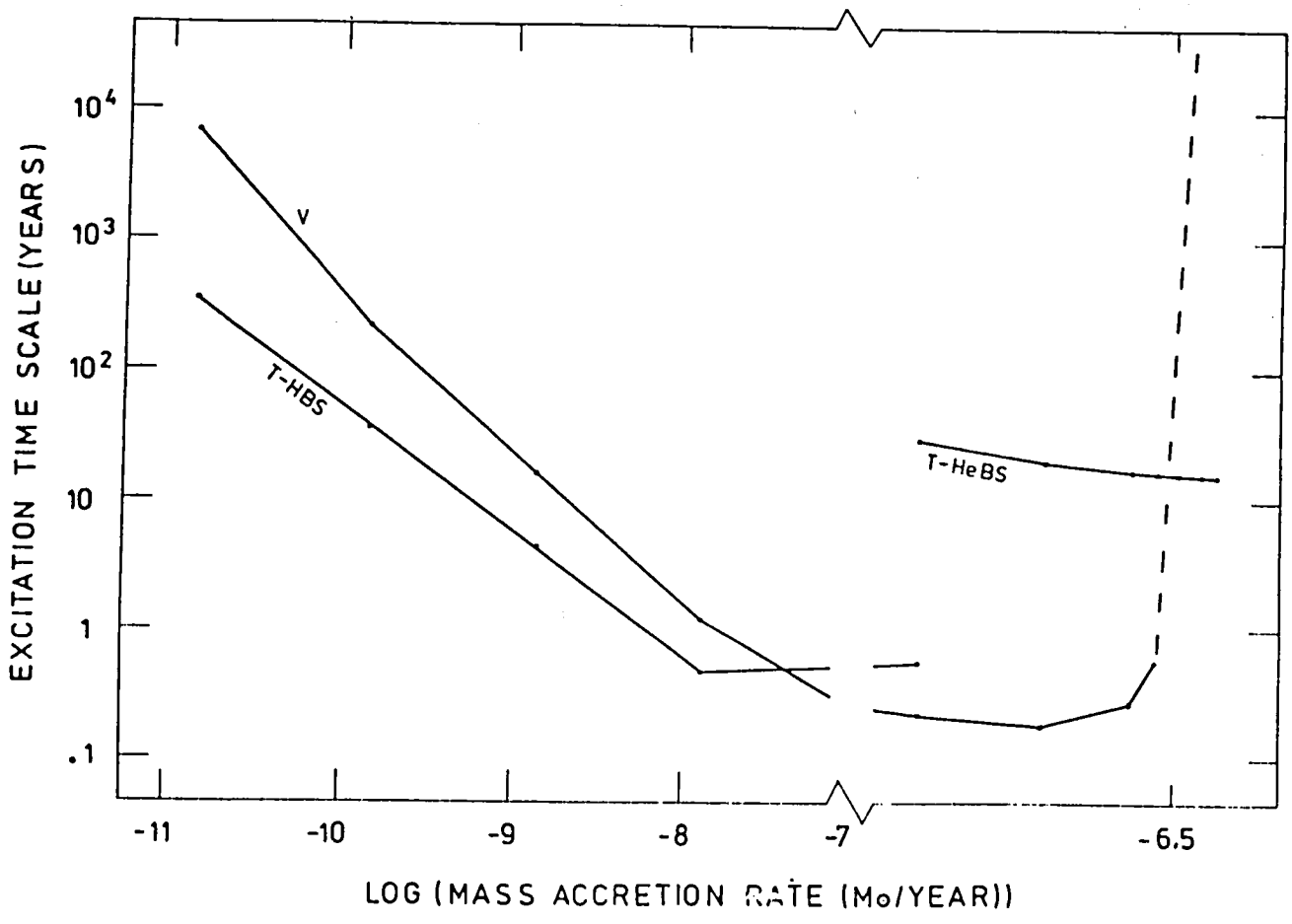

Fig. 6 - Characteristic timescales for the growth of thermal and vibrational instabilities, taken from Sienkiewicz and Dziembowski (1978) for white dwarfs undergoing steady-state accretion and nuclear burning. The curves labelled T-HBS and T-HeBS give the growth timescales for thermal instabilities in the H- and He- burning shells, respectively. The curve marked V gives the excitation timescale for vibrational instability in the most unstable mode; this is the fastest-growing instability for accretion rates in the range $4 \times 10^{-8} M_\odot yr^{-1} \lesssim \dot{M} \lesssim 3 \times 10^{-7} M_\odot yr^{-1}$.

theorists have begun to carry out considerably refined calculations for increasingly realistic stellar models, and some have begun to attack the extremely complex and important problems associated with the effects of rotation on non-radial stellar oscillations. Preliminary work has also been done in a few cases involving accretion and nuclear burning.

Among the many problems that need attention before we can claim an understanding of the oscillations of white dwarfs, the following appear to this writer to be some of the more important ones:

1. How does the layered compositional structure of a white dwarf affect the frequencies and excitation rates of non-radial oscillations? In particular, the location and extent of the He ionization zone is expected to depend rather sensitively upon the thickness of the overlying hydrogen layer; how does this affect the excitation rates? Does the depth of the hydrogen layer determine whether or not a white dwarf lying in the instability strip will be a variable? Also, do the H/He or He/C interfaces introduce additional g-modes ("surface waves") into the non-radial oscillation spectrum? If so, what are the periods of these modes; can they explain the 800-1000 second period oscillations?

2. What effect does the coupling between convection and oscillations have for the white dwarfs? For the purposes of a preliminary investigation of this problem, the use of a very simple form of time-dependent mixing-length theory may be sufficient; certainly this seems to be a logical and necessary first step.

3. From the standpoint of observations, can refined versions of the period-amplitude plot shown in Fig. 4 provide further clues to the nature of the ZZ Ceti oscillations? In addition, is it possible to achieve sufficient frequency resolution in the large-amplitude ZZ Ceti stars to determine

whether the variability of the mode amplitudes observed here is due tp beating between colsely-spaced high -k modes, as the period-amplitude correlations tend to suggest?

4. Also in regard to observations, is Wolff's model of beating between rotationally=split g-modes supported or rejected by observations of the rotation-broadening of the Balmer lines in the ZZ Ceti stars? If it is confirmed, the theoretical basis for the model requires further devleopment.

5. The toroidal r-modes introduced by Paploizu and Pringle need to be investigated carefully in the context of improved stellar models. What are the mode frequencies and excitation rates in such models? Do these modes play a role in the long-period ZZ Ceti stars as well as in the cataclysmic variables? Is there direct observational evidence of the required rotation in either type of system?

6. Can the interaction between the accretion disk and the white dwarf in cataclysmic variables drive oscillations of the star? How can this be calculated, and under what conditions (if any) can such excitation occur?

7. Finally, is there observational evidence for the existence of high-luminosity degenerate variables?

With the interest and activity on problems of white dwarf oscillations that has now been generated, perhaps it is not too much to hope that significant progress is answering these and related questions may be achieved before the next pulsation conference.

Acknowledgments

This work has been supported by the National Science Foundation under grants AST 76-80203 and AST 76-80203 A01.

References

Aizenman, M.L., and Cox, J.P. 1975, Ap.J., 195, 175.

Aizenman, M.L., and Smeyers, P. 1977, Astrophys. Space Sci., 48, 123.

Angel, J.R.P., Illing, R.E., and Landstreet, J.D. 1972, Ap.J., 175, L85.

Baglin, A. 1976, in Multiple Periodic Variable Stars, ed. W.S. Fitch (Reidel: Dordrecht), p. 223.

Brickhill, A.J. 1975, M.N.R.A.S., 170, 405.

Buchler, J.R. 1978, Ap.J., 220, 629.

Cameron, A.G.W. 1975, Astrophys. Space Sci., 32, 215.

Carson, T.R. 1976, Ann. Rev. Astron. Ap., 14, 95.

Chandrasekhar, S. 1961, Hydrodynamic and Hydromagnetic Stability, (Clarendon Press: Oxford).

Christensen-Dalsgaard, J. 1975, M.N.R.A.S., 174, 87.

Cowling, T.G. 1941, M.N.R.A.S., 101, 367.

Cox, J.P. 1974, unpublished lecture notes, University of Colorado.

———. 1976, Ann. Rev. Astron. Ap., 14, 247.

Cox, J.P., and Giuli, R.T. 1968, Principles of Stellar Structure (Gordon and Breach: New York).

DeGregoria, A.J. 1977, Ap.J., 217, 175.

Demaret, J. 1975, Astrophys. Space Sci., 45, 31.

Demaret, J., and Perdang, J. 1978, preprint.

Denis, C. 1975, Mem. Soc. R. Liege, 8° (Belgium), 8, 253.

Deupree, R.G. 1976, in Proc. Solar and Stellar Pulsation Conference, ed. A.N. Cox and R.G. Deupree, LASL report LA-6544-C.

Durisen, R.H. 1977, Ap.J., 213, 145.

Dziembowski, W. 1977a, Acta Astron. 27, 203.

———. 1977b, Acta Astron., 27, 1.

———. 1978, preprint.

Gallagher, J.S., and Starrfield, S.G. 1978, Ann. Rev. Astron. Ap., 16, in press.

Goldreich, P., and Keeley, D.A. 1977a, Ap.J., 211, 934.

———. 1977b, Ap. J., 212, 243.

Gough, D.O. 1977, Ap.J., 214, 196.

Greenstein, J.L., and Peterson, D.M. 1973, Astron. Ap., 25, 29.

Greenstein, J.L., Boksenberg, A., Carswell, R., and Shortridge, K. 1977, Ap.J., 212, 186.

Hansen, C.J., Aizenman, M.L., and Ross, R.R. 1976, Ap.J., 207, 736.

Hansen, C.J., Cox, J.P., and Carroll, B.W. 1978, preprint.

Hansen, C.J., Cox, J.P., and Van Horn, H.M. 1977, Ap.J., 217, 151.

Hendon, A.A., and Cox, A.N. 1976, in Proc. Solar and Stellar Pulsation Conference, ed. A.N. Cox and R.G. Deupree, LASL report LA-6544-C, p.167.

Kippenhahn, R., and Thomas, H.-C. 1978, Astron. Ap., 63, 265.

Koester, D. 1976, Astron. Ap., 52, 415.

Lamb, D.Q., and Van Horn, H.M. 1975, Ap.J., 200, 306.

Ledoux, P. 1951, Ap.J., 114, 373.

———. 1974, in Stellar Stability and Evolution, ed. P. Ledoux, A. Noels, and A.W. Rodgers (Reidel: Dordrecht), p. 135.

Ledoux, P., and Walraven, Th. 1958, Handbuch der Physik, 51, 353.

Liebert, J., Angel, J.R.P., Stockman, H.S., Spinrad, H., and Beaver, E.A. 1977, Ap.J., 214, 457.

Lynden-Bell, D., and Pringle, J.E. 1974, M.N.R.A.S., 168, 603.

McGraw, J.T. 1977, Ph.D. thesis, University of Texas (Austin).

McGraw, J.T., and Robinson, E.L. 1976, Ap.J., 205, L155.

Osaki, Y., and Hansen, C.J. 1973, Ap.J., 185, 277.

Ostriker, J.P., and Bodenheimer, P. 1968, Ap.J., 151, 1089.

Paczynski, B. 1971, Acta Astron., 21, 417.

Papaloizu, J., and Pringle, J.E. 1978, M.N.R.A.S., 182, 423.

Perdang, J. 1968, Astrophys. Space Sci., 1, 355.

Pringle, J.E. 1977, M.N.R.A.S., 178, 195.

Robinson, E.L. 1976, Ann. Rev. Astron. Ap., 14, 119.

———. 1978, this conference.

Robinson, E.L., and McGraw, J.T. 1976, Proc. Solar and Stellar Pulsation Conference, ed. A.N. Cox and R.G. Deupree, LASL report LA-6544-C, p. 98.

Robinson, E.L., Nather, R.E., and McGraw, J.T. 1976, Ap.J., 210, 211.

Sastri, V.K., and Simon, N.R. 1973, Ap.J., 186, 997.

Schatzman, E. 1958, White Dwarfs (North-Holland: Amsterdam).

Shaviv, G., and Kovetz, A. 1976, Astron. Ap., 51, 383.

Sienkiewicz, R. 1975, Astron. Ap., 45, 411.

Sienkiewicz, R., and Dziembowski, W. 1978, preprint.

Simon, N.R. 1977, Astrophys. Space Sci., 51, 205.

Sion, E.M., Acierno, M.J., and Turnshek, D.A. 1978, Ap.J., 220, 636.

Sion, E.M., and Vila, S.C. 1976, Ap.J., 209, 850.

Smeyers, P. 1966, Bull. Acad. R. Belge, Cl. Sc., 5^{me} Série, 52, 1126.

Sparks, W.M., Starrfield, S.G., and Truran, J.E. 1977, in Novae and Related Stars, ed. M. Friedjung (Reidel: Dordrecht), p. 189.

Stothers, R. 1977, Ap.J., 213, 791.

Sweeney, M.A. 1976, Astron. Ap., 49, 375.

Vandakurov, Yu. V. 1977, Soviet Astron. Letters, 3, 249.

Van Horn, H.M. 1976, in Multiple Periodic Variable Stars, ed. W.S. Fitch (Reidel: Dordrecht), p. 259.

Van Horn, H.M., and Savedoff, M.P. 1976, in Proc. Solar and Stellar Pulsation Conference, ed. A.N. Cox and R.G. Deupree, LASL report LA-6544-C, p. 109.

Vauclair, G., and Reisse, C. 1977, Astron. Ap., 61, 415.

Vemury, S.K. 1976, Ap.J., 221, 258.

Vila, S.C. 1977, Ap.J., 217, 171.

Vila, S.C., and Sion, E.M. 1976, Ap.J., 207, 820.

Warner, B. 1976a, in Multiple Periodic Variable Stars, ed. W.S. Fitch (Reidel: Dordrecht) p. 247.

———. 1976b, in Structure and Evolution of Close Binary Systems, ed. P. Eggleton, S. Mitton, and J. Whelan (Reidel: Dordrecht), p. 85.

Warner, B., and Robinson, E.L. 1972, Nature Phys. Sci., 239, 2.

Wolff, C.L. 1974, Ap.J., 193, 721.

———. 1977, Ap.J., 216, 784.

Discussion

Sobouti: I would have to dispute your formula for the expansion of the g-mode. There are certain criteria for any perturbation expansion, which in the case of g-modes are not met. In perturbation expansions, you always have an energy denominator which is the difference of two energies. If you look at the spectra of g-modes, you can find an infinite number of pairs of energy levels which are infinitely small and infinitely close to each other, and if you insert these into the denominator the series won't converge. So the g-modes cannot accept the perturbation expansion.

Van Horn: Thank you, I hope you will say more about this in your paper later on. All I can say is, this is the classical expression that has been quoted since Ledoux.

Sobouti: That formula is fine for p-modes, but not for g-modes, I am afraid.

Van Horn: Will you say something about this in your talk?

Sobouti: I don't know. I am only allowed twelve minutes. [Laughter]

Cahn: Would you like to continue the discussion into the planetary aspects?

Van Horn: I can tell you in one word what I was going to say, and that is that Stothers has looked at some models for planetaries recently using the new Carson opacities, and he finds that a mysterious bump which occurs in those opacities drives instability at high luminosity for an effective

temperature range from 100,000 K down. He doesn't know where it terminates. It is apparently a difference in the Los Alamos opacities and the Carson opacities.

Wolff: I would like to make two further suggestions to the observers about testing this model of mine, which Van Horn summarized so nicely. There may be a tendency for the light curve to repeat itself after an interval of one or two weeks. The precise interval is proportional to the rotation period, and the theory says what this interval is for each star. So, do an auto-correlation of the light curve, displaced by a certain amount, and measure the tendency for repetition. The other suggestion that I would make is that if you observe a few stars intensively, that would be a great deal of help in testing these models.

Nather: I will exercise the Chairman's prerogative and make one comment while the next speaker is coming up here. The one star that has been observed most intensively is R548, and there we do find splitting which is inconsistent with rapid rotation. It has to be slow.

THE PERIOD STRUCTURE OF THE ZZ CETI VARIABLES

John T. McGraw
Department of Astronomy and McDonald Observatory
The University of Texas at Austin

The ZZ Ceti variables are a class of pulsating white dwarfs (cf. the previous review by Robinson) which show a large variety in the appearance of their light curves. The approximate range in amplitude, period and pulse shape is shown in Figure 1 which contains segments of the light curves of HL Tau-76 (the prototypical ZZ Ceti star), GD 154 (the variable with the longest period), and ZZ Ceti itself (R548), the most extensively observed variable. Time-

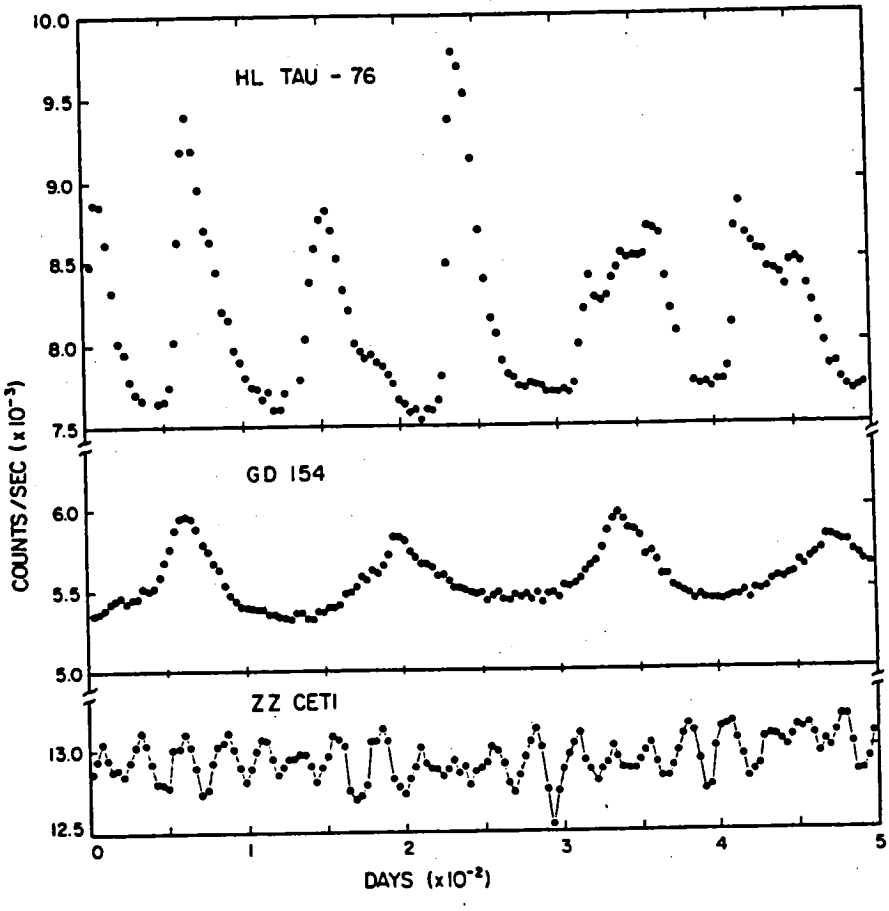

Figure 1: Segments of the light curves of HL Tau-76, GD 154 and ZZ Ceti. The ordinate is expressed in detected photons per second in "white" light, corrected for atmospheric extinction.

resolved photometry in unfiltered light has yielded a wealth of information about the period structure of these stars. Though we are faced by a broad range of period structure, we believe it is possible to explain most of the features of the light curves of ZZ Ceti variables by invoking reasonable mechanisms; we interpret the period structure in terms of nonradial pulsations which are modulated by rotation of the star and which, for the large amplitude variables, can become nonlinear. Theoretical models of pulsating white dwarfs will ultimately confirm or reject our suggestions. The purpose of this paper, then, is to review the current observational status of the period structure of the ZZ Ceti stars. We will discuss in particular those features which appear to be the most important for theory to explain, or which may be relevant to the directions of theoretical development.

The shortest primary period for a ZZ Ceti variable is about 192 s, seen in L19-2, and the longest is the primary period of GD 154, about 1186 s. In general, the light curves of these variables are so complex that, apart from an estimate of the primary period, little can be determined from them directly. Power spectra of the light curves are used to investigate the period structure in detail. Using this technique, the light curve of every ZZ Ceti variable has been shown to contain at least two independent periods, that is, periods which are not simply harmonics. Figure 2 shows a power spectrum of the light curve of L19-2. The ratio of the periods represented by the two prominent peaks in this spectrum is $P_1/P_2 \simeq 194\ s/114\ s \simeq 1.7$.

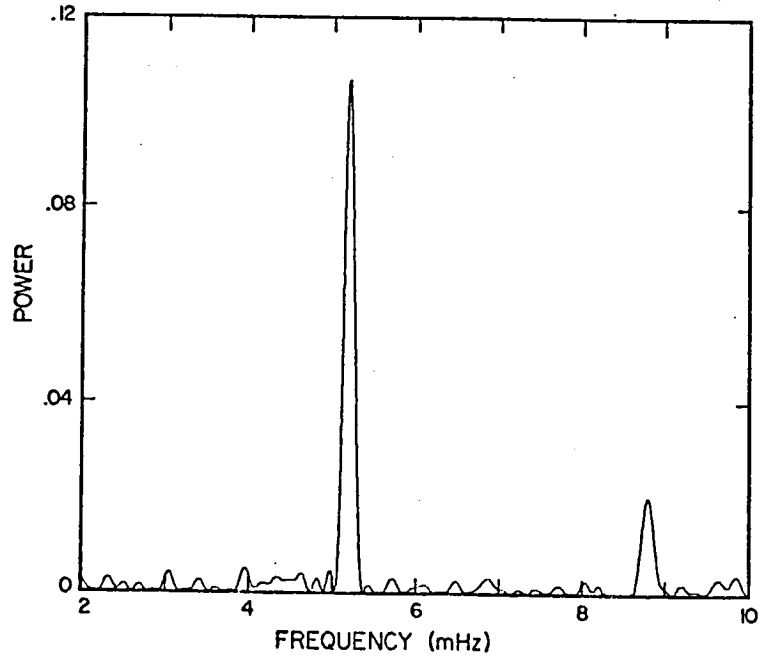

Figure 2: The power spectrum of the light curve of L19-2. The ordinates of all power spectra in this paper are directly comparable.

The variety of photometric complexity seen in the light curves is reflected in their power spectra. Figure 3 shows the power spectra for HL Tau-76, GD 154 and ZZ Ceti.

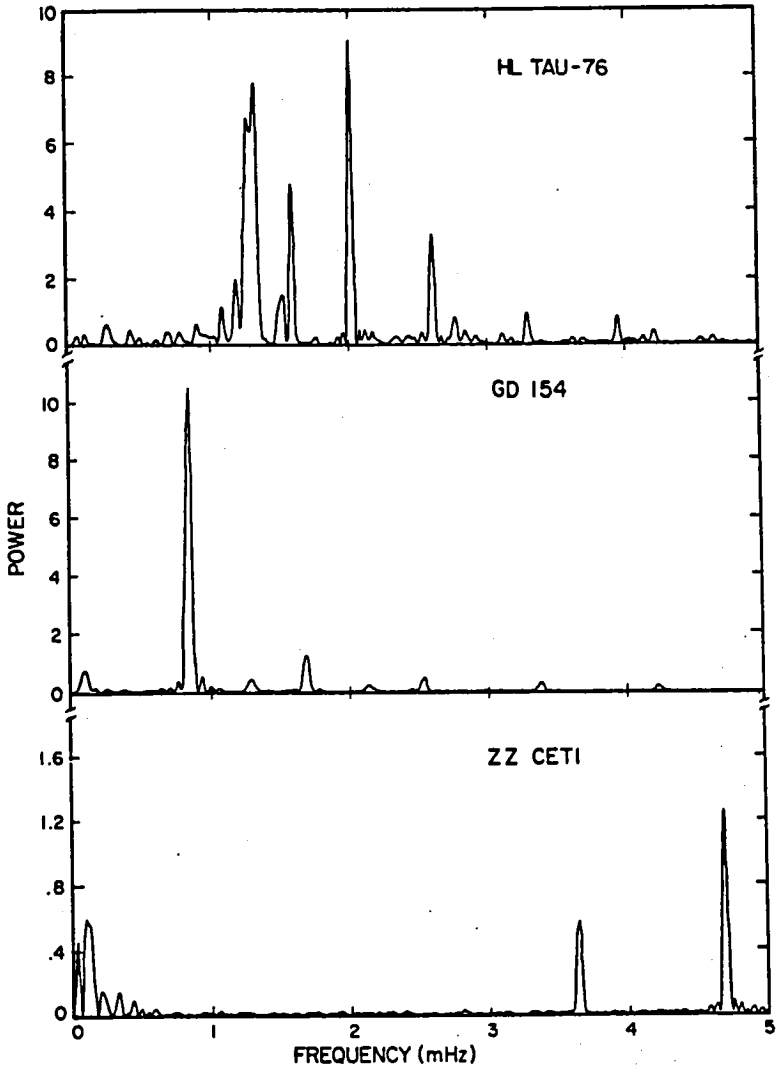

Figure 3: Power spectra of the light curves of HL Tau-76, GD 154 and ZZ Ceti. Segments of the light curves from which these spectra were derived are shown in Figure 1.

This figure illustrates an approximate correlation between the amplitude of the variable and the complexity of its power spectrum: large amplitude variables tend to have complex, multi-peaked spectra while low amplitude variables have simpler spectra with fewer peaks (Robinson and McGraw 1976). Originally it was suggested that this correlation also included the period as a parameter and that large amplitude variables with complex spectra also had long

periods. GD 154, with a spectrum of intermediate complexity (cf. Figure 3), negates this earlier suggestion - amplitude and complexity appear to be the relevant parameters (Robinson et al. 1978).

Power spectra of the light curves of most of the ZZ Ceti variables change on time scales ranging from minutes to days. Two power spectra for one night's data on G29-38 are shown in Figure 4. The light curve, a run of five hours duration, was halved and each half was transformed separately. The two spectra look totally different, showing that significant changes to the period structure of this star occurred

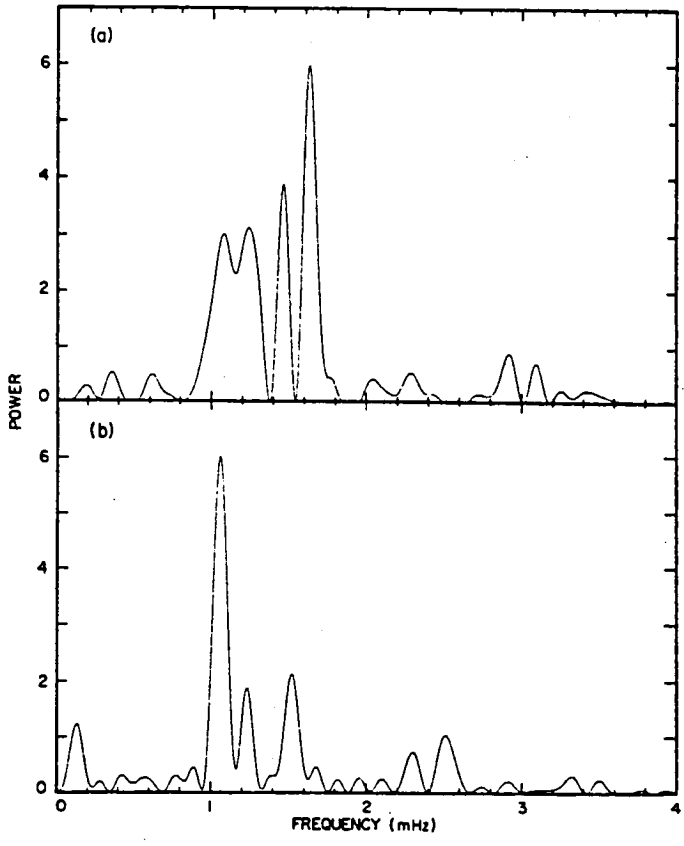

Figure 4: Power spectra of the light curve of G29-38 obtained on one night. These spectra, (a) derives from the first half of the run and (b) from the second, show typical changes in frequency and amplitude which occur during a run.

within this run. Figure 5 shows power spectra derived from runs on two separate nights. Again, there are significant changes in both the frequencies and amplitudes of the peaks in this spectrum.

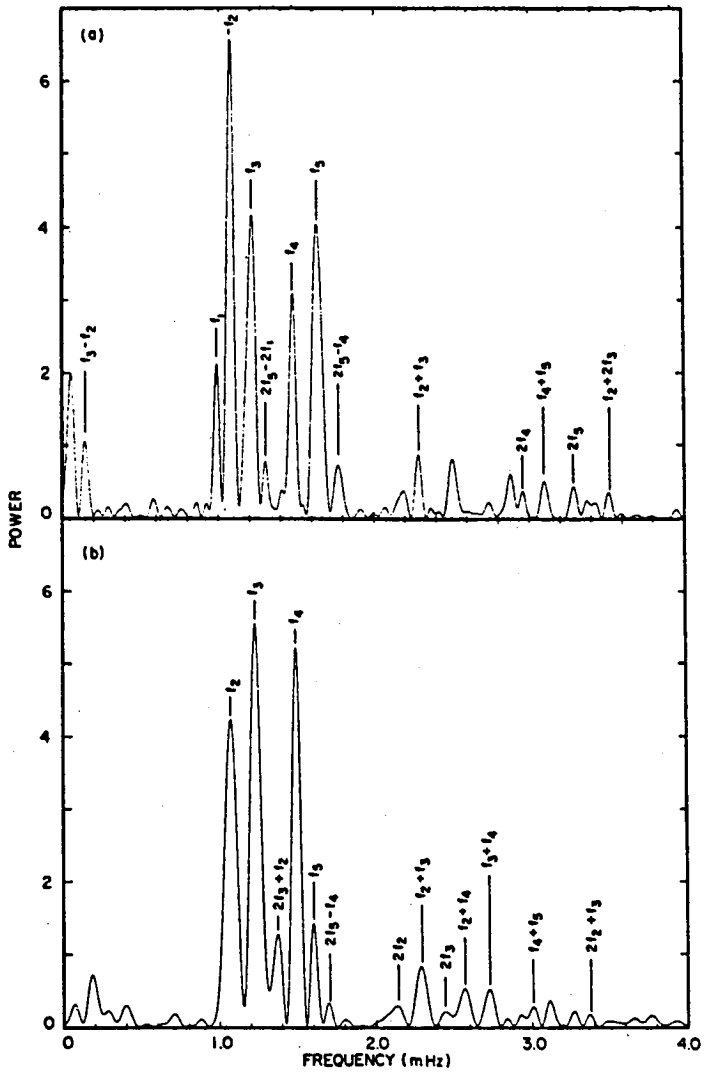

Figure 5: Power spectra of the light curve of G29-38 derived from runs obtained on consecutive nights. Five major peaks and some of the peaks identified with linear combinations of major peaks are indicated.

This figure also illustrates two numerical relationships among frequencies of peaks in the power spectra of several of the ZZ Ceti light curves. The first relationship, the occurrence of "cross-frequencies", is seen in the spectra of about half of the variables. If we pick the one to five strongest peaks in a spectrum and denote the frequencies of these peaks as primary frequencies, some, but not all, of the secondary peaks in the spectrum have frequencies, f, given by a linear combination of primary frequencies: $f = nf_i \pm mf_j$, where i and j specify primary frequencies and n and m are small integers. The second relationship, a pattern of equally spaced frequencies, occurs in the

spectra of G29-38 and two other variables. In Figure 5, the average frequency spacings $\langle f_3 - f_2 \rangle \simeq \langle f_5 - f_4 \rangle \sim 0.14$ mHz and $\langle f_4 - f_3 \rangle \simeq 0.26$ mHz $\simeq 2 \times 0.14$ mHz can be seen.

An additional feature of the period structure of the ZZ Ceti variables has been seen in the light curves of BPM 31594 (McGraw 1976) and GD 154 (Robinson et al. 1978). These stars have been observed to change their primary periods by factors of about 2 and 2/3, respectively, within 24 hours. Figure 6 shows the power spectrum derived from the light curve of BPM 31594 obtained on the discovery night (above) and that from the light curve obtained the next night (below). The primary frequency decreased by a factor of about 1.99 (significantly different from 2), but a smaller peak remained at the approximate frequency seen the first night. In addition, in the later spectra significant power appeared at frequencies near 3/2 and 5/2 the primary frequencies. GD 154 exhibited the opposite behavior. On

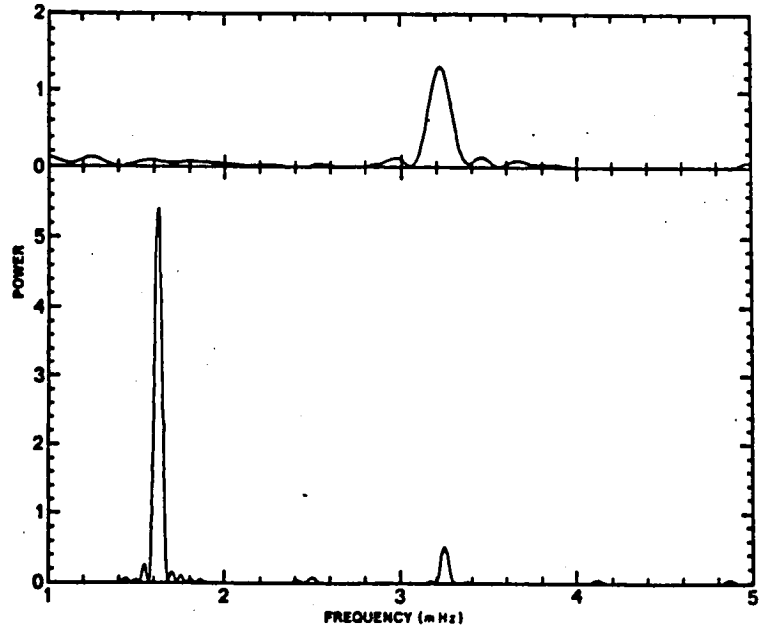

Figure 6: Power spectra of the discovery run (upper) and the run obtained the following night (lower) on BPM 31594. Note the change in frequency of the primary peak in the spectra and the appearance of peaks at frequencies near 3/2, 2, 5/2 and 3 times the frequency of the major peak in the latter spectrum.

the first nine nights it was observed it showed one principal peak and four harmonics of this frequency, plus peaks near 3/2, 5/2 and 7/2 of the principal frequency. On the tenth night it was observed, the peak near 3/2 the frequency of the original principal peak had become the dominant peak in

the spectrum. Since the original ten runs, this star has been observed in each of its "states", showing that the period change is not an isolated incident.

Amidst the photometric complexity, three low amplitude variables, ZZ Ceti, L19-2 and G117-B15A, show a refreshing simplicity and regularity. ZZ Ceti has been shown to be a variable with four very stable periods (Robinson, Nather and McGraw 1976). The periods occur in closely spaced pairs, each pair forming a single peak in a power spectrum derived from a light curve of reasonable ($\lesssim 6^h$) length. The close spacing causes a modulation of the amplitudes and frequencies of the two peaks in the power spectrum ("beating"). The modulation itself has a period of about 1.5 days. Stover et al. (1977) have used data from two observing seasons to show that for each of the four pulsations $Q \equiv |\dot{P}|^{-1} > 10^{11}$. Additional data from Cerro Tololo, supplied by Jim Hesser and Barry Lasker, will extend the baseline of observations to about eight years. On the assumption that $\dot{P}$ reflects the evolution of the star, these data should improve the measurement of Q by another order of magnitude.

Table 1 summarizes the observed photometric properties of the ZZ Ceti stars. GD 154 and BPM 31594 have been included as "moderately" stable pulsators because these stars have been observed to change their basic pulsational periods. When in one "state" the period stability can be very high - a $Q > 10^8$ was derived for GD 154 from an ephemeris constructed for the data gathered on the first nine nights it was observed (Robinson et al. 1978).

TABLE 1

PHOTOMETRIC PROPERTIES OF THE ZZ CETI STARS

Star	Basic Periods (seconds)	Mean Amplitude (magnitude)	Harmonics	Cross-Frequencies	Period Stability	Ref.
BPM 30551	823	0.18	No	No	Moderate	(12, 15)
ZZ Ceti	213, 274	0.02	No	No	$Q > 10^{11}$	(2, 14, 18)
BPM 31594	310, 617	0.21	Yes	No	Moderate	(13)
HL Tau-76	384, 494, 625, 746	0.28	Yes	Yes	Low	(1, 3, 4, 5, 6, 7, 9)
G38-29	925, 1020	0.22	Yes	Yes	Low	(8)
GD 99	350, 476, 595	0.07	Yes	Yes	Moderate	(11)
G117-B15A	216, 272	0.05	No	No	High	(11)
GD 154	780, 1186	0.10	Yes	No	Moderate	(17)
L19-2	114, 192	0.03	No	No	High	(15, 16)
R808	513, 830	0.15	Yes	Yes?	Low	(11)
G207-9	292, 318, 557, 739	0.06	No	Yes	High?	(10)
G29-38	494, 625, 746	0.28	Yes	Yes	Low	(8)

REFERENCES

1) Landolt 1968
2) Lasker and Hesser 1971
3) Warner and Nather 1970
4) Warner and Nather 1972
5) Warner and Robinson 1972
6) Page 1972
7) Fitch 1973
8) McGraw and Robinson 1975
9) Desikachary and Tomaszewski 1975
10) Robinson and McGraw 1976
11) McGraw and Robinson 1976
12) Hesser et al. 1976
13) McGraw 1976
14) Robinson et al. 1976
15) McGraw 1977
16) Hesser et al. 1977
17) Robinson et al. 1978
18) Stover et al. 1978

A rather simple and self-consistent model for the general period structure of the ZZ Ceti variables, incorporating most of the data presented above, can now be proposed. The fact that multiple, highly stable periods occur in these stars definitely confirms that the luminosity variations are produced by pulsations, as has been pointed out earlier by Robinson. Even the shortest ZZ Ceti period is too long by an order of magnitude to be associated with the longest theoretically predicted radial pulsation periods for white dwarfs of reasonable mass (cf. Ostriker 1971), but periods calculated for nonradial modes match more closely. In particular, periods of nonradial g-modes calculated for white dwarfs most closely approximate the periods observed for the ZZ Ceti variables (Brickhill 1975, Osaki and Hansen 1973). The correspondence of the theoretical to the observed periods is not good enough to allow identification of individual pulsation modes, however. For linear, adiabatic pulsations, the period of a nonradial mode is specified by three integers: k, which specifies the radial overtone, ℓ, the number of surface node lines, and the degenerate parameter, m, which may assume values $|m| \leq \ell$. Periods for g-modes on white dwarfs and approximate relationships for g-mode periods as a function of k, ℓ and m are given by Brickhill (1975). For Brickhill's model which most closely resembles a ZZ Ceti ($0.6\ M_\odot$, $T_e = 13000$ K), he derives periods $P_{k\ell} : P_{12} = 136$ s, $P_{22} = 178$ s and $P_{32} = 218$ s. This last period approximates the shortest periods observed in ZZ Ceti variables. Note that there is no a priori or observational limit on k - with $k \lesssim 30$, theoretical periods matching the longest observed periods can be generated. There is, however, an observational constraint on ℓ. If ℓ becomes large, the surface of the star becomes dissected into many segments of varying surface brightness and the luminosity variations will be rapidly smoothed out, thus the star will not be detected as a variable.

Nonradial pulsations can also account for some of the multiple periods seen in the power spectra of ZZ Ceti variables. Multiple, independent pulsations have been suggested to explain the two principal periods (213 s and 274 s) of ZZ Ceti (Robinson, Nather and McGraw 1976) and the four strongest periods in BPM 30551 (Hesser, Lasker and Neupert 1976). For ZZ Ceti, the period ratio indicates that the 213 s period is associated with a $k = 1$, $\ell = 2$ mode and the 274 s period is associated with a $k = 2$, $\ell = 2$ mode. The period ratio of 1.7 for L19-2 might, by analogy, be associated with Brickhill's periods corresponding to modes with $k = 1$, $\ell = 1$ and $k = 1$, $\ell = 2$. Periods of other variables with these period ratios might be associated with similar modes. The point of this is that, though period ratios do recur, the period spectrum of nonradial modes is so complex that, until theory gives us reasons to choose particular modes, the identification of

the modes in which the variables are really pulsating is virtually impossible. The most likely source of multiple, independent periods in low amplitude ZZ Ceti variables is, however, multiple, independent pulsations.

The fact that the power spectra of the light curves of ZZ Ceti stars change with time can be partially explained by nonradial pulsations on a slowly rotating star. Rotation destroys the spherical symmetry of a star, thus removing the degeneracy of the index m. This results in "rotational splitting" of modes with periods $P_{k\ell}$ into additional modes $P_{k\ell m}$: $P_{k\ell m} = 1/\sigma_{k\ell m} = |\sigma_{k\ell} - m\,(1 - C_{k\ell})\Omega|^{-1}$, where $C_{k\ell}$ is a constant which depends on the structure of the star and can assume values $0 \leq C_{k\ell} \leq [\ell(\ell + 1)]^{-1}$, and Ω is the rotational frequency (cf. Brickhill 1975). The closely spaced periods produced by this mechanism can modulate the light curve. For ZZ Ceti, the changes with time seen in the power spectra occur because the period of modulation is greater than the length of a photometric run. If closely spaced periods occur in the power spectra of other ZZ Ceti variables, they too will change with time, as is observed. If observing runs longer than the beat period could be obtained, the power spectra of these stars may appear stable. Robinson et al. (1978) suggest that rotational splitting of the $\ell = 2$ g-mode periods creates the closely spaced pairs of periods in ZZ Ceti. It is reasonable that white dwarfs rotate; therefore, this mechanism almost certainly contributes to the changes in the power spectra. This mechanism is not unique, however. Any periods sufficiently closely spaced, arising for example from two independent pulsation modes, will result in a modulation of the power spectra. Another possibility, which I would rather not admit, is that some of these stars, especially the large amplitude variables, are fundamentally unstable in their period structure.

The period changes observed in the moderate amplitude variables BPM 31594 and GD 154 have been interpreted as a transfer of pulsational energy from one mode to another by (weak) nonlinear coupling (McGraw 1976, Robinson et al. 1978). For radial pulsations, Ledoux and Walraven (1958) derive nonlinear coupling coefficients between modes with frequencies f and f_o: $k(f,f_o) \propto (f - 2f_o)^{-1}$. In the absence of similar theory for nonradial modes, we generalize this to $k(f_i,f_j) \propto (nf_i - mf_j)^{-1}$. The coupling can become very efficient near the resonances. The suggestion is, then, that the observed changes occurred between modes where n = 1 and m = 2. In terms of the indices k, ℓ and m, changes in ℓ and m do not readily account for the observed period changes, but if k is allowed to change value by at least 3, modes near this resonance may be found (McGraw 1976). For larger amplitude variables which are presumably more nonlinear, the coupling is more efficient and periods corresponding to

many resonances can appear. This can explain the appearance of the cross-frequencies observed in the power spectra of larger amplitude variables. In addition, nonlinear pulsations produce nonsinusoidal pulses in the light curve (cf. Figure 1). The pulse shape will then contribute to the frequency structure in the power spectrum. Elementary Fourier analysis tells us that the first additional frequencies to appear will be harmonics of the pulse repetition frequency. These two effects, harmonics and cross-frequencies, both of which are related to increasing nonlinearity, are responsible for the complexity/amplitude correlation. Apparently, ZZ Ceti variables of low amplitude are linear pulsators but large amplitude variables are highly nonlinear.

In summary, the light curves of ZZ Ceti variables range from simple to very complex, but even the most complex can apparently be explained by several simple effects. Multiple nonradial modes, probably corresponding to different radial overtones, may be simultaneously excited in each star. The excitation energy of individual stars is distributed among permitted modes by nonlinear resonant coupling. In addition, "rotational splitting" of the nonradial modes can produce closely spaced periods which results in modulation of the light curve. The amplitude/spectral complexity correlation results from the appearance in the power spectrum of harmonics and cross-frequencies which are the effects brought on by increasing nonlinearity of the pulsations.

When theoretical models of these stars are done, the rewards are likely to be great. Certainly we will increase our understanding of the fundamental evolution of white dwarfs. A program already underway is to directly measure the cooling times of linearly pulsating variables. Osaki and Hansen (1975) have shown that there exists a period-luminosity relationship for nonradial pulsations on white dwarfs. Measuring the highly stable pulsations of stars like R548 over a baseline of 50-100 years will allow a significant determination of the rate of change of the period and thus give a measurement of the cooling time of the star. A more immediate result might be to set limits on the core composition of the variables by measuring the baseline over which $\dot{P}$ does not appear to change. For example, $\dot{P}$ for an iron white dwarf is more than a factor of two greater than for a carbon core white dwarf.

Observers are beginning to find that nonradial pulsations are ubiquitous. In addition to the ZZ Ceti variables they are observed in the β CMa and B stars (Smith 1977). There is evidence that they occur in δ Scuti stars (Millis 1973), they have been suggested as the pulsation modes of white dwarfs in cataclysmic variables (Chanmugam 1972, Warner and Robinson 1972), and of course they occur in the sun (cf.

Rhodes, Ulrich and Simon 1977). Because of their short periods and the ease with which they can be observed, the ZZ Ceti stars are probably the most extensively observed class of nonradially pulsating stars. When the theory of pulsation on these stars can explain the observations, the ZZ Ceti stars will be a laboratory of linear and nonlinear nonradial pulsations, from which investigations into the pulsational instabilities in other stars may be firmly launched.

REFERENCES

Brickhill, A. J. 1975, M.N.R.A.S., 170, 405.
Chanmugam, G. 1972, Nature, 236, 83.
Desikachary, K. and Tomaszewski, L. 1975, IAU Colloq. No. 29, p. 283.
Fitch, W. S. 1973, Ap. J. (Letters), 181, L95.
Hesser, J. E., Lasker, B. M., and Neupert, H. E. 1976, Ap. J., 209, 853.
_____. 1977, Ap. J. (Letters), 215, L75.
Landolt, A. U. 1968, Ap. J., 153, 151.
Lasker, B. M. and Hesser, J. E. 1971, Ap. J. (Letters), 163, L89.
Ledoux, P. and Walraven, Th. 1958, Handbuch der Physik, 51, 353.
McGraw, J. T. 1976, Ap. J. (Letters), 210, L35.
_____. 1977, Ap. J. (Letters), 214, L123.
McGraw, J. T. and Robinson, E. L. 1975, Ap. J. (Letters), 200, L89.
_____. 1976, Ap. J. (Letters), 205, L155.
Millis, R. L. 1973, P.A.S.P., 85, 410.
Osaki, Y. and Hansen, C. J. 1973, Ap. J., 185, 277.
Ostriker, J. P. 1971, Ann. Rev. Astron. and Astrophys., 9, 353.
Page, C. G. 1972, M.N.R.A.S., 159, 25p.
Rhodes, E. J., Jr., Ulrich, R. K. and Simon, G. W. 1977, Ap. J., 218, 901.
Robinson, E. L. and McGraw, J. T. 1976, Ap. J. (Letters), 207, L37.
Robinson, E. L., Nather, R. E. and McGraw, J. T. 1976, Ap. J., 210, 211.
Robinson, E. L., Stover, R. J., Nather, R. E. and McGraw, J. T. 1978, Ap. J., 220, 614.
Smith, M. A. 1977, Ap. J., 215, 574.
Stover, R. J., Robinson, E. L., and Nather, R. E. 1977, P.A.S.P., 89, 912.
Warner, B. and Nather, R. E. 1970, M.N.R.A.S., 147, 21.
_____. 1972, M.N.R.A.S., 156, 1.
Warner, B. and Robinson, E. L. 1972, Nature, 239, 2.

Discussion

Aizenman: You mentioned that the m = 0 mode was missing. Would you explain this further?

McGraw: Well, I'll try. When we see patterns of what we call equally spaced frequencies in the power spectrum, we generally assume an $\ell = 2$ mode and that what we are seeing is $m = \pm 2, \pm 1$, but in two cases that I can recall the m = 0 mode would be missing in that interpretation. I have no idea why that kind of selection would occur. In the case of ZZ Ceti, the detailed analysis of its light curve showed a high stability, and an attempt was made at mode identification, in which case the m = 2 mode was picked. But we can't really give a justification why the m = 0,1 modes aren't present as well.

A. Cox: I want to ask a technical question. Where are your side bands? Why don't you have side bands on all these? Aliases?

McGraw: You do have to contend with them, but the amplitude is very low. We have long data streams to begin with, and we "window" the data. I think what you are driving at is whether we are seeing significant peaks.

A. Cox: I was just wondering why you don't have those wiggles on the side?

McGraw: They are very low amplitude, compared to the amplitudes that we are measuring.

THE g-MODES OF WHITE DWARFS*

Y. Sobouti, M.R.H. Khajehpour and V.V. Dixit

Department of Physics and Biruni Observatory

Pahlavi University, Shiraz, Iran

SUMMARY

The neutral g-modes of a degenerate fluid at zero temperature are analyzed. The g-modes of a degenerate fluid at finite but small temperatures are then expanded in terms of those of the zero temperature fluid. For non-relativistic degenerate fluids it is found that (a) the g-eigenvalues are proportional to $T\,\mu_e^6\,\mu_i^{-1}$, where T is the internal temperature of the fluid, μ_e and μ_i are the mean molecular weights of electrons and ions, respectively; (b) the ion pressure is solely responsible for driving the g-modes. For white dwarfs of about a solar mass,the periods of the g-oscillations are in the range of a few hundred of seconds.

I. INTRODUCTION

It has been suggested that the short period oscillations observed in the cataclysmic variables are connected with the g-modes of the white dwarf component of these objects (e.g. Warner and Robinson, 1972; Osaki and Hansen, 1973). The thrust of the argument behind this suggestion is that the observed periodicities, of the order of several tens of seconds, are too long to be attributed to the p-modes. In connection with the longer periodicities of DA white dwarfs, of the order of several hundreds of seconds, some authors have also called upon the

---

*Contribution No. 4, Biruni Observatory

g-modes. For example, Wolff (1977) has proposed that the interaction of a slow rotation with the g-modes is capable of accounting for such periodicities. Most of these propositions have, at most, had partial acceptability by investigators in the field. Modifications to the theories have been proposed (e.g., Papaloizou and Pringle, 1978), and alternative explanations, not requiring the intervention of g-modes, have been put foreward (e.g., Bath 1973, and Bath et al., 1974).

In recent years, Baglin and Schatzman (1969) have calculated some g-frequencies of white dwarfs with finite temperatures, Harper and Rose (1970). Osaki and Hansen (1973), and Brickhill (1975), each have analyzed the problem in varying details. Practically all previous works on non-radial oscillations of white dwarfs are attempts to integrate the differential equations governing the small displacements of the fluid. Some information on the eigenfrequencies and, to a lesser extent, on the eigenfunctions has been accumulated over the years.

The authors wish to draw attention to an alternative approach to the problem: The operator generating small displacements of a fluid, including those of a degenerate structure, is self-adjoint (Chandrasekhar, 1964). The normal modes of the fluid belong to a Hilbert space. If there is access to a basis set for this space, then one can expand the actual eigendisplacements of the fluid in terms of this basis set, transform the differential equations of motions into a matrix equation, and obtain the expansion coefficients by variational calculations. This alternative route is followed in the present paper. It provides more information on the eigenvalues and eigenfunctions of the system, and gives deeper insight into their behavior and their dependence on the physical properties of the fluid.

(6) is an exact solution of Equations (1) corresponding to $\varepsilon = 0$. This completes the demonstration of the existence of neutral modes in the zero temperature fluid, the neutral g-modes.

IV. THE BASIS-SET

The neutral state of the zero temperature fluid is infinitely degenerate. Any displacement vector $\underset{\sim}{\xi}$ satisfying Equation (6), but otherwise arbitrary, is an eigenfunction of $\varepsilon = 0$. Sobouti (paper I) has used this arbitrariness to propose a set of basis-vectors for the space of the g-modes of the neutral fluid. Thus, let $\underset{\sim}{\xi}^j$, $j = 1,2,\ldots$, have the following spherical harmonic expansion

$$\underset{\sim}{\xi}^j : \left(\frac{\psi^j(r)}{r^2} Y_\ell^m , \frac{1}{\ell(\ell+1)} \frac{\chi^{j\prime}(r)}{r} \frac{\partial Y_\ell^m}{\partial \theta} , \frac{1}{\ell(\ell+1)} \frac{\chi^{j\prime}(r)}{r} \frac{1}{\sin\theta} \frac{\partial Y_\ell^m}{\partial \phi}\right), \qquad (11a)$$

where $\chi' = d\chi / dr$.

Substitution of Equation (11a) in Equation (6) gives

$$\chi^{j\prime} = \psi^{j\prime} + \frac{\rho'}{\rho} \psi^j. \qquad (11b)$$

One of the two functions ψ^j and χ^j could be chosen arbitrarily. Equation (11b) can then be used to obtain the other one. One now appreciates the immense simplification that Equation (6), or equivalently Equation (11b), brings into the problem. These equations reduce the task of specifying a vector $\underset{\sim}{\xi}^j$ to the determination of only one scalar function, ψ^j, say. The following expression for ψ^j is used in the numerical calculations of this paper:

$$\psi^j = -\frac{3}{4\pi G} pp'\rho^{-2} r^{\ell+2j-2} , \quad j = 1,2,\ldots. \qquad (11c)$$

We note the following: (a) On the surface of star ψ vanishes, while χ', the non-radial component of the displacement, remains finite. (b) The exponent of r is chosen such that $\underset{\sim}{\nabla}.\underset{\sim}{\xi}$ behaves as r^ℓ near the origin and is an even or odd polynomial depending on whether ℓ is even or odd; these properties are shown to be required by Hurley, Roberts and Wright (1966). (c) The polynomials in r are helpful in acheiving the completeness of the proposed vectors of

II. THE MODEL AND THE EQUATIONS OF MOTION

A fluid consisting of non-relativistic degenerate electrons and non-degenerate ions will be considered. It will be assumed that the temperature is constant throughout the fluid, except in a thin envelope. In this envelope, the temperature will decrease to zero in a manner determined by whether the envelope is in convective or in radiative equilibrium.

i) Equations of Motion: Adiabatic Lagrangian displacements of the fluid, $\underset{\sim}{\xi}(\underset{\sim}{r})\ \exp(i\ \varepsilon^{1/2}\ t)$, are governed by the following equations:

$$\mathcal{W}\underset{\sim}{\xi} = \varepsilon\rho\underset{\sim}{\xi}, \tag{1a}$$

where

$$\mathcal{W}\underset{\sim}{\xi} = \underset{\sim}{\nabla}\delta p - \frac{1}{\rho}\delta\rho\underset{\sim}{\nabla}p - \rho\underset{\sim}{\nabla}\delta\Omega, \tag{1b}$$

$$\delta\rho = -\rho\underset{\sim}{\nabla}.\underset{\sim}{\xi} - \underset{\sim}{\nabla}\rho.\underset{\sim}{\xi}, \tag{2a}$$

$$\delta p = -\left(\frac{\partial p}{\partial\rho}\right)_{ad}\rho\underset{\sim}{\nabla}.\underset{\sim}{\xi} - \underset{\sim}{\nabla}\rho.\underset{\sim}{\xi}, \tag{2b}$$

$$\nabla^2\delta\Omega = -4\pi G\delta\rho, \tag{2c}$$

and ρ, p and Ω are the density, pressure and gravitational potential of the fluid in hydrostatic equilibrium, respectively.

ii) The Equation of State: The pressure of the fluid is the sum of the partial pressures of the degenerate free electronsand the non-degenerate ions. Thus,

$$p(\rho,T) = p_e(\rho,T) + p_i(\rho,T). \tag{3a}$$

No correction for charge separation is allowed in Equation (3a). The number density of the free electrons and the positive ions is assumed to be proportional to each other, so as to maintain macroscopic charge neutrality. Therefore, both p_e and p_i are given in terms of the same density ρ. At temperatures

T, much below the Fermi temperature T_F of electrons, temperature corrections in p_e are of the order of $(T/T_F)^2$. In contrast, the ions treated as a perfect gas have their pressure p_i proportional to the temperature. Thus, up to and including the first order terms in T/T_F, Equation (3a) gives

$$p(\rho,T) = p_e(\rho) + \frac{k}{\mu_i H}\rho T = \frac{k}{\mu_e H}\rho T_F\left[\frac{2}{5} + \frac{\mu_e}{\mu_i}\frac{T}{T_F}\right] \quad , \quad T_F \propto \rho^{2/3}, \qquad (3b)$$

where the first term on the right hand side is the electron pressure at zero temperature, μ_e and μ_i are the mean molecular weights of electrons and ions, k and H are the Boltzmann constant and the mass of hydrogen atom, respectively. As a simplifying assumption, μ_e and μ_i will be considered to be constant throughout the star and also in the course of any thermodynamic process which may take place in it.

iii) The Adiabatic Processes: The entropy of the fluid is the sum of the electronic and ionic contributions, s_e and s_i, respectively. Thus, the change in the entropy is

$$ds = ds_e + ds_i. \qquad (4a)$$

For the unit mass of ions, treated as a perfect gas, one has

$$ds_i = \frac{k}{\mu_i H}\left(\frac{3}{2}\frac{dT}{T} - \frac{d\rho}{\rho}\right). \qquad (4b)$$

The entropy per unit mass of non-relativistic degenerate electrons is $s_e = (\frac{1}{2}\pi^2 k/\mu_e H)T/T_F$ (see for example, Landau and Lifshitz, 1959; Morse, 1965). From the last expression, and considering the fact that T_F is proportional to $\rho^{2/3}$, one obtains

$$ds_e = \frac{1}{2}\pi^2\frac{k}{\mu_e H}\frac{T}{T_F}\left[\frac{dT}{T} - \frac{2}{3}\frac{d\rho}{\rho}\right] = \frac{\pi^2}{3}\frac{\mu_i}{\mu_e}\frac{T}{T_F}ds_i. \qquad (4c)$$

One observes that (a) ds_e is smaller than ds_i by a factor of T/T_F, and (b) in the course of an adiabatic process (in which by definition $ds = 0$) both ds_e and

ds_i vanish simultaneously. These results simplify the forthcoming calculations considerably. Thus, one obtains

$$\left(\frac{\partial p}{\partial \rho}\right)_{ad} = \left(\frac{\partial p_e}{\partial \rho}\right)_{s_e} + \left(\frac{\partial p_i}{\partial \rho}\right)_{s_i} = \frac{5}{3}\frac{p_e}{\rho} + \gamma \frac{p_i}{\rho}, \tag{5}$$

where $\gamma = 5/3$ is ratio of the specific heats of the ion gas.

III. THE NEUTRAL MODES OF THE ZERO TEMPERATURE FLUID

At zero temperature the g-modes of a degenerate fluid are neutral, that is, the g-eigenvalues become zero (e.g., Harper and Rose, 1970). We intend to analyze these neutral modes in some detail and subsequently use them as a basis set to expand the modes of the finite temperature model. The formalism is the same as that of Sobouti (1977a, henceforth referred to as paper I) for the g- and p-modes of ordinary fluids.

Let us investigate if there is a displacement $\underset{\sim}{\xi}(\underset{\sim}{r}) \neq 0$ which is a solution of Equation (1) and for which the corresponding $\delta\rho$ is zero. This last condition, by Equation (2a), requires that

$$\delta\rho = -\rho \underset{\sim}{\nabla}.\underset{\sim}{\xi} - \underset{\sim}{\nabla}\rho.\underset{\sim}{\xi} = 0. \tag{6}$$

Substitution of Equation (6) in Equation (2b) gives

$$\delta p = -\left[\left(\frac{\partial p}{\partial \rho}\right)_{ad} - \left(\frac{\partial p}{\partial \rho}\right)_{st}\right] \rho \underset{\sim}{\nabla}.\underset{\sim}{\xi}, \tag{7}$$

where we have utilized the fact that in hydrostatic equilibrium p is a function of ρ alone and $\underset{\sim}{\nabla}P = (\partial p/\partial\rho)_{st}\underset{\sim}{\nabla}\rho$. The expression $(\partial p/\partial\rho)_{st}$ is the derivative of p with respect to ρ as prevailing in the equilibrium structure. The subscript "st" is inserted to distinguish this derivative from the adiabatic derivative $(\partial p/\partial\rho)_{ad}$. From Equation (3b) one has

$$\left(\frac{\partial p}{\partial \rho}\right)_{st} = \left(\frac{\partial p_e}{\partial \rho}\right)_{st} + \frac{k}{\mu_i H} T + \frac{k}{\mu_i H} \rho \left(\frac{\partial T}{\partial \rho}\right)_{st}. \tag{8a}$$

The first derivative on the right hand side of Equation (8a) will be calculated for the zero-temperature structure and is equal to $\frac{5}{3} p_e/\rho$. With regards to $(\partial T/\partial \rho)_{st}$, let us define γ' as follows:

$$\left(\frac{\partial T}{\partial \rho}\right)_{st} = (\gamma' - 1)\frac{T}{\rho} . \tag{8b}$$

We observe that in the isothermal core, $\gamma' = 1$. In the envelope, where the temperature decreases outwards, one has the following information: (a) In any region in convective equilibrium, $\gamma' > \gamma$. (b) In any convectively neutral region, $\gamma' = \gamma$. (c) In any region in radiative equilibrium, $\gamma' < \gamma$. From the theory of g-modes in ordinary fluids one knows that in case (a) some unstable g-motions (or g-modes, if they develop into standing patterns) arise. These are, however, confined to the convective layers. In case (c) stable g-modes develop and again are confined to the radiative region. We shall assume that the envelope is convectively neutral, case (b). By this assumption the envelope will not contribute to the g-modes of the system and the role of the degenerate core will be singled out. In view of these considerations, Equation (8a) becomes

$$\left(\frac{\partial p}{\partial \rho}\right)_{st} = \frac{5}{3}\frac{p_e}{\rho} + \frac{p_i}{\rho} , \text{ in the core,} \tag{8c}$$

$$= \frac{5}{3}\frac{p_e}{\rho} + \gamma'\frac{p_i}{\rho} , \text{ in the envelope.} \tag{8d}$$

Substitution of Equations (5), (8c) and (8d) in Equation (7) gives

$$\delta p = -(\gamma - 1)p_i \nabla\cdot\xi = -(\gamma - 1)\frac{k}{\mu_1 H} T \rho \nabla\cdot\xi, \text{ in the core,} \tag{9a}$$

$$= 0, \text{ in the envelope } (\gamma = \gamma'). \tag{9b}$$

This completes the reduction of δp. From Equations (2c) and (6) one has

$$\delta\Omega = 0. \tag{10}$$

We now observe that at zero temperature, $\delta\rho$, δp, and $\delta\Omega$, generated by the displacements prescribed by Equation (6), vanish identically. Thus ξ of Equation

Equations (11) in the g-subspace of the normal modes of the neutral-fluid. The completeness of the proposed vectors, though not yet estabilished theoretically, has, however, been born out by numerical computations of Sobouti (1977b) and of this paper. Variational calculations with the basis vectors of Equations (11) enable one to isolate the g-modes of a fluid systematically and with satisfactory accuracies.

We have only discussed the g-modes of the neutral fluid. A second basis set for the p-modes can be generated from the requirement that the p-set is orthogonal to the g-set. These two basis sets may then be used to expand the eigendisplacement vectors of any other fluid at finite temperatures (see paper I for the p-basis set and for further details). Silverman and Sobouti (1978), and Sobouti and Silverman (1978) have carried out such an expansion for ordinary fluids. Their analysis shows that in the limit of small departures from the neutral state (the limit of small T in the present problem), the g-modes, as given in terms of the vectors of Equations (11), are independent of the p-basis vectors. This property stems from the fact that the g-states at $T = 0$ are degenerate. In the language of linear vector spaces, to a degenerate state there corresponds a subspace of the normal modes of the system. The effect of a small perturbation is to specify the principal directions of this subspace but it leaves the subspace unaltered. Thus, up to the order T/T_F, the g-eigendisplacements can be expanded in terms of the basis set of Equation (11) alone. No intervention of the p-basis set will be necessary.

V. THE EQUATION GOVERNING THE g-MODES:

Let $\underset{\sim}{\xi}^j$, $j = 1,2,\ldots$ be a sequence of the g-eigendisplacements of the finite temperature fluid. The Eulerian variations $\delta\rho$, δp and $\delta\Omega$, generated by these vectors are given by Equations (6), (9) and (10), respectively. Substitution of these in Equations (1) gives

$$\mathcal{W}\underset{\sim}{\xi}^j = \underset{\sim}{\nabla}\delta^j p = \varepsilon^j \rho \underset{\sim}{\xi}^j. \tag{12}$$

The density ρ in Equation (12), and in Equation (9) for $\delta^j p$, is the density of the zero temperature fluid. This does not imply, however, that the density and the pressure are approximated by their values at $T = 0$. We have been able to show that Equation (12) is correct up to the terms of first order in T/T_F. The terms arising from δp, $\delta\rho$ and $\delta\Omega$ in Equations (1), on account of the fact that the density distribution at $T \neq 0$ is different from that at $T = 0$, cancel out each other.

Let $\underset{\sim}{\xi}^j$ have the following expansion in terms of the basis set of Equations (11):

$$\underset{\sim}{\xi}^j = \Sigma \underset{\sim}{\zeta}^k Z^{kj}; \; k, j = 1,2, \ldots. \tag{13}$$

The expansion coefficients Z^{kj} can be considered as the elements of a matrix Z. Thus,

$$Z = \left[Z^{kj} \right]; \; k, j = 1,2, \ldots . \tag{14a}$$

Each column of Z is an eigenvector of the system. Let E be the diagonal matrix of the eigenvalues ε^j,

$$E = \left[\varepsilon^j \right]^{\text{diagonal}}; \; j = 1,2, \ldots . \tag{14b}$$

In connection with Equation (13), let us introduce the following matrices:

$$W^{kj} = \int \underset{\sim}{\zeta}^{k*} . \mathcal{W} \underset{\sim}{\zeta}^j dv, \tag{15a}$$

$$S^{kj} = \int \rho \underset{\sim}{\zeta}^{k*} . \underset{\sim}{\zeta}^j dv. \tag{15b}$$

We are now ready to convert the differential Equation (12) into an equivalent matrix equation. Let us substitute Equation (13) in Equation (12), premultiply the resulting equation by ζ^{i*} (say), and integrate over the volume of the fluid. We obtain the (i,j)th element of the following matrix Equation:

$$WZ = SZE. \tag{16a}$$

The matrix Z simultaneously diagonalizes W and S. A normalization condition on the eigendisplacements $\underset{\sim}{\xi}^j$, or on the eigenvectors Z, could be imposed such that S diagonalizes to a unit matrix I (see Silverman and Sobouti, 1978). Thus

$$Z^{\dagger} S Z = I. \tag{16b}$$

Given the matrices W and S, the eigenvalue matrix E and the eigenvector matrix Z can be solved from Equations (16).

The W-and S-Matrices: From Equations (15a), (12), and (9), after an integration by parts, one obtains

$$W^{kj} = \int (\gamma - \gamma') \; p_i \underset{\sim}{\nabla}\cdot\underset{\sim}{\xi}^{k*} \; \underset{\sim}{\nabla}\cdot\underset{\sim}{\xi}^{j} dv, \tag{17a}$$

where γ' is defined by Equation (8b). The value of γ' is equal to unity in an isothermal core; and is equal to γ, the ratio of specific heats of ions, in a convectively neutral envelope. Substitution of Equation (11) in Equation (17a) and an integration over the solid angle gives

$$W^{kj} = (\gamma - 1) \frac{kT}{\mu_i H} \int_0^R \frac{\rho 12}{\rho} \psi^k \psi^j \, r^{-2} \, dr, \tag{17b}$$

where R is the radius of the star. The assumption of a convectively neutral envelope confines the domain of integration to the core of the star. (i) The thickness of the envelope, however, is proportional to T and to R/M. The latter is, in turn, proportional to T_{Fc}^{-1}. Therefore, the ratio of the thickness of the envelope to the radius of the star is of the order of T/T_{Fc}. (ii) The density, temperature, and pressure tend to zero at the surface. These two factors make the contribution of the envelope to the W-matrix of the second order in T/T_{Fc}. Therefore, extending the domain of integration over the whole star does not introduce first order errors. This completes the reduction of the W-matrix. For the S-matrix, after an integration over the angles, one gets

$$S^{kj} = \int_o^R \rho\left[\frac{\psi^k\psi^j}{r^2} + \frac{1}{\ell(\ell+1)} \chi^{k'}\chi^{j'}\right] dr. \qquad (18)$$

The symmetry and positive definiteness of the W-and S-matrices are manifest from Equations (17) and (18).

VI. SOME PROPERTIES OF THE EIGENVALUES AND EIGENVECTORS

i) The Sign and the Asymptotic Behavior of the Eigenvalues: From Equations (12) and (9) one can readily write down the following integral expression for ε^j:

$$\varepsilon^j = (\gamma - 1)\frac{kT}{\mu_i H}\int \rho\nabla.\underset{\sim}{\xi}^{j*}\nabla.\underset{\sim}{\xi}^j dv \Big/ \int \rho\underset{\sim}{\xi}^{j*}.\underset{\sim}{\xi}^j dv. \qquad (19)$$

Either from Equation (19) or from Equations (17) and (18) for the W-and S-matrices, one can draw the following conclusions:

a) The numerator and the denominator in Equation (19) are both positive for any $\underset{\sim}{\xi}^j$, or, the W-and S-matrices are symmetric and positive definite. Therefore, all eigenvalues ε^j are positive. That is, the g-modes of a degenerate fluid are all stable. This, of course, is not surprising. The g-modes are prototypes of convective motions. An isothermal core is highly subadiabatic and is stable against convective motions.

b) In Equation (19), as the mode-number j increases, the numerator becomes progressively smaller than the denominator. This can be seen from Equations (17b) and (18), where the integrations over the solid angles have been carried out. This asymptotic behavior is well estabilished for the g-modes of ordinary fluids (e.g., Ledoux and Walraven 1958).

ii) The Unit and the Order of Magnitude of the Eigenvalues: In Equation (19), let us use a dimensionless radius variable x = r/R. Thus, one obtains

$$\varepsilon^j = (\gamma - 1)\frac{k}{\mu_i H}\frac{T_{Fc}}{R^2}\frac{T}{T_{Fc}}\epsilon^j, \qquad (20a)$$

$$\epsilon^j = \int \rho \nabla_x \cdot \underset{\sim}{\xi}^{j*} \nabla_x \cdot \underset{\sim}{\xi}^j d^3x \Big/ \int \rho \underset{\sim}{\xi}^{j*} \cdot \underset{\sim}{\xi}^j d^3x, \qquad (20b)$$

where T_{Fc} is the Fermi temperature at the center. In Equation (20a) the factors (T/T_{Fc}) and ϵ^j are dimensionless. The first of these factors depends on the model under study. The second factor is calculated for a zero temperature star and is given in Tables1,2, and 3. The remaining factor in Equation (20a) has physical dimensions. On expressing T_{Fc} and R in terms of the central density ρ_c (see Chandrasekhar, 1939) one gets

$$\varepsilon^j = \frac{4\pi G\rho_c}{\eta_1^2} (\gamma - 1) \frac{\mu_e}{\mu_i} \frac{T}{T_{Fc}} \epsilon^j, \qquad (21a)$$

where η_1 is the Emden radius of the polytrope 1.5 (we note that the structure of a non-relativistic degenerate fluid at zero temperature is that of the polytrope 1.5). The p-eigenvalues of the fluid are of the order of $4\pi G\rho_c / \eta_1^2$. Therefore, the g-eigenvalues of the white dwarfs are smaller than the p-eigenvalues by a factor of T/T_{Fc}. Upon expressing ρ_c in terms of the total mass of the star, one obtains an alternative expression for ε^j (see Chandrasekhar, 1939),

$$\varepsilon^j = \frac{128\pi^2}{125} \frac{G^4}{K^3} \eta_1^{-6} \left(\frac{d\Theta}{d\eta}\right)_1^{-2} (\gamma - 1)\mu_e^5 \frac{\mu_e}{\mu_i} \left(\frac{M}{M_\odot}\right)^2 \frac{T}{T_{Fc}} \epsilon^j, \qquad (21b)$$

where $(d\Theta/d\eta)_1$ is the surface value of the derivative of the Emden temperature, and k is defined by the relation $p = K(\rho/\mu_e)5/3$. The oscillation period $P^j = 2\pi / \sqrt{\varepsilon^j}$, in the cgs units, is given by

$$P^j \text{ (sec)} = 69.0(\gamma - 1)^{-1/2} \mu_e^{-5/2} \left(\frac{\mu_i}{\mu_e}\right)^{1/2} \frac{M_\odot}{M} \left(\frac{T_{Fc}}{T}\right)^{1/2} (j)^{-1/2}. \qquad (22a)$$

For $\gamma = 5/3$, $\mu_e = 2$, and $\mu_i = 4$, one has

$$P^j \text{ (sec)} = 21.1 \frac{M_\odot}{M} \left(\frac{T_{Fc}}{T}\right)^{1/2} (\epsilon^j)^{-1/2} \qquad (22b)$$

iii) Behavior of the Eigendisplacements at the Center and at the Surface: Once the eigenvector matrix Z is calculated from Equation (16), the

eigendisplacement vectors $\underset{\sim}{\xi}^j$, can be obtained by Equations (13) and (11). We note the following properties of $\underset{\sim}{\xi}^j$:

a) At the center $\underset{\sim}{\nabla}.\underset{\sim}{\xi}$ tends to zero as r^{ℓ}. See the remarks following Equation (11c).

b) At the surface, the radial component of $\underset{\sim}{\xi}$ tends to zero as r-R. The non-radial component and $\underset{\sim}{\nabla}.\underset{\sim}{\xi}$ remain finite. These requirements from the g-modes of any fluid are analyzed in paper I.

VII. NUMERICAL RESULTS

Equation (16) is solved in a Rayleigh-Ritz approximation, that is, by approximating the infinite matrices of Equation (13)-(16) by finite matrices. The matrix size was varied from one by one to seven by seven. Values of ℓ = 1,2,3,4,5 and 6 were considered. For ℓ = 1 and 2 the dimensionless eigenvalues ϵ^j, Equation (21b), and the eigenvectors Z at various Rayleigh-Ritz approximations are given in Tables 1 and 2. The eigenvalues are displayed in lines marked by an asterisk. The column below each eigenvalue is the corresponding eigenvector. The eigenvectors are normalized according to Equation (16b). For ℓ = 3,4,5, and 6 the dimensionless eigenvalues are given in Table 3. The convergence of eigenvalues is satisfactory. The same ansatz, Equation (11c), for non-degenerate fluids, however, gives much faster convergence (Sobouti, 1977b). Motivated by this observation a search for a more suitable ansatz for degenerate fluids is being made.

VIII. CONCLUDING REMARKS:

The salient features of our model can now be summarized. The white dwarf core is taken to be an isothermal fluid, composed of ions and non-relativistic degenerate electron gas. In this formalism, corrections up to first order in T/T_{Fc} are included, where T is the temperature of the core and T_{Fc} is the Fermi

Table 1. The eigenvalues and the eigenvectors of the g-modes of white dwarfs, corresponding to $\ell = 1$. The eigenvalues (Equation 20b) are displayed in rows marked by asterisks. The column below each eigenvalue is the corresponding eigenvector. Computations are in the Rayleigh-Ritz approximation, using from one to seven variational parameters. The last two digits in the entries represent the exponents of 10.

					* 0.5184+00	
						0.6600-02
				* 0.2654+00	0.6724+00	
				-0.8996-02	0.1352-02	
				0.3167-01	0.2471-01	
			* 0.1684+00	0.3497+00	0.7312+00	
			0.1109-01	-0.2199-02	0.3254-02	
			-0.8377-01	-0.3596-01	-0.3898-02	
			0.1183+00	0.1072+00	0.6105-01	
		* 0.1172+00	0.2166+00	0.3999+00	0.7494+00	
		-0.1307-01	0.3303-02	-0.4963-02	0.1705-02	
		0.1607+00	0.4027-01	0.2508-01	0.1985-01	
		-0.4936+00	-0.3102+00	-0.1706+00	-0.4368-01	
		0.4151+00	0.3772+00	0.2980+00	0.1223+00	
	* 0.8629-01	0.1461+00	0.2500+00	0.4288+00	0.7554+00	
	-0.1501-01	-0.4496-02	0.6698-02	-0.1810-02	0.2531-02	
	0.2673+00	-0.3400-01	-0.5606-01	-0.4056-01	-0.1341-02	
	-0.1340+01	0.6051+00	0.3828+00	0.2621+00	0.9413-01	
	0.2449+01	-0.1707+01	-0.1227+01	-0.7487+00	-0.2043+00	
	-0.1452+01	0.1283+01	0.1104+01	0.7824+00	0.2482+00	
* 0.6619-01	0.1043+00	0.1673+00	0.2743+00	0.4471+00	0.7580+00	
-0.1690-01	0.5793-02	-0.8360-02	-0.2535-02	-0.3873-02	0.1855-02	
0.4082+00	0.1235-01	0.1018+00	-0.5969-01	0.3168-01	0.1848-01	
-0.2958+01	-0.9435+00	-0.7592+00	0.6453+00	-0.4014+00	-0.8743-01	
0.8779+01	0.4760+01	0.3378+01	-0.2605+01	0.1705+01	0.4633+00	
-0.1124+02	-0.8043+01	-0.6298+01	0.4901+01	-0.3108+01	-0.7988+00	
0.5136+01	0.4376+01	0.3830+01	-0.3225+01	0.2161+01	0.5804+00	
* 0.5163-01	0.7871-01	0.1190+00	0.1842+00	0.2924+00	0.4594+00	0.7593+00
-0.1879-01	0.7072-02	-0.9869-02	-0.3549-02	0.5469-02	-0.1605-02	0.2360-02
0.5878+00	-0.2476-01	0.1642+00	-0.6866-01	-0.6653-01	-0.4936-01	-0.1686-02
-0.5740+01	-0.1264+01	-0.1440+01	0.1195+01	0.8952+00	0.5724+00	0.1523+00
0.2444+02	0.1042+02	0.7994+01	-0.6686+01	-0.5338+01	-0.3339+01	-0.7685+00
-0.5036+02	-0.2968+02	-0.2277+02	0.1854+02	0.1475+02	0.9375+01	0.2229+01
0.4927+02	0.3544+02	0.2926+02	-0.2444+02	-0.1953+02	-0.1237+02	-0.2916+01
-0.1830+02	-0.1508+02	-0.1347+02	0.1185+02	0.9812+01	0.6348+01	0.1519+01
g_7	g_6	g_5	g_4	g_3	g_2	g_1

Table 2. The eigenvalues and the eigenvectors of the g-modes of white dwarfs, corresponding to $\ell = 2$. See the legend for Table 1 for further details

					*	0.1199+01
						0.2148-01
					* 0.6630+00	0.1567+01
					-0.3548-01	-0.1502-02
					0.9286-01	0.7693-01
				* 0.4339+00	0.8694+00	0.1733+01
				0.5113-01	-0.9241-03	0.1076-01
				-0.2908+00	-0.1505+00	-0.4392-01
				0.3389+00	0.3096+00	0.1990+00
			* 0.3077+00	0.5522+00	0.1002+01	0.1800+01
			0.6907-01	0.5869-02	-0.2000-01	-0.2757-03
			-0.6427+00	0.2205+00	0.1333+00	0.8814-01
			0.1635+01	-0.1083+01	-0.6853+00	-0.2668+00
			-0.1200+01	0.1080+01	0.8935+00	0.4554+00
		* 0.2299+00	0.3798+00	0.6367+00	0.1088+01	0.1830+01
		0.8946-01	-0.1280-01	0.3036-01	0.1464-02	0.8014-02
		-0.1208+01	-0.2673+00	-0.2734+00	-0.2184+00	-0.6347-01
		0.5007+01	0.2499+01	0.1672+01	0.1198+01	0.5345+00
		-0.7972+01	-0.5668+01	-0.4258+01	-0.2937+01	-0.1167+01
		0.4257+01	0.3722+01	0.3237+01	0.2499+01	0.1085+01
	* 0.1783+00	0.2765+00	0.4334+00	0.6996+00	0.1146+01	0.1846+01
	0.1124+00	0.2150-01	-0.4239-01	0.8077-03	-0.1678-01	0.2506-03
	-0.2053+01	0.2660+00	0.4999+00	0.3583+00	0.2248+00	0.1108+00
	0.1227+02	-0.4656+01	-0.3549+01	-0.2946+01	-0.2093+01	-0.7626+00
	-0.3160+02	0.1816+02	0.1324+02	0.1036+02	0.7459+01	0.2920+01
	0.3630+02	-0.2644+02	-0.2105+02	-0.1683+02	-0.1200+02	-0.4595+01
	-0.1523+02	0.1296+02	0.1136+02	0.9706+01	0.7239+01	0.2855+01
* 0.1408+00	0.2105+00	0.3129+00	0.4770+00	0.7500+00	0.1191+01	0.1857+01
0.1377+00	0.3290-01	0.5618-01	-0.5112-02	-0.2624-01	0.3197-02	0.7393-02
-0.3255+01	0.1637+00	-0.8548+00	-0.5043+00	0.4246+00	-0.3363+00	-0.9939-01
0.2617+02	-0.7301+01	0.7055+01	0.5960+01	-0.4739+01	0.3396+01	0.1279+01
-0.9649+02	0.4443+02	-0.3412+02	-0.2857+02	0.2349+02	-0.1684+02	-0.6090+01
0.1780+03	-0.1078+03	0.8399+02	0.6946+02	-0.5700+02	0.4117+02	0.1507+02
-0.1594+03	0.1152+03	-0.9583+02	-0.8137+02	0.6736+02	-0.4870+02	-0.1778+02
0.5511+02	-0.4508+02	0.4019+02	0.3571+02	-0.3048+02	0.2246+02	0.8291+01
g_7	g_6	g_5	g_4	g_3	g_2	g_1

Table 3. The g-eigenvalues of white dwarfs (Equation 216), corresponding to ℓ=3,4,5, and 6. See the legend for Table 1 for further details.

ℓ = 3						
						0.2005+01
					0.1146+01	0.2645+01
				0.7623+00	0.1496+01	0.2967+01
			0.5477+00	0.9626+00	0.1733+01	0.3122+01
		0.4135+00	0.6708+00	0.1109+01	0.1896+01	0.3204+01
	0.3237+00	0.4941+00	0.7637+00	0.1221+01	0.2014+01	0.3254+01
0.2612+00	0.3788+00	0.5557+00	0.8381+00	0.1310+01	0.2105+01	0.3289+01
ℓ = 4						
						0.2942+01
					0.1694+01	0.3916+01
				0.1136+01	0.2206+01	0.4444+01
			0.8231+00	0.1427+01	0.2565+01	0.4724+01
		0.6266+00	0.1003+01	0.1643+01	0.2823+01	0.4888+01
	0.4947+00	0.7447+00	0.1139+01	0.1812+01	0.3017+01	0.4995+01
0.3997+00	0.5785+00	0.8341+00	0.1250+01	0.1952+01	0.3173+01	0.5074+01
ℓ = 5						
						0.4023+01
					0.2299+01	0.5395+01
				0.1546+01	0.2993+01	0.6174+01
			0.1126+01	0.1934+01	0.3492+01	0.6614+01
		0.8620+00	0.1366+01	0.2229+01	0.3862+01	0.6887+01
	0.6841+00	0.1021+01	0.1551+01	0.2463+01	0.4149+01	0.7074+01
0.5445+00	0.7978+00	0.1151+01	0.1712+01	0.2669+01	0.4393+01	0.7221+01
ℓ = 6						
						0.5260+01
					0.2960+01	0.7096+01
				0.1986+01	0.3856+01	0.8166+01
			0.1450+01	0.2481+01	0.4514+01	0.8798+01
		0.1115+01	0.1755+01	0.2861+01	0.5014+01	0.9205+01
	0.8802+00	0.1320+01	0.1998+01	0.3176+01	0.5417+01	0.9500+01
0.2131+00	0.1089+01	0.1512+01	0.2174+01	0.3359+01	0.5615+01	0.9625+01
g_7	g_6	g_5	g_4	g_3	g_2	g_1

temperature at the center.

From Equations (21), it is seen that the eigenvalues for g-mode oscillations are proportional to the internal temperature T. We also note that the factor $(\gamma - 1)$ appears in Equation (21a) because of the assumption of an isothermal core. If there is any decrease in the temperature outwards, this factor should be replaced by $(\gamma - \gamma')$, where γ' is defined by Equation (8b). This replacement will result in a decrease in the eigenvalues.

Again, from Equation (21b) we see that the eigenvalues are very sensitive functions of the mean molecular weight of the electrons, varying as μ_e^6. Dependence on μ_i, the mean molecular weight of the ions, is not so pronounced. These features should be compared with Brickhill's remark that the periods of gravity oscillations of white dwarfs do not depend critically on the composition of the stars.

The periods of g-modes are given by Equation (23), where the values of ϵ^j are of the order of unity (see Tables 1,2, and 3). Thus, the periods of oscillations come out to be of the order of a few hundred seconds. As the harmonic number ℓ increases, the periods decrease. These conclusions, as well as the linear dependence of our eigenvalues on the temperature are in agreement with similar results obtained, through an entirely different approach, by Papaloizou and Pringle.

Let us also emphasise an important difference between the g-modes of a degenerate structure and those of an ordinary fluid. According to Cowling (1941), the pressure fluctuations associated with the g-modes of an ordinary fluid are less prominent than the corresponding density fluctuations. For degenerate fluids, the opposite appears to be the case. Equations (12) and (9a) show that the Eulerian changes in ionic pressure are mainly responsible for the g-modes. The effects of Eulerian changes in the density and in the electronic pressure remain unimportant (in the limit of non-relativistic

degeneracies). That the g-modes are primarily driven by the buoyancy forces remains valid for degenerate as well as for non-degenerate fluids.

These calculations have been carried out for non-relativistic fluids. There are strong indications that in a relativistic case, the oscillation periods will decrease.

ACKNOWLEDGMENT

The authors are grateful to Dr. A. Sanyal for many stimulating discussions. Numerical calculations of this paper were carried out in the Computing Center of Pahlavi University. The research was supported in part by the Ministry of Science and Higher Education of Iran.

REFERENCES

Baglin, A., Schatzman, E.: 1969, in Low Luminosity Stars, ed. S.S. Kumar (New York: Gordon and Breach), p. 385

Bath, G.T.: 1973, Nature Phys. Sci. 246, 84

Bath, G. T., Evans, W.D., Pringle, J.E.: 1974, M.N.R.A.S. 166, 113.

Brickhill, A.J.: 1975, M.N.R.A.S. 170, 405

Chandrasekhar, S.: 1939, An Introduction to the Study of Stellar Stellar Structure (Chicago: University Press)

Chandrasekhar, S.: 1964, Astrophys. J., 139, 664

Cowling, T.G.: 1941, M.N.R.A.S. 101, 367

Harper, R.V.R., Rose, W.K.: 1970, Astrophys. J. 162, 963.

Hurley, M., Roberts, P.H., Wright, K: 1966, Astrophys.J. 143, 535

Landau, L.D., Lifshitz, E.M.: 1959, Statistical Physics (London: Pergamon Press)

Ledoux, P. and Walraven, Th.: 1958, Handbuch der Physik, 51, 353-604

Morse, P.M. 1965: Thermal Physics (New York: W.A. Benjamin Inc.)

Osaki, T., Hansen, C.L.: 1973, Astrophys. J. 185, 277

Papaloizou, J., Pringle, J.E.: 1978, M.N.R.A.S. 182, 423

Silverman, J.N., Sobouti, Y.: 1978, Astron. Astrophys., 62, 355

Sobouti, Y.: 1977a, Astron. Astrophys., 55, 327 (paper I)

Sobouti, Y.:1977b, Astron. Astrophys., Suppl. Series, 28, 463

Sobouti, Y., Silverman, J.N.: Astron. Astrophys. 62, 365

Warner, B., Robinson, E.L.: 1972, Nature Phys. Sci. 239, 2

Wolff, C.L.: 1977, Astrophys. J. 216, 784

MIRA VARIABLES: AN INFORMAL REVIEW

ROBERT F. WING
Astronomy Department, Ohio State University

The Mira variables can be either fascinating or frustrating -- depending on whether one is content to watch them go through their changes or whether one insists on understanding them. Virtually every observable property of the Miras, including each detail of their extraordinarily complex spectra, is strongly time-dependent. Most of the changes are cyclic with a period equal to that of the light variation. It is well known, however, that the lengths of individual light cycles often differ noticeably from the star's mean period, the differences typically amounting to several percent. And if you observe Miras -- no matter what kind of observation you make -- your work is never done, because none of their observable properties repeats exactly from cycle to cycle.

The structure of Mira variables can perhaps best be described as loose. They are enormous, distended stars, and it is clear that many different atmospheric layers contribute to the spectra (and photometric colors) that we observe. As we shall see, these layers can have greatly differing temperatures, and the cyclical temperature variations of the various layers are to some extent independent of one another. Here no doubt is the source of many of the apparent inconsistencies in the observational data, as well as the phase lags between light curves in different colors. But when speaking of "layers" in the atmosphere, we should remember that they merge into one another, and that layers that are spectroscopically distinct by virtue of their vertical motions may in fact be momentarily at the same height in the atmosphere.

I sometimes find it helpful to think of Miras as jellyfish. As they move through the water, their general oscillatory motion can be expected to continue, but it is impossible to predict all the details of their changes in shape and appearance; if you tweek a jellyfish on one side, you don't know if, when, and with what amplitude the disturbance will reach the other. If you think of Miras this way, you will stop worrying about their failure to repeat exactly in their variations.

No one has ever called Miras a theoretician's delight. Certainly they have not been very useful in testing theories of stellar pulsation. There is just too much going on -- it's hard to know which observable properties are even relevant to pulsation. In fact the question has sometimes been raised as to whether the Miras are pulsating at all. Merrill (1955) wrote that "the evidence for volume pulsation is so meagre that skepticism is warranted", and Wallerstein (1977) has proposed that the apparent radius changes in Miras are caused not by the outward movement of the gas but simply by changes in the atmospheric opacity. Recent results from infrared spectroscopy (Hinkle 1978) have clarified the picture considerably, basically by allowing us to look more deeply into the atmosphere, and I think that the last doubts that Mira variables are pulsating have finally been laid to rest.

A scheme has recently been devised by Cahn and Wyatt (1978) by which one can estimate the masses and luminosities (and hence ages) of individual Miras from two readily observable quantities, the mean period and the mean spectral type at maximum. This scheme is based on the assumption that Miras are pulsating stars, more specifically that they are pulsating in the first overtone. Since we have few opportunities of determine masses and luminosities of individual Miras directly, it will be difficult to decide observationally whether this picture is correct. At this stage the question is not whether the relations of Cahn and Wyatt will eventually need recalibrating, but whether they exist at all. However, the fact that Cahn and Wyatt were able to construct a self-consistent picture suggests that they may be on the right track, and that it may indeed be possible to understand the gross observable properties of individual Miras, such as surface temperature and mean period, in terms of their masses and evolutionary states.

In describing to you the observed behavior of Miras, I will attempt to select those particular observations that have a bearing on the question of pulsation -- although, as I have already indicated, it is not always obvious which observations these are. The discussion will be centered around the sizes of these stars, or more particularly the evidence for changes in size. No mention will be made of their absolute magnitudes, ages, chemical compositions, population types, galactic distribution, statistical properties, or other matters not directly related to pulsation. Rather, we will be concerned with the variations of individual stars, and with some spectroscopic peculiarities that are related to the enormous sizes of their atmospheres.

As soon as we try to talk about the sizes of Mira variables, we run into a serious problem. The reason that we can see so many different atmospheric layers at the same time is that the continuous opacity -- between the spectral lines and bands -- is extremely low. A Mira is about as translucent as a jellyfish: you can practically see right through it. Some regions contributing to the spectrum are much farther from the center of the star than others, and this is all within the region we call the "photosphere". In order to speak of the size of a Mira, we must specify the wavelength precisely. Furthermore, there may be no real discontinuity between the photosphere and the circumstellar shell that contributes zero-volt absorption lines and infrared emission, since presumably the shell consists of material which has drifted away from the star, and which may receive new contributions with every light cycle. In this respect, Miras are worse than jellyfish. Although the radius of a jellyfish is both time-dependent and angle-dependent, at least there is a membrane to show us where the jellyfish ends and the ocean begins. The size of a jellyfish is certainly difficult to measure, but at least the creature has a size.

The methods that can be used to determine the sizes of Miras fall into three classes:

(1) Direct. Angular diameters of Miras have been measured directly with Michelson interferometers, by observations of lunar occultations, and by speckle interferometry. The distance must be known to calculate the ab-

solute size, but useful information about changes in size can be obtained directly from the observed changes in angular diameter.

(2) Photometric. If you know the luminosity L (or equivalently the absolute bolometric magnitude M_{bol}) and the effective temperature T_e, you can calculate the size of the emitting surface area and hence the stellar radius R, since $L = 4\pi R^2 \sigma T_e^4$. If you don't know the distance and have only the apparent bolometric magnitude m_{bol}, you can still calculate the change in radius from the observed changes in T_e and m_{bol}.

(3) Spectroscopic. Measurements of radial velocities of absorption and emission lines give information about vertical motions in the atmosphere. Integration of the radial velocity curve then gives the distance moved by the gas producing the lines.

All of these methods are clear-cut in concept, and all of them are known to "work" in the sense that they give reasonable results for the sizes of other kinds of stars. But all of them get into trouble when they are applied to the Miras, and in general the results from the three methods are in poor agreement.

For example, Figure 1 shows a famous illustration from the paper by Pettit and Nicholson (1933). From the variations in bolometric magnitude (obtained from the observed radiometric magnitudes, with crude corrections for absorption by the earth's atmosphere) and temperature (from a very broad-band color index, which compares the radiation shortward and longward of 1.3 μ), they computed the variation in the angular diameter of Mira (o Cet). Differentiation of the diameter curve then gave the "radiometric radial velocity curve", which is compared to the radial velocity curve measured spectroscopically by Joy (1926) for the mean absorption spectrum of Mira. The two curves have similar amplitude but are badly out of phase -- in fact, they are nearly mirror images of one another. Similar comparisons for three other Miras have recently been published by Wallerstein (1977); the higher quality of the data used in his analysis did not make the discrepancy go away.

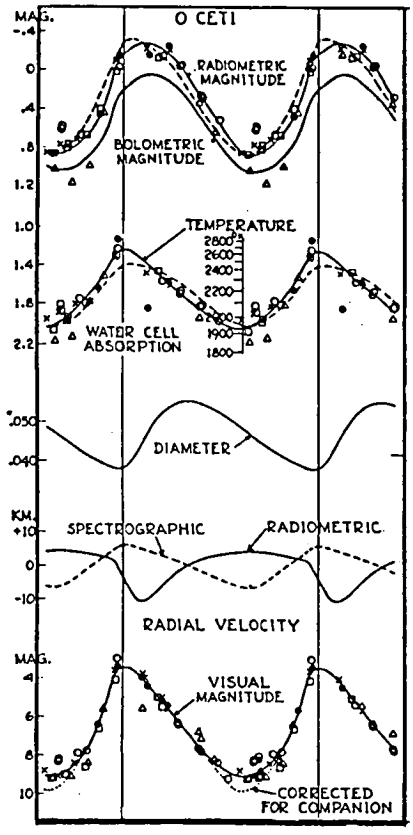

Fig. 1 - The variations of o Cet (Mira), according to Pettit and Nicholson (1933). Note that the color temperature variations are in phase with the visual light curve but not the bolometric curve. The diameter curve is computed from the temperature and bolometric magnitude. Its derivative, the radiometric radial velocity curve, disagrees with the radial velocities determined spectroscopically.

What is the problem? It's not that the observations of Miras are so difficult. All three methods (including Michelson interferometry) had been applied to Miras by the 1920's, and in general the measurements by each method are reproducible to sufficient accuracy. Also, impressive advances in each of the three areas of observation have been made within the past decade, and yet the discrepancies persist. The problem, it seems to me, is simply that when we observe a Mira by any of these methods, we don't know what we're looking at.

For most of the remainder of my talk, I will give examples of the use of each method, focusing attention on the problems of interpretation. I think it will be clear why observers can derive a lot of pleasure from the study of Miras, and why theoreticians, for the most part, can not.

THE DIRECT APPROACH

The basic problem with the direct approach to measuring the sizes of Miras is that it really is not very direct. We don't measure the size of an image with a ruler. Rather, we observe some optical phenomenon that is related to the size of the star -- the visibility of interference fringes at different mirror separations, or the degree of degradation of the diffraction pattern as the star disappears behind the moon, or the character of the speckles in the seeing disk. In each case, a model for the distribution of light in the true stellar image must be assumed before the observed quantity can be related to image size.

How much limb darkening (or brightening) is there? Is the star round? Does it have spots on it? If the answer assumed for any of these questions is wrong, so is the angular diameter that we get. Nevertheless, the results obtained by these techniques have certainly been instructive. The main problem with using these results is that there haven't been enough of them.

The angular diameter of Mira was measured with a Michelson interferometer in January 1925 by Pease at Mount Wilson (see Kuiper 1938). Unfortunately, the method could be employed only when the variable was at maximum light.

Diameter measurements of Miras by lunar occultation observations are a rather recent innovation, since a time resolution of a few milliseconds is needed to resolve the diffraction pattern. A few years ago Nather and Wild (1973) succeeded in observing an occultation of R Leo at V = 8 on the declining branch. Its phase was estimated to be 0.27, so that it should have been very nearly at its maximum diameter if the diameter curve of Pettit and Nicholson (Figure 1) is valid. The light curve of this event is shown in Figure 2. Anyone who has seen occultation data for just about any other star will recognize that R Leo is enormous. The diffraction pattern is completely smeared out. From the slope of the decline, Nather and Wild computed a uniform-disk diameter of 0.067 arcsec.

For stars as large as this, the occultation technique runs into a

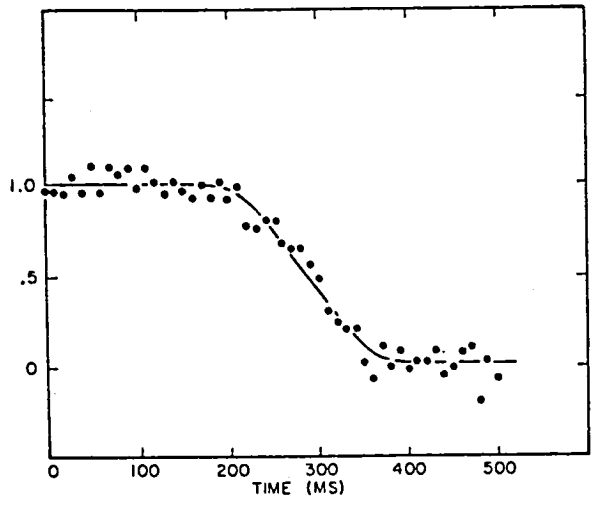

Fig. 2 - Light curve of the occultation of R Leo on 19 May 1972, as measured by Nather and Wild (1973). The computed angular diameter is 0.067 arcsec.

snag, as Nather and Wild point out. Since there is no diffraction pattern, there is no information as to the slope of the lunar limb at the point of contact. One rock could spoil the result. Fortunately this problem can be overcome by planning simultaneous observations at different observatories. It does not arise if the star is, say, one-quarter to one-tenth the size of R Leo; there are many Miras in this range of angular size, but of course they are correspondingly fainter, and photon noise becomes a problem.

Occultation observations of Miras are now being pursued vigorously by Ridgway and his colleagues at Kitt Peak (Ridgway, Wells, and Joyce 1977). Most of their measurements are being made at 2 μ in the infrared, so that daytime observations are possible. Since it is impossible to control the motion of the moon, this method will never produce a true diameter curve for any single star. However, even a simple pair of observations of the same Mira could be useful in indicating whether the spectroscopic or the photometric diameter curve tends to be confirmed by the direct method. Occultation measurements of U Ori were recorded by Ridgway, Wells, and Joyce in two different lunations, and they indicate that the diameter is several percent larger at phase 0.36 than at phase 0.99. This result appears to confirm the photometric diameter curve, but unfortunately no conclusion can be drawn. The two observations were made with different filters, one in the continuum

and one in an H_2O band, and it is quite possible that the measured change in diameter has more to do with wavelength dependence than with time dependence.

Exciting results obtained by speckle interferometry have recently been published by Labeyrie, Koechlin, Bonneau, Blazit, and Foy (1977). R Leo and o Cet were found to be twice as large at wavelengths affected by strong TiO bands as they are at continuum wavelengths. Information about changes in diameter with phase is still very limited, but the indications are that changes with wavelength at a given phase are much more dramatic than changes with phase at a given wavelength. The acquisition of further speckle data, especially if timed to cover a substantial portion of the light cycle of a single Mira, would be enormously valuable.

THE PHOTOMETRIC APPROACH

The formula $L = 4\pi R^2 \sigma T_e^4$ is straightforward enough, but the Miras are not. One problem is that the formula assumes the stars are round -- not shaped like jellyfish. We now examine the problems associated with determining L and T_e.

Observationally, it takes a lot of work to determine L, or even the apparent quantity m_{bol}. But at least m_{bol} -- the total radiation from the star reaching the top of our atmosphere -- is a well-defined quantity. Since the time of Pettit and Nicholson (1933), much more sophisticated methods have been applied to the determination of m_{bol}, including the use of Stratoscope scans to interpolate between the various infrared magnitudes measured from the ground (Smak 1966). A few observations of Miras have also been made from high-altitude aircraft (Strecker, Erickson, and Witteborn 1978). I am currently collaborating with J. Smak on the determination of m_{bol} for a large set of Miras from extensive wide- and narrow-band photometry. My impression is that if you are willing to do the work and are careful about the photometric calibrations, you can determine m_{bol} to an accuracy of a few percent. Recent work on this problem has not changed the character of the bolometric light curves derived by Pettit and Nicholson. In other words, I don't think

errors in the determination of m_{bol} can be responsible for the discrepancies mentioned above.

Light curves measured at carefully-chosen continuum points in the infrared can give a good approximation to the bolometric light curve. Lockwood and Wing (1971) have published light curves for 25 Miras in I(104), measured photoelectrically with a narrow bandpass at 10400 Å, and they were found to have the same amplitudes and phasing as the bolometric light curves of Pettit and Nicholson. Since I(104) is very much easier to measure than m_{bol}, it is nice to know that it provides essentially the same information.

The I(104) light curves have proved quite interesting, especially since each measurement of magnitude has been part of a set of narrow-band photometry which also gives the spectral type (from the strengths of TiO and VO bands) and the near-infrared continuum color. When I started this work in 1965, my hope was that the I(104) curve of any Mira would repeat so well from cycle to cycle that its characteristics could be established once and for all. Several Miras were followed through two or three cycles to test this idea, and the first results seemed promising. Figure 3 shows the visual and I(104) curves for W Peg in two successive cycles. The V curves, measured photoelectrically with a UBV photometer, show typical cycle-to-cycle differences: one maximum is 0.3 mag brighter than the other, and it occurred ahead of schedule; the slopes on the declining branches are also different. On the other hand, the I(104) magnitudes followed the same curve in both cycles. I would like to be able to tell you that the differences in the visual maxima were caused by differences in blanketing of the visual region by TiO, but the fact of the matter is that W Peg attained the same spectral type, M7.0, at both maxima.

These observations of W Peg, from 1965 and 1966, were made with a spectrum scanner. Since 1969 I have been using a set of eight interference filters to obtain similar information. In addition, Lockwood (1972) has published extensive photometry of Miras on a five-color system in the same near-infrared spectral region. These three systems have enough in common that it has been possible to work out the transformations between them (Lockwood and Wing 1971; Wing and Lockwood 1973); in particular, all three measure I(104).

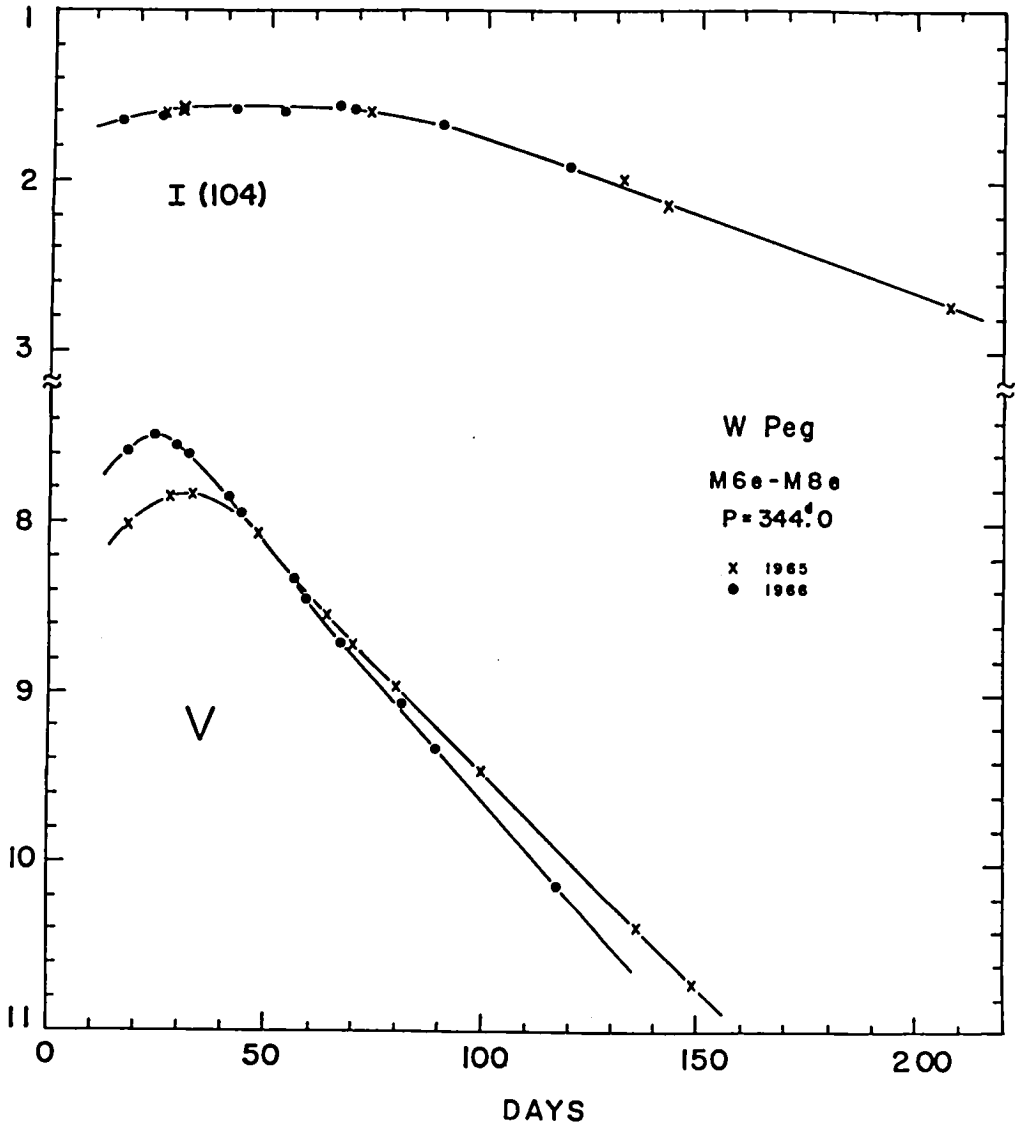

Fig. 3 - Photoelectric light curves in V and I(104) for W Peg, a typical Mira variable, during the accessible portions of two consecutive cycles. In this case the differences in the visual curves are not reflected in the I(104) curve. Note also that the infrared maximum occurs well after the visual maximum. From Wing (1967).

When Lockwood and I combined our data to form I(104) light curves for several Miras over a number of cycles, it became clear that cycle-to-cycle differences do occur in the I(104) curves quite commonly, and that the nice behavior shown by W Peg in Figure 3 is the exception rather than the rule. Several of these I(104) light curves are shown in Figure 4, where different

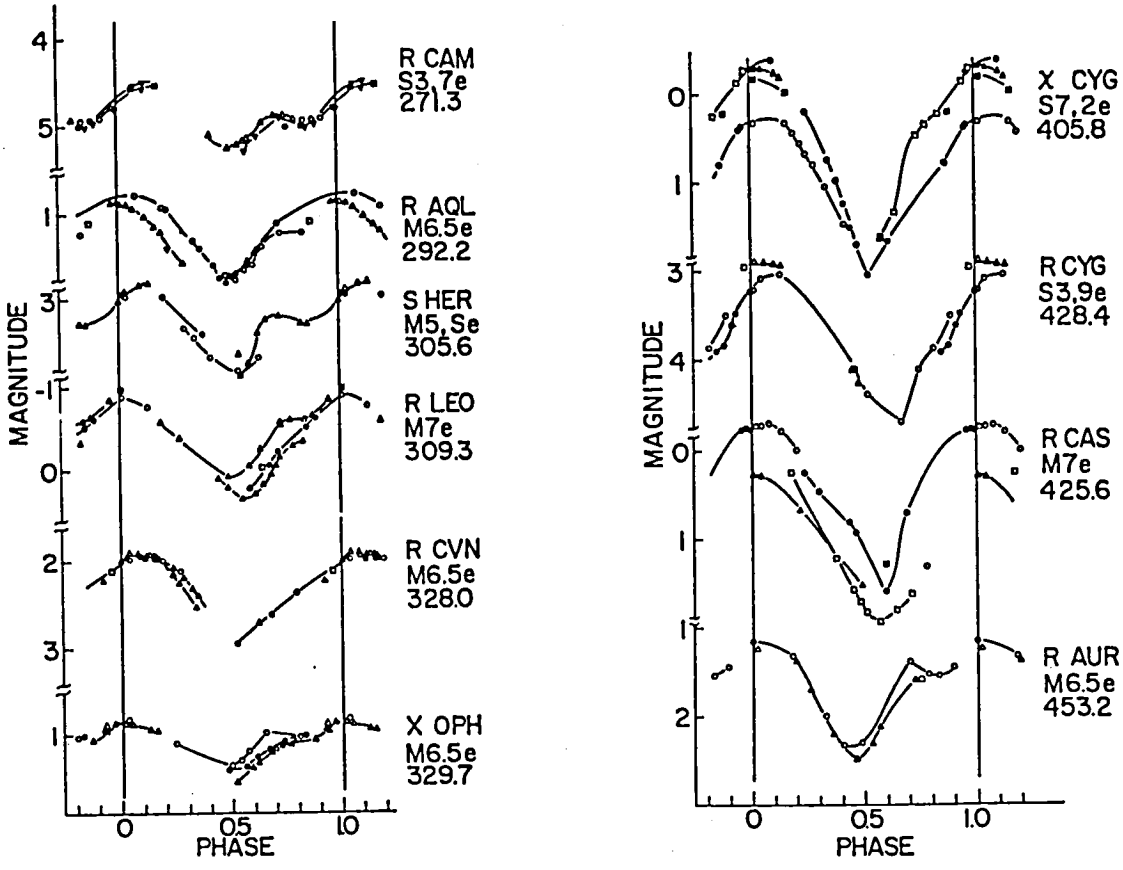

Fig. 4 - Light curves in I(104), an infrared continuum point, for Miras of relatively short period (left) and long period (right). Below the name of each star is its mean spectral type at maximum light (Keenan 1966) and the mean period used in calculating the phases. From Lockwood and Wing (1971).

symbols have been used to distinguish the different cycles. The stars of relatively short period usually repeat fairly well, while the large-amplitude, 400-day Miras show more substantial cycle-to-cycle differences. From an analysis of these differences in terms of the simultaneously measured spectral types and color temperatures, we were forced to conclude that cycle-to-cycle differences affect the bolometric curves as well.

Several of the stars in Figure 4 show humps on the rising branch, at about phase 0.7. Similar humps have long been known to occur in the visual light curves of certain Miras, and it was not known whether they are caused by superficial changes in spectroscopic features or by more basic changes in the continuum radiation. Now we see that the humps are present in the continuum radiation; blanketing changes do not affect the I(104) magnitude, and

in any case the spectral types were observed to remain constant, at their latest value, throughout the interval from phase 0.6 to 0.8, whether or not a hump occurred in the light curve. The TiO and VO bands used for spectral classification are evidently formed very far from the layer emitting the continuum; these molecules do not start to dissociate until a month or two after the photospheric temperature has started to rise.

The infrared data show that humps on the rising branch are quite common: most stars observed in two or more cycles show a hump in at least one cycle. On the other hand, few stars seem to have humps in every cycle.

It is difficult to avoid the conclusion that humps also occur in the bolometric light curve, whenever they occur in I(104). If we know the shape of the bolometric curve, we can use the color temperatures measured in the infrared continuum, along with the usual formula, to inquire how the radius changes when a hump occurs. Interestingly, the color temperatures are observed to increase smoothly and monotonically, from minimum to visual maximum, no matter whether a hump occurs in the light curve or not; there is never a hump in the temperature curve. Thus the leveling-off or decrease in luminosity following a hump must be the result of a rapid decrease in radius prior to maximum light. Lockwood and I suggested that the occurrence (or not) of a hump of the rising branch is simply the result of the interplay between rising temperature and decreasing radius during this part of the cycle.

This brings us to the question of what temperature is really appropriate to use in the formula $L = 4\pi R^2 \sigma T_e^4$. The fundamental problem with applying this formula to the Mira variables, it seems to me, is that the effective temperature T_e is <u>defined</u> by this formula and has meaning <u>only</u> if we can attach a meaning to the radius R. Since the star has no membrane, we have to think of the radius as the distance from the center of the star at which the optical depth takes on some value, such as unity; as we have seen, the radius is then strongly wavelength-dependent and may vary by as much as a factor of two over the width of a strong spectral feature. Some kind of averaging is needed, but it is not clear what kind of mean opacity, or mean radius, corresponds to the "effective" temperature. There are

innumerable ways of estimating the temperature of a Mira spectroscopically or photometrically, but different methods often give substantially different results, in part because they refer to different layers of the atmosphere which really do have different temperatures, and in part because most line ratios and photometric color indices are not pure indicators of temperature.

So what do we do? The usual response is to go ahead and use the formula anyway. That is, we determine m_{bol} as best we can, estimate T_e from a color index that we hope is representative (or worse, from the spectral type), and bravely plug them into the formula to compute the size. This gives us a number, but we really don't know how this number is related to the size of the star.

Applications of the photometric method to Mira variables do at least give internally consistent results, as exemplified by Pettit and Nicholson's diameter curve in the center of Figure 1. The size (or rather, this number) is smallest near the time of visual maximum, and it increases most rapidly between the times of visual maximum and bolometric maximum, which occurs one or two months later. Nearly all spectroscopic and photometric temperature indicators agree that the highest temperature occurs very close to the time of visual maximum; if the temperature really drops during the following month or so, a rapid increase in the size of the emitting region is needed to account for the increase in bolometric flux.

There are three further results from the narrow-band photometry of Miras which, although not clearly related to radius variations, do tell us a good deal about the structure and extent of their atmospheres: (1) the temperatures measured in the continuum are usually much higher than would be expected from the spectral type; (2) spectral types determined from different TiO bands are often grossly discordant; and (3) the variations in spectral type are only loosely coupled to the variations in color temperature. While each of these findings came as a surprise, I believe they are all manifestations of the same thing, namely the great stratification of these stars' atmospheres.

Color temperatures that are abnormally high for the spectral type do not always occur -- as a consequence of the loose coupling indicated in

the third result above, the effect can go either way -- but most Miras have high temperatures for their spectral types at most phases. The effect is most conspicuous (and best established) in the early-type Miras near maximum light, when the near-infrared color temperatures are completely free from blanketing effects. For example, R Tri at its 1965 maximum attained a color temperature as high as that of a normal K4 giant, but its spectral type was never earlier than M3 (Spinrad and Wing 1969). I interpret this as meaning simply that the continuum and the absorption spectrum are formed very far apart, in regions of very different temperature. In other words, the atmosphere of a Mira is more stratified than that of a normal giant (Wing 1967).

A recent study of hydrodynamical phenomena in Mira variables (Willson and Hill 1979) lends credence to the conclusion that their atmospheres may be more distended than those of non-variable M giants of the same luminosity. There is simply not enough time for the atmosphere to recover from the effects of one shock wave before the next shock starts to propagate through it. The atmosphere is thus never in a "normal" state, and although the star has the energy output of a giant, the physical characteristics of its atmosphere, such as density and temperature structure, may more closely resemble those of a supergiant. Indeed, Mira variables seem spectroscopically to have the luminosities of supergiants, if their pressure-sensitive line ratios are interpreted in the usual way. For this reason, Keenan has always refrained from assigning luminosity classes to Mira variables (Keenan 1966; Keenan, Garrison, and Deutsch 1974). Unfortunately, not all investigators have exercised such restraint, and supergiant luminosity classifications have been published for several Miras, leading to possible confusion as to their actual luminosities.

The second of the results from narrow-band photometry mentioned above refers to the assignment of temperature classes. For the Miras, temperature classification becomes ambiguous as soon as we consider two different classification criteria -- even if they are just different bands of the same molecule. In Figure 5, we see that the relative strengths of the TiO bands measured by filters 1 and 3 on the eight-color system are not the same in the Mira as they are in the giant. For the giant we get the same spectral type from both TiO bands and from the continuum color, while for the Mira we get

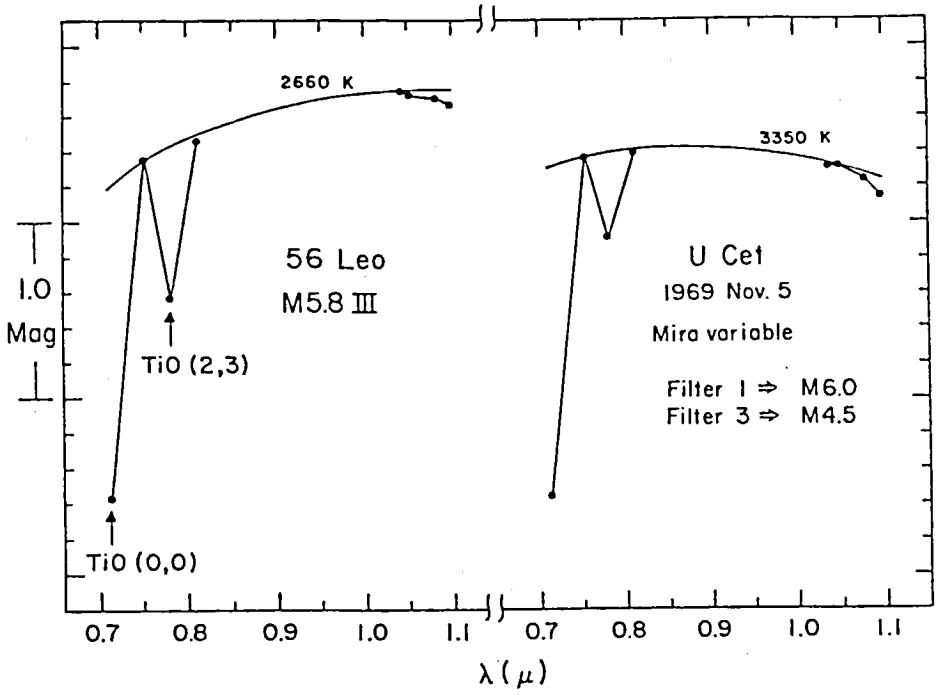

Fig. 5 - Eight-color photometry for 56 Leo, a normal, unreddened giant, and U Cet, a Mira variable. The two stars have nearly the same TiO strength at filter 1 but different TiO strengths at filter 3 and very different color temperatures. From Wing (1974).

M6 from the zero-volt TiO band, M4.5 from the excited TiO band, and M3 from the color. Clearly we must be careful in using spectral classifications of Miras; in particular, we should not use them to infer the temperature of the photosphere. At the same time, these results encourage me to hope that the infrared color temperature from the eight-color photometry may indeed be suitable to use in calculations of the radius, since it appears to refer to the same deep layer from which most of the total flux is emitted.

The loose coupling between color temperature and band strength is illustrated in Figure 6. The loops executed by Miras are really enormous -- the band strengths can differ by a factor of two or more between phases of the same color temperature. Because of this, bolometric corrections for Miras must be tabulated as two-dimensional functions of band strength and color, rather than as one-dimensional functions of spectral type as have always been used in the past. Another consequence of these loops is that they render the band-strength data virtually useless for abundance determinations.

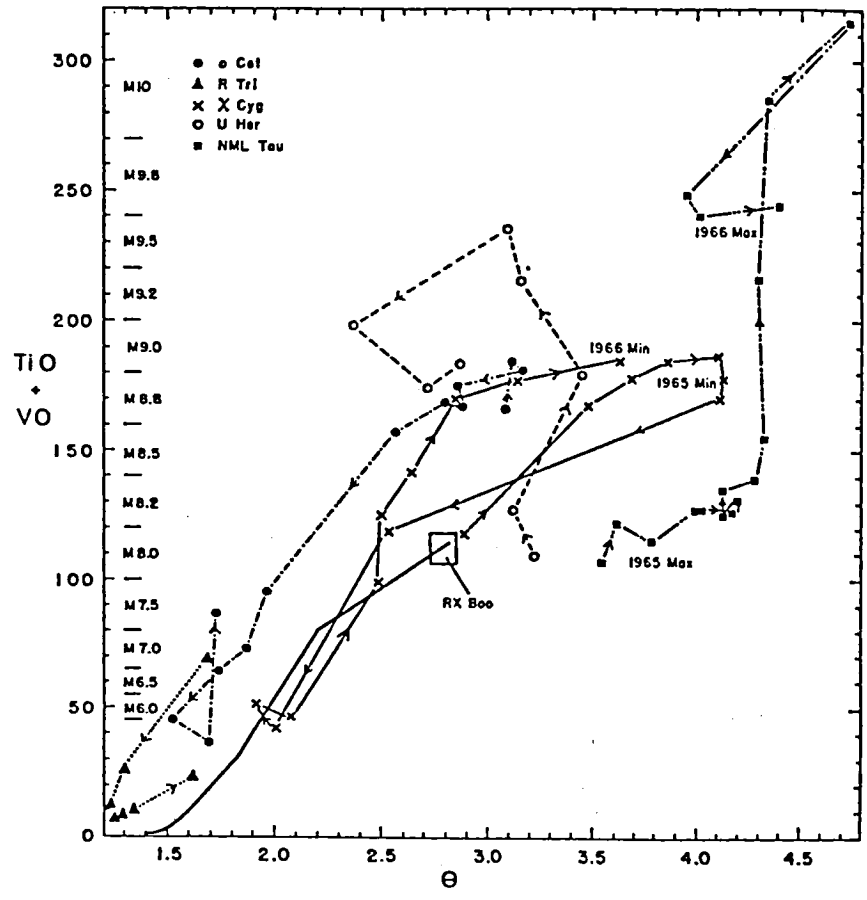

Fig. 6 - An index of molecular band strength is plotted against the reciprocal color temperature (5040/T), both measured in the near infrared with a scanner (Wing 1967). Normal giants define the heavy line ending in the box labeled RX Boo, whereas Mira variables execute large loops. See Spinrad and Wing (1969) for details.

These loops can be interpreted in the same way as the other phenomena we have discussed -- the band strengths and the continuum color refer to widely separated regions, the temperature variations in which are out of phase. This behavior could be modeled if all Miras showed loops that were at least qualitatively similar, but they're all different! In Figure 6, χ Cyg goes clockwise while U Her goes counter-clockwise. In fact, the loops shown by the same star in different cycles are not necessarily any more similar than the loops of two different stars.

Well, what do you expect of a jellyfish? Remember that the layers contributing to the spectra are near-perfect vacua separated by millions of miles, and you will be able to excuse their poorly-coordinated performance.

THE SPECTROSCOPIC APPROACH

The spectra of Miras are incredibly complex. They are dominated in the ultraviolet and blue regions by atomic absorption lines, in the visual and near infrared by bands of metallic oxide molecules, and in the infrared beyond 1.5 μ by innumerable lines from the rotation-vibration transitions of CO and H_2O. In addition to these absorption features, emission lines of various descriptions are present. Hydrogen lines of the Balmer, Paschen, and Brackett series are strong in emission during more than half the cycle, from just before maximum to approximately the time of minimum light; since absorption lines can be seen (and identified) within the broad emission profiles of the Balmer lines, it is clear that the hydrogen emission is produced in a deep layer of the atmosphere (Joy 1947). Some of the weaker emission lines are known to be produced by fluorescence, and although I will not discuss these particular lines further here, I should mention that the careful study of fluorescence mechanisms in Miras can provide important information about the structures and motions of their atmospheres (Wing 1964; Willson 1976). In fact, the very fact that fluorescence mechanisms are operative shows that these atmospheres are so rarefied that the populations of excited levels in atoms are governed by radiative processes rather than by collisions. Other metallic emission lines seem to be produced by recombination, some remain unidentified, and still other emission lines have been found to have molecular origins. Interesting reviews of the line spectra of Miras have been published by Merrill (1960) and Willson (1976).

Recent observations of Miras have revealed additional emission lines. Just six weeks ago, the first emission lines to be detected in the ultraviolet spectrum of a Mira variable below the atmospheric cut-off were recorded in R Leo with the IUE satellite (Wing and Carpenter 1978). At the other end of the spectrum, lines emitted by OH, H_2O, SiO, and CO have been detected in the microwave region.

Spectroscopic studies of the pulsational properties of Miras are based on the measurement of radial velocities. Unfortunately, an accurate measurement is not enough; there are three problems with which we must deal before

the radial-velocity data can be converted into information about the expansion and contraction of the atmosphere. First, because of projection effects, the measured radial velocity does not tell us immediately the motion of the surface of the star; we must apply a very uncertain correction for geometry and limb darkening. Emission lines are particularly difficult to use, since they may be either limb-darkened or limb-brightened, depending on the depth of their formation. This problem has been discussed recently by Wallerstein (1977). A more important problem, also discussed by Wallerstein, is that it is not sufficient to know the absolute motion of the surface; we must also know the radial velocity of the center of mass of the star before we can tell whether the surface is moving up or down. Finally, when we find that different spectral features have different radial velocities, we must somehow decide which feature to use as an indicator of the photospheric velocity.

For many years, most of the radial-velocity work on Miras was done at Mount Wilson Observatory, mainly by Merrill and Joy. The spectroscopic radial-velocity curve shown in Figure 1 was taken from an early study of Mira by Joy (1926); 28 years later Joy (1954) published a second study of Mira, from which Figure 7 was taken. Quite generally, the emission lines show smaller radial velocities than absorption lines, i.e. the emitting regions are moving outward and/or the absorbing regions are falling inward. [The only red-shifted emission lines that have been identified in Miras are certain fluorescent lines that are excited by off-center coincidences (Wing 1964)]. Different emission lines, however, display very different behavior: note in particular the curves for Joy's "standard" metallic emission lines, the Fe II lines, and the hydrogen lines in panels (b) and (d) of Figure 7. The behavior of the absorption spectrum is also rather complex: Merrill, in several papers, reported that the radial velocities of absorption lines show a dependence upon excitation potential -- another indication of extreme stratification. In addition, a few instances of doubling of atomic lines have been reported, and evidence of incipient line doubling (fuzzy or irregular line profiles) is rather common.

Faced with the many different velocities that are present in the spectrum at any given phase, how can we decide which velocity best represents

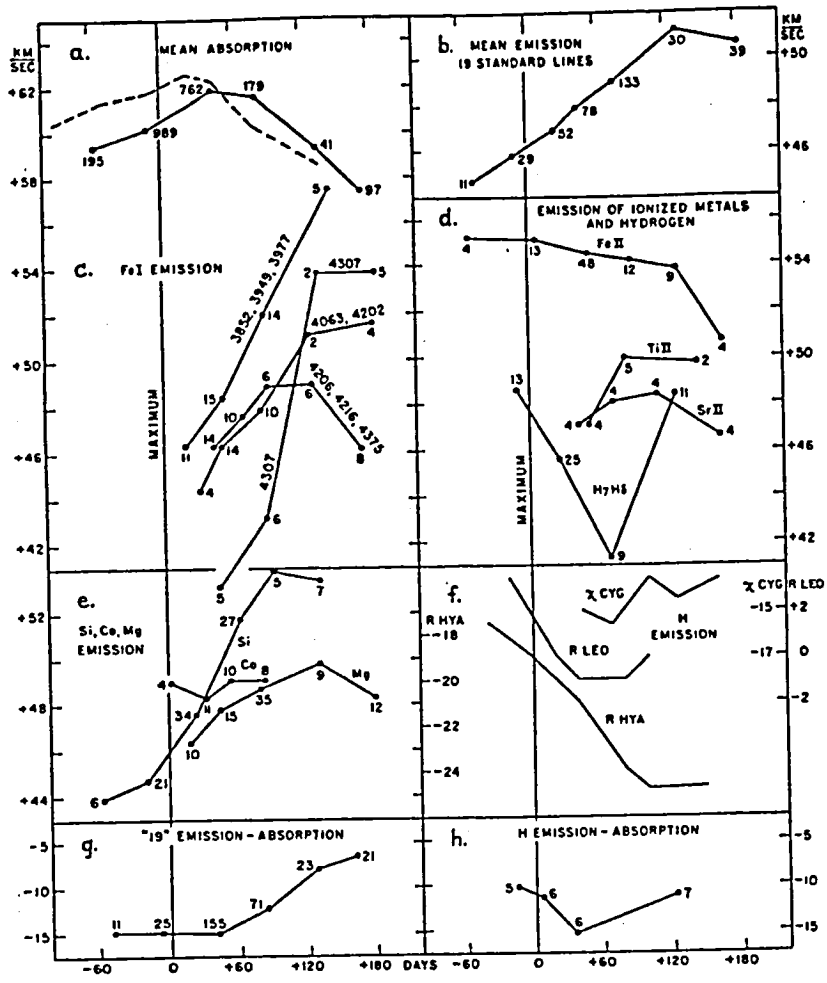

Fig. 7 - Radial velocities measured in the spectrum of Mira, from Joy (1954). Absorption and emission lines, all from the blue spectral region, have been grouped according to their behavior. Numbers next to the points indicate the number of measurements entering the mean.

the motion of the photosphere and which the motion of the center of mass? Many approaches to this question have been tried. Usually some kind of average of the atomic absorption-line velocities is taken to be the photospheric velocity. Common choices for the center-of-mass velocity are the mean absorption velocity at the time of maximum light, the velocity of Fe II emission lines (which appear to be formed in the chromosphere and show relatively little velocity variation with phase), and the velocities of certain molecular microwave emission lines (which are formed still farther out). Unfortunately, all these velocities are different.

For 7 stars with high-quality optical and microwave velocity data, Wallerstein (1975) prepared Figure 8 to illustrate the differences in the

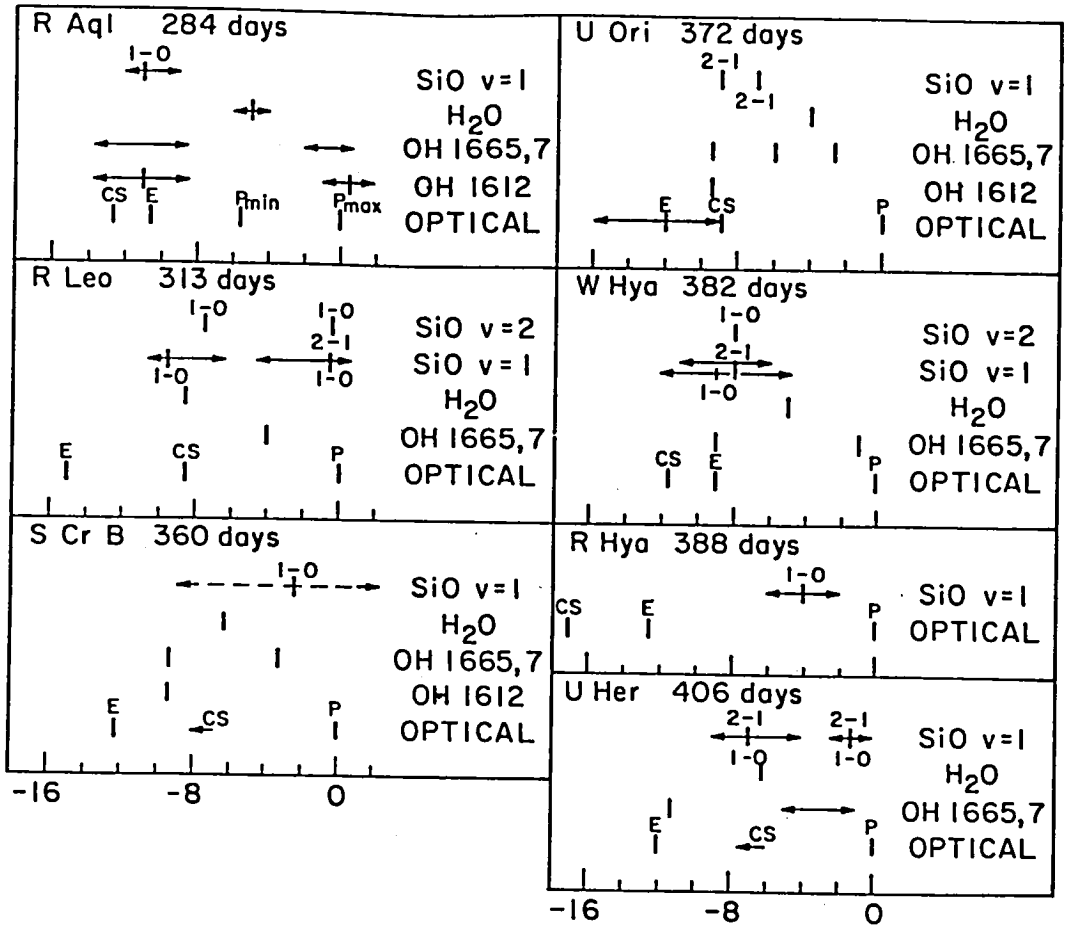

Fig. 8 - Radial velocities of various optical and radio lines plotted relative to the velocity obtained from high-excitation absorption lines (labeled P for "photospheric") for 7 well-studied Mira variables. Characteristic velocities of optical emission (E) and circumstellar (CS) lines are plotted as well as the velocities of radio lines of SiO, H_2O, and OH. From Wallerstein (1975).

various observed velocities which might be considered to represent the motion of the center of mass. Also included are the characteristic velocities of optical emission lines and circumstellar absorption components. The reference velocity in each case is that of the absorption spectrum and is labeled P for "photospheric". Because of the dependence of the absorption-line velocity upon excitation potential, Wallerstein used only high-excitation lines, which are formed in deeper layers than the low-excitation lines, in the determination of P. Even with this precaution, however, it is doubtful whether this velocity refers to a layer as deep as the true photosphere, and in fact the results from the infrared CO lines discussed below seem to show that it does not.

Since Figure 8 was originally drawn, thermal (as opposed to maser) SiO emission has been detected from several Miras. Since this emission must arise in a large, low-density region, it should indicate fairly directly the center-of-mass velocity of the star. According to Reid and Dickinson (1976), the circumstellar emitting region has a modest velocity of expansion (as inferred from the SiO line profile), and the center-of-mass velocity is smaller than the velocity derived from atomic absorption lines at bright phases, i.e. the gas producing the absorption is seen falling back in.

Once the necessary decisions have been made, the radial-velocity curve can be integrated to determine the distance moved by the gas producing the measured lines. The corresponding change in surface area can then be calculated and compared to that obtained by the photometric method. Whenever this exercise has been carried out, as for example by Pettit and Nicholson (see Figure 1) and more recently by Wallerstein (1977), it has revealed a disturbing discrepancy: the motion of the gas inferred from the photometry is simply not confirmed by the measured radial velocities. In fact, Wallerstein showed that a discrepancy exists no matter what value is assumed for the center-of-mass velocity, since part of the problem is that the amplitude of the radial-velocity variations -- at least for atomic lines in the blue -- is much too small to correspond to the photometric variations.

If, like Wallerstein, we choose to assume that the atomic absorption-line velocities are indicating the actual motion of the photosphere, then we are forced to look for an error in the interpretation of the photometry. Wallerstein's (1977) suggestion is that we have been fooled by an opacity effect: the apparent increase in size between the times of visual and bolometric maxima is not due to an actual outward movement of the gas but is simply the result of an increase in the atmospheric opacity as the temperature drops and molecules and grains form. However, this explanation has a fatal flaw. Although an increase in opacity can indeed cause an increase in the apparent size as measured directly (say by an interferometer of some kind), there is no way that it can produce an increase in size as "seen" by a photometer, since an increase in opacity cannot make the star become bolometrically brighter.

If, on the other hand, we assume that there is nothing basically wrong with the conventional interpretation of the photometry, we must conclude that the atomic absorption lines seen in the blue spectral region, even those of high excitation, do not arise in the photosphere, i.e. the layer producing most of the bolometric radiation seen by a photometer. This could be the case if the opacity is much greater in the blue than in the infrared. Evidence in favor of this conclusion has finally been produced by studies of high-resolution infrared spectra which show lines which do have the radial velocities, and the large velocity amplitudes, that are expected for the motion of the photosphere.

The real break-through, it seems to me, came from investigations of line doubling, particularly Maehara's (1968) study of the doubling of atomic lines on near-infrared spectrograms of χ Cyg, an S-type Mira. Instances of line doubling in Miras had been reported earlier -- in the S star R And (Merrill and Greenstein 1958; Spinrad and Wing 1969) and in the carbon star R Lep (Phillips and Freedman 1969) -- but Maehara was the first to carry out a spectroscopic analysis of each set of lines separately and to establish that the blue component is produced in much hotter gas than the other. He therefore was able to construct a reasonable model involving a layer of shock-heated gas rising through a stratum of cooler gases.

Maehara also measured the velocities of the lines of TiO and CN on his near-infrared plates of χ Cyg. These were not doubled, but they didn't have the same velocity, either. The CN lines were found to be formed in the warm, rising layer, while the TiO lines were formed in the cooler layer. No wonder it has been hard to interpret the molecular band strengths of Miras in terms of a single-slab model!

With a two-component model, it is not difficult to see how the discrepancy between the photometric and spectroscopic results might be resolved. We must simply suppose that, during the maximum and post-maximum phases, most of the light comes from the deep, rising layer -- which brightens bolometrically as it swells and rises above the sources of continuous and molecular opacity in the cooler, in-falling layer -- while most of the absorption lines seen spectroscopically are produced in the in-falling layer.

It is only when double lines can be seen in the spectrum that we can measure the temperatures and motions of both layers and thus obtain the information we need to specify the parameters of a two-component model. Spectrograms of Miras in the blue region generally do not show double lines; evidently the opacity in the blue is too great to allow the deep layer to be seen. Rayleigh scattering, with its λ^{-4} dependence, is likely to contribute to the opacity in the blue, along with TiO bands and the overlapping wings of atomic lines. The advantage gained by Maehara (1968) in using the near-infrared and by Spinrad and Wing (1969) in using the one-micron region is considerable. It is also no mere coincidence that all reported instances of atomic line doubling have been found in S- and C-type Miras, which have lower atmospheric opacities than the much more common M-type Miras. [I do not count the doubled lines reported in o Cet by Adams (1941), since the displaced components that he saw were from an expanding circumstellar shell, rather than a deep layer of rising gas].

Much more complete information about the two-component model has come from the study of the infrared lines of carbon monoxide. The two-micron region where the first-overtone CO bands lie corresponds to the minimum opacity due to H^-, which in any case is seriously depleted at the cool temperatures of Miras because of the shortage of free electrons. Although the CO lines themselves are strong, they are not very densely packed, and it is possible to see down to the photosphere between these lines. Furthermore, the CO molecule is very stable and can exist at the high temperatures of the shock-heated photosphere. Hence it is possible to see photospheric CO absorption lines whenever the motion of the photosphere displaces them from the corresponding lines formed in the cool outer envelope.

Figures 9 and 10 show a section of the spectrum of χ Cyg in the region of the first-overtone CO bands on two different dates. They were obtained with a Fourier-transform spectrometer at the Kitt Peak National Observatory. Wavenumber increases from upper left to lower right. Most of the absorption features visible in these spectra are due to CO, although telluric H_2O lines are also present. For orientation I have labeled the (3,1) and (2,0) band heads of $C^{12}O^{16}$ on the third and fourth strips, respectively, of Figure 9.

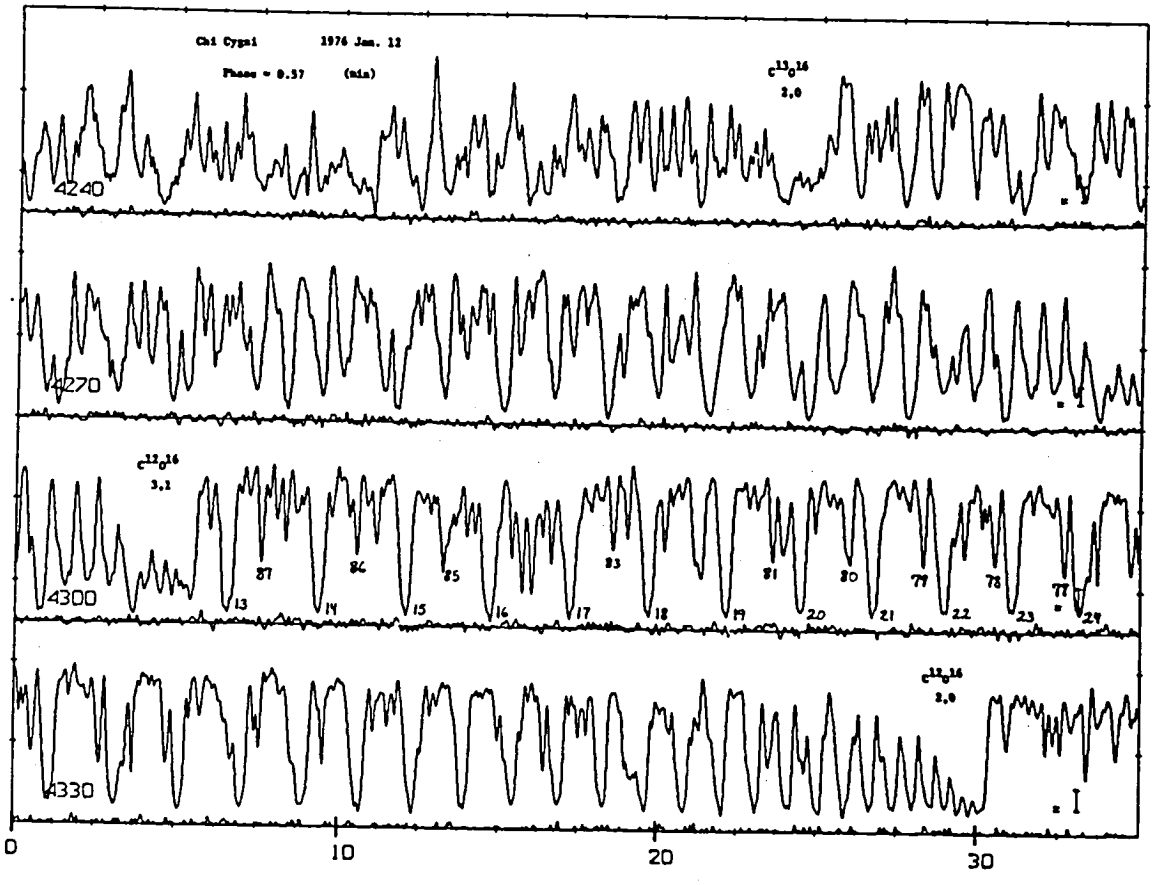

Fig. 9 - The spectrum of χ Cyg from 4240 to 4360 cm^{-1} (2.36 to 2.29 μ) on 1976 Jan. 12, when the star was at minimum light (phase 0.57). The (2,0) and (3,1) heads of $C^{12}O^{16}$ and the (2,0) head of $C^{13}O^{16}$ are labeled, as are the rotational quantum numbers of some of the lines of the (2,0) band (in the third strip). All CO features are sharp and single. From an unpublished Kitt Peak spectrum (courtesy D. N. B. Hall, S. T. Ridgway, and K. H. Hinkle).

The (4,2) head is in the left half of the first strip, where the spectrum is messy because of H_2O contamination, and the (2,0) head of the isotopic molecule $C^{13}O^{16}$ is clearly visible in the right half of the first strip. I have also labeled, on the third strip, the rotational quantum numbers of some of the R-branch lines of the (2,0) band of $C^{12}O^{16}$; the two sequences can, of course, be followed into the fourth strip, but they become blended together as they approach the band head, which occurs at about quantum number 50.

The spectrum shown in Figure 9 was taken at minimum light when the CO lines are sharp and single. The one shown in Figure 10 was obtained seven

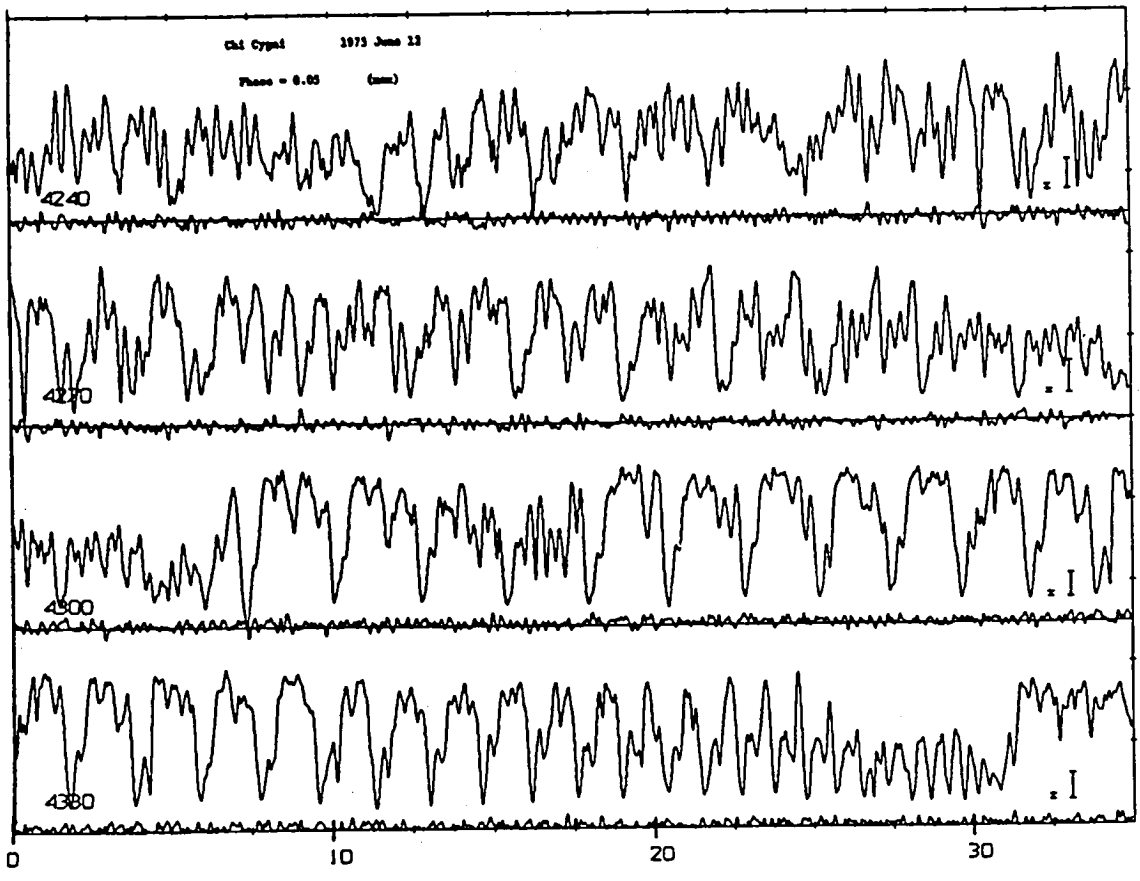

Fig. 10 - The same as Figure 9, except that the date was 1975 June 12, when χ Cyg was at maximum (phase 0.05). Here the CO features are double.

months earlier when the variable was at maximum, and we see at once that all the CO features, including the band heads, are doubled. The doubling is particularly obvious in the fourth strip. The weaker components, shifted to shorter wavelengths, can be identified with the deeper, warmer layer.

The comparison of Figures 9 and 10 points out two great advantages of the infrared CO bands in studies of line doubling, in addition to those already mentioned. First, since Miras have relatively small light amplitudes in the infrared, spectra of the same high quality can be obtained throughout the cycle. Second, because the doubling is shown by a large number of lines covering a substantial range in excitation, it is possible to measure the velocities and temperatures of both atmospheric layers with high precision.

The first report of the doubling of CO lines in a Mira variable was published by Maillard (1974), who described the spectrum of R Leo. Two extensive programs of infrared spectroscopy of Miras have also been undertaken: one the recently-completed Ph.D. dissertation of K. H. Hinkle, supervised by T. G. Barnes and D. L. Lambert, at the University of Texas, and the other an on-going project at Kitt Peak National Observatory, where D. N. B. Hall and S. T. Ridgway, who initiated it, have now been joined by Hinkle. The Texas results for R Leo, the star observed most extensively, have been published (Hinkle 1978 - CO and OH bands) or are in press (Hinkle and Barnes 1979 - H_2O bands). These papers are extremely illuminating, and I hope that the brief summary I will give here will inspire you to read them. Results from the Kitt Peak program have not yet been published, but since it uses even higher spectral resolution and involves extensive coverage of several stars, it may be expected to shed still more light on the Mira phenomenon.

From the positions and strengths of lines of both CO and OH measured between 1.6 and 2.5 μ in the spectrum of R Leo at nine distinct phases, Hinkle (1978) has been able to give a much clearer picture of the velocity and temperature structure and the manner in which these quantities vary through the cycle. Line doubling is most apparent just before maximum light, since at that time we begin to see the blue-shifted components from the deep part of the photosphere, which has just encountered the shock wave of a new cycle, while the infalling material from the previous cycle has not yet faded from visibility. In addition, Hinkle identified a third layer, a cool outer shell which produces only low-excitation lines and is falling slowly back toward the star; thus some of the infrared lines, at certain phases, were actually seen as triple.

These results are shown in Figure 11, in which velocity is plotted against phase. This figure is based on the first-overtone OH bands; similar results were obtained for the first- and second-overtone CO bands. For the purposes of the present discussion, two results stand out as being the most important. (1) The velocities of the warm, blue-shifted component near maximum light are algebraically much smaller than any previously seen in the absorption spectrum and are similar to those of the hydrogen emission lines;

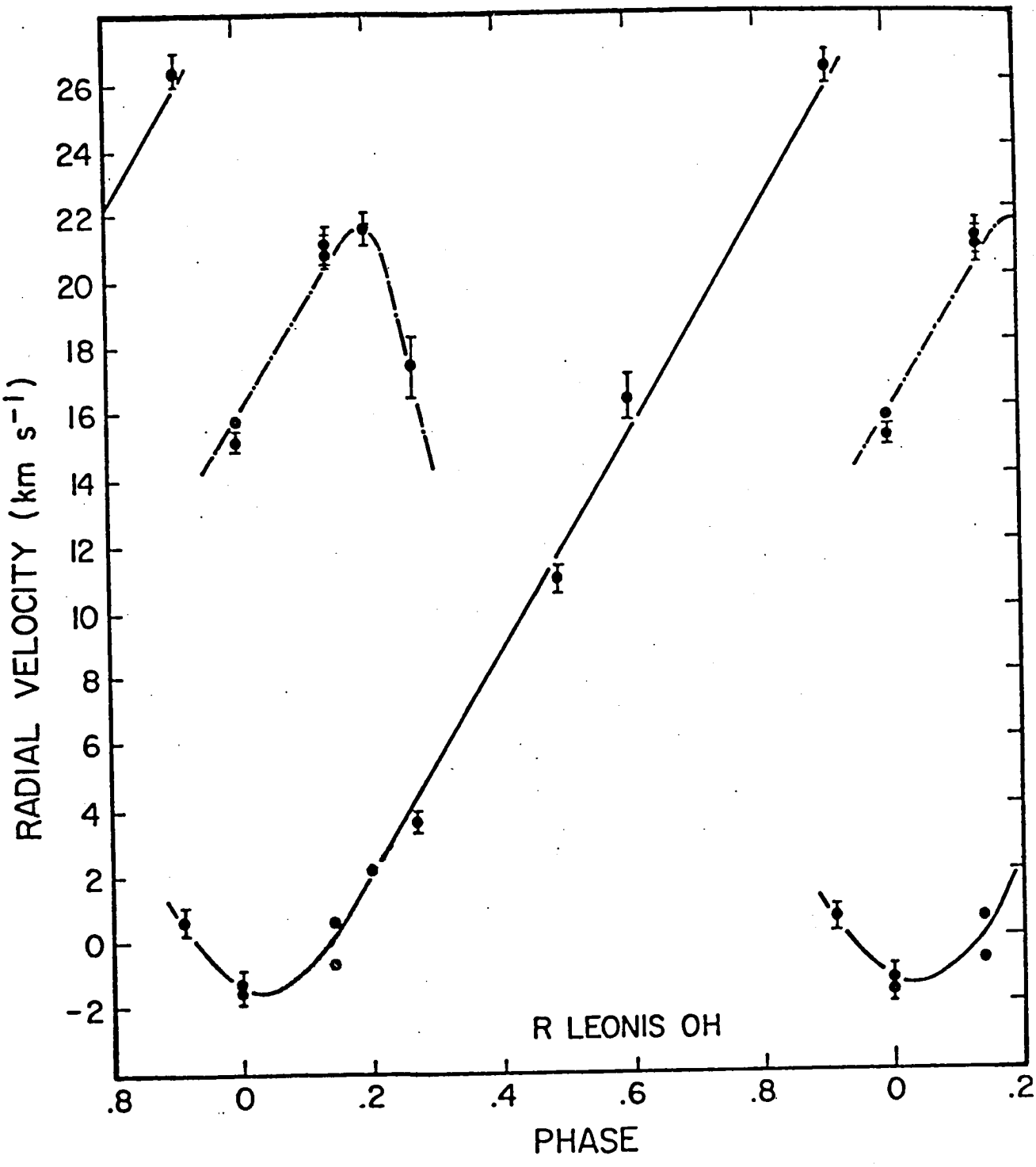

Fig. 11 - Velocity variations shown by OH lines in R Leo. Near maximum light (phase 0) the velocity is smallest as the gas rises rapidly; the motion can be followed for a full cycle as the gas decelerates and falls back in, and near phase 0.9 it is possible to see the photospheric layers from two successive cycles. In addition, the low-excitation OH lines show another component (dot-dash curve) which is identified with the cool circumstellar shell. From Hinkle (1978).

this is, in fact, the sort of velocity required for the expanding photosphere inferred from the photometry between the times of the visual and bolometric maxima. (2) The amplitude of the velocity variation, 27 km s^{-1}, is larger than any previously found and is, for the first time, consistent with the photometric results. The same gas can be seen throughout a complete cycle as it rises, decelerates, and falls back in.

Hinkle (1978) finds that a consistent pulsational model for R Leo can be derived if the center-of-mass velocity is 8 ± 1 km s^{-1}. This value is significantly smaller than most of the absorption-line velocities measured in the blue, which range from 7 to 15 km s^{-1} as a function of phase (Merrill 1946, 1952). This displacement of the mean absorption velocity from the center-of-mass velocity, which indicates that the absorbing material is falling in, is consistent with the suggestion of Reid and Dickinson (1976) discussed earlier.

Another molecule that produces a great many lines in the infrared spectra of Miras is H_2O, and its lines, too, are double throughout much of the cycle (Hinkle and Barnes 1979). The spectrum of H_2O is so complicated that the doubling of its lines might have gone unnoticed, were it not for the fact that the H_2O lines are sometimes sharp and single. The component that is always present can be identified with the cool circumstellar layer which also produces CO and OH lines of the same velocity. The other, which shows a greater range in velocity, comes from the photosphere. The behavior of the H_2O spectrum is thus similar to that of CO and OH, but there is an interesting difference. At maximum light, when the warm layer is moving rapidly outward and the doubling of the CO and OH lines is easily seen, the H_2O lines are single. Hinkle and Barnes offer a simple explanation for this difference: the H_2O molecules are dissociated at the high temperatures of the photosphere near maximum light, and they do not start to form in appreciable numbers until about 0.1 cycle later, when the photospheric temperature has dropped sufficiently.

Figure 12 illustrates the doubling of H_2O lines in R Leo. Nearly all the absorption in this spectral interval is due to stellar H_2O. In the upper spectrum, taken at maximum light, the lines are single and only the

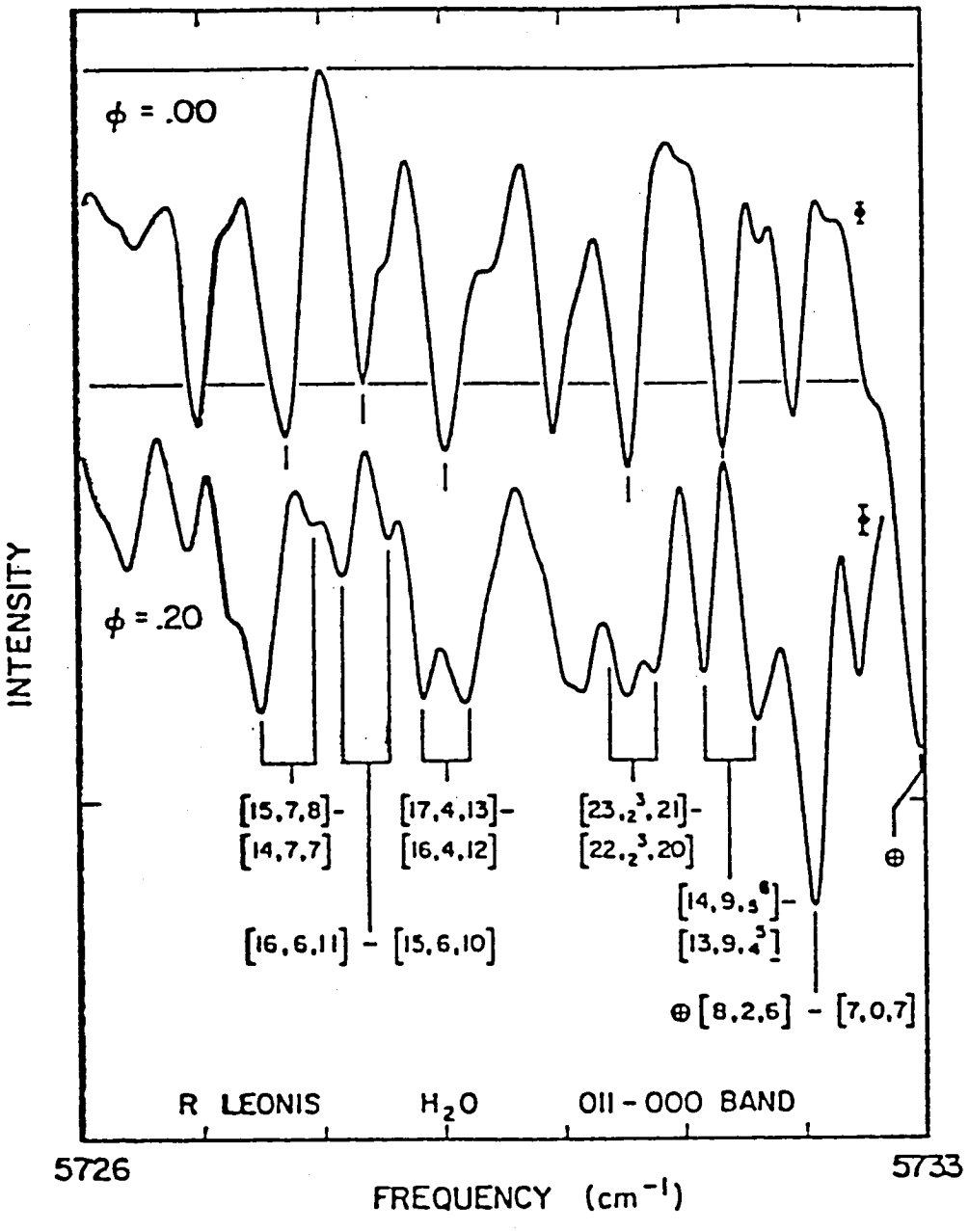

Fig. 12 - A section of the infrared spectrum of R Leo dominated by lines of H_2O. The lines are single at maximum light (upper spectrum) and double at phase 0.2 (lower spectrum). From Hinkle and Barnes (1979).

cool shell component is present. In the lower spectrum, taken 0.2 cycle later, the shell component of each line is shifted to the left as the material falls back into the star, and a second component from the rising photosphere appears, shifted to the right.

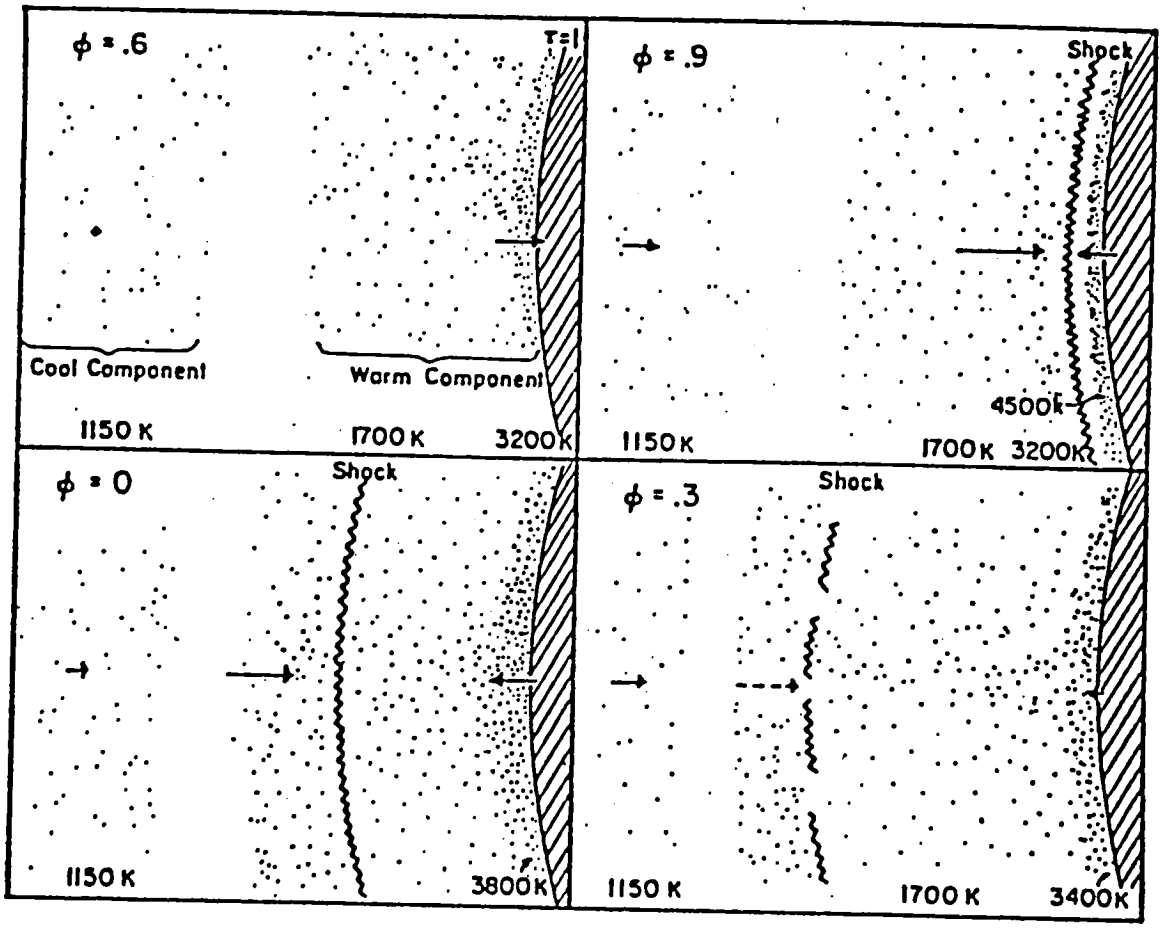

Fig. 13 - Schematic representation of the outer atmosphere of a Mira variable at phases 0.6, 0.9, 0.0, and 0.3, based on infrared spectroscopy of R Leo. The arrows represent gas velocities. From Hinkle and Barnes (1979).

Hinkle and Barnes (1979) have summarized in Figure 13 the picture of R Leo that they have put together from their infrared observations. At all phases a cool circumstellar shell is present, contributing low-excitation lines. The stellar photosphere pulsates and is at all times hotter than the temperatures conventionally ascribed to Miras -- a result anticipated by narrow-band photometry in the infrared (Wing 1967). Intermediate temperatures occur in the star's upper atmosphere, where most of the atomic and molecular absorption lines are formed and through which the shock wave propagates.

I find the recent results from infrared spectroscopy extremely encouraging. On the one hand they show that the spectroscopic approach can indeed give information about the pulsational properties of Miras. At the same time

they show us how to construct a model which, at least in its broad outline, is consistent with the photometric as well as the spectroscopic observations.

CONCLUDING REMARKS

This review has touched upon a wide variety of topics; the common theme has been the great extent of the observable atmospheres of the Mira variables. We have considered various methods for measuring the sizes of these atmospheres, and more particularly the manner in which the size changes through the cycle. The results obtained by different methods have been compared, and the differences thus found have reminded us that observations of Miras are not always easy to interpret.

I have emphasized the problems of interpretation because it seems to me that these are not always given sufficient attention. I hope I have distinguished between the problems that are the star's fault (such as departures from spherical symmetry) and those which, dear Brutus, are our own (such as unwittingly combining results which refer to different parts of the star). While the Miras will always be difficult objects to treat, some of the problems that have baffled astronomers for decades have recently disappeared. In particular the famous discrepancy between the photometric and spectroscopic diameter curves turns out not to be a real discrepancy at all, since the two methods are not looking at the same gas. The discrepancies between molecular band strength and continuum color temperature can be accounted for in the same way.

A simple model for the atmospheric structure and motions of Miras, based on Hinkle's recent observations of the doubling of infrared molecular lines, has been described. This model, consisting of two atmospheric layers plus a circumstellar shell, has been remarkably successful in providing a physically plausible picture of the atmosphere which is consistent with the photometrically-measured magnitude and temperature variations as well as the spectroscopic data. However, it is of course much <u>too</u> simple to account for <u>all</u> the observations. For example, in Figure 13 the outer atmosphere is

represented by a large region at the uniform temperature of 1700°K, whereas we have long known that temperature and velocity gradients must exist since the measured velocities of absorption lines show a dependence on excitation potential. In another paper at this conference, Pilachowski, Wallerstein, and Willson (1979) treat the absorption-line velocities as functions of excitation potential, ionization potential, wavelength, and line strength; their results for the outer atmosphere should now be combined with the broader picture given by studies of line doubling to obtain a more complete and realistic model for the atmosphere.

Much observational work on Miras remains to be done. In particular I would like to encourage work in three areas. First, it is important to find out how well the radial velocity variations of the infrared molecular lines repeat from cycle to cycle. In the work done to date it has been necessary to combine observations from different cycles, and this procedure generally has not been very successful with other kinds of observations of Miras. The current program of infrared spectroscopy at Kitt Peak should settle this point. Second, measurements of molecular band strengths and photospheric color temperatures should be made around the cycle by narrow-band photometry, but unlike previous measurements of this kind, they should be accompanied by high-resolution spectroscopy so that the region of formation of each spectral feature can be identified from its radial velocity. Such combined data could form the basis for a more detailed model of the atmosphere. Finally, direct diameter measurements through as much of the cycle as possible, by speckle interferometry in well-defined wavelength bands, are badly needed. Now that it is possible to derive diameter curves from photometry and spectroscopy that are at least qualitatively the same, we must be brave and ask whether the same result can be obtained by direct measurement.

I would like to thank Dr. Kenneth H. Hinkle for showing me his results prior to publication, and for providing the Kitt Peak spectra shown in Figures 9 and 10. I also thank Dr. George Wallerstein for helpful correspondence.

REFERENCES

Adams, W. S. 1941, *Ap. J.* 93, 11.

Cahn, J. H., and Wyatt, S. P. 1978, *Ap. J.* 221, 163.

Hinkle, K. H. 1978, *Ap. J.* 220, 210.

Hinkle, K. H., and Barnes, T. G. 1979, *Ap. J.* (in press).

Joy, A. H. 1926, *Ap. J.* 63, 281.

Joy, A. H. 1947, *Ap. J.* 106, 288.

Joy, A. H. 1954, *Ap. J. Suppl.* 1, 39.

Keenan, P. C. 1966, *Ap. J. Suppl.* 13, 333.

Keenan, P. C., Garrison, R. F., and Deutsch, A. J. 1974, *Ap. J. Suppl.* 28, 271.

Kuiper, G. P. 1938, *Ap. J.* 88, 429.

Labeyrie, A., Koechlin, L., Bonneau, D., Blazit, A., and Foy, R. 1977, *Ap. J. (Letters)* 218, L75.

Lockwood, G. W. 1972, *Ap. J. Suppl.* 24, 375.

Lockwood, G. W., and Wing, R. F. 1971, *Ap. J.* 169, 63.

Maehara, H. 1968, *Publ. Astron. Soc. Japan* 20, 77.

Maillard, J.-P. 1974, *Highlights of Astronomy* 3, 269.

Merrill, P. W. 1946, *Ap. J.* 103, 275.

Merrill, P. W. 1952, *Ap. J.* 116, 337.

Merrill, P. W. 1955, "Some Questions Concerning Long Period Variable Stars", in *Studies of Long Period Variables*, ed. L. Campbell (Cambridge: Amer. Assoc. of Variable Star Observers), p. ix.

Merrill, P. W. 1960, in *Stellar Atmospheres*, ed. J. L. Greenstein (Chicago: University of Chicago Press), p. 509.

Merrill, P. W., and Greenstein, J. L. 1958, *Publ. Astron. Soc. Pacific* 70, 98.

Nather, R. E., and Wild, P. A. T. 1973, *Astron. J.* 78, 628.

Pettit, E., and Nicholson, S. B. 1933, *Ap. J.* 78, 320.

Phillips, J. G., and Freedman, R. S. 1969, *Publ. Astron. Soc. Pacific* 81, 521.

Pilachowski, C., Wallerstein, G., and Willson, L. A. 1979, in *Current Problems in Stellar Pulsation Instabilities,* ed. D. Fischel, J. R. Lesh, and W. M. Sparks (NASA; in press).

Reid, M. J., and Dickinson, D. F. 1976, *Ap. J.* 209, 505.

Ridgway, S. T., Wells, D. C., and Joyce, R. R. 1977, *Astron. J.* 82, 414.

Smak, J. I. 1966, *Ann. Rev. Astron. Ap.* 4, 19.

Spinrad, H., and Wing, R. F. 1969, *Ann. Rev. Astron. Ap.* 7, 249.

Strecker, D. W., Erickson, E. F., and Witteborn, F. C. 1978, *Astron. J.* 83, 26.

Wallerstein, G. 1975, *Ap. J. Suppl.* 29, 375.

Wallerstein, G. 1977, *J. Roy. Astron. Soc. Canada* 71, 298.

Willson, L. A. 1976, *Ap. J.* 205, 172.

Willson, L. A., and Hill, S. J. 1979, *Ap. J.* (in press).

Wing, R. F. 1964, *Publ. Astron. Soc. Pacific* 76, 296.

Wing, R. F. 1967, Ph.D. dissertation, University of California, Berkeley.

Wing, R. F. 1974, *Highlights of Astronomy* 3, 285.

Wing, R. F., and Carpenter, K. G. 1978, *Bull. Amer. Astron. Soc.* 10, 444.

Wing, R. F., and Lockwood, G. W. 1973, *Ap. J.* 184, 873.

PERIOD RATIOS OF RED GIANTS AND SUPERGIANTS

Kam-Ching Leung

Behlen Observatory
Department of Physics and Astronomy
University of Nebraska
Lincoln, Nebraska

and

Office of Energy Research
U. S. Department of Energy
Washington, D. C. U.S.A.

It is a general belief that all late-type giants and supergiants are unstable. The variabilities tend to be more regular and with large amplitudes (in visible light) for the giants - long period variables (LPV). They tend to be much less regular and or erratic and with much smaller amplitudes for the supergiants - semi-regular variables (SRV). Since their light curves change from cycle to cycle, it is not possible to describe a red variable by just a single period and shape of light variation. We would like to investigate whether the light variation can be interpreted as superimposition of two/or more periodic light curve components of arbitrary shape (i.e. non-sinusoidal shape). Should this be successful we would like to determine the values of the period ratios of these red variables.

The visual observations of selected stars published passim in Harvard Annals and AAVSO Quarterly by the American Association of Variable Star Observers (AAVSO) were employed. The method of analysis has been briefly described previously by Leung (1971). The observations used for a red variable usually cover an interval of about 50 years.

Supergiants - SRV. In the case of SRV the erratic changes in both period and shape of the light curve are common, therefore a satisfactory representation of the observations is extremely difficult to achieve. The primary periods and secondary periods of M - type supergiants were summarized by Stothers and Leung (1971). Their results are listed in Tables 1 and 2. The periods are functions of temperature (Spectral type) and radius (liminosity class). The primary period is associated with large amplitude light variation.

Table 1. *Primary periods (in days) of variable* M-*type supergiants*

Class	M1	M2	M2.5	M3	M3.5	M4
Ia	...	586	...	670 459	900	968
Iab	184 182	290	378 325	467 460	500	689
Ib	...	165	...	...	365	415

Table 2. *Secondary periods (in days) of variable* M-*type supergiants*

Class	M1	M2	M2.5	M3	M3.5	M4
Ia	...	5000 4500	...	...	...	...
Iab	1733	2800 2200	...	3060	...	2900
Ib	...	2050	...	...	2950	4100

The period ratio (secondary to primary) was found to be about 10 for the M supergiants. Stothers and Leung connected the primary period to the pulsational period, and the long secondary period to the convective turnover time of the giant cells in the stellar envelope. S Per (Leung and Stothers 1977) is a more regular variable among the SRV. The observations and the computed light curve from 2 period - components are shown in Figure 1. The light curve of S Per resembles LPV even though the period ratio does not.

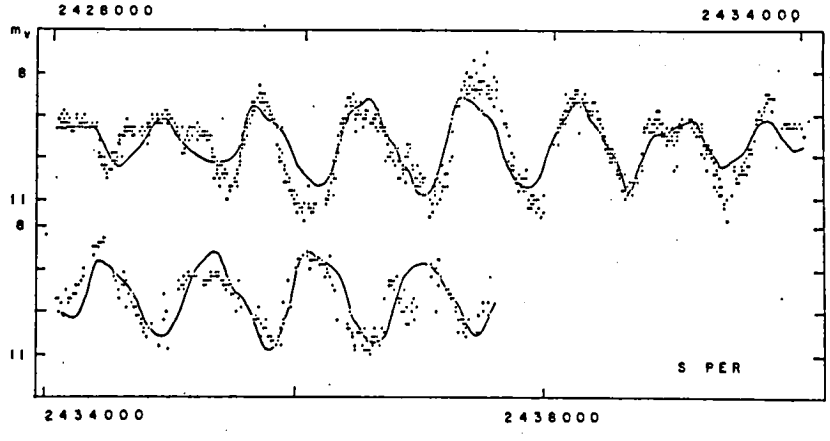

Fig. 1 AAVSO observations of S Per (six-day-mean). Computed light curve (smooth curve) based on 2 period-components. Abscissa is Julian day.

Giants - LPV. Seven LPV; O Cet, R And, T Cep, T Cas, R Hya, S CrB and T Cen, were analyzed. Examples of the observations and their computed light curves are shown in Figures 2 and 3.

The crosses are observations not included in the data set in deriving the period-components. Thus, these sections of the light curves, represents the predictions by the computer light curves.

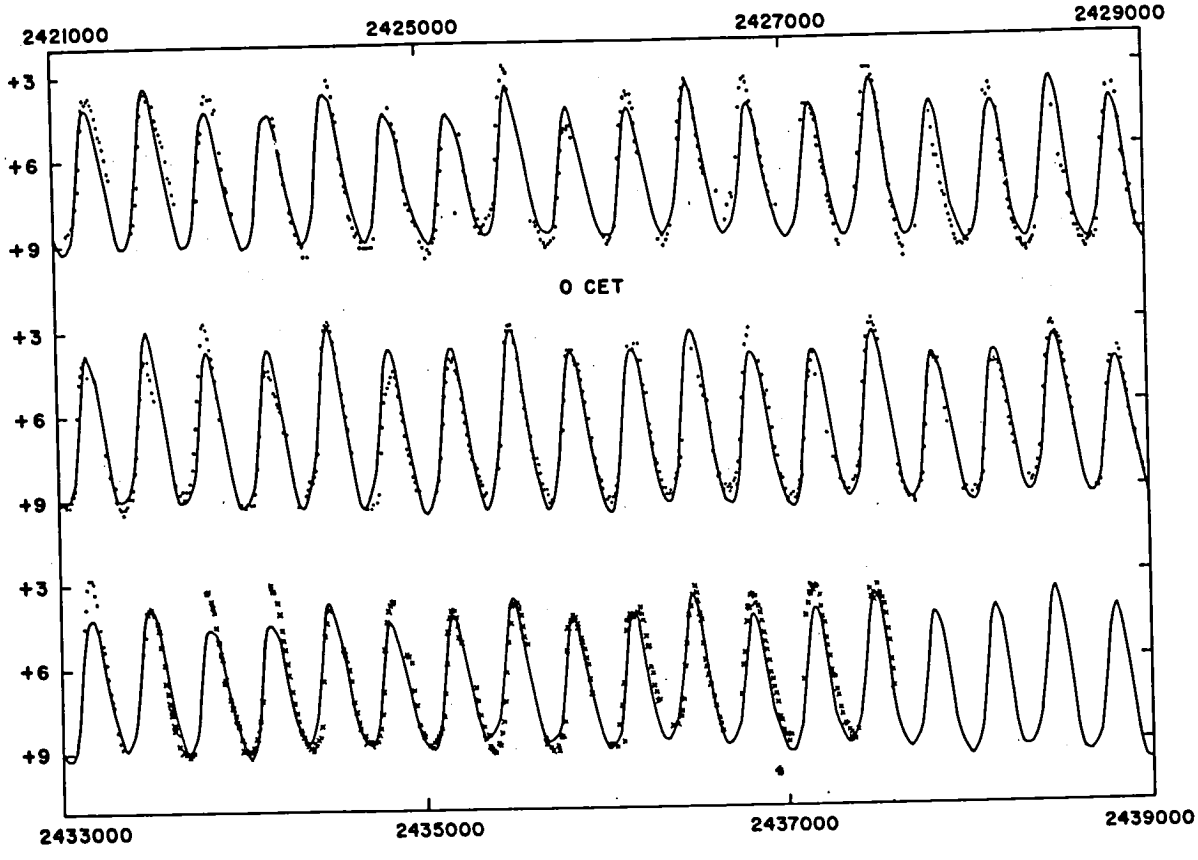

Fig. 2 AAVSO observations of O Cet (ten-day-mean). Computed light curve (smooth curve) based on 3 period-components. Observations not included in the determination of period-components are denoted as crosses. Abscissa is Julian day.

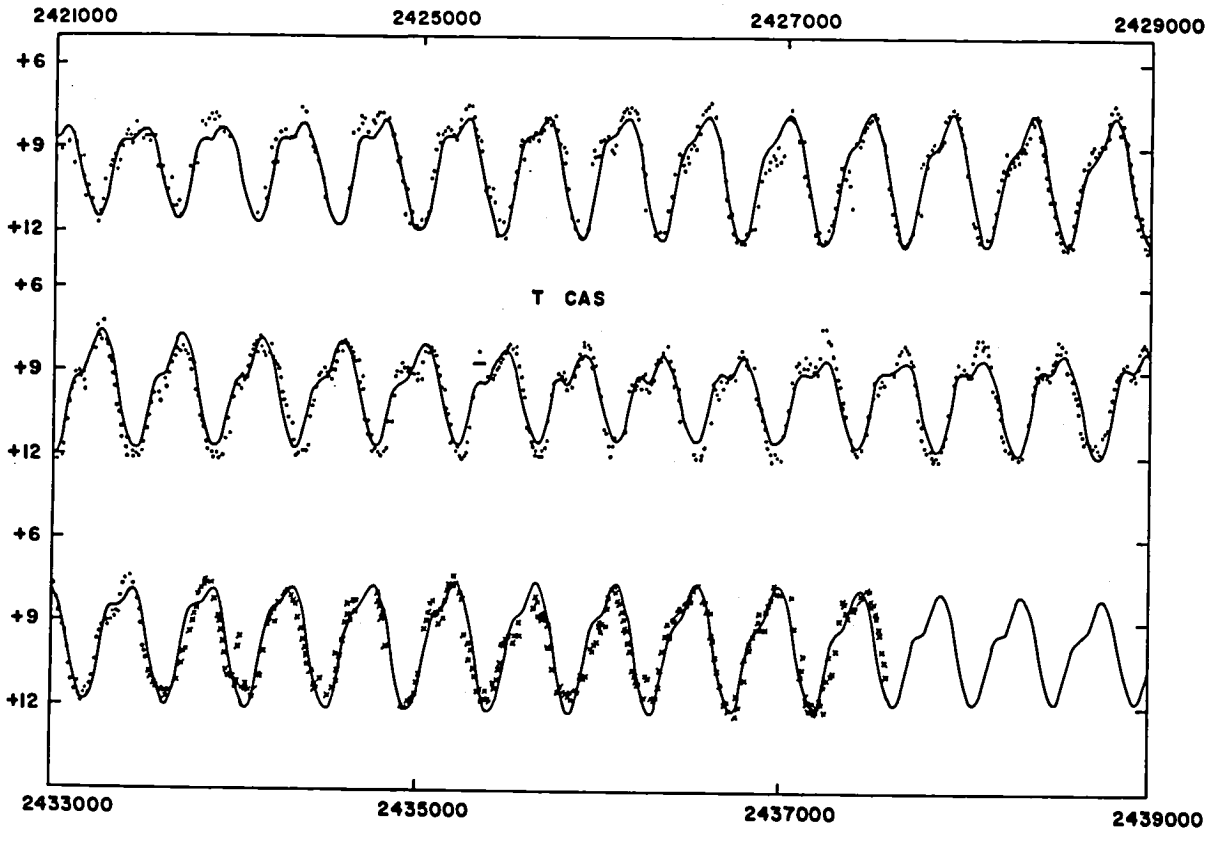

Fig. 3 AAVSO observations of T Cas (ten-day-mean). Computed light curve (smooth curve) based on 2 period-components. Observations not included in the determination of period-components are denoted as crosses. Abscissa is Julian day.

The computed light curves in general for all selected variables fit the observations quite satisfactorily. The root-mean-squared errors are ranging from 0.4 to 0.6 of a magnitude. Two period-components were determined for each of the selected LPV, except for O Cet where 3 period-components were employed. The period ratios (P2/P1) for 5 variables are centered around 1.04. The shorter period P1 is associated with the larger amplitude of variation. The amplitude ratios

(A2/A1) range from 0.15 to 0.28. The period and amplitude ratios of T Cen and S CrB do not fit into the general behavior described above. The unusual carbon star V Hya (Leung 1973) has very peculiar light variation. Four distinct period-components were found for this variable.

We believe that the primary period, P1, is the pulsational period, and the modulating period, P2, may be derived from a non-radial mode.

REFERENCES

Leung, K. C. 1971, Bull. Amer. Astron. Soc. 3, 485.

_____ 1973, Bull. Amer. Astron. Soc. 5, 415.

Leung, K. C., and Stothers, R. 1977, J. British Astron. Assoc. 87, 263

Stothers, R., and Leung, K. C. 1971, Astron. and Astrophys. 10, 290.

Discussion

Stellingwerf: If you have a period ratio of 1.05, it seems that you would see beats every 20 periods or so. Did you try period ratios around 20?

Leung: In this kind of technique you don't force the period to be what you want. You have a bunch of observations, and you find the fundamental period almost by just looking at them, which is fairly easy. You try to find the best fit light curve (period and slope), which is normally skewed, or with humps. Then you prewhiten the observations and you perform a periodogram analysis, which gives a more or less sinusoidal fit. You don't want that, so when you find the period from the periodogram analysis -- the normal technique of spectrum analysis -- you go to the much more time-consuming technique of a least-squares fit in the non-sinusoidal light curve. Then whatever peak you get, can't be forced to a particular ratio.

Stellingwerf: But if you have a period ratio of 1.05, you should have another one at about 20. I was wondering whether you saw one.

Leung: No. Normally we use observations covering about 50 years.

P. Wood: Have you made any statistical tests on these secondary periods to see how significant they are?

Leung: We do that by studying the (o - c) and see how much the residues are reduced. There is no way you can fit a light curve with a single period, given the differing maxima, differing humps, and differing positions. Take T Cas -- not only does the hump appear in different places, but the height of the hump is different.

P. Wood: Did you perform a spectral analysis on one of these things?

Leung: No, because you cannot do that. The normal periodogram analysis, or power spectrum, gives the wrong answer, because the shape is not anything like sinusoidal. The very steep rise and gradual descent are of the RR Lyrae type. That's why the subroutine for power spectrum analysis is only one subroutine.

A. Cox: Do you imply that you have found all the periods, or are there more?

Leung: For Miras, for example, I get three. The fourth one is of very small amplitude, in the noise level. I don't want to hold myself to the fourth one. For our stars, the amplitude of the third one is very small. The problem is that we are dealing with amateur observations. After removing two periods, the σ is generally about 0.5 mag. That is precisely the observational error of amateur observations.

A. Cox: Have you tried professional observations of these stars?

Leung: I need 15-30 years of observations, and so far, none of them has been observed that long. I don't think I intend to do it myself! [Laughter]

VELOCITY STRUCTURE IN LONG PERIOD VARIABLE STAR ATMOSPHERES

C. Pilachowski and G. Wallerstein
University of Washington
Seattle, Washington

L. A. Willson
Iowa State University
Ames, Iowa

ABSTRACT

A regression analysis of the dependence of absorption line velocities on wavelength, line strength, excitation potential, and ionization potential is presented, and conclusions are drawn regarding the velocity structure of the atmosphere and the regions of formation of different lines.

I. MOTIVATION

A. Observational Considerations and Method.

High dispersion absorption line spectra of long period (Mira) variables show much larger velocity scatter (∿5-8 km/s) than similar quality observations of more normal M giants (∿1-2 km/s, approaching the expected velocity resolution of the plates used in this study).

Previous investigators have noticed correlations between the velocity of absorption lines and the excitation potential of the lower levels (see for example Merrill, 1964a,b for U Ori, R Ser, R Hya; Adams 1941 and Joy 1954 for o Ceti; Merrill 1952 for T Cas, R LMi, W Hya and T Cep). Preliminary inspection of the plates in the present study suggested the possibility of a strong correlation with ionization potential also for some of the plates.

For any atmosphere with a velocity gradient in the reversing layer the velocity determined from a given spectral line will depend on the equivalent width or line strength which determines the region of formation of the line. Maehara (1971) found a fairly strong dependence of the velocity of absorption lines on the line intensity for χ Cyg. In addition, if the continuum opacity is strongly wavelength dependent, then one might hope to discover a correlation between the wavelength of the line and its velocity.

The present study is therefore an attempt to understand the systematic effects on the absorption line velocities of the four parameters excitation potential (χ_e), ionization potential (χ_i), line strength (S), and wavelength (λ). For line strength a visual estimate on an integer

scale where most measured lines fall between 1 (very weak) and 4 (strong) has been used. The procedure has been to solve for coefficients in a multiple linear regression (least squares fit) with the four independent variables:

$$v = C_o + C_{f(\lambda)} \cdot f(\lambda) + C_S \cdot S + C_i \cdot \chi_i + C_e \cdot \chi_e \qquad (1)$$

When a group of lines contains a wide spread of parameter values, such as excitation potentials from 0 eV to 3.5 eV or wavelength from 3800 Å to 4400 Å, then the correlation coefficients derived are not very sensitive to small errors in v. If the group contains only lines with similar parameter values, such as ionization potentials from 7.4 eV to 7.9 eV or wavelengths from 4000 Å to 4075 Å, then small errors in v lead to large variations in the coefficients. For this reason, as well as to reduce everything to a common set of velocity units to facilitate comparisons between coefficients, we tabulate the results in terms of parameter ranges X_R defined by

$$X_R = C_X(X_{max} - X_{min}) \qquad (2)$$

where C_X is the coefficient for parameter X, X_{max} the maximum value assumed by the parameter in the sample, and X_{min} the minimum value assumed. Note that for wavelength we have allowed for the use of functions of λ; correlations have been calculated for $f(\lambda) = \lambda$, $1/\lambda$, $1/\lambda^2$, and $1/\lambda^4$. In general there were no differences in the results between $f(\lambda) = \lambda$ and $f(\lambda) = \lambda^{-4}$, with a very slight improvement in the significance of the fit as $f(\lambda)$ was changed from λ to $1/\lambda$, $1/\lambda^2$, and $1/\lambda^4$ in a few cases. We have therefore chosen to tabulate coefficients in terms $1/\lambda$ as an intermediate "standard case".

We expect some relationships to hold between the signs of the four coefficients based on simple arguments. The ionization potential and excitation potential dependence should reflect the velocity as a function of distance from the source of excitation and ionization; the simplest models are therefore expected to have excitation potential coefficients and ionization potential coefficients of the same sign ($C_i \cdot C_e > 0$). If the continuum opacity decreases from $\sim$3600 Å to $\sim$7800 Å (for example if the principal opacity source is Rayleigh scattering $\propto \lambda^{-4}$) then lines in the blue region of the spectrum will be formed at higher atmospheric levels than will the lines in the red region. Also, strong lines are formed higher in the atmosphere than weak ones. Hence the coefficients in λ and S should have opposite signs, or those in $1/\lambda$ and S the same sign ($C_\lambda \cdot C_s < 0$ or $C_{1/\lambda} \cdot C_s > 0$). Table 1 summarizes the four expected configurations based on these arguments, and the simplest general interpretation of each case.

B. Theoretical motivation and shock model interpretation.

The interpretation of emission lines in long period variable stars as produced in a moderately strong shock front rising from the photosphere once each cycle has proven very effective in interpreting those features (Willson 1976; Willson and Hill 1976) and is also confirmed by infrared observations (Hinkle 1978). A schematic velocity profile of a simple model for the shocked atmosphere (from Hill and Willson 1978) is shown in Figure 1. Important features of the models for the present study are:

1. The atmosphere typically contains two shocks. The lower shock, of large amplitude, produces the hydrogen emission lines and the visual continuum; the upper shock is in the reversing layer and is the direct cause most of the observed scatter in the velocities of the absorption lines.

2. The amplitude of the upper shock is expected to be $\sim$10-20 km/s for stars with masses $\sim$1 $M_\odot$ and periods from 150^d to 350^d.

3. The magnitude of the inward preshock velocity at a given shock is $\gtrsim$ the magnitude of the outward postshock velocity for the zero mass loss strictly periodic case.

Note that in a few cases the absorption lines in the red have been observed to be split, with components differing in velocity by typically 10-20 km/s (Shinkawa 1973 for S Car; Maehara 1971, for χ Cyg and o Ceti; present study plates DAO 7641 (RT Cyg) and EC 2688 (Z Oph)).

In Figure 1 we have also included an idealized distribution of velocities for A) Circumstellar lines, B and F) 0-1.0 eV lines, C and E) 1-3 eV lines, C) absorption lines of ionized elements, D) emission lines of ionized metals, and H) emission lines of hydrogen. This idealized distribution is based mainly on the results of the present study which indicate typical regions of line formation in the shock wave model for each of these classes of lines.

An interpretation of the coefficients of the regression analysis (cases a-d of Table 1) using the velocity profile of Figure 1 is presented in Table 2. There are two possible interpretations of cases c and d with the shock model, with different corollary behavior expected

as noted in the table. Isothermal hydrodynamic calculations (Willson and Hill 1976, Hill and Willson 1978) suggest a reasonable likelihood of a small region of increasing outward velocity behind the shock, as in case c1. There is, however, no very strong theoretical justification of a similar region of decreasing inward velocity ahead of the shock (case d1) although Hall (1978) sees a "hook" in the velocity of the high excitation components of molecular lines in the infrared vs. time that may result from such a decrease. In the present study the corollary behavior of the case d results strongly favors the second interpretation, unresolved splitting of low excitation lines, as does the fact that case d and mixed cases c, d account for a majority of the plates. Also in one case (DAO 7641) where the splitting is resolved, omitting the red components of the doubled lines converts this case d into a clear post shock case b.

Internal consistency for the regression analysis was judged on the basis of the following criteria:

1. Is the result a permitted model (one of cases a-d), i.e. physically reasonable?

2. Does the velocity distribution satisfy the "corollary behavior" of Table 2?

3. Does the exclusion or inclusion of an arbitrary set of lines leave the result unchanged?

4. Does the set of all regression fits satisfy our expectations for the simplest models ($C_i \cdot C_e > 0$ and $C_{1/\lambda} \cdot C_s > 0$ or cases a-d)?

Plots of the ranges of $1/\lambda$ vs. S and of χ_i vs. χ_e for all the plates are shown in Figures 2 and 3. The "forbidden regions" have been shaded beyond the minimal error of 2 km/s from each axis. Error bars on each point are pre-fit standard deviations. Clearly the plates do generally satisfy the fourth consistency criterion. The few exceptions for Z Oph are red plates which turn out to have lines present representing both shocks, and for which our simple cases therefore do not apply.

In Figures 4 and 5 are plotted the coefficient ranges $1/\lambda$ vs. χ_i and S vs. χ_e, with error bars as in Figures 2 and 3. The quadrants are marked according to the case each represents. The expected corollary behavior of small scatter plus small coefficients is seen for the preshock case a. For cases c and d large scatter and large coefficient ranges are both found - this is the corollary behavior expected if c and d both represent mixtures of lines from both sides of the shock.

The sensitivity of the results to the inclusion or exclusion of a few lines was investigated both through a series of calculations made deleting successively the most deviant lines in the sample (ones most likely to be misidentified, for example, with very high excitation or very high residual velocity) and through a "running solution". The running solution was a calculation of coefficients for sequential groups of ten lines. In Figure 6 the coefficient ranges for a running solution for S Car (D 895) are shown as a function of the average wavelength for the ten lines. Each successive group of ten lines includes five lines from the previous set. The conclusion suggested by our criteria regarding coefficient ranges and standard deviations, namely that the coefficients for χ_i and χ_e are the only ones which are significant, is clearly

supported by the trends in the running solution. The coefficients which the general analysis suggests are not significant show mostly a random scatter about zero.

The running solution is not only useful as a consistency check, it is also an efficient means of locating misidentified lines. Such lines generally cause an abrupt change in the coefficient ranges in the running solutions. In the example for S Car such "deviant" lines near 4500 Å may explain the overall lack of correlation for S even though most of the 10 point S coefficients are negative. There are in this case no obviously bad lines, however, so we have chosen to consider C_S not significant.

Note however that the running solution is a very poor means of checking the wavelength coefficient, since for lines listed in order of λ the wavelength interval for each set of ten lines is much smaller than the overall wavelength interval. For this reason a further check of the wavelength coefficient was made for those dates where two plates in different wavelength regions were available by calculating a single set of regression coefficients for these plates. In cases (such as DAO 10157 and 10162 of RT Cyg) where lines in both wavelength regions appear to be formed on the same side of the shock, the wavelength coefficients for the combined plates are consistent with those for each plate taken separately. For pairs of plates (such as Pc 3237 and 3238 of Z Oph) where there is clear evidence that the lines are formed on different sides of the shock, the combined plates create a very strong apparent wavelength dependence and yield a strong case d -- further evidence in favor of the cross shock interpretation for the case c and d results.

II. ANALYSIS OF THE OBSERVATIONAL MATERIAL

In order to interpret the actual data in terms of the schematic models of Section I we must first develop criteria for the significance or lack of significance of the coefficients, and means of evaluating the regression fits for validity. Two approaches have been used: requiring internal consistency plus comparison with a "null" case, plate DAO 10936 of β Peg, with minimal observed scatter and for which velocity gradient effects are not expected.

The requirements for a significant fit can be summarized as follows:

1. No fit for fewer than 10 lines can be considered significant.

2. The fit must significantly decrease the scatter. Mathematically we insist that

$$SD^f/SD^o \leq .9$$

where SD^o is the standard deviation of the observed velocities in the sample and SD^f is the standard deviation for the differences between observed and predicted (from the regression fit) velocities for each line in the sample. Ideally this requirement should be written in terms of a function of n, the number of lines in the sample. However, after samples containing less than 10 lines have been eliminated, and considering the relatively limited typical sample sizes (25-100 lines) used here, the constant .9 should suffice.

3. A coefficient in the regression fit is deemed <u>significant</u> if and only if the range for that coefficient is greater than the original standard deviation SD^o:

$$X_R \geq SD^o \ . \qquad (4a)$$

The coefficient is marginally significant if

$$X_R \geq SD^f \quad . \tag{4b}$$

In Table 3 the results of the regression for one plate each of β Peg, L^2 Pup and S Car, for 8 plates of RT Cyg, and for 7 plates of Z Oph are summarized. Those coefficients which satisfy Equation 4a are underlined with a solid line; those which satisfy Equation 4b are underlined with a dashed line; coefficients without underlining are not significant. Reassuringly, β Peg is found to contain no significant velocity correlations by our criteria. The case from Tables 1 and 2 which best describes each plate is listed in Table 3 also; parentheses and double assignments are used for cases which do not satisfy criterion 2 or where only one of the coefficients is significant by Equation 4a.

An immediately striking result is the large number of d and c,d results for plates with fairly large scatter. In an attempt to further clarify the interpretation of these cases, to distinguish between the two possible interpretations suggested in Table 2, we have plotted histograms of velocity for various groups of lines: low excitation (0-1 eV) absorption lines (0), moderate excitation (1-3 eV) absorption lines (X), high excitation (>3 eV) absorption lines (+), absorption lines of ions (II), emission lines of neutral atoms other than H (Fe, Cr, etc.) and ions (EII), and emission lines of hydrogen (H,H'). Such plots are shown in Figures 7 to 12 for β Peg, L^2 Pup, S Car, RT Cyg at maximum (DAO 10157, 10162) and at $+33/34^d$ (DAO 7631, 7641) and Z Oph at $+47^d$ (Pc 3237, 3238). These particular examples were selected as those

which most clearly illustrate the interpretation of several different cases with the shockwave model.

For β Peg (DAO 10936, Figure 7) we find a nearly Gaussian distribution with small scatter, mostly low excitation lines (n(1-3 eV)/n (0-3 eV) = .35 and no lines with χ_e > 3 eV) and no emission lines. This agrees with our expectation that β Peg does not have extensive velocity gradients, and suggests that our method produces significant results only for stars which are truly "abnormal".

The histogram of velocities for L^2 Pup (Figure 8) suggests that most of the lines are formed above the shock. The most probably stellar velocity is ∿53 km/s giving pre-shock infall velocity ∿5 km/s and post-shock outward velocity also ∿5 km/s. The lower shock (from the emission lines of H and Si) is near ∿40 km/s, i.e., rising with velocity relative to the star ∿13 km/s.

For S Car (Figure 9) the interpretation is less straightforward. From the location of the H emission lines the lower shock post shock velocity appears to lie 280 km/s; from the absorption lines of the ions there appears to be preshock infalling material at ∿300 km/s. There are peaks in low excitation at 288 km/s (= most likely stellar velocity?) and ∿291 km/s and peaks in 1-3 eV lines around 283 km/s and 294 km/s. Following the notation of Figure 1 it seems likely that we are seeing both shocks, with velocities A = 288 km/s, C = 294 km/s, D = 283 km/s, G = 300 km/s and H = 280 km/s. This means outward velocities relative to the star of 5 km/s (upper shock) and 8 km/s (lower shock), inward velocities of 6 km/s and 12 km/s for the two shocks, or total shock

amplitudes of 11 km/s and 20 km/s for the two shocks. This is in exact agreement with Shinkawa (1973) who found velocity curve amplitudes of 11 km/s (visual) and 20 km/s (infrared).

A common feature of all the velocity histograms is the concentration of the absorption lines of certain ions on the red edge of the main velocity peak. The interpretation of this was suggested by Figure 2: these lines are probably formed in the region immediately ahead of the shock where radiative ionization of Ba, Sr, Sc, etc. has taken place. These lines are then the best indicators of the limiting infall velocity of the material ahead of the shock.

In Figures 10-12 the velocities A-H have been indicated as far as it is possible to locate them. For RT Cyg near maximum both the red plate (DAO 10157) and the blue plate (DAO 10162) give the same mean absorption line velocity, the same scatter, and the similar ratios of low excitation to high excitation lines, suggesting both show lines from the same region. The red plate includes one possible split line, VI(19) λ 6292, with $\Delta v \approx 15$ km/s which may be the amplitude of the upper shock. The red component of this line agrees with the absorption lines of ions (in DAO 10162) in placing the pre-shock infall velocity (C) near -109 km/s. The emission line velocities from hydrogen are particularly unreliable near maximum, when overlying absorption is strongest, but all the lines together suggest the existence of shocks with post shock velocities D $\simeq$ -125 km/s and H $\simeq$ -131 km/s.

Figure 11 shows the clearest case of resolved line splitting, plate DAO 7641 of RT Cyg at 34^d, with the blue plate DAO 7631 taken one day

previously. There clearly are two groups of velocities peaking near -113 km/s and -128 km/s. In Table 3 two analyses of 7641 are listed: one for a set of velocity measurements made with a single average velocity used for the split lines (7641 A) and one set of measurements (7641 B), plotted in Figure 12, which includes separate determinations for each component. The first determination yielded case d2 (unresolved doubling, large scatter); this became case b (post shock region) when the red components of the doubled lines were excluded from the fit. This pair of plates thus provides dramatic confirmation of the shock interpretation of the regression coefficients for the absorption line velocities.

A final very interesting pair of consecutive plates of Z Oph are shown in Figure 12. Pc 3237 is a red plate ($\lambda\lambda$ 5567-6707 Å) and Pc 3238 is a blue plate (4156-4571 Å) both taken at phase $+47^d$. In the red we are clearly seeing below the shock, with a preponderence of high excitation lines, large scatter, and $\langle v \rangle$ = -93 km/s or net outward velocity (based on an estimated stellar velocity of -85 km/s) of $\sim$8 km/s. The lines in the blue plate, on the other hand, clearly originate above the shock, with more low excitation lines, less scatter, and $\langle v \rangle$ = -80 km/s suggesting infall velocity $\sim$5 km/s. Confirmation here also comes from the "anomalous" absorption and emission lines in the blue plate, which extend past the mean velocity of the red plate.

In Table 4 we summarize some known properties of the four long period variable stars in this study, with the shock amplitudes and stellar velocities suggested by the present analysis. For these four

stars, within the accuracy of the present analysis, the amplitude of the reversing layer shock near maximum light appears to be 15 ± 5 km/s, with no obvious dependence on period or spectral type.

III. GENERAL CONCLUSIONS

The scatter which is frequently found in velocity measurements of absorption lines in long period variables is probably the result of a shock of moderate amplitude (10-20 km/s) located in or near the reversing layer. The frequently observed correlations of velocity with excitation and ionization potential are a result of the velocity gradients produced by this shock in the atmosphere. A straight-forward linear regression analysis with parameters λ, S, χ_e, and χ_i is an effective way of determining the region of formation of the absorption lines for a given date and wavelength region. We have presented here a simple interpretation of the signs of the coefficients of the regression analysis in terms of case a: preshock; case b: post shock; cases c or d: across the shock, together with criteria for evaluating the validity of the fit. Finally, careful analysis of a series of plates for four long period variable stars has allowed us to estimate the amplitude of the reversing layer shock and also the most probable stellar velocity for these stars (Table 4). The results are in substantial agreement with previous velocity observations where such are available.

ACKNOWLEDGEMENTS

We are pleased to acknowledge the assistance of the Directors of these observatories: Dominion Astrophysical Observatory, Hale Observatories, Cerro Tololo Interamerican Observatory, and Lick Observatory, for the use of their telescopes and spectrographs, as well as the Astronomy Department of the California Institute of Technology for use of the Grant measuring engine. This research was support by grants from the National Science Foundation.

BIBLIOGRAPHY

Adams, W. S., 1941, Ap. J. 93, 19.

Campbell, L, 1955, Studies of Long Period Variables, AAVSO, Cambridge, MA.

Clayton, M. L. and Feast, M. W., 1969, MNRAS 146, 411.

Feast, M. W., 1963, MNRAS 125, 367.

Hall, D., 1978, (private communication).

Hill, S. J. and Willson, L. A., [in preparation].

Hinkle, K., 1978, Ap. J. 220, 210.

Joy, A. H., 1954, Ap. J. Suppl 1, 39.

Kukarkin, B. V. et al., General Catalogue of Variable Stars, Moscow, 1, 1958, 2, 1965, 3, 1971.

Maehara, H., 1968, PASJ 20, 77.

Maehara, H., 1971, PASJ 23, 503.

Merrill, P. W., 1964a, Ap. J. 102, 348.

Merrill, P. W., 1964b, Ap. J. 103, 6.

Merrill, P. W., 1952, Ap. J. 116, 18.

Merrill, P. W., and Greenstein, J. L., 1958, PASP 70, 98.

Shinkawa, D., 19 , Ap. J. Suppl. 25, 253.

Willson, L. A., 1976, Ap. J. 205, 172.

Willson, L. A. and Hill, S. J., 1976, Stellar Pulsation Conference (Los Alamos Scientific Laboratory) p. 279.

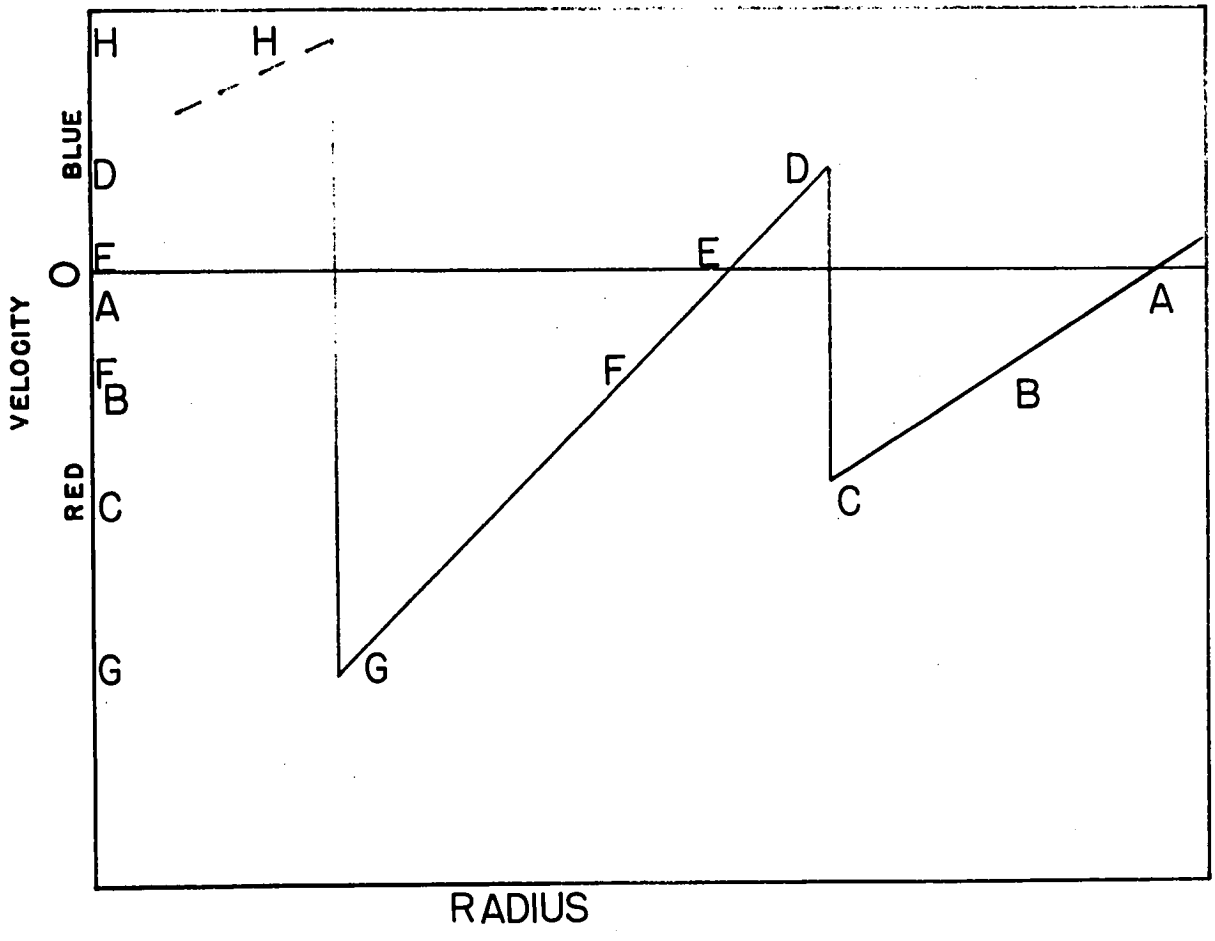

Figure 1. Schematic shock structure and regions of line formation: A, stellar velocity; B to C: increasing excitation pre shock velocities; D: post shock velocity; D to E or F: decreasing excitation; G: higher excitation pre shock region for the lower shock; H: rising post shock region, hydrogen emission line formation.

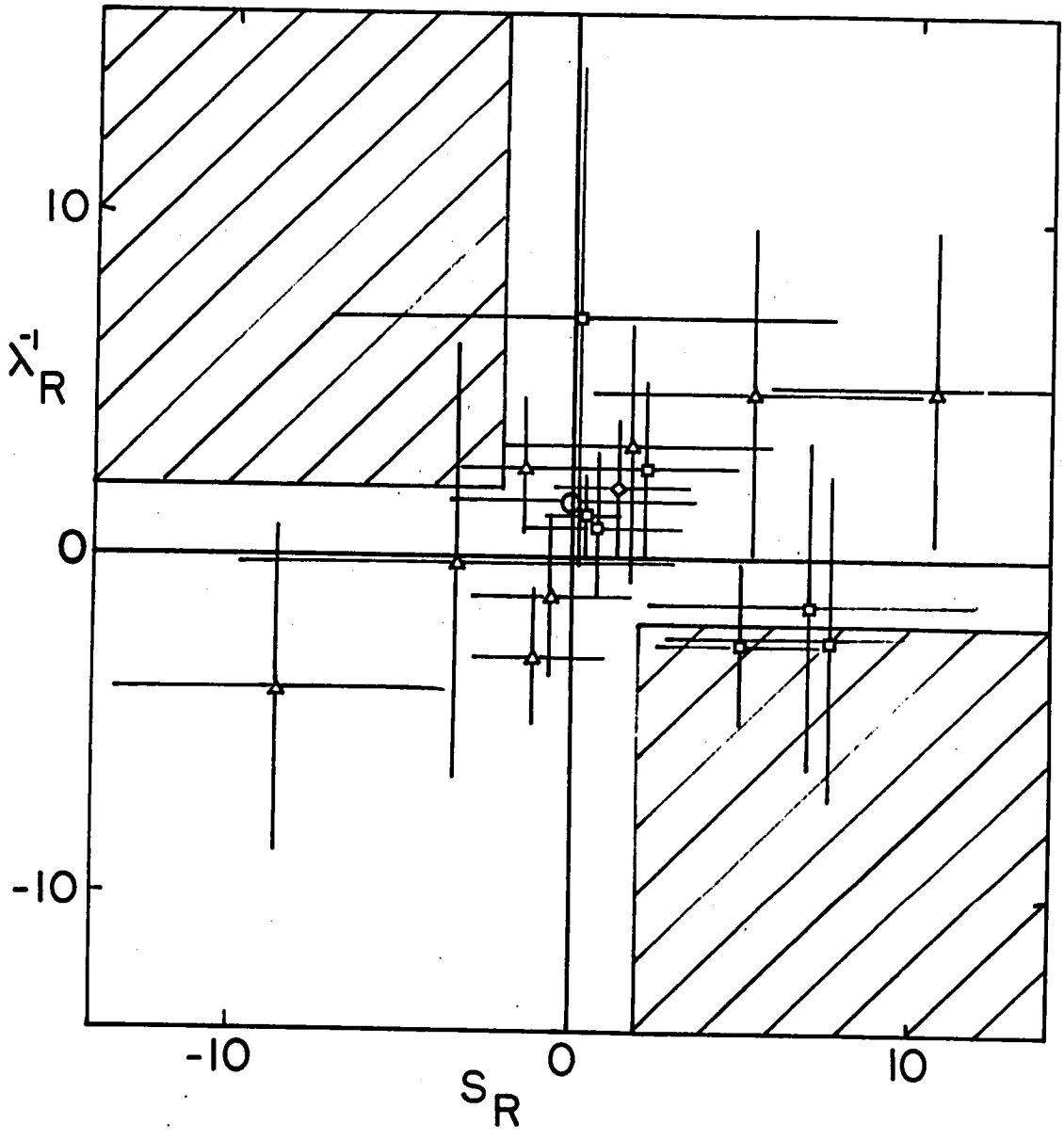

Figure 2. Plot of range of $1/\lambda$ coefficient vs. range of S coefficient for RT Cyg (Δ), Z Oph ($\square$), S Car (0), and L^2 Pup ($\diamond$). Error bars are standard deviations of observed velocities. Shaded region is forbidden region according to cases a-d of Table 1 and assuming a residual scatter of $\sim$2 km/s.

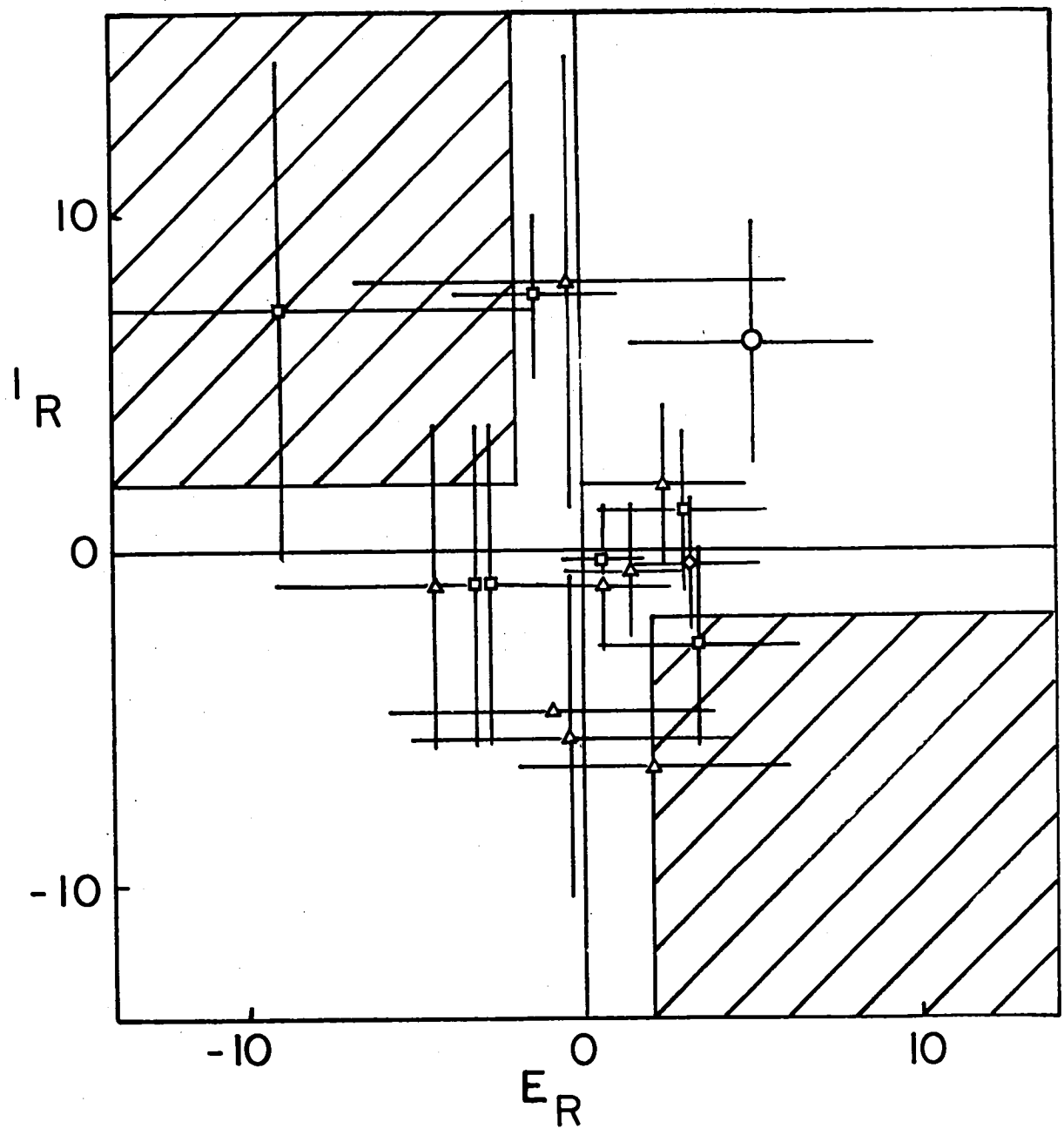

Figure 3. Coefficient ranges for χ_i vs. χ_e. Symbols and shading as for Figure 2.

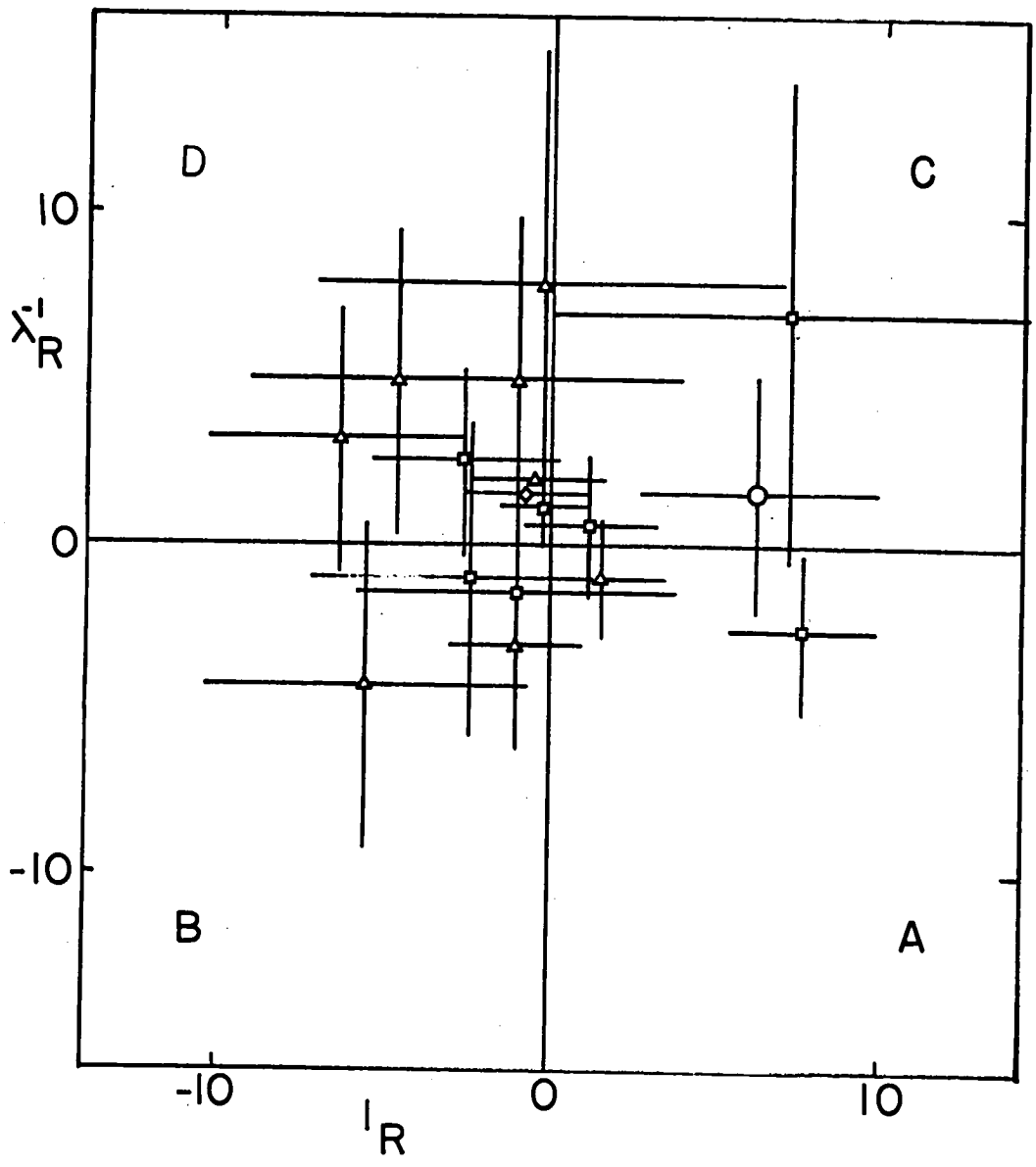

Figure 4. Coefficient ranges for $1/\lambda$ vs. χ; symbols as in Figures 1 and 2. Each quadrant represents one case of Table 1 and is labelled accordingly.

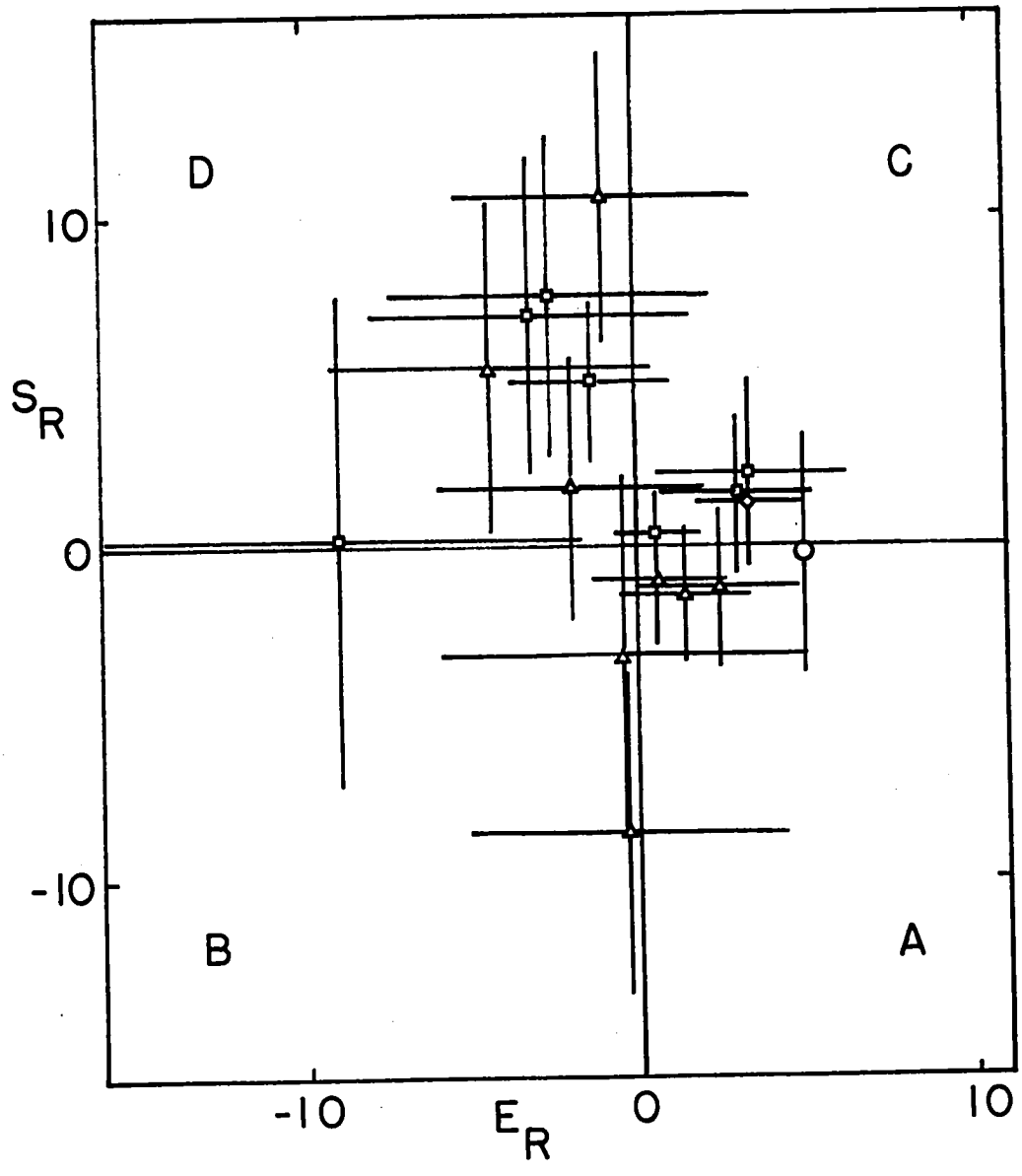

Figure 5. Coefficient ranges for S vs. χ_i; symbols and labelling of cases as in Figure 4.

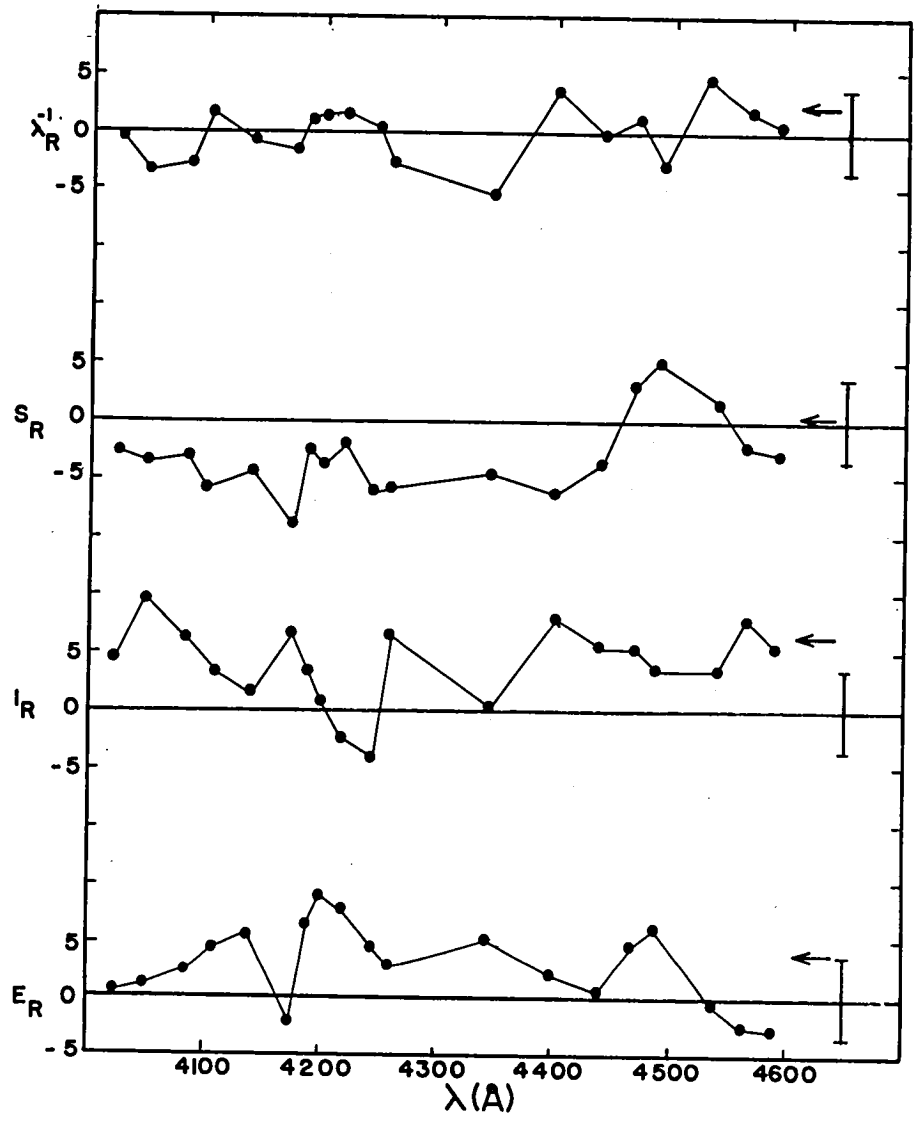

Figure 6. Running solution for S Car D895. The error bars represent ±SD, the standard deviation of the observed velocities. The arrows indicate the coefficients for the fit for the entire plate. The positive χ_i dependence is clearly supported by the running solution; the two points which are negative come from the two sets of ten lines containing λ4226.73 of CaI (2) which has an "anomalous" velocity of 288.8 km/s for its low inoization potential of 6.09 eV.

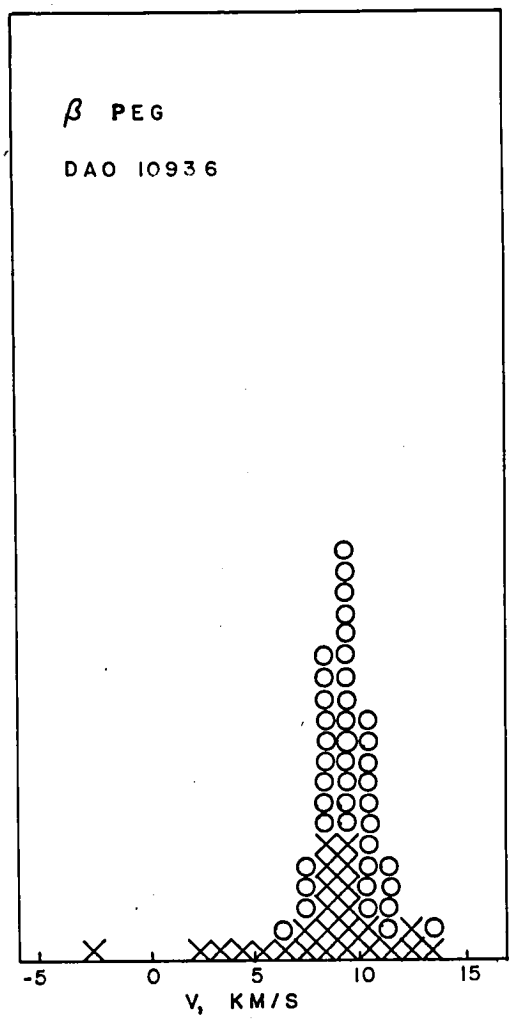

Figure 7. Heliocentric velocity histogram for β Peg. The mean absorption line velocity is 9.3 km/s. The larger scatter in the higher excitation lines may arise in part from misidentification of some lines as high excitation atomic lines rather than e.g. molecular features. Symbols for Figures 7-12: 0 = lines from 0-1 eV levels; X: 1-3 eV; +: >3 eV; II: absorption by ions; EII, Cr, Fe, H, etc. = emission lines.

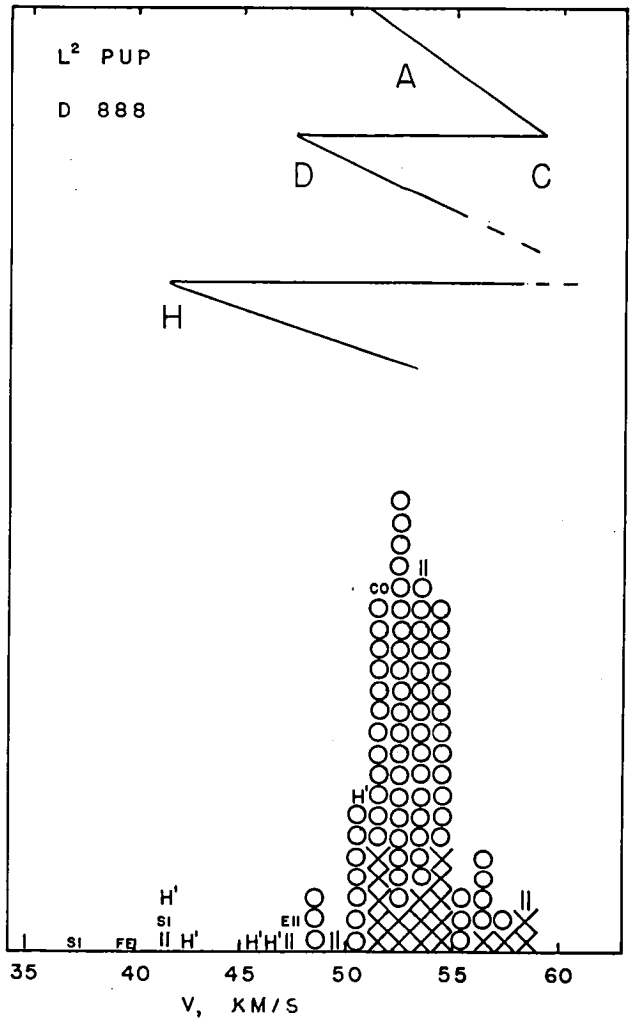

Figure 8. Heliocentric velocities histogram for L Pup. Probably location of velocities as characterized by Figure 1 are indicated: A = steller velocity = 53 km/s; C = preshock velocity of upper shock 59 km/s; D = post shock velocity of upper shock ≈ 47 km/s, H = psot shock velocity of lower shock ≈ 43 km/s.

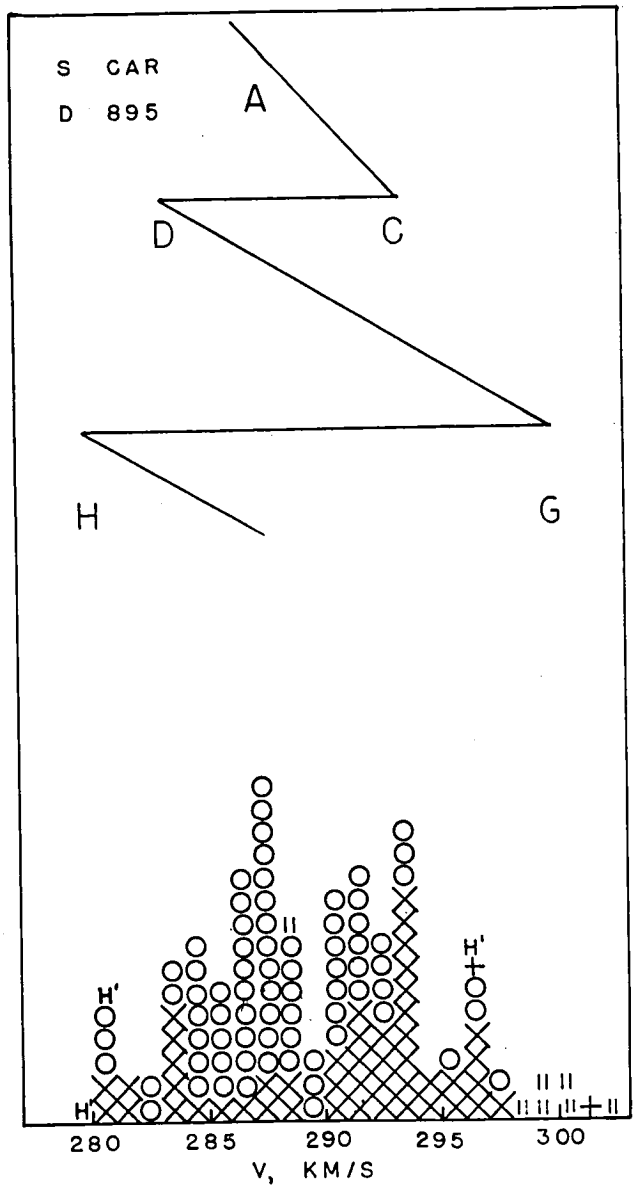

Figure 9. Heloicentric velocity histogram for S Car. Velocities as characterized by Figure 1 are indicated: A ≈ 288 km/s, C ≈ 294 km/s, G ≈ 300 km/s, D ≈ 283 km/s, and H $\leq$ 280 km/s.

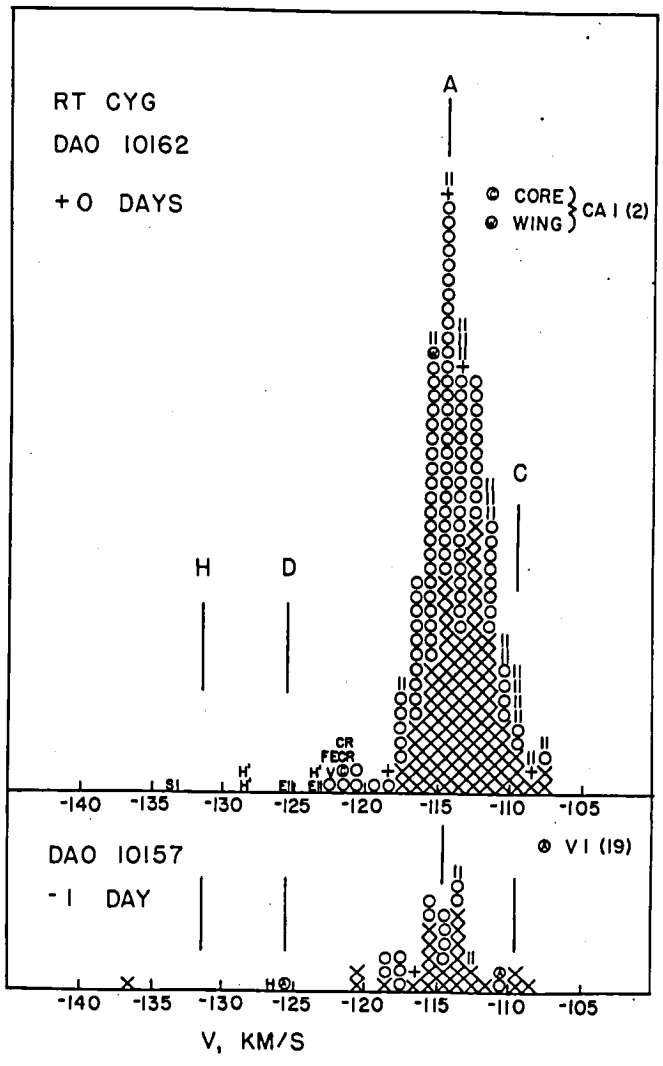

Figure 10. Velocity histogram for RT Cyg at maximum: DAO 10157 (∿6000 Å) and DAO 10162 (∿4000 Å). Assignment of velocities A (stellar), D (post shock), C (pre shock) and H (hydrogen emission) are noted as for Figures 8, 9. (There is an additional hydrogen emission line at -147 km/s which is not shown.)

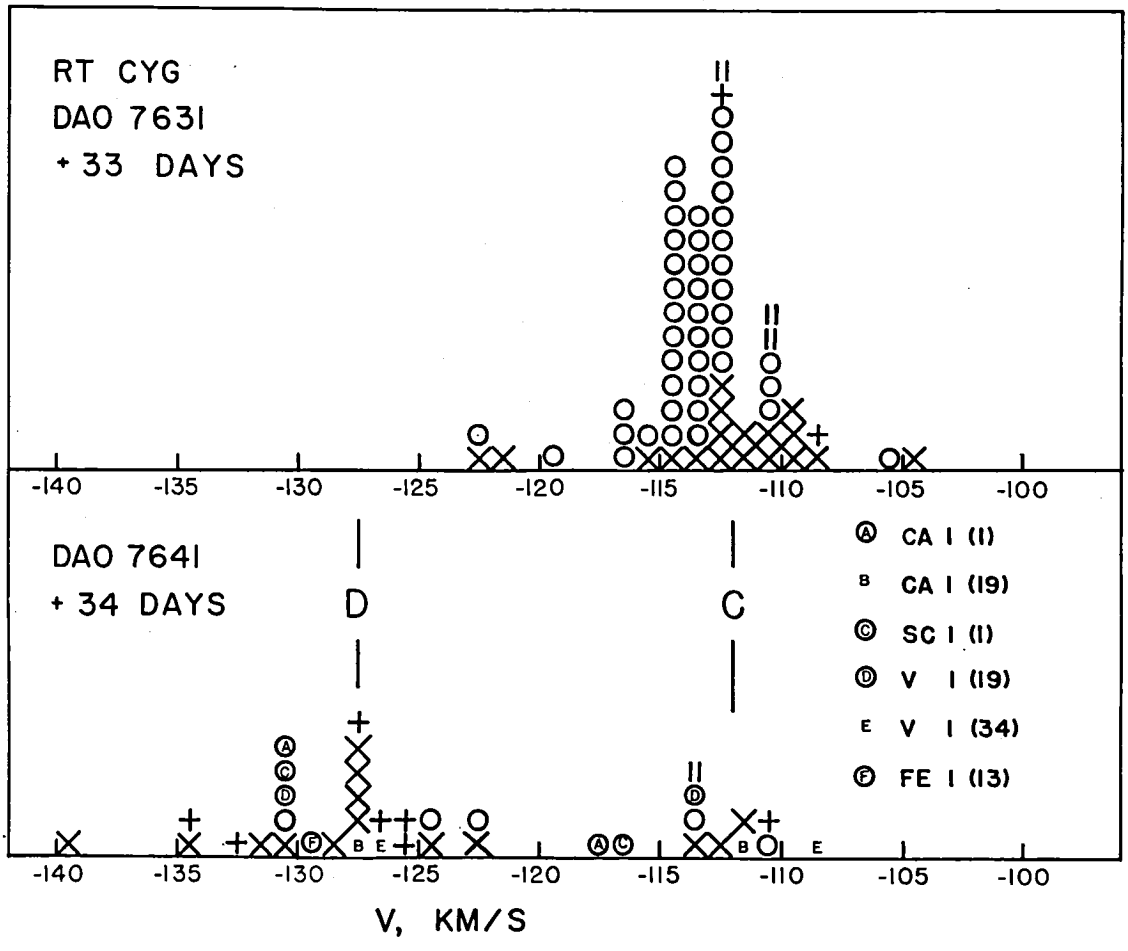

Figure 11. Velocity histograms for RT Cyg at +33/34[d]: DAO 7631 (∿4000 Å) and 7641B (∿6000 Å, with components of doubled lines indicated).

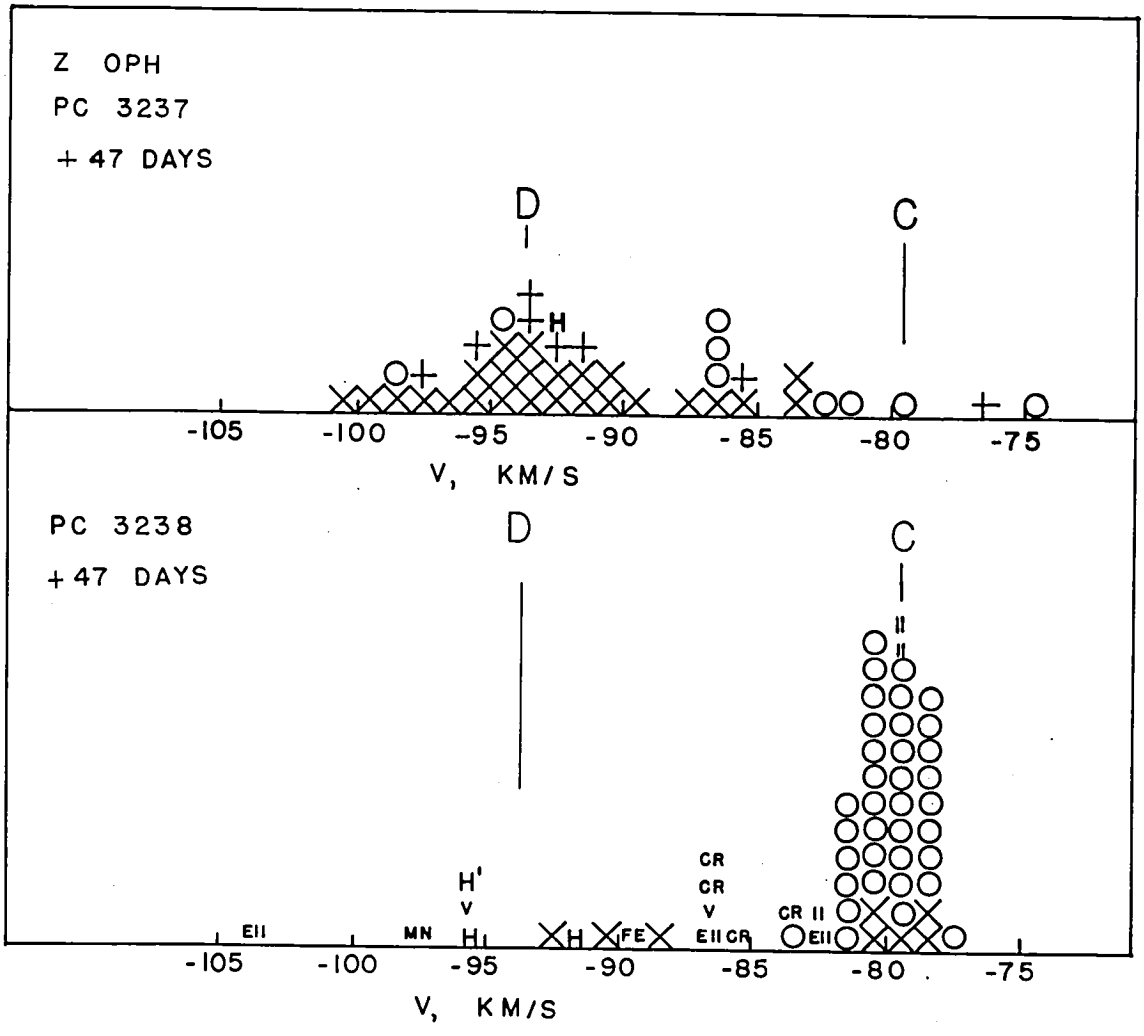

Figure 12. Velocity histogram for Z Oph at 47: PC 3237 (red) and 3238 (blue). The blue plate clearly indicates the pre-shock velocity C = -80 km/s; the red plate gives the post shock velocity D = -93 km/s.

Table 1. Allowed Coefficient Signs

Case	X = 1/λ	S	χ_i	χ_e	Position of reversing layer relative to source of excitation	Velocity gradient (outward velocity positive)
a	-	-	+	+	above	positive
b	-	-	-	-	below	positive
c	+	+	+	+	below	negative
d	+	+	-	-	above	negative

Table 2. Shock Model Interpretation of Regression Coefficients

Case	Region	Expected corollary behavior
a	above shock	•mostly low excitation lines ($\lesssim$ 1 eV) •lines redshifted ($\lesssim$ 10 km/s) •higher excitation lines more redshifted •small scatter in velocity
b	below shock	•many higher excitation lines ($\gtrsim$ 1 eV) •larger scatter than case a •lines at v_* to blueshifted ($\lesssim$ 5 km/s) •higher excitation lines more blueshifted •dependence on ionization potential
c	c1. immediate post-shock region	•very strong χ_i dependence •moderate scatter •blueshift predominant
	c2. Unresolved doubling and mixture of pre and post shock lines, especially high excitation lines	•very large scatter •two velocities-favored in histograms •broad features and apparent blends at intermediate velocities •lines both redshifted and blueshifted compared to v_* •exclusion of high excitation lines should convert case c2 to case a, with lower scatter.
d	d1. immediate pre shock region	•strong χ_e and χ_i dependence •small scatter
	d2. unresolved doubling of low excitation lines	•χ_e dependence •large scatter •broad features and apparent blends •exclusion of low excitation lines converts d to b, with smaller scatter.

Table 3. Results of the Regression Analysis

Plate[1]	Phase	λλ	(n0-3eV)	<v>	$\frac{n(1-3)}{n(0-3)}$	SD^o	SD^f/SD^o	1/λ	S	χ_i	χ_e	Case
β Peg DAO 10936		4325-4606	63	9.3	.36	1.4	.97	- .7	- .4	- .1	-1.0	--
L^2 Pup D 888		3770-4427	89	53.2	.20	1.8	.88	+ 1.9	+ 1.4	- .5	+3.2	c
S Car D 895		3835-4693	106	291.7	.37	3.6	.67	+ 1.6	- .1	+6.3	+4.9	a,c
RT Cyg:												
DAO 10157	- 1^d	5866-6599	36	-113.9	.64	2.4	.85	- 1.2	- .6	+1.9	+2.5	a,c
DAO 10162	0^d	3797-4586	190	-113.6	.45	2.0	.89	+ 2.6	- 1.4	- .6	+1.5	c,d
10157+10162			226	-113.7	.48	4.3	.93	+ 4.9	+ .8	+ .5	+ .0	c,d
Pb 14597	+ 8^d	6141-6599	12	-111.1	.6	6.6	.88	- .1	- 3.3	+8.0	- .5	a,c
Pb 14598[2]	+ 8^d	7511-7714	3	-120.4	.3	7.9	--	--	--	--	--	--
14597+14598			15	-112.6	.5	7.0	.94	+ 2.6	- 2.2	+2.3	-6.4	--
DAO 9345	+10^d	5866-6563	26	-136.7	.81	4.6	.59	+ 4.9	+10.7	-4.7	-1.0	d
DAO 9351	+11^d	5889-6678	55	-125.7	.80	3.9	.72	+ 3.2	+ 1.8	-6.4	+2.1	(d)
9345+9351			81	-129.2	.80	4.2	.72	+ 3.4	+ 5.2	-6.1	-2.1	d
DAO 7631	+33^d	4351-4722	55	-113.2	.29	2.0	.88	- 2.9	- 1.1	-1.1	+ .6	a,b
DAO 7641A[3]	+34^d	5889-6632	30	-125.1	.80	4.8	.83	+ 4.8	+ 5.3	- .9	-4.5	(d)
DAO 7641B[3]	+34^d	6090-6613	20	-123.7	.63	4.9	.86	- 4.1	- 8.7	-5.6	- .4	b
7631+7641B			75	-116	.38	3.3	.94	- 1.2	- 2.0	-2.8	-2.5	--
Z Oph:												
Pc 10318	- 8^d	3905-4482	22	- 81.8	.30	2.3	.88	+ .7	+ .8	+1.3	+2.9	a,c
Pc 3184	+ 5^d	5857-6624	15	- 86.4	.73	7.5	.81	+ 7.0	+ 0.2	+7.2	-8.9	c,d
EC 2688[4]	+36^d	4861-6172	28	- 87.5	.46	2.5	.74	- 2.6	+ 5.0	+7.6	-1.4	c,a
Pc 7840	+44^d	3770-4496	42	- 84.7	.19	2.8	.88	+ 2.7	+ 2.2	-2.7	+3.5	c,d
Pc 7846	+44^d	5426-6743	44	- 88.5	.68	4.9	.82	- 1.4	+ 7.0	-1.0	-3.2	c,d
7840+7846			86	- 86.6	.44	4.4	.82	+ 5.3	+ 4.2	-2.9	- .6	c,d
Pc 3237	+47^d	5567-6707	30	- 92.2	.83	4.8	.84	- 2.4	+ 7.6	-1.0	-2.7	c,d
Pc 3238	+47^d	4156-4571	41	- 79.9	.12	1.2	.95	+ 1.2	+ .4	- .3	+ .5	(a)
3237+3238			71	- 85.1	.42	6.9	.46	+13.4	+ 2.8	-1.2	-3.7	d

[1] Plate coding and dispersions: DAO: Dominion Astrophysical Observatory 48"; blue plates 6 Å/mm, red plates 10 Å/mm. Pb: Hale Observatories 200"; 7 Å/mm. Pc: Hale Observatories 200"; blue plates 9 Å/mm, red plates 13.5 Å/mm. D: Cerro Tololo Interamerican Observatory 60"; blue plates 9 Å/mm. EC: Lick Observatory 120"; 16 Å/mm.

[2] Some high excitation lines split, with v = -113 km/s, -127 km/s

[3] 7641A treats all lines as single; 7641B resolves split lines with v = -128 km/s, -113 km/s.

[4] This plate contains several split lines and many broad ones.

Table 4. Properties of the four stars studied. Periods, mean spectral types, and maximum visual magnitudes from Clayton and Feast (1969) and Feast (1963); visual amplitudes from Campbell (1955) and Kukarkin et al., GCVS; velocities and shock amplitudes from the present study. Both v_* and Δv are uncertain by ±3 km/s.

	L^2 Pup	S Car	RT Cyg	Z Oph
Period	141^d	150^d	191^d	350^d
Spectral Type at maximum	M5e	M0e	M2e	K4ep
m_v (mean max.)	2.6	5.7	7.3	8.1
Δm_v	3.4	2.7	4.5	4.0
v_*, km/s	53	288	-113	-85
Δv, km/s	17	20 11	13-16	13-16

Discussion

Belserene: Did you discuss the objectivity of your statistical criteria with a mathematician, perhaps?

Willson: That's a terrible question. I showed them to a mathematician. He made very little comment. It's a semi-empirical rule. I'm sure that there are mathematical arguments, but they depend on sample size, the reliability of the measurements, etc. Those parameters are so uncertain that the rule of thumb and iterative consistency seem to be pretty good for the first round. Actually, because so many cases turn out to be across the shock, I'm not sure that we learn too much from the coefficients themselves. I tend to like the histograms better, but we started off with the other part.

PULSATION AND MASS LOSS IN MIRA VARIABLES

P. R. Wood
Mount Stromlo and Siding Spring Observatory
Research School of Physical Sciences,
Australian National University

Abstract

The behaviour of pulsation in the outer layers of a "typical" Mira variable ($M = M_\odot$, $L = 10^4 L_\odot$, $T_{eff} = 2750K$, $P = 373$ days) has been studied in the adiabatic and isothermal limits. A shock wave propagates outward once per period and the radial velocity obtained from observations of hydrogen emission lines is identified with the velocity of gas in the post-shock region. In the adiabatic case, mass loss in the form of a steady stellar wind was produced. However, the mass loss rate is far too large (0.02 $M_\odot yr^{-1}$) if approximate observational estimates of the photospheric density are adopted. In the isothermal case, no continuous mass loss was produced but occasional ejection of shells occurs. The time-averaged mass loss rate produced by this process is $\approx 10^{-12} M_\odot yr^{-1}$. Pulsation introduced into a star undergoing steady mass loss as a result of radiation pressure acting on grains caused the mass loss rate to increase by a factor of ~ 40 while the terminal velocity of the flow was almost unaltered.

I. INTRODUCTION

The occurrence of violet displaced resonance line absorption in the spectra of luminous M giants and supergiants has long been interpreted as evidence for the existence of matter flowing outward from these stars at ~ 10 km sec^{-1} (Deutsch 1960, Weyman 1963), although the mass loss rates are still very uncertain (Sanner 1976, Reimers 1977, Bernat 1977). In addition, infra-red (IR) observations have shown the existence of a cool emission component in many M giants and supergiants which is taken to indicate the presence of dusty circumstellar material. Mass loss rates have been derived from the IR observations by Gehrz and Woolf (1971). The production of mass outflow in late-type stars is usually attributed to a radiation pressure force acting on grains (Hoyle and Wickramasinghe 1962, Kwok 1975) or possibly on molecules (Weyman 1962, Maciel 1977), or to chromospheric heating produced by sound generation in the extensive convection zones of these stars (Fussi-Pecci and Renzini 1976, Renzini et al. 1977). However, in the case of the Mira variables, a large amplitude shock wave is injected into the outer layers of the star once each pulsation cycle so that mass loss may be produced by pulsation alone, or the pulsation may substantially increase the rate of mass loss which results from either of the above mechanisms. In this paper, the production of mass loss by pulsation and the effect of pulsation on mass flows produced by radiation pressure acting on grains are examined.

II. OBSERVATIONAL DATA

It will be assumed here that the variability of Miras is the result of a radial pulsation which causes a shock to propogate into the outer layers of the star once each pulsation cycle. The bright hydrogen emission lines that are apparent during much of a Mira pulsation cycle are assumed to originate from the relaxation region behind the outward propagating shock wave. In this situation, the velocity of the hydrogen emission lines represents the velocity of the material behind the shock front. Similarly, the velocity of the violet-shifted cores of strong resonance absorption lines is taken as a measure of the velocity of a steady stellar wind far above the shocked region near the photosphere.

The existence of a characteristic double-peaked maser emission from a number of Mira variables provides an accurate means of determining centre-of-mass (cms) radial velocities for these stars. According to the maser models of Elitzer, Goldreich and Scoville (1976) and Reid et al. (1977), the double-peaked structure results from maser amplification on the near and far sides of a spherically symmetric flow of matter from the central star. The velocity separation of the two peaks, which is observed to be time invariant (Harvey et al. 1974), is assumed to be twice the terminal flow velocity. A comparison of maser and thermal radio emission velocities (Reid and Dickinson 1976) confirms the prediction that the mean of the radial velocities of the two maser emission peaks coincides with the cms radial velocity of the associated star.

Table 1 lists cms radial velocities derived for all Mira variables for which either thermal radio emission or well-defined twin maser emission peaks could be found in the literature. Also listed are hydrogen emission line velocities and absorption line velocities (Feast 1963, Wallerstein 1975) relative to the cms of the star (a positive entry indicates motion outward from the star): these velocities are obtained at, or shortly after, maximum. No correction factor (usually 24/17) has been applied to the emission line velocities to account for sphericity and limb darkening effects. In fact, for an optically thick shock or an optically thin shock with overlying absorption, the peak emission line intensity should occur at the shock velocity and therefore no correction factor should be applied in these cases. Column 8 of Table 1 gives the estimate of the terminal stellar wind velocity obtained from resonance line absorption (Wallerstein 1975) while column 9 gives the terminal velocity estimate which is equal to half the velocity separation of the twin OH maser emission peaks.

The velocities given in Table 1 are plotted against the period of pulsation in Figures 1 and 2. In most stars, the post-shock velocity lies in the range 5 to 10 km s^{-1} near maximum light, with some evidence for an increase in the outward velocity with period. Absorption line velocities lie in the range -5 to -10 km s^{-1}, but these velocities are of little use in the present situation since a lack of knowledge of their region of formation in the shocked atmosphere precludes any comparison of these velocities with theoretical models. The terminal flow velocities (Fig. 2) obtained from circumstellar absorption lines and from the separation of the twin maser emission peaks seem to agree reasonably well and they are concentrated in the range 3-6 km s^{-1}. There is an apparent increase in the terminal flow velocity with period which is generally consistent with the relation obtained from the larger sample of stars which includes the semi-regular variables with periods $\gtrsim$ 500 days (Dickinson, Kollberg and Yngvesson 1975).

Table 1

MIRA RADIAL VELOCITIES

Star	Period	v_{cms}	v^W_{abs}	v^F_{abs}	v^W_{em}	v^F_{em}	v_{cs}	$\frac{1}{2}\Delta v_{OH}$	Source
Z Cyg	263	-171.0				2.0		2.2	1
R Aql	284	30.1	-5.4	- 3.9	5.1	9.1	7.1	6	2
R Leo	313	7.2	-7.8	- 4.8	7.2	9.2	0.7		3
O Ceti	332	50.9		-13.9		2.9			4
U Mic	335	- 63.0		- 9.0		5.0		3	5
RS Vir	353	- 25.0				15.0		3.5	1
SY Aql	356	- 71.1				11.9		3.5	1
S Cr B	360	- 15.6	-6.3	-14.6	5.9	6.4		3.5	1
U Ori	372	- 26.0	-6.0	- 4.0	6.0	8.0	3.0	3.5	10
V Mic	381	- 0.1						5.6	6
W Hya	382	37.7	-7.3	- 4.3	~1.7	9.3	4.2	4	7,3,8
R Hya	388	- 12.3	-5.8	- 6.3	6.7	6.7	11.2		11
RW Sco	388	- 78.8				9.2		5	5
W Vel	393	4.0		- 4.0		8.0		3.5	5
RR Aql	394	12.6				11.6		5	2
U Her	406	- 33.0	-6.0	- 5.0	6.0	11.0		5	10
χ Cyg	407	- 8.9	-8.9	- 8.9	7.1	7.1	7.6		4
WX Ser	425	- 10.5						7.5	2
R Cas	431	16.6	-6.4	- 9.4	8.1	6.6	3.6	3.5	3,9
W Aql	490	- 39.6				- 1.6			11
IK Tau	~500	46.3					~9.7	17	2

Notes: Period is in days and velocities are in km s^{-1}. v_{cms} is the heliocentric radial velocity of the star and all other velocities are measured relative to this value. v^W_{abs} and v^F_{abs} (v^W_{em} and v^F_{em}) are absorption (emission) line velocities measured near maximum by Wallerstein (1975) and Feast (1963) respectively. v_{cs} are circumstellar absorption line velocities from Wallerstein (1975) and $\frac{1}{2}\Delta v_{OH}$ is half the velocity separation of the twin OH maser emission features. Sources of v_{cms} are: (1) Dickinson, Kollberg and Yngvesson (1975); (2) Wilson and Barrett (1972); (3) Reid and Dickinson (1976); (4) Lo and Bechis (1977); (5) Bowers and Kerr (1977); (6) Caswell, Robinson and Dickel (1971); (7) Dickinson and Kleinmann (1977); (8) McGee, Newton and Brooks (1977); (9) Nguyen-Quang-Rieu, Fillet and Gheudin (1971); (10) Wilson et al. (1972); (11) Dickinson et al. (1978).

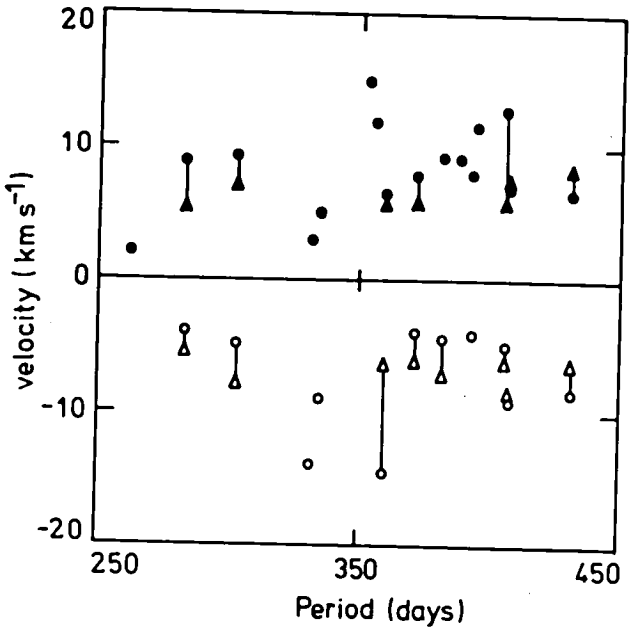

Fig. 1 Emission line (solid symbols) and absorption line (hollow symbols) velocities near maximum plotted against period. Circles are from Feast (1963) and triangles from Wallerstein (1975). Lines join measurements of the same star by the two different authors. All velocities are measured relative to the centre-of-mass of the star.

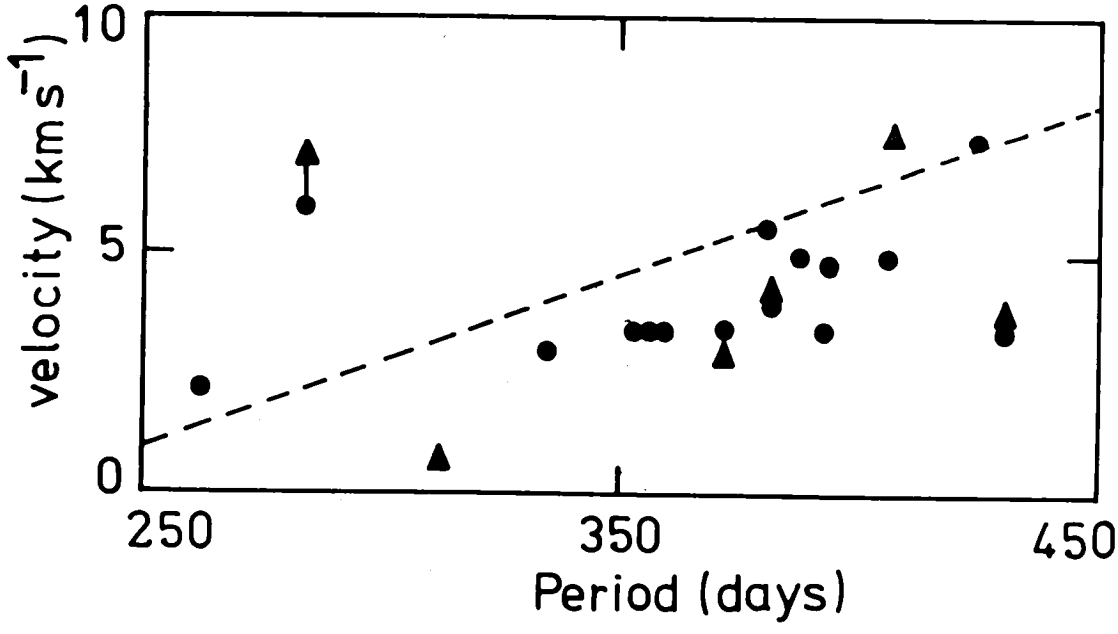

Fig. 2 Stellar wind flow velocity obtained from circumstellar optical absorption lines (triangles) and half the velocity separation of twin OH maser emission peaks (circles) plotted against Mira period. Lines join observations of the same star. The dotted line is the relation obtained by Dickinson, Kollberg and Yngvesson (1975) for a larger sample of stars including semi-regular variables with periods > 500 days.

The most useful observational property for comparison with theoretical models is the variation in the hydrogen emission line (i.e., post-shock) velocity with phase. However, the existing emission line velocity curves seem rather ambiguous. Early velocity curves obtained at dispersions of 35-65 A mm^{-1} for O Ceti (Joy 1926) and U Ori, R Leo, χ Cygni and R Cas (Merrill and Burwell 1930) are shown in Figure 3a after conversion to velocity relative to the stellar centre-of-mass. These curves generally show a rise to maximum at phase ~ 0.2 and decline thereafter. However, more recent higher dispersion results (~ 10 A mm^{-1}) by Joy 1954, Merrill 1945, 1945a, 1947, 1952, 1953 and Wallerstein 1975 (Fig. 3b) do not show any consistent pattern, e.g., R Leo and O Ceti show a maximum velocity at phase ~ 0.2 as found in earlier results whereas R Hya shows a continually increasing velocity and χ Cygni and U Ori show a continually decreasing velocity. In view of the discrepancy between the two sets of results, perhaps all that one can say from the observations is that the velocities of the hydrogen emission lines lie in the range 5-10 km s^{-1}.

III. NUMERICAL METHODS AND PHYSICAL ASSUMPTIONS

This study uses an implicit difference scheme based on the Eulerian fluid dynamical equations expressed in conservation law form. The calculations were performed on a model with parameters $L = 10^4 L_\odot$, $M = M_\odot$ and composition (X,Y) = (0.7, 0.3). These parameters were chosen since the Mira pulsation period (373 days) obtained for the star from the formulae of Wood and Cahn (1977) lies near the centre of the observed period distribution (Wood and Cahn 1977). A period of 373 days is also representative of the periods of those Miras which are observed to have maser emission.

For the hydrostatic starting models, an effective temperature T_{eff} = 2750K is derived by assigning the star to the old disk giant branch (Wood and Cahn 1977) and a photospheric radium r_{phot} is defined by the relation $L = 4\pi r_{phot}^2 T_{eff}^4$. The radial temperature distribution in the starting models (and at all times in the isothermal model sequences) is given by

$$T = \tfrac{1}{2} T_{eff} \left(1 + \tfrac{3}{2} \tau\right) f \qquad (1)$$

where $f = 1$, if $r < r_{phot}$,

$$= 1 - \left(1 - \frac{r_{phot}^2}{r^2}\right)^{\frac{1}{2}} \quad , \text{if } r > r_{phot}.$$

The factor f accounts for geometric dilution of radiation at large distances from the photosphere. A fictitious optical depth τ is defined as an explicit function of r by

$$\tau = \tfrac{2}{3} \exp\left\{-\frac{(r - r_{phot})}{\lambda}\right\}$$

where the scale height λ is chosen so that $T = 10^4$K on the inner boundary which is situated at $r = 0.8\ r_{phot}$. The inner boundary conditions were applied at $0.8\ r_{phot}$ since Mira variables appear to be first overtone pulsators (Wood 1975) and first overtone pulsation models have a node near $0.8\ r_{phot}$. Stellar interior models constructed using radiative diffusion and mixing-length convection for energy transport indicate that the temperature at $0.8\ r_{phot}$ is ~ 10^4K, although this is dependent on the molecular opacity

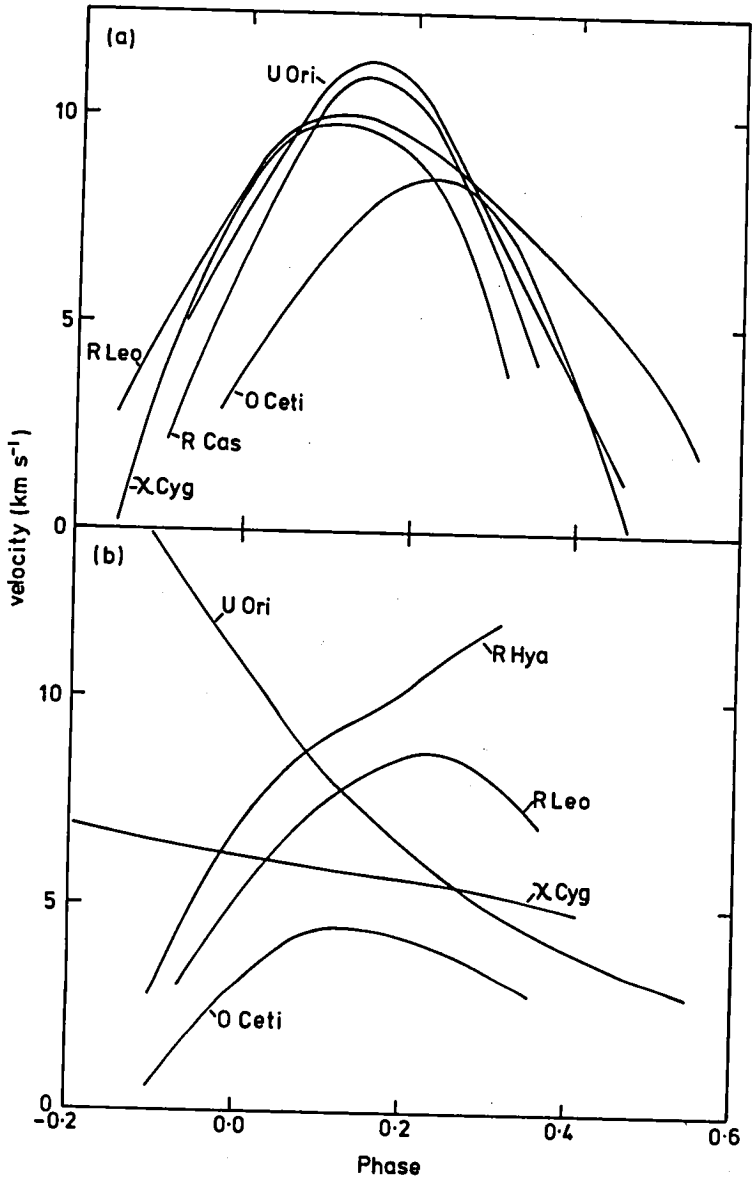

Fig. 3a Emission line velocity relative to the stellar centre-of-mass plotted against phase of the pulsation cycle. The curves are eye-fits to the data of Merrill and Burwell (1930) and Joy (1926).

Fig. 3b Same as Figure 3a except data are from Merrill 1945, 1945a, 1947, 1952, 1953 and Wallerstein (1975).

assumed in the photospheric layers.

In the hydrostatic models, the pressure Π_o applied at the inner boundary was adjusted so that, at fictitious optical depth $\tau = \frac{2}{3}$, the gas pressure $P_g = 10^2$ dynes cm^{-2}($\rho \approx 6 \times 10^{-10}$ gm cm^{-3}) to agree with observational and model atmosphere estimates of the photospheric density in late type giants and Miras (Auman 1969, Fujita 1970). Pulsation of the star is simulated by varying the pressure Π applied at the inner boundary according to the formula

$$\ln\Pi = \ln\Pi_o + A \sin \frac{2\pi t}{P} \quad , \tag{2}$$

where P is the Mira pulsation period (373 days).

In models where an approximate simulation of a mass flow produced by radiation pressure acting on grains is required, it is assumed that the gas and grains are coupled and that all grains condense out over a small temperature interval. In this situation, the radiation force per unit mass of gas is approximated by

$$f_{rad} = \frac{Q_{eff}}{1 + \exp \frac{T - T_{con}}{\Delta T}} \frac{L}{R^2} \tag{3}$$

where Q_{eff} is a constant, T_{con} is a condensation temperature and ΔT is a temperature interval over which all material condenses out. The values T_{con} = 1500K and ΔT = 100 K are used here.

The equation of state allows for the formation of molecular hydrogen but ionization of hydrogen and helium (applicable only in the innermost zones) had to be omitted because of numerical problems at the inner boundary.

In all calculations, the outer boundary was placed at $10r_{phot}$ and zone spacing δr increased with r according to the formula $\delta r \propto r^{\frac{1}{2}}$. The radius r and the Eulerian coordinate x are related by the formula

$$r = 8.88 \times 10^7 \ (501 - x)^{-2} \ (R_\odot) \ .$$

For the adiabatic and isothermal calculations not involving radiation pressure 360 zones were used while 180 zones were used in the calculations involving radiation pressure induced flows.

IV. ADIABATIC MODELS

Using an amplitude A = 1 in equation 2, a sequence of adiabatic models was constructed covering 17 pulsation periods, by which time a steady periodic situation had been reached. Figure 4 shows the propagation of the first 10 shocks from the inner to the outer boundary as a function of time while Figure 5 shows the radial density, temperature and velocity distributions at one value of the phase of the pulsation cycle in the steady periodic limit.

In Figure 4, it is noticeable that the first shock which propagates into the hydrostatic atmosphere travels much faster than succeeding shocks.

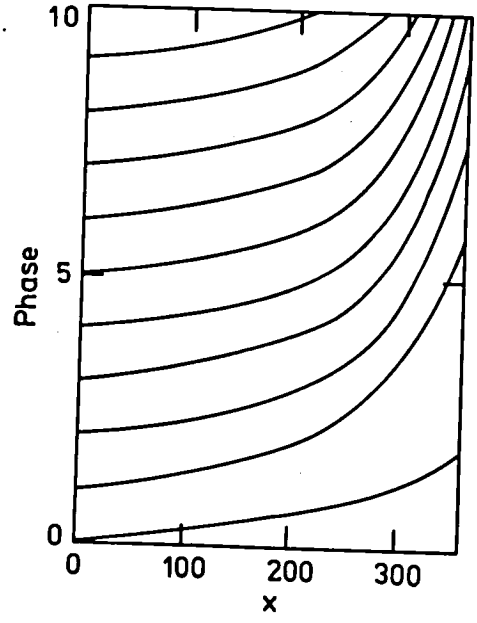

Fig. 4 Propagation of the first 10 shocks of the adiabatic calculations. x is the Eulerian coordinate (see § III).

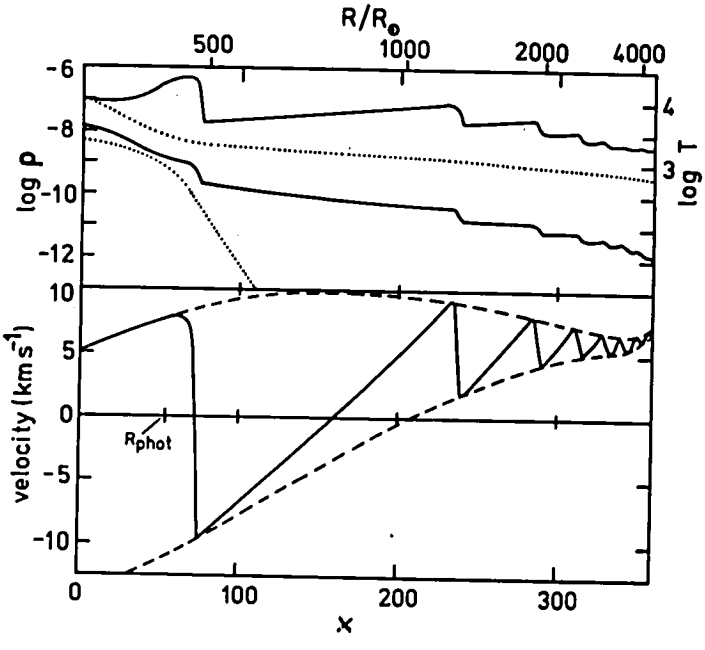

Fig. 5 Temperature, density and velocity profiles at a single phase of the adiabatic calculations after a steady state has been reached (continuous curves). Dotted lines show temperatures and density distributions in the initial hydrostatic models. Dashed lines mark an envelope for the velocity curves.

The rapidity of the first shock is due to two factors (a) the large density gradient in the hydrostatic atmosphere which causes the first shock to speed up (Zeldovich and Raiser 1966) more than later shocks when the density gradient has been reduced (see Fig. 5), and (b) the fact that all shocks but the first are impeded by the ram pressure of material falling inward after the passage of the previous shock. A further complication arises from the fact that in the steady periodic situation, the shocks are superimposed upon an underlying outward flow which causes the velocity amplitude of the shocks to decrease with time and radius even though they are propagating down a density gradient. These considerations show that the first shock is atypical and that therefore studies of the propagation of an individual shock into a hydrostatic atmosphere (e.g., Slutz 1975) do not give an accurate picture of the propagation of large-amplitude periodic shocks.

In the steady state, the shock waves are dissipated in the region above the photosphere and produce a steady mass outflow far from the star. Since the flow becomes supersonic before it reaches the outer boundary, the outer boundary conditions can not affect the flow, which must meet the interstellar medium in a shock front beyond the region studied here. Near the outer boundary, the velocity increases rapidly due to the formation of molecular hydrogen. The rate of continuous mass loss produced by the adiabatic pulsations is $\sim 0.02\ M_{\odot}\,yr^{-1}$, which is much greater than observational estimates of $\sim 2 \times 10^{-6}\ M_{\odot}\,yr^{-1}$ (Gehrz and Woolf 1971). However, the velocity of the outflow is similar to the observed values given in Figure 2.

The reason for the large mass loss rate is the high gas density in the flow. For a perfect gas, it is easy to show that the differential equations governing the continuous parts of the flow, and also the Hugoniot equations relating quantities across shocks embedded in the flow, are unaffected by a change of scale in the density. (Due to dissociation of hydrogen, the gas in the flow is not perfect at all points but the present arguments should remain essentially correct.) Thus the density at any point in the flow is proportional to the density or pressure specified at the inner boundary, while the flow velocity and temperature will remain unaltered following a change in scale of the inner boundary density or pressure. These considerations show that the mass loss rate could be lowered to observed values by reducing the inner boundary pressure by a factor of $\sim 10^4$. However, the resulting photospheric pressure and density are then considerably less than the observed values given earlier.

Another severe problem with these adiabatic models is the large region of high gas temperature ($T > 10^4$k) produced by pulsation. Assuming the high temperature post-shock region is optically thin to Balmer and higher series radiation, the cooling time at the densities involved for $T > 10^4$K is < 1 second. The adiabatic assumption is clearly violated in this situation. In view of the above considerations, it appears that adiabatic calculations do not accurately represent the behaviour of pulsation in the outer layers of Mira variables.

V. ISOTHERMAL MODELS

In these calculations, the temperature is time-invariant and has the radial distribution given by equation 1. A long series of models was computed covering 92 pulsation periods with a pressure variation amplitude

A = 1.0 (equation 2) at the inner boundary. Although no continuous mass loss was produced, occasional ejection of shells of material does occur.

The essential features of the dynamics of the situation can be explained with reference to Figure 6, in which the radii of the first 14 shocks are plotted against time. As in the adiabatic case, the first shock propagates rapidly outward down the density gradient in the hydrostatic atmosphere. Material behind the shock is decelerated by gravity and begins to fall in toward the star. The second shock begins to travel outward into the infalling material but is eventually halted and pushed backward. Each shock propagating outward reduces the amount of infalling material and the fourth shock actually overtakes and coalesces with shocks 2 and 3. This type of behaviour continues until after 14 cycles the inner regions (out to $\sim 600R_{\odot}$) become reasonably periodic. Typical velocity and density profiles after many cycles are shown in Figure 7. In the extended calculations, the continual coalescing of shocks beyond the periodic region eventually (after 80 cycles) built up a single strong shock which was able to propagate outward and escape through the outer boundary. By repeated events of this type, a Mira variable could build up a circumstellar shell and possibly produce a mass outflow. However, the mass loss rate (calculated by dividing the mass lost in the single ejection event by the time required to produce this event) is very small ($\sim 10^{-12} M_{\odot} yr^{-1}$).

The variation of post shock velocity with phase is shown in Figure 8. It is interesting that the rise to maximum at phase 0.1 - 0.2 and subsequent decline is similar to the results obtained from the early observations shown in Figure 3a. The maximum value of the theoretical post-shock velocity lies well within the range of emission line velocities exhibited by the sample of stars in Figure 1.

A recent observation (Hinkle 1978) which can be compared with the present isothermal calculations is the infra-red absorption line radial velocity curve of R Leo (Fig. 9), which indicates infall velocities much greater than those previously obtained from optical observations (Fig. 1). Although the precise point of origin of the IR absorption lines in the dynamical atmosphere is not known, the maximum infall velocity in the atmosphere at any time must be at least as large as that obtained from the IR observations. It can be seen from Figure 9 that the infall velocity at the nominal photosphere ($\tau = \frac{2}{3}$) of the isothermal models accelerates at almost the same rate as the infall velocity observed in R Leo, except for the flat spot on the velocity curve of the models (caused by the hydrogen dissociation region moving close to the photosphere as the pressure falls). This indicates that the surface gravity g (or more precisely, g times the pulsation period P) of R Leo is approximately the same as that of the present models but that the temperature in the models should be raised slightly to prevent formation of molecular hydrogen in the photospheric region. This latter suggestion is also consistent with the fact that Hinkle (1978) derives temperatures > 3000K for the regions in which the lines used to derive the velocities in Figure 9 are formed. Although R Leo has a shorter period (312 days) than the models (373 days), the formulae of Wood and Cahn (1977) predict an effective temperature for R Leo which is only 50K hotter than that in the models and a value of gP only 6% greater.

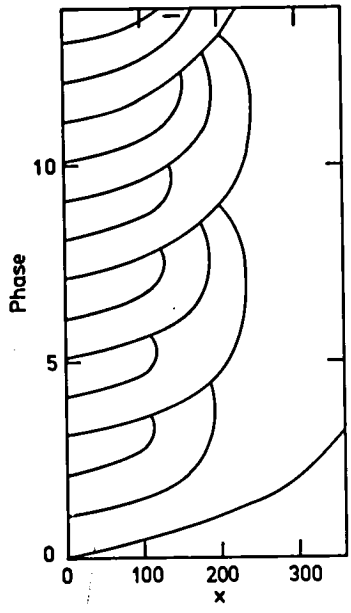

Fig. 6 Propagation of the first 14 shocks of the isothermal calculations.

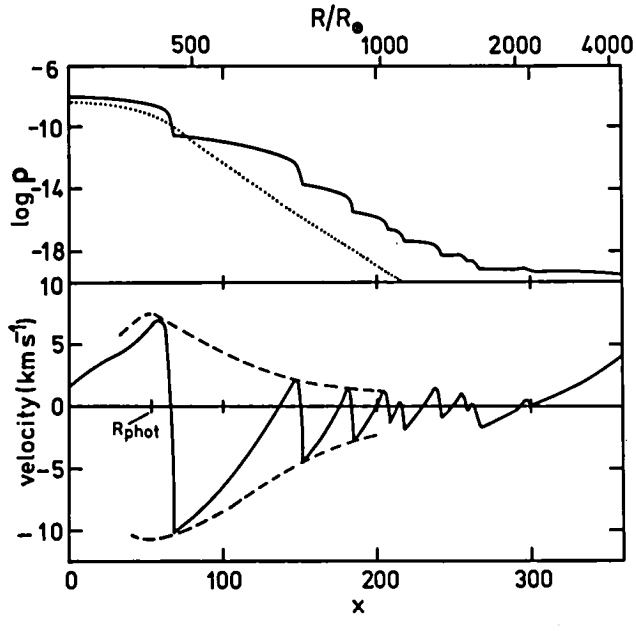

Fig. 7 Density and velocity profiles at a single phase of the isothermal calculations (continuous curves). The dotted line shows the density distribution in the hydrostatic starting model. The upper dashed curve is drawn through the post-shock velocity maxima and the lower dashed curve indicates maximum infall velocity. The positive velocity at the outer boundary was caused by passage of a shock (see text).

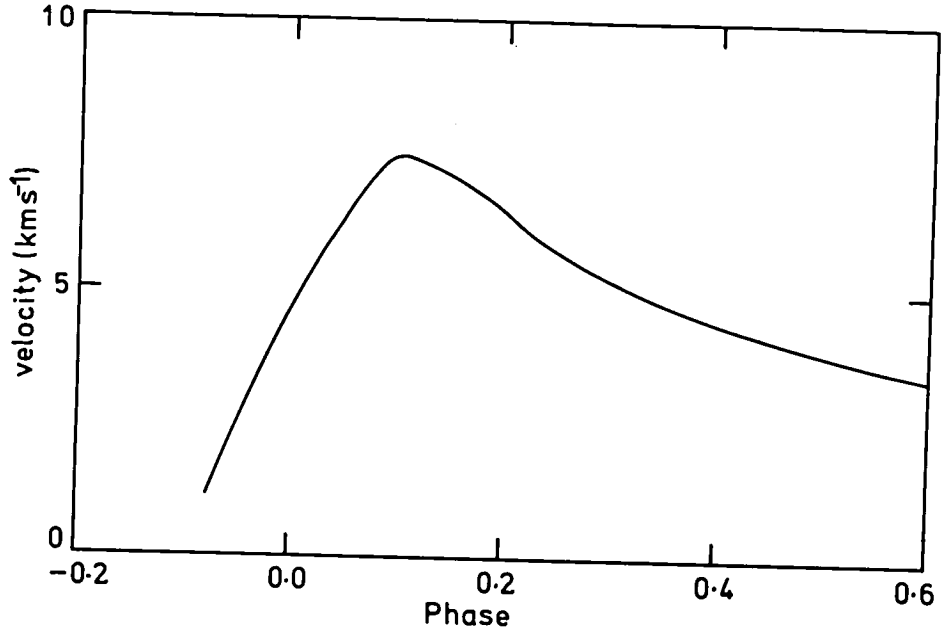

Fig. 8 Post-shock velocity plotted as a function of phase in the isothermal models. The zero point of phase is shifted so that the velocity maximum occurs near the phase of the observed velocity maximum in Figure 3a.

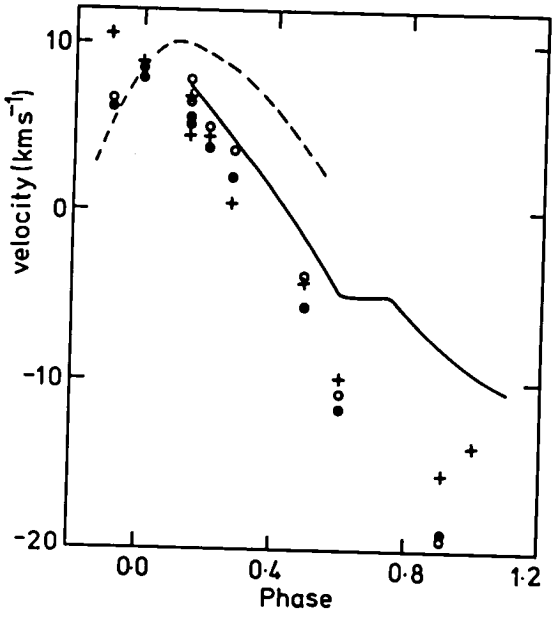

Fig. 9 The velocity at the nominal photosphere ($\tau = \frac{2}{3}$) of the isothermal models plotted against phase (continuous curve). The symbols are infra-red absorption line velocities of R Leo (relative to the centre-of-mass given in Table 1) from Hinkle (1978): ,CO Δv = 3 lines; +,CO Δv = 2 high excitation lines; O,OH Δv = 2 lines. The dashed curve is the hydrogen emission line velocity of R Leo from Figure 3a.

VI. THE EFFECT OF PULSATION ON A MASS FLOW PRODUCED BY RADIATION PRESSURE

Using the approximations given in § III for grain formation and acceleration by stellar radiation, the effective grain radiation cross-section parameter Q_{eff} was adjusted (keeping the inner boundary pressure constant) until a steady outward flow was obtained with a velocity at the outer boundary of ~ 5 km s^{-1} (Fig. 10). Integrating the flow from the

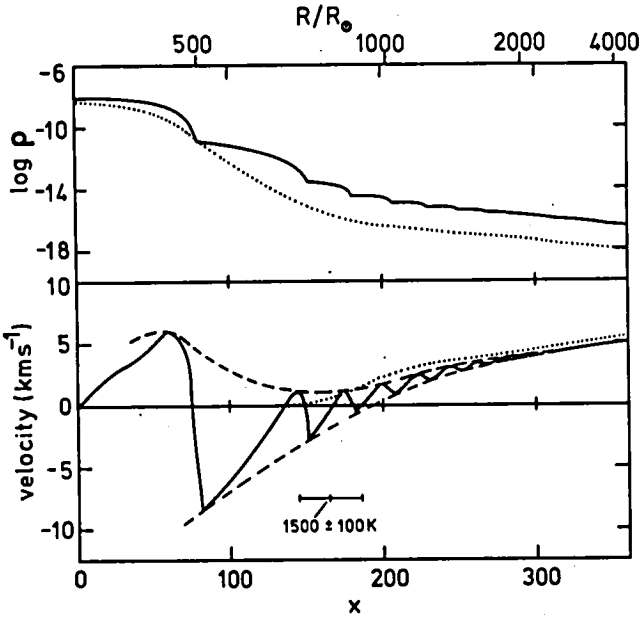

Fig. 10 Density and velocity profiles at a single phase in the models which include a radiation pressure-induced mass flow as well as pulsation. Dotted lines show density and velocity profiles in the initial steady state mass outflow model. The dashed curves are an envelope to the velocity profiles.

outer boundary to infinity gives a terminal velocity of 7 km s^{-1}, which is well within the range of observed flow velocities (Fig. 2). The mass loss rate Φ resulting from the flow is 7×10^{-9} $M_\odot yr^{-1}$. However, this value is not very meaningful since Φ is directly proportional to the pressure Π specified at the inner boundary (see § IV.). Any value of Φ can be obtained by adjusting Π, while the flow velocity will remain unaltered.

The effect of a pulsating atmosphere (isothermal approximation) at the base of the steady mass outflow was examined by varying the pressure at the inner boundary (using an amplitude A = 1.0 in equation 2) so that pulsation and shock waves were produced as before. Figure 10 shows the initial density and velocity distributions and the distributions which resulted when an equilibrium situation had been attained. The two main results of this calculation are (1) the flow velocity far from the star is only slightly different from that which existed in the absence of pulsation, and (2) the mass loss rate is increased by a factor of ~ 40. The latter result is due

to the lowering of the time-averaged density (or pressure) scale height in the pulsating regions below the sonic point causing the sonic point density to be raised.

As a final point, it is noted that in the region where pulsation velocities are much greater than the underlying flow velocity (radius $< 600R_\odot$), the behaviour of pulsation is almost identical to that which occurs when there is no radiation pressure-induced mass loss (the maximum post-shock velocity is slightly smaller in these calculations but this is purely a result of the increased numerical smoothing of the velocity profile behind the shock caused by the doubling of the zone spacing used in the isothermal models without grains). Since the emission lines in the model come from shocks at radii $< 600R_\odot$, no information relating to the mass outflow can be obtained from shock emission.

VII. SUMMARY

It has been shown that adiabatic pulsation in the surface layers of a star with parameters similar to those of a Mira variable can produce a steady stellar wind with a terminal velocity similar to that observed in the stellar winds associated with Mira variables and cool luminous red giants. However, two direct consequences of the adiabatic models conflict with observations (1) with observational estimates of the photospheric density, the mass loss rate is $\sim 10^4$ times larger than observed, and (2) an extensive region with a temperature $> 10^4$K exists behind the innermost shock and since the cooling time for this region is much shorter than the pulsation period, the assumption of complete adiabaticity is clearly incorrect.

Mira-type pulsation in the envelope of a red giant is found incapable of producing a continuous mass outflow when the radial temperature distribution is held constant in time (isothermal approximation). However, the coalescing of many shock waves in the outer layers of the envelope causes occasional ejection of shells of matter. The mass loss rate estimated for this process is $\sim 10^{-12} M_\odot yr^{-1}$. Since this mass loss rate is much smaller than observed mass loss rates, another mass loss mechanism, such as the action of radiation pressure on grains, must exist on the giant branch. The magnitude of the post-shock velocity in the isothermal models is shown to agree reasonably well with the velocity of the hydrogen emission lines observed in Mira variables.

In order to investigate the effect of pulsation on a stellar wind produced by the action of radiation pressure on grains, a model was first produced with a steady radiation pressure-induced mass outflow and then pulsation was introduced into the star. The flow velocity far from the star was almost unaltered by the pulsation but the mass loss rate was enhanced by a factor of ~ 40. Thus Mira variables can be expected to lose mass at a rate which is considerably faster than that in non-variable red giants of similar luminosity and spectral type. The enhancement in the mass loss rate is due to the reduced density gradient in the pulsating atmosphere and the consequent increase in the density at the sonic point of the flow.

This work was performed while the author was in receipt of a Queen Elizabeth II Fellowship at the Australian National University.

References

Auman, J. R.: 1969, Ap.J. 157, 799.
Bernat, A. P.: 1977, Ap.J. 213, 756.
Bowers, P. F. and Kerr, F. J.: 1977, Astr. and Ap. 57, 115.
Caswell, J. L., Robinson, B. J. and Dickel, H. R.: 1971, Astrophys. Letters 9, 61.
Deutsch, A. J.: 1960, in Stellar Atmospheres (Chicago: University of Chicago Press), ed. J. L. Greenstein, P.543.
Dickinson, D. F. and Kleinmann, S. G.: 1977, Ap.J.(Letters). 214, L135.
Dickinson, D. F., Kollberg, E. and Yngvesson, S.: 1975, Ap.J. 199, 131.
Dickinson, D. F., Reid, M. J., Morris, M. and Redman, R.: 1978, Ap.J. 220, L113.
Elitzur, M., Goldreich, P. and Scoville, N.: 1976, Ap.J. 205, 384.
Feast, M. W.: 1963, M.N.R.A.S. 125, 367.
Fujita, Y.: 1970, Interpretation of Spectra and Atmospheric Structure in Cool Stars (Tokyo: University of Tokyo Press), p. 89.
Fussi-Pecci, F. and Renzini, A.: 1976, Astr. and Ap. 39, 413.
Gehrz, R. D. and Woolf, N. J.: 1971, Ap.J. 165, 285.
Harvey, P. M., Bechis, K. P., Wilson, W. J. and Ball, J. A.: 1974, Ap.J. Suppl. 27, 331.
Hinkle, K. H.: 1978, Ap.J. 220, 210.
Hoyle, F. and Wickramasinghe, M. C.: 1962, M.N.R.A.S. 124, 417.
Joy, A. H.: 1926, Ap.J. 63, 281.
1954, Ap.J.Suppl. 1, 39.
Kwok, S. 1975, Ap.J. 198, 583.
Lo, K. Y. and Beckis, K. P.: 1977, Ap.J. (Letters), 218, L27.
Maciel, W. J.: 1977, Astr. and Ap. 57, 273.
McGee, R. X., Newton, L. M. and Brooks, J. W.: 1977, M.N.R.A.S. 180, 91p.
Merrill, P. W.: 1945, Ap.J. 103, 6.
————————: 1945a, Ap.J. 103, 275.
————————: 1947, Ap.J. 106, 274.
————————: 1952, Ap.J. 116, 337.
————————: 1953, Ap.J. 118, 453.
Merrill, P. W. and Burwell, C. G.: 1930, Ap.J. 71, 285.
Nguyen-Quang-Rieu, Fillet, R. and Gheudin, M.: 1971, Astr. and Ap. 14, 154.
Reid, M. J. and Dickinson, D. F.: 1976, Ap.J. 209, 505.
Reid, M. J., Muhleman, D. O., Moran, J. M., Johnston, K. J. and Schwartz, P.R.: 1977, Ap.J. 214, 60.
Reimers, D.: 1977, Astr. and Ap. 61, 217.
Renzini, A., Cacciari, C., Ulmschneider, and Schmitz, F.: 1977, Astr. and Ap. 61, 39.
Sanner, F.: 1976, Ap.J.Suppl. 32, 115.
Slutz, S.: 1976, Ap.J. 210, 750.
Wallerstein, G.: 1975, Ap.J.Suppl. 29, 375.
Weyman, R. J.: 1962, Ap.J. 136, 476.
————————: 1963, Ann. Prev. Astr. and Ap. 1, 97.
Wilson, W. J. and Barrett, A. H.: 1972, Astr. and Ap. 17, 385.
Wilson, W. J., Schwartz, P. R., Neugebauer, G., Harvey, P. M., and Becklin, E. E.: 1972, Ap.J. 177, 523.
Wood, P. R.: 1975, M.N.R.A.S. 171, 15p.
Wood, P. R. and Cahn, J. H.: 1977, Ap.J. 211, 499.
Zel'dovich, Ya. B. and Raizer, Ya. P.: 1966, Physics of Shock Waves and High-Temperature Phenomena (London: Academic Press).

Discussion

J. Wood: In one of your earlier slides, where you showed the series of shocks asymptotically approaching 7 km/sec, at what point does the escape velocity fall to this value?

P. Wood: At about 2000 solar radii, or a bit beyond. It has become supersonic at that point.

J. Cox: I don't understand why you had to assume it is isothermal. When you do the calculation, the energy equation...

P. Wood: Either you have to know all the physics of the shock -- that is, how much energy is being radiated in lines behind the shock, etc. -- or you can do the simple thing by assuming it's adiabatic (and then you use the energy equation), or you can assume it's isothermal (in which case, you assume that in a region which is very thin relative to the separation of the two shocks, all the energy is radiated). Those are the two limits I took, adiabatic and isothermal, without doing all the detailed physics.

Willson: We also did the same calculation and found the same results, that the isothermal model does not show mass loss. 10^{-12} is the number that we estimated in the same fashion as you did. I am very pleased to see that you calculated the combination of dust with the isothermal case, and I was as startled as anyone else to find that it only gives you a factor of 40, which is not enough to give you the six orders of magnitude that you need. Although we have not yet run the right masses, we found that if you look carefully at what's happening in the shock, the isothermal model should break down at

several stellar radii, because the recombination length of hydrogen in the shock becomes comparable to other scales of the problem. At that point, you start to convert to the adiabatic approximation. At that point you lose a lot of mass. If you estimate where that point occurs and calculate the mass loss, it is within a factor of 10 of 10^{-6}. As I said, we haven't run the exact models, but that looks like the right ball-park estimate; that's closer than anything else that's been done.

P. Wood: By the time you get into those regions, the shock is so "thick" that it's meaningless to talk about a shock wave.

Unknown: Barkat would argue with you that you can't do it with pulsation. He said that you could do it by a series of puffs blown off by individual pulsations which sort of build up, pop, and then settle down.

P. Wood: Yes, these are relaxation oscillations, which are of much larger amplitude. They don't bear any resemblance to what you see in a Mira. That is something later in the evolution.

Keller: Are you aware of Sanford's IR image tube observations, which show a very extended dust cloud around α Ori? He just recently published these 1 μ observations. In other unpublished work, he has seen a large cloud around R Leo, which would extend out to enormous distances, as you might expect.

Van Horn: To more than 100 stellar radii?

Keller: Oh, yes.

P. Wood: R Leo has a larger IR excess than most Miras of the same type.

Nather: There are occulation measurements of R Leo in the IR at Hale Observatory, that are 10-100 times larger than what we see in the optical region. That would tend to bear this out.

SATELLITE INFRARED OBSERVATIONS OF LATE-TYPE VARIABLE STARS

Stephen P. Maran

Andrew G. Michalitsianos

Laboratory for Astronomy and Solar Physics
NASA-Goddard Space Flight Center
Greenbelt, Maryland 20771

Thomas F. Heinsheimer

Thomas L. Stocker

The Aerospace Corporation
El Segundo, California 90009

To appear in

Current Problems in Stellar Pulsation Instabilities

June, 1978

ABSTRACT

Intensive monitoring of late-type variable stars with satellite-borne infrared sensors has yielded useful light curves extending over 4-1/2 years for some objects. These are the most detailed and extensive infrared light curves yet obtained for variable stars. They facilitate the cycle-to-cycle comparison of the photometric behavior of long-period stars and permit the investigation of "irregular" variables for possible recurrent photometric activity. The long-period variables omicron Ceti and S Canis Minoris are shown to have infrared minima that repeat accurately, but maxima that vary widely. The Mira-type star R Cancri was not included in our previously reported observations, however we have now obtained a good series of measurements on one of its maxima.

The Aerospace Corporation and the NASA-Goddard Space Flight Center are engaged in a program of systematic infrared astronomy with U.S. Air Force satellites. This includes an on-going survey of infrared sources within 10° of the celestial equator (Sweeney et al. 1977, Heinsheimer et al. 1978) as well as the intensive monitoring of selected late-type variable stars that began in 1971 (Maran et al. 1976, 1977). A summary of the detailed results on each well-observed variable star through early 1975 will be published by Chapman et al. All of the observations in our program consist of wide-band photometry at wavelength 2.7 μ m.

We recently began to study a more extensive set of light curves, which carry the measurements through mid-1976. Since early 1975, when the earlier series of observations ended, we have observed a few sources that were not previously monitored with the satellite sensors. An example is R Cancri (Figure 1), a Mira-type star with period 362 days, visual range 6.2 - 11.8 magnitude and spectral type M7e, according to the General Catalogue of Variable Stars (GCVS). Although relatively close, R Cnc (distance modulus 7.7 mag.) is not a detected H_2O or OH maser source (Lépine and Paes de Barros 1977, Bowers and Kerr 1977) but has been observed as a 7-mm wavelength, J = 1-0 SiO maser by Spencer et al. (1977). The latter authors published spectra of the v = 1 and v = 2 lines taken on 29 January 1976 and 20 February 1976, respectively. These dates are near the maximum of the 2.7-μm light curve, as seen from Figure 1. Comparison of more extensive series of SiO observations with the satellite measurements might provide information on whether the SiO maser in this star is saturated.

The satellite light curve of R Cnc is presented in units of flux density. Each point represents the mean of several observations on the same

day. The points at the bottom of Figure 1 are the standard deviations corresponding to the mean measurements plotted directly above. Note the prominent stillstand on the ascending branch of the light curve.

We have previously suggested that the infrared light curve of a Mira-type star is very variable at maximum light and yet remarkably reproducible at minimum light (Maran et al. 1976, 1977), a circumstance that is compatible with Ikaunieks' (1975) conclusion that minimum light may correspond to the "normal state of a long-period variable." This result, similar to Eggen's (1975) findings* in the visual seems consistent with the shock-wave theory as proposed to account for the velocity curves found in visual-light spectroscopy of these stars (cf.: Wallerstein 1977, Willson 1976). We have attempted to demonstrate this by the superposed epoch method in the case of omicron Ceti (Figure 2). Here, only the data for our shorter time base, through early 1975, have been included. Using the new series of data through mid-1976, the effect is obvious in the light curve of the Mira variable S Canis Minoris (Figure 3). The Figure shows four well-observed maxima and five well-observed minima, as well as part of a fifth, poorly-measured maximum. Note in particular the strong contrast between the 1973 and 1974 maxima, but the good agreement in flux density level at all five minima.

We thank the U.S. Air Force for continued cooperation with the program of infrared astronomy from earth orbit.

*Note, however, that William Herschel, in the late Eighteenth Century, already remarked on the pronounced variability of the magnitude of omicron Ceti at visual maximum!

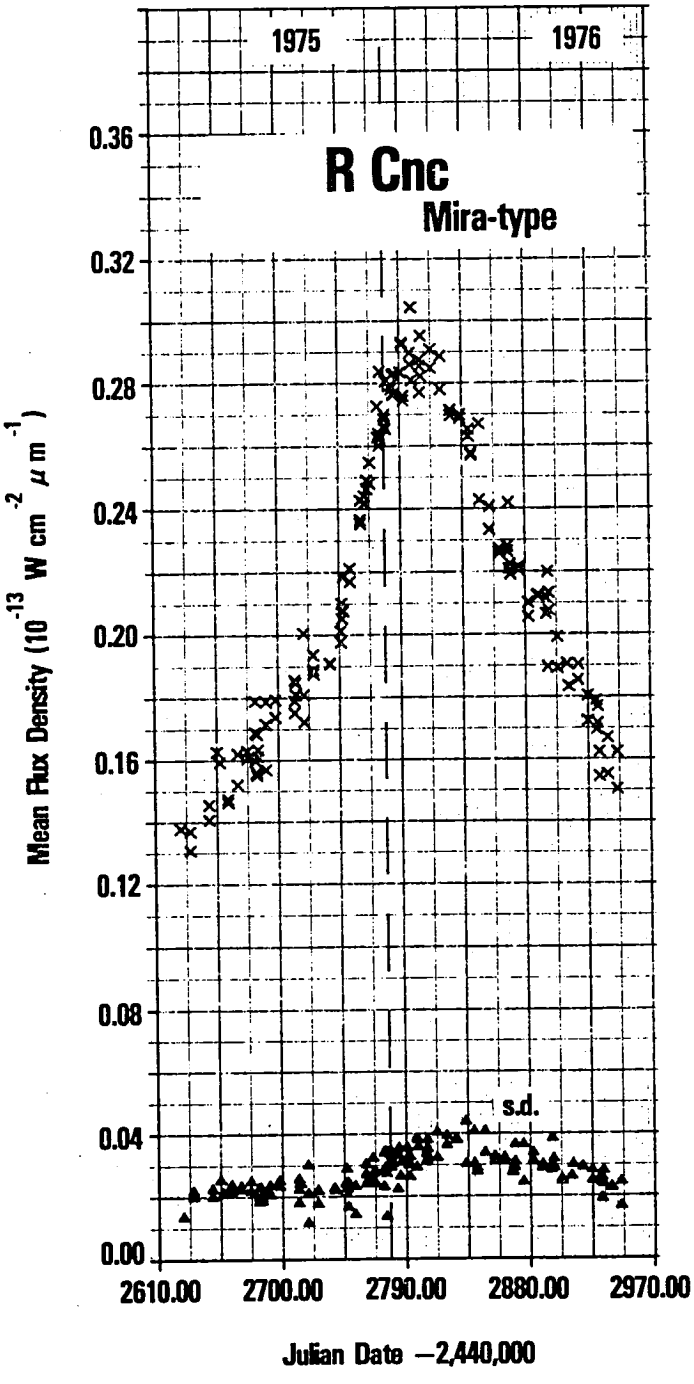

Figure 1.--Top--Infrared light curve of R Cancri, based on observations made at wavelength 2.7 μm with U.S. Air Force satellite sensors. Each point is the mean of several measurements. Flux density is plotted versus Julian date.

Bottom--Standard deviations of the observations plotted above, in the same units.

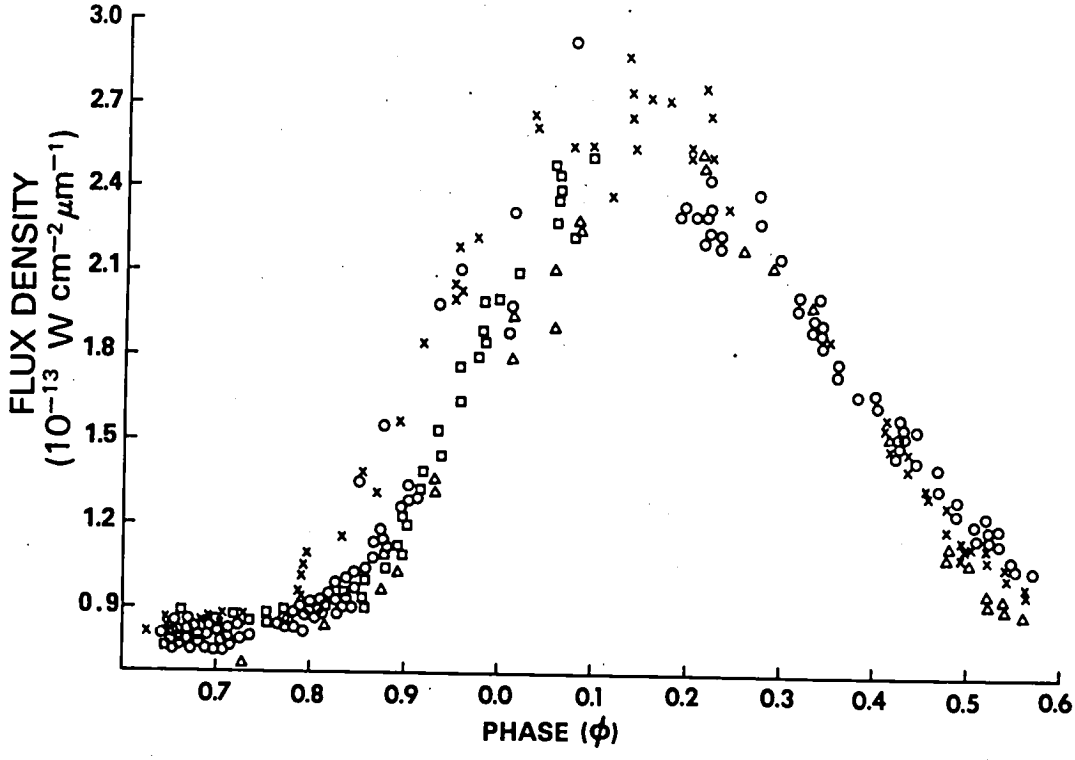

Figure 2.--Superposed-epoch light curve for omicron Ceti, based on 2.7-μm satellite measurements during four consecutive cycles of the long-period variable star in 1972-1975. Flux density is plotted versus phase. Phase 0.0 corresponds to maximum visual light, as determined from light curves prepared by the American Association of Variable Star Observers. Symbols distinguish measurements from the four stellar cycles. Note the region from phase 0.8 to phase 0.2 in which cycle-to-cycle variation is pronounced.

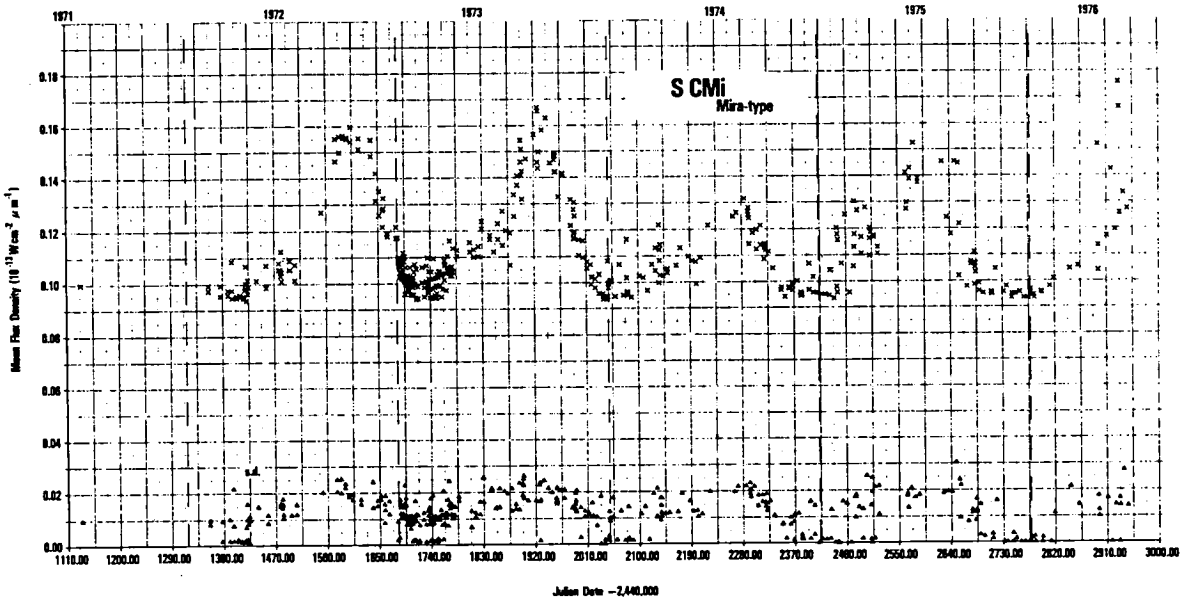

Figure 3.--Infrared light curve and corresponding standard deviations for S Canis Minoris. Details of the format are the same as in Figure 1. Note the pronounced cycle-to-cycle variability at maximum light, which can be contrasted with the well-reproduced flux density at minimum light.

REFERENCES*

Bowers, P. F., and Kerr, F. J. 1977, Astron. Astrophys., 57, 115.

Chapman, R. D., Michalitsianos, A. G., Maran, S. P., Hobbs, R. W., Heinsheimer, T. F., and Stocker, T. L. 1978, in preparation.

Eggen, E. J. 1975, Astrophys. J., 195, 661.

Heinsheimer, T. F., Sweeney, L. H., Yates, F. F., Maran, S. P., Lesh, J. R., and Nagy, T. A. 1978, to appear in Proc. SPIE.

Ikaunieks, J. 1975, in Pulsating Stars, ed. B. V. Kukarkin (New York: Wiley), p. 259.

Lépine, J. R. D., and Paes de Barros, M. H. 1977, Astron. Astrophys., 56, 219.

Maran, S. P., Heinsheimer, T. F., Stocker, T. L., Anand, S. P. S., Chapman, R. D., Hobbs, R. W., Michalitsanos, A. G., Wright, F. H., and Kipp, S. L. 1977, Infrared Physics, 17, 565.

Maran, S. P., Heinsheimer, T. F., Stocker, T. L., Chapman, R. D., Hobbs, R. W., and Michalitsanos, A. G. 1976, Proc. SPIE, 95, 23.

Spencer, J. H., Schwartz, P. R., Waak, J. A., and Bologna, J. M. 1977, Astron. J., 82, 706.

Sweeney, L. H., Heinsheimer, T. F., Yates, F. F., Maran, S. P., Lesh, J. R., and Nagy, T. A. 1977, Proc. SPIE, 124, 125.

Wallerstein, G. 1977, J. Royal Astron. Soc. Canada, 71, 298.

Willson, L. A. 1976, Astrophys. J., 205, 172.

---

*Bibliographical note: due to a change in spelling, author Michalitsanos (1977 and earlier) is now Michalitsianos.

Discussion

Keller: What accounts for the large variations in the data? What is the cause of the noise?

Maran: I don't know, but I can make guesses. There is sometimes noise due to what may be spacecraft reflections of the moon. Also, if you compare the infrared and visible light curves, you see that the satellite looks closer to the Sun than the AAVSO observers do. So unlike IUE, which has large avoidance cones, there are other effects. Supposedly, bad data points are removed before we see the data, but it's clear that there are occasional bad points in the 1976 data.

Wing: Aren't the 2.7 μ observations affected by stellar water absorption bands?

Maran: Since we have a wide band, the answer is probably "no" or "not much." But you may be right for the following reason: the largest amplitude we've seen in a Mira variable is about 3 magnitudes (ratio of maximum to minimum flux). That's 20% larger than any ground-based IR observations I've seen in the K and L bands, which bracket our band. If that difference is real, then you are probably right, although it may be due to the fact that our curves are better defined, so we are less conservative about estimating the amplitude.

AN INDEPENDENT CEPHEID DISTANCE SCALE: CURRENT STATUS

Thomas G. Barnes III
Department of Astronomy
University of Texas at Austin

I. INTRODUCTION

For the past two years my collaborators and I at the University of Texas at Austin have worked toward establishing an independent distance scale for Cepheid variables. The basis of our approach is to make use of the apparent magnitude and the visual surface brightness, inferred from an appropriate color index, to determine the angular diameter variation of the Cepheid. When combined with the linear displacement curve, obtained from the integrated radial velocity curve, the distance and linear radius are determined. The great attractiveness of the method is its complete independence of all other stellar distance scales. Even though a number of practical difficulties currently exist in implementing the technique, our preliminary results may nonetheless be useful by virtue of this independence.

II. VISUAL SURFACE BRIGHTNESSES

The critical component of this technique is the relation between a color index and the visual surface brightness parameter F_V, defined by

$$F_V = 4.2207 - 0.1V_o - 0.5\log \phi \ , \qquad (1)$$

where V_o is the apparent visual magnitude corrected for interstellar extinction and ϕ is the stellar angular diameter in milliseconds of arc. Measured values of the stellar angular diameter are now available for nearly one hundred stars (Barnes, Evans, and Moffett 1978). Of the readily available photometric indices for these stars, we have found the Johnson (1966) V-R index to be the most tightly correlated with F_V (Barnes and Evans 1976; Barnes, Evans, and Parsons 1976; Barnes *et al.* 1978). Knowledge of $(V-R)_o$ alone permits F_V to be inferred from the mean relation with a typical uncertainty of ± 0.033 over the spectral type range O4 - M8. This uncertainty is entirely attributable to the observational errors. No luminosity class effects are apparent in the relation.

Although no Cepheid variable has an observed angular diameter, the presence of several other kinds of variables on the relation, even though observed at random times in their cycles, led Barnes, Evans and Parsons (1976) to suggest that the F_V - $(V-R)_o$ calibration would apply to Cepheids throughout their pulsations. Barnes *et al.* (1977) examined this

assumption by the strategem of exploring its consequences when applied to Cepheids for which the requisite photometry and radial velocities had been published. They found the assumption to be verified within the rather loose constraints permitted by the quality of the data (see also Evans 1977).

In the present discussion I will explore the validity of this assumption by determining the F_V - $(V-R)_o$ relation from Cepheids themselves and comparing the result to the relation for stars of known angular diameter. (This work will be published elsewhere in its entirety by T.G. Barnes and B.J. Beardsley.)

III. CEPHEID SURFACE BRIGHTNESSES: THE SLOPE

Thompson (1975) has devised a method for determining the visual surface brightness of a Cepheid, to within an unknown additive constant, from photometry and radial velocities. His method requires *a priori* knowledge of the star's linear radius, but not of the distance or luminosity. To obtain the linear radii, we have adopted Balona's (1977) recent results for the Cepheid period-radius relation:

$$\log R/R_o = 1.213 + 0.6021 \log P \ . \qquad (2)$$

This relation assumes a conversion factor between radial velocity and pulsational velocity of p=1.31.

The photometric and radial velocity data were essentially the same as used by Barnes *et al.* (1977) and referenced therein. Color excesses were taken from Parsons and Bell (1975). We adopted R = 3.3 and E(V-R)/E(B-V) = 0.84.

To ensure that the problem of phase-matching the photometric and radial velocity data was minimized, we used only those eleven Cepheids (with BVRI data) for which simultaneous photometry and radial velocities have established the relative phases (Breger 1967, Evans 1976). We simply shifted the radial velocity phases until minimum radial velocity occurred at the appropriate phase relative to the V light curve. (The mean shift was -0.005 in phase.)

For each Cepheid, Thompson's method yields the variation in F_V with color index to within an unknown constant. Figure 1 shows a representative result. In all eleven cases the data are consistent with a linear relation between F_V and $(V-R)_o$ and with no distinction between rising and falling branches of the light curve. This confirms the observational and theoretical arguments for linearity given by Barnes *et al.* (1977).

Figure 2 shows that the slopes are independent of period and have a scatter about their mean value in accordance with the observational uncertainities. The mean slope is -0.360 $\pm$ 0.010 (s.e.m.). This slope is somewhat less negative than the best fit to the A-F-G stars of known angular diameter given by Barnes *et al.* (1977), in agreement with their, and Evans' (1977), suspicions.

Both the linearity and common slope are also found if the surface brightness is correlated with $(B-V)_o$. In this case we obtain -0.211 $\pm$ 0.003 (s.e.m.), in comparison with Thompson's value of -0.211 $\pm$ 0.003 and Balona's value of -0.215 $\pm$ 0.002.

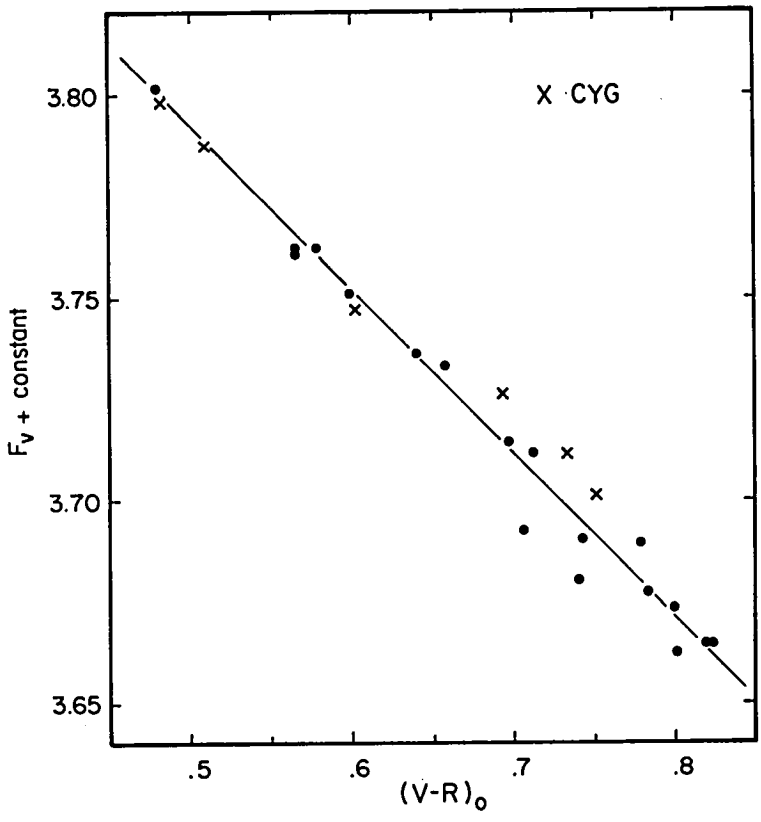

Figure 1: The variation in F_V with $(V-R)_o$ for X Cygni. Dots represent phases of falling light and crosses, phases of rising light. The line is a least-squares fit to the data.

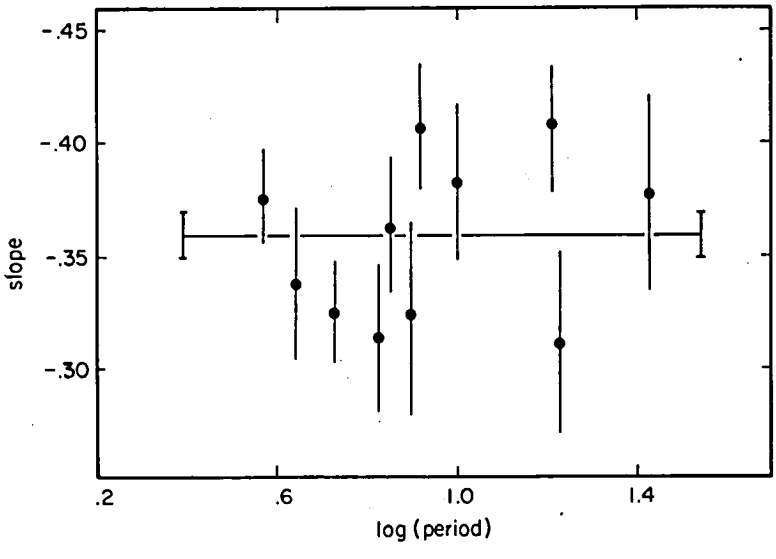

Figure 2: The individual Cepheid slopes plotted against the logarithm of the period. The error bars are one sigma values based on the uncertainities in the photometry, the phase-matching, and the adopted linear radii. The mean slope and its uncertainity are shown.

IV. CEPHEID SURFACE BRIGHTNESSES: THE ZERO POINT

Until a Cepheid angular diameter is actually measured, the zero point must be acquired either by assuming that Cepheids have surface brightnesses similar to non-variable F supergiants or by using model atmosphere results. Happily, both choices give the same result for the short period Cepheids.

Parsons (1969, 1970a, 1971) has demonstrated that his model atmosphere fluxes for F and G supergiants accurately match the observed fluxes in the blackbody six-color system for a large selection of variables and non-variables. One parameter obtained in the fitting procedure is the stellar angular diameter, tabulated by Parsons (1970b) and Parsons and Bouw (1971). The uncertainities in the angular diameters are ± 0.03 dex from the fitting procedure (Parsons 1971), ± 0.02 dex from the model physics (Parsons 1978, private communication), and ± 0.02 dex from the interstellar extinction (our estimate). The last uncertainty cancels out when eq. (1) is used to compute the visual surface brightness parameter.

Only one star in Parsons' lists has an observed angular diameter, the F8Ia star δ CMa. Parsons (1970b) gives $\log \phi = 0.56 \pm 0.04$, whereas Hanbury Brown et al. (1974) measured 0.56 ± 0.06. This gives us considerable confidence that his mean angular diameters for Cepheids are accurate.

There are eighteen Cepheids with both angular diameters and BVRI photometry. We have computed visual surface brightnesses for these using eq. (1). Recall that the interstellar extinction term in the computation of $\log \phi$ cancels the same term in eq. (1) leaving F_V independent of interstellar extinction. (Interstellar reddening still enters to the extent that incorrect elimination of it affects the fit of the model fluxes to the observed fluxes.)

Figure 3 compares the visual surface brightnesses of the Cepheids to those for similar temperature stars of known angular diameter. For Cepheids bluer than $(V-R)_o = 0.6$ the agreement is excellent. In particular note the agreement with δ CMa at $(V-R)_o = 0.47$. Because of the paucity of observed angular diameters in this color range, the mean curve from Barnes et al. (1978) is very poorly determined. It could easily be altered to fit simultaneously the short period Cepheids and the few observed angular diameter stars.

The long period Cepheids are clearly discordant. After examining the uncertainities involved, we are convinced that the long period Cepheids cannot lie on the same relation as the non-variable stars of measured angular diameter.

Ignoring the Cepheids to the red of $(V-R)_o=0.6$, we find the model atmosphere values of F_V to be represented by the regression line

$$F_V = \underset{\pm .025}{3.945} - \underset{\pm .048}{0.338}\ (V-R)_o\ . \qquad (3)$$

The slope of this relation is in agreement with the value found in the previous section by a total different approach. However, the uncertainty in the slope in eq. (3) is considerably larger than found earlier. Hence we have adopted the previous value of the slope and used the model atmosphere results to establish the zero point:

$$F_V = \underset{\pm .006}{3.957} - \underset{\pm .010}{0.360}\ (V-R)_o\ , \qquad (4)$$

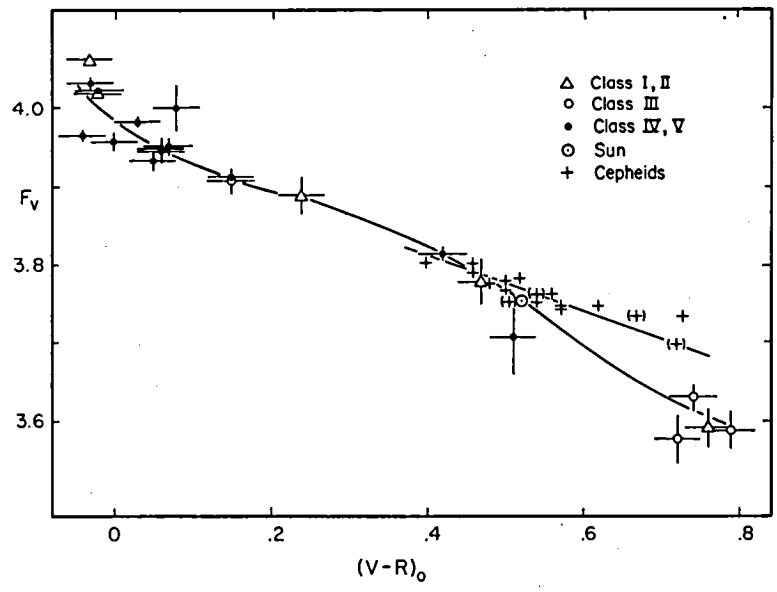

Figure 3: The relation between visual surface brightness parameter and $(V-R)_o$ for Cepheids (plus signs) and for stars of measured angular diameter (all other symbols). Uncertain values are enclosed in parentheses. The smooth curve is the fit adopted by Barnes et al. (1978).

where both uncertainities are standard errors of the mean. This line is shown in Figure 3.

V. A PRELIMINARY DISTANCE SCALE

With the relation between F_V and $(V-R)_o$ now established, we return to the determination of the Cepheid distances. We have used eq. (4) and the technique described by Barnes et al.(1977) to determine distances for the seven short-period Cepheids for which the requisite data exist and for which Evans (1976) has established phase matching (η Aql, RT Aur, δ Cep, W Gem, ζ Gem, S Sge, and T Vul). A weighted mean of the seven yields a distance scale (14.2 $\pm$ 6.8)% larger than the Fernie and Hube (1968) scale and (18.2 $\pm$ 6.3)% larger than the Sandage and Tammann (1969) scale.

The above uncertainities are the random uncertainities only, whereas more realistic values should include the contributions of systematic errors. There are three of these to consider:

1) The uncertainty in the conversion factor from radial velocity to pulsational velocity enters directly into the distance scale. With a conservative estimate of p = 1.31 $\pm$ 0.06, this contributes $\pm$4.6%.

2) The uncertainty in the slope in eq. (4) enters in a manner dependent upon the mean color and amplitude of the Cepheid. The uncertainty in the distance due to this ranges from $\pm$4.2% to $\pm$13.5%, with a mean of $\pm$7.2% which we will adopt.

3) The uncertainty in the zero point in eq. (4) enters exponentially, giving $\pm$2.8%. However, this represents only the observational and theoretical scatter in the zero point and does not include any systematic

uncertainty in the model physics. As mentioned earlier, the uncertainty in model physics leads to $\pm$0.02 dex in log ϕ, or another 4.7% in distance.

Altogether the systematic errors are $\pm$10.2% in distance.

Combining the variances, we find a preliminary distance scale (14.2 $\pm$12.2)% larger than Fernie and Hube, and (18.2 $\pm$12.0)% larger than Sandage and Tammann. Averaging these and expressing the result as a change in absolute magnitude, we find the short-period Cepheids 0.33 $\pm$ 0.23 mag. brighter than on the old distance scale. This is quite consistent with the currently recommended change in the Hyades distance modulus.

In conclusion, we have shown that the surface brightnesses of Cepheid variables may be determined from the Cepheids themselves, that for short-period Cepheids the resultant values are in good agreement with non-variables of the same color, and that the preliminary distance scale to which these values lead supports full effect of the new Hyades distance scale upon Cepheid luminosities.

ACKNOWLEDGEMENTS

It is a pleasure to acknowledge the many contributions of my collaborators B.J. Beardsley, D.S. Evans, T.J. Moffett, and S.B. Parsons, without whom this work would not have been accomplished. Discussions with J.D. Fernie were also most valuable. Financial support from NSF through grant AST76-21316 is gratefully acknowledged.

REFERENCES

Balona, L.A. 1977. Mon.Not.R.Astr.Soc., 178, 231.
Barnes, T.G. and Evans, D.S. 1976. Mon.Not.R.Astr.Soc., 174, 489.
Barnes, T.G., Dominy, J.F., Evans, D.S., Kelton, P.W., Parsons, S.B. and Stover, R.J. 1977. Mon.Not.R.Astr.Soc., 178, 661.
Barnes, T.G., Evans, D.S. and Moffett, T.J. 1978. Mon.Not.R.Astr.Soc., 183, 285.
Barnes, T.G., Evans, D.S. and Parsons, S.B. 1976. Mon.Not.R.Astr.Soc., 174, 503.
Breger, M. 1967. Mon.Not.R.Astr.Soc., 136, 61.
Evans, N.R. 1976. Ap.J.Suppl., 32, 399.
Evans, N.R. 1977. Mon.Not.R.Astr.Soc., 181, 85P.
Fernie, J.D. and Hube, J.O. 1968. Astr.J., 73, 492.
Hanbury Brown, R., Davis, J. and Allen, L.R. 1974. Mon.Not.R.Astr.Soc., 167, 121.
Johnson, H.L. 1966. Ann.Rev.Astr.Ap., 4, 193.
Parsons, S.B. 1969. Ap.J.Suppl., 18, 127.
Parsons, S.B. 1970a. Ap.J., 159, 951.
Parsons, S.B. 1970b. Warner and Swasey Obs. Preprint No. 3.
Parsons, S.B. 1971. Mon.Not.R.Astr.Soc., 152, 121.
Parsons, S.B. and Bell, R.A. 1975. Dudley Observ. Rep., 9, 73.
Parsons, S.B. and Bouw, G.D. 1971. Mon.Not.R.Astr.Soc., 152, 133.
Sandage, A.R. and Tammann, G.A. 1969. Ap.J., 157, 683.
Thompson, R.J. 1975. Mon.Not.R.Astr.Soc., 172, 455.

Discussion

Schmidt: Could you tell us how the radii are affected by the zero point?

Barnes: I haven't done that for this group of Cepheids. It will increase the radii somewhat over what I have obtained previously.

Wesselink: What does the value -0.33 mean?

Barnes: The -0.33 magnitude is the shift in the mean distance modulus or the mean absolute magnitude that is implied by this result on seven Cepheids.

Evans: In your graph for X Cyg, in the surface brightness-(V-R) relation, do you think you would get a somewhat steeper slope if you confined yourself to the descending branch of the light curve? You'd definitely get different slopes from different branches.

Barnes: There are typically only a few points on the rising branch; I think that there are only four for X Cyg. I don't think that it is statistically significant that three lie above and only one below the curve. Looking at the other 10 Cepheids, there seems to be a random scatter of the points about the rising and falling branches.

A. Cox: You've already published data from seven Cepheids. Are these the same stars, and is this the same answer? If not, how different is it?

Barnes: The 1977 paper used these seven Cepheids plus two others. The present result is different by about 1.5 σ -- about 0.3 mag brighter than the previous result in absolute magnitude. The reason for that is threefold.

In our early work, we didn't know about Nancy Evans' work on relative phasing, so we just shifted the curves until they looked right. Secondly, we have an improved technique for interpolating in the displacement curve at the phases for which photometry exists. Finally, the 1977 computations were based on a preliminary surface brightness -- color relation from stars of known angular diameter. The present results are based on a relation inferred from the Cepheids themselves.

THE BARNES-EVANS COLOR-SURFACE BRIGHTNESS RELATION: A PRELIMINARY THEORETICAL INTERPRETATION

Harry L. Shipman

University of Delaware

ABSTRACT

Model atmosphere calculations from the published literature are used to assess the claim of Barnes, Evans, and their collaborators that their empirically derived relation between V-R and surface brightness is independent of a variety of stellar parameters, including surface gravity. This relationship is being used in a variety of applications, including the determination of the distances of Cepheid variables using a method based on the Baade-Wesselink method. The principal conclusion here is that the use of a main-sequence relation between V-R color and surface brightness in determining radii of giant ($\log g = 2$) stars is subject to systematic errors that are smaller than 10 % in the determination of a radius or distance for temperatures cooler than 12,000 K. The application of a main-sequence relation to white-dwarf stars is also considered; the error in white-dwarf radii determined from a main sequence color-surface brightness relation is again roughly 10 %.

I. INTRODUCTION

Stellar diameters derived from lunar occultations and Johnson UBVRI photometry have been used to develop an empirically calibrated relation between the surface brightness of a star and its V-R color (Barnes and Evans 1976; Barnes, Evans, and Parsons 1976; Barnes, Evans, and Moffett 1978). This relation, often called the Barnes-Evans relation, can be

used for a variety of purposes. Since comparable techniques generally require observations having considerably higher spectral resolution, the Barnes-Evans relation, if it is indeed widely applicable, presents considerable promise for a variety of astrophysical problems. Yet this relation is empirically derived using measurements of nearby stars, mostly main sequence stars, and many of its most interesting applications (including those relevant to the variable star field) involve the extension of this relation to other types of objects. How valid is this extension? The range of applicability of a relation of the Barnes-Evans type is the central focus of this paper.

The surface brightness parameter used in the Barnes-Evans relation is

$$F_V = 4.2207 - 0.1\ V_o - 0.5 \log \phi', \qquad (1)$$

where V_o is the apparent visual magnitude corrected for interstellar extinction and ϕ' the stellar angular diameter in milliseconds of arc. Barnes, Evans, and their colleagues argue empirically that the relation between F_V and the Johnson (1966) V-R color is a single-valued one. This relation has been used to measure the radii of nearby stars (Lacy (1977b) and of white-dwarf stars (Moffett, Barnes, and Evans 1978). It has been used to determine distances of eclipsing binaries (Lacy 1977a), of Cepheid variables (Barnes et al. 1977) and of a nova (Barnes 1976). It has also been applied tentatively to solar flares, and a variety of other applications are contemplated (Evans 1978). A theoretical assessment is timely.

II. THEORETICAL FRAMEWORK

A disadvantage of dealing with broad-band photometric systems from a theoretical viewpoint is that broad-band photometry does not isolate some easily calculable part of the spectrum, but rather measures the

integrated intensity of a broad spectral region containing both continuum emission and also the contamination of spectral lines. It is this feature of broad-band photometry that makes it extremely economical in terms of telescope time. A thorough evaluation of the applicability of the Barnes-Evans F_V versus V-R relation would require a consideration of all the lines that could affect these bands at all temperatures and gravities. There are considerable difficulties involved in computing synthetic Johnson colors, and they are only beginning to be solved for the UBV colors (Buser and Kurucz 1978). The ambition of this investigation is far more modest. Here I ask how badly changes in gravity and chemical composition affect the continuum fluxes at the central wavelengths of the V and R bands. Since at the temperatures considered here, line blanketing is minimal, changes in the continuum fluxes should provide a reasonable idea of changes in the V-R colors.

To recast the color-surface brightness relation into theoretically tractable terms, use the following relations:

$$\phi' = 206,264,806.2\ (2R/D), \tag{2}$$

$$V_o - 0.04 = -2.5 \log (f_V/3.52 \times 10^{-20}), \text{ and} \tag{3}$$

$$f_V = 4\pi\ (R/D)^2\ H_V, \tag{4}$$

where R is the stellar radius, D its distance, V_o the Johnson V magnitude, ϕ' is in milliseconds of arc, f_V is the stellar flux at the Earth in the central wavelength of the V band and H_V is the Eddington flux at the stellar surface at the central wavelength of the V band in ergs cm^{-2} sec^{-1} $ster^{-1}$ Hz^{-1}. Note that H is normalized so that $\int H_\nu d\nu = \sigma T_{eff}^4/4\pi$. For the purposes of this paper, the effective wavelengths are presumed constant at 0.55 microns (V) and 0.7 microns (R). Variations in effective wavelength with temperature are presumed to be second-order effects when considering the change in H_V versus V-R when gravity or

chemical composition is altered. Equation (3) takes the V magnitude of Vega as 0.04 and takes the visual flux at 5556 A as 3.52×10^{-20} ergs cm^{-2} sec^{-1} Hz^{-1}, averaging the results of Hayes and Latham (1975), the corrected results of Oke and Schild (1970), and the recent calibration of Tug et al. (1977). Uncertainties in the transformation of monochromatic magnitudes to V-magnitudes undoubtedly exist and will affect the calibration of the zero point to some small degree; for present purposes they are not material. Equations (1) through (4) can be combined to yield the following definition of the surface brightness parameter F_v:

$$F_v = 5.047 \pm 0.002 + 0.25\ H_v\ , \qquad (5)$$

where the uncertainty in the constant comes from a presumed 2 % uncertainty in the absolute flux calibration.

For present purposes a continuum color is defined:

$$v'-r' = -2.5 \log (H_v/H_r), \qquad (6)$$

using the effective wavelengths noted above. Ideally this color would be equal to the Johnson V-R color plus an additive constant. Blanketing and changes in effective wavelength with temperature cause reality to fall short of the ideal. But in narrow color regions, one can presume that a change in the H_v versus v'-r' relation is paralleled by a change in the broadband color index V-R and the broadband flux F_v. It may be possible to calibrate the V-R index in absolute terms in the future (Buser 1978; Buser and Kurucz 1978).

III. RESULTS

Figure 1 illustrates the central results of this paper, Here the monochromatic Eddington fluxes H_v are plotted against the monochromatic v'-r' color index. These fluxes and colors are taken from a variety of

models: those of Kurucz, Peytremann, and Avrett (1974) for main sequence (log g = 4.5) and giant (log g = 2) models with T_{eff} higher than 8,000 K, or v'-r' = -0.118; those of Carbon and Gingerich (1969) for main sequence (here log g = 4 because more models were available) and giant (log g = 2) models for T_{eff} between 4,000 and 8,000 K; and mine (Shipman 1972, 1977; McGraw and Shipman 1978) for the white-dwarf models (log g = 8). Since white-dwarf stars are either essentially pure H or essentially pure He, models for both compositions are shown. Also shown is the black body relation for a gray atmosphere where $H_v = B_v/4$ given the normalization of H.

The sets of models chosen for Figure 1 are worth noting. All models, except the He-rich white-dwarf models, include line blanketing to some extent. The Carbon-Gingerich models are fairly old, and do not use the most modern, elaborate treatment of line blanketing. However, published grids of models which cover the T_{eff} range that the Carbon-Gingerich models are used for here (Peytremann 1974, Bell et al. 1975) do not directly provide tables of emergent fluxes. Gustafsson et al. (1975) show that their models, which do include a state-of-the-art, elaborate statistical treatment of line blanketing, have temperature gradients quite similar to those of Carbon and Gingerich (1969) that are used here. Under the circumstances, the use of the Carbon-Gingerich models is probably justified, particularly since no models cooler than T_{eff} = 4000 K, where blanketing by TiO bands can greatly affect integrated fluxes in the V and R bands, are considered here. A test of the accuracy of the Carbon-Gingerich models is provided by the T_{eff} range between 8,000 K and 10,000 K, where the Carbon-Gingerich grid overlaps the Kurucz, Peytremann, and Avrett (1974) grid (which includes a fairly elaborate treatment of line blanketing). Differences between the H_v versus v'-r' relations provided by the two sets of models are less than 2 % in H_v.

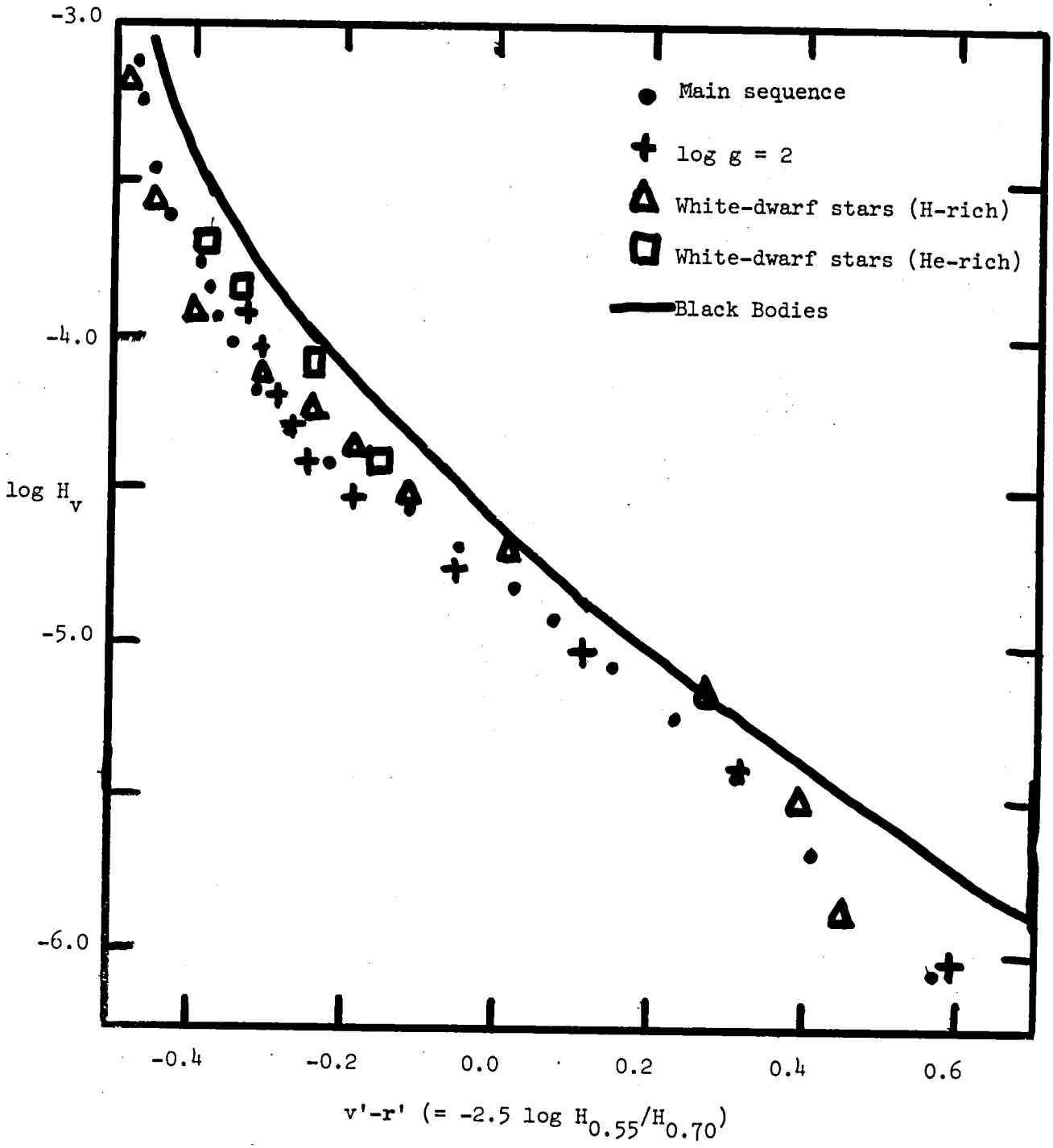

Figure 1. Color-Surface Brightness relations. The relation between Eddington flux in the visual band (effective wavelength 0.55 microns) and the monochromatic color index v'-r' is shown for a variety of model atmospheres and for black bodies. References to the specific model calculations is provided in the text.

It is worth examining the sensitivity of the conclusions presented here to the assumptions used, particularly to the simplified treatment of line blanketing used in the Carbon-Gingerich models. For most models, the observed blanketing coeffecients (defined as the fraction of the total flux removed by lines) in the V and R bands are 5 % or less, as tabulated by Carbon and Gingerich. Differential effects on the V and R colors should be smaller still. The effects are somewhat larger but still less than 20 % for the cooler T_{eff} = 5,000 and 4,000 K models. Carbon and Gingerich argue that the continuum energy distribution is relatively insensitive to the way that line blanketing is treated. Thus the approximate treatment of line blanketing will not affect the conclusions here for T_{eff} > 6,000 K, and will probably not affect the results at cooler temperatures. Stars cooler than 4,000 K were not included in this investigation; an examination of the M-dwarf models of Mould (1976) indicated that TiO blanketing could seriously affect the R colors, so that the behavior of v'-r' might differ from the behavior of the observed color V-R.

The results in Figure 1 show that H_v (or equivalently F_v, see equation 5) is quite tightly correlated with the v'-r' color. Figure 2 shows the difference between the value of H_v calculated from the models and the value derived from a piecewise-linear fit to the main sequence relation. This difference should parallel the difference between the empirical Barnes-Evans relation, derived for main sequence stars, and the true relation for giant stars or for white-dwarf stars. Cooler than v'-r' = -0.3, or T_{eff} = 12,000 K, the main-sequence and giant (log g = 2) relations coincide within 0.1 in log H_v or (equation 5) 0.025 in F_v. This correspondence agrees with the observations of Barnes et al. (1978). They

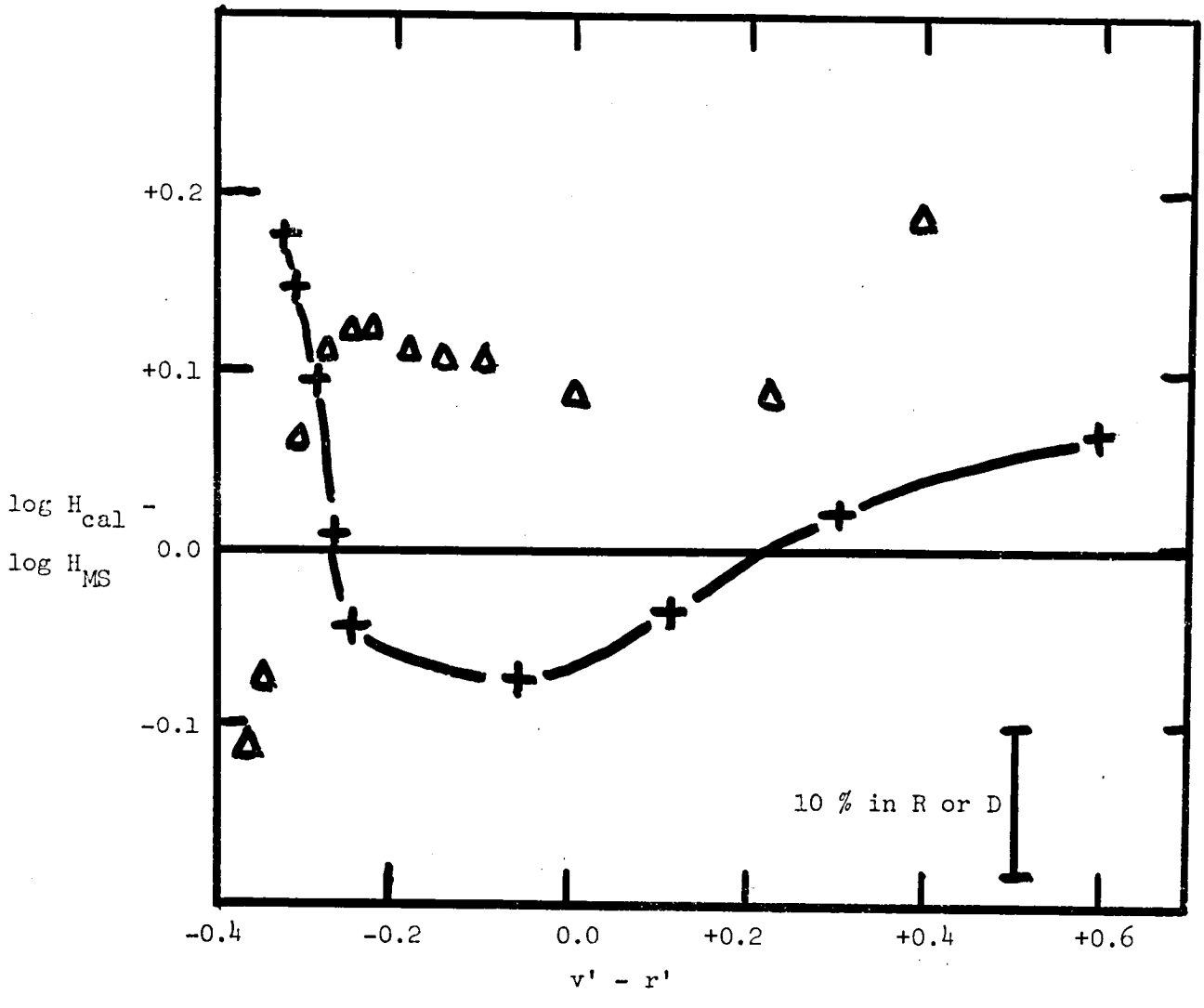

Figure 2. The difference between the visual flux calculated from the models and the flux determined from a main-sequence H_v vs. v'-r' relation. Plus signs and solid curve: log g = 2. Triangles: H-rich white-dwarf stars (log g = 8). The scale bar shows the change in H_v that corresponds to a 10 % change in a radius or distance measured using a surface-brightness method.

state that the scatter in the F_v versus V-R relation, a relation presumably very similar to the theoretical H_v versus v'-r' relation plotted in Figures 1 and 2, is 0.033; they attribute this to observational uncertainties, meaning that the cosmic scatter caused by gravity and composition changes is less than this. For the white-dwarf stars, the main-sequence relation is within 0.15 in log H_v of that given for the white-dwarf models for all but the coolest one (T_{eff} = 5,000 K) one plotted in Figure 2. Even the He-rich models fall within 0.2 in log H_v of the main-sequence line. The coincidence between the color-surface brightness relations for the two types of white-dwarf stars was noted by Shipman (1978) in connection with the monochromatic g - r color (this discovery provided the motivation for the present paper). In applications, the Barnes-Evans relation is generally used to determine stellar radii or distances, and a 10 % error in either of these quantities is shown in Figure 2. Note that there are some additional uncertainties when the slope of the Barnes-Evans relation is used to determine distances to variable stars; see the discussion below.

IV. PHYSICAL BASIS OF THE RELATION

A natural question to ask now is why? Why is v'-r', or equivalently V-R, such a good predictor of the visual flux H_v? Why does the Barnes-Evans relation work? This section provides some nonrigorous arguments directed towards a qualitative answer to this question.

Consider two model atmospheres with the same visual flux H_v. They are thus characterized by the same temperature at visual optical depth 2/3, where the flux in the V band is produced. Were these atmospheres isothermal --were the temperatures at τ_v = 2/3 and τ_r = 2/3 the same-- there would be no dependence of v'-r' on gravity, composition, or anything

else, for it would be the wavelength (not depth) dependence of the source function which would drive the dependence of H_v on v'-r' color. In such a case, the H_v versus v'-r' color would follow the black body line. The relation almost follows the black body line (Figure 1), reflecting the fact that the v' and r' fluxes come from almost the same layer in the stellar atmosphere, but the coincidence is not exact.

The deviation of the H_v versus v'-r' relation from the black body line is caused by the fact that the v' and r' bands sample different layers in the stellar atmosphere. In all cases, the opacity in the v' band is less than the opacity in the r' band, and the stellar atmosphere is bluer than a black body with the same H_v (same temperature at visual optical depth = 2/3) would be. In cool (T_{eff} less than 8,000 K) stars, opacity in the 0.5 - 0.7 micron region comes from H^-. H^- is a very gray opacity source, with less than a 30 % change from 0.55 microns to 0.7 microns. Further, since both giant and dwarf stars have H^- as the principal opacity source in this wavelength region, the relative change in the opacity from v' to r' is the same in both types of stars, as well as in the white-dwarf stars. Thus we can understand the relative independence of the H_v versus v' -r' relation on surface gravity at cool temperatures. The V-R Johnson index is the only line-free index that samples two parts of the same continuum. A color index that samples two sides of a discontinuity (for example, U - V or V - I) would produce greater gravity effects, in all probability.

For the hotter stars, with temperatures exceeding 8,000 K and v'-r' colors bluer than -0.25, Figure 2 shows that the character of the H_v versus v'-r' relation changes drastically. This change can be attributed to a change in opacity source, since at these temperatures neutral H rather than H^- dominates in the v' and r' bands. Atomic H is

less gray than H^-; the opacity doubles when going from the v' band to the r' band. The character of the difference between main sequence and giant stars changes. For white-dwarf stars, this transition occurs at slightly higher temperatures but similar values of the v'-r' color index (see Figure 2). At the extremely high temperatures, exceeding $T_{eff} = 12,000$ K (v'-r' = -0.30), the main sequence relation is no longer such a good predictor of H_v. However, at such high temperatures, the slope of the H_v versus v'-r' relation is such that this type of relation is less useful--observational uncertainties in the measured color indices translate into larger uncertainties in the surface brightness parameter H_v (or equivalently the parameter F_v).

V. CONCLUSIONS

Figures 1 and 2, the centerpiece of this paper, indicate that the relation between surface brightness H_v (equivalent to the Barnes-Evans parameter F_v) and the v'-r' color is independent of surface gravity at the level of approximately 0.1 in log H_v for stars cooler than $T_{eff} = 14,000$ K, with errors not too much larger at higher temperatures where the slope of the relation makes v'-r' a less useful estimator of F_v. As long as differential blanketing effects are unimportant, and we believe that they are, the monochromatic v'-r' color should behave the same as the broadband V-R color, and therefore this claim can be made of the Barnes-Evans relation as well. This paper does not consider the problem of the cool stars (T_{eff} less than 4,000 K), where TiO blanketing effects could be important.

Consequently distance measurements of stars hotter than $T_{eff} = 4,000$ K, such as those made by Lacy (1977a, 1977b) should not be seriously affected

by systematic errors. While there are some errors at the 10% level in measuring white-dwarf radii using a main-sequence relation of the Barnes-Evans type, these errors reverse sign at T_{eff} = 12,000 K and consequently measurements of the radii of a group of stars should be relatively free from systematic errors. Parallax errors are generally larger than 10 %, so that use of the Barnes-Evans relation should not introduce any significant additional errors in most applications. The value of this relation lies in its applicability with small telescopes; the broad bands of the V and R filters reduce the requirements of telescope size or observing time.

When the Barnes-Evans relation is used to determine the distances to Cepheid variables using an extension of the Baade-Wesselink method (Barnes et al. 1977), a problem arises because it is the slope of the relation that enters the distance-finding method. Is the slope of the H_v versus v'-r' relation the same for Cepheids (log g = 1.5 to 2) as it is for main-sequence stars? In the 6,000 K to 8,000 K range, the slope from model atmospheres changes from -0.445 at log g = 4 to -0.397 at log g = 2. Small uncertainties in the models could produce large changes in this conclusion, and these models are affected by convection, which produces uncertainties in the models (Relyea and Kurucz 1978). At the present time it is only possible to state that a change in slope of this magnitude cannot be ruled out, and that a change in slope greater than this might be possible but a significantly greater change in slope is unlikely. This possibility of a change in slope should be considered as a possible uncertainty in an evaluation of radii using the method of Barnes et al. (1977).

This investigation has some limitations. Perhaps the most severe is that it is restricted to continuum colors. In the temperature range

being considered, line blanketing is a relatively minor effect in the V and R bands, and differential line blanketing (which would affect the V-R color through changes in line strengths with surface gravity) should be smaller still. Thus the extension of the present line of work to models including a more thorough treatment of line blanketing should probably not affect the principal conclusions of this paper. In addition, the present investigation does not include stars larger than log g = 2 and M-type stars.

Within these uncertainties, the principal conclusion of this paper is that a main-sequence relation between V-R and F_v such as that proposed by Barnes and Evans can be applied to stars with surface gravities between log g = 2 and log g = 8 and produce radii or distances with systematic errors of 10 % or less in most cases. Precise values of the errors as a function of T_{eff} and log g can be determined by examining Figures 1 and 2.

I thank Drs. T. G. Barnes and J. T. McGraw for encouragement. This work has been partially supported by NASA under grant NSG 5144 and by the NSF under grant AST76-20723.

Barnes, T. G. 1976. Mon. Not. R. A. S. 177, 53p-58p.

Barnes, T. G., Dominy, J. F., Evans, D. S., Kelton, P. W., Parsons, S. B., and Stover, R. J. 1977. Mon. Not. R. A. S. 178, 661-674.

Barnes, T. G., Evans, D. S., and Parsons, S. B. 1976. Mon. Not. R. A. S. 174, 503-512.

Barnes, T. G., and Evans, D. S. 1976. Mon. Not. R. A. S. 174, 489-502.

Barnes, T. G., Evans, D. S., and Moffett, T. J. 1978, Mon. Not. R. A. S. (submitted).

Bell, R. A., Erikson, K., Gustafsson, B., and Nordlund, A. 1975. Astron. Astrophys. Suppl. 23, 37.

Buser, R. 1978. Astron. Astrophys. 62, 411-424.

Buser, R., and Kurucz, R. L. 1978. Astron. Astrophys. (submitted).

Carbon, D., and Gingerich, O. 1969. in O. Gingerich, ed., Theory and Observation of Normal Stellar Atmospheres, Cambridge: MIT Press.

Evans, D. S. 1978. Bull. Amer. Astron. Soc. 9, 643-644.

Gustafsson, B., Bell, R. A., Eriksson, K., and Nordlund, A. 1975. Astron. Astrophys. 42, 407-432.

Hayes, D. S., and Latham, D. W. 1975. Ap. J. 197, 593-601.

Johnson, H. L. 1966. Ann. Rev. Astron. Ap. 4, 193.

Karp, A. H. 1975. Ap. J. 200, 354.

Kurucz, R. L., Peytremann, E., and Avrett, E. H. 1974. Blanketed Model Atmospheres for Early-Type Stars, Washington: Smithsonian Press.

Lacy, C. H. 1977a. Ap. J. 213, 454.

Lacy, C. H. 1977b. Ap. J. Suppl. 34, 479-492.

McGraw, J. T., and Shipman, H. L. 1978. In preparation.

Moffett, T. J., Barnes, T. G., and Evans, D. S. 1978. Astron. J. (submitted).

Mould, J. R. 1976. Astron. Astrophys. 48, 443.

Oke, J. B., and Schild, R. E. 1970. Ap. J. 161, 1015.

Peytremann, E. 1974. Astron. Astrophys. Suppl. 18, 81.

Relyea, L. S., and Kurucz, R. L. 1978. Ap. J. Suppl. 37 (in press).

Shipman, H. L. 1972. Ap. J. 177, 723-743.

Shipman, H. L. 1977. Ap. J. 213, 138-144.

Shipman, H. L. 1978. Ap. J. (submitted).

Tug, H., White, N.M., and Lockwood, G.W. 1978. Astron, Astrophys. 61 , 679-684.

Discussion

Smith: The previous question as to why the Barnes-Evans relationship works was actually answered, ironically, several years ago by Cayrel, who was interested in looking at the competing effects of backwarming and line blocking in model atmospheres when you went from normal composition to metal-poor stars. He came to the conclusion that (G-R) -- if I remember correctly -- on the Stebbins-Kron system was just the right color for these two effects to cancel out. And this also tends to explain why the (V-R) color works as a black-body indicator in this relationship.

Shipman: Good, I'm glad to get the history straight.

Wesselink: Have you any idea how much the effect of the bandwidth might be, if you change from a narrow band to a broad band?

Shipman: I don't have a good estimate of the uncertainty of the broad-band filters, but the bad estimate I have is that the absolute value of the line blocking in all of these filters is only around 10%. What I worry about is the differential line blocking between main sequence stars and giant stars. But even if that has not been done correctly in the Gingerich and Carbon models, I would say the error is probably 0.05 mag or less.

Nather: You stopped at 4000° going redward, but the relationship seems to work appreciably redward of that. Do you have any feeling as to why?

Shipman: I really don't know why. The reason I stopped there is that I took a look at some models for M dwarf stars, and there were TiO bands all over the place. So I can't argue that the continuum color resembles a broad-band color in that case.

EVIDENCE FOR THE EXISTENCE OF NONRADIAL SOLAR OSCILLATIONS: SOLAR ROTATION*

Thomas P. Caudell and Henry A. Hill
Department of Physics
University of Arizona

I. INTRODUCTION

In the recent work of Hill and Caudell (1978) the solar origin of the observed long period oscillations in apparent diameter was demonstrated. One of the strongest pieces of evidence obtained at SCLERA† for this conclusion was the phase coherency of six oscillations over a two-week period in which seven days of equatorial diameter measurements in the 1973 solar oblateness data of Hill and Stebbins (1975) were analysed. This analysis further showed, through examination of the ratio of oscillatory power at two different scan amplitudes in the finite Fourier transform edge definition, the FFTD (see Hill, Stebbins, Oleson 1975 for discussion of diameter measurement technique), that the four higher frequency modes were likely to be p-modes while the two lower to be g-modes with large values of $\ell \approx 20\text{-}40$, where ℓ is the principal order number in the spherical harmonic expansion of the eigenfunction. The discovery that g-modes of large ℓ value are excited to an observable level allows one to place new constraints on solar models (Hill and Caudell 1978).

This paper extends this form of analysis through inclusion of an additional day of data, which falls between the first four and the last three days of the previous analysis. When placed on the phase diagrams, this subsequent addition confirms the original choice of phase solutions and strengthens the solar normal mode hypothesis. The power of the oscillations as a function of day for the p-modes are also analysed for periodicity. We observe that the power fluctuates for each of the peaks in a well defined manner, going nearly to zero at the minima. This implies the existence of beating between states of approximately equal amplitudes, an interpretation which in the light of the properties of the FFTD suggests that the beating is not between states of the different ℓ values. It further suggests that the beating is between rotational split states that differ only in m, the azimuthal order number, and is reminiscent of Wolff's (1977) work on rotation in DA white dwarfs. With this interpretation, mode identification of these oscillations is made, allowing inference of the eigenfunction weighted internal rotation rate of the sun (Hill 1978).

II. PHASE COHERENCY

The phase as defined by the Fourier transform for each peak in the power spectrum was computed and shifted to a common time of day. Since this is observationally determined to within a multiple of 2π, the solution was picked which gave the best fit for a constant phase shift per day (see Hill and Caudell 1978 for details). In Figure 1 is plotted the phase solutions for the equatorial observations as a function of date, with the new point on the 17th included. These are indeed unique solutions in that displacing the last three days up or down multiples of 2π increases significantly the χ^2 variant of the linear fit. To illustrate this proposition, the square root of χ^2 for a given fit to the original seven-days observations for each peak is given in Figure 2 plotted against the displacement in phase of the last three days as a unit. The standard deviation of an individual observation has been set arbitarily to unity. Note the parabolic nature of these curves and that it is unlikely that a phase shift of 2π has occurred between the four- and three-day sets of observations. This indicates that the oscillations observed at SCLERA are phase coherent over periods of two weeks, further proof of their solar origin.

III. TEMPORAL POWER VARIATIONS

The phase coherency of the oscillatory power over a two week period implies a relatively high level of stability, i.e. low damping. This fact allows one to examine the power of the oscillations as a function of day without such complicating factors that lead to a change in the mode during the interim. Variations in power will arise if beating occurs between different unresolved eigenfrequencies within a single observed peak (Wolff 1976). The beating pairs of modes may differ in m value as well as ℓ value when solar rotation is accounted for (Gough 1977). Due to the theoretically possible values of ℓ in the observed peaks and the variation in detection sensitivity with ℓ and m of the FFTD used in these diameter measurements, the temporal dependence of power can be valuable in distinguishing between the two cases.

In Figure 3 is plotted the equatorial oscillatory power against date for the four p-mode peaks. Through the data points have been fit a function of the form $A^2\cos^2(\Omega_b t + \phi)$ where amplitude A, beat frequency Ω_b and phase ϕ were adjusted to minimize the χ^2 variant. The resultant functions have been drawn in the figure. Here ν represents the frequency of the mode in milliHertz and Ω_b the best fit beat frequency in radians per day. Both quantities are listed in the first two columns of Table 1. Because of the sampling in the time on a daily basis there are higher aliased values of Ω_b which will give equally good fits.

There are several major conclusions to be drawn from the power plots. First, the cosine squared function of a single beat frequency does indeed fit the observations quite well. This indicates that perhaps only one pair of states dominates the beating in each peak. Second, the power at the minimum goes nearly to zero, often by a factor of 100 below the maximum value. Only if the amplitudes of the two constituent states are equal to within 20% will this be possible. If the beating states were of different ℓ value, this observational result requires that their amplitudes vary with ℓ just as the variation of the FFTD sensitivity with ℓ (see Hill 1978 for discussion of ℓ dependence of the sensitivity of the FFTD). This must be true for each of the observed peaks. However, such an assumption regarding the ℓ dependence of the amplitudes is not required if the beats occur between rotationally split modes. Since the FFTD favors the mode of highest ℓ and $|m|$, the beating in a given peak of the power spectrum will be dominated by the two modes with $m = \pm\ell$. This appears to be the most likely phenomenon to occur in light of the observations to date.

In the following we present an interpretation based on the case where modes of nonzero ℓ value are excited and the beating pattern is dominated by the associated $m = \pm\ell$ states. Beats between states with $|m| < \ell$ only add lower beat frequencies commensurate with those for the $|m| = \ell$ states. This will allow extraction of information about the internal rotation of the sun.

IV. ROTATIONAL SPLITTING AND INTERNAL ROTATION

The hydrogen atom, when given an axis of symmetry through the imposition of an external magnetic field, splits the otherwise energy degenerate m states and produces a multiplet of states, $2\ell + 1$ in number for each ℓ value. As in the hydrogen atom, when the sun is given an axis of symmetry by rotation, a degenerate set of states with a given ℓ value will split its eigenfrequency into a $2\ell + 1$ multiplet (Gough 1977, Ledoux and Walraven 1958). The eigenfunction in the presence of rotation has the form,

$$\vec{\xi}_{k\ell m}(\vec{r},t) = \vec{\xi}_{k\ell m}(\vec{r}) \exp\left\{i(2\pi\nu_{k\ell}t + m\beta_{k\ell}\bar{\Omega})\right\} \qquad (1)$$

where

$$\beta_{k\ell}\bar{\Omega} = \frac{\int_0^{R_\odot} \rho\Omega \left\{ \left(\xi_{k\ell} + \eta_{k\ell}\right)^2 + [\ell(\ell+1) - 2]\eta_{k\ell}^2 \right\} r^2 dr}{\int_0^{R_\odot} \rho \left\{ \xi_{k\ell}^2 + \ell(\ell+1)\eta_{k\ell}^2 \right\} r^2 dr} \quad , \qquad (2)$$

Ω is the local rotational frequency, ρ the mass density, r the radius of the mass element, and the remaining functions are defined as components of the displacement vector for a normal mode of a nonrotating star written as

$$\left\{ \xi_{k\ell}(r) P_\ell^m(\cos\theta) e^{im\phi} \quad , \quad \eta_{k\ell}(r) \frac{d}{d\theta} P_\ell^m(\cos\theta) e^{im\phi} \quad , \right.$$

$$\left. im\, \eta_{k\ell}(r) \frac{1}{\sin\theta} P_\ell^m(\cos\theta) e^{im\phi} \right\} \quad . \tag{3}$$

The angles θ and ϕ are the standard spherical coordinates, $P_\ell^m(x)$ the associated Legendre polynomial and k is the radial order related to the number of radial nodes in the eigenfunction. Clearly $\beta_{k\ell}\overline{\Omega}$ is the eigenfunction weighted mean of the internal rotational frequency. Identification of the modes contributing to the four p-mode oscillations as well as the spatial filtering for SCLERA type diameter measurements must be clarified before $\beta_{k\ell}\overline{\Omega}$ can be determined.

The theoretical eigenfrequency spectrum of the sun is rich in states of differing ℓ value, many of which lie close together in frequency (Iben 1976 and Wolff 1978a). Due to the low resolution of an eight hour data run, several of these states may form the constituents of a single observed peak in power (Hill 1978, §2.2.3). The detection sensitivity to a particular ℓ value for the diameter measurements made at SCLERA depends on the dimensions of the aperture and the latitude of the measurement. Hill (1978) calculated the detection sensitivity for oscillations as a function of ℓ value at the equator using the solutions to the wave equation given by Hill, Rosenwald and Caudell (1978). It was found in the region between ℓ = 0 and 12 the relative detection sensitivity increases with the ℓ value by a factor of nearly 4 in power. Out of this analysis also came the result that for a given ℓ value, the relative sensitivity to m reaches a pronounced maximum when $m = \pm\ell$ and is a minimum for the m = 0 case. Combining these two theoretical results we conclude that although several different eigenmodes may be contributing to a given oscillation, the largest ℓ value will be detected the easiest. If rotationally split, the $m = \pm\ell$ states will produce the strongest detectable effect.

Consulting the eigenfrequency spectrum associated with a standard solar model (Iben 1976, Wolff 1978a), a tentative mode identification can be made for the modes that dominate the observed power spectrum. This is accomplished by picking the theoretical frequencies which fall within the observed peaks. The k value and the maximum ℓ values associated with each observational peak are listed in columns 3 and 4 of Table 1. Applying the results of the previous paragraph, we

conclude that beating must be occurring between the plus and minus m states for these largest ℓ values. Column 5 of the table is the result of dividing the appropriate alias of the beat frequency by these maximum ℓ values to give the smoothest variation in rotation rate; column 6 is the inverse of column 5 in days where the standard deviation has been estimated to be one day. There is also another solution giving a smoother rotation curve. For this solution, the rotation rate increases more rapidly than the one given in the table.

The last column in Table 1 gives estimates of the depth to which the p-mode has substantial amplitude (Wolff 1978b, Figure 2). Inside this point, the amplitude exponentially decreases to the center, thus weighting the rotational velocity curve exterior to this point. These numbers illustrate the tenet that the various beat frequencies contain the requisite information to extract the depth dependence of solar rotation.

The correlation between columns 6 and 7 in Table 1 appears to be statistically significant. Based on this analysis the interior of the sun appears to be rotating at a somewhat larger rate over the surface, a result not inconsistent with the recent work on the five-minute oscillation (Ulrich, Rhodes, and Deubner 1978) and Gough's (1977) interpretation of 12.2 day periodicities reported in the Princeton solar oblateness observations (Dicke 1976).

V. CONCLUSION

The addition of a new data point on the phase plots of Hill and Caudell (1978) confirms the coherent properties of the observed oscillations. The two large ℓ g-mode oscillations identified in the previous work may be candidates for the slowly rotating mode-locked structures of Wolff (1976). For the four low frequency p-modes, periodic nature is observed in the daily power levels, varying with periods of several days. This is attributed to beating between rotationally split m states for a given ℓ value, an effect similar to that suggested for the DA white dwarfs (Wolff 1977). In any case, nonradial modes are a major contribution to the observed solar oscillations; the nonradial character of the observed modes allows the depth dependence of the internal solar rotation to be investigated.

The authors wish to acknowledge the use of the computing facilities of Kitt Peak National Observatory and the assistance of Mr. Ross Rosenwald with the numerical techniques.

*This work was supported by the National Science Foundation and the Air Force Geophysical Laboratories.

†SCLERA is an acronym for the Santa Catalina Laboratory for Experimental Relatively by Astrometry and is a research facility jointly operated by the University of Arizona and Wesleyan University.

Table 1

ν(mHz)	$\Omega_b\left(\frac{\text{rad}}{\text{day}}\right)$	k	ℓ	$\beta_{k\ell}\bar{\Omega}\left(\frac{\text{rad}}{\text{day}}\right)$	T_{rot}(days)	$r_{eff}/R_\odot$
0.606	0.57	1	10	0.258	24.4 ± 1.0	.77
0.539	1.15	1	8	0.249	25.2 ± 1.0	.75
0.463	1.41	1	6	0.288	21.8 ± 1.0	.72
0.414	1.05	1	4	0.263	23.9 ± 1.0	.64

REFERENCES

Dicke, R. H. 1976, Solar Phys., 37, 271.

Gough, D. G. 1977, M.N.R.A.S., submitted.

Hill, H. A. 1978, The New Solar Physics, ed. J. A. Eddy (Westview Press, Boulder, Colorado).

Hill, H. A. and Caudell, T. P. 1978, M.N.R.A.S., in press.

Hill, H. A., Rosenwald, R. D., and Caudell, T. P. 1978, Ap. J., in press.

Hill, H. A. and Stebbins, R. T. 1975, Ap. J., 200, 471.

Hill, H. A., Stebbins, R. T., and Oleson, J. R. 1975, Ap. J., 200, 484.

Iben, I., Jr., and Mahaffy, J. 1976, Ap. J. (Letters), 209, 39.

Ledoux, P., and Walraven, Th. 1958, Handbuch der Physik, Vol. LI., ed. S. Flugge (Berlin, Springer-Verlag), 353.

Ulrich, R. K., Rhodes, E. J., and Deubner, F. L. 1978, preprint.

Wolff, C. L. 1976, Ap. J., 205, 612.

Wolff, C. L. 1977, Ap. J., 216, 784.

Wolff, C. L. 1978a, see §2.2.3 of Hill 1978.

Wolff, C. L. 1978b, submitted for publication.

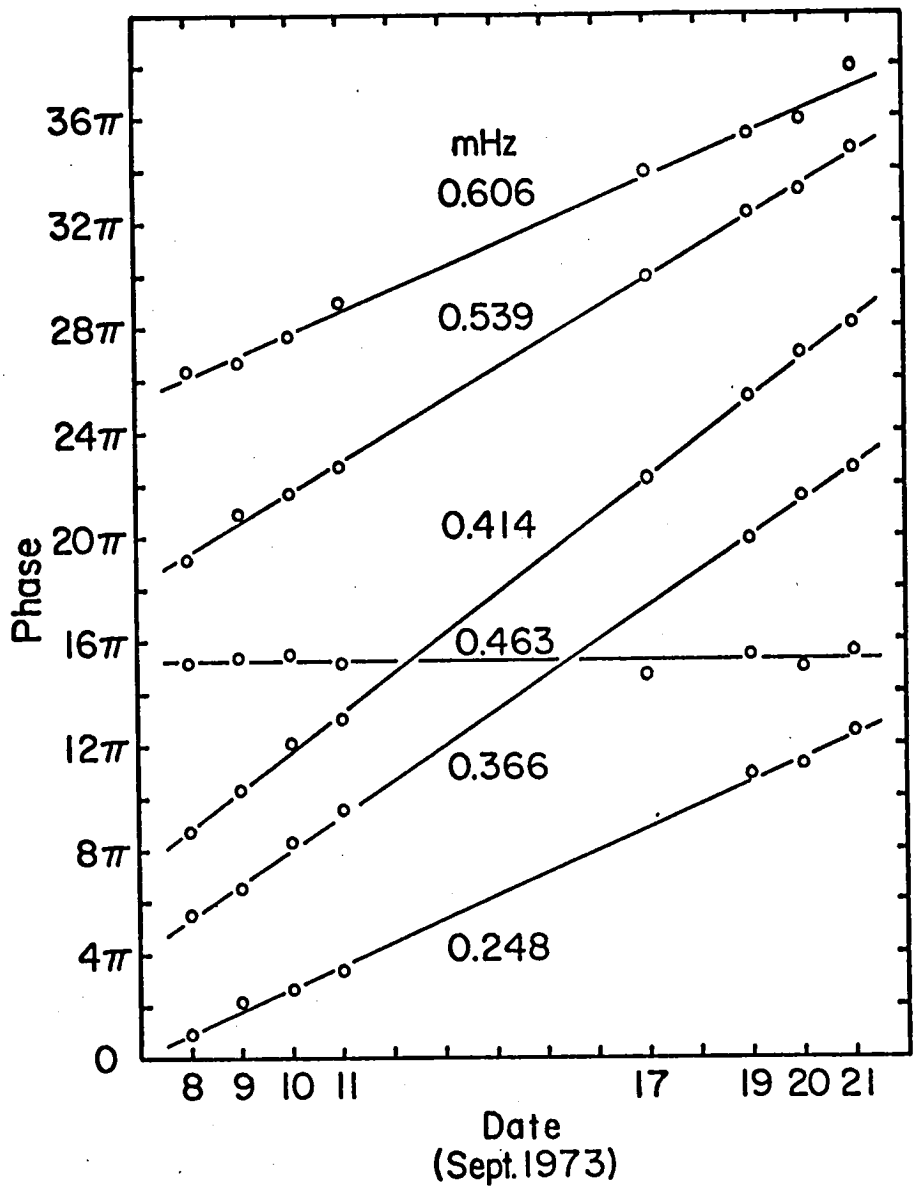

Fig. 1. The phase as defined by the Fourier transform of the observed oscillations as a function of date. The phase for a given day and predetermined time of day is defined to within an additive multiple of 2π radians. For this plot the multiple has been previously choosen (Hill and Caudell 1978) to yield the best fit to the data not including the 17th of September. The results of the 17th have been added making no change in the previous fits. The frequency for each oscillatory period obtained from these observations is listed on the figure in mHz.

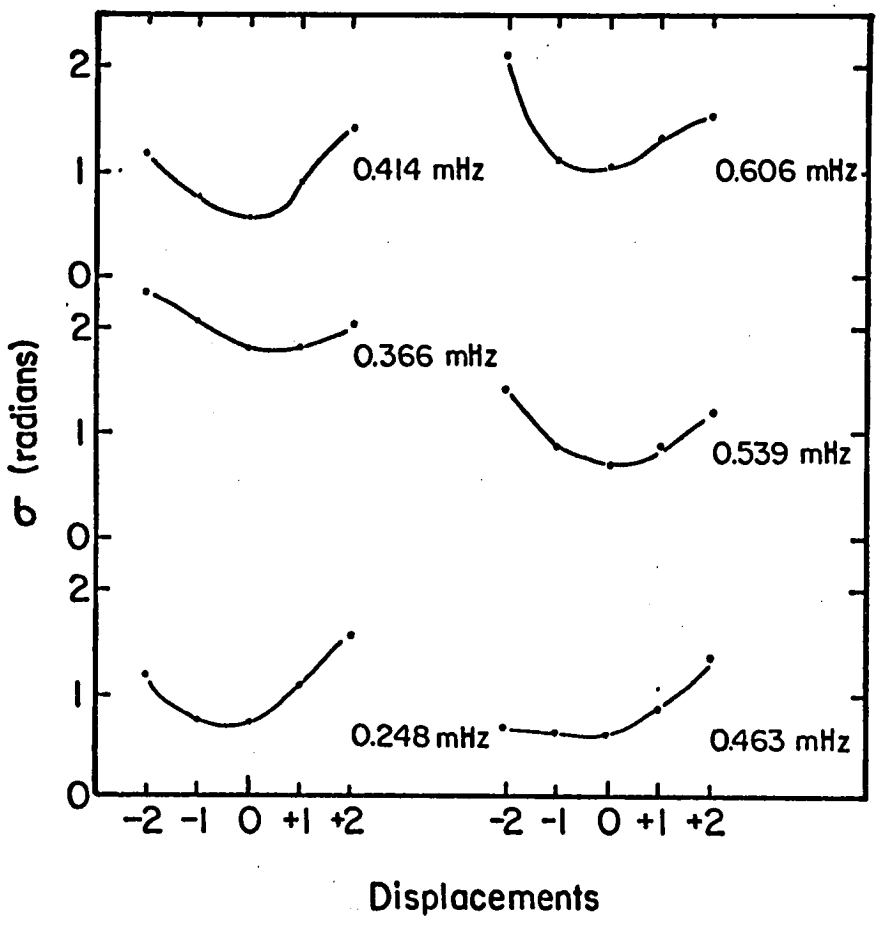

Fig. 2. The square root of the χ^2 variant of the linear fits in Fig. 1 where the last three days have been displaced up and down multiples of 2π. The standard deviations for the individual observations have been set to one. The zero of the horizontal scale is taken as the solutions plotted in Fig. 1.

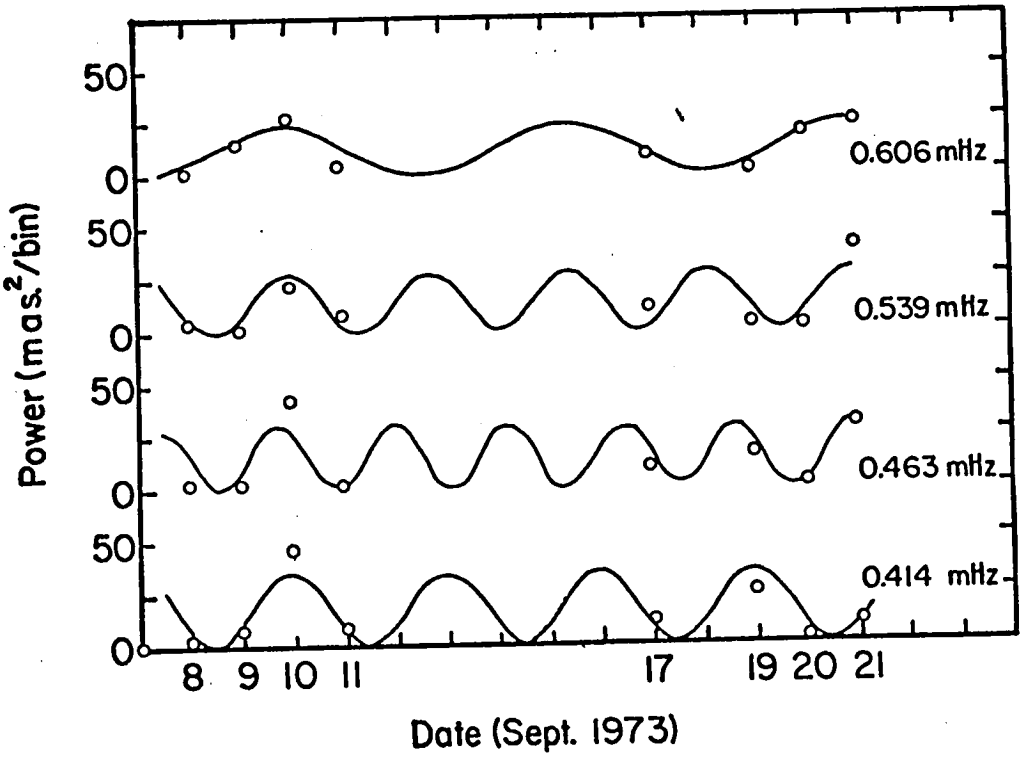

Fig. 3. The power level in units of milli-arcsec squared per frequency bin (0.03 - mHz) for the four p-mode oscillations as a function of date. The smooth curve is the least square fit to the points with the function $A^2\cos^2(\Omega_b t + \phi)$.

Discussion

[Questions interjected during the paper]

Stellingwerf: What determines the slopes in Fig. 1?

Hill: For instance, if there were exactly 24 periods of oscillation in one day, the slope can, for example, be either 0, +1, +2, -1, or -2. But if the period comes out to be, say, 45.5 minutes -- that's 31.65 periods in a day, then it's the 0.65 that determines the slope.

A. Cox: What is the 0.463 mHz oscillation like in Fig. 1?

Hill: This one is quite close to being diurnal -- it's off by about 1 .

[After Talk]

J. Cox: One question about differential rotation -- if you imagine that the rotational angular frequency is constant on a cylinder, isn't the interpretation ambiguous because of the variation from latitude to latitude in the rotation rate, i.e. differential rotation?

Hill: But if the oscillation is coherent over a time long compared to the period of oscillation, then when one measures rotational splitting, one measures an average over the entire Sun. So it doesn't matter whether it's a longitudinal slice in cylinders or a slice in spherical surfaces. One doesn't measure the splitting locally; it's a weighted average. The equation that was written down by van Horn had Ω outside the integral because he had uniform rotation, but as soon as you have non-uniform rotation, Ω goes inside the integral and you get a weighted average of Ω over the entire volume.

Wesselink: Did I see that the rotational period was decreasing as you go down?

Hill: Yes, the period was decreasing as you went in.

Wesselink: Then it goes up again?

Hill: No, I think that's just scattering. The scatter was around one day in the period. There must be several interpretations, and what I've presented is just one interpretation. If you want to use it, you must conclude there's a trend there. There may also be more structure.

A PRELIMINARY ATTEMPT TO INTERPRET THE POWER SPECTRUM OF THE SOLAR FIVE MINUTE OSCILLATIONS IN TERMS OF THE GLOBAL OSCILLATION MODEL.

D.A.Keeley
Lick Observatory, Board of Studies in Astronomy and Astrophysics
University of California, Santa Cruz

To be presented at the Conference on Current Problems in Stellar Pulsation Instabilities, Goddard Space Flight Center, Greenbelt, Maryland June 1-2, 1978.

ABSTRACT

The observed power spectrum of the solar five minute oscillations is discussed from the viewpoint that the oscillations are excited by turbulent convection. The observations place significant constraints on the theory, and suggest constraints on the solar model structure.

I. INTRODUCTION

The solar five minute oscillations provide a sensitive probe of the properties of the solar atmosphere and upper convection zone, and a challenge to theories which attempt to explain the amplitude of the oscillations as a function of frequency and spatial wave number. This paper discusses some properties of the power spectrum of the oscillations, in the context of the specific excitation mechanism described by Goldreich and Keeley (1977). It also discusses the effect of the atmospheric temperature profile, and the mechanical boundary condition. In § III the observed power spectrum as a function of aperture size is used to suggest constraints on the theoretical surface velocity of individual normal modes having periods near five minutes. It has already been noted by Ulrich and Rhodes (1977), that the frequency spectrum is better represented by solar models with mixing length equal to two or three pressure scale heights. It is shown in § IV that the steep low frequency side of the peak in the power spectrum is also more readily explained if the mixing length is greater than one scale height. The high frequency end of the power spectrum is also discussed.

II. BRIEF DESCRIPTION OF OBSERVATIONAL DATA

The main observational data to be considered here are the shape of the power spectrum, and the dependence of the power density at a given frequency, on the horizontal scale observed. Examples of the data available are given by Fossat and Ricord (1975), and Fossat, Grec, and Slaughter (1977). For observations through circular apertures, the power spectrum shows a rather sharp peak very near 5 minute period, and the position and shape are rather insensitive to aperture diameter over the range from 22" up to

several minutes of arc. One of the most striking features is the steep rise on the low frequency side of the peak; the power density increases by a factor of about 6.5 between about 7 minutes and 5 minutes. On the high frequency side, the drop-off is roughly half as steep. An additional piece of information is the fall-off in power density at the peak, as a function of aperture size. The data of Fossat and Ricord (1975) suggest a drop by a factor $\sim$2.5 in power density, when the aperture diameter goes from 22" to 60".

III. THE RELATIVE CONTRIBUTION OF DIFFERENT SPHERICAL HARMONIC MODES

a) Theoretical result of the averaging process.

Consider observations made through a circular aperture sufficiently small that the region viewed on the solar surface subtends a small solid angle at the center of the sun. Then the sphericity of the surface can be neglected and the vertical component of velocity can be written in the form

$$V(\theta, \phi, t) = \sum_{Lm} v_{Lm} \; Y_{Lm}(\theta,\phi) e^{-i\omega_{Lm} t},$$

in which θ and ϕ are spherical polar coordinate angles, Y_{Lm} is a spherical harmonic, and ω is the oscillation frequency. v_{Lm} is the velocity amplitude for a given Lm mode. The spatial averaging can be carried out most simply if the polar axis of the coordinates is chosen to be the line of sight. Let θ_o be the angular radius of the disc as seen from the center of the sun. Then

$$V = \sum_{Lm} v_{Lm} e^{-i\omega_{Lm} t} \frac{1}{\Delta\Omega} \int_{\cos\theta_o}^{1} Y_{Lm} \, d\Omega$$

$$= \sum_{L} v_{Lo} e^{-i\omega_{Lo} t} \frac{2\pi}{\Delta\Omega} \left(\frac{2L+1}{4\pi}\right)^{\frac{1}{2}} \sin\theta_o P_L^{-1}(\cos\theta_o),$$

where P_L^{-1} is an associated Legendre function. For $L\theta_0 \ll 1$, but $\theta_0 \ll 1$

$$V = \sum_L v_{Lo} e^{-i\omega_{Lo} t} \left(\frac{2L+1}{4\pi}\right)^{\frac{1}{2}}$$

and for $L\theta_0 \gg 1$, but $\theta_0 \ll 1$,

$$V = \sum_L v_L \left(\frac{2}{\pi \theta_0^{\frac{1}{2}}}\right) \left(\frac{1}{L\theta_0}\right) \cos\left[(L+\tfrac{1}{2})\theta_0 - \frac{3\pi}{4}\right]$$

The theoretical calculations give mean square velocities for each normal mode; these are assumed to add incoherently. Thus the formulae above yield

$$V^2 = \sum_L v_L^2 \left(\frac{2L+1}{4\pi}\right), \quad L\theta_0 \ll 1, \text{ and}$$

$$V^2 = \sum_L v_L^2 \frac{4}{\pi^2 \theta_0} \frac{1}{(L\theta_0)^2} \cos^2\left[(L+\tfrac{1}{2})\theta_0 - \frac{3\pi}{4}\right], \quad L\theta_0 \gg 1.$$

To compare with observations made with a finite bandwidth $\Delta\omega$, the sum over L's is taken for all modes having frequencies within that band. If $\Delta\omega$ is not too small, there will be one or more modes with no radial nodes, one or more with one radial node, one or more with two radial nodes, etc., contributing. Within each such group the L value will vary over a range depending on the bandwidth $\Delta\omega$, and the L values involved in different groups will be quite different except when L itself is small or the bandwidth is wide. From the calculated relation between frequency and L for modes with a fixed number of radial nodes, $\frac{\Delta L}{L} \approx 2 \frac{\Delta\omega}{\omega}$. Thus the number of modes expected in $\Delta\omega$ is $\sim 2 L \frac{\Delta\omega}{\omega}$, provided this number is greater than unity;

if the bandwidth is very small some groups may not contribute at all. In this case, the bandwidth of the individual normal modes may be important. If within each group it is assumed that V_L^2 is the same, the power can then be written as

$$V^2 = \frac{\Delta\omega}{\omega} \sum_L v_L^2 \left(\frac{2L+1}{4\pi}\right) (2L), \quad L\theta_0 \ll 1$$

$$V^2 = \frac{\Delta\omega}{\omega} \sum_L v_L^2 \frac{4}{\pi^2\theta_0} \frac{1}{(L\theta_0)^2} (2L)\cos^2\left[(L+\tfrac{1}{2})\theta_0 - \frac{3\pi}{4}\right], \quad L\theta_0 \gg 1 .$$

where the sum now is over the central L values of each group. The power per unit frequency interval follows directly from these formulae.

b) Trial distributions of v_L^2

It is instructive to plug in some trial distributions for v_L^2 as a function of L, to see whether any clues to the actual distribution of mode energies in the sun can be obtained. The L values for the groups depend on ω; for definiteness, a frequency $\omega = 2 \times 10^{-2}$ sec^{-1} was chosen. Approximate L values for groups near this frequency are as follows, for a model with mixing-length equal to one pressure scale height: 1004, 620, 386, 270, 195, 150, 120, 98, 80, 68, 56, 50, 43, 36, 30, 25, 19. Relative power densities were calculated corresponding to the following three cases: Case 1) $v_L^2 = 1$ for all L. Case 2) $v_L^2 = L$. Case 3) $v_L^2 = L^{-1}$. The calculations were simplified by omitting the $\cos^2$ factor, and by using the asymptotic form for small $L\theta_0$ up to the point where it intersected the form for large $L\theta_0$. This occurred at $L\theta_0 \approx 2\pi^{-\frac{1}{3}}$. The results are shown for six different aperture sizes, in table 2. The most important point to note is that in all three cases, the ratio of power densities at 22" and 60" is greater than the observed ratio of 2.5 noted earlier. Although these

calculations are extremely crude, they suggest that there may be problems if v_L^2 is constant or an increasing function of L. In fact, current calculations (Keeley 1977) suggest that v_L^2 increases with L for periods longer than ~3.5 minutes, if turbulence provides the only damping mechanism. This suggests that it will be worthwhile to repeat the calculations presented in table 1, using an accurate representation of the Legendre function. Results similar to those of the crude calculation may present a severe challenge to the turbulent excitation theory, and a significant constraint on any theory which predicts amplitudes of individual normal modes. If, on the other hand, the observations at 22" suffer from seeing or guiding effects which reduce the power observed at high spatial wave number, then the results may be compatible.

IV. THE SHAPE OF THE POWER SPECTRUM

Since the observations suggest that the shape is relatively independent of aperture size, it is convenient to discuss the power spectrum corresponding to fixed values of L. Results for L = 100, 200, and 300, all of which contribute to the power at periods as long as about 10 minutes, are considered in detail below. The discussion naturally divides into consideration of the energy to which an individual mode is excited, and the shape of the eigenfunction for the velocity amplitude. Of course, these are not totally independent, but this separation will be useful.

The preliminary results reported by Keeley (1977) showed that for models with mixing length equal to one or two pressure scale heights, the surface $(\text{velocity})^2$ for $200 \leq L \leq 600$ had a peak near $\omega \approx 2 \times 10^{-2}$ (period ~5.25 minutes). The peak was steepest on the low frequency side, in general agreement with observations. However, it was noted at that time

that the peak was not nearly sharp enough. These calculations include only turbulent dissipation in the calculation of the excitation energy, and the eigenfunctions were calculated for the adiabatic case.

a) The shape of the eigenfunctions

It is convenient to define an effective mass as the excitation energy required to produce a v^2 (averaged over the surface, and in time) of $(1\ \mathrm{cm/sec})^2$, at any particular depth in the atmosphere. This depends on the shape of the eigenfunction, but not on the actual excitation energy. The actual v^2 is obtained as the quotient of the excitation energy and the effective mass.

On the low frequency side of the peak, the increase in v^2 is due to an initial decrease in effective mass as the number of radial nodes in the eigenfunction increases. Physically, this occurs because the kinetic energy of the higher modes is more concentrated in the surface region, where the density is lower, and less energy is required to produce a given velocity. In the models discussed by Keeley, the excitation energy decreased with ω, but this effect was more than compensated by the decrease in effective mass, for $\omega < 2 \times 10^{-2}$. At higher frequencies (in a sequence with fixed L) the effective mass dropped off relatively slowly, and the net result was the high-frequency cut-off noted above.

The problem of insufficient steepness at low frequency can be approached from two directions. The first is to construct models in which the fall-off of effective mass is more rapid in the frequency range $\omega = 1.5 \times 10^{-2}$ to 2×10^{-2}, and the second is to find models in which the excitation energy decreases more slowly with ω, at least for periods greater than about 5 minutes. The latter problem is discussed in b) below. The ratio of

effective masses over a given frequency range is conveniently expressed as $-\log (m(\omega_2)/m(\omega_1))/\log(\frac{\omega_2}{\omega_1})$. In table 2 this ratio is shown for solar models with three different values of the mixing length. The eigenfrequencies are not the same in these three cases, but $\omega_1 \approx 1.5 \times 10^{-2}$ and $\omega_2 \approx 2 \times 10^{-2}$ for the functions chosen. It is clear from the table that the model with largest mixing length is the most favorable, at all L values considered. If the excitation energies were roughly equal over this frequency range, the slope would be almost steep enough. Of course, the exact comparison with observations through a circular aperture requires that the results for various L values be combined as discussed in §III above. The results shown in table 2 are for models which have a fairly realistic atmosphere out to a temperature minimum of 4180°K.

Some preliminary calculations of nonadiabatic eigenfunctions have also been done. Including turbulent viscosity in the equations of motion does not have a significant effect on the shape of the eigenfunction, as reflected in the effective masses for the low frequency, low L modes studied so far. On the other hand, a fully nonadiabatic treatment of the radiative dissipation has a significant effect, apparently because the dissipation is very strongly localized near the top of the convection zone. For the cases studied, the result is to steepen the decrease in effective masses with increasing frequency, and thus to steepen the low-frequency side of the peak of the power spectrum. The nonadiabatic calculations can't at present be done correctly with a realistic solar atmosphere, since the radiationflux is not given simply in terms of the temperature gradient, as in the approximation usually used for stellar interiors. Also, the effects of convection are not included.

i) Effect of surface temperature and the mechanical boundary condition.

Models computed using the diffusion approximation all the way to the surface had surface temperatures of about 4880°. A more realistic value of T at the temperature minimum is about 4180° (Allen 1976). Adiabatic eigenfunctions and frequencies were computed for the diffusion models, and for models in which the empirical temperature profile was used at the surface. In addition, the models were computed with two different boundary conditions, one being that the Lagrangian pressure perturbation vanish at the surface, and the other that an outgoing wave existed (evanescent or propagating) with radial wave number determined as if the surface had an isothermal region attached to it at the boundary point of the model. The effect of a lower temperature at the surface is to make the waves more evanescent, and is expected to be most important at high frequency. At periods $\lesssim$ 5 minutes, it was found that with the $\delta^L P = 0$ boundary condition the low T model had lower effective masses (at optical depth 10^{-3}) and a slightly steeper decline in effective masses with increasing ω than the high surface temperature model. With the outgoing wave condition the situation was the opposite for both the magnitude of the effective mass, and the ratios of effective masses. In general, for either surface temperature, models with the outgoing wave condition had lower effective masses. The differences were largest at the highest frequency, where the waves were closest to being able to propagate. Significant changes in eigenfrequencies occurred only when the modes were close to propagating. Otherwise, the two atmosphere models and two boundary conditions gave nearly equal frequencies for the same physical oscillation modes.

b) The Excitation Energy

In the theory described by Goldreich and Keeley (1977), the expression for the excitation energy of a normal mode is given in the form of a quotient of two numbers. The denominator is the damping rate of the normal mode, and the numerator is a double integral, over depth in the model, and over eddy sizes at a given depth. An improved approximation to the inner integral has been used in the calculations described here.

i) Low frequency behaviour

In the discussion of the low frequency side of the peak in the power spectrum, it was noted that if the excitation energies over that frequency range were roughly equal, then the steep decline in effective mass for the high mixing-length models produced a slope much more in line with the observations. However, for all three mixing lengths tested, the excitation energy decreased significantly with increasing frequency. One way of equalizing the excitation energies for periods greater than about 5 minutes is to make all modes derive the main contribution to their excitation energy from a single set of eddies. The desired result will then be expected, provided the equipartition argument (Goldreich and Keeley 1977) is approximately valid. The result can be achieved, in fact, by a decrease in the correlation time for eddies in the outer part of the convection zone. If $\omega \tau_c < 1$ at $\omega \lesssim 2 \times 10^{-2}$ for the largest, most energetic eddies at a given depth, then all modes with $\omega < 2 \times 10^{-2}$ will tend towards energy equipartition with these eddies. If $\omega \tau_c > 1$ for the largest eddies, then the modes will tend to equipartition with a smaller, less energetic eddy having a correlation time satisfying $\omega \tau \approx 1$. In the present theory, the correlation time for the largest eddies is taken to be the mixing length divided by the convective velocity, and is scaled to

smaller eddies by assuming a Kolmogoroff spectrum. Then the integral over eddy sizes depends on the correlation time assumed for the largest eddies in the form

$$\mathcal{L}(\omega) = \tau_c \int_0^1 \frac{dx}{x} \, x^{7.5} \exp\left(-\frac{1}{4}\omega^2 \tau_c^2 \, x^2\right)$$

This is a slow function of ω for $\omega \tau_c \ll 1$, but drops like $\omega^{-7.5}$ for $\omega \tau_c \gg 1$. The changeover between the two types of behaviour is rather gradual; thus a change in τ_c which shifts the low frequency modes into the flat region results in a slower fall-off of the excitation energy, and therefore of the power spectrum, at high frequency.

The behaviour of excitation energy expected from the above discussion was verified by artificially increasing the convective velocity near the surface of the convection zone. A factor of less than two was sufficient to achieve the desired result. Thus it appears possible to reproduce, more or less, the steep rise in the power spectrum by a decrease in correlation time, in combination with a model with large mixing length. Of course, some of this gain is at the expense of the high-frequency fall-off.

ii) High frequency behaviour

The power spectrum as presently computed does not fall off very fast at high frequencies, at fixed L, except for L > 1000 or so (Keeley 1977). If such high L values do make substantial contribution to the power observed through typical apertures, they will improve the shape of the high frequency end substantially. However, it seems likely that radiative damping will play a significant role in decreasing the excitation energy

for high-frequency modes. The only published nonadiabatic results on radiative damping are those of Ando and Osaki (1975, 1977). They find that the modes around 5 minutes are linearly unstable, but that modes near 3 minutes are stable. Strong damping sets in at somewhat lower frequency in their 1977 calculations, which include a chromosphere and corona. For the present models, the turbulent damping exceeds the radiative driving in all cases, but they are comparable for some modes. The result of a negative contribution to the damping would be an increase in the excitation energy of those modes; this could have a significant effect on the spectrum. For periods greater than about 7 minutes, the radiative growth or decay rate is relatively small compared to the turbulent decay rate. One important source of uncertainty is the calculation of the damping by the turbulent viscosity approximation. In addition, the calculations by Ando and Osaki do not include convection, and also do not calculate the radiative flux perturbation strictly correctly in the part of their model which employs an empirical $T(\tau)$ relation. Some preliminary nonadiabatic calculations using models with the high-temperature boundary, but no convective perturbations, find stability for all modes checked in the 3 to 10 minute range, without the effect of turbulent viscosity. A further source of uncertainty is the convective velocity profile (and magnitude) in the outer part of the convection zone, since this region contributes strongly to both the turbulent damping, and the total excitation.

V. SUMMARY OF RESULTS

The crude calculation of the power density near five minute period, as a function of aperture size, is not in agreement with observations; if a more accurate calculation establishes this discrepancy more firmly, then the observations may provide a powerful constraint on any theory of the excitation of the oscillations. In the present state of the theory, it seems possible to explain the steep low frequency side of the power spectrum peak. This requires, however, that the mass distribution of the sun be more like that of a model with a mixing length of three pressure scale heights, than one scale height. Important uncertainties in the damping due to radiative and convective energy transport preclude any strong statements about the high frequency end of the power spectrum; if there is linear driving comparable to the turbulent damping for periods near five minutes, this could have a significant effect on the sharpness and position of the peak.

This work was supported in part by NASA grant NGL-05-002-003.

REFERENCES

Allen, C. W. 1976, Astrophysical Quantities, (Third edition, London: Athlone Press).

Ando, H. and Osaki, Y. 1975, Publ. Astron. Soc. Japan, 27, 581.

Ando, H. and Osaki, Y. 1977, Publ. Astron. Soc. Japan, 29, 221.

Fossat, E., Grec, G., and Slaughter, C. 1977, Astron. and Astrophysics, 60, 151.

Fossat, E. and Ricord, G. 1975, Astron. and Astrophys. 43, 243.

Goldreich, P., and Keeley, D. 1977, Ap. J. 212, 243.

Keeley, D. 1977. Proceedings of the Symposium on Large Scale Motions on the Sun, Sacramento Peak Observatory, Sept. 1-2, 1977.

Ulrich, R. K., and Rhodes, E. J. 1977, Ap. J. 218, 521.

TABLE 1

Power density as a function of aperture size for three different assumptions about the velocities.

Case 1: $v_L^2 = 1$
Case 2: $v_L^2 = L$
Case 3: $v_L^2 = L^{-1}$

	Aperture diameter	<2"	5"	10"	22"	60"	120"
	θ_o	< .00135	.00325	.0065	.0143	.0390	.078
	L_c	> 1004	418	209	95	35	17
Case 1	Power density $L < L_c$	3.25×10^6	4.66×10^5	2.13×10^5	4.38×10^4	3.85×10^3	~0
	Power density $L > L_c$	0	3.87×10^5	1.65×10^5	6.83×10^4	1.33×10^4	3.02×10^3
	Total	3.25×10^6	8.53×10^5	3.78×10^5	1.12×10^5	1.72×10^4	3.02×10^3
Case 2	Power density $L < L_c$	2.69×10^9	1.84×10^8	2.97×10^7	2.63×10^6	1.01×10^5	~0
	Power density $L > L_c$	0	2.96×10^8	7.40×10^7	1.39×10^7	1.20×10^6	$\sim 1.82 \times 10^5$
	Total	2.69×10^9	4.80×10^8	1.03×10^8	1.65×10^7	1.30×10^6	$\sim 1.82 \times 10^5$
Case 3	Power density $L < L_c$	6.52×10^3	3.27×10^3	1.95×10^3	8.23×10^2	1.51×10^2	~0
	Power density $L > L_c$	0	5.32×10^2	4.45×10^2	4.68×10^2	2.29×10^2	8.7×10^1
	Total	6.52×10^3	3.80×10^3	2.40×10^3	1.29×10^3	3.80×10^2	8.7×10^1

TABLE 2

Logarithmic slope $\frac{\Delta \log (\text{effective mass})}{\Delta \log (\omega)}$ between $\omega \approx 1.5 \times 10^{-2}$ and $\omega \approx 2 \times 10^{-2}$, at three optical depths, for three values of mixing length/pressure scale height.

	Mixing length	1	2	3
	$\tau = 10^{-3}$	2.596	4.306	4.944
L = 100	$\tau = 10^{-2}$	2.087	3.929	4.563
	$\tau = 0.7$	1.213	3.072	3.688
	$\tau = 10^{-3}$	2.846	4.491	5.060
L = 200	$\tau = 10^{-2}$	2.426	4.150	4.719
	$\tau = 0.7$	1.561	3.378	3.949
	$\tau = 10^{-3}$	2.756	4.746	5.337
L = 300	$\tau = 10^{-2}$	2.323	4.419	5.011
	$\tau = 0.7$	1.517	3.676	4.271

Discussion

A. Cox: You have this high value of the mixing length -- three pressure scale heights -- so how deep in either mass or temperatures does the eigenfunction have any size? Does it go in very deep -- 2000°K? Half way into the Sun?

Keeley: Well, if you mean 0.1 of the surface amplitude, it goes in a very short distance -- a few percent of the radius. It doesn't go very deep into the convection zone. For a reasonably low ℓ value -- say $\ell = 10$, which I haven't shown -- then it goes a lot deeper. For $\ell = 1000$ it really stays way out at the surface.

Shipman: Presumably, it does go more than one mixing length, however.

Keeley: Yes, the scale height is around $10^7 - 10^8$ cm, and it goes in farther than that.

Concluding Remarks

A. J. Wesselink

I have often wondered about a zoologist's reaction, who, by looking over an astronomer's shoulder, acquaints himself with the terms we are using in our science. The collection: giant, dwarf, Cetus (whale), fishes, Taurus (bull), Camelopardalis (giraffe) and many others is hardly second to that he is using in his own field. Our zoological manners of doing astronomy seem to continue unto today -- o Ceti was referred to as a jelly-fish by one of us during this conference.

There are still problems with the absolute magnitudes of RR Lyrae variables as derived from statistical parallaxes despite the accurate work on proper motions and radial velocities that has been done. It is not our intention to elaborate here on the method of statistical parallax but the three results that are obtained for the same group of stars should be independent. However, in the case of the RR Lyrae's it is found that these are positively correlated, which indicates the presence of errors in the photometry, the only element common to the three methods. This problem could be solved by securing mean apparent magnitudes for all RR Lyrae's on a homogeneous photometric system. Another difficulty of our problem is our lack of sufficient knowledge of the velocity-ellipsoid, which unfortunately is more difficult to remedy. Observations in the Small Magellanic Cloud revealed the presence of a type of "RR Lyrae variable" about a magnitude brighter than the normal type. How many such bright "RR Lyrae's" exist in our galaxy is not known as there is no known way recognizing them there. Clearly, the presence in sensible percentages of these stars would

disturb the statistical method, which assumes the same absolute magnitude for all stars of a group.

This conference has shown the relevance of studying periods, light curves and period-changes by both observation and theory. For many years the RR Lyrae variables in globular clusters have been observed for period changes by photography. This photographic method, the only one available twenty and more years ago, has the merit of being efficient as many variables are photographed simultaneously on a single plate. Unfortunately the epochs, the periods and the period changes are scarcely accurate enough to check whether the rates of change of these periods are either constant (as demanded by evolution) or variable (which would apply in the case evolution and semi-convection would both operate). The electronic camera, already available for some time, has not yet been employed for this type of work. Although it is just as efficient as the photographic plate, its superior accuracy would determine the rate of change of the periods with the precision required. I would like to recommend the use of the electronic camera for the study of variable stars in globular clusters for observatories in the Eastern parts of the United States as good results in this program are guaranteed despite the often mediocre atmospheric conditions.

We have heard some illuminating lectures on the Beta Cep variables. The light and velocity variations in these stars are both small and the older methods of observing, mostly photographic, have often been too crude to unravel the complicated period structure. This situation caused O. Struve, in the early forties, to call them: "The skeletons in the closet", although we owe the most vivid descriptions of these stars to him. Modern Knowledge of the Beta Cep variables has been acquired mainly by the photoelectric

methods of observing and it is unlikely that the degrading qualification, mentioned before, will be remembered for long. Much progress has also been made through high dispersion spectroscopy and the study of line profiles. More photoelectric photometry on the Beta Cep variables is required now. I think it is a myth that first class photometric results necessarily require "photometric Skies". The comparison photometer first designed by Walraven and further developed by McCord eliminates most of the ill effects of uneven transparency and clouds by the rapid succession of comparisons between the variable and a constant star. I hope that this type of photoelectric photometry will soon be used on Beta Cep variables, Delta Scuti variables and other short period variables at observing sites in the Eastern parts of the United States where, as we mentioned before, the observing conditions are only average.

According to a number of speakers at this conference there is a discrepancy between the masses of RR Lyrae variables as deduced from pulsation theory and evolution theory. The problem has apparently no obvious solution in either the choice of the stellar model or the identification of the mode. The mass as found from pulsation theory is sensitive to the adopted radius. A systematic error in the latter of 10% is quite possible and would explain most of the discrepancy found for the mass derived by means of the two theories.

Hanbury Brown's measures of the angular diameters of a number of bright stars with his intensity interferometer are rightly admired. The existing instrument at Narrabri, Australia is unfortunately not powerful enough to measure even the brightest pulsating variables. We hear that a bigger instrument is being built, which will be large enough to measure the

brightest Cepheids. We are looking forward to Hanbury Brown's report that pulsating variables really do.

Including Baker's after dinner speech there have been forty-two lectures and 54 contributing authors. A. N. Cox contributed to four different papers, which is more than anybody else did. Would you please show your appreciation to Art in the usual manner (applause).

This has been a good conference. It is surprising how many new and interesting things one can hear in only two days.

Our thanks go to both the scientific and the local organizing committees. We thank the speakers for preparing and delivering their talks. We are grateful to the Goddard Space Flight Center for the hospitality. I may conclude with the wish of seeing you all again at the next meeting on pulsating variable stars.

BIBLIOGRAPHIC DATA SHEET

1. Report No.	2. Government Accession No.	3. Recipient's Catalog No.
NASA TM-80625		

4. Title and Subtitle	5. Report Date
Current Problems in Stellar Pulsation Instabilities	May 1980
	6. Performing Organization Code

7. Author(s)	8. Performing Organization Report No.
David Fischel, Janet Rountree Lesh and Warren M. Sparks	

9. Performing Organization Name and Address	10. Work Unit No.
National Aeronautics and Space Administration Goddard Space Flight Center Greenbelt, MD 20771	11. Contract or Grant No.
	13. Type of Report and Period Covered
12. Sponsoring Agency Name and Address	Technical Memorandum
National Aeronautics and Space Administration Washington, D.C. 20546	14. Sponsoring Agency Code

15. Supplementary Notes

16. Abstract The fourth meeting in the series of stellar pulsation conferences sponsored alternately by the Los Alamos Scientific Laboratory and the Goddard Space Flight Center was held at GSFC in Greenbelt, Maryland, on 1-2 June 1978. In contrast to previous conferences in this series, the topics of discussion included all kinds of pulsating variable stars, rather than Cepheids alone. In recognition of this broader scope, this conference was entitled "Current Problems in Stellar Pulsation Instabilities."

The Scientific Organizing Committee consisted of Drs. Morris L. Aizenman, Annie Baglin, Arthur N. Cox, David Fischel, R. Edward Nather, Kurt von Sengbusch, and Warren M. Sparks (chairman). On the Local Organizing Committee were Drs. David Fischel, Warren M. Sparks, and Janet Rountree Lesh (chairman). We made a concerted effort to gain international participation in the meeting, and about 60 scientists from 10 countries attended.

Dr. Adriaan J. Wesselink, whose pioneering work is the basis of many modern variable star studies, was an honored guest at the conference. We wish to thank Dr. Wesselink for his many perceptive comments during the discussion periods, and also for his concluding remarks.

Thanks are also due to the session charimen, and to Dr. Norman Baker for his witty contribution to the conference dinner. We gratefully acknowledge financial support for this meeting from the National Aeronautics and Space Administration.

17. Key Words (Selected by Author(s))	18. Distribution Statement
Stellar Pulsation, Stellar Instabilities, Cepheids, Beta Cepheid Star	Unclassified - Unlimited Subject Category 90

19. Security Classif. (of this report)	20. Security Classif. (of this page)	21. No. of Pages	22. Price*
Unclassified	Unclassified	710	$21.50

*For sale by the National Technical Information Service, Springfield, Virginia 22161

*U.S. GOVERNMENT PRINTING OFFICE: 1980 635-050/4 1-3

National Aeronautics and
Space Administration

Washington, D.C.
20546

Official Business
Penalty for Private Use, $300

SPECIAL FOURTH CLASS MAIL
BOOK

Postage and Fees Paid
National Aeronautics and
Space Administration
NASA-451

NASA

POSTMASTER: If Undeliverable (Section 158
Postal Manual) Do Not Return